

# Three-Membered Silacycles and Silylenes in Thermal and Photochemical Curing of Polysiloxanes

Matthias Fabian Nobis

Vollständiger Abdruck der von der TUM School of Natural Sciences der Technischen Universität München zur Erlangung eines  
**Doktors der Naturwissenschaften (Dr. rer. nat.)**  
genehmigten Dissertation.

Vorsitz: Prof. Dr. Angela Casini

Prüfer\*innen der Dissertation:

1. Prof. Dr. Dr. h.c. Bernhard Rieger
2. Prof. Dr. Shigeyoshi Inoue
3. Prof. Dr. Rainer Haag

Die Dissertation wurde am 19.01.2023 bei der Technischen Universität München eingereicht und durch die TUM School of Natural Sciences am 27.02.2023 angenommen.



WACKER-Institut für Siliciumchemie

The following work was carried out from March 2019 to November 2022 at the “Institute for Silicon Chemistry” at the Technical University of Munich within the WACKER-Chair of Macromolecular Chemistry under the supervision of Prof. Dr. Dr. h.c. Bernhard Rieger. This work was financially supported by a doctoral scholarship of the WACKER Chemie AG.

## Acknowledgements

First, I want to thank my supervisor Prof. Dr. **Bernhard Rieger** for giving me the opportunity to pursue a doctorate at his chair and giving me the trust and liberty to define my own research objectives. I fully enjoyed working on this fascinating topic and I am grateful for all the support and helpful discussions concerning this research project. With his guidance, I had the chance develop my full potential and hopefully become a better researcher.

My sincere gratitude also goes to my mentor Prof. Dr. **Shigeyoshi Inoue** who advised me throughout the progression of my thesis and beyond. I am especially thankful for the constant help and prompt support at any given time. His openness to fully welcome me at his chair as an external member allowed me to further expand my knowledge in the field of low-valent silicon chemistry.

Furthermore, I would like to thank my collaboration partners Dr. **Maximilian Moxter**, Dr. **Jan Tillmann**, Dr. **Thomas Renner**, and Dr. **Wolfram Schindler** from the WACKER-Chemie AG for our joint project work, the fruitful and inspiring discussions, and the productive and pleasant atmosphere at our regular meeting. In addition, I want to give a big thanks to **Belinda Dombret** for her countless assistance and help with any rheological measurements.

In addition, I thank Dr. **Carsten Troll** for his persistent efforts to maintain this chair as it is. This includes not only the professional side of the chair, such as maintenance of our analytic instruments and chemical supplies but also the internal and social connection within the chair, by organizing various barbecue events and spoiling us with ice cream and drinks. I further thank Dr. **Sergei Vagin** for the fundamental discussions and motivating interest for my research. Beyond that, I want to thank **Annette Bauer** for her welcoming spirit and the support in all of the bureaucratic obstacles and the excellent organization.

To all former and current members of our and Inoue's chair, I enjoyed the cheerful atmosphere and helpful community within and across the different labs. I especially thank **Andreas Saurwein** for the long and lasting companionship throughout my entire studies, from the first practical lab course to the last shared day at the chair.

I thank my students **Sarah, Jonas, Matthias, Magdalena** and **Megan** for their hard-working dedication and excellent lab work, which helped me to complete this thesis.

---

I am extremely grateful for all the close friendships I have found along this way. Therefore, I would like to give a big thank to **Marc Julian Kloberg**, **Jonas Futter**, **Thomas Pehl**, **Moritz Kränzlein** and **Paula Großmann** for being such good friends and creating this memorable time.

Furthermore, I would like to express my gratitude to my predecessor and friend **Fabian Herz**, who guided me through my master's thesis and supported me in any situation. His humor and kindness have always helped me to stay curious and be in a good mood during that time. To have continued his excellent work and research as his successor fills me with pride and joy.

And finally, I would like to express my thankfulness and gratitude to my brother **Sebastian** and my parents **Kirsten** und **Peter** for their continuous support and unconditional love.

## Table of Content

Acknowledgements.....	I
Table of Contents .....	III
List of Abbreviations.....	V
List of Publications .....	VIII
Abstract.....	1
Zusammenfassung.....	2
1. Introduction – Building a Network.....	3
2. Silicon based materials.....	5
2.1. Polysilanes.....	5
2.2. Polycarbosilanes.....	8
2.3. Polysilazanes.....	10
2.4. Polysiloxanes .....	12
2.4.1. History and Origin .....	13
2.4.2. Synthesis and Production.....	13
2.4.3. Properties and Application .....	18
2.5. Curing of Polysiloxanes .....	20
2.5.1. Condensation Curing.....	21
2.5.2. Addition Curing .....	23
2.5.3. Radical Curing.....	25
2.5.4. Alternative Approaches.....	27
2.6. Organosilicon Compounds .....	33
2.6.1. Silylenes.....	34
2.6.2. Silacyclopropanes.....	40
2.6.3. Silacyclopropenes .....	46
3. Motivation and Aim – Innovative Curing of Polysiloxanes.....	52
4. Silacyclopropanes as Crosslinker in Thermal Silicone Curing .....	54
4.1. Bibliographic data.....	54
4.2. Abstract graphic (TOC) .....	54
4.3. Content.....	55
4.4. Manuscript .....	56

5. Modular silacyclopropenes: synthesis and application .....	65
5.1. Bibliographic data.....	65
5.2. Abstract graphic (TOC) .....	65
5.3. Content.....	66
5.4. Manuscript .....	67
6. Silacyclopropenes: Photo-Activity and Curing Application.....	71
6.1. Bibliographic data.....	71
6.2. Abstract graphic (TOC) .....	71
6.3. Content.....	72
6.4. Manuscript .....	73
7. Summary and Prospects .....	81
8. Literature.....	84
9. Appendix .....	94
9.1. List of Figures .....	94
9.2. List of Schemes.....	95
9.3. List of Tables.....	96
9.4. Supporting Information .....	97
9.4.1. Supporting Information for Chapter 4.....	97
9.4.2. Supporting Information for Chapter 5.....	150
9.4.3. Supporting Information for Chapter 6.....	184
9.5. License Agreements.....	265
9.5.1. License Agreement for Chapter 4 .....	265
9.5.2. License Agreement for Chapter 5 .....	267
9.5.3. License Agreement for Chapter 6 .....	269
9.6. Statutory Declaration.....	271

## List of Abbreviations

**Table 1:** General abbreviations.

Sign	Signification
Adm	adamantyl
BCF	tris(pentafluorophenyl)boran
Bp	boiling point
BuLi	Butyllithium
D <sub>3</sub>	hexamethylcyclotrisiloxane
D <sub>4</sub>	octamethylcyclotetrasiloxane
DCM	dichlormethane
DME	dimethoxyethane
DVTMS	divinyltetramethyldisiloxane
Et	Ethyl
et al.	et alia (lat. “and others”)
HMDS	hexamethyldisiloxane
HT	high temperature
HTV	high temperature vulcanization
in situ	lat. “on the spot”
iPr	Iso-propyle
KHMDS	potassiumhexamethyldisilazide
Me	methyl
Mes	mesityl
MMA	methylmetacrylate
NHC	<i>N</i> -heterocyclic carbene
NHSi	<i>N</i> -heterocyclic silylene
NTMS	bis(trimethylsilyl)amide
PDMS	polydimethylsiloxane
Ph	phenyl
PMHS	polymethylhydrosiloxane
ROP	ring-opening polymerization
RT	room temperature

## List of Abbreviations

---

RTV	room temperature vulcanization
sBu	<i>sec</i> -butyl
<i>t</i> Bu	<i>tert</i> -butyl
THF	tetrahydrofurane
TMCTS	2,4,6,8-tetramethylcyclotetrasiloxane
TMEDA	tetramethylethylenediamin
TMS	trimethylsilyl-
UV	ultraviolet

---

**Table 2:** Abbreviations for formula signs.

---

Sign	Signification [Unit]
Å	Ångström [Å]
cSt	centistokes [cSt]
d	Days [d]
$\mathcal{D}$	polydispersity index [-]
$G^*$	complex shear modulus [Pa]
$G'$	storage modulus [Pa]
$G''$	loss modulus [Pa]
h	hour [h]
$\lambda$	wavelength [nm]
$M_n$	number average molecular weight [kg/mol]
$M_w$	weight average molecular weight [kg/mol]
$M_{n,abs}$	absolute molecular weight [kg/mol]
$M_{n,rel}$	relative molecular weight [kg/mol]
min	minutes [min]
nm	nanometer [nm]
ppm	part per million [-]
T	temperature [°C]
$T_d$	degradation temperature [°C]
$T_g$	glass transition temperature [°C]
$T_m$	melting temperature [°C]
tan ( $\delta$ )	dissipation factor [-]

---



**Table 3:** Abbreviations for methods.

---

Sign	Signification
AFM	atomic force microscopy
ATR-IR	attenuated total reflection infrared spectroscopy
CA	contact angle
CI	chemical ionization
COSY	correlation spectroscopy
DLS	dynamic light scattering
DSC	differential scanning calorimetry
EA	elemental analysis
ESI-MS	electron spray-ionization mass spectrometry
EPR	electron paramagnetic resonance
GPC	gel-permeation chromatography
HMBC	heteronuclear multiple bond correlation
ig	inverse gated
inept	insensitive nuclei enhanced by polarization transfer
LIFDI-MS	liquid injection field desorption ionization mass spectrometry
NMR	nuclear magnetic resonance spectroscopy
SCXRD	single-crystal X-ray diffraction
SEC	size-exclusion chromatography
TGA	thermogravimetric analysis

---

## List of Publications

### Journal Article

1. F. Herz, † M. Nobis, † D. Wendel, P. Pahl, P. Altmann, J. Tillmann, R. Weidner, S. Inoue, B. Rieger, “Application of multifunctional silylenes and siliranes as universal crosslinkers for metal-free curing of silicones”, *Green Chemistry*, **2020**, *22*, 4489-4497. (Highlighted as “2020 Green Chemistry Hot Articles”)
2. M. Nobis, S. Inoue, B. Rieger, “Modular silacyclopropenes: synthesis and application for Si–H containing substrate functionalization”, *Chemical Communications*, **2022**, *58*, 11159-11162.
3. M. Nobis, J. Futter, M. Moxter, S. Inoue, B. Rieger, “Photo-Activity of Silacyclopropenes and their Application in Metal-Free Curing of Silicones”, *ChemSusChem*, **2022**, e202201957. (Highlighted as “VIP - Very Important Paper”)

† = these authors contributed equally.

### Patent Application

4. M. Nobis, F. Herz, B. Rieger, R. Weidner, “Silirane compounds as stable silylene precursors and their use in the catalyst-free preparation of siloxanes”, filed as PCT/EP2019/083744, published as WO2021110265A1 (04.12.2019).
5. M. Nobis, M. Moxter, B. Rieger, R. Weidner, “Silirene-functionalized compounds and mixtures thereof for preparation of and promotion of adhesion by siloxanes”, filed as PCT/EP2021/064438 (28.05.2021).
6. M. Nobis, M. Moxter, B. Rieger, “Modulare Silirene: Herstellung und Anwendung von monofunktionellen Silirenen zur variablen Funktionalisierung von Substraten mittels Hydrosilylierung”, filed as PCT/EP2022/067772 (28.06.2022).

### Publications beyond the scope of this thesis

7. A. Saurwein, M. Nobis, S. Inoue, and B. Rieger, “Synthesis of a Triphenylphosphinimide-Substituted Silirane as a “Masked” Acyclic Silylene”, *Inorganic Chemistry*, **2022**, *61*, *26*, 9983–9989.

### Conference Contributions

8. M. Nobis, F. Herz, B. Rieger, “Application of multifunctional silylenes and siliranes as universal crosslinkers for metal-free curing of silicones”, 19th International Symposium on Silicon Chemistry **2021**, Toulouse, France; Poster Presentation awarded: *Chemical Communications* Outstanding Poster Prize Presentation.

## Abstract

Polysiloxanes have become by far the most important material in the class of inorganic polymers, with a vast and still growing industry located in various countries around the globe.<sup>[1-3]</sup> Amongst the different types of polysiloxanes, the segment of cured elastomers leads the silicone market with a global share of 41 % in 2020.<sup>[4]</sup> Silicone elastomers are usually produced via addition or condensation curing by means of platinum- or tin-based catalysts. The employed metal remains in the cured product and can only be recovered through extensive purification efforts, thus creating environmental and economic challenges. In this work, different methods for alternative curing of polysiloxanes without the utilization of metal catalysis are investigated and described. The first method that will be addressed is based on multifunctional silacyclopropanes (siliranes) as thermally controlled linker scaffolds to crosslink different functionalized polysiloxanes. Herein, the described siliranes act as stable precursors and can be activated to generate the respective transient silylenes via fragmentation at temperatures above 120 °C. This highly active low valent silicon species reacts with the silicone functionalities (Si-H or Si-OH) in an insertion reaction, thus curing the liquid polymer chains to the desired elastomer. Broadening the scope of alternative curing methods, a light mediated curing is described via the introduction of silacyclopropenes (silirenes) as photo-labile silylene precursors. A model study confirms the required coupling reactivity upon irradiation and reveals an undesired side reaction, which attenuates the curing effectiveness. To counteract this issue, a method to create higher functional silirenes is described. This technique allows the functionalization of Si-H containing substrates with vinyl substituted silacyclopropenes in a hydrosilylation reaction. Providing an efficient and versatile technique to generate multi-functional silacyclopropene derivatives, ranging from small molecules to polymeric materials like polysiloxanes. This way, access is given to polymeric silirene linker scaffolds and their application as UV-active curing agents for crosslinking liquid silicones, including hydride, hydroxy, or vinyl terminated PDMS. By combining these curing methods, two different approaches are reported to produce catalyst and additive free silicone elastomers, thus creating genuine alternatives to the conventional curing methods.

## Zusammenfassung

Polysiloxane sind im Laufe der Zeit zu einem der wichtigsten Materialien innerhalb der Klasse der anorganischen Polymere geworden, aufgebaut und gestützt durch eine enorme und immer noch wachsende Industrie, in den verschiedensten Ländern der Welt.<sup>[1-3]</sup> Unter den verschiedenen Sorten an Polysiloxanen führt das Segment der vernetzten Elastomeren den Silikon Markt mit einem globalen Anteil von 41 % in 2020.<sup>[4]</sup> Silikonelastomere werden normalerweise durch Additions- oder Kondensationsvernetzung, mithilfe von Platin oder Zinn basierten Katalysatoren, hergestellt. Das eingesetzte Metall verbleibt im vernetzten Produkt und kann nur unter aufwendigen Reinigungsmethoden wieder entfernt werden, was somit umwelttechnische und ökonomische Herausforderungen erzeugt. In dieser Arbeit werden verschiedene Methoden für alternatives Vernetzen von Polysiloxanen, ohne den Gebrauch von Metallkatalyse, beschrieben. Die erste Methode basiert auf multifunktionellen Silacyclopropanen (Siliranen) als thermisch kontrollierbare Linkerstrukturen, welche unterschiedlich funktionalisierte Polysiloxane vernetzt. Die hierbei beschriebenen Silirane agieren als stabile Vorstufen und können aktiviert werden, um die entsprechenden kurzlebigen Silylene durch Abspaltung bei Temperaturen oberhalb von 120 °C zu erzeugen. Diese hochreaktiven niedervalenten Siliciumspezies reagieren mit den Silikonfunktionalitäten (Si-H oder Si-OH) in einer Insertionsreaktion, welches die flüssigen Polymerketten zu dem gewünschten Elastomer vernetzt. Um den Einsatzbereich der alternativen Vernetzungsmethoden zu erweitern, wird zusätzlich eine lichtvermittelte Vernetzung durch das Einführen von Silacyclopropenen (Silirenen) als lichtlabile Silylenevorstufe beschrieben. Eine Modellstudie bestätigt die erforderliche Kupplungsreaktion mittels Bestrahlung und zeigt eine ungewünschte Nebenreaktion, welche die Vernetzungseffektivität abschwächt. Um diesem Problem entgegenzuwirken, wird eine Methode beschrieben die höher funktionelle Silirene erzeugt. Dieses Verfahren erlaubt die Funktionalisierung von Si-H enthaltenden Substraten mit vinylsubstituierten Silacyclopropenen durch eine Hydrosilylierung. Auf diese Weise ist es möglich, polymere Silirenlinkerstrukturen zu erzeugen und diese als UV-aktive Vernetzer für die Verbrückung von flüssigen Silikonen (hydrid-, hydroxy-, oder vinylterminierte PDMS) zu nutzen. Kombiniert man diese Vernetzungsmethoden, erhält man zwei unterschiedliche Ansätze, um katalysator- und additivfreie Silikonelastomere zu erhalten, welche tatsächliche Alternativen zu den konventionellen Vernetzungsmethoden darstellen.

## 1. Introduction – Building a Network

The conceptual introduction of polymers as long chains of relatively simple repeating units by Herman Staudinger in 1920, marks the beginning of a new class of materials: the class of macromolecules.<sup>[5,6]</sup> Though their emergence only began in the middle of the last century, today, polymers and their applications are numerous and play an essential role in our modern world. Many products, ranging from simple commodities to essential components for advanced space rockets are based on innovative research to create new polymer materials. Even though there is a plethora of different polymers available today, not all polymers meet the desired properties depending on their application. Thus, further modification of these materials is key and will help to widen their application scope. There are various techniques to modify polymers, affect their chemical or physical properties and combine a variety of functions in a single material. The creation of polymer networks is one of the most effective modification techniques, which can be realized through grafting, crosslinking or blending.<sup>[7]</sup> Grafted copolymers are macromolecules, which consist of a main polymer chain as backbone with branches of different polymers attached to it. This covalent attachment process is irreversible and forms a hybrid material network. Depending on the production process a polymer can either be grafted *to*, in which the functionalized polymer branch is directly attached to the backbone, or grafted *from*, where the branching results from an in situ polymerization onto the backbone.<sup>[8,9]</sup> The creation of a network by multidirectional chain extension through the formation of covalent bonds is defined as crosslinking. This irreversible process can be the result of the polymerization of monomers with more than two functionalities or the formation of covalent bonds between premade polymer chains. This inter- or intramolecular bond formation can either be accomplished by chemical reactions (sulfur vulcanization, peroxide curing, metal catalysis, etc.) or irradiation. Once the polymer network has formed covalent linkages, the polymer chains are immobilized and generate an elastic, amorphous polymer. This transformation renders the material more robust towards solvents, light, heat, or other mechanical agencies.<sup>[10-12]</sup> Blending describes the process of mixing two or more different polymers to obtain a macroscopic homogeneous mass. The resulting blend combines the favorable properties of all its constituents and provides a completely new material. Due to their nature, most polymers are immiscible and mixing them results in an arbitrary dispersed polymer matrix. This *quasi-binary* mixture does not provide a

true two-phase or single-phase structure but something in between, without the creation of a distinct interface of the involved phases. Thus, this multi-phased material depends on a variety of factors, such as the relative concentration of the polymers in each phase, the extent of phase separation, the interaction of the respective polymers, the character of the predominant phase, or the nature of the dispersed phase. <sup>[12,13]</sup>

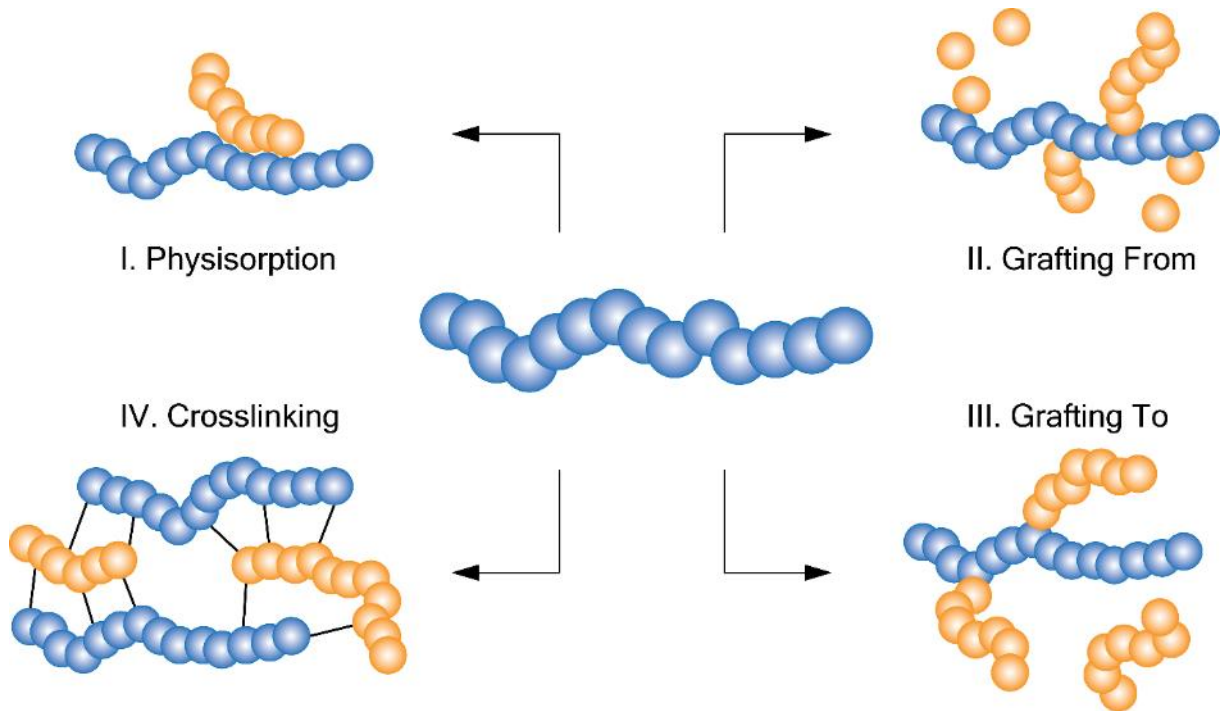


**Figure 1.** Schematic overview of different polymer association. (I) “Physisorption” describes the reversible attachment of polymers through physical attractive forces. (II) “Grafting from” is the covalent attachment of a monomer to a polymer chain followed by a polymerization, while (III) “grafting to” is referred to the functionalization of the polymer backbone with already finished polymer to create branches. (IV) “Crosslinking” describes the irreversible formation of a polymer network via chemical bonding of the individual polymer chains.

There are many different approaches to modify polymers and thus even more polymer materials with different properties. However, the technique of crosslinking, polysiloxane crosslinking in particular, is primarily considered and discussed as polymer modification in this thesis.

## 2. Silicon based materials

Silicon based materials have gained increasing relevance over the last decades due to their numerous practical applications as useful ingredients, additives, ceramics, or polymeric materials. This involves the various technical fields: Solar cells and photovoltaic applications are highly dependent on polycrystalline silicon as base material, while the development of microelectronic and optoelectronic devices have become interested in the utilization of silicon nanowires (SiNWs), crystalline or amorphous silicon (c-, a-Si) as high performance materials.<sup>[14]</sup> Silica, silicates and other functional silanes are frequently used as filler materials or additives in various industrial processes, whereas many high-tech ceramic materials derive from organosilicon scaffolds, like silicon nitride ( $\text{Si}_3\text{N}_4$ ), silicon carbide (SiC), or silicon oxycarbide (SiCO) ceramics.<sup>[15,16]</sup> Yet, one of the most successful silicon based materials are the class of polysiloxanes and other silicone derived polymers, like polysilanes, polycarbosilanes, or polysilazanes, due to their vast range of application in different products and industries.<sup>[1]</sup> In the following these silicon based polymers will be further described, regarding synthesis, properties and applications thereof.

### 2.1. Polysilanes

Polysilanes are polymers with a backbone consisting solely of silicon atoms. Different substitution at the silicon allows the creation of a variety of polymers with variable properties. Although the general chemical structure of polysilanes seems rather simple and comparison with their carbon-based analogues seems obvious, the polymerization of these macromolecules is characterized by difficult to control and harsh synthesis conditions as well as product formations with broad and polymodal molecular weight distributions.<sup>[17]</sup>

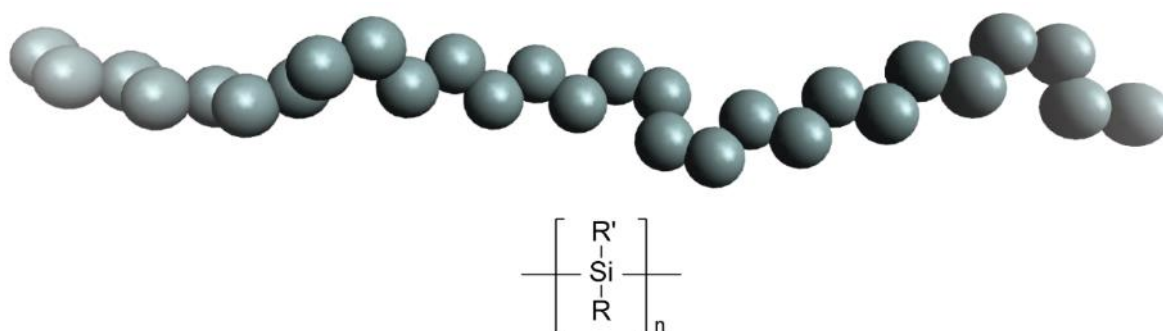
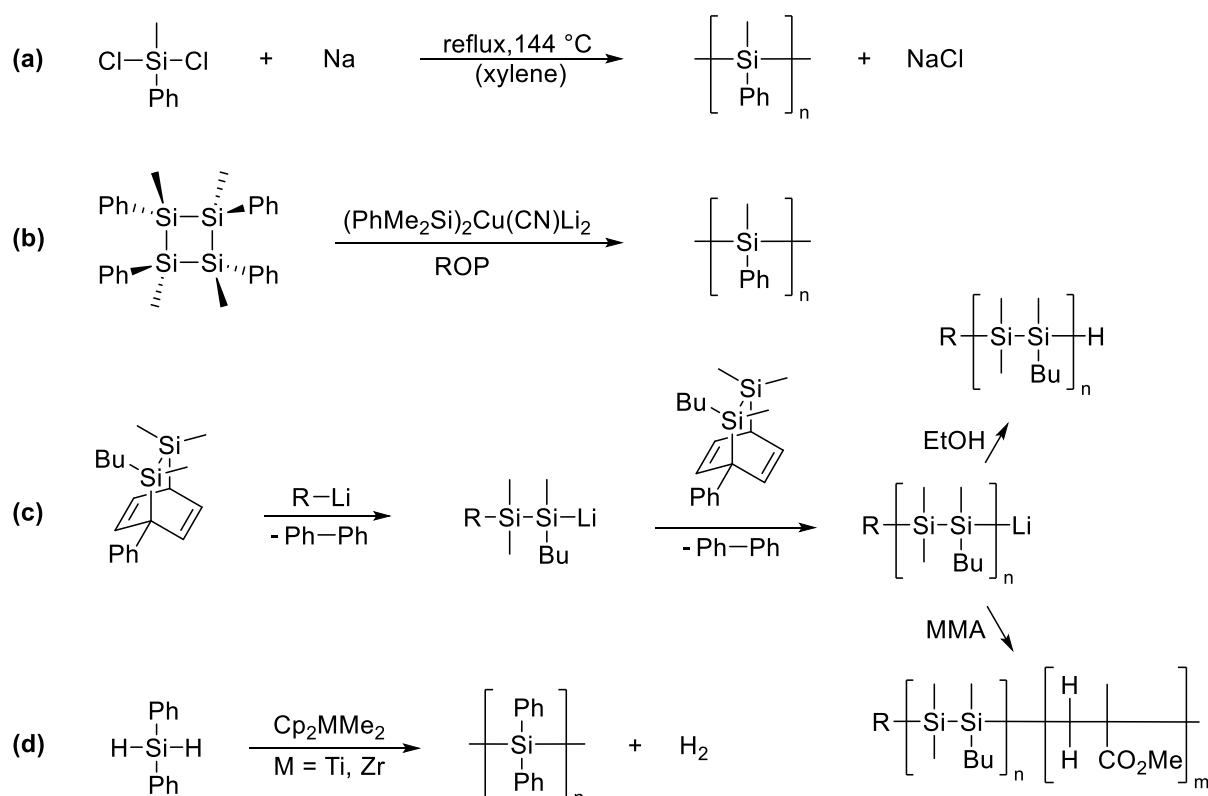


**Figure 2.** Representation and chemical structure of polysilanes consisting of a continuous silicon-silicon bond.

Since its first preparation by Kipping in the late 1920s, the most common procedure to create polysilanes is the reaction of dichlorosilanes with dispersed alkali metals via the Wurtz-type reduction.<sup>[18,19]</sup> Conducting the reaction in boiling aromatic solvents, most commonly in toluene or xylene, bears the risk of spontaneous ignition and attenuates the scope of employable functional groups, which can withstand these conditions, to a minimum.<sup>[17,20–22]</sup> Different approaches have been investigated to improve the reaction control and obtain a set of better manageable conditions. Variation of the reducing agents confirmed that alkali metals show the highest activity for producing polysilanes. Lithium favors the formation of cyclic oligomers, due to its lower reactivity compared to sodium.<sup>[23]</sup> While Na/K alloys or pure potassium metal promote polymer growth, also polymer degradation and back-biting is favored under these conditions.<sup>[24]</sup> The usage of toluene/diglyme mixtures<sup>[25]</sup> as well as different crown ethers or cryptands<sup>[26–28]</sup> in low concentrations often enhance product yields but affect the molecular weights towards lower values. To avoid these hard to control reaction conditions alternative procedures have been reported to successfully produce polysilanes.



**Scheme 1.** Overview of synthetic processes to generate polysilanes. (a) Reductive Wurtz-type coupling of dichlorosilanes. (b) Ring-Opening Polymerization of cyclotetrasilanes. (c) Anionic polymerization of masked disilenes mediated by organolithium compounds. (d) Dehydrogenative coupling of organosilanes by metallocene based catalysts.



The first one describes the ring-opening polymerization (ROP) of small strained cyclosilanes. Matyjaszewski polymerized tetramethyl-tetraphenyl-cyclotetrasilane in nearly quantitative yield by employing  $(\text{PhMe}_2\text{Si})_2\text{Cu}(\text{CN})\text{Li}_2$ . This way, polysilanes with predominant heterotactic tacticity, molecular weights up to 30 kg/mol and a PDI of 1.5 could be realized.<sup>[29,30]</sup> Further, various transition metal catalysts have been investigated to mediate the ROP, although only the formation of dimers could be achieved by utilizing Pd- or Pt-based compounds.<sup>[31]</sup> A different approach is offered by the anionic polymerization of masked disilenes in combination with an organolithium initiator.<sup>[32]</sup> The repetitive attack of the polysilanyl anion at the silicon atom of the monomer results in the propagation of the polymer anion. Subsequent addition of ethanol terminates this living-type polymerization, whilst adding methylmethacrylate (MMA) at low temperatures creates a block copolymer.<sup>[33–36]</sup> In addition, a very promising alternative derives from the dehydrogenative coupling of organosilanes by applying metallocene based catalysts. The catalytic disproportionation of the Si-H bond to create the respective Si-Si bond allows much milder reaction conditions, thus decreasing the limitation of applicable substituents and further increasing the control of the product's molecular weight and tacticity.<sup>[37–39]</sup> Due to various synthetic challenges and the problematic instability of polysilanes under UV-light, it is no surprise that this polymer class is only of minor interest for possible industrial applications. Nevertheless, first approaches to implement polysilanes as functional material have been made, as Yajima reported the rearrangement reaction of polydimethylsilane for the generation of  $\beta$ -siliconcarbide fibers in the late 1970s.<sup>[40]</sup> The discovery of unique photophysical properties, caused by interactions and electronic delocalization within the  $\sigma$ -bonded silicon backbone, gave access to the semiconductor industry and the application in electronic devices.<sup>[41]</sup> Today, polymethylphenylsilane is applied as emitter material in the production of various OLEDs,<sup>[42]</sup> or as semiconductor layers in organic field-effect transistors (OFET).<sup>[43]</sup> However, the still challenging generation of polysilanes, especially of high purity for applications in the semiconductor industry, remains the dominant issue in applying polysilanes as functional material.

## 2.2. Polycarbosilanes

Polycarbosilanes are referred to as a broad class of silicon-based polymers, in which the polymer backbone generally consists of the elements silicon and carbon in alternate positions.<sup>[44]</sup> Other definitions describe polycarbosilanes as organosilicon polymers composed of substituted silicon atoms and difunctional organic groups which bridge these silicon atoms,<sup>[45]</sup> or simply as a polymer containing silicon-carbon bonds as a backbone.<sup>[5]</sup> The most relevant members of these polymers are linear polycarbosilanes with a regular -Si-C- framework structure, yet their hyperbranched analogues have currently gained interest as base material to silicon carbide ceramics.<sup>[46,47]</sup>

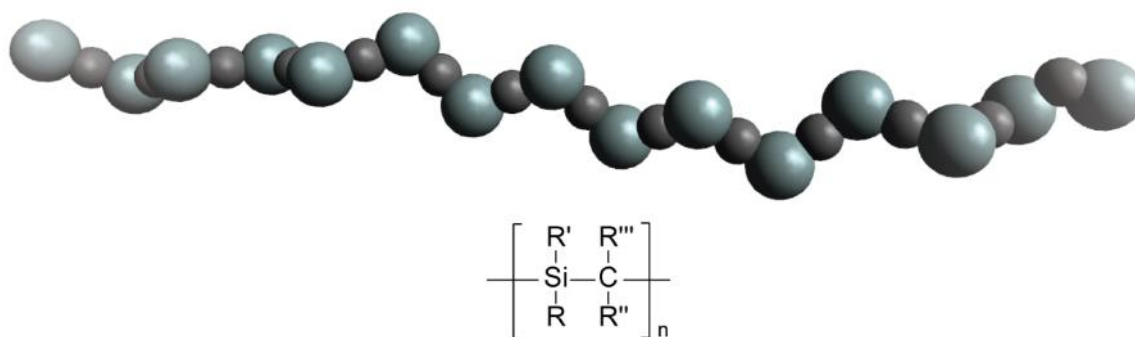
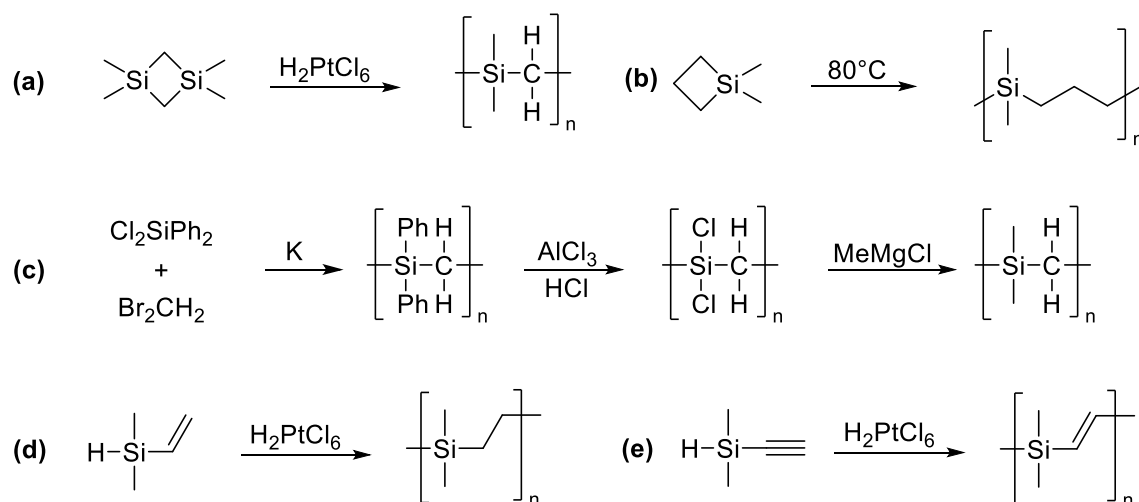


**Figure 3.** Depiction and chemical structure of linear polycarbosilanes of alternating silicon-carbon bonds.

The creation of polycarbosilanes coincides with the origin of organosilicon chemistry in the first half of the 20<sup>th</sup> century. In the beginning alkylation of chlorosilanes with zinc or mercury reagents, or the utilization of sodium in a Wurtz-Fittig coupling to combine alkyl halides with chlorosilanes, was the initial methodology to synthesize the required silicon carbon bonds. Later, organolithium and Grignard reagents have become more extensively applied over the last century and still continue to be widely used in the creation of carbosilanes to this day. However, novel approaches including hydrosilylation of alkenes and alkynes, electrolysis, ring-opening of cyclic organosilanes or gas phase pyrolysis have been investigated to form carbosilanes in recent years.<sup>[3]</sup> The first identified poly(silylenemethylene) (PSM) was formed in low molecular weight via the coupling reaction of (chloromethyl)chlorodimethylsilane in combination with sodium.<sup>[48]</sup> Soon after, the ring-opening polymerization (ROP) of disilacyclobutane was established to afford high molecular weight PSM.<sup>[48,49]</sup> The greatest driving force for the either thermal or transition metal-catalyzed ROP has been assigned to the strain energy (17.2 kcal/mol) of the disilacyclobutane monomer.<sup>[48]</sup> Saturated and unsaturated polycarbosilanes with a general Si-C-C- backbone scaffold are mainly created by

a hydrosilylation reaction, promoted by chloroplatinic acid ( $\text{H}_2\text{PtCl}_6$ ).<sup>[50,51]</sup> Whereas the thermal ROP of monosilacyclobutane affords polycarbosilanes with an even greater amount of carbon atoms incorporated into the polymer chain.<sup>[52]</sup> Numerous PSMs have been reported in addition to the parent poly(silylenemethylene) over the last years, which demonstrate their unique position between the class of organic polyolefins and the class of truly inorganic polysilanes or polysiloxanes.<sup>[53]</sup> A glass transition temperature of  $T_g = -87^\circ\text{C}$  for poly(silylenemethylene) shows this intermediate between poly(isobutylene) ( $T_g = -20^\circ\text{C}$ ) and polydimethylsiloxane ( $T_g = -150^\circ\text{C}$ ).



**Scheme 2.** General procedures to create different polycarbosilanes. (a) Platin catalyzed ROP of disilacyclobutane.<sup>[48]</sup> (b) thermal ROP of monosilacyclobutane.<sup>[52]</sup> (c) Initial Wurtz coupling reaction, subsequent reduction with  $\text{AlCl}_3$  and final substitution via Grignard coupling.<sup>[54]</sup> (d) Hydrosilylation polymerization of vinyl dimethylsilane<sup>[50]</sup> and (e) hydrosilylation polymerization of acetylenedimethylsilane.<sup>[51]</sup>

This observation is consistent with the expected barrier decrease for the chain torsion and an increase in the chain flexibility as the carbon-carbon bond is replaced by the elongated silicon-carbon bond and finally substituted by the silicon-oxygen bond.<sup>[55]</sup> While its thermal stability seems to be significantly higher than that of a polysiloxane in inert atmosphere, the oxidation of bridging  $\text{CH}_2$  groups decreases its thermal stability in air.<sup>[56]</sup> Even though this polymer class exhibits interesting properties and promising features, there are only few industrial applications of polycarbosilanes, most of them involve the production of silicon carbide ceramics or related SiC-based fibers.<sup>[46,47]</sup>

### 2.3. Polysilazanes

Polysilazanes are characterized as polymers containing repeating Si-N bonds in the main chain. Albeit polysilazanes represent the nitrogen bridged analogues to the isoelectronic polysiloxanes, their industrial importance is rather small in comparison.<sup>[2,57]</sup> As we have seen before, this is mainly the result of their comparably high reactivity towards protic reagents, just as a lack of suitable synthesis procedures to afford high molecular weight polymers.<sup>[58]</sup> Most endeavors to produce linear polysilazanes result in the generation of oligomers or cyclic compounds with rather complex scaffolds.<sup>[59-61]</sup>

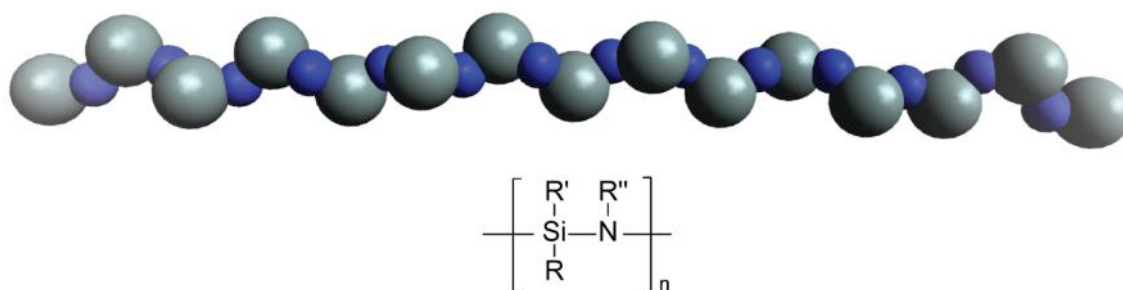
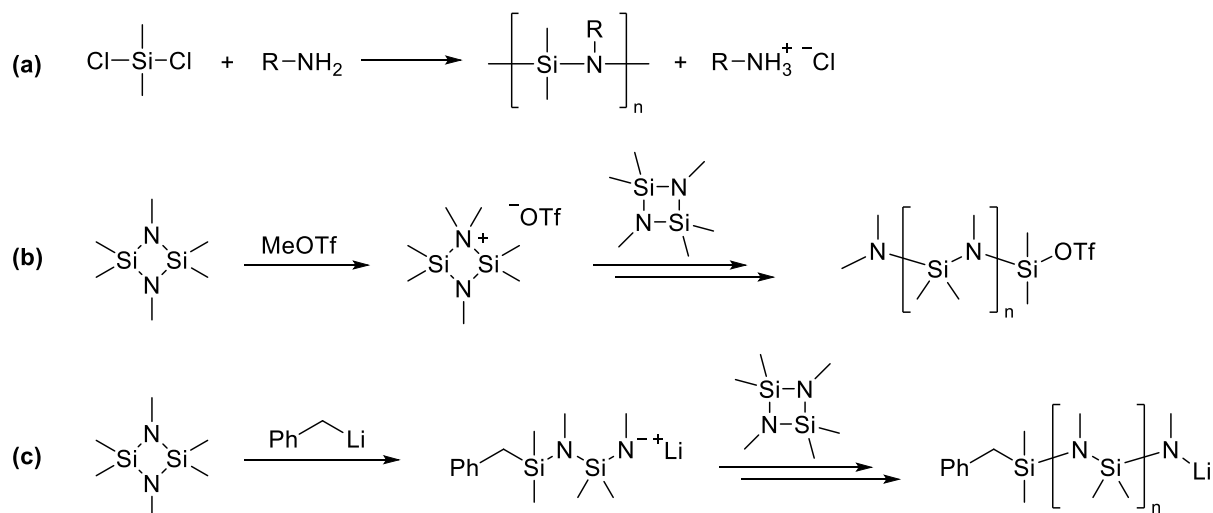


**Figure 4.** Depiction and chemical structure of linear polysilazanes, with a backbone of repeating Si-N bonds.

However, there are two general approaches to create linear polysilazanes. Most of them involve a polycondensation process by employing di- or trichlorosilanes and amines.<sup>[47,60]</sup> Due to its simplicity and its analogy to the generation of polysiloxanes, the aminolysis reaction has become the preferred route for producing polysilazanes. First reports on this subject were provided by Stock et al. in the early 1920s,<sup>[62]</sup> followed by other groups over the last decades.<sup>[60,61,63]</sup> It has been shown that the product formation and selectivity is strongly dependent on the steric properties of both the chlorosilane as well as the amine. The usage of dichlorosilane and ammonia results in the formation of oligomers, whereas with increasing demand of the substituents the generation of three- or four-membered cyclosilazanes is favored.<sup>[61]</sup> The obtained oligomeric or cyclic structures are usually chemically unstable and are predominantly used as ceramic precursors under pyrolysis.<sup>[15,16]</sup> However, these cyclic silazanes can be applied as monomer units in a ring-opening polymerization to afford polysilazanes with increased molecular weights. Some attempts have been made to introduce transition metal-based catalysts for the ROP of cyclosilazanes, yet only oligomeric structures could be obtained.<sup>[60,64]</sup> Till now, solely cationic and anionic ROP lead to longer polysilazane chain-lengths and higher molecular weights. For these processes cyclodisilazane is primarily

utilized, due to its high ring strain.<sup>[65]</sup> In addition, the substitution at the nitrogen is of significant importance for the polymerization initiation as well as propagation. With increasing steric hinderance the reaction slows down and decreases the final molecular weight, thus mostly N-methyl cyclosilazanes are used for the ROP. Various initiators have been tested for the cationic ROP, such as MeCOCl/AgSbF<sub>6</sub>, TfOH, BF<sub>3</sub>/Et<sub>2</sub>O or Me<sub>3</sub>OBF<sub>4</sub>, however methyl triflate (MeOTf) has been reported as most effective amongst them.<sup>[66]</sup> Despite the high reactivity, back-biting reactions remain a major concern in cationic ROP, which leads to depolymerization and storage incapability. This is not the case for the anionic ROP, in which organo-alkali reagents mediate the polymerization of cyclodisilazanes.<sup>[67]</sup> The employment of lithium amides, alkyl lithium/aryl lithium, or naphthyl sodium are reported in literature.<sup>[68]</sup> In the case of benzyl lithium linear polysilazanes with molar masses higher than 100 kg/mol could be afforded. In addition, no end- or back-biting could be observed over a long period, allowing a controllable and stable generation of linear polysilazanes.



**Scheme 3.** Synthesis overview for producing polysilazanes. (a) Polycondensation via aminolysis reaction of dichlorosilane with amines. (b) Cationic ROP initiated by methyl triflate to polymerize cyclodisilazane. (c) Anionic ring opening polymerization of cyclodisilazane mediated via benzyl lithium.

In general, polysilazanes exhibit promising properties regarding their thermal stability and mechanical features. Although the Si-O bond energy with 432 kJ/mol lies above the one of the Si-N bond (316 kJ/mol),<sup>[59,69]</sup> polysilazanes are reported to be more thermally stable. This stability manifests in an almost 50 °C higher degradation temperature ( $T_d = 450$  °C) compared to polysiloxanes.<sup>[70]</sup> Nevertheless, polysilazanes are quite labile towards strong bases and acids, resulting in the depolymerization of the polymer chains.<sup>[71]</sup> Furthermore, the long term stability is of major concern, but can be avoided by applying anionic ring opening

polymerization processes. So far, the only industrial application for polysilazanes is in the field of ceramics as precursors for silicon nitride  $\text{Si}_3\text{N}_4$  or silicon carbonitride  $\text{Si}_x\text{N}_y\text{C}_z$  in pyrolysis processes.<sup>[47,60,72]</sup> Albeit their similarity to polysiloxanes, no other potential application as functional material was reported so far and still has to be discovered.

## 2.4. Polysiloxanes

Polysiloxanes commonly known as silicones are by far the most important material among the inorganic and semi-inorganic polymers. Numerous patents and publications regarding synthesis, properties, and applications of polysiloxanes showcase their commercial relevance in our present world, created by a large industry in various countries.<sup>[14,70,72–90]</sup> The backbone of polysiloxanes consists of repetitive Si-O units, which provides this polymer class different unique and intriguing properties.<sup>[1]</sup>

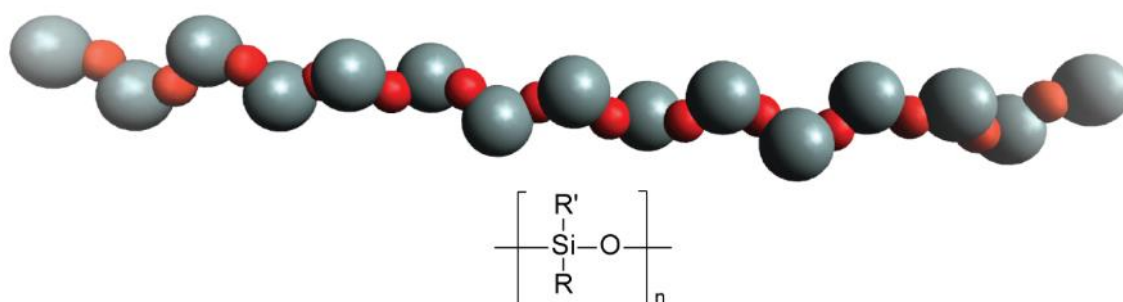


**Figure 5.** General depiction and chemical structure of the Si-O backbone present in a polysiloxane chain.

One of them is the high thermal stability of silicones due to the strength of the silicon-oxygen bond, which is crucial for the utilization in high-temperature applications. The chemical properties of typical side groups create polymer chains with considerable low surface free energy, thus applications as waterproof coating, mold-release agents, or biomedical compounds can be realized. The distinct difference in atom size of silicon and oxygen and their respective bond angles create a very irregular cross section within the polymer chain, resulting in a characteristic amorphous state and unique equation-of-state properties.<sup>[91,92]</sup> Due to the general importance, as well as their major part as research subject in this thesis, the history, synthesis, production, properties, and applications of polysiloxanes will be described more extensively in the following chapters.

### 2.4.1. History and Origin

The first appearance of polysiloxanes dates back to the year 1872, when Landenburg observed the unintentional formation of a viscous oil by reacting  $\text{Et}_2\text{Si}(\text{OEt})_2$  in acidic water. To his surprise this polymeric material exhibited a high decomposition point and did not freeze at  $-15\text{ }^\circ\text{C}$ .<sup>[70,93,94]</sup> However, F.S. Kipping is considered to be the actual discoverer and name giver of the polysiloxanes, by his attempts to synthesize a  $\text{R}-(\text{Si}=\text{O})-\text{R}$  double bond in 1901. The strongly polarized Si-O bond and the resulting tendency to polymerize however resulted in the formation of polysiloxanes.<sup>[95]</sup> Yet, the first synthesis of a silanone was realized almost a century later, due to its unexpected high reactivity.<sup>[96,97]</sup> Due to Kipping's original objective, this new material was named silicoketones or silicones, in analogy to the carbon-based ketones  $\text{R}-(\text{C}=\text{O})-\text{R}$ .<sup>[1]</sup> Although the term of "silicones" is a misnomer, it has persisted to this day and is commonly accepted as description for this polymer class, albeit the term "polysiloxane" is technically more accurate and preferred by researchers working in this field. The actual introduction of polysiloxanes as an industrial product however took another 30 years with the discovery of the Müller-Rochow process in 1940. The direct synthesis of elemental silicon with methyl chloride and subsequent hydrolysis creates polydimethylsiloxane and remains the method of choice for producing linear polysiloxanes to this day.<sup>[98]</sup> The constant search for new applications and their vast implementation in numerous fields has allowed the polysiloxane industry to grow continuously over the last century. This renders the polysiloxanes the most successful inorganic polymer and a highly relevant polymeric material in our present world.<sup>[99]</sup>

### 2.4.2. Synthesis and Production

Most sources of polysiloxane monomers are functional silanes  $\text{R}_{4-n}\text{SiX}_n$  with moieties that can readily be hydrolyzed, for instance  $\text{X} = \text{Cl}, \text{NR}_2, \text{OR}, \text{OCOR}$ . One of the most common precursors is dimethyldichlorosilane  $\text{Me}_2\text{SiCl}_2$  (DDS) for the synthesis of polydimethylsiloxane (PDMS). Due to the fact that organosilicon compounds are solely artificial and cannot be retrieved from a natural source, all polysiloxane monomers are afforded on a synthetic route. Elemental silicon is used as a base material for this technology, which is obtained by electrochemical reducing of mineral silica  $\text{SiO}_2$  in a carbothermal reaction. This major industrial process requires high temperatures of about  $2000\text{ }^\circ\text{C}$  and provides elemental silicon in a purity of 99.8%.<sup>[100-105]</sup> For the usage as semiconductor material additional purification

methods have to be applied to afford even higher levels of purity. The production of polysiloxanes however relies primarily on this “raw” material due to its availability and cost-benefit efficiency.<sup>[1]</sup>

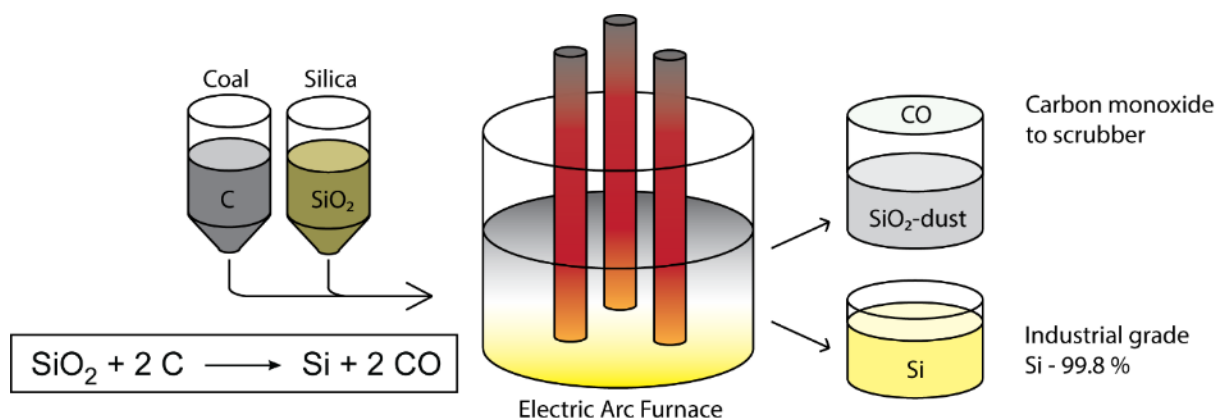
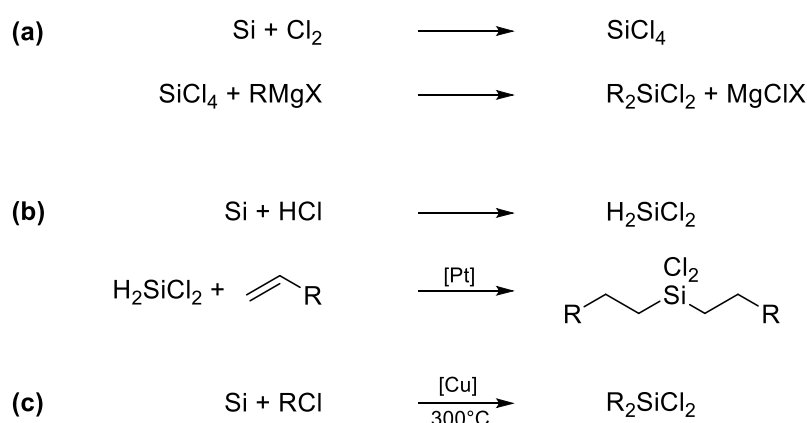


**Figure 6.** Industrial refinement of silica  $\text{SiO}_2$  to elemental silicon by a reductive carbothermal reaction.

The generated silicone is then transformed into the respective organosilicon species via different approaches. The reaction of silicon with chlorine and subsequent substitution by organic groups with the help of organolithium, Grignard reagents or organic zinc compounds allows the formation of a variety of organosilicons.<sup>[104,105]</sup> Converting silicon into silyl-hydrides and subsequent addition of multiple bonds in a hydrosilylation reaction represents another method. Nevertheless, the most significant process is the Müller-Rochow process or “Direct Process”, which transforms elemental silicon directly into the desired organosilicon compound.<sup>[106–108]</sup>

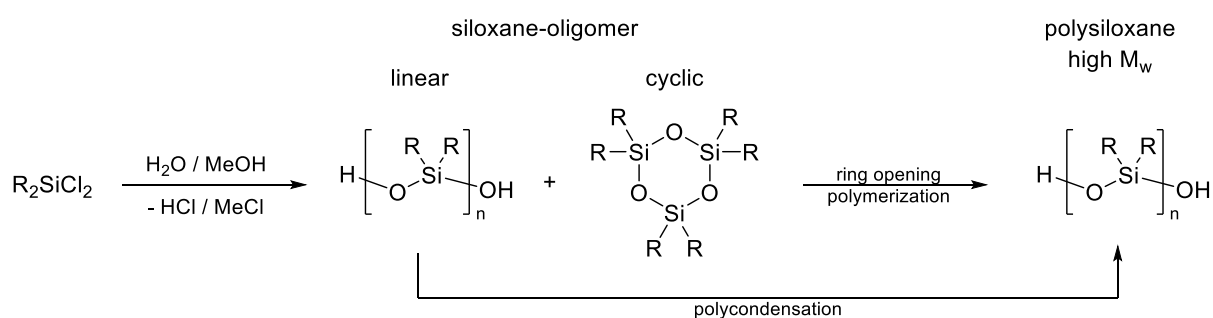


**Scheme 4.** Transformation of elemental silicon to organosilicon compounds. (a) Chlorination of silicon, followed by a Grignard reaction. (b) Transformation of silicon into silyl hydrides with subsequent hydrosilylation reaction. (c) “Direct Process” or “Müller-Rochow-Process” to convert silicon directly into the organosilicon species.

The present silicone industry is primarily based on the employment of  $\text{Me}_2\text{SiCl}_2$  (DDS), which is exclusively synthesized via the Direct Process. Gaseous methyl chloride  $\text{MeCl}$  is reacted on



contact with solid silicon in combination with a copper catalyst at temperatures between 250-300 °C to afford a mixture of different methylchlorosilanes ( $\text{Me}_n\text{SiCl}_{4-n}$ ,  $n=0-4$ ).<sup>[106]</sup> Process parameters like the purity of the reagents, the preparation of the contact mass, or the applied reaction temperature strongly affect the product distribution, with the result that more than 90 % DDS can be achieved.<sup>[109,110]</sup> By applying other alky/aryl chlorides a variety of organochlorosilanes for the synthesis of more complex polysiloxanes can be obtained. The subsequent polymerization of the organochlorosilane monomer involves an industrial process consisting of two steps. Firstly, a hydrolysis reaction converts the chlorosilane into hydroxy silanes, which will then condense to afford the basic Si-O repeating unit. This first process step results in the formation of linear and cyclic oligosiloxanes. Depending on the reaction conditions the product distribution can be controlled to create either mostly cyclic or linear polysiloxanes.<sup>[111-115]</sup> Many efforts have been made to optimize this reaction towards purely linear or cyclic oligomers.<sup>[114]</sup> In addition, the replacement of the hydrolysis by a methanolysis process allows the direct formation of methyl chloride, which can be utilized in the Direct Process again, thus creating a beneficial cycle process.<sup>[89,94,98]</sup>

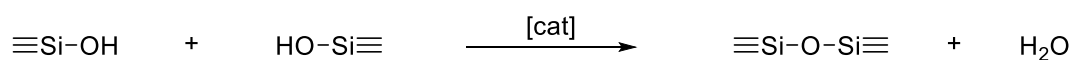


**Scheme 5.** Two-step process to afford polysiloxanes. Initial hydrolysis/methanolysis of the organochlorosilane to obtain linear or cyclic siloxane oligomers. Subsequent polymerization via polycondensation or ROP.

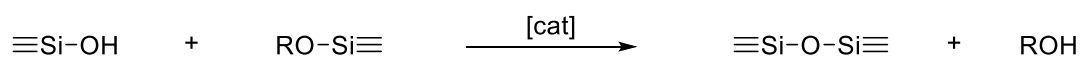
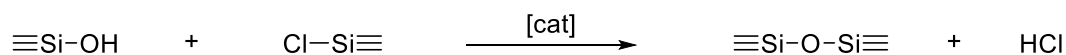
The second step is the final polymerization of the siloxane oligomers to high  $M_w$  polysiloxanes. Linear siloxane oligomers are thus transformed by a polycondensation process to obtain the desired product. Different approaches are utilized to perform the respective polycondensation. The most important one is the homofunctional polycondensation, which is inherent to a variety of catalyst systems, including protic acids, Lewis acids, strong charged bases, stannous salts, phosphonitrile chlorides or other heterogeneous catalysts.<sup>[115-120]</sup> To shift the equilibrium reaction towards longer polymers, the accruing water from the polycondensation is removed by a continuous distillation during the process. However, disproportionation reactions usually accompany acid or base initiated polycondensation reactions and can

become unfavorable to provide precise product attributes.<sup>[121–124]</sup> Other approaches involve heterofunctional polycondensation processes by reacting hydroxy functionalized siloxanes with different substituted ones. The silanol moiety presents reactivity towards a broad range of silyl functionalities, such as Si-H, Si-Cl, Si-OR, Si-OCOR or Si-NR<sub>2</sub>.<sup>[115]</sup> Yet, condensation with chlorosilanes (Si-Cl) and alkoxy silanes (Si-OR) are particularly important for the synthesis of polysiloxanes. The condensation with chlorosilanes requires basic or nucleophilic catalysts (triethylamine or pyridine) since acidic catalysts favor the protonation of the silanol and promote a self-condensation.<sup>[125]</sup> Whereas condensation of alkoxy silanes with hydroxy-terminated polysiloxanes is exploited for creating block copolymers or even polysiloxane networks.<sup>[126,127]</sup> Realization of this reaction can be promoted by various catalysts, like Sn<sup>II</sup> carboxylates,<sup>[116,128]</sup> trifluoroacetic acid,<sup>[129]</sup> or phosphazanium salts.<sup>[130]</sup>

#### homofunctional polycondensation



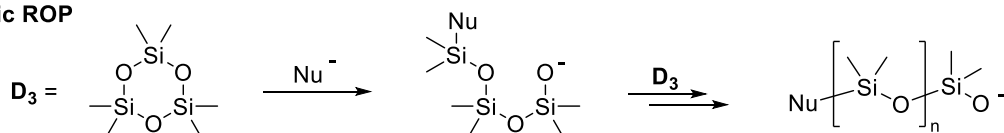
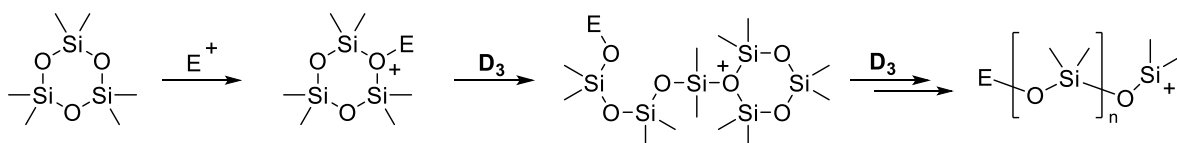
#### heterofunctional polycondensation



**Scheme 6.** Polycondensation processes to obtain polysiloxanes via homo- or heterofunctional approaches.

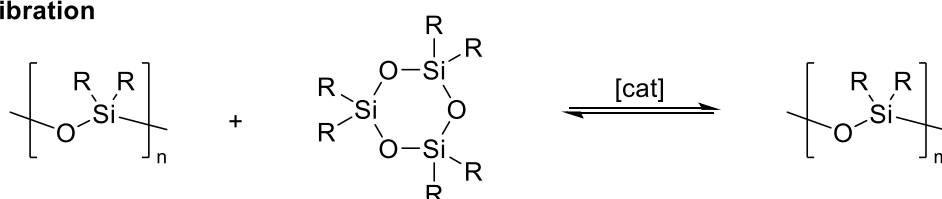
Despite everything, the hydrolytic polycondensation to generate high M<sub>w</sub> polysiloxane has been mostly replaced by the ring-opening polymerization of cyclic tri- and tetramers by ionic initiators.<sup>[75,102,131]</sup> The nature of this process is a reversible one, albeit the correct choice of monomer, initiator and reaction conditions provides an essentially irreversible method in practice. For instance, one crucial requirement is the elimination of all initiator/catalyst from the final product via neutralization of the ionic species, thermolysis and volatilization of the initiator. Anionic ROP usually involves the employment of hydroxides, alkali-metal oxides, or bases in general.<sup>[89,132–136]</sup> The polymerization commences through a nucleophilic attack on the monomer. Consequently, the ring gets opened, which is followed by a propagation attack on the next siloxane ring, resulting in the chain elongation.<sup>[1]</sup> In contrast to most other polymerizations the driving force of this process is not an decrease in enthalpy but rather an increase in entropy caused by an increase of internal molecular freedom due to the transformation of a strained cyclic structure to a linear chain.<sup>[1,131]</sup> The cationic ROP is of less

industrial importance, although polymerization yields and product distribution are comparable to the anionic ROP method. Typical catalysts are conventional Lewis acids, tin-based catalysts, or combinations of metal sulfonates and acid chlorides.<sup>[136,137]</sup> The complete mechanism of the cationic ROP is still under consideration. While the formation of a siloxonium ion as the initiation step is widely accepted, the propagation is assumed to proceed either through a chain-growth or a step-growth polymerization.<sup>[137-140]</sup> In all ionic ROP an end group blocking is performed to prevent potential back-biting or re-equilibration reactions. In addition, this technique allows to introduce reactive end groups, that can be used for subsequent modifications.<sup>[141,142]</sup>

**Anionic ROP****Cationic ROP**

**Scheme 7.** Anionic and cationic ring opening polymerization processes of cyclic siloxane monomer units.

Another powerful tool is the equilibrium polymerization, often referred to as equilibration. It utilizes the equilibrium state of the polymerization to control the average molecular weight of the final polysiloxane. This way, mixtures of cyclic and linear polysiloxanes of different chain lengths and weight distributions can be equilibrated to form polysiloxanes with homogenous characteristics. The equilibrium of the constant chain formation and chain deconstruction is influenced by the reaction conditions, such as distillation of volatile small siloxanes, or the choice of catalyst. Thus, the equilibration represents a very useful method to obtain polysiloxanes with distinct properties or create copolymers by mixing different functionalized siloxanes.<sup>[94,143]</sup>

**Equilibration**

**Scheme 8.** Equilibration of linear and cyclic polysiloxanes to create high molecular polysiloxane material.

### 2.4.3. Properties and Application

The combination of unique thermal properties over a vast range of temperatures and mechanical features like an exceptional elasticity contribute to the technological and industrial importance of polysiloxanes. It has become the preferred material for applications under extreme conditions. With a  $T_g$  of  $-125\text{ }^\circ\text{C}$  and an onset of thermal degradation up to  $350\text{ }^\circ\text{C}$ , polysiloxanes satisfy given requirements to withstand an exceptional range of low or high temperatures. Most of these properties originate from the basic structure of the polysiloxane backbone and thus are expressed in almost every member of this polymer class. Of paramount importance is the fundamental nature of the siloxane bond, which exhibits partially double-bond and partly ionic character. The Si-O bond is relatively long with a typical length of  $1.64\text{ \AA}$ , yet smaller than the simple addition of the respective atomic radii (Si  $1.17\text{ \AA}$  and O  $0.66\text{ \AA}$ ).<sup>[144]</sup> This is a result of the large difference in electronegativity of silicon with a value of 1.8 and oxygen with 3.5 (according to Pauling),<sup>[145]</sup> which implicates an estimated ionic character of up to 51%.<sup>[146]</sup> At the same time, an additional attraction originates from the overlap of the oxygen's p orbital and the low-lying vacant 3d orbital of the silicon resulting in the partial double-bond character and a  $\pi$ -back donation.<sup>[147]</sup>

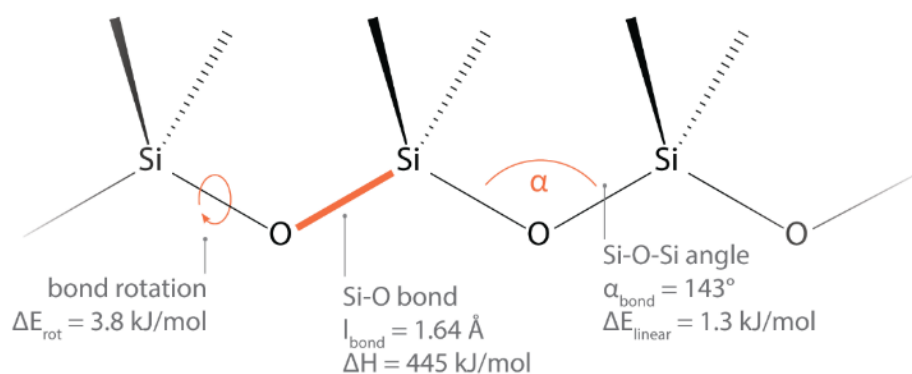


**Figure 7.** Characteristic properties of a polydimethylsiloxane chain, such as bond length, enthalpy, or angle.

The combination of these attributes defines the exceptional strength of this bond and further contributes to the conformational flexibility of the polysiloxane chain. This flexibility is the result of the prior described Si-O bond length as well as the Si-O-Si bond angle. The elongated bonds in the polymer backbone create an increase in spatial separation and hence reduce the hinderance for the organic substituents at the silicon. This allows the rotation of these substituents and facilitates the resulting “umbrella-type” motion even at temperatures as low

as  $-196\text{ }^{\circ}\text{C}$ .<sup>[148]</sup> In addition, the Si-O-Si bond angle is considered to be comparable “soft” with an energy barrier to linearize of  $1.3\text{ kJ/mol}$ , thus allowing considerable bending and stretching of the polysiloxane chain.<sup>[58,149,150]</sup> Due to this constellation the Si-O bond exhibits a surprisingly small rotation energy barrier of only  $3.8\text{ kJ/mol}$ .<sup>[151]</sup> As a consequence, the polymer can readily minimize internal strain by rotating and bending its siloxane backbone. This freedom of motion was shown to be the main reason for their high degree of flexibility and their low-lying glass transition point of around  $T_g = -123\text{ }^{\circ}\text{C}$ .<sup>[152]</sup> Another crucial effect originates from the relatively weak intermolecular interaction between the individual polymer chains. Thus, only small friction forces and low viscosities are associated with these polymers with activation energies for a viscous flow below  $40\text{ kJ/mol}$  in general. However, these mechanical properties are dependent of and increase with the molecular weight of the polymer chains as well as with the size of the substituted organic side groups.<sup>[153,154]</sup> Polysiloxanes show surprisingly constant Newtonian fluidity over the entire applicable temperature range. At low temperatures the siloxane backbone is structured in a coiled helical conformation, which in turn shifts the organic substituents outwards towards the neighboring chains. As a consequence, the polar siloxane backbone experiences effective shielding from the pendent organic substituents as well as only weak attraction or interpenetration of the individual chains, due to the weak interaction of the respective side groups.<sup>[14]</sup> By increasing the temperature this helical scaffold converts gradually to a more random coil formation, which attenuates the described shielding effect and allows more entanglement and interactions. On the other hand, the increase in temperature results in a general decrease of viscosity, which counterbalances the previous effect. This interplay of effects retains the Newtonian-type flow characteristic of polysiloxanes and allows to use this constant behavior in a wide range of temperatures.<sup>[155,156]</sup> This property and the high thermal stability render polysiloxanes particularly suitable fluid materials in many high or low temperature applications. In general, silicones are a highly stable material, since they are considerably resistant towards hydrolysis, oxidation, or UV-irradiation under ambient conditions.<sup>[89,157]</sup> However, due to the partially ionic bond character in the backbone, the siloxane chain is prone to decompose in both strong basic as well as acidic conditions.<sup>[70]</sup> In contrast to common opinion, polysiloxanes are considered ecologically compatible since they undergo degradation with natural clay and their degradation products are non-toxic and consist mostly of simple silica  $\text{SiO}_2$ .<sup>[158]</sup> Thus, polysiloxane products are available in various forms either as

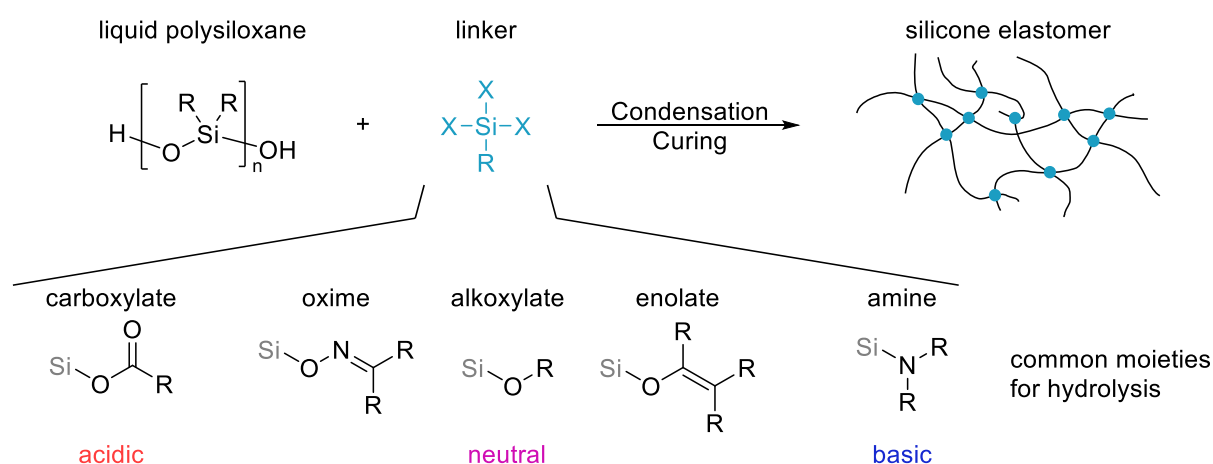
bulk material or in surface applications. A first commercial utilization was development as silicon-based damping fluid by the US Air Force during the Second World War.<sup>[159]</sup> These days, established silicone applications are provided as fluids, surfactants, greases, gels, coatings, foams, resins, or even elastomers. Silicone fluids can be found as hair conditioners, polishes, antifoaming agents, or lubricants.<sup>[3,160]</sup> The exceptional weather resistance and water repellent properties render polysiloxanes ideal as coating material for outdoor applications. While silicone elastomers are used as flexible rubbers in our daily life, they have become particularly useful as outdoor high voltage insulation.<sup>[161]</sup> By incorporating different fillers and additives like silica to increase tensile strength or alumina trihydrate to improve heat conductivity for instance, these elastomers can be readily modified for their specified applications. This renders this material applicable in a vast variety of industries ranging from automotive, aerospace, metallurgy, insulation, electronic or household appliance. However, one of the most relevant commercial segments is the field of medical applications. The stability, inertness, and pliability of polysiloxanes is crucial for medical tubing, catheters, prostheses, or artificial organs. In combination with its high permeability, silicones are found as contact lenses, artificial skin, or drug delivery systems.<sup>[80,87,162,163]</sup>

## 2.5. Curing of Polysiloxanes

The described benefits and applications from silicone fluids render them valuable materials in a vast range of industries. However, many use cases require solid materials, which do not flow. In contrast to most carbon-based polymers, polysiloxanes do not show a high degree of entanglement and experience only very weak attractive forces towards each other, thus simple chain elongation does not result in solidification of this material.<sup>[89,111]</sup> As a result, the polysiloxane chains need to be crosslinked to form covalently linked silicone networks. These cured silicones range from soft gels and coatings to highly flexible elastomers and rigid resins. Most curing processes include either the utilization of tri- or tetrafunctional silanes as reactive joints affording solely siloxane bridged networks or the implementation of organic residues (Si-Me, Si-vinyl, Si-H), which results in silicone material linked by organic spacers.<sup>[89]</sup> Today, the large majority of industrial silicone rubbers is produced by three different curing methods each providing specific advantages and disadvantages: the moisture or condensation cure, the transition metal-catalyzed or addition cure, and the heat controlled or radical cure.

## 2.5.1. Condensation Curing

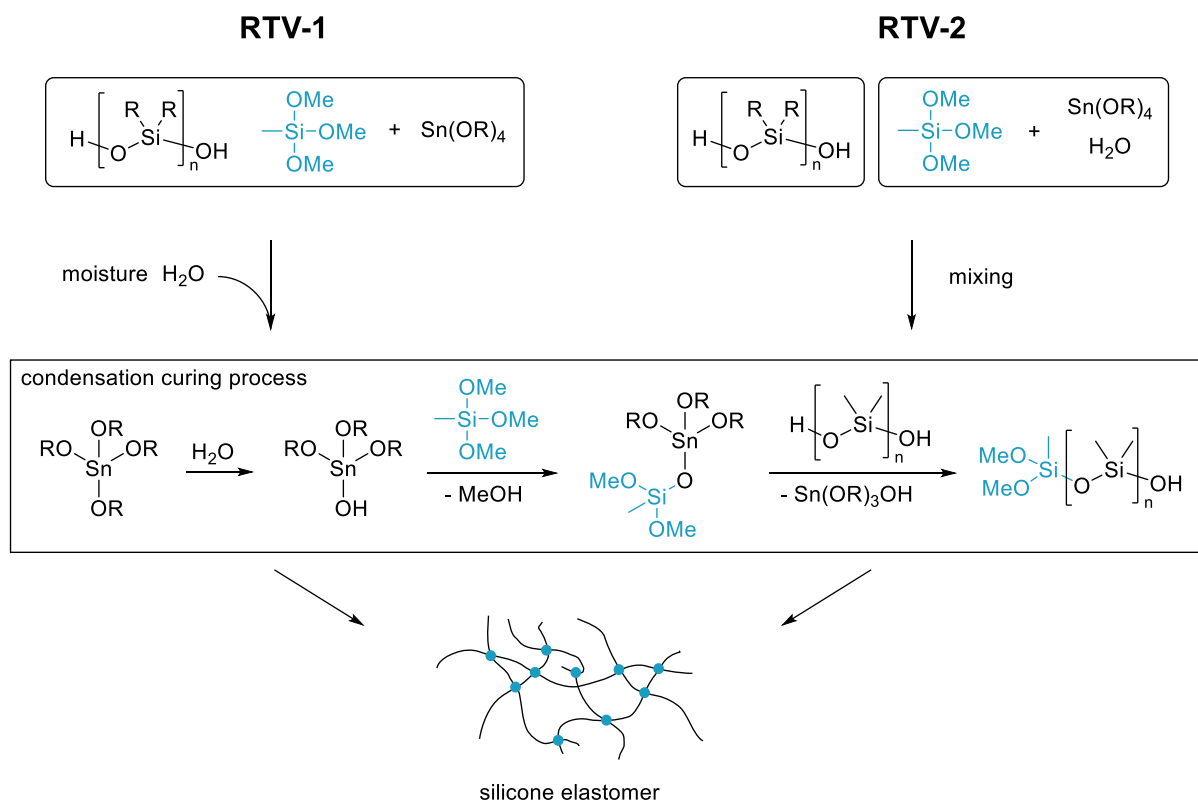
In general, hydroxy terminated polysiloxanes (Si-OH) react with multifunctional compounds in a condensation reaction to form the desired elastomer. Due to the fact that hydroxy moieties in polysiloxanes occur exclusively at terminal positions no curing is feasible by employing just polysiloxanes. Thus, using at least trifunctional linkers ensure the effective formation of a silicone network, most common are tri- or tetrafunctional silanes (RSiX<sub>3</sub>, SiX<sub>4</sub>). To create stable curing mixtures, the linkers are protected by hydrolysable substituents. The respective leaving group on the linker controls the reaction rate, consequently the curing rate as well. Chlorosilanes would react fast and are widely available, however the formation of hydrochloric acid (HCl) excludes them for practical application. More common is the incorporation of carboxylates, oximes, alkoxides, or amines as effective leaving groups for the condensation curing. Depending on the formed byproduct the curing mixture can react acidic, neutral, or basic, which can be crucial for choosing a suitable linker besides its curing rate.<sup>[89]</sup>



**Scheme 9.** Condensation curing of hydroxy-terminated polysiloxanes with a variety of silane derivative linkers.

The curing reaction occurs at room temperature, which is the reason why this process is also referred to as room temperature vulcanization (RTV). However, the respective hydrolysis usually requires additional catalysis, conducted by tin- and titanium-based catalysts, acids, or bases. All procedures share the necessity of H<sub>2</sub>O being present in form of moisture as a cocatalyst for the hydrolysis reaction.<sup>[164]</sup> Acid catalysts are employed to accelerate the hydrolysis reaction by protonation of the respective leaving group on the linker, hence increasing its leaving ability. Basic catalysts, on the other hand, realize the deprotonation of the terminal hydroxy functionality of the polysiloxane, thus improving its nucleophilicity. Several studies have shown that stronger acids, like trichloroacetic acid were more efficient

than weaker ones. Similar results were obtained by comparing triethylamine as a strong base with weaker bases like pyridine.<sup>[165,166]</sup> Even bifunctional catalysis can promote this reaction by employing simple buffer solution as a combination of both acidic and basic catalysts.<sup>[167,168]</sup> Metal based catalysis for the condensation curing are usually tin or titanium derived alkoxides and esters. The requirement of water as an initiator for the active catalyst species allows the preparation of a one component system, hence the classification as RTV-1. The hydrolysis of the catalyst upon contact with moisture creates the actual hydroxy metal catalyst. Consecutive substitution of the linker silane generates the activated metal alkoxide, followed by the nucleophilic attack of the silanol to produce the polysiloxane elastomer and regenerate the activated catalyst. Adjustment of the reaction humidity allows a simple way to control the respective curing rate. With increasing activity of the employed tin catalysts some curing systems are prepared as a two-component system, one containing the hydroxy terminated polysiloxane, the other the catalyst in combination with the multifunctional linker and a defined amount of water. Due to their two-part segmentation, these curing systems are called RTV-2. Upon mixing the condensation reaction is initiated instantly, generating the desired elastomer.<sup>[89,169]</sup>



**Scheme 10.** Comparison of the condensation curing process RTV-1 (one-component system) and RTV-2 (two-component system) by using tin-based catalysis to generate silicone elastomers.

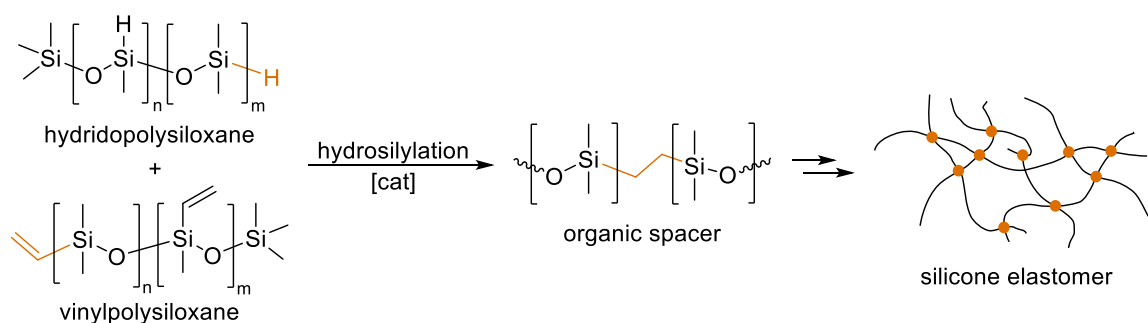


Due to the nature of the condensation reaction, all condensation curing processes generate elimination products during the reaction progress. The resulting shrinkage and mass loss of the final elastomer product must be considered. Moreover, volatile elimination products might create safety and health concerns, thus limiting its application range.<sup>[170]</sup> The same applies to the limitation of creating thicker elastomer layers, since the hydrolysis reaction with moisture is dominated by the diffusion of H<sub>2</sub>O in the polysiloxane. Nevertheless, their simplicity, practicality, and robustness towards catalyst poisons render this type of curing one of the most successful for general, unspecified applications.<sup>[89]</sup>

### 2.5.2. Addition Curing

The second curing method is the addition curing also referred to as hydrosilylation curing, due to the defining type of reaction for this crosslinking type. In general, two different polysiloxanes, a vinyl-functionalized and a hydrid-functionalized silicone are combined with a catalyst to perform the hydrosilylation reaction, thus affording the cured elastomer. Since this curing method is prepared as a two-component system and conducted at room temperature it is technically categorized as an RTV-2 system as well. Platinum or rhodium based catalysts are most commonly employed for this type of addition reaction, however a variety of different transition metals can be utilized likewise.<sup>[171,172]</sup>

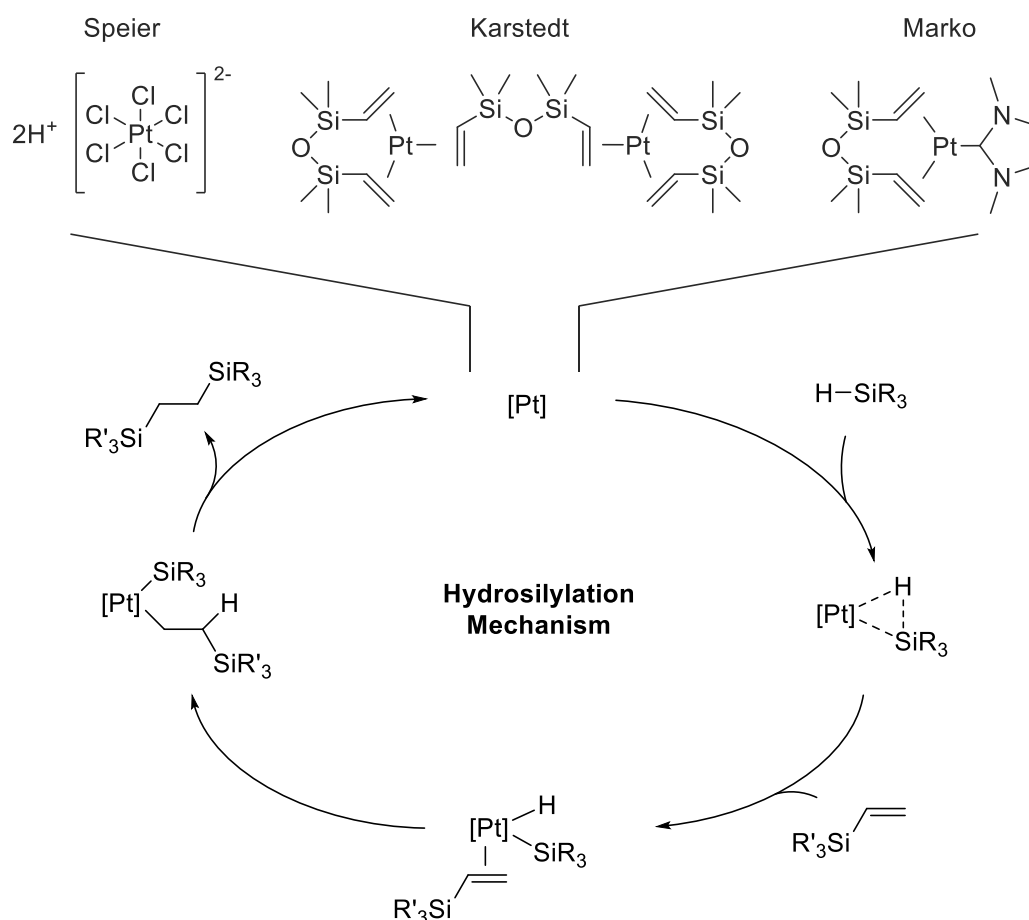
#### Addition Curing



**Scheme 11.** Addition curing of hydrid- and vinyl-functionalized PDMS via a transition metal catalyzed hydrosilylation reaction.

The curing is initiated by mixing the two components together. Usually, the vinylpolysiloxane is combined with the hydrosilylation catalyst in one component and the hydridopolysiloxane in the other. The resulting curing rate is comparable fast, yet an increase of temperature or pressure contributes to an additional acceleration of the reaction speed. Well known catalyst

systems are the Speier- and Karstedt-catalyst as Pt-based or the Wilkinson-catalyst as Rh-based option. Nevertheless, continuous efforts have been made to improve the catalyst efficiency or reduce its required concentration, by employing platinum carbene complexes for a new generation of hydrosilylation catalysts.<sup>[173]</sup> The respective catalytic mechanism was proposed by Chalk and Harrod in 1965 on the basis of the Speier catalyst  $\text{H}_2\text{PtCl}_6$ .<sup>[174]</sup> Reduction of the Pt(II) complex affords the active Pt(0) species, which forms a hydrido-silyl-complex with the hydrosilane in the initial oxidative addition. Subsequent coordination of the olefin to the metal center, is followed by a migratory insertion of the olefin into the Pt-H bond. As a last step, the alkyl silane is cleaved of the catalyst complex in a reductive elimination, forming the desired product and regenerating the active Pt-catalyst. In general, this reaction is regioselective, forming in most cases the anti-Markovnikov product. The original mechanism was proposed via an insertion reaction of the olefin into the Pt-H bond, however recent studies suggest the prior described pathway, which also allows the transformation of vinyl- or allylsilanes by a  $\beta$ -hydride elimination.<sup>[175]</sup>

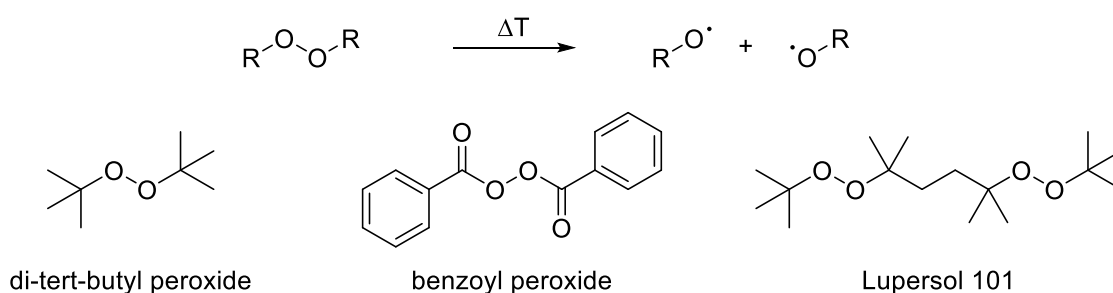
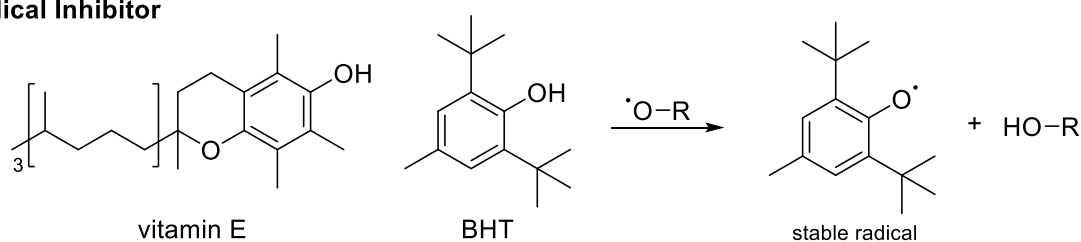


**Figure 8.** Hydrosilylation mechanism via oxidative addition of the hydrosilane to the platinum, followed by the insertion of the olefine, and finalization by the reductive elimination of the carbosilanes closes the reaction cycle.

The processing time can be manipulated by the use of different inhibitors or filler materials. This way even heat initiated one component systems can be prepared by choosing the right inhibitor.<sup>[89,94]</sup> Additionally, also photosensitive catalyst are employed to allow an one-component curing system at ambient temperatures.<sup>[1]</sup> Due to the nature of the hydrosilylation reaction as an addition reaction no elimination product is formed, hence no significant shrinkage or mass reduction is observed. Albeit the celerity and effectiveness of this curing method, one of the biggest issues is the entrapment of the metal catalyst in the final silicone elastomer. This results in the simple loss and waste of very expensive and rare transition metals in most cases, as well as an alteration of the elastomer properties over time. The employed Pt-catalyst agglomerates in the polymer matrix, forming nanoparticles and resulting in a yellowish discoloring of the product. A recovery of the metal is economically not beneficial due to the low concentration of the employed catalyst. However, by combining of the global production of silicone elastomers, an estimated loss of up to 6 tons of pure platinum is assumed each year.<sup>[1]</sup>

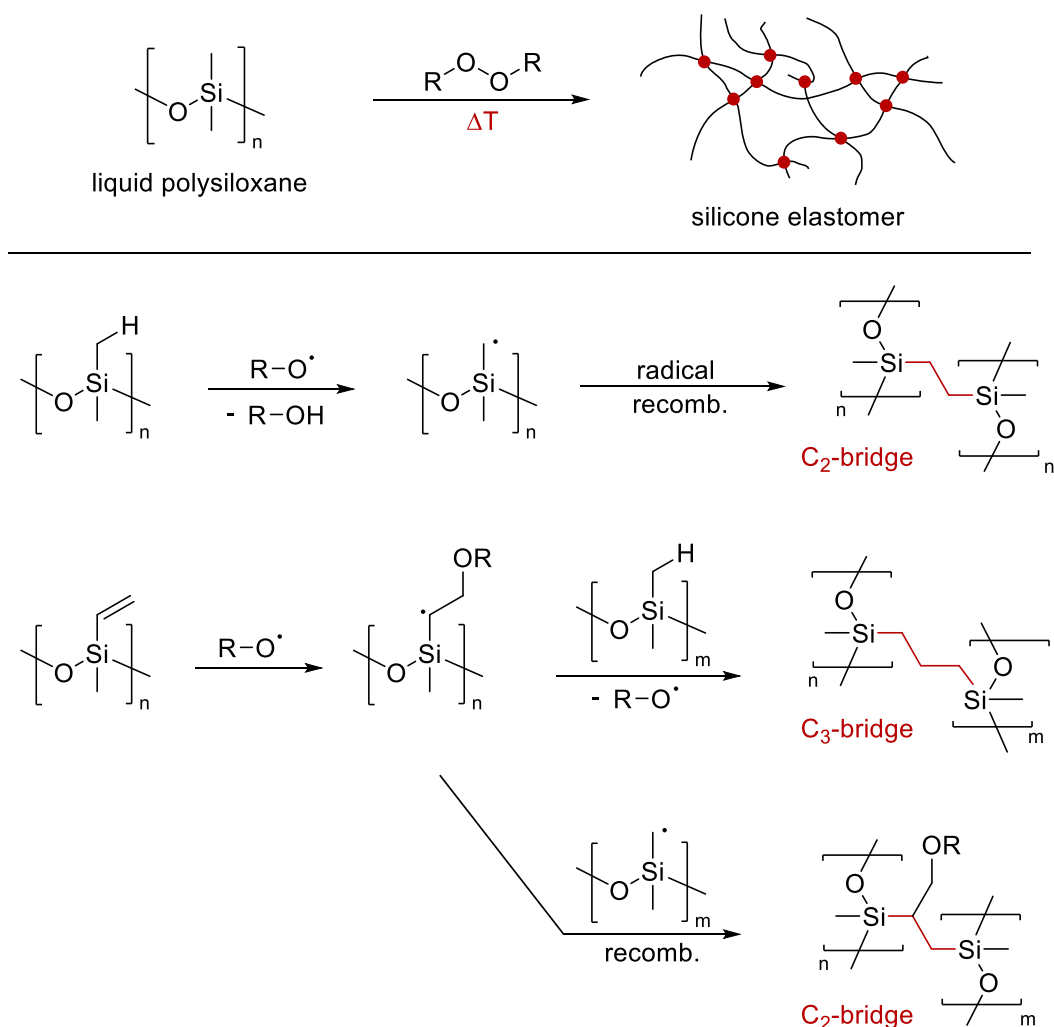
### 2.5.3. Radical Curing

The third industrial relevant process to create silicone elastomers is the radical curing process. Due to the necessity of employing high-temperature conditions, this type of curing is also referred to as high temperature vulcanization (HTV) and shares similarities to the traditional rubber production. Organic peroxides are commonly used as comparably stable precursors for the generation of radical species at elevated temperatures. Examples of applicable initiators are benzoyl peroxide, di-*tert*-butyl peroxide, *m*-chlorobenzyl peroxide, or commercially available peroxides like Lupersol 130 (2,5-bis(*tert*-butylperoxy)-2,5-dimethyl-3-hexyne) and Lupersol 101 (2,5-bis(*tert*-butylperoxy)-2,5-dimethyl-hexane).<sup>[89,94]</sup> The effective curing temperature is dependent on the peroxide structure and stability, therefore common temperature conditions range from 110-200 °C.<sup>[176]</sup> The active peroxides, usually employed in a concentration range from 0.02 to 1.0 mol %, can be inhibited by various antioxidants (radical traps) to increase the stability and storability of the one-component curing mixtures. Widely applied are 2,6-di-*tert*-butyl-4-methylphenol (BHT) and vitamin E as radical inhibitors, due to their availability and low costs. These bulky phenol derivatives react readily with the free radical to form stable phenoxyl radicals.

**Radical Initiator****Radical Inhibitor**

**Scheme 12.** Overview of commonly used radical initiators and inhibitors for the HTV curing process of silicones. There are essentially two types of radical reactions utilized for the HTV process of polysiloxanes. The first one proceeds via an abstraction of a hydrogen atom from a pendent methyl group of the PDMS chain, after initial thermal activation and homolytic fission of the peroxide. The resulting Si-CH<sub>2</sub><sup>•</sup> radicals couple in a recombination reaction and subsequently form an ethyl-bridged network. Increasing conversion of the elastomer affords an increase in the reaction viscosity, thus attenuating the rate and efficiency of the curing by restricting the movement of the free radicals in the material.<sup>[177]</sup> Accruing hazardous phenol byproducts need to be removed through heat stripping or by superficial neutralization with NaHCO<sub>3</sub>.<sup>[89]</sup> The higher activity of vinyl moieties towards radical addition compared to the radical abstraction of alkanes is exploited for the second type of radical curing. This allows lower curing temperatures and milder process conditions, thus reducing production costs. In addition, less reactive peroxides provide a better control of the crosslinking reaction, for instance di-*tert*-butyl peroxide exclusively reacts with vinyl-containing polysiloxanes.<sup>[176]</sup> As a first step, the highly reactive radical initiator reacts in an addition reaction with the vinyl group at the polysiloxane. Subsequent coupling of the polymer attached radical with pendant methyl-groups (Si-Me) result in the formation of a propyl-bridge and the creation of the elastic network, while eliminating and regenerating the initial radical. Alternative reaction paths enable the recombination of a vinyl-originating radicals with a methyl radicals, while recombination of vinyl-derived radicals is generally not observed.<sup>[89]</sup>

## Radical Curing - HTV



**Scheme 13.** HTV or Radical curing of polysiloxanes with organic peroxides. Overview of possible reaction pathways dependent on the type of polysiloxane functionality and crosslinking conditions.

Electron beams,  $\gamma$ - or high energy UV-radiation represent additional methods to create free radicals for the curing of polysiloxanes.<sup>[89]</sup> The respective C-H or Si-C fission allows analogous radical curing to the peroxide based HTV process. However, these alternative techniques bear almost no industrial significance, due to their high costs and complex production set-ups.

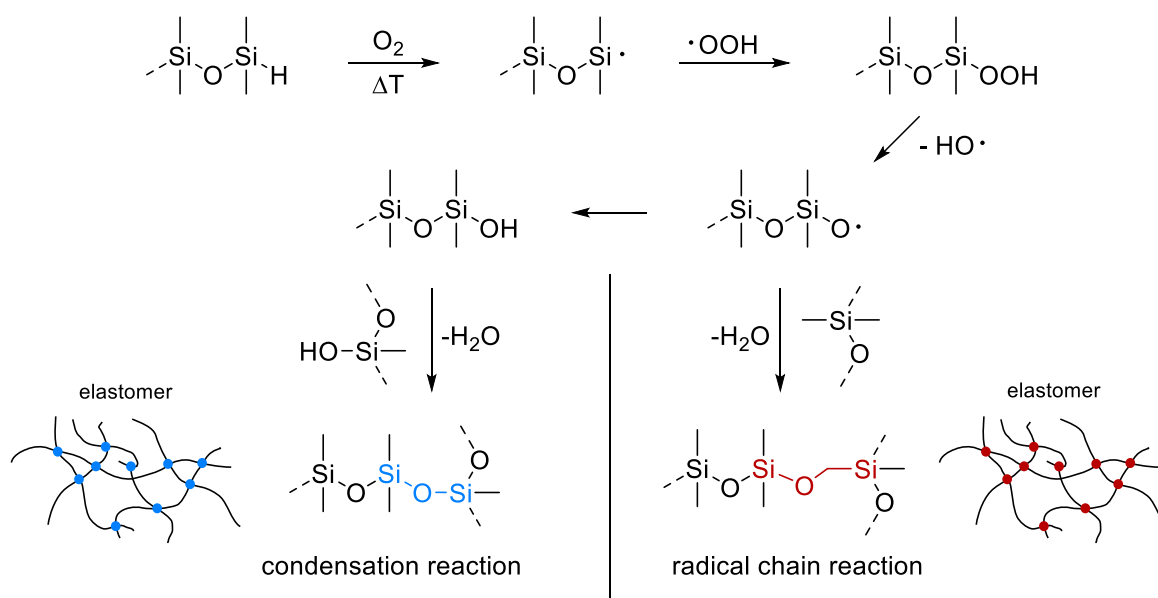
## 2.5.4. Alternative Approaches

The presented curing methods via condensation, addition or radical crosslinking showcase the efficiency and potential of these curing processes to create silicone elastomers for a plethora of different applications. Regardless of their many advantages, each crosslinking type bears specific drawbacks like shrinkage of the elastomer due to the formation of side

products, or entrapment of the employed catalyst in the elastic material, among others. These issues emphasize the need of alternative silicone crosslinking for a more sustainable creation and safer use of these materials in the future. In the following a selection of different approaches will be presented to highlight recent and promising advances in the field of silicone curing.

A facile, metal-free method to obtain polysiloxane elastomers from inexpensive and readily available liquid PDMS via an autoxidation process was presented by Book et al. in 2019.<sup>[178]</sup> By oxidizing hydrosilane functionalized polymers at temperatures above 250 °C in air, a silyl radical is generated by a facile hydrogen abstraction of the molecular oxygen. The respective silyl radical either converts into a silanol, followed by a condensation reaction, or initiates a radical chain reaction, resulting in silyl ether linked polysiloxane elastomers. While lower temperatures favor the condensation pathway, higher temperatures up to 300 °C facilitate the latter process. Subsequent research emphasizes the curing controllability of this method through the ratio of hydrosilanes in the starting material, the reaction temperature and time, and the type of functionality (lateral, terminal, pendant, telechelic moiety).<sup>[179]</sup> This simple process allows catalyst free curing of hydrosilane functionalized polysiloxanes. However, the reported process suffers from long curing durations and the employment of cost intensive, high temperatures, which limits its applicability and attenuates its economic benefit.

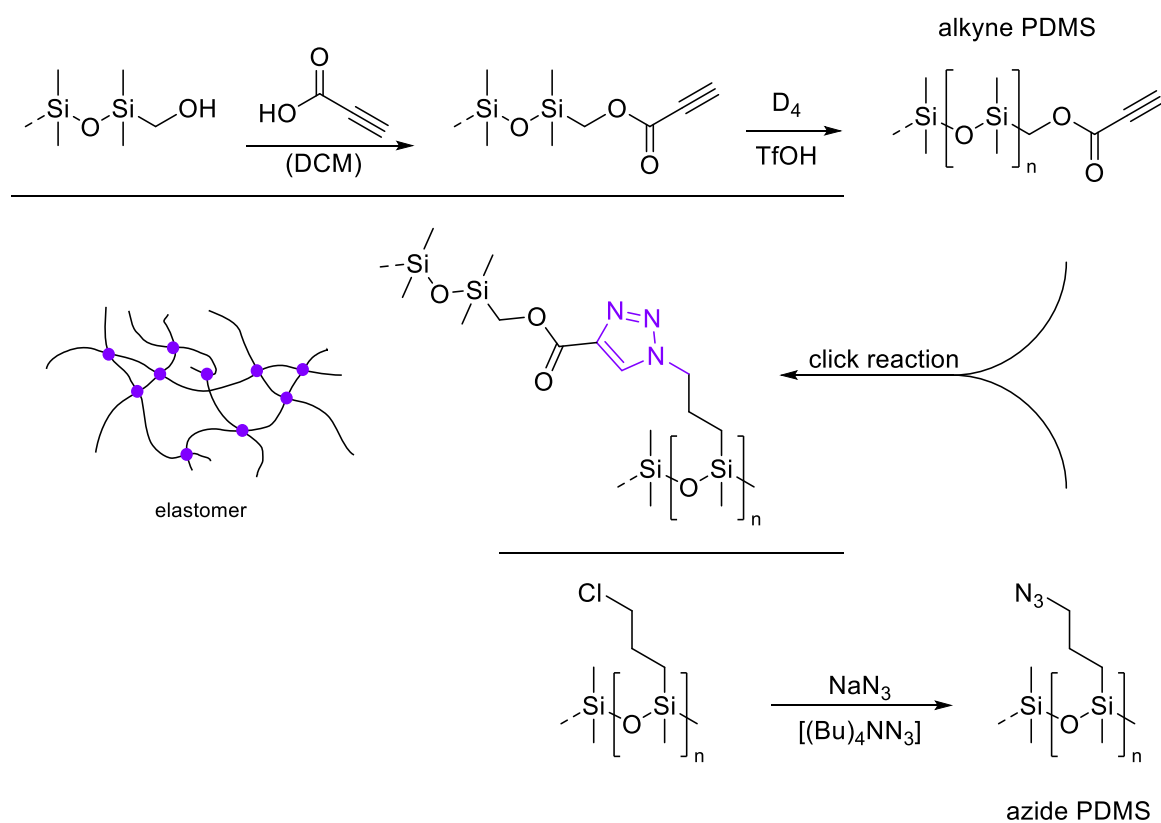
#### Autoxidation Curing



**Scheme 14.** Thermal oxidative crosslinking of hydrosilane functionalized PDMS by employing molecular oxygen.

A different approach for metal free curing was realized through the usage of the click reaction, introduced by the same group of Brook et al. in 2012.<sup>[180]</sup> This process required the synthesis of alkyne and azido functionalized polysiloxanes as reagents for the respective cycloaddition. The formation of alkyne terminated polysiloxanes was conducted by introducing the alkyne moiety through a condensation reaction onto small siloxane-diols and subsequent acidic equilibration of D<sub>4</sub> (octamethyl-cyclotetrasiloxane) units to create the polymeric backbone. The counterpart reagent, the polysiloxane functionalized with pendant azido-propyl branches, was afforded by reacting commercially available chloropropyl functionalized polysiloxane with sodium azide (NaN<sub>3</sub>) in the presence of tetra-*n*-butylammonium azide ((Bu)<sub>4</sub>NN<sub>3</sub>) as a phase transfer catalyst. Depending on the electronic properties of the employed alkyne, the final curing could be enabled thermally in the range of 60-90 °C, resulting in the described cycloaddition (click) reaction and the formation of the metal-free elastomer. However, the necessary preparation of these different functionalized polysiloxanes affords complex synthetic challenges, while the UV-lability of the ligating triazole rings further reduces their stability, and limiting their application range.<sup>[181]</sup>

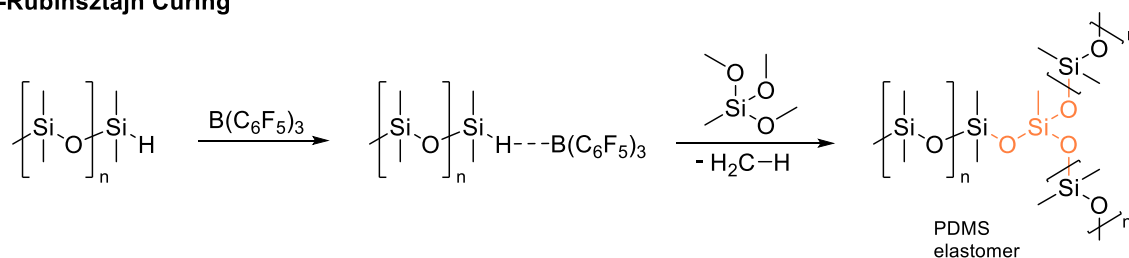
### Click Ligation Curing



**Scheme 15.** Schematic overview of the metal free curing via click ligation of alkyne and azide functionalized PDMS.

Additional efforts have been made by Brook et al. to exploit the reactivity of the Piers-Rubinstein reaction for the crosslinking of hydride functionalized polysiloxanes with alkoxy silanes.<sup>[182]</sup> This way, highly stable siloxane bridged polysiloxane networks can be created through the utilization of  $B(C_6F_5)_3$  (BCF) as catalyst for the hydrogen abstraction. The biggest advantage is the employment of readily available hydride polysiloxanes and multifunctional silyl-ethers as crosslinking joints. However, the need of a strong Lewis acid as catalyst is the major disadvantage of this method. Since comparably high concentrations of the catalyst (10 mol%) are required for a successful curing, the resulting catalyst ratio in the final elastomers remains at a high level. In addition, the lasting activity of this strong Lewis acid facilitates the catalytic degradation of the silicone network. Moreover, the elimination of a volatile alkane due to the nature of the Piers-Rubinsztajn reaction results in a shrinkage of the elastic material.

#### Piers-Rubinsztajn Curing

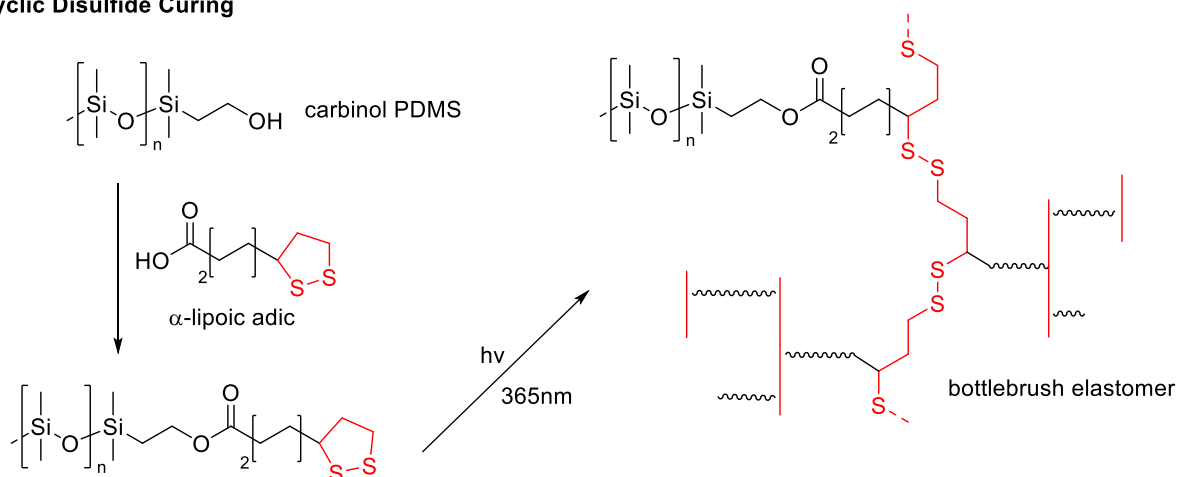


**Scheme 16.** Piers-Rubinsztajn catalyzed curing of hydride functionalized with multifunctional silyl-ethers.

A recent alternative process based on cyclic disulfides allows light mediated curing of bottlebrush silicone elastomers, without using any catalysts, additives, or solvents.<sup>[183]</sup> Introduction of  $\alpha$ -lipoic acid onto carbinol terminated PDMS by a condensation reaction affords the required disulfide functionalized PDMS. Irradiation under UV-light connects the respective cyclic units in a ring-opening polymerization. The resulting disulfide backbones are branched and intersected by the original polysiloxane backbone, thus creating the desired elastomer. Subsequent irradiation of these elastomers allows dynamic redistribution of the disulfide bonds, which can be utilized for light mediated self-healing or on demand degradation. Even though the curing process is rather a creation of a secondary polymer backbone within the polysiloxane matrix, this method showcases the possibility to create elastic hybrid materials by introducing different types of polymer networks. At the same time, the introduction of this disulfide backbone narrows the application range of this product in terms of thermal and photochemical lability to highly specific use cases.



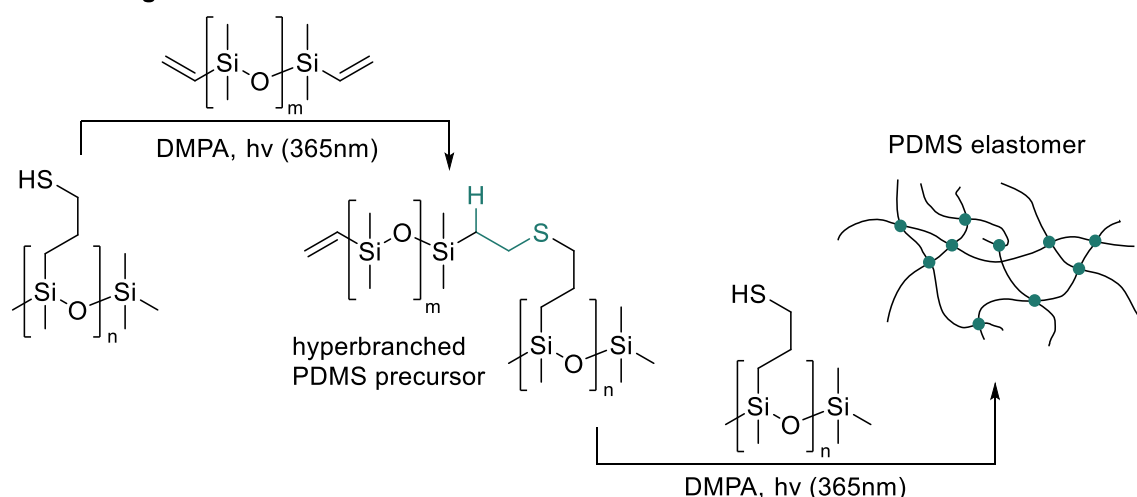
## Cyclic Disulfide Curing



**Scheme 17.** Crosslinking of cyclic disulfide functionalized PDMS through UV-light mediated initiation to afford bottlebrush elastomers containing two different types of polymer backbones.

Another light controlled curing process is the photoinitiated thiol-ene curing of vinyl-terminated PDMS with lateral propyl-thiol functionalized PDMS, reported by Daugaard et al in 2014.<sup>[184]</sup> By preparing short chained hyperbranched PDMS precursors in a first step, the second thiol-ene reaction results in the formation of highly flexible PDMS elastomers. The utilization of DMPA (2,2-dimethoxy-2-phenylacetophenone) is required as a photo-initiator to promote the UV-controlled reaction. Albeit the benefits of this metal free option, the comparable slow curing rate and the necessity of a two-step crosslinking process hinders its use for a broader field of application.

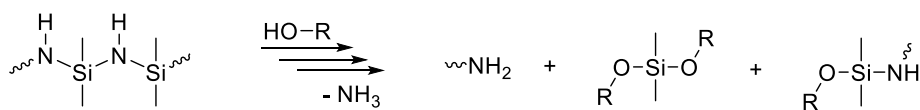
## Thiol-ene Curing



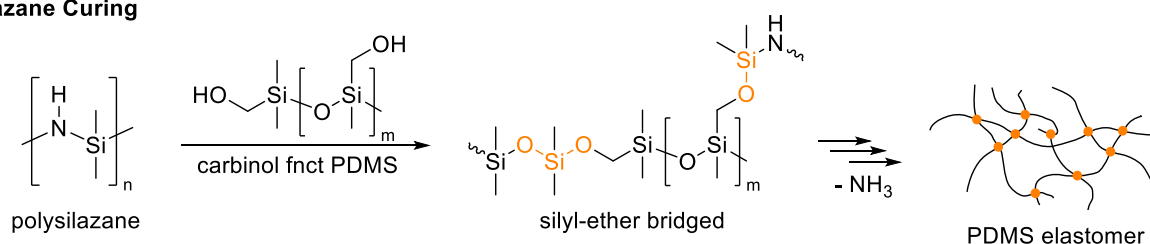
**Scheme 18.** Thiol-ene based curing to create PDMS elastomers from vinyl- and thiol-functionalized polysiloxanes. A recent study from Daugaard et al. in 2022 reports of an unexpected fragmentation mechanism of polysilazanes, which enables catalyst free curing of carbinol functionalized

polysiloxanes.<sup>[185]</sup> As described earlier, polysilazanes are primarily used as ceramic precursors, however this new curing method casts a new light on this type of material. The proposed mechanism of fragmentation is initiated by the reaction of a carbinol moiety and proceeds via the Si-N bond fission in the polysilazane backbone. The subsequent elimination of ammonia is the consequence of the formation of the respective silyl-ether and the silicone network. This way, soft silicone elastomers can be generated at ambient conditions without the use of any catalyst. Yet, the formation of a side product can cause shrinkage or foaming of the final elastomer. In addition, the nature of ammonia as a Brønsted-base facilitates the ionic degradation of the polysiloxane backbone and thus its long-term stability. However, it is worth noting that polysilazanes can be employed as curing agents for silicone elastomers.

#### Silazane Fragmentation

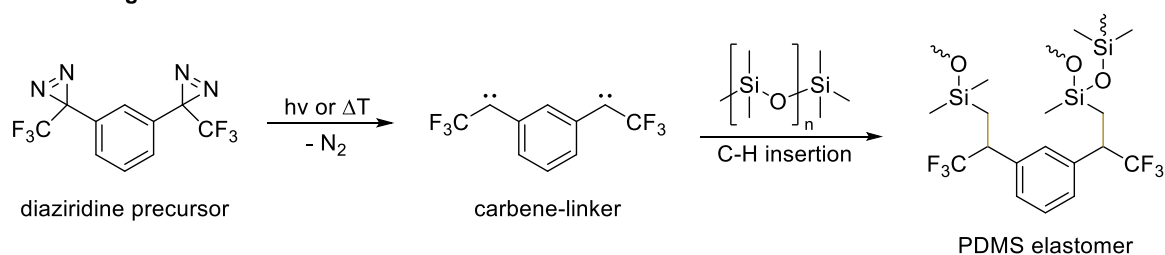


#### Silazane Curing



**Scheme 19.** Overview of the underlying polysilazane fragmentation mechanism (top) and the resulting curing concept based on the reaction with carbinol functionalized PDMS (bottom).

In 2019, Wulff et al. reported of the utilization of *in-situ* generated carbenes for curing of a variety of different polymer types, such as polyolefins or polysiloxanes.<sup>[186]</sup> Diaziridines are employed as comparably stable precursors to afford the carbene-linker scaffolds through thermal or photochemical initiated elimination of  $\text{N}_2$ . The high reactivity of these compounds facilitates C-H insertion reactions and enables crosslinking of polymers, which are usually unreactive towards post-modification. This way, facile polysiloxanes without specific attached functional groups can be cured at mild process conditions. However, the necessity of perfluorinated moieties incorporated in the linker structure raise ecological or health concern. Moreover, the instability of the diaziridine functionalities and the elimination of molecular nitrogen bears a relatively high explosive potential, resulting in additional safety precautions and specific storage and application measures.

**Carbene Curing**

**Scheme 20.** Carbene based curing of polysiloxane through thermal or light induced activation of bis-diaziridines. These reports of recent efforts to introduce alternative methods to prepare polysiloxane rubber materials show the necessity of new, more sustainable, more economical, and safer curing options. Many of these processes focus on metal free crosslinking as a major advantage, due to the increasing scarcity of rare noble metals as catalyst material. Others try to establish new fields of application and expand the beneficial properties of elastic polysiloxanes for other use cases.

## 2.6. Organosilicon Compounds

In general, organosilicon compounds are referred to as a combination of the metalloid silicon and the most basic organic atom carbon. However, compounds consisting of silicon and other heteroatoms, like oxygen, nitrogen, or sulfur amongst others, are also included in this description of organosilicon compounds. Naturally occurring silicon is found almost exclusively as silicate, thus the nature of organosilicon compounds is solely a synthetic one.<sup>[89]</sup> With an electronegativity of 1.9 (Pauling), silicon is considered a classical metalloid and sits between actual metal like lithium or aluminum (1.0-1.6) and the organic carbon (2.55). Thus, most organosilicon compounds exhibit polarized bonds. Yet, this polarization is weaker compared to classical organometallic compounds which grants the respective silicon-based species a comparable higher stability. In analogy to their carbon counterparts, organosilicon moieties can be found in a variety of (hetero)cycles, chains, or aromatic compounds. Albeit their similarities, the reactivity of organosilicon compounds is usually distinctly higher and can differ quite drastically. There are several reasons to explain this, the most important ones are the already mentioned difference in electronegativity as well as their respective atom radii of 1.06 Å (Si) and 0.66 Å (C), which influences their orbitals and the energetic position thereof.<sup>[89]</sup>

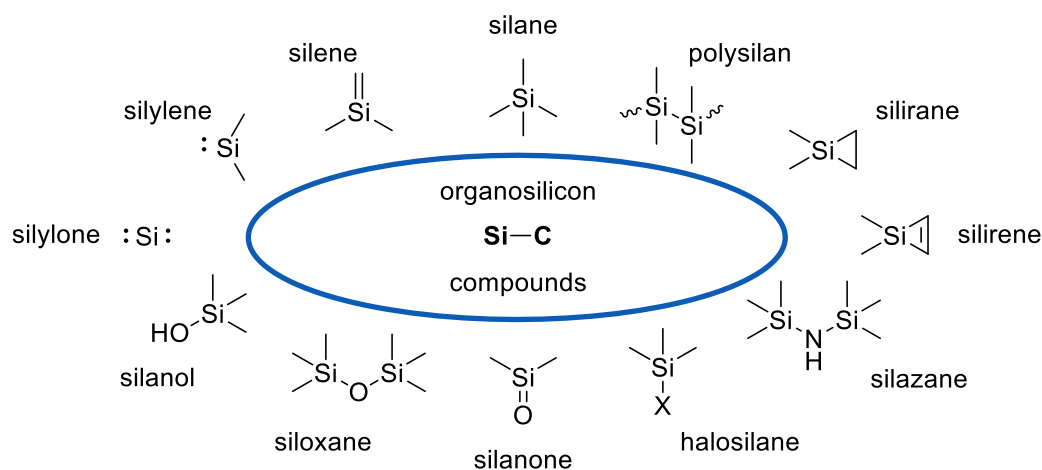
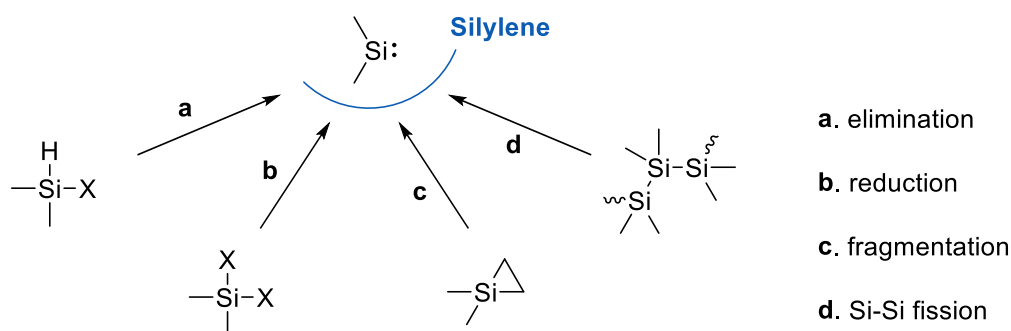


**Figure 9.** Selection of relevant organosilicon compounds and their description (X = F, Cl, Br, I).

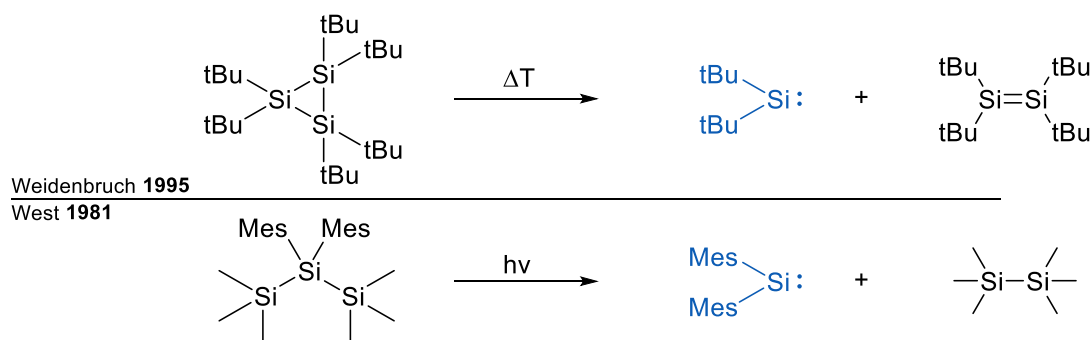
### 2.6.1. Silylenes

A particular interesting case of organosilicon species are the silylene compounds, due to their unique oxidative state of (+II). The majority of organosilicon compounds share the common oxidative state (+IV), which is why silylenes are also referred to as low-valent silicon species. Compounds of this kind were considered unstable and impossible to obtain synthetically.<sup>[89]</sup> However, through sufficient thermodynamic and kinetic stabilization, a plethora of different silylenes is now synthetically available and draws increasing attention towards academic and industrial applications. One of these intended applications is the introduction of low-valent silicon as potential catalyst, since there is a general tendency to substitute rare and unsustainable transition metals with more abundant and safer metals like iron or even metalloids like silicon.<sup>[96,187]</sup> The difficulty of silicon based catalysts to provide similar properties like transition metals is aggravated by the limited number of oxidative states, provided solely by valence electrons of the *s*- and *p*-block. In general, silylenes are highly reactive and tend to undergo immediate consecutive reactions like polymerization or disproportionation. Thus, adequate stabilization is key to control these silylenes according to their specific application.<sup>[89]</sup>

There are various approaches to synthesize silylenes. Depending on the respective synthesis strategy, different types of organosilicon precursors can be employed. Some of the most commonly used methods to obtain the desired silylene species are either by reduction of halosilanes, pyrolysis of silanes, degradation of polysilanes or fragmentation of strained silacycles.



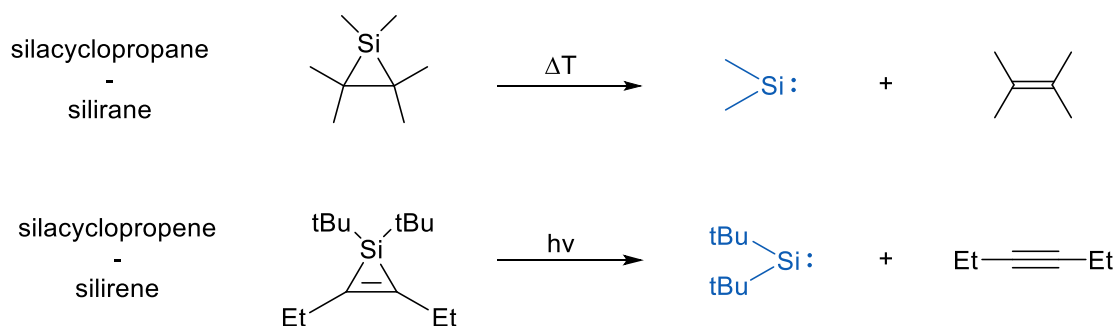
**Scheme 21.** Common synthetic approaches to create silylenes by employing different types of silicon precursors. One of the most common synthetic approaches to generate silicon (II) species is the degradation of polysilanes through cleavage of the comparably weak Si-Si bond. Silanes consisting of at least three consecutive coupled silicon atoms occupy the necessary molecular structure, thus cyclic or linear polysilanes are an obvious choice for this purpose. Cyclic trisilanes represent an ideal silylene source. Due to their small ring size, the resulting ring strain facilitates the Si-Si fission. Either thermolysis at high temperatures or photolysis with hard UV-light can be employed to enable to required reactivity. In addition, transition metal catalysts can be utilized as well, albeit their examples in literature is rather scarce.<sup>[188-190]</sup>



**Scheme 22.** Exemplary synthesis of silylenes through thermal or photochemical induced Si-Si cleavage.

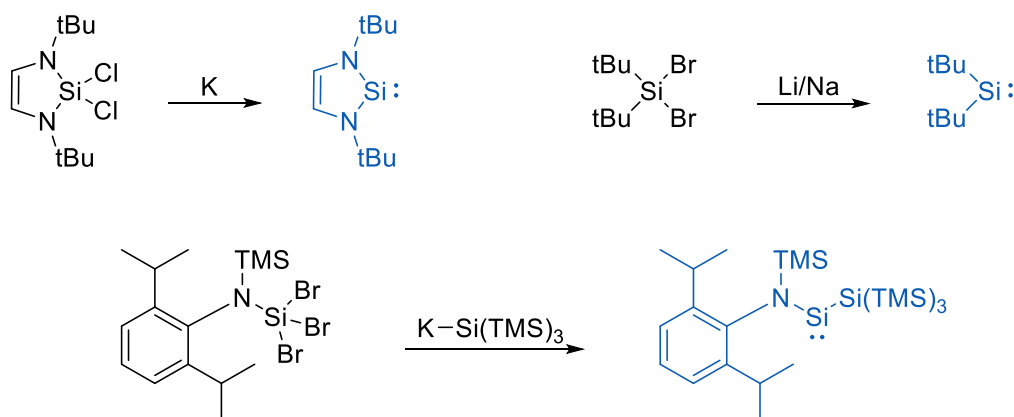
The fragmentation reaction of small silacycles is driven by the release of the ring strain within these circular scaffolds. Although in theory, all silacycles are suitable for generating silylenes, only the highly strained siliranes (silacyclopropanes) are practically capable of doing so. The thermal or photochemical induced fragmentation of the three-membered Si-C ring results in the formation of an alkene and the desired silylene. This type of reaction was initially reported for the fragmentation of the stable hexamethylsilacyclopropane into dimethylsilylene under thermolytic conditions by Seyferth et al. in 1975.<sup>[191]</sup> Formally, silacyclopropanes are the addition product of a silylene and an olefine. Thus, they are referred to as “trapped” silylenes and can be considered as a stabilized precursor of highly reactive but unstable silylenes.<sup>[192,193]</sup>

In addition, silacyclopropenes as an unsaturated version of the respective silacyclopropanes can undergo similar fragmentation reactions, resulting in the formation of the aimed silylene and an alkyne. Many silacyclopropenes can be photochemically activated even at higher wavelengths, due to the pseudo- $\pi$  aromatic character of these compounds.<sup>[194–196]</sup>



**Scheme 23.** Fragmentation of stable three-membered silacycles to obtain the desired silylenes.

Another frequently used method is the reduction of dihalosilanes in combination with strong reduction agents. Commonly used reductants are metals like lithium, sodium, potassium, magnesium, and alloys thereof or compounds like  $KC_8$ , lithium- or sodium-naphthalene. Depending on the stability of the dihalosilanes the choice of the reductant and thus its reduction potential is key to successfully obtain the aimed silylene. Due to the increasing bond strength with decreasing atomic number ( $F > Cl > Br > I$ ), fluorosilanes are less favored candidates for this reaction. Chloro-, bromo-, or iodo-silanes on the other hand can be reduced much easier and are therefore commonly employed as silylene precursors. To accelerate the reduction, this type of reaction is usually performed in polar, aprotic solvents.<sup>[89,197,198]</sup> This way, the first stable silylene at ambient conditions was isolated via the reaction with potassium to form the first *N*-heterocyclic silylene (NHSi) by Denk et al. in 1994.<sup>[199]</sup>



**Scheme 24.** Reduction of dihalosilanes with different reducing agents to afford the respective silylenes.

Among the low-valent silicon species, the divalent silylene occupies the most important place. The name “silylene” is derived from their carbon-based analogue, the carbene, which are well studied and broadly employed as  $\sigma$ -donating ligands in a variety of different catalyst systems in organometallic chemistry.<sup>[200]</sup> All members of the tetrels possess four valence electrons in the general configuration of  $(ns)^2(np)^2$ . However, it has become apparent that carbenes differ significantly in regard of their electronic properties from their related, yet heavier elements of group 14. The reason for this difference lies in the respective electronic ground state. Typically, carbenes are found in the triplet ground state consisting of two valence electrons with the same spin, resulting in a diradical. This property originates from the negative singlet-triplet splitting ( $\Delta E_{S,T} = -14$  kcal/mol) of  $H_2C(II)$ , generating a stabilizing effect in the triplet state.<sup>[201]</sup> This singlet-triplet energy difference increases significantly along the elements of group 14. Thus, the singlet ground state is already favored in the case of silylenes due to a positive value of  $\Delta E_{S,T} = +16.7$  kcal/mol for  $H_2Si(II)$ , with an even more distinct tendency towards the singlet-ground state for the heavier analogues (Ge, Sn, and Pb).<sup>[201]</sup>

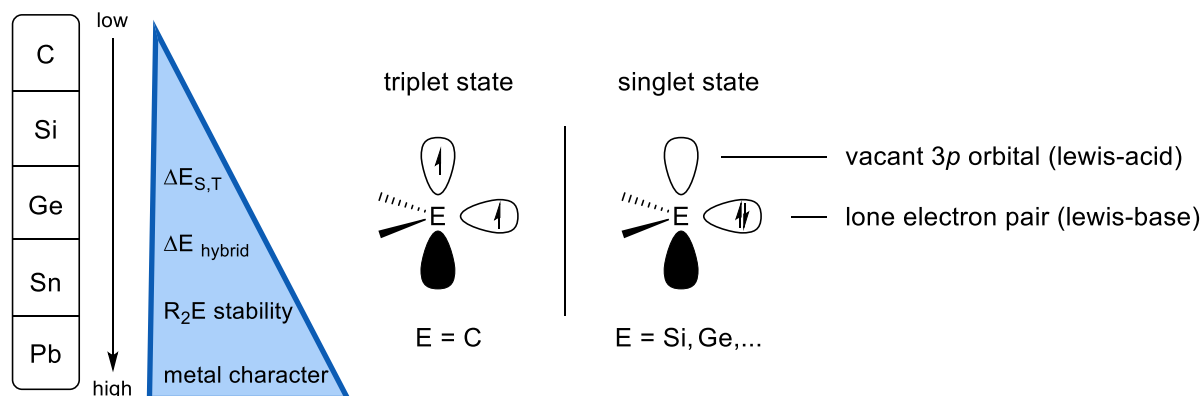


**Figure 10.** Comparison of singlet-triplet energy difference, hybridization energy, stability and metal character of the divalent compounds within the group 14 elements and orbital depiction of the triplet and singlet ground states.

Similar tendencies can be observed for the energy of hybridization ( $E_{\text{hybrid}}$ ) increase along the heavier atoms of this group. A higher effective nuclear charge and a reduced overlap between the s- and p-orbitals can explain the resulting increase in energy separation as well as the spatial separation of these orbitals. As a consequence, silylenes and their heavier analogues exhibit a filled  $sp^2$ -type orbital with a high s-character, while the respective bonding orbitals show a particular high p-character. This is further demonstrated by the decrease of the interligand bond angle for  $H_2M(II)$ : from  $134^\circ$  for  $H_2C(II)$ , over  $92.7^\circ$  for  $H_2Si(II)$ , to eventually  $90.5^\circ$  for  $H_2Pb(II)$ . The bond angle for the respective carbene in the triplet ground state approaches the ideal orbital geometry of  $180^\circ$  for a  $sp$ -hybridized orbital and further

emphasizes the significant difference to the heavier tetrels.<sup>[201]</sup> The comparable small energy of hybridization for the carbon-atom enables a variety of differently bonded carbon-compounds, thus a combination of two carbenes results in the generation of a  $sp^2$ -hybridized and planar C=C double bond.<sup>[202]</sup> In the light of classical consideration, no such bonding is possible for silylenes or heavier analogues, due to the interatomic Pauli-repulsion of the inner-shell electrons in combination with the lone pair repulsion between the two compounds.<sup>[203]</sup> However, West et al. succeeded in creating the first known disilene, which disproved the original bonding hypothesis and resulted in the creation of an adapted bonding model by Carter-Goddard-Malrieu-Trinquier. The CGMT-model describes the bond as an electron donor-acceptor interaction between the filled  $sp^2$ -hybridized orbital and the vacant p-orbital of the second fragment. The combination of these interactions generates a bonding with effective double-bond character, revealing a *trans*-pyramidal geometry. The degree of deflection is strongly related to the singlet-triplet energy difference ( $\Delta E_{S,T}$ ), resulting in a greater distortion from the original planarity with an increased value for the energy difference.<sup>[204]</sup>

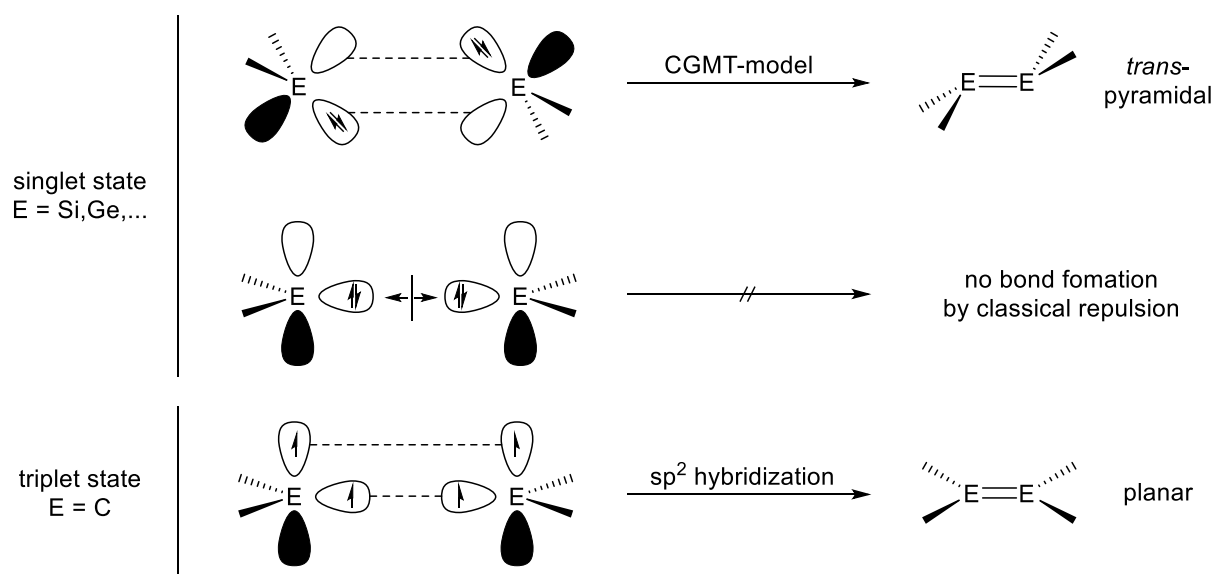
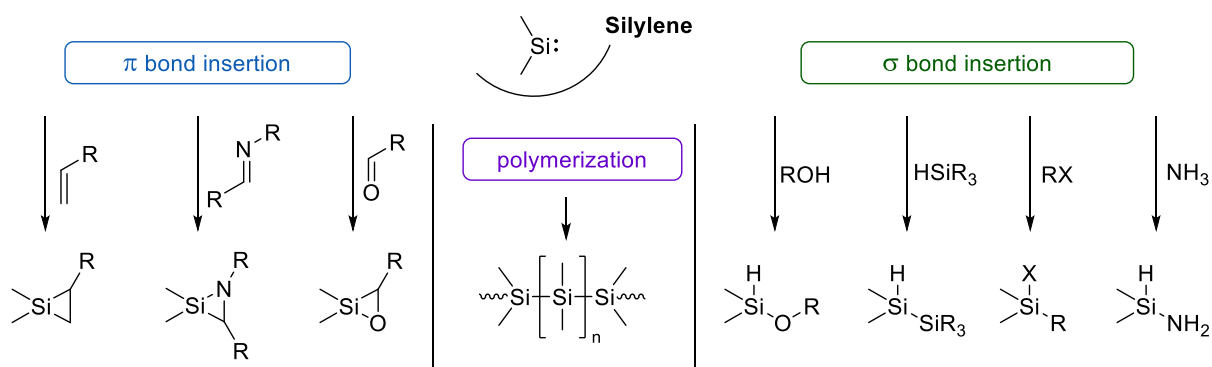


**Figure 11.** Different bonding models for the dimerization of single- and triplet-ground state fragments and their resulting molecular geometry.

The resulting electronic properties of these low-valent species are strongly influenced through the bound ligands, which enable an effective degree of reactivity control. Silylenes exhibit an amphiphilic character, due to their singlet-ground state. The vacant p-orbital provides the possibility to act as a Lewis-acid, while the electron lone-pair acts as a Lewis-base. In regard of the octet rule, silylenes possess solely six valence electrons and are formally



in a state of electron deficiency. The resulting high reactivity is showcased through polymerization-, dimerization-, insertion-, or addition-reactions and emphasizes the instability of this compound class. Even the respective dimerization products are usually highly instable and tend to polymerize, due to a small HOMO-LUMO gap (approx. 3 eV) and a weak  $\pi$ -orbital overlap.<sup>[205]</sup>



**Scheme 25.** Silylene reactivity overview of  $\sigma$ -,  $\pi$ -bond insertion as well as dimerization and polymerization reactions.<sup>[206]</sup>

As a result, effective stabilization and protection is key to isolate the respective silylene species as such. In general, two potential stabilization methods are employed to achieve the desired silylene properties and guarantee their stability. One method is the introduction of sterically demanding ligands, effectively blocking the silicon atom. This kinetic control protects the Si(II) center from nucleophilic attacks or dimerization, and polymerization reactions. Over the years, a variety of different ligands with controllable steric demand have been developed and introduced, such as silyl-, aryl-, or alkyl-based ligands. Through exaggeration of the steric bulk, a counteracting destabilization and repulsion of the ligands takes places, which leads to an increase of the ligand bond angle and eventually the transition towards a triplet ground state. The second method relies on the thermodynamic stabilization of the silicon atom, in which mostly heteroatom-based ligands have proven themselves as useful. The effective stabilization can originate from ligand substitution either through  $\sigma$ -acceptor or  $\pi$ -donor effects. Electron withdrawing ligands with heteroatoms like nitrogen, oxygen, sulfur, or phosphor drain electron density from the non-bonding orbital (HOMO) at the silicon. This way, the orbital and the respective singlet ground state is stabilized, by lowering its energy and increasing its s-character. Additional stabilization is possible through electronic resonance, caused by the  $\pi$ -donor effects of the ligand. The donating electron density affects the vacant p-orbital (LUMO), resulting in a less electrophilic character as well as a larger HOMO-LUMO energy difference,<sup>[203]</sup> eventually stabilizing the silylene.<sup>[203]</sup>

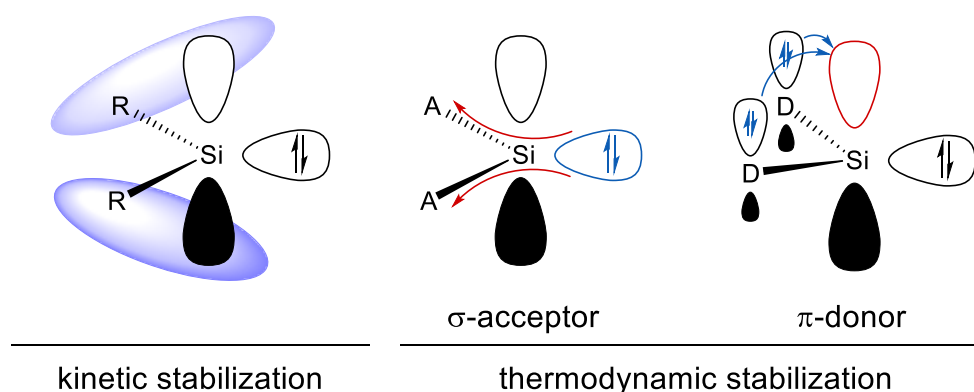


**Figure 12.** Depiction of stabilization methods for silylene compounds via kinetic or thermodynamic control.

On the basis of these techniques, Jutzi et al. succeeded in creating the first stable silylene thus laying the foundation of low valent silicon chemistry in 1986.<sup>[207]</sup> In 1994, West et al. were able to isolate another stable silylene based on the framework of *N*-heterocyclic silylenes.<sup>[208]</sup> By combining these stabilizing ligand effects, it was possible to create entirely new and unknown compounds. Since then, the scope of available and stable silylenes has increased significantly, while the introduction of future ligand systems will ensure new horizons.<sup>[209–211]</sup>

### 2.6.2. Silacyclopropanes

Silacyclopropanes, also referred to as siliranes are three-membered silicon heterocycles. In regard to their electronic properties, silacyclopropanes do not belong to the class of low-valent silicon compounds, however they represent a highly reactive precursor species for the generation of the prior described silylenes. Silacyclopropanes exhibit a strong structural resemblance with the all-carbon based cyclopropanes, yet their respective reactivities and properties differ significantly. Siliranes show a higher strained ring system, experience less stabilization and are consequently more reactive than their carbon-based analogues. This distinct difference is shown by comparing bond-lengths and angles of the respective cycles.<sup>[212]</sup>

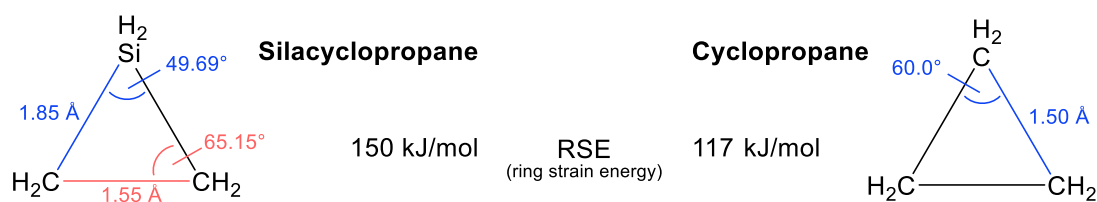
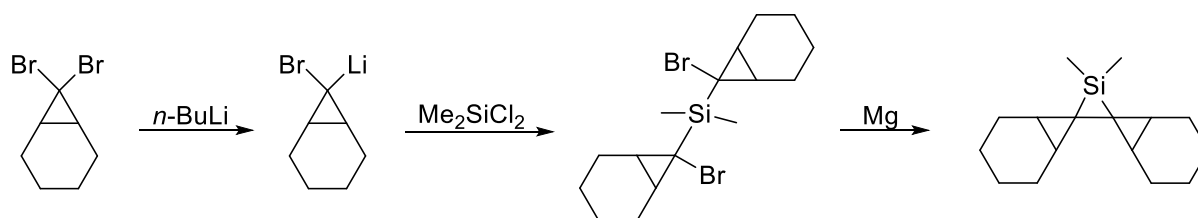


**Figure 13.** Comparison of silacyclopropanes and cyclopropanes in regard to bond-lengths, angles, and ring strain.

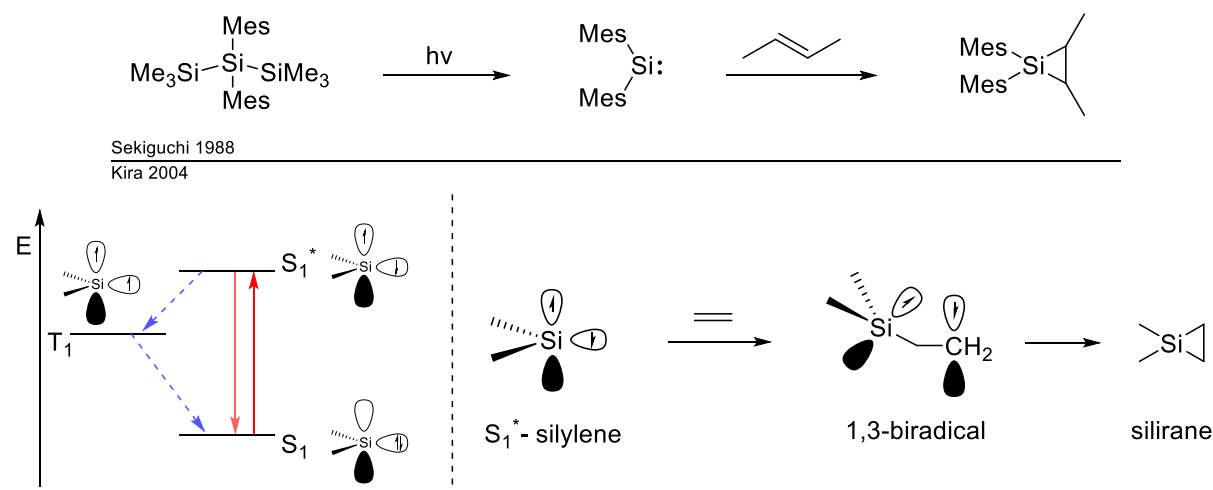
In the case of cyclopropane, the bond-angles are all equivalent with a value of  $60.0^\circ$ , resulting in the generation of a comparably low value for the respective ring strain. The different bond angles and lengths in the case of silacyclopropane deform the ring system further and thus increase its ring strain energy. Another effect occurs from the polarized  $\text{Si}^{\delta+}-\text{C}^{\delta-}$  bond, which facilitates nucleophilic or electrophilic attacks in the case of the heteroatomic silacyclopropane. In addition, the attenuated interaction of the  $3p$ -orbital of the silicon and the  $2p$ -orbital of the carbon atoms further destabilizes the silicon containing ring system. In accordance with the Dewar-model, cyclopropanes are stabilized through the  $\sigma$ -aromaticity of the delocalized six bonding-electrons within the ring. It is considered that this aromaticity is primarily responsible for the low ring-strain energy in cyclopropanes.<sup>[213-215]</sup> Due to the difference in orbital size and energy in the case of siliranes, this type of stabilization is less probable and decreases the delocalization of the contributing electrons. As a result, silacyclopropanes are generally less stable compounds compared to cyclopropanes, yet exhibit a significantly more interesting and higher reactivity.<sup>[216]</sup> This instability manifests in a high reactivity towards moisture or oxygen, which prohibits the handling of this compound class under ambient conditions in most cases.

Initial attempts to synthesize silacyclopropanes originated from the generation of cyclopropanes via the Gustavson-reaction, by reacting 1,3-dihalopropane with zinc to afford the desired three-membered ring.<sup>[217]</sup> Unfortunately, this reactivity could not simply be transferred to siliranes, due to the emergence of various side and consecutive reactions. The first successful isolation of a stable silirane was reported by Seyferth et al. in 1972 by employing magnesium in a Wurtz-coupling reaction.<sup>[218]</sup>



**Scheme 26.** First synthesis of a stable silacyclopropane by Seyferth et al. in 1972 via the Wurtz-coupling reaction. Since then, various approaches have been presented to enable alternative synthesis pathways for their generation. One of them is based on the photolysis of polysilanes to generate silylenes by irradiation with UV-light. The photo lability of the Si-Si silane bond allows homolytic scission thereof to afford the highly reactive low valent silylene species. This

concept was initially introduced by Ishikawa and Kumada 1972, by irradiating dodecamethylcyclohexasilane at a wavelength of 250 nm for several hours.<sup>[219]</sup> The actual creation of the silirane proceeds through the addition of an olefin to the respective silylene. This way, the isolation of diaryl substituted silylenes with 2-butene was first reported by Ando and Sekiguchi in 1988.<sup>[220]</sup>

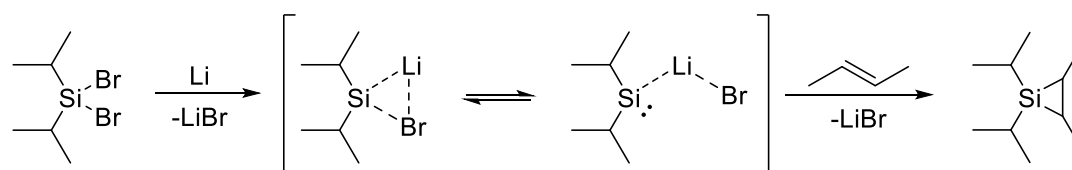


**Scheme 27.** Silane photolysis reaction to create the silirane in the presence of butene reported by Sekiguchi, as well as the mechanistic theory to explain the respective reaction pathway, provided by Kira et al.

To explain the reaction mechanism, Kira et al. suggested that the photo-addition of the olefins proceeds over the excitation of the electronic ground state of the silylene. The respective singlet-ground state  $S_1$  gets excited by the energy input of the photon to reach the higher lying singlet state  $S_1^*$ . This transient species can subsequently react with the present olefin forming a biradical compound, which will eventually recombine the two radicals in a ring-closure reaction to form the desired silacyclopropane.<sup>[221]</sup> Even though this technique provides a powerful tool to create siliranes, the necessity to generate highly reactive silylene species in the process can be critical in regards of side reactions.

Besides the prior mention reduction of 1,3-dihalosilanes via the Wurtz-coupling reaction, the direct reduction at the silicon center has become comparably prominent for the generation of silacyclopropanes. Strong reducing agents are employed for the direct reduction of the 1,1-dihalosilane in combination with an olefin as a trapping agent. Typical reducing agents are alkali metals, sodium-naphthalene, or potassium graphite.<sup>[222,223]</sup> The respective silanes are usually substituted by chloride or bromide, while a higher reaction rate is observed for the latter one, based on the better polarizability of the bromide compared to the chloride.<sup>[224]</sup> Thus, the correct choice of reducing agents is crucial for an effective synthesis of the desired silirane

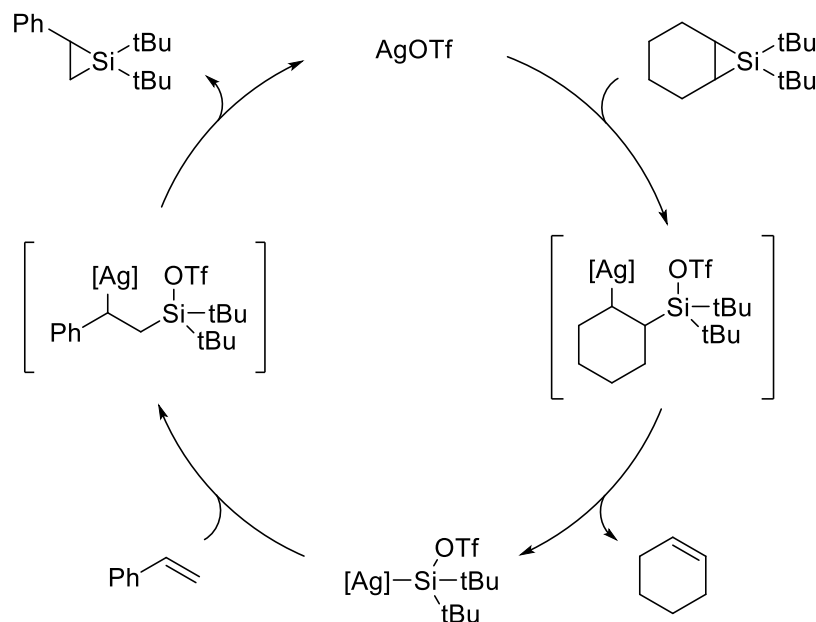
and can prevent consecutive reactions or other side reactions. Based on the wide range of different substituted halosilanes this method bears many possibilities to create a variety of silacyclopropanes. The mechanism behind this reduction is believed to involve the generation of a silylenoide intermediate, which is considered a radical reaction process and proceeds through the cycloaddition of the present olefin. Boudjouk et al. were the first to present this hypothesis,<sup>[225]</sup> while Lee et al. later showed the synthesis of various siliranes by employing lithium-bromosilylenoide emphasizing this theory even further.<sup>[226]</sup>



**Scheme 28.** Lithium based reduction of 1,1-dibromosilane through the formation of a silylenoide species.

A different and effective concept of altering existing silacyclopropane compounds is the silylene-transfer reaction. The incorporated olefine can be exchanged by another olefine to afford a new silirane through the transient formation of the respective silylene species. This equilibrium reaction is dependent on the reaction conditions and the difference in stability of the respective siliranes. In order to initiate the reaction, the reactant silirane species has to be activated, which can either be done thermally, photochemically, or via metal catalysis. Depending on the stability of the silirane temperatures between 60 °C for hexamethylsilirane and 110 °C for cyclohexyl-di-tert-butylsilirane are required in order to activate them and release the silylene species.<sup>[223,227]</sup> Photochemical activation, on the other hand, is less prominent for the silylene-transfer reaction, however some examples have been reported in the past for the analogue reaction with alkynes to form silirenes.<sup>[223]</sup> The last, yet most utilized approach is the metal catalyzed silylene-transfer reaction. Thorough research has been done by Woerpel et al. to establish the metal catalyzed version of this reaction over the years.<sup>[228-251]</sup> Exploiting the high ring strain in cyclohexyl-di-tert-butylsilirane and its consecutive lability, a variety of different di-tert-butyl substituted siliranes were accessible in high yields. The main advantage of this approach are the mild reaction conditions, which allows even the creation of thermally labile siliranes with ease. Various metal-based catalysts can be employed, albeit the use of copper or silver-based catalysts has shown to be most effective, with fast reaction rates as well as a broad tolerance for different olefins or other trapping agents.<sup>[228-250]</sup> In 2004, Driver et al. proposed a reaction mechanism for the catalytic transfer

of cyclohexyl-di-tert-butylsilirane with styrene in the presence of AgOTf.<sup>[230]</sup> It has been shown that the olefine addition to the transient silylene species proceeds stereospecific, and results in the respective cis- or trans-product.<sup>[225]</sup>



**Scheme 29.** Proposed mechanism of the silver-catalyzed silylene transfer reaction in the presence of styrene.

With these synthesis methods at hand, it was possible to create a variety of silirene species, yet their stability still is highly dependent on the electronic and steric protection by the substituents. While mostly steric effects have been utilized for the isolation of the first siliranes by Seyferth,<sup>[218]</sup> also electronic stabilization via hyperconjugation resulted in the successful generation of various siliranes.<sup>[218,227]</sup> Over the time, stable siliranes containing different heteroatoms have been reported by Boudjouk,<sup>[225]</sup> Power,<sup>[232]</sup> Rieger,<sup>[233]</sup> or Inoue.<sup>[96]</sup> Usually these compounds have to be handled under protective atmospheres, however Fink,<sup>[234]</sup> Gaspar,<sup>[235]</sup> and Kira each reported examples of a stable silirane, withstanding ambient conditions.<sup>[220]</sup>

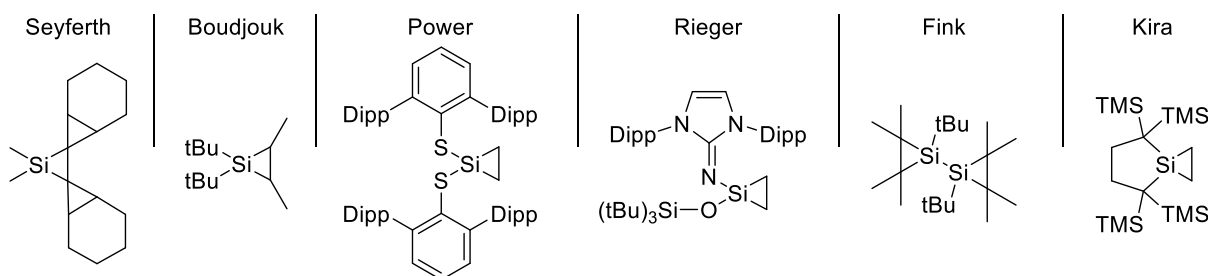
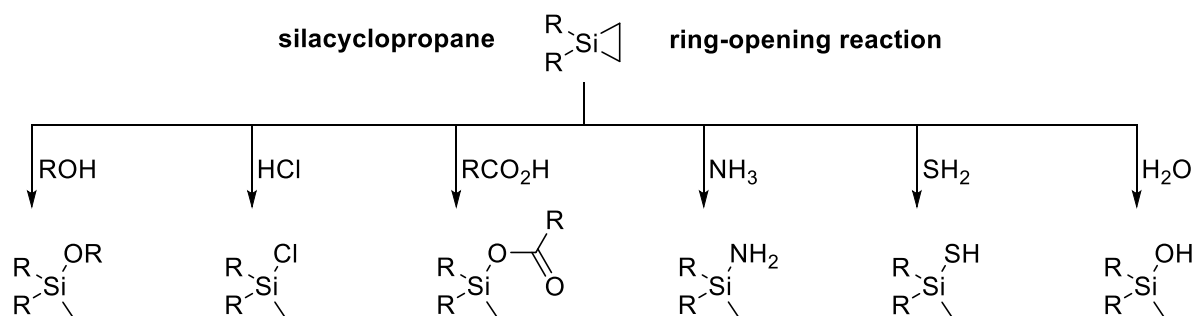


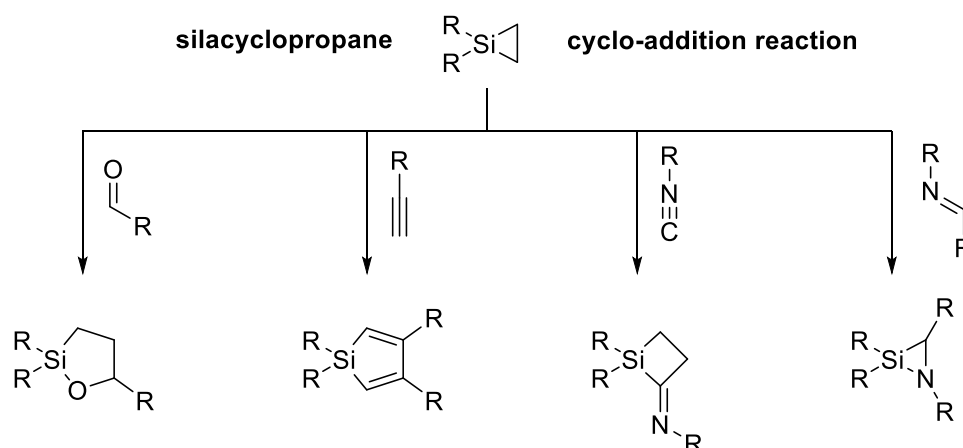
**Figure 14.** Overview of some literature known stable and isolable silacyclopropanes.

In general, silacyclopropanes exhibit a strong tendency towards ring opening reactions as a result of the highly polarized Si-C bond and the ring strain energy. The respective attack of the nucleophile always proceeds at the positive polarized silicon atom and thus initializes the ring opening.<sup>[218]</sup> Exemplary are the reactions of siliranes with alcohols, acids, thiols, amines, or water, resulting in the formation of the respective ring-opening product.<sup>[236]</sup>



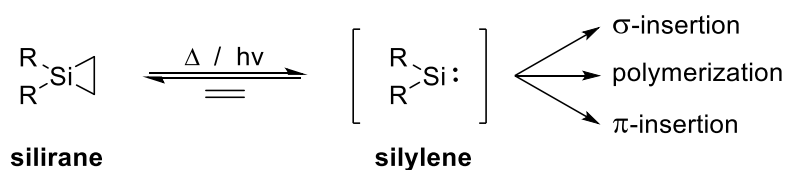
**Scheme 30.** Selection of ring-opening reactions of various nucleophiles with silacyclopropanes.

Besides the ring opening reaction, the reaction of alkynes, carbonyls, imines, or isocyanides results in the insertion and cycloaddition into silacyclopropanes. Employing carbonyl moieties in form of aldehyds, formamides, esters, or ketones affords the creation of the respective oxasilacyclopentane scaffold in high yields and selectivity.<sup>[237–239]</sup> Iminosilacyclobutanes are the product of the reaction with isocyanides at elevated temperatures, which can readily be transformed in the prior mentioned oxasilacyclopentane by hydrolysis.<sup>[240]</sup> With the help of the silylene-transfer reaction, either thermally or catalytically controlled, silaazaridines can be created in the presence of imines, by releasing the respective olefin in the process.<sup>[241]</sup>



**Scheme 31.** Overview of different cycloaddition reactions with carbonyls, alkynes, isocyanides, and imines.

However, one of the most useful and broadly exploited reaction of silacyclopropanes is the generation of transient silylenes by the elimination of the respective olefin. This fragmentation can be initiated either thermally, or photochemically and provides a controllable access to various silylene species. Due to this fact, siliranes are considered as “masked silylenes”, which usually need less stabilization and can be easier synthesized. In most cases, the respective transient silylenes are not stabilized enough to be isolated, thus consecutive reactions are inevitable due to their high reactivity. As earlier described the silylenes can undergo various types of reactions, including different insertion reactions.<sup>[225,242]</sup>



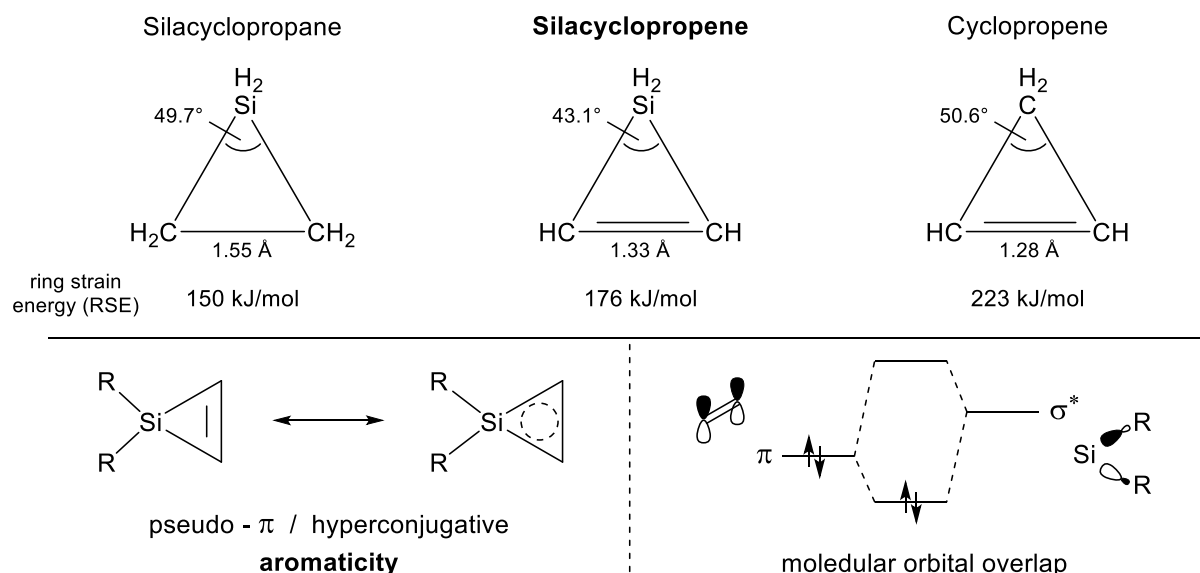
**Scheme 32.** Equilibrium reaction of siliranes and silylenes, with possible consecutive reactions of the transient silylene.

### 2.6.3. Silacyclopropanes

Silacyclopropanes (silirenes) belong to the class of three-membered sila-cycles as well and represent the unsaturated version of the prior described silacyclopropanes. Albeit their resemblance towards siliranes or cyclopropanes, their stability and reactivity differ significantly based on their unique electronic structure. Comparing the calculated C-C bond lengths and the respective apex bond angle C-Si-C would indicate that silacyclopropanes exhibit a higher degree of ring deformation and thus a higher ring strain energy.<sup>[243,244]</sup> However, comparably low values for the ring-strain energy ( $RSE_{\text{silirene}} = 175.5 \text{ kJ/mol}$ ) in silirenes suggest that these ring systems experience a significant stabilization through increased aromatization within the ring. The participation of the completely vacant 3d-orbital of the Si-atom with the two electrons at the  $\pi$  bonding C=C bond enable the delocalization of these electrons, thus affording an increased amount of aromaticity. This effect is attenuated in the case of Ge or Sn due to the decreased participation of the 4d or 5d-orbitals respectively. Whereas cyclopropene exhibits no aromatic character at all because of the sheer lack of any d-orbitals in the carbon atom, hence explaining the comparable high ring strain energy in the cyclopropene ring ( $222.6 \text{ kJ/mol}$ ).<sup>[243]</sup> The stabilization of silirenes is further consolidated by the hyperconjugation and the strong molecular orbital (MO) overlap of the C=C  $\pi$ -bond orbital



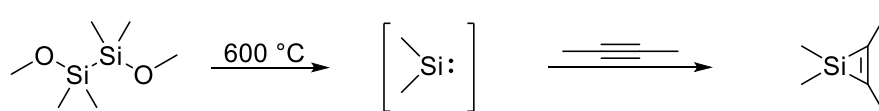
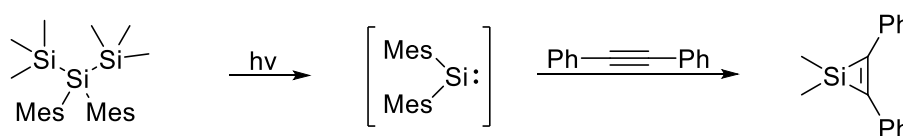
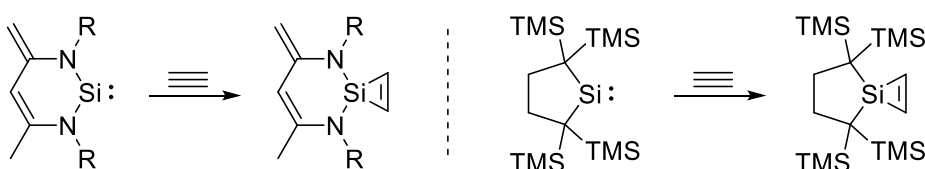
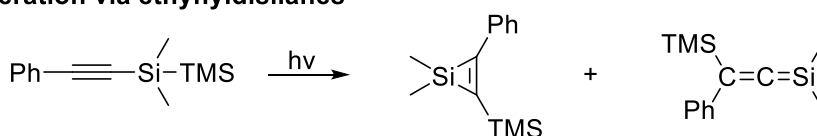
with the vacant low-lying antibonding  $\sigma^*$ -orbital of the  $\text{SiR}_2$  fragment. Due to these effects, this type of stabilization is referred to as “pseudo- $\pi$ ” or “hyperconjugative” aromaticity in the literature.<sup>[194]</sup> As a consequence, silacyclopropenes are generally more stable than their saturated counterparts and exhibit an unusual absorption band at higher wavelengths above 300 nm, which can be exploited for their photochemical reactivity.<sup>[196,245]</sup>



**Figure 15.** Top: Comparison of the calculated C=C bond lengths and apex bond angles of silacyclopropanes, silacyclopropenes, and cyclopropenes in combination with their resulting ring strain energy (RSE).<sup>[243]</sup> Bottom: Depiction of the aromaticity in silacyclopropenes and their respective MO overlap.<sup>[194]</sup>

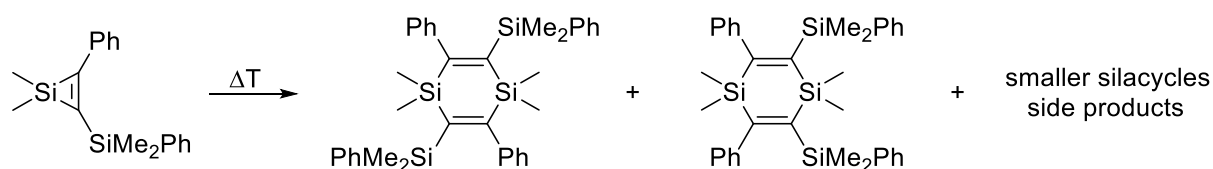
First synthetic attempts have been reported by Volpin et al. in 1962 for the reaction of dimethylsilylene with diphenylacetylene,<sup>[246]</sup> however Atwell and Weyenberg later demonstrated the formation of a disilane as the only reaction product, not the creation of a silacyclopropene.<sup>[247,248]</sup> It were Conlin and Gasper, who successfully isolated the first literature known silacyclopropene through a gas-phase flow-pyrolysis at 600 °C by reacting 1,2-dimethoxytetramethyldisilane with 2-butyne.<sup>[249]</sup> Seyferth et al. followed soon after with the thermolysis of hexamethylsilacyclopropane in the presence of bis(trimethylsilyl)-acetylene to afford 2,3-bis(trimethylsilyl)-1,1-dimethyl-1-silacyclopropene in good yields.<sup>[250,251]</sup> In general, the synthesis of silacyclopropenes is based on the initial generation of an unstable transient silylene species, which undergoes a cycloaddition reaction with a present alkyne compound. Besides the thermally controlled synthesis routes, photolysis of cyclic and acyclic polysilanes can be exploited for this purpose as well. Photochemically generated silylenes react with various alkynes to afford the desired silacyclopropenes.<sup>[252,253]</sup> However the photo-lability of many silacyclopropenes facilitates side reactions and

attenuates or prevents an effective isolation of these compounds under irradiation. Rearrangement reactions arising from a 1,2-hydrogen or TMS shift in the three-membered rings are well known side reactions occurring through the irradiation of the respective silacyclopropenes.<sup>[253]</sup> With the first introduction of stable silylenes in the 1990s, the possibility to construct silacyclopropenes on the basis of N-heterocyclic, acyclic, or carbocyclic silylenes allowed a controlled and facile access to generate a variety of new silacyclopropenes.<sup>[254–257]</sup> The exclusive generation of silirenes via the addition of silylenes to alkynes was expanded in the year 1977 by the photolysis of alkynyl-substituted disilanes to afford silacyclopropenes on a much more convenient route.<sup>[258]</sup> Since then several procedures have been reported for the photochemical reaction of (phenylethynyl)disilanes yielding the desired silacyclopropenes in high yields by utilizing a low-pressure mercury lamp.<sup>[259,260]</sup> Most silacyclopropenes are unstable towards air and moisture, however introduction of sufficiently bulky substituents at all participating atoms of the ring system leads to the formation of stable and comparably inert silacyclopropenes. Various examples have been reported for the isolation of air-stable silirenes, which can be handled without protective measures or special care.<sup>[245,261]</sup>

**Pyrolysis via silylene****Photolysis via silylene****Generation via stable silylenes****Generation via ethynyldisilanes**

**Scheme 33.** Overview of various synthesis methods to generate silacyclopropenes through different approaches.

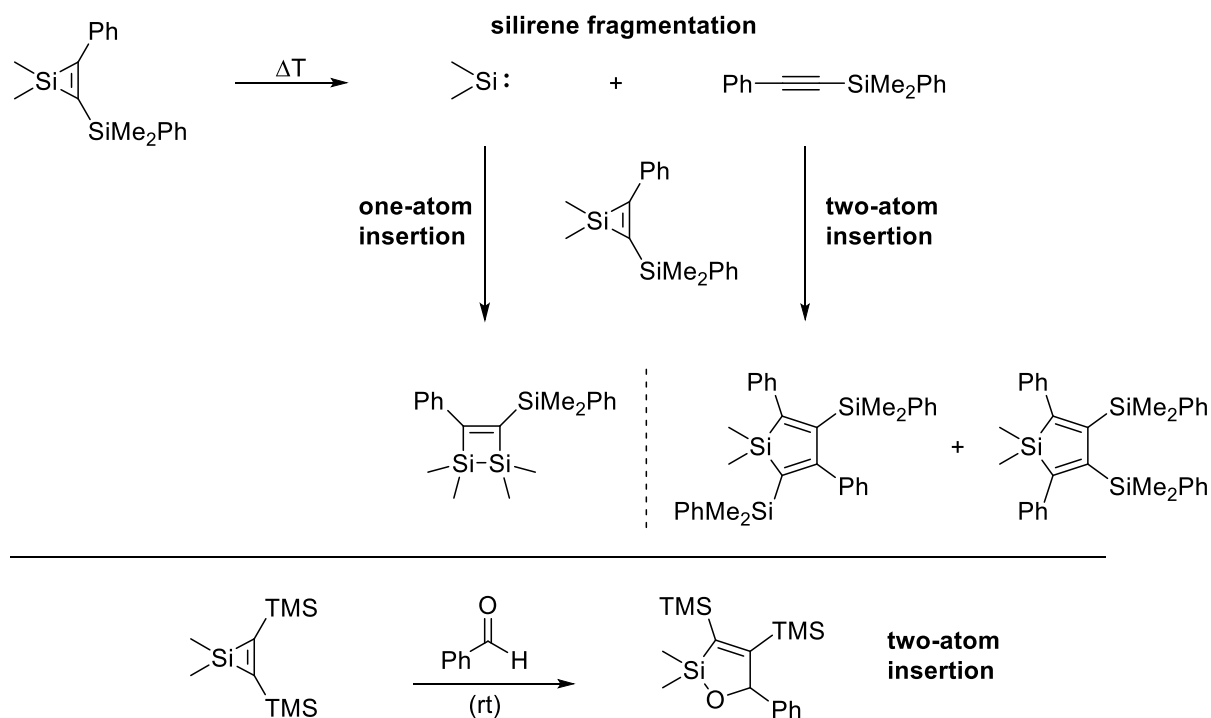
The thermal and photochemical reactivity of silacyclopropenes is highly influenced by the respective substituents at the silicon and carbon atoms of the unsaturated ring system. In general, the thermal reactions of silacyclopropenes can be divided in five different reaction types. Silylene fragmentation,<sup>[245,250,251,253,261]</sup> dimerization,<sup>[262–264]</sup> insertion,<sup>[248,251,264–267]</sup> isomerization,<sup>[245,262]</sup> and polymerization reactions have been reported in the literature.<sup>[196,245]</sup> Upon thermal activation, the silacyclopropene can eliminate the respective acetylene to afford the in situ generated silylene again. The silylene can thus undergo various insertion or other reactions as prior described. Because of this behavior, silacyclopropenes are also referred to as masked silylenes, just like the saturated silacyclopropanes. However,  $\sigma$ -dimerization reactions occur regularly through thermolysis of these compounds as well. The respective head to tail dimerization yields in the formation of six-membered silacycles, while affording side products such as smaller five- or four-membered ring systems as well. Due to the nature of this dimerization, only trans isomers are generated in this thermolysis indicating that steric control is key in this type of reaction. The reaction mechanism is believed to proceed through a concerted pathway, since no evidence for a homolytic scission of the Si-C bond could be observed. In addition, molecular orbital calculations are in accordance with this hypothesis.<sup>[264]</sup>



**Scheme 34.** Thermal dimerization reaction of silacyclopropenes to afford dimeric six-membered silacycles.

The insertion reaction of different compounds into the Si-C bond of the silirene ring is a well-known reaction type. Most of them include one- or two-atom insertion, which can also be seen as ring expansion reactions in fact. A facile one-atom insertion occurs from the reaction of silacyclopropenes with silylenes to afford the respective 1,2-disilacyclobutene. Seyferth and Atwell have reported a variety of silylene based insertion reactions under thermolytic conditions.<sup>[266,268]</sup> Prominent two-atom insertions include the reaction of silirenes with alkynes or related compounds containing triple bonds. While the one-atom insertion results in the formation of a silacyclobutene ring, this two-atom insertion generates the respective silacyclopentadiene as a product. Since the thermolysis of silirenes can yield the silylene and acetylene fragmentation respectively, this type of insertion reactions usually occurs as side

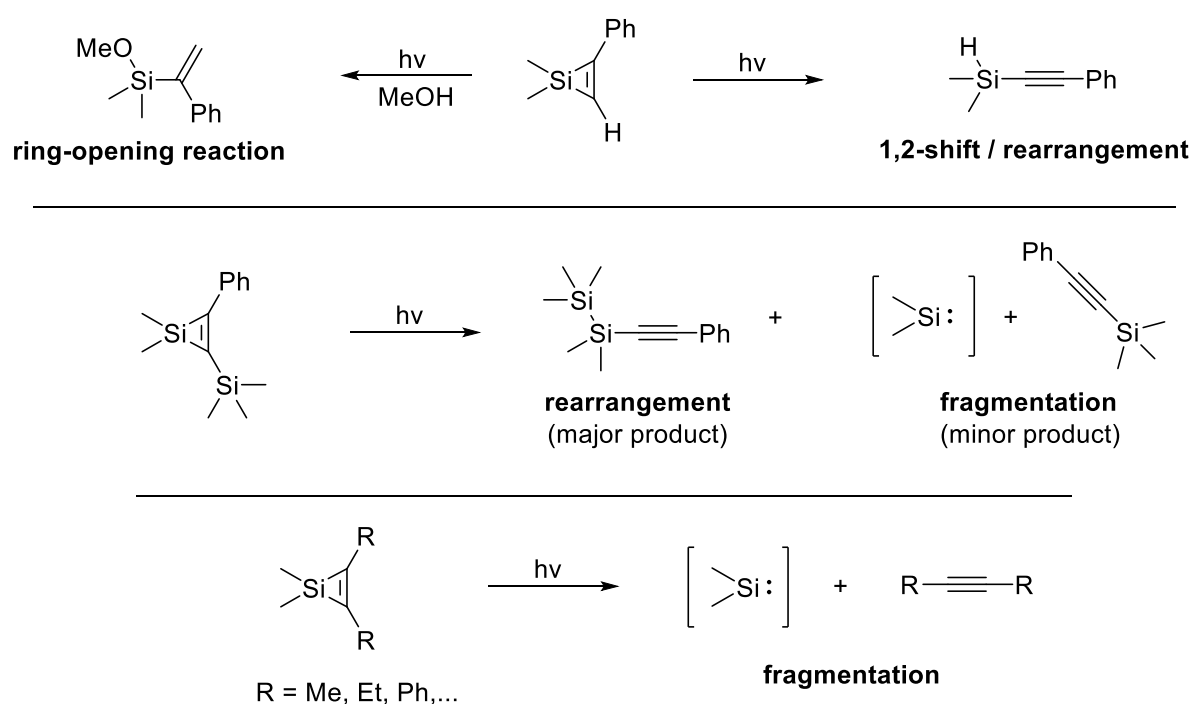
reaction upon thermolysis conditions.<sup>[260,263]</sup> Another two-atom insertion reaction is based on reactivity of silirenes with aldehydes and ketones, in which the carbonyl C=O bond gets inserted into the ring system. For instance, Seyferth et al. reported the reaction of dimethyl-bistrimethylsilyl-silacyclopropene with benzaldehyde to afford the respective 1-oxa-2-silacyclopent-3-ene in high yields at room temperature.<sup>[268]</sup>



**Scheme 35.** Insertion reactions of silacyclopropenes via one- and two-atom insertion. One-atom insertions proceed via the reaction with silylenes, while two-atom insertions occur in combination with alkynes or aldehydes.

The photochemical behavior of silacyclopropenes depends strongly on the type of substituent attached to the silacycles. In general, silirenes containing a hydrogen on one of the participating carbon atoms originate from the photolysis reaction of an ethynyl-disilane and are in most cases thermally as well as photochemically labile. In the presence of a trapping agent like methanol, a consecutive ring-opening reaction occurs without the possibility to isolate any intermediate compounds. In the absence of methanol as a trapping agent, undefined polymerization or rearrangement reactions can be observed. The latter reaction can be understood as a 1,2-hydrogen shift to afford the respective ethynyl-hydrosilane.<sup>[260]</sup> Similar rearrangement reactions were also reported through the migration of silyl-based substituents, like trimethylsilyl, to generate the respective ethynyl-disilanes via the 1,2-shift of these silyl-substituents from the carbon to the silicon atom.<sup>[269]</sup> However, 2,3-disubstituted silirenes bearing no hydrogen or silyl-moieties undergo selective fragmentation under

irradiation to generate the silylene species in combination with the respective acetylene. This type of reaction can be readily exploited for the selective and controlled generation of silylenes, due to the nature of silirenes as masked silylenes. In general, hydrogen and silyl-substituted silacyclopropenes can perform this type of fragmentation as well, however the respective rearrangement cannot be prevented and the effective formation of the silylene species remains compromised.<sup>[269]</sup> In contrast to the saturated silacyclopropanes, the photolability of the silacyclopropenes arising from the aromatic nature of this type of compound, bears great potential to be utilized for photochemical reactions and light-controlled applications.



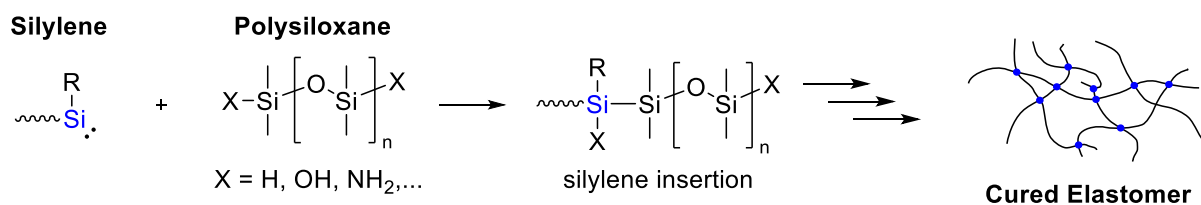
**Scheme 36.** Overview of differently substituted silacyclopropenes and their different behavior upon irradiation.

### 3. Motivation and Aim – Innovative Curing of Polysiloxanes

The industrial importance of silicones is emphasized by their outstanding physical and chemical properties, yielding in numerous applications for a variety of different industries. Silicone-based elastomers have become the most relevant segment within the polysiloxane industry. While silicones are used as fluids, gels, or resins, the segment of cured elastomers led the global silicone market with a share of more than 41% in 2020.<sup>[4]</sup> However, conventional curing strategies primarily proceed through hydrosilylation or condensation by employing metal catalysts based on tin or platinum, which become non-recoverable in the polymer networks. For instance, this results in the waste of 4-6 tons of pure platinum each year, solely attributed to the hydrosilylation curing process.<sup>[270]</sup> Disadvantages of the respective condensation curing include the elimination of small and volatile compounds, such as alcohols or carboxylic acids, resulting in a mass loss and shrinkage of the final material.

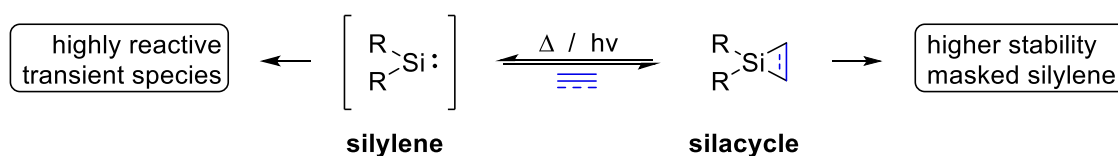
With regard to the resulting environmental, social, and financial challenges arising from the continuous utilization of these conventional processes, development of innovative and more sustainable methods for the crosslinking of polysiloxanes are the main focus of this work. By excluding metal catalysts or additives in the curing process, the environmental impact and financial expenses can be effectively reduced, while preventing to deterioration of the final elastomer properties through contamination.

The fundamental idea to eliminate metal catalysts in the curing process is to replace these catalysts with highly active crosslinker-molecules. These should be able to connect the functional groups present on the polysiloxane-chains thus forming a polymer network and the desired silicone rubber. By this process the crosslinker will be introduced into the silicone and will be a part of the final rubber itself, thus it would be desirable to keep contamination and implementation of foreign heteroelements by addition of these crosslinkers low. A suitable candidate to achieve this task is the general motif of the low valent Si(II) species, the silylenes. In general, silylenes are difficult to isolate and have to be stabilized kinetically or thermodynamically. At the same time, this instability renders silylenes a very reactive species which are known to react with various moieties.



**Scheme 37.** Conceptual crosslinking method based on the application of silylenes with functionalized silicones.

To create an effective crosslinker compound it is crucial to combine at least three active silylene functionalities on one scaffold. Each silylene reacts with the functional group of individual silicone-chains, thus generating the desired silicone network. Furthermore, due to the chemical composition of the silylene-motif itself, the introduction of foreign elements in the polysiloxane matrix can be prevented. This way, the consistency of the final silicone rubber will be maintained and contamination is reduced to a minimum. Consequently, the backbone of the silylene based crosslinker scaffold will be composed of a silicone-based structure to further ensure this homogeneity.



**Scheme 38.** Protecting of the silylene through silacyclopropane precursor structures, gaining synthesis and application control.

The high reactivity of the silylene is key to obtain fast and efficient crosslinking reactions. However, the silylene instability under ambient conditions complicates the direct isolation and usage of these structures. Three-membered silacycles act as masked silylenes and represent stable precursors, which can readily be employed for this type of usage. This way, the crosslinkers can be isolated and stored without decomposition, allowing facile one component curing mixtures. The silacyclopropane moiety allows thermal ( $\Delta T$ ), while the silacyclopropene moiety enables photochemical ( $h\nu$ ) activation to form the respective transient silylene. This way control over the synthesis and crosslinking process will be obtained. The final step in the project is the usage and application of the synthesized crosslinker molecules with various types of polysiloxanes and their respective functional groups. The curing process itself as well as the resulting silicon rubbers will be investigated to gain insights into the reaction and to assess the network formation potential compared to the established metal catalyzed curing processes.

## 4. Silacyclopropanes as Crosslinker in Thermal Silicone Curing

### 4.1. Bibliographic data

Title: “Application of multifunctional silylenes and siliranes as universal crosslinkers for metal-free curing of silicones”<sup>[271]</sup>

Status: Research Article, Publication Date: 05.06.2020

Journal: Green Chemistry

Publisher: Royal Society of Chemistry (RSC)

DOI: 10.1039/D0GC00272K

Authors: Fabian A. D. Herz, **Matthias Nobis**, Daniel Wendel, Philipp Pahl, Philipp J. Altmann, Jan Tillmann, Richard Weidner, Shigeyoshi Inoue, Bernhard Rieger ‡

### 4.2. Abstract graphic (TOC)

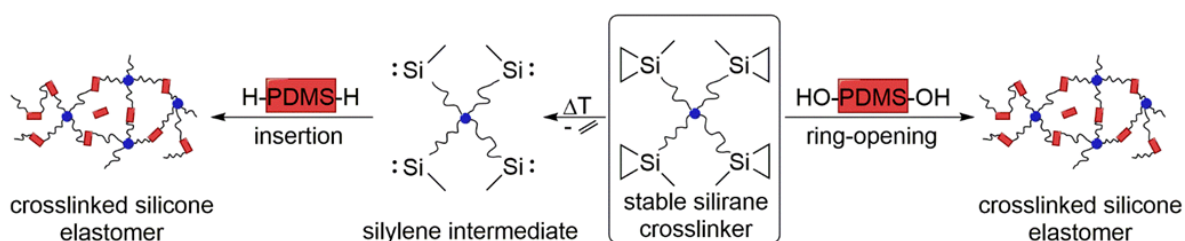


**Figure 16.** Table of Content for the manuscript titled “Application of multifunctional silylenes and siliranes as universal crosslinkers for metal-free curing of silicones”

‡F. Herz and M. Nobis contributed equally by planning and executing all experiments and preparing the manuscript. D. Wendel, P. Pahl, J. Tillmann, and R. Weidner helped with data analysis and by revising the manuscript. P. Altmann conducted all SC XRD-measurements and managed the processing of the respective data. All work was performed under the supervision of B. Rieger and S. Inoue.




### 4.3. Content

Conventional industrial crosslinking of silicones is usually done by the well-established tin-catalysed condensation, platinum-catalysed addition, or peroxide curing. The choice of the appropriate crosslinking method is always a trade of individual advantages and disadvantages. The introduction of new crosslinking methods for silicone rubbers allows to combine their beneficial attributes, while reducing drawbacks with the help of highly reactive silylenes and silacyclopropanes. These new crosslinking methods are not dependent on non-recoverable Pt- or toxic Sn-catalysts and enable the production of clean polysiloxane elastomers. The reactive silylene species is generated by thermal decomposition of stable silirane precursors and reacts with various functionalities of silicone building blocks. This way, curing of hydride or hydroxy functionalized PDMS is possible through silylene insertion reactions into the respective moieties. Due to the nature and stability of the synthesized silirane linker structures, a thermally controlled activation allows the preparation of stable one-component mixtures and their direct application. Alternatively, polymeric multifunctional silirane linkers can be ring-opened by nucleophilic compounds like siloxanols, facilitating an alternative curing with standard nucleophilic siloxanes. The utilization of curing temperatures below the silylene-activation facilitates this second crosslinking pathway. By combining these two related concepts, most functional groups in siloxane chemistry can be crosslinked with just one universal cross-linking agent. Considering the growing importance of green chemistry and sustainable solutions, the renouncement of non-recoverable noble or toxic metals (Pt/Sn) is a seminal improvement which could become a relevant resource-saver. Silylenes play a big role in organometallic chemistry but unlike their carbon analogues (carbenes) only very few applications have been reported so far. The herein described alternative crosslinking method acts as basic concept of silirane crosslinking, including the synthesis of the multifunctional siliranes as model compounds and their application. To our knowledge this is the first application of silylenes in the field of applied polymer chemistry and comes with a broad spectrum of advantageous characteristics, which are ready to be utilized.

Cite this: *Green Chem.*, 2020, **22**, 4489

## Application of multifunctional silylenes and siliranes as universal crosslinkers for metal-free curing of silicones†

 Fabian A. D. Herz,<sup>‡a,b</sup> Matthias Nobis,<sup>‡a,b</sup> Daniel Wendel,<sup>a,b</sup> Philipp Pahl,<sup>a</sup> Philipp J. Altmann,<sup>c</sup> Jan Tillmann,<sup>d</sup> Richard Weidner,<sup>d</sup> Shigeyoshi Inoue <sup>b</sup> and Bernhard Rieger <sup>\*a,b</sup>

Conventional industrial crosslinking of silicones is usually done by the well-established tin-catalysed condensation, platinum-catalysed addition or peroxide curing. We report the first application of highly reactive multifunctional silylenes as universal crosslinkers for catalyst-free curing of standard industrial silicones. The reactive silylene species is generated by thermal decomposition of stable silacyclopropane precursors and reacts with various functionalities of silicone building blocks in an addition reaction. Alternatively, the multifunctional silacyclopropanes can be ring-opened by nucleophilic compounds like siloxanols, which can also be employed for network formation with standard nucleophilic siloxanes. These new crosslinking methods are not dependent on non-recoverable Pt- or toxic Sn-catalysts and enable the production of clean, extractable-free elastomers. We describe the synthesis of multifunctional siliranes as model compounds and their application in silicone curing.

Received 21st January 2020,  
Accepted 4th June 2020

DOI: 10.1039/d0gc00272k

rsc.li/greenchem

### Introduction

Polysiloxanes (silicones) have become omnipresent in our daily lives, mostly due to their outstanding physical and chemical properties. In contrast to conventional carbon-based polymers, long siloxane chains are still able to flow to some degree. Therefore the polymeric chains need to be crosslinked in order to form a non-flowing solid material.<sup>1</sup> Industrial crosslinking is mainly focused on the three conventional methods hydrosilylation, condensation curing and radical curing. They each exhibit different advantages and disadvantages and are used based on the product requirement. Condensation curing for instance is an easy and robust method which utilizes inexpensive silanol-terminated siloxanes. Besides the low cost and easy handling this method

requires long curing durations and a condensation catalyst (e.g. Sn-based). Volatile condensation products and the resulting shrinkage further limit its application. Addition-cured silicone rubbers are made by noble-metal-catalysed hydrosilylation of a two-component mixture of siloxanes bearing silicon hydrides and vinyl groups. The greatest benefits of addition curing are the absence of small volatile byproducts, low shrinkage and the high reaction rate. Although metals like Pt or Rh are highly active and used in ppm concentrations it makes hydrosilylation the most expensive curing process. Furthermore, the homogeneous catalysts remain in the final product and cannot be recovered. In case of platinum this results in a loss of 4–6 tons of metal each year.<sup>2</sup> Besides the high expenses and the environmental impact, the remaining catalyst is a contaminant in the product. Whether it is colloidal metal, condensation products or peroxide residues, extractables play a role in every mentioned curing method. Despite the disadvantages, catalysts remain indispensable components in silicone curing due to the lack of alternatives with equivalent reaction rates. Further improvements in catalyst design allow lower catalyst concentrations and better control over side reactions but do not tackle the overall problem.<sup>3</sup>

Our goal was to develop a new crosslinking method for siloxanes that functions without metal catalysts but features the same advantages as conventional methods. To compete with highly active catalysts, it is obvious to utilize highly reac-

<sup>a</sup>Technical University of Munich, WACKER-Chair of Macromolecular Chemistry, Lichtenbergstraße 4, 85748 Garching bei München, Germany. E-mail: rieger@tum.de

<sup>b</sup>Technical University of Munich, WACKER-Institute of Silicon Chemistry, Lichtenbergstraße 4, 85748 Garching bei München, Germany

<sup>c</sup>Technical University of Munich, Catalysis Research Center, Ernst-Otto-Fischer-Straße 1, 85748 Garching bei München, Germany

<sup>d</sup>WACKER Chemie AG, Consortium für elektrochemische Industrie, Zielstattstraße 20, 81379 München, Germany

† Electronic supplementary information (ESI) available. CCDC 1953911. For ESI and crystallographic data in CIF or other electronic format see DOI: 10.1039/d0gc00272k

‡ These authors contributed equally to this work.

## Paper

tive species based on an atom type which is already present in the polymer to avoid contamination. Divalent silicon(II) compounds (silylenes), which offer a broad and high reactivity, live up to these requirements. Since the discovery of the first Si(II)-compound in 1986 by Jutzi *et al.* silylenes have been intensely investigated and are still a hot topic in silicon chemistry.<sup>4</sup> Unlike their carbon analogues (carbenes), which have various useful applications,<sup>5</sup> silylenes are up to date of no particular industrial use. The reactivity is comparably broad as carbenes and covers addition reactions with nucleophiles as well as insertions in various chemical bonds and activation of small molecules.<sup>6–11</sup> Permanent silylenes, which are stable at ambient temperatures, require kinetic and electronic stabilization by complex ligands (Chart 1).

This strategy is not ideal for polymer chemistry since stability and reactivity are mutually dependent. The required stabilization for persistent silylenes as reactive groups would not only limit the reactivity but cannot be economically justified.

A more convenient approach is to use stable silylene precursors which can be activated in order to release the reactivity when needed. A similar approach which employs *in situ* generated carbenes was published by Steele *et al.*<sup>12</sup> Silacyclopropanes (siliranes) are an excellent candidate for this strategy since they are known as an effective silylene source. In contrast to silylenes, siliranes are much more stable at ambient temperature and even examples of air stable compounds are known. Due to the high ring-strain and polarization of the Si–C bonds they still show a high level of reactivity and offer a broad synthetic potential.<sup>7,13,14</sup> Stability beyond room temperature requires kinetic stabilization by shielding groups such as <sup>t</sup>Bu or thermodynamic stabilization by  $\pi$ -donating groups such as amides.<sup>7,13,14</sup> Compounds 1–4 are examples of ambient temperature stable siliranes, 2 is even stable in air.<sup>7,14–16</sup> Siliranes can be obtained by trapping the corresponding transient silylenes in a [2 + 1] cycloaddition. The C<sub>2</sub>-moiety of siliranes can be exchanged either by thermal degradation or by catalytic silylene transfer which was reported by Woerpel *et al.*<sup>17–20</sup>

Siliranes are highly reactive towards polar reagents and can be ring-opened with nucleophiles like alcohols, carboxylic acids and water.<sup>21</sup> Furthermore, they are sources of highly reactive transient silylenes, which can be generated by photolysis or thermolysis<sup>22</sup> (Scheme 1). These transient silylenes insert into various bonds *via* addition reaction. Functionalities worth mentioning are Si–H, –OH and Si–OR.<sup>22,23</sup> These two reactiv-

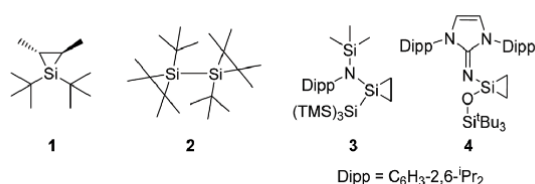
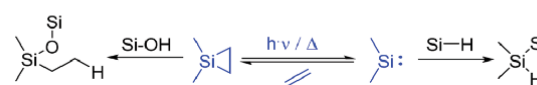


**Chart 1** Literature known examples of room-temperature stable silacyclopropanes.



**Scheme 1** Reactivity pathways of siliranes. Ring-opening with nucleophiles and degradation to silylenes followed by insertion into various bonds.

ities cover the range of all common functional groups used in industrial silicone chemistry (Si–H, Si–OH, Si–Vinyl, Si–OR) which makes siliranes a versatile functional group for crosslinking reactions.

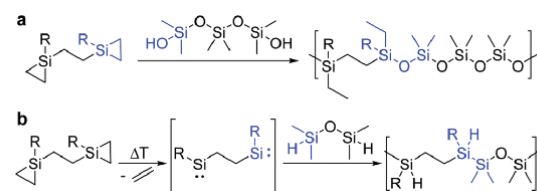
### Novel crosslinking concepts

The two reaction pathways of siliranes enable two different approaches for crosslinking of siloxanes. The ring-opening concept (Scheme 2a) utilizes the reaction of siliranes with nucleophiles, such as the standard industrial Si–OH terminated siloxanes.

Similar to the hydrosilylation the ring-opening reaction is an addition reaction and therefore forms no byproduct in the curing process. An advantage of siliranes over hydrosilylation is the ability to form siloxane bonds upon ring-opening with silanols, which sustains the motif of the siloxane backbone. As silylene precursors which can be thermally or photochemically activated,<sup>15,23</sup> multifunctional silirane compounds are thereby also suitable crosslinkers for Si–H and Si–OR functionalized siloxanes. In this scenario Si–Si bonds are formed *via* insertion of the transient silylene into the respective functional groups (Scheme 2b). Semenov *et al.* reported an approach which involves photochemically generated, not linker-bound silylenes for crosslinking. This method turned out to be ineffective for bulk crosslinking (low UV-penetration) and generally includes a lot of side-reactions.<sup>24–27</sup>

### Design of silirane crosslinkers

We designed multifunctional silirane-compounds based on Si, O, C, and H to keep the structures as simple as possible and avoid additional heteroatoms, which can deteriorate the rubber properties. For easier feasibility we avoided complex functional groups and favoured the modification of already existing compounds from industry. A facile approach is to exploit the silylene transfer reaction in order to transform



**Scheme 2** (a) Schematic crosslinking reaction of siloxanes with nucleophilic groups (e.g. Si–OH, C–OH) with siliranes *via* ring-opening. (b) Schematic crosslinking of siloxanes with hydrosilane functionalities *via* silylene insertion.

## Green Chemistry

industrial vinyl-compounds into multifunctional silirane-crosslinkers.

This one-step synthesis requires stable monofunctional siliranes like compound **1**, which are transferred to vinyl-groups of a multifunctional substrate. This method allows the simple and convenient synthesis of crosslinkers for byproduct free ring-opening crosslinking.

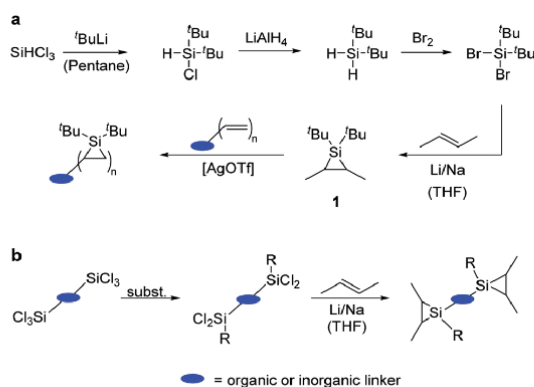
However, thermal degradation of these compounds cleaves off free unlinked silylenes and reforms the multifunctional vinyl-substrates, which are both not capable of insertion-crosslinking. In order to achieve crosslinking *via* silylene insertion as well, it is necessary to link the silicon atoms of the siliranes together (Scheme 3b). These crosslinkers can react *via* both addition and insertion. The synthesis of such structures requires the reduction of multi-dihalosilanes with subsequent trapping of the generated silylenes (Scheme 3b). These precursors can also be synthesized from common industrial building blocks. Hydrosilylation allows an easy addition of trichlorosilane to multifunctional vinyl compounds, introducing the two halogen atoms necessary for reduction and one for easy substitution and reactivity tuning.

Another important consideration is the number of silirane moieties per crosslinker. Crosslinkers for silirane ring-opening need to be at least trifunctional to form nodal points with difunctional siloxanols. Hydride functionalized PDMS is available with a variable amount of Si-H and requires only difunctional siliranes for silylene-insertion crosslinking.

## Results and discussion

## Synthesis of ring-opening crosslinkers 5–10

We were able to synthesize a broad variety of multifunctional silirane compounds (**5–10**, Chart 2) based on the silylene



**Scheme 3** (a) General synthesis pathway of silirane **1** and its utilization for multifunctional silirane ring-opening crosslinkers. (b) General synthesis of universal silirane-crosslinkers for silylene-insertion and ring-opening. The Si-atoms must be linker-bound to enable multifunctional silylenes.

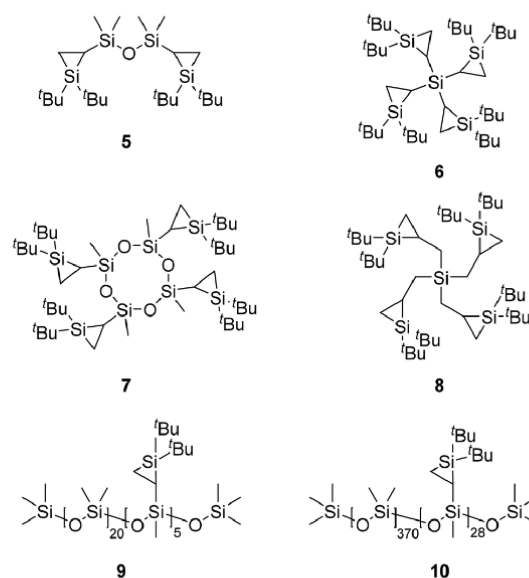


**Chart 2** Synthesized multifunctional siliranes for ring-opening crosslinking.

transfer reaction. This procedure requires stable and simple monofunctional siliranes which can be transferred.

Several “monosiliranes” were synthesized *via* dihalosilane reduction for comparison. Literature known <sup>t</sup>Bu<sub>2</sub>-silirane **1** turned out to be the best compromise between stability and reactivity. Lowering the steric shielding by exchange of one <sup>t</sup>Bu to <sup>s</sup>Bu resulted in unstable siliranes. Liquified 2-butene was used as olefinic trapping agent in the reduction step, since it is cost efficient and easy to remove. High concentrations of up to 40 eq. 2-butene efficiently suppressed side reactions. The most effective reducing agent turned out to be a Li/Na alloy (2.5% Na). Coordinating solvents are essential to this reduction, low concentrations prevent the reaction at all. THF afforded the highest reaction rates combined with little side-reactions. Coordinating solvents with a smaller environmental impact like 2-MeTHF can also be used. Bromides have proven to be good starting materials since they react fast and selective and afforded high yields. Dichlorides required heating and sonication and were often accompanied by side-products. Even though full conversion was achieved (<sup>29</sup>Si-NMR), the overall yield of **1** was lowered by workup loss.

The subsequent silylene transfer was tested with silirane **1** and **11** (DVTMS, divinyltetramethylsiloxane) in various manners. Only the catalytic silylene transfer, as reported by Woerpel *et al.*, reached complete conversion of all substrate vinyl groups. The release of volatile side-product 2-butene from the reaction mixture forces the equilibrium reaction towards the multifunctional product. The best results were obtained using a slight excess of silirane **1** (1.1 eq.) in relation to the number of vinyl groups in the substrate. The reactions were carried out in toluene with AgOTf as catalyst. Reaction

temperatures between 40 and 60 °C allowed fast conversion and eased butene release. Nonetheless we preferred at least 24 h reaction time, since this leads to the precipitation of the catalyst as visible small particles in solution and a precipitate on the glass surface. The catalyst then could easily be removed by filtration over carbon black and dry neutral  $\text{Al}_2\text{O}_3$ . Excess **1** and solvent could be removed in vacuum.

Catalytic silylene transfer enabled the transformation of every tested vinyl compound into multifunctional siliranes. We used tetra vinylsilane, tetra vinyl-tetramethylcyclo-tetrasiloxane and tetraallylsilane as substrates for tetrafunctional siliranes **6**, **7** and **8**, as well as TMS-terminated PDMS (polydimethylsiloxane) with varying chain length and vinyl content for **9** and **10** (statistical distribution). Bissilirane **5** was synthesized as an exemplary model for screenings and is only capable of chain elongation. All synthesized crosslinkers are colourless viscous oils or resins. Under argon siliranes **5–10** endured storage at ambient temperature for a long time and even survived heating to 140 °C for 16 h, if no reaction partner was present.  $^{29}\text{Si}$ -NMR suggests high purities for the purified products and showed new silirane signals in the characteristic range of around  $-50$  ppm. In  $^{19}\text{F}$ -NMR small amounts of fluorine could be detected, possibly due to  $\text{OTf}^-$  adducts. Compounds **6–8** have many diastereomeric forms, caused by the chiral centres at the silirane ring. This can be observed in  $^{29}\text{Si}$ -NMR. In case of crosslinker **8** there are 4 silirane signals which show a 1:3:3:1 distribution. This reflects perfectly the theoretical distribution for all *R,S*-combinations and indicates a non-stereoselective addition of silylene to the double bond. It was possible to crystallize one of the many diastereomers (*R,R,S,S*) of compound **6** from solution. The crystal structure (Fig. 1)

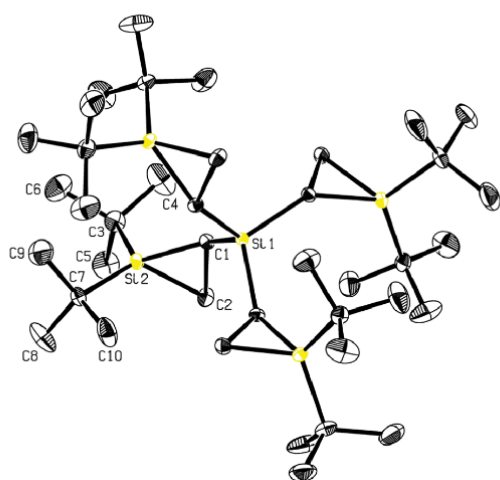


Fig. 1 Molecular structure of **6** in the solid state with ellipsoids set at the 50% probability level. Only one of many diastereomers crystallized from the mixture. For clarity, hydrogen atoms are omitted. For bond length and angles see ESI.†

reveals the surrounding  $t\text{Bu}$ -shielding which leads to the high stability.

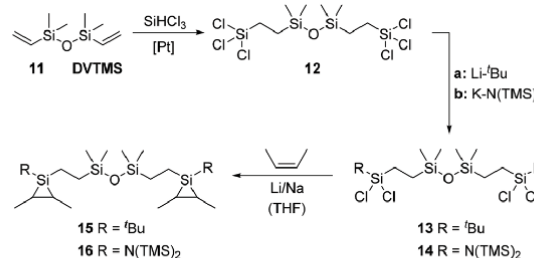
#### Synthesis of insertion crosslinkers **15** & **16**

For demonstrational purposes we chose DVTMS (**11**) as starting material. This allows the synthesis of difunctional siliranes (Scheme 4). The addition of trichlorosilane to **11** by hydrosilylation was performed in high yields and gave the expected chlorosilane-compound **12**. Further modification was feasible by employing *tert*-butyl (**13**) or HMDS (**14**) as substituents and gave the necessary tetrachloro-precursors. Side reactions and oligomerization processes are a great issue in the subsequent reduction step. Best results could be obtained with a Li/Na alloy (2.5% Na) in THF similar to the preparation of silirane **1**. Reducing the solvent concentration while keeping a great excess of olefin (2-butene, 40 eq.) resulted in a significant reduction of side reactions. Although a distinct deceleration of the reaction rate could be observed under these conditions. Bissiliranes **15** and **16** required up to 7 days reaction time. The reduction in alternative polar aprotic solvents like  $\text{Et}_2\text{O}$  or DME resulted in considerably lower yields.

With optimized reaction conditions, oligomerization reactions of butene could not entirely be prevented. We separated the polymeric side product by reversed-phase chromatography, which afforded **15** and **16** in sufficient purity for following crosslinking experiments. NMR-measurements revealed three distinct silirane species originating from silylene addition to also *trans*-butene and 1-butene, which are common impurities. Upon thermal activation (120 °C) all three species effectively cleaved off the incorporated olefin and formed the reactive silylene species. Thus, separation or isolation of the isomeric products was not necessary.

#### Reactivity of mono- and multifunctional siliranes

The required reactivity of siliranes for siloxane crosslinking was tested with silirane **1** and Si-based screening compounds. The screening compounds were chosen to represent all common functional groups from industrial silicones. All screening reactions were performed in benzene solution and products were identified *via* 2D- $^{29}\text{Si}$ - $^1\text{H}$ -NMR spectroscopy. **1** reacted fast and selectively with silanols, alcohols and other nucleophiles as expected *via* ring-opening.  $\text{Ph}_3\text{SiOH}$  reacted already at r.t., sterically demanding alcohols like  $\text{TMS-CH}_2\text{OH}$

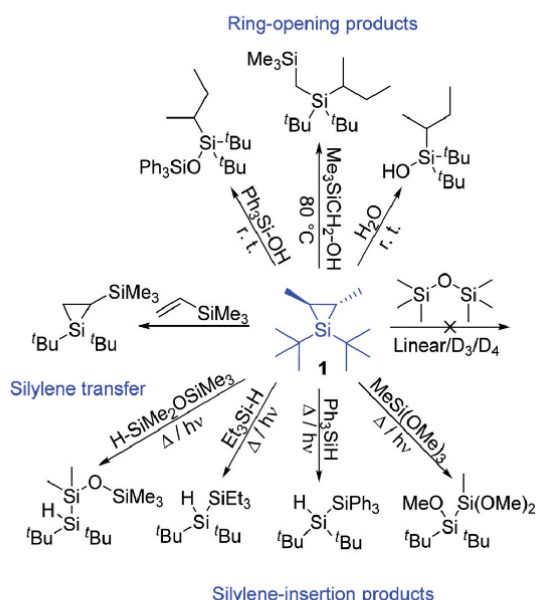


Scheme 4 Synthetic route for bifunctional siliranes **15** and **16**.

and  $t\text{BuOH}$  required heating ( $80\text{ }^\circ\text{C}$ ). In every example  $-\text{OH}$  attacked at the silicon atom of **1**, forming a siloxane bond. Furthermore **1** showed no reactivity towards  $\text{Si-H}$ ,  $\text{Si-OMe}$  and dimethylsiloxanes at  $T < 120\text{ }^\circ\text{C}$ , which is a requirement for the ring-opening concept. Silylene transfer from **1** to substrates like tetramethyl-vinyl-disiloxane or vinyl-trimethylsilane was observed without heating or addition of catalyst. Since this is an equilibrium reaction, it did not reach full conversions. Thermal decomposition of **1** at  $140\text{ }^\circ\text{C}$  generated the reactive  $t\text{Bu}_2$ -silylene which could be efficiently trapped with compounds bearing  $\text{Si-H}$  or  $\text{Si-OMe}$ . The products were identified as the expected insertion-products (Scheme 5). Under these conditions, siliranes showed no reactivity towards PDMS compounds.

Based on reports from Boudjouk and Fink on photolytic silirane cleavage we investigated the potential for photochemical curing.<sup>15,22,23</sup> UV-VIS measurements revealed absorption maxima for siliranes **1**, **6–10**, **15** and **16** in the range of 210–230 nm. UV-Photolysis of **1** at 254 nm in presence of screening compounds gave the expected insertion products (analogously to thermolysis). Due to insufficient absorption this reaction required long irradiation. The requirement for highly energetic UV-C radiation, which is not compatible with siloxanes, disqualifies compounds **6–10**, **15** and **16** for photocrosslinking.

Bissiliranes **15** and **16** were able to insert into  $\text{Si-H}$ ,  $\text{Si-Vinyl}$  and  $\text{Si-OH}$ . Transient silylenes were not observed directly but the existence can be assumed by formation of trapping products and the formation of butene gas. Both compounds were tested with triethylsilane, pentamethyl-disiloxane and



**Scheme 5** Reactivity of  $t\text{Bu}_2$ -silirane **1** with various screening compounds bearing functional groups of common silicone building blocks.

1,1,1,3,5,5,5-heptamethyltrisiloxane as model compounds and yielded the expected disilane products.  $120\text{ }^\circ\text{C}$  turned out to be the minimal temperature for silylene formation. Silirane **15** degraded in air as expected. Fortunately, amide-stabilized silirane **16** turned out to be very stable and withstood storage in air. In contrast to the  $t\text{Bu}$  analogue we observed no ring opening reaction for **16** with  $\text{MeOH}$  or  $\text{Ph}_3\text{SiOH}$ , but the insertion of its bissilylene into  $\text{Si-OH}$ . This reactivity qualifies **16** for insertion crosslinking with siloxanols as well.

#### Monomer preparation

Generally, all siloxanes for crosslinking experiments were degassed and dried to avoid problems with oxygen and water. For vinyl- and hydrosiloxanes the application of high vacuum and heat was sufficient. Carbinol and silanol terminated siloxanes were additionally flashed over dry neutral alumina and  $3\text{ \AA}$  molecular sieve. Even though siloxanols tend to self-condensation, we observed only little chain elongation after drying and 6-month storage under argon and molecular sieve. The effectivity of this drying process was confirmed by successful crosslinking with dried siloxanes. The use of unrefined siloxanes resulted in sticky gels due to silirane quenching.

#### Silirane ring-opening crosslinking

We tested the crosslinking capability of siliranes **5–10** with PDMS of varying length and different nucleophilic functions. We used PDMS with termination of  $\text{Si-OH}$  ( $n \approx 57, 131, 486$ ),  $\text{Si-CH}_2\text{OH}$  ( $n \approx 89, 182$ ),  $\text{Si-C}_3\text{H}_6\text{OH}$  ( $n \approx 11$ ),  $\text{Si-C}_3\text{H}_6\text{NH}_2$  ( $n \approx 16$ ). The respective combination of siloxane and silirane crosslinker was mixed under inert atmosphere until it was homogenous. For highly viscous crosslinkers mixing at elevated temperatures for a short time was necessary. At curing temperatures between  $80\text{--}120\text{ }^\circ\text{C}$  the mixtures solidified after 0.5–4 h. The mixtures were stable at ambient temperatures for a prolonged time. Mixtures which contained remains of AgOTf from silirane-crosslinker synthesis cured at r.t. within 6 weeks and resulted in coloured, turbid elastomers with low crosslinking density (sticky surface, gel-like).

Crosslinkers **7–10** were able to form solid elastomers with every tested siloxane. Silirane **6** turned out to be too unreactive, presumably attributed to its surrounding shielding (Fig. 1). The crosslinked products were generally colourless, clear elastomers. For mixing ratios of 1 : 1–1.8 : 1 (molar ratio of silirane groups to  $-\text{OH}$ ), non-sticky elastomers were obtained – which indicates a fully cured product (stickiness/tackiness is a measure for the crosslinking degree and occurs for polymers with a significant sol fraction<sup>28</sup>). Shore A hardness (ShA) for elastomers made with **7–10** ranged between 1 and 33. This is in the typical range of siloxane elastomers and can be further adjusted by addition of fillers and additives.<sup>29</sup> Curing of  $\text{Si-OH}$  terminated PDMS with polymeric crosslinkers **9** and **10** showed a rising ShA-hardness with rising silirane content. For low silirane content crosslinker **8** the highest ShA was achieved with a 1 : 1 mixing ratio – higher silirane contents made it softer. We assume that this behaviour is caused by the formation of lesser valency nodal points when **8** is used in excess

(less crosslinks cause softer polymers). Curing in air was tested at 110 °C for crosslinkers 6–10 but gave an unusable sticky glue-like gel in every case.

We further investigated the curing process in a rheometer with compounds 8 and 9 as representatives for star-shaped and linear polymeric crosslinkers. The experiments were conducted with Si–OH terminated PDMS ( $n \approx 131$ ) and varying silirane contents (Fig. 2, N<sub>2</sub>-atmosphere, 110 °C). Oscillation rheology monitors the complex viscosity, which describes viscoelastic properties of the material and the degree of curing progression, as well as elastic modulus  $G'$  and loss modulus  $G''$ . Completion of curing was assumed when the viscosity reached a plateau and required roughly 10–24 h. We found that crosslinkers 8 and 9 differed strongly in terms of curing duration, elastic properties and end-viscosity. In experiments containing compound 9, it took 50–80 min for the mixture to solidify and 90–110 min for compound 8 (solidification at  $G' = G''$ ).<sup>30</sup> However, the overall time for a full cure was generally shorter for crosslinker 8. We assume that polymeric crosslinker 9 reacts faster in the beginning due to lower steric hindrance compared to 8 but requires longer overall reaction times owing to a hindered accessibility of the last remaining

silirane groups. Dissipation factor  $\tan(\delta)$  can be used for judgement of the elastomeric properties. After maximum conversion (steady viscosity) elastomers with crosslinker 9 reached  $\tan(\delta)$  values as low as 0.002 already at a 1 : 1 mixing ratio. Increasing silirane-contents had no adverse effects on the results and indicate a high ring-opening efficiency and high crosslinking density. For crosslinker 8 the optimum (0.005) was reached at a 1.5 mixing ratio. This can presumably be attributed to a high steric crowding at the crosslinker for triple nodal points which impedes another addition of Si–OH. The slight marching of viscosity (Fig. 2b) hints towards this behaviour. The idle, poorly accessible silirane groups must therefore be compensated by a higher silirane concentration to achieve full curing. In general, the low dissipation factors reflect almost ideal elastic properties and suggest high conversions.<sup>30</sup>

### Silylene insertion crosslinking

Bissilirananes 15 and 16 were tested for their crosslinking ability with hydride functionalized PDMS 17 ( $M_n \approx 2.4 \text{ kg mol}^{-1}$ , 29% Si–H) and 18 (55 kg mol<sup>-1</sup>, 0.8% Si–H) with lateral Si–H groups (Chart 3). Mixtures of varying functional group ratios were tested at a curing temperature of 140 °C. The crosslinking degree of crosslinked elastomers was evaluated by swelling measurements in toluene. The conducted crosslinking experiments were successful for all tested hydrosiloxanes and yielded, depending on the conditions, soft gels, firm elastomers or brittle solids.

Crosslinking PDMS 18 with 15 in equimolar ratio of silirane to hydride, the gel fraction reached a value of 0.73. Excess use of crosslinker 15 (up to 5×) resulted in brittle polymers with gel fractions greater than 0.97 and shore A0 hardness up to 80. The low hydride concentration (0.8%) of the used PDMS monomer 18 offers only few moieties for the silylene intermediate to interact. Thus, these short-lived silylenes are less likely to crosslink the respective polymer chains before deactivation. Low molecular weight hydro-PDMS 17 (29% Si–H) yielded hard elastomers at the same curing conditions already in under-stoichiometric silirane amounts. Ratios from 0.5 to 1 resulted in gel fractions of 0.85 to 0.98 with shore A0 hardness greater than 60, demonstrating the dependence of crosslinking efficiency on the functional group density and chain length. Generally, the high gel fraction values (up to 0.98) imply that all PDMS monomers are successfully crosslinked.

In addition to hydrosiloxanes we tested industrial difunctional silanol-terminated PDMS 19 ( $M_n \approx 9.8 \text{ kg mol}^{-1}$ ) and 20 (36 kg mol<sup>-1</sup>). Various polymerizations with 15 or 16 in varying crosslinker to Si–OH ratios were performed. Curing reactions with 15 did not result in silicone elastomers in any tested ratio (0.5–2). According to the previous screenings, 15

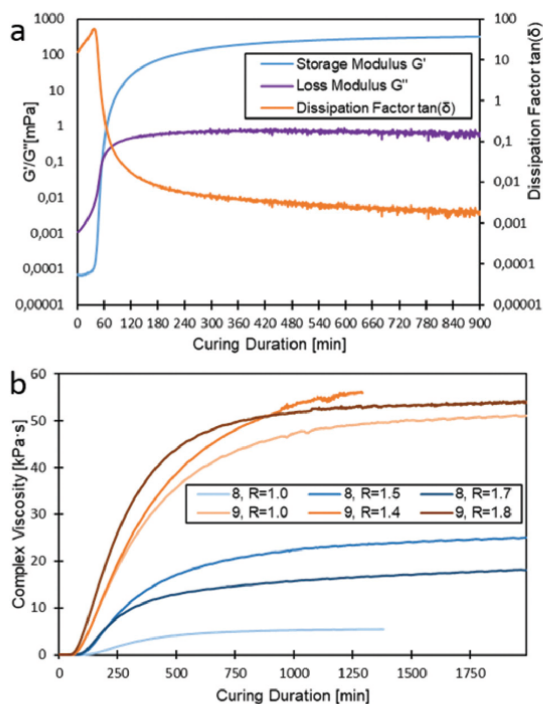


Fig. 2 (a) Exemplary curing curves of crosslinker 9 with Si–OH terminated PDMS ( $n \approx 131$ ) at 110 °C, mixing ratio  $R = 1.4$ . Storage- and loss modulus [kPa] vs. time and the resulting dissipation factor  $\tan(\delta)$  ( $f = 1$  Hz, gradually decreasing amplitude). (b) Complex viscosity of crosslinkers 8 and 9 measured by oscillatory rheology ( $f = 1$  Hz, gradually decreasing amplitude). Curing was conducted at 110 °C with PDMS (Si–OH terminated,  $n \approx 131$ ) under nitrogen. The molar ratio  $R$  describes the ratio of silirane to silanol groups.

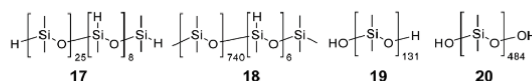


Chart 3 Tested PDMS prepolymers for silylene-insertion crosslinking.

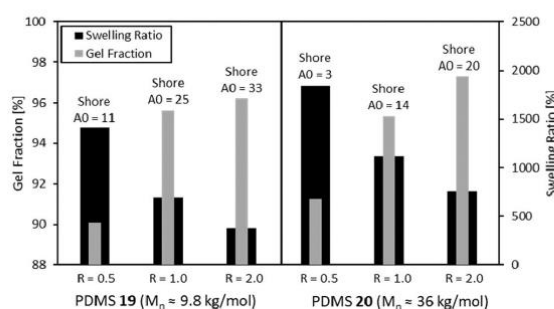


Fig. 3 Swelling ratio  $S = (W_{\text{swollen}} - W_{\text{dried}})/W_{\text{dried}}$ , gel fraction and shore A0 hardness measurements of crosslinked OH-terminated PDMS 19 and 20 with silylene crosslinker 16 in various silirane to Si–OH mixing ratios R.

did most likely undergo the expected ring opening reaction. Due to the bifunctional nature of hydroxy functionalized PDMS, only chain elongation is possible. The chain elongation was observed in rheologic measurements in terms of a slight rise in viscosity. Bissilirane 16, which did not undergo ring-opening reactions with hydroxides in screenings, generated clear, colourless elastomers. Silirane to Si–OH ratios from 0.5–2 resulted in soft elastomers with a Shore A0 hardness ranging from 11–33 (19) and 3–20 (20).

Increasing silirane content resulted in a higher crosslinking density, manifested by a higher rigidity and dropping swelling ratios S. High gel fraction values of over 90% were measured for elastomers consisting of 19/20 and 16, suggesting that most prepolymer was crosslinked (Fig. 3). The absence of stickiness strengthens this indication and rules out solidification by chain elongation.

These findings suggest that crosslinker 16 unexpectedly undergoes a different reaction path than 15, which allows the formation of crosslinked siloxane networks. Based on the polymerization and screening results, we act on the assumption that the transient silylenes insert into the terminal Si–OH and consequently form a hydrosilane as conjunctive group. These hydrosilanes can further be attacked by another silylene *via* insertion, thus forming a trifunctional nodal point. Since the result of a silylene insertion into hydrosilanes is always another hydrosilane, a network-forming consecutive multi-step reaction is possible (Fig. 4a).

The curing process of Si–OH terminated PDMS with crosslinker 16 was further monitored with rheological measurements to verify and evaluate the crosslinking behaviour (silirane/Si–OH = 2, Fig. 4b and c). Heating the polymer mixture to 75 °C for 4 hours did not result in any measurable increase of viscosity, thus no crosslinking or chain elongation occurred. At 125 °C the crosslinking reaction started instantly with a high reaction rate, reaching liquid–solid transition ( $\tan(\delta) = 1$ ) already after 10 min at 138 °C (Fig. 4c). Additional curing for 60 min at 140 °C yielded the final elastomer.

The high storage modulus and low dissipation factor clearly prove successful silylene insertion with bifunctional hydroxy-

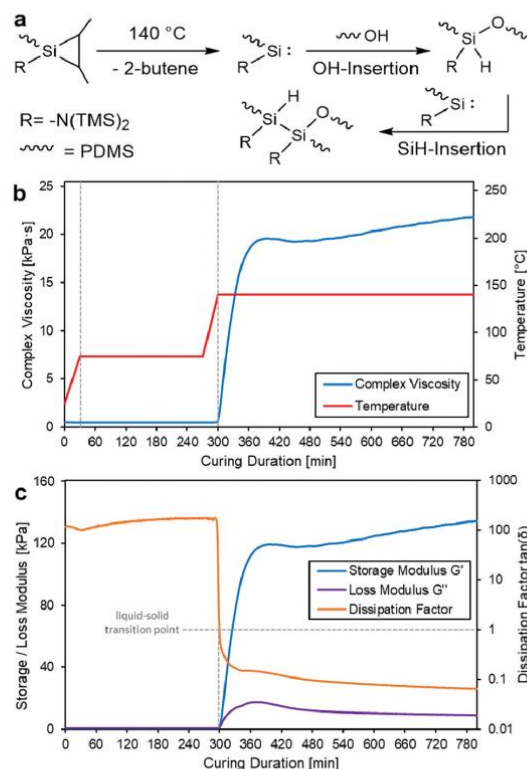


Fig. 4 (a) Possible crosslinking reaction of difunctional crosslinker 16 with hydroxy terminated PDMS-chains by the proposed multi-step insertion mechanism. (b) Dynamic viscosity curves ( $f = 1$  Hz, gradually decreasing amplitude) during curing for crosslinker 16 with PDMS 19 in a silirane to Si–OH ratio of 2. (c) Storage- and loss modulus vs. time and the resulting dissipation factor  $\tan(\delta)$  for the same curing reaction.

PDMS in a network forming manner and rule out simple ring-opening. Furthermore, crosslinking experiments with air-stable bissilirane 16 and hydro-PDMS 17 at 140 °C gave a positive result in air, yielding colourless non-sticky elastomers. The polymers made with crosslinker 16 were hydrolytically stable and could be stored in air for several months.

## Conclusion

Herein we demonstrated that the crosslinking concepts based on multifunctional siliranes serve as a catalyst-free alternative to the established PDMS crosslinking methods. Multifunctional silirane crosslinkers were successfully obtained in few synthetic steps by modification of standard industrial compounds. Investigation of silirane reactivity with small model compounds and industrial PDMS building blocks provide evidence for the high efficiency of both silirane ring-opening and silylene insertion crosslinking. The mechanical properties of the elastomers can be controlled by the mixing-ratio and the nature of the crosslinker. The crosslinked poly-



mers contained no reinforcing additives and fillers but already exhibited good elastic characteristics. Ring-opening curing with compounds 7–10 covers conventional Si–OH terminated siloxanes and features byproduct-free thermal crosslinking. The total absence of byproducts or catalysts enables the production of clean silicone elastomers – free of extractables and unrecoverable precious metals. Especially the elastomers which are crosslinked *via* ring-opening could be beneficial for medical purposes and in the electronics industry. Additionally, siliranes are suitable for crosslinking of *e.g.* hydride functionalized silicones *via* a silylene insertion reaction. Novel bifunctional siliranes (15, 16) have proven to be a reliable silylene source for this purpose and provide the required reactivity. To our knowledge this is the first application that utilizes transient silylenes in applied chemistry. The lability of exemplary silirane crosslinkers (5–10, 15) towards O<sub>2</sub> and H<sub>2</sub>O required storage and application under inert gas – just as most unvulcanised industrial siloxane systems.<sup>29</sup> Bissilirane 16 however exhibited high stability and even enabled effective curing in the presence of air. This result demonstrates that the stability of siliranes can be tailored by thermodynamic and kinetic stabilization without the loss of their diverse reactivity. It was proven that siliranes are a very versatile and suitable basis for reactions with all common functional groups in silicone chemistry. Our structures are exemplary compounds that require further optimization in terms of synthesis, air-stability and reaction rates. Especially the reduction of halosilanes with alkali metals must be considerably improved in order to make the entire process environmentally friendlier. A possible solution to increase the atomic efficiency and to cut out problematic chemicals could be the electrochemical synthesis of siliranes.

Nevertheless, it is shown that multifunctional siliranes are a serious alternative to conventional crosslinking methods with several advantages. With regard to the increasing global consumption and the limited availability of rare noble metals (*e.g.* Pt), alternative concepts like silirane crosslinking could become useful for saving resources. A major advantage over the conventional Pt-catalysed hydrosilylation is also the possibility of storage as a readily mixed one-component system. This feature gives the user more latitude, since it makes pot-times obsolete. The easy accessibility of multifunctional siliranes by modification of existing industrial compounds makes the concept economically and ecologically worthwhile.

## Experimental

Further details of used materials, experimental procedures, measurements techniques and analytical data are given in the ESI.†

### General synthesis for multifunctional siliranes 5–10

2.80 mmol (1.00 eq.) of the respective vinyl-functionalized reagent and  $x \cdot 1.20$  eq. silirane 1 were mixed with 5 mL toluene in a 20 mL Schlenk-tube ( $x$  = number of vinyl-moieties at the

reagent). While stirring 1 mg (4.01  $\mu$ mol, 0.0014 eq.) AgOTf was added to the reaction. The mixture was heated up to 60 °C and stirred for 16 h. Emerging butene gas was released over a relief valve. Full conversion was verified by <sup>1</sup>H-NMR (absence of vinyl-H). The solvent and remaining 1 were removed by high vacuum (60 °C, 10<sup>-5</sup> mbar) from the product. Separation of the catalyst was carried out by diluting the crude product in 5 mL pentane and subsequent filtration over an appropriate amount of aluminium oxide (Al<sub>2</sub>O<sub>3</sub>). The aluminium oxide was further washed with 2 mL pentane. At last the solvent was removed *in vacuo* to obtain the silirane crosslinkers as colourless viscous fluids.

### General synthesis for bifunctional silylene-crosslinkers 15–16

A 250 mL high-pressure Schlenk-tube with a PTFE sealed screw cap was equipped with a PTFE-coated stir bar and was loaded with 20.0 mmol (1.00 eq.) of the dichloro-silane reagent. 50 mL THF and 20 mg (0.09 mmol, 0.001 eq.) 3,5-di-*tert*-butyl-4-hydroxytoluene (BHT). The reaction tube was cooled down to –78 °C with a dry ice/isopropanol mixture. Present argon atmosphere was removed *in vacuo* and 33.6 g (600 mmol, 30.0 eq.) *cis*-2-butene was condensed into the cooled reaction mixture by pressurizing it with 1.80 bar of the respective gas. After re-pressurizing with argon, 2.10 g (300 mmol, 15.0 eq.) Li/Na alloy chunks (2.5% Na) were added to the reaction mixture, followed by vigorous stirring at room temperature for 7 days. By the end of the reduction, *cis*-2-butene gas and remaining solvent was removed under vacuum. The crude slurry was diluted in 50 mL pentane to precipitate and separated the generated lithium chloride by filtration. The product was collected by removing the remaining solvent *in vacuo* to afford the silylene-crosslinker.

### Monomer preparation

Generally, all siloxanes for crosslinking experiments were degassed and dried to avoid problems with oxygen and water. For vinyl- and hydrosiloxanes the application of high vacuum and heat was sufficient. Carbinol and silanol terminated siloxanes were additionally flashed over dry neutral alumina and 3 Å molecular sieve. Even though siloxanols tend to self-condensation, we observed only little chain elongation after drying and 6-month storage under argon and molecular sieve. The effectivity of this drying process was confirmed by successful crosslinking with dried siloxanes. The use of unrefined siloxanes resulted in sticky gels due to silirane quenching.  $M_w$  was determined by <sup>1</sup>H- and <sup>29</sup>Si-NMR. For length determination of Si–OH terminated PDMS we used an adapted TAI (trichloroacetyl isocyanate) method; for reference terminal Me groups are integrated.<sup>31</sup>

### Ring-opening crosslinking procedure

Ring-opening crosslinking was tested with dried and degassed PDMS (Si–OH terminated of  $M_n$  = 9.8 or 36 kg mol<sup>-1</sup>). The respective crosslinker (6–10) was mixed with PDMS in a 0.7 to 2.0 ratio (silirane to –OH ratio). After vigorous stirring with a PTFE-coated magnetic stirring bar the homogeneous reaction

mixture was heated up to 110 °C for 24 h under a protective argon atmosphere. The resulting networks were non-sticky, clear and colourless elastomers.

#### Preparation of PDMS elastomers with silylene-crosslinkers

Dried and degassed hydromethyl-PDMS of  $M_n = 2.4$  to 55 kg mol<sup>-1</sup> or hydroxy-terminated PDMS of  $M_n = 9.7$  to 36 kg mol<sup>-1</sup> was mixed with the respective silylene-crosslinker (15, 16) such that silylene to PDMS functional moiety (Si-H or Si-OH) ratio was 0.5 to 3.3. The mixture was diluted in 5 mL pentane to obtain a homogeneous mixture and stirred vigorously with a PTFE-coated magnetic stirring bar. The solvent was subsequently removed under vacuum. The mixture was activated by heating to 140 °C for 24 h under a protective argon atmosphere. The curing process was performed in an open vial to prevent internal pressure build-up by the release of butene-gas. The resulting elastomers were cloudy to clear polymers with small defects of gas enclosure as a result of the gas formation.

#### Conflicts of interest

The authors declare the following conflicts of interest: two patent applications were filed, covering the methods in this paper.

#### Acknowledgements

We acknowledge our principal funding source for this work, the WACKER Chemie AG. Dr E. Fritz-Langhals, Dr Maximilian Moxter and Dr Niklas Wienkenhöver are acknowledged for helpful discussions and advice. We also thank Belinda Dombret and Peter Winter for rheological measurements.

#### Notes and references

- M. A. Brook, *Silicon in Organic, Organometallic, and Polymer Chemistry*, Wiley & Sons Ltd, New York, 1999.
- N. R. Council, *The Role of the Chemical Sciences in Finding Alternatives to Critical Resources: A Workshop Summary*, The National Academies Press, Washington, DC, 2012.
- I. E. Markó, S. Stérin, O. Buisine, G. Mignani, P. Branlard, B. Tinant and J.-P. Declercq, *Science*, 2002, **298**, 204.
- P. Jutzi, D. Kanne and C. Krüger, *Angew. Chem., Int. Ed. Engl.*, 1986, **25**, 164–164.
- M. Fèvre, J. Pinaud, Y. Gnanou, J. Vignolle and D. Taton, *Chem. Soc. Rev.*, 2013, **42**, 2142–2172.
- D. Wendel, A. Porzelt, F. A. D. Herz, D. Sarkar, C. Jandl, S. Inoue and B. Rieger, *J. Am. Chem. Soc.*, 2017, **139**, 8134–8137.
- D. Wendel, W. Eisenreich, C. Jandl, A. Pöthig and B. Rieger, *Organometallics*, 2016, **35**, 1–4.
- D. Wendel, T. Szilvási, C. Jandl, S. Inoue and B. Rieger, *J. Am. Chem. Soc.*, 2017, **139**, 9156–9159.
- D. Wendel, T. Szilvási, D. Henschel, P. J. Altmann, C. Jandl, S. Inoue and B. Rieger, *Angew. Chem., Int. Ed.*, 2018, **57**, 14575–14579.
- I. Safarik, V. Sandhu, E. M. Lown, O. P. Strausz and T. N. Bell, *Res. Chem. Intermed.*, 1990, **14**, 105–131.
- V. Y. Lee, *Organosilicon Compounds*, Academic Press, Cambridge (Massachusetts), 2017.
- J. Ping, F. Gao, J. L. Chen, R. D. Webster and T. W. J. Steele, *Nat. Commun.*, 2015, **6**, 8050.
- D. H. Pae, M. Xiao, M. Y. Chiang and P. P. Gaspar, *J. Am. Chem. Soc.*, 1991, **113**, 1281–1288.
- K. R. Pichaandi, J. T. Mague and M. J. Fink, *J. Organomet. Chem.*, 2011, **696**, 1957–1963.
- P. Boudjouk, U. Samaraweera, R. Sooriyakumaran, J. Chrusciel and K. R. Anderson, *Angew. Chem.*, 1988, **100**, 1406–1407.
- D. Wendel, D. Reiter, A. Porzelt, P. J. Altmann, S. Inoue and B. Rieger, *J. Am. Chem. Soc.*, 2017, **139**, 17193–17198.
- T. G. Driver and K. A. Woerpel, *J. Am. Chem. Soc.*, 2003, **125**, 10659–10663.
- T. G. Driver and K. A. Woerpel, *J. Am. Chem. Soc.*, 2004, **126**, 9993–10002.
- J. Ćiraković, T. G. Driver and K. A. Woerpel, *J. Am. Chem. Soc.*, 2002, **124**, 9370–9371.
- T. G. Driver, in *Silver in Organic Chemistry*, ed. M. Harmata, John Wiley & Sons, Hoboken, 2010, ch. 7, pp. 183–227.
- D. Seyferth, *J. Organomet. Chem.*, 1975, **100**, 237–256.
- P. Boudjouk, U. Samaraweera, R. Sooriyakumaran, J. Chrusciel and K. R. Anderson, *Angew. Chem., Int. Ed. Engl.*, 1988, **27**, 1355–1356.
- K. R. Pichaandi, J. T. Mague and M. J. Fink, *J. Organomet. Chem.*, 2015, **791**, 163–168.
- V. V. Semenov and N. F. Cherepennikova, *Dokl. Akad. Nauk SSSR*, 1989, **309**, 119–122.
- V. V. Semenov, N. F. Cherepennikova, S. B. Artemicheva and G. A. Razuvaev, *Appl. Organomet. Chem.*, 1990, **4**, 163–172.
- V. V. Semenov, E. Y. Ladilina, N. F. Cherepennikova and T. A. Chesnokova, *Russ. J. Appl. Chem.*, 2002, **75**, 127–134.
- V. V. Semenov, *Russ. Chem. Rev.*, 2011, **80**, 313–339.
- M. Mikrut, A. Wilk, J. W. M. Noordermeer and G. Verbeek, *J. Adhes.*, 2009, **85**, 395–412.
- W. Noll, *Chemistry and Technology of Silicones*, Academic Press Inc., London, 1968.
- T. G. Mezger, *The Rheology Handbook*, Vincentz Network, Hannover, 2014, 4th edn.
- A. R. Donovan and G. Moad, *Polymer*, 2005, **46**, 5005–5011.

## 5. Modular silacyclopropenes: synthesis and application

### 5.1. Bibliographic data

Title: “Modular silacyclopropenes: synthesis and application for Si–H containing substrate functionalization”<sup>[272]</sup>

Status: Communication, Publication Date: 09.09.2022

Journal: Chemical Communications

Publisher: Royal Society of Chemistry (RSC)

DOI: 10.1039/D2CC04565F

Authors: **Matthias Nobis**, Shigeyoshi Inoue, Bernhard Rieger ‡

### 5.2. Abstract graphic (TOC)

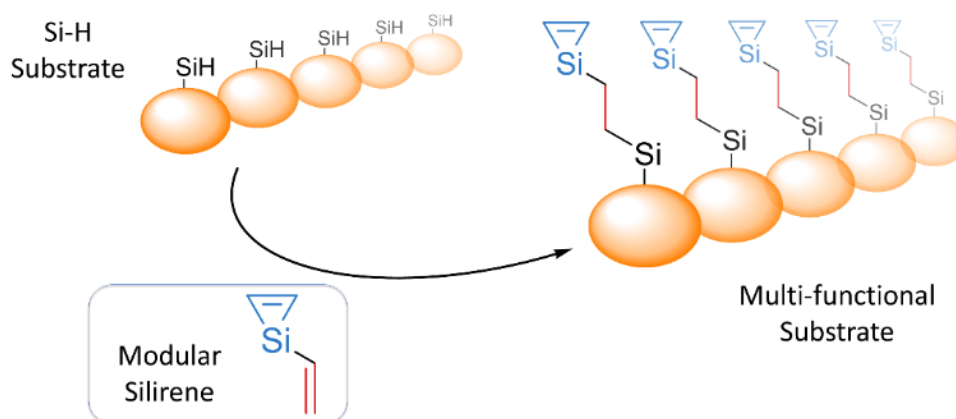


**Figure 17.** Table of content for the manuscript titled “Modular silacyclopropenes: synthesis and application for Si–H containing substrate functionalization”

---

‡M. Nobis provided the original idea, planned, and executed all experiments, performed the data analysis, and prepared the manuscript. All work was performed under the supervision of B. Rieger and S. Inoue.

### 5.3. Content

Silacyclopropenes are known since the early 1970s and can be considered as stable precursors for transient silylenes. To this day, applications of these compounds remain scarce beyond the world of organosilicon chemistry. Disadvantages are their complex synthetic accessibility and their limitation as monofunctional compounds. Consequently, there is no particular use for silacyclopropenes in other academic or industrial fields at the moment. To address these challenges, a novel concept of “modular” silacyclopropenes as building blocks was reported which can simply be attached to various Si-H containing substrates. A facile synthetic access for these modular compounds was described to create a variety of different substrates, ranging from small molecules to siloxane polymers. This way introduction of multifunctional silacyclopropenes will be feasible without synthetic complications since the coupling reaction is performed via hydrosilylation reaction with common and widely applied catalysts. The described method renders the class of silacyclopropenes applicable for various fields including surface or nanomaterial modification as well as a source for multifunctional transient silylenes. These findings demonstrate the first creation of higher-functional silacyclopropenes and hence could enable this compound class for a broad spectrum of applications. In the context of the superior purpose of this thesis to develop new and alternative curing concepts for silicone rubbers, the synthesis of higher multifunctional silirene compounds was a key prerequisite to facilitate the creation of silirene based linker scaffolds. The complex synthesis of this compound class prohibited the generation of higher functional scaffolds via the established synthesis procedures. The reduced reactivity and stability with an increasing number of silirene-moieties per linker molecule results in longer reaction times and higher ratios of side reactions. The introduction of the modular silirenes provides a facile synthesis procedure by creating the silacyclopropene moiety in the beginning as a monofunctional unite, thus eliminating the prior described disadvantages. This reactive silirene unit can then be grafted on a hydroxy functionalized PDMS to afford the desired polymeric linker structure. The presented technique could be applied for a diverse introduction of silacyclopropenes on different types of substrates or surfaces, extending towards other fields of application than just PDMS crosslinking.

## 5.4. Manuscript

ChemComm



COMMUNICATION

View Article Online  
View Journal | View IssueCite this: *Chem. Commun.*, 2022, 58, 11159Received 16th August 2022,  
Accepted 8th September 2022

DOI: 10.1039/d2cc04565f

rsc.li/chemcomm

## Modular silacyclopropenes: synthesis and application for Si–H containing substrate functionalization†

Matthias Nobis,<sup>ab</sup> Shigeyoshi Inoue<sup>ib</sup> and Bernhard Rieger<sup>ib</sup>\*<sup>ab</sup>

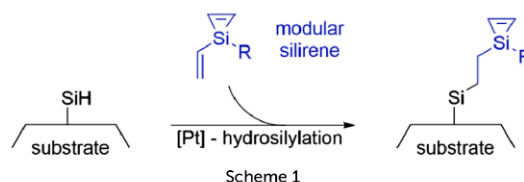
A method to functionalize Si–H containing substrates with vinyl substituted silacyclopropenes has been developed. This provides an efficient and versatile technique to generate multi-functional silacyclopropene derivatives, ranging from small molecules to polymeric materials like polysiloxanes. Thus, access is given to a new class of functionalized materials that exhibits potential in a variety of possible applications.

Since the 1970s silacyclopropenes (silirenes) have gained considerable attention in organosilicon chemistry.<sup>1–3</sup> These three-membered silicon heterocycles are considered as stable sources for highly reactive transient silylenes. The thermal<sup>4,5</sup> and photochemical<sup>4,6</sup> reactivity of silirenes allows the *in situ* generation of silylenes and their use in classical inorganic chemistry. However, they could even enable possible applications in various fields like polymer, surface, or nano-material chemistry. The first report of a silirene is given by Colin and Gaspar in 1976,<sup>7</sup> where they obtained tetramethyl-silacyclopropene by reacting dimethoxy-tetramethyldisilane with 2-butyne in a gas phase pyrolysis. In the same year Seyferth *et al.* succeeded in synthesizing a thermally stable silacyclopropene from the reaction of hexamethylsilacyclopropane with bis(trimethylsilyl)-acetylene.<sup>8</sup> There are various approaches to synthesize silacyclopropenes, most of them involve the addition of a silylene to alkynes,<sup>7–10</sup> or the photolysis of the respective ethynyl-disilane derivatives.<sup>10,11</sup> However, most of these compounds are designed as mono-functional silirenes and share relatively challenging synthesis routes. Hence, the development of effective strategies to generate multi-functional silirene derivatives is crucial to establish possible applications for silacyclopropenes.

In this work, we describe a method to utilize simple silacyclopropenes as “building blocks” which can be used to

functionalize respective Si–H containing substrates in a coupling reaction (Scheme 1). Specific molecular design must be considered to enable these modular silirenes for the hydrosilylation reaction, a reaction which is well known and widely used in industry or academia.<sup>12</sup> Taking advantage of the relatively simple synthesis of these modular silirenes, one can attach these building blocks to a variety of materials. This way, complex and demanding syntheses can be avoided, and a broad application scope can be achieved. Crucial for the hydrosilylation reaction with an Si–H substrate is the introduction of an unsaturated moiety at the silirene. At the same time the silirene must receive sufficient stabilisation by its second substituent R to withstand the conditions of the subsequent hydrosilylation reaction.

With these conditions in mind, we designed silirenes 4–6 starting from the basic organosilicon compound trichlorovinylsilane (Scheme 2). Implementation of hexamethyl-disilazane  $-N(TMS)_2$  as substituent was performed by the addition of potassium bis(trimethylsilyl)amide (KHMDS) in THF. The stabilizing effects of the silazane moiety as a  $\pi$ -donor and its steric protection were essential for the synthesis of silacyclopropanes 2 and 3. Substitution with  $-N(iPr)_2$ ,  $-Ph$  (less steric demanding), or  $-tBu$  (no  $\pi$ -donating effect) could be realized as well. However, the respective derivatives did not form any silacyclopropanes and emphasize the requirement of a suitable substituent for further reactions. For the subsequent generation of silacyclopropane 2 and 3, we converted corresponding dichlorosilane 1 with lithium and 2-butene or cyclohexene respectively. Best results could be obtained with a lithium/

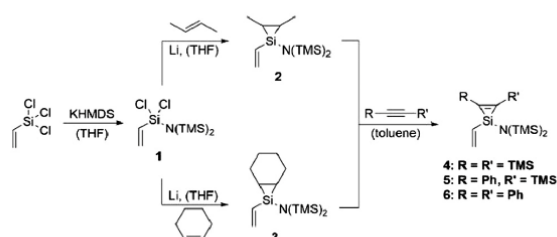


<sup>a</sup> Technical University of Munich, WACKER-Chair of Macromolecular Chemistry  
Lichtenbergstraße 4, 85748, Garching bei München, Germany.  
E-mail: rieger@tum.de

<sup>b</sup> Technical University of Munich, WACKER-Institute of Silicon Chemistry  
Lichtenbergstraße 4, 85748, Garching bei München, Germany

† Electronic supplementary information (ESI) available. See DOI: <https://doi.org/10.1039/d2cc04565f>

## Communication

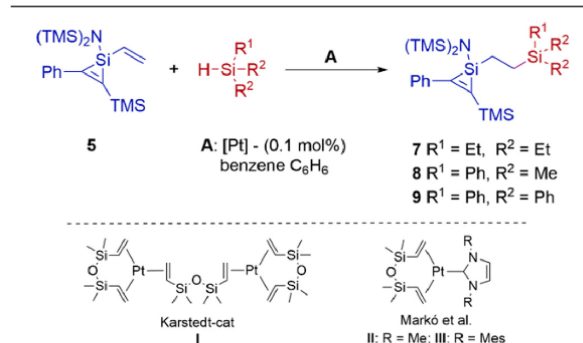


Scheme 2 Synthetic pathway for silacyclopropenes **4**, **5** and **6** via the conversion of silacyclopropanes **2** and **3** in a silylene-transfer reaction.

sodium alloy (2.5 wt% Na) as reducing agent in THF and high ratios (up to 30 eq.) of the respective olefin. Due to higher yields as well as a simpler purification procedure, we preferred the creation of silacyclopropane **2** and its utilization for the final synthesis step. Here, we transformed the silacyclopropane into the desired silacyclopropene *via* a silylene-transfer reaction. This type of reaction can either be thermally induced<sup>13</sup> or mediated by various metal catalysts based on Cu, Ag or Pd.<sup>14</sup> The silylene-transfer was conducted with bis(trimethylsilyl)-acetylene, 1-phenyl-2-trimethylsilyl-acetylene and diphenyl-acetylene and resulted in the formation of silacyclopropenes **4**, **5** and **6** respectively. It could be observed that with increasing number of phenyl groups the thermal stability of the silirene ring system increases. Thus, **4** renders the least stable silirene, which starts to decompose at 110 °C, while **5** withstands temperatures of 140 °C. Silirene **6** could even be heated up to 180 °C without any observable decomposition. Because of this lability silirene **4** was synthesized under milder conditions *via* the catalytic pathway using AgOTf. Meanwhile **5** and **6** could readily be obtained without any catalyst *via* the thermally induced synthesis route. This way we have three silacyclopropenes at hand, which meet our initial criteria as modular silacyclopropenes for the subsequent function-alization reaction.

At the beginning, we examined the capability of our modular silirene **5** to be hydrosilylated with triethylsilane, dimethylphenylsilane, and triphenylsilane as model compounds. As illustrated in Table 1, hydrosilylation with a selected variety of catalysts (**I–IV**) lead to the desired functionalized products **7–9**. In general, best results could be obtained at elevated temperatures (65 °C). However, increasing the reaction temperature over 100 °C resulted in the destruction of the silacyclopropene moiety. Among the applied catalysts, the well-known Karstedt catalyst<sup>15</sup> **I** proved to be the most active one. Two other Pt(0)-carbene complexes **II** and **III**, reported by Markó *et al.*<sup>16</sup> exhibited a slightly lower activity compared to **I**. In general, catalyst loadings higher than 4 mol% resulted in a decreased ratio of product formation, while we observed the depletion of the silirene moiety. Generation of the respective acetylene and various new signals in the TMS-region support this assumption of decomposition. Because of this lability we tried to reduce the catalyst loading to minimize the destruction of the silirene moiety in the process. In summary, the hydrosilylation reaction can be performed by well-established Pt(0)-catalysts that are commonly employed in industry and research.<sup>17</sup> The reaction progress of the hydrosilylation reaction can be monitored

Table 1 Catalysed hydrosilylation of modular silirene **5** with different silanes



Entry	[Catalyst]	Temp. [°C]	Yield <sup>a</sup> [%]	
			7/8/9	
1	<b>I</b> (Karstedt)	25	52/55/40	
2	<b>I</b> (Karstedt)	65	70/83/79	
3	<b>II</b> (Markó)	65	71/82/80	
4	<b>III</b> (Markó)	65	68/79/72	

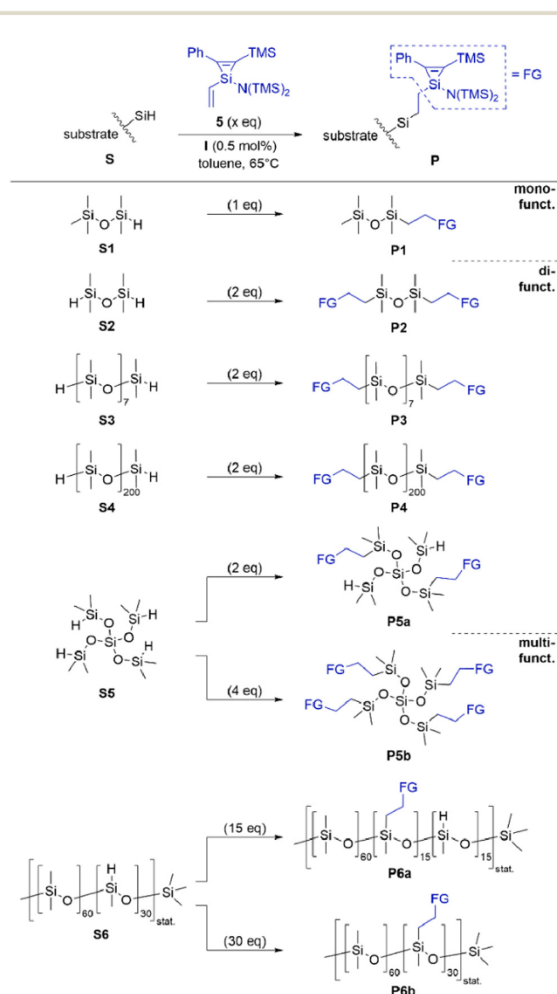
<sup>a</sup> Isolated yields were determined after reaction finalization (full depletion of modular silirene **5**) and additional vacuum distillation.

by NMR-spectroscopy with ease. In the <sup>1</sup>H-NMR spectrum in the case of triethylsilane, one can see the depletion of the Si-H signal at 3.88 ppm as well as the signals of the vinyl moiety from 6.00 to 6.14 ppm, while the proton signals for the newly formed ethyl-bridge emerge at 1.10 and 1.27 ppm (Fig. S15 and S22 in ESI<sup>†</sup>). In the <sup>29</sup>Si-NMR a downfield shift for the silicon-signal of the ring-system from -97.5 ppm to -81.0 ppm is observed. Likely, the conversion of the vinyl- to an ethyl-moiety creates a decrease of electron-density at the silicon-atom hence resulting in the observed deshielding effect (Fig. S17 and S24 in ESI<sup>†</sup>). Comparable results could be observed for the hydrosilylation reaction of silirene **5** with dimethylphenylsilane and triphenylsilane respectively. The chemical shift of the hereby formed silirenes in the <sup>29</sup>Si-NMR can be found at -81.1 ppm for Me<sub>2</sub>PhSiH and -81.2 ppm for Ph<sub>3</sub>SiH respectively (Fig. S29 and S32, ESI<sup>†</sup>). This way, both aliphatic as well as aromatic silanes were applicable for the coupling reaction with modular silirene **5**. In comparison with these three model compounds, the reaction of dimethylphenylsilane resulted in the highest yield of 83%, after the product was isolation *via* vacuum distillation. The hydrosilylation reaction of silirene **6** with triethylsilane could be realized as well by employing Karstedt catalyst **I** at 65 °C. After a reaction time of 3 h full conversion of **6** yielded in the respective modification of triethylsilane. In the <sup>29</sup>Si-NMR, the change of chemical shift from -96.2 ppm to -79.4 ppm for the silirene group indicates the successful coupling reaction. No destruction of the sensitive silacyclopropene functionality under the described catalytic conditions could be noticed for silirenes **5** and **6**, providing the required stability for further substrate modification. In contrast, silacyclopropene **4** did not survive hydrosilylation reactions with the given catalysts, all attempts yielded in the decomposition of the silacyclopropene moiety. At the same time, we can observe the formation of bis(trimethylsilyl)acetylene as

an elimination product of the silirene depletion. This is in accordance with the already observed thermal lability of **4**. Evidently, we tried to hydrosilylate silacyclopropane **2** and **3** with triethylsilane as well. However, no successful coupling reaction could be observed under the given conditions (Table 1). Solely, the depletion of the silacyclopropane moiety was observed. These results let us surmise that **2** and **3** do not hold sufficient stabilization to withstand the applied catalytic conditions. This assumption is supported by the general higher lability of silacyclopropanes compared to silacyclopropenes.<sup>3,18</sup>

Since we were able to confirm our general concept in test reactions with alkyl- and aryl-substituted silanes, we wanted to expand the scope of employable Si-H substrates. Hence, we investigated the functionalization of various siloxy-based substrates **S** with the modular silirene **5** under the conditions given in Scheme 3. First, we modified pentamethyldisiloxane (**S1**) as additional mono-functional substrate. Next, we functionalized **S2–S4** as difunctional compounds, which represent both molecular

as well as polymeric substrates. By varying the stoichiometry of silirene to substrate, variable modifications of **S5** can be achieved. This way, we could create partially functionalized substrate **P5a** by using 2 equivalents or fully functionalized substrate **P5b** by using 4 equivalents of **5**, respectively. In a similar fashion, “semi”-modified PMHS **P6a** or fully modified PMHS **P6b** were created by variation of the applied silirene ratio. The substrate modification was evaluated by NMR-spectroscopy. Again, the depletion of the Si-H signal from the respective silane **S** in the <sup>1</sup>H-NMR and <sup>29</sup>Si-NMR can be monitored and provide evidence for a successful functionalization. At the same time, the development of a new silirene signal between –81.0 ppm and –80.7 ppm (in contrast to modular silirene **5** with –97.5 ppm) emphasizes this assumption and proves the preservation of the silirene functionality. We assume comparable chemical environments in close proximity of the silirene group as the hydrosilylation reaction always creates an ethyl-bridge for each substrate. As a result, the chemical shifts for the new silirene moieties can be found in a narrow range (±0.5 ppm) for all functionalized substrates **P**. Chemical shifts for the silirene-moiety of the prior synthesized compounds **7**, **8** and **9** could also be found in a similar range around –81 ppm, which provides further evidence towards a successful modification. Additional proof can be provided by UV/Vis-spectroscopy. In general many silacyclopropenes exhibit characteristic absorption bands in the near ultraviolet region.<sup>2,8</sup> This property can be assigned to the “pseudo-π” aromaticity resulting from the interaction of the carbon π bond orbital with the vacant low-lying σ\* orbital of the silicon-atom and its substituents.<sup>3,19</sup> In the UV/Vis-spectrum modular silirene **5** shows a distinct absorption band at λ<sub>max</sub> = 323 nm (Fig. S18 in ESI†). After the functionalization reaction, the modified substrates **P** exhibit a slightly blue shifted absorption band around λ<sub>max</sub> = 316 nm (Fig. S26 in ESI†). These findings support our assumption that the preservation of the silacyclopropene functionality can be accomplished under the described conditions. We observed that with an increasing number of Si-H functionalities per substrate the reaction time increases likewise. To reduce the reaction time, we increased the catalyst concentration compared to the test reaction with triethylsilane (Table 1) from 0.1% mol to 0.5 mol%. Under these conditions higher conversion and better functionalization can be realized within 4 h for monofunctional **S1**, while bifunctional **S2–S4** require up to 12 h of reaction time. Full modification of **S6** as multifunctional substrate was achieved within 24 h with the described catalyst concentrations. Filtration over aluminium oxide (Al<sub>2</sub>O<sub>3</sub>) and subsequent drying under vacuum were conducted to remove any utilized catalyst and volatile side products from the functionalized substrates (see ESI† for respective yields). This way all tested substrates could be functionalized with the respective silirene-moiety, hence giving easier synthetic access or even the only possibility to approach higher functional silirenes. The fact that established catalysts like the Karstedt catalyst can be employed in this modification, allow an easier implantation of this methodology and a broader acceptance in other scientific fields. One can imagine using this technique for nanomaterials like silicon nanosheets (SNS) or silicon nanocrystals (SNC), since



Scheme 3 **S5** to obtain mono-, bis- or multi-functional substrate **P**.

functionalization is key to modify their properties such as solubility<sup>20</sup> or photoluminescence.<sup>21</sup> We were able to functionalize linear polysiloxanes to create polymeric silirene scaffolds. Moreover, we created a reagent to post-modify polymeric substrates, which offers the potential for tuning polymer properties or introducing photo-sensitive moieties, even after polymerization. In a similar fashion this method could be utilised in surface chemistry as a reactive substrate to alter surface characteristics. Furthermore, coatings or adhesion promoters could be facilitated by introducing silirenes moieties as a coupling agent on the surface.

In conclusion, we established a versatile and applicable method to modify a variety of substrates with silacyclopropene functionalities. For this purpose, we present the concept of modular silacyclopropenes and the synthesis thereof. Sufficient substituent stabilisation of the ring system was key for the preparation as well as the preservation of this functionality in the coupling reaction. Commercially available and widely used catalysts like the Karstedt catalyst can be employed in the hydrosilylation reaction. The tested substrates range from small monofunctional molecules to polymeric multifunctional structures. Further efforts will be made to expand the scope to Si–H containing surfaces or silicon nanomaterials and possible applications of multifunctional silacyclopropenes as polymer curing agents. By presenting this method, we hope to shine a new light on silacyclopropenes as applicable and useful functionalities as photo-active moieties and stable precursors for highly active silylenes.

We acknowledge our principal funding source the WACKER Chemie AG. We especially thank Dr Maximilian Moxter and Dr Niklas Wienkenhöver for constructive advice and helpful discussions. We thank Andreas Saurwein for revising the manuscript and valuable discussions. We also like to thank Maximilian Muhr for LIFDI-MS measurements.

## Conflicts of interest

The authors declare the following conflicts of interest: one patent application (PCT/EP2022/067772) was filed, covering the methods in this paper.

## Notes and references

- (a) M. Ishikawa and M. Kumada, *Adv. Organomet. Chem.*, 1981, **19**, 51; (b) Y.-N. Tang, in *Reactive Intermediates*, ed. R. A. Abramovitch, Springer US, Boston, MA, 1982, pp. 297–366;
- (c) D. Seyferth, D. C. Annarelli and S. C. Vick, *J. Organomet. Chem.*, 1984, **272**, 123.
- M. Ishikawa, A. Naka and J. Ohshita, *Asian J. Org. Chem.*, 2015, **4**, 1192.
- R. R. Aysin, L. A. Leites and S. S. Bukalov, *Organometallics*, 2020, **39**, 2749.
- M. Ishikawa, K. Nishimura, H. Sugisawa and M. Kumada, *J. Organomet. Chem.*, 1980, **194**, 147.
- (a) D. Seyferth, D. P. Duncan and S. C. Vick, *J. Organomet. Chem.*, 1977, **125**, C5; (b) J. Ohshita, N. Honda, K. Nada, T. Iida, T. Mihara, Y. Matsuo, A. Kunai, A. Naka and M. Ishikawa, *Organometallics*, 2003, **22**, 2436.
- (a) A. Sekiguchi, T. Tanaka, M. Ichinohe, K. Akiyama and S. Tero-Kubota, *J. Am. Chem. Soc.*, 2003, **125**, 4962; (b) D. Seyferth and S. C. Vick, *J. Organomet. Chem.*, 1977, **125**, C11.
- R. T. Conlin and P. P. Gaspar, *J. Am. Chem. Soc.*, 1976, **98**, 3715.
- D. Seyferth, D. C. Annarelli and S. C. Vick, *J. Am. Chem. Soc.*, 1976, **98**, 6382.
- (a) F. Lips, A. Mansikkamäki, J. C. Fettinger, H. M. Tuononen and P. P. Power, *Organometallics*, 2014, **33**, 6253; (b) S. Santra, *ChemistrySelect*, 2020, **5**, 9034; (c) S. Ishida, T. Iwamoto and M. Kira, *Heteroat. Chem.*, 2011, **22**, 432; (d) J. A. Baus, N. Laskowski and R. Tacke, *Chem. Ber.*, 2016, **2016**, 5182; (e) M. Ishikawa, K.-I. Nakagawa, M. Ishiguro, F. Ohi and M. Kumada, *J. Organomet. Chem.*, 1978, **152**, 155.
- Y. E. Türkmen, in *Comprehensive Heterocyclic Chemistry IV*, ed. D. Black, Elsevier Science & Technology, San Diego, 2022, pp. 506–533.
- (a) H. Sakurai, Y. Kamiyama and Y. Nakadaira, *J. Am. Chem. Soc.*, 1977, **99**, 3879; (b) M. Ishikawa, H. Sugisawa, T. Fuchikami, M. Kumada, T. Yamabe, H. Kawakami, K. Fukui, Y. Ueki and H. Shizuka, *J. Am. Chem. Soc.*, 1982, **104**, 2872.
- (a) K. Maeda and K. Morokura, *J. Jpn. Pet. Inst.*, 2020, **63**, 1; (b) Y. Naganawa, K. Inomata, K. Sato and Y. Nakajima, *Tetrahedron Lett.*, 2020, **61**, 151513; (c) J. V. Obligation and P. J. Chirik, *Nat. Rev. Chem.*, 2018, **2**, 15; (d) T. Galeandro-Diamant, M.-L. Zanota, R. Sayah, L. Veyre, C. Nikitine, C. de Bellefont, S. Marrot, V. Meille and C. Thieuleux, *Chem. Commun.*, 2015, **51**, 16194; (e) D. Troegel and J. Stohrer, *Coord. Chem. Rev.*, 2011, **255**, 1440.
- (a) D. Seyferth and D. C. Annarelli, *J. Am. Chem. Soc.*, 1976, **117**, C51; (b) J. Belzner, H. Ihmels, B. O. Kneisel, R. O. Gould and R. Herbst-Irmer, *Organometallics*, 1995, **14**, 305; (c) T. G. Driver and K. A. Woerpel, *J. Am. Chem. Soc.*, 2003, **125**, 10659.
- (a) W. S. Palmer and K. A. Woerpel, *Organometallics*, 1997, **16**, 4824; (b) T. G. Driver and K. A. Woerpel, *J. Am. Chem. Soc.*, 2004, **126**, 9993; (c) C. Z. Rotsides and K. A. Woerpel, *Dalton Trans.*, 2017, **46**, 8763.
- (a) B. D. Karstedt, *General Electric*, US Pat., US3715334A, 1973; (b) P. B. Hitchcock, M. F. Lappert and N. J. W. Warhurst, *Angew. Chem., Int. Ed. Engl.*, 1991, **30**, 438.
- I. E. Markó, S. Stérin, O. Buisine, G. Berthon, G. Michaud, B. Tinant and J.-P. Declercq, *Adv. Synth. Catal.*, 2004, **346**, 1429.
- Y. Nakajima and S. Shimada, *RSC Adv.*, 2015, **5**, 20603.
- M. S. Gordon, *J. Am. Chem. Soc.*, 1980, **102**, 7419.
- I. Fernández, J. I. Wu and P. v R. Schleyer, *Org. Lett.*, 2013, **15**, 2990.
- M. A. Islam, R. Sinelnikov, M. A. Howlader, A. Faramus and J. G. C. Veinot, *Chem. Mater.*, 2018, **30**, 8925.
- M. Dasog, G. B. de los Reyes, L. V. Titova, F. A. Hegmann and J. G. C. Veinot, *ACS Nano*, 2014, **8**, 9636.



## 6. Silacyclopropenes: Photo-Activity and Curing Application

### 6.1. Bibliographic data

Title: “Photo-Activity of Silacyclopropenes and their Application in Metal-Free Curing of Silicones”<sup>[269]</sup>

Status: Research Article (Open Access), Publication Date: 29.11.2022

Journal: ChemSusChem

Publisher: Wiley-VCH (Chemistry Europe)

DOI: 10.1002/cssc.202201957

Authors: **Matthias Nobis**, Jonas Futter, Maximilian Moxter, Shigeyoshi Inoue, Bernhard Rieger ‡

### 6.2. Abstract graphic (TOC)

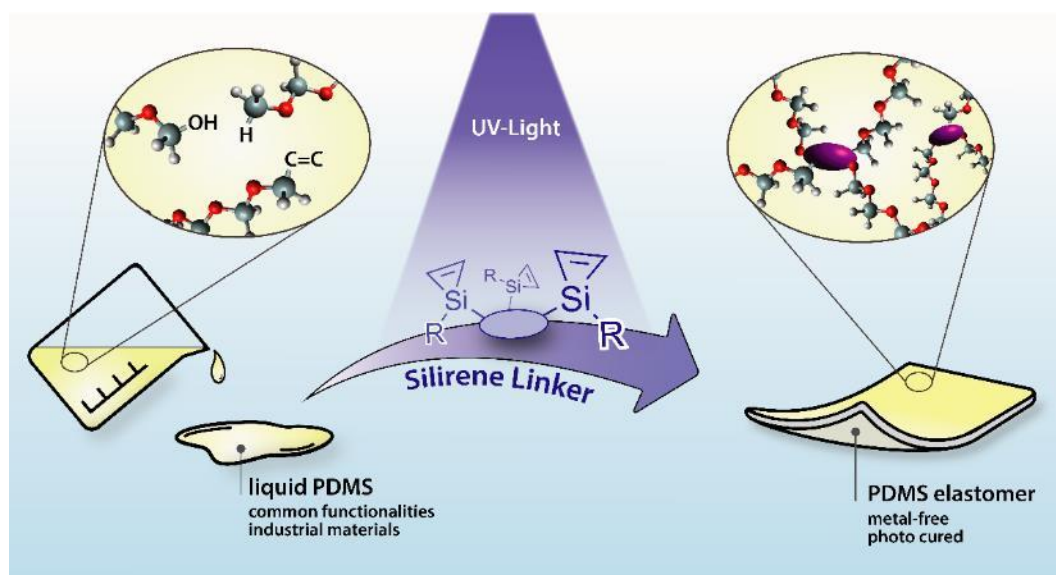


**Figure 18.** Table of content for the manuscript titles “Photo-Activity of Silacyclopropenes and their Application in Metal-Free Curing of Silicones”.

---

‡M. Nobis provided the original idea and prepared the manuscript. M. Nobis and J. Futter planned and executed all experiments and performed the data analysis. M. Moxter helped with data analysis and revising the manuscript. All work was performed under the supervision of B. Rieger and S. Inoue.

### 6.3. Content

The concept of multifunctional silacyclopropenes as photo-active linker scaffolds for PDMS curing was introduced. Silirenes display characteristic absorption bands in the near ultraviolet regions, due to their "pseudo- $\pi$ " aromatic ring-system. This property is crucial, because although polysiloxanes exhibit an excellent transmittance in the visible and near-ultraviolet light spectrum, the absorbance of the polymer at wavelengths shorter than 280 nm increases significantly. Thus, all photo-based curing efforts below this limit are considered improbable, including the utilization of silirane based linker scaffolds for such purposes. To establish a fundamental understanding of this compound class, the general reactivity of various monofunctional silirenes towards different substrates under UV-irradiation was investigated. For this purpose, different di-tert-butyl substituted silirenes were synthesized and examined for their photo reactivity towards insertion reactions with common PDMS functionalities, including silanes (Si-H), silanols (Si-OH), and vinylsilanes (Si-C=C). As a main challenge, the occurrence of an undesired side product, originating from a light-induced rearrangement reaction, could be observed. Attenuation of the respective side reaction ratio could be achieved through low-temperature control or variation of the chemical structure. It could be shown that with decreasing reaction temperatures the yield of the desired insertion reaction could be improved to higher yields (up to 90 %). As a result, the reaction time and consequently the curing duration increase significantly. The alteration of the chemical configuration of the silirene itself allowed better product ratios without the disadvantage of gaining longer reaction times. This way, the most suitable silirene candidates could be identified which met the necessary reactivity and crosslinking criteria. The subsequent synthesis of multifunctional silirene linkers based on these candidates was accessible via the prior discussed technique of modular silirenes. Final curing of functionalized PDMS provides the general proof of concept for this alternative curing system by employing the synthesized linker scaffolds based on the most suitable silirenes. The described method renders this class of crosslinker scaffolds applicable for a variety of differently functionalized polysiloxanes. These findings demonstrate the many possibilities of light controlled curing and its potential as a metal- and additive-free alternative to the conventional methods. In addition to the prior discussed silirane curing of chapter 4, this concept represents an even more gentle crosslinking method, suitable for thermo-sensitive applications as well.

 Very Important Paper

## Photo-Activity of Silacyclopropenes and their Application in Metal-Free Curing of Silicones

Matthias Nobis,<sup>[a, b]</sup> Jonas Futter,<sup>[b]</sup> Maximilian Moxter,<sup>[c]</sup> Shigeyoshi Inoue,<sup>[a]</sup> and Bernhard Rieger<sup>\*[a, b]</sup>

Silicone elastomers are usually produced via addition or condensation curing by means of platinum- or tin-based catalysis. The employed catalysts remain in the final rubber and cannot be recovered, thus creating various economic and environmental challenges. Herein, a light-mediated curing method using multifunctional silacyclopropenes as crosslinker structures was introduced to create an effective alternative to the conventional industrial crosslinking. To evaluate the potential of the photoreaction a model study with small monofunctional silirenes was conducted. These investigations confirmed the required coupling reactivity upon irradiation and

revealed an undesired rearrangement formation. Further optimization showed the reaction selectivity to be strongly influenced by the substitution of the three-membered ring system and the reaction temperature. The synthesis of multifunctional silirenes was described based on the most suitable model compound to create active crosslinker scaffolds for their application in silicone curing. This photo-controlled process produces catalyst and additive free elastomers from liquid silicones, including hydride-, hydroxy-, or vinyl terminated polydimethylsiloxanes.

### Introduction

One of the most relevant inorganic polymers is the class of polysiloxanes commonly known as silicones. They can be found in a vast range of applications due to their outstanding physical and mechanical properties, as well as their thermal robustness and chemical stability.<sup>[1]</sup> This renders this material dominant across a variety of sectors from the construction, automotive, textile, and cosmetic to pharmaceutical and biomedical industries.<sup>[2]</sup> While silicones are used as fluids, gels, or resins, the segment of cured elastomers led the global silicone market with a share of more than 41% in 2020.<sup>[3]</sup> Conventional crosslinking strategies are centered on the addition (hydrosilylation) or condensation curing of polydimethylsiloxane (PDMS). Silicone rubber created via condensation is inexpensive and easy to handle; however, volatile elimination products and long curing durations restrict its application. Although addition


curing benefits from fast crosslinking reactions and low network shrinkage, it is limited to a more expensive two-component mixture of hydride- and vinyl-functionalized PDMS. Both techniques share the need for a metal catalyst such as platinum (addition) or tin (condensation) to cure PDMS at room temperature.<sup>[4]</sup> Furthermore, the implemented metal catalysts and respective degradation products will remain in the final silicone network, thus creating economic challenges and raising environmental questions. Even though catalyst amounts could be reduced to ppm concentrations by improving catalyst design,<sup>[5]</sup> the thriving demand for silicone elastomers results in the waste of 4–6 tons of pure platinum each year.<sup>[6]</sup> All this emphasizes the necessity for novel metal-free crosslinking methods. Alternative curing via autoxidation,<sup>[7,8]</sup> silacyclopropanes,<sup>[9]</sup> thiol-enes,<sup>[10]</sup> polysilazanes,<sup>[11]</sup> or cyclic disulfides<sup>[12]</sup> has been introduced over the past years. While autoxidative curing can use readily available hydride-terminated silicones, it is restricted to temperatures above 220 °C.<sup>[8]</sup> Another heat-controlled method is the curing of hydroxy-terminated PDMS by using silacyclopropanes in a ring-opening reaction. Respective UV-based curing can be realized by using thiol-ene-functionalized polysiloxanes as crosslinkers to create soft PDMS-networks with vinyl-terminated silicones.<sup>[10]</sup> Comparable efforts to cure with UV-light were made by employing cyclic disulfides as terminal functionalities on the PDMS chains. Further ring-opening polymerization afforded the respective bottlebrush elastomers.<sup>[12]</sup> All of these methods are limited by either high temperatures or the necessity of a specific PDMS functionality. To tackle these issues, we wanted to create a catalyst-free method, which can be applied at room temperature for a broad range of commonly used PDMS functionalities.


For this, we introduce a curing strategy by utilizing multifunctional silacyclopropenes (silirenes) as crosslinker scaffolds. Collin and Gaspar reported the first synthesis of a silacyclopro-

[a] M. Nobis, Prof. Dr. S. Inoue, Prof. Dr. B. Rieger  
WACKER-Institute of Silicon Chemistry  
Technical University of Munich  
85747 Garching bei München (Germany)  
E-mail: rieger@tum.de

[b] M. Nobis, J. Futter, Prof. Dr. B. Rieger  
WACKER-Chair of Macromolecular Chemistry  
Technical University of Munich  
85747 Garching bei München (Germany)

[c] Dr. M. Moxter  
Consortium für elektrochemische Industrie  
WACKER Chemie AG  
Zielstattstraße 20, 81379 München (Germany)

 Supporting information for this article is available on the WWW under <https://doi.org/10.1002/cssc.202201957>

 © 2022 The Authors. ChemSusChem published by Wiley-VCH GmbH. This is an open access article under the terms of the Creative Commons Attribution Non-Commercial License, which permits use, distribution and reproduction in any medium, provided the original work is properly cited and is not used for commercial purposes.

prene in 1976.<sup>[13]</sup> Since then the moiety of silirenes have gained considerable attention and various synthesis strategies have been reported. Most of them involve a [2 + 1] cycloaddition of an alkyne to the respective silylene.<sup>[14]</sup> These three-membered ring systems, known to undergo various reactions in response to heat<sup>[15,16]</sup> or UV irradiation,<sup>[15,17]</sup> serve as stable precursors for transient silylenes. The high reactivity of these silylenes ensures a fast curing reaction with the respective silicone functionalities to compete with the conventional crosslinking methods. The general feasibility of a silylene-based curing of linear PDMS was reported by our group in 2020.<sup>[9]</sup> However, the presented curing strategy can only be performed at high temperatures above 140 °C and limitations of the applicable silicone functionalities reduce its effectiveness and scope. By setting up a silirene-based crosslinking concept we are able to present a UV-light controlled curing for hydride-, hydroxy-, and vinyl-functionalized linear PDMS. In this work our aim is to combine the benefits of light-mediated, room-temperature curing with the expansion of employable silicone functionalities, yielding metal-, catalyst-, and additive-free silicone elastomers.

#### Curing concept, design, and conditions

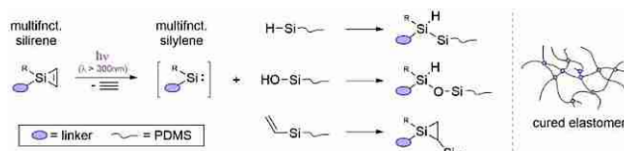
For creating a catalyst-free curing concept for silicones, we were drawn to the motif of silacyclopropenes. The three-membered ring of the silirene can be opened under UV-light to generate transient silylenes. These highly reactive low-valent silicon species can easily react with commonly used silicone functionalities like Si–H, Si–OH, or Si–vinyl.<sup>[15,18]</sup> We surmised that this reactivity could be used to crosslink the silicone chains and create the desired elastomers (Scheme 1). Additionally, the class of silirenes shows a high stability, compared, for example, to their saturated analogues, the silacyclopropanes.<sup>[19,20]</sup> This property is key for creating stable curing mixtures and a defined curing initiation. Furthermore, silirenes display characteristic absorption bands in the near ultraviolet regions, due to their “pseudo- $\pi$ ” aromatic ring-system.<sup>[19]</sup> This property is crucial, because although polysiloxanes exhibit an excellent transmittance in the visible and near-ultraviolet light spectrum, the absorbance of the polymer at wavelengths shorter than 280 nm increases significantly,<sup>[21]</sup> thus rendering all photo-based curing efforts below this limit improbable. Another benefit arises from the chemical composition of the silirene linker structures itself, which consist only of atoms already present in polysiloxanes.

Hence, we can avoid introducing additional heteroatoms and possibly deteriorating the final elastomer properties.

## Results and Discussion

### Model compounds

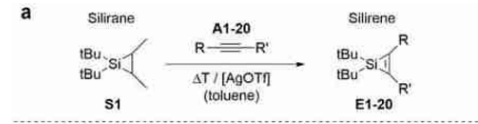
We began our search for an effective crosslinker by investigating suitable silirenes. Initial syntheses of small monofunctional silirenes as model compounds were performed to study potential candidates for the intended photoreactions. In order to synthesize a broad variety of silirenes **E1–E20** (Table 1), we employed the silylene-transfer reaction, by converting literature-known silacyclopropane **S1** in the presence of acetylenes **A1–A20**.<sup>[22]</sup> Commercially unavailable acetylenes were synthesized by literature-known procedures either via cross-coupling of bis(trimethylsilyl)acetylene,<sup>[23]</sup> reduction of tetrachloroethylene with lithium,<sup>[24]</sup> or treatment of trichloroethylene or phenylacetylene with *n*-butyllithium in combination with the respective halogen substrate.<sup>[25]</sup> The subsequent reaction to afford the respective silacyclopropene **E1–E20** could be realized either thermally ( $T > 120$  °C), or catalytically (AgOTf, 1.0 mol%). Best results were observed using a small excess (1.1 equiv.) of acetylene **A** compared to silirane **S1**. While higher yields were observed for the catalytically controlled reaction in most cases, phosphine-substituted silacyclopropene **E19** and **E20** could only be synthesized thermally. Further, no product formation could be noticed for silirenes **E6**, **E11**, and **E12** through the presented procedures. We surmise that with increasing steric demand of the acetylene the formation of the silacyclopropene becomes improbable and no reaction occurs, since this affects only acetylenes with larger substituents. We then conducted UV/Vis-measurement with the new silirenes **E1–E20** to assess their potential for a light induced reaction. We can conclude that the solely alkyl/aryl-substituted silacyclopropenes (**E1–E5**) show the lowest absorption maxima around 270 nm, whereas silyl-substituted silirenes (**E7–E10**) convene the highest observed absorption maxima from 324 up to 348 nm. Asymmetric Si/C-substituted silirenes (**E13–E17**) can be found between these two silirene classes, with absorption maxima located around 320 nm. This tendency can also be correlated to the respective chemical shifts in the <sup>29</sup>Si nuclear magnetic resonance (NMR) spectra. We observed that an upfield shift of the signal of the central silicon atom corresponds to an absorption maximum at higher wavelengths. We hypothesize that the



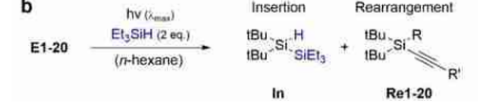
**Scheme 1.** Light-mediated curing strategy: multifunctional silirene scaffolds form PDMS elastomers with hydride-, hydroxy-, and vinyl-functionalized silicones via photo-induced generation of transient silylene-linkers.

**Table 1.** Overview of (a) the synthesis of model silirenes **E1–E20** via silylene transfer reaction with silirane **S1** and (b) the relative ratio of insertion (In) to rearrangement (Re) product in the photoreaction with triethylsilane.

**a**



**b**



E	R	R'	Yield <sup>[a]</sup> E [%]	Abs. λ [nm]	In/Re <sup>[b]</sup>
1	Me	Me	78	246	100:0
2	Et	Et	72	225	100:0
3	Ph	Me	82	260	100:0
4	Ph	Ph	84	290	– <sup>[c]</sup>
5	<i>m</i> -xylyl	<i>m</i> -xylyl	45	296	– <sup>[c]</sup>
6	<i>o</i> -xylyl	<i>o</i> -xylyl	– <sup>[d]</sup>	–	– <sup>[c]</sup>
7	SiMe <sub>3</sub>	SiMe <sub>3</sub>	75	348	35:65
8	SiMe <sub>2</sub> Et	SiMe <sub>2</sub> Et	58	324	34:66
9	SiMe <sub>2</sub> tBu	SiMe <sub>2</sub> tBu	60	327	37:63
10	SiEt <sub>3</sub>	SiEt <sub>3</sub>	53	328	33:67
11	SiPh <sub>3</sub>	SiPh <sub>3</sub>	– <sup>[d]</sup>	–	–
12	Si( <i>i</i> Pr) <sub>3</sub>	Si( <i>i</i> Pr) <sub>3</sub>	– <sup>[d]</sup>	–	–
13	SiMe <sub>3</sub>	Me	65	278	63:37
14	SiMe <sub>3</sub>	Ph	79	325	65:35
15	SiEt <sub>3</sub>	Ph	70	323	66:34
16	SiMePh <sub>2</sub>	Ph	55	327	61:39
17	Si( <i>i</i> Pr) <sub>3</sub>	Ph	58	325	65:35
18	GeMe <sub>3</sub>	GeMe <sub>3</sub>	51	333	0:100
19	P(Ph) <sub>2</sub>	P(Ph) <sub>2</sub>	57	315	– <sup>[c]</sup>
20	P(Ph) <sub>2</sub>	Ph	61	325	– <sup>[c]</sup>

[a] All yields given for isolated pure compounds. [b] Relative yields were calculated via <sup>1</sup>H and <sup>29</sup>Si NMR spectroscopy by comparing the respective integrals. [c] No photoreaction at any given wavelength (254–420 nm) could be observed. [d] No product formation was observed. Starting material could not be recovered.

observed shielding effect is caused by an increase of electron density at the ring-system, which could shift the excitation of the silirene towards higher wavelengths.

### Si–H photoreactivity

To establish the desired reactivity, we tested our silirenes in a photo-mediated reaction with triethylsilane in a model study by using <sup>1</sup>H and <sup>29</sup>Si NMR spectroscopy. For this, we mixed the reagents in *n*-hexane and irradiated the solution for 30 min at different wavelengths (254–420 nm). We observed the desired insertion reaction into the Si–H bond with the alkyl/aryl-substituted silirenes **E1–E3**; however, activation of these compounds was only achievable with hard UV-light (254 nm FLT). Thus, rendering this compound class ineffective for an application in silicone curing, since an activation above 280 nm is required. Although **E4** shows a distinct absorption maximum at 300 nm, no reaction at any given wavelength could be observed. Next, we investigated the group of silyl-substituted

silirenes **E7–E10**, due to their characteristic absorbance at higher wavelengths above 325 nm. This time activation and subsequent insertion of the silirene was performed with a 365 nm LED. In the case of **E7** even radiation at 420 nm could be employed with equal results. While silyl substituents shift the activation towards higher wavelength, the selectivity of the photoreaction decreases. The formation of an additional side product was observed, which could be assigned to the respective rearrangement product **Re** of the silirene. This type of rearrangement is known in literature for silyl- and hybrid-substituted silirenes in particular.<sup>[26]</sup> Unfortunately, the rearrangement product does not react further with any silane, hence reducing the capability of the silirene to crosslink Si–H functionalized polysiloxanes severely. To our surprise, silirenes **E7–E10** yielded in comparable product distributions. Relative ratios of approximately 33–66% were determined for the insertion/rearrangement products, which appears to be independent from the steric demand of the employed silyl-substituent. However, improved insertion ratios were measured by employing asymmetric silirenes **E13–E17**, substituted with both an alkyl/aryl- as well as a silyl-moiety. Due to the reduction to only one silyl-based, rearrangeable substituent in these scaffolds, the relative yield of the rearrangement reaction was significantly decreased to 34% under the described conditions. Nevertheless, activation of the respective silirenes was achieved at 365 nm, which meets our criteria for a UV-based curing process. Germyl-silirene **E18** afforded solely the respective rearrangement product under irradiation, while phosphine based silirenes **E19** and **E20** were entirely inactive towards any exposure of light in the range from 256 to 420 nm. It can be concluded that fully alkyl/aryl-substituted silirenes are unfit for our purpose, due to their low absorption and activation properties. Silyl-substituted silirenes show activation at higher wavelength but the primarily formation of the rearrangement product attenuate their effectiveness. By choosing asymmetric, aryl- and silyl-substituted silirenes the best compromise for both desired characteristics, possible activation above 300 nm and a higher selective photoreaction towards the insertion product, can be found. To further improve the photoreaction additional screenings were conducted to improve the reaction selectivity. (Table 2) For this optimization, silirene **E7** and **E14** were selected due to their described photo-activity, their good synthetic accessibility, and to represent the respective groups of disilyl- (**E7**) and aryl/silyl-substituted (**E14**) silirenes. First, a variation of the triethylsilane amount was investigated. In the absence of any silane the respective silirene reacts exclusively to the rearrangement product **Re**, without the formation of any other side products, whereas increasing the amount of silane from 2 to 10 or even 100 equiv. did not change in the reaction selectivity considerably. Hence, we assume that the reaction is not limited by reactant accessibility. Similar results can be concluded for the variation of the activation wavelength to 300 or 420 nm. Changing the solvent to toluene or cyclohexene also did not result in any notable shift. However, by reducing the reaction temperatures, we detected a significant change towards higher yields of the desired insertion product **In**. At –40 °C we observe that for **E7** both reaction products are

**Table 2.** Photoreaction of silirenes **E7** and **E14** with triethylsilane and variation of the reaction parameters to optimize the reaction selectivity.

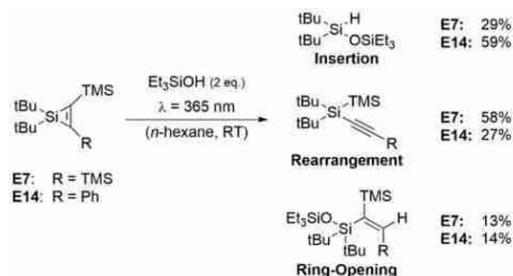
Deviation from standard conditions	$t^{[a]}$ [h]	In/Re <sup>[b]</sup> [%]	
		E7	E14
none <sup>[c]</sup>	0.5	34:66	65:35
0 equiv. Et <sub>3</sub> SiH	0.5	0:100	0:100
10 equiv. Et <sub>3</sub> SiH	0.5	34:66	64:36
100 equiv. Et <sub>3</sub> SiH	0.5	36:64	65:35
$\lambda_{\text{max}}=300$ nm	0.5	35:65	63:37
$\lambda_{\text{max}}=420$ nm	0.5	34:66	– <sup>[d]</sup>
toluene as solvent	0.5	33:67	65:35
C <sub>6</sub> D <sub>12</sub> as solvent	0.5	35:65	64:36
$T=-40$ °C	24	50:50	81:19
$T=-80$ °C	72	79:21	93:07

[a] Reaction time was determined after full conversion of the respective silirene. [b] Relative yields were calculated via <sup>1</sup>H and <sup>29</sup>Si NMR spectroscopy by comparing the respective integrals. [c] Reaction conditions as written in scheme above. [d] No photo reaction at 420 nm could be observed.

present in equal shares, while the insertion product is formed predominantly with a relative ratio of 79% at a temperature of  $-80$  °C. A similar tendency can be noted for **E14**, which afforded yields of the insertion greater than 90% at such low temperatures. Unfortunately, the improvement reaction selectivity is accompanied by a substantial increase in the reaction time. Full conversion of the respective silylene requires 24 h at  $-40$  °C or even up to 72 h at  $-80$  °C. Even though controlling the photoreaction through temperature bears great potential, the increase of the reaction time to several days and the actual implementation of a silicone curing process at  $-80$  °C do not seem applicable or efficient. Hence, the most effective control to regulate the photoreaction stays the modification of the chemical scaffold itself.

#### Si–OH photoreactivity

To evaluate the capability of our model system to react with silanols, silirene **E7** and **E14** were irradiated in the presence of triethylsilanol (Scheme 2). Again, we observed the photoreaction of both silirenes at 365 nm and the formation of the desired insertion, as well as the rearrangement product. The transient silylene inserts into the O–H bond of the silanol resulting in a siloxane, in contrast to the disilane formation in the reaction with triethylsilane. However, the respective rearrangement product, arising from the intramolecular reaction of the silirene, does not differ from the previous test reactions. Additionally, a second side reaction can be noted, which could be assigned to the ring-opening product. This literature known reaction is triggered by the increased nucleophilicity of the silanol compared to the silane.<sup>[15,27]</sup> Contrary to the rearrangement the ring-opening product does not reduce the curing efficiency of the silirene, since it creates a covalent bond with

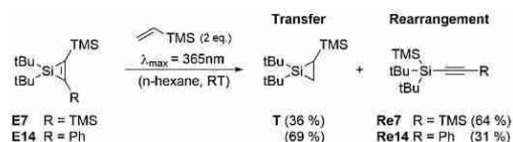

**Scheme 2.** Photoreaction of silirene **E7** and **E14** with triethylsilanol. Respective formation and relative ratio of the insertion, rearrangement, and ring-opening product.

the silanol. Consequently, curing with hydroxy-terminated siloxanes could be performed through both reactions, the insertion and the ring-opening. Again, silirene **E14** shows the higher selectivity towards the insertion product with 59% relative yield, while **E7** afforded only 29% relative yield.

Interestingly for both silirenes the respective ring-opening reaction occurred in comparable yields (13 and 14%, respectively). This could indicate a thermally induced reaction, which is not affected by the photoactivity of the silirene, since the ring-opening reaction is usually reported via heat control. To investigate this behavior, we conducted thermal control reactions. Heating the reaction mixtures up to 70 °C, no conversion of the silirenes could be detected over a period of 24 h. At temperatures above 80 °C small amounts of the ring-opening product were observable. By increasing the temperature to 110 °C the reaction could be accelerated to afford full conversion within 4 h. Even though **E7** and **E14** show a relatively high thermal stability towards triethylsilanol, we hypothesize that the irradiation and activation of the silirenes may facilitate this reaction even at lower temperatures. Additionally, reducing the reaction temperature to  $-40$  °C results in an increase of the photoreaction selectivity. This time both relative yields of the rearrangement, and the ring-opening product were reduced to 16 and 5%, respectively, while the ratio of the insertion product was increased to 79% for the irradiation of **E14** under reduced temperature. Yet again, the respective reaction time increases likewise and durations of up to 30 h are required to afford full conversion under these conditions.

#### Si–vinyl photoreactivity

At last, we studied the reactivity of silirene **E7** and **E14** towards vinyl-silanes to outline the curing potential for vinyl-functionalized polysiloxanes. Photoreactions were prepared by combining the respective silirene with vinyl-trimethylsilane. The mixtures were subsequently irradiated at 365 nm for 30 min and afforded the analogue rearrangement product as well as the desired transfer product (Scheme 3). This silylene-transfer-reaction

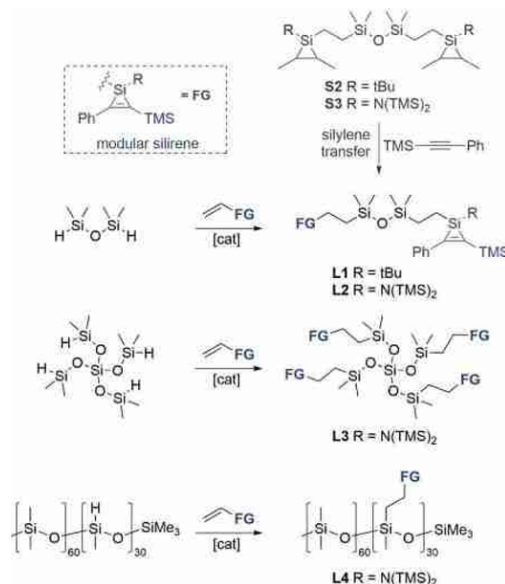


**Scheme 3.** Photoreaction of silirene **E7** and **E14** with vinyltrimethylsilane. Respective formation and relative ratio of the insertion and rearrangement product.

describes the transformation of a silirene to a silirane. As earlier described, these saturated silacycles lack the required photo-activity at higher wavelengths above 300 nm and will not react further under the employed irradiation at 365 nm once they are formed. Hence, the reaction with vinyl-triethylsilane results in the formation of the desired silirane product. Once again, we observed that **E14** affords higher yields in the photoreaction towards the transfer product with a relative yield of 69%, whereas **E7** results predominantly in the rearrangement product and only a relative ratio of 36% can be observed for the transfer reaction. In accordance with this, irradiating the reaction mixture at lower wavelengths ( $\lambda_{\max} = 265$  nm), resulted only in the formation of small amounts of the rearrangement product **Re** without the generation of any stable silirane. We presume that further decomposition of the intermediary formed silirane is caused by the use of hard UV-light, since this type of reactivity is well reported for siliranes at such low wavelengths.<sup>[28]</sup> Similar results could be obtained for the improvement of the photoreaction selectivity by reducing the reaction temperature. At  $-40$  °C the relative yields of the transfer product were elevated to 78% for the light-mediated reaction of **E14**, while the reaction time was extended from 30 min to almost 30 h. We can summarize that our investigated silirenes **E7** and **E14** can react with the three mainly used silicone functionalities (Si–H, Si–OH, Si–vinyl) via photo-activation at 365 nm. The undesired side reaction (rearrangement) can be minimized by substitution of the silirene with both silyl- and aryl-moieties as well as by low temperature control.

### Crosslinker-scaffolds

In order to create effective curing agents, we need to generate multifunctional silirene structures. These can react with the provided functionalized polysiloxane chains and act as joints in the final silicone elastomer. Based on the obtained results from our model study, the motif of silirene **E14** was chosen as suitable candidate for these crosslinkers. As a result, the following multifunctional silirenes **L1–L4** have been synthesized accordingly (Scheme 4). We initially synthesized bifunctional silirenes **L1** and **L2** from the earlier reported<sup>[9]</sup> bifunctional silacyclopropanes **S2** and **S3** via the silylene transfer reaction as previously described for the model silirene compounds **E1–E20**. Best results were obtained through the thermally controlled reaction at 120 °C and an excess of 3 equiv. of acetylene. However, this procedure was only applicable for bi- or trifunc-



**Scheme 4.** Synthesis of multifunctional silirene crosslinker **L1–L4** via silylene transfer or modular silirenes.

tional silirene scaffolds, due to the advancing complexity of the precursor synthesis with an increasing number of silirane-moieties. To tackle this issue, we recently reported a method to generate higher functional silirenes via the employment of “modular silirenes”.<sup>[29]</sup> Monofunctional silirene units can be grafted onto various Si–H-containing substrates, while avoiding the synthesis of complex precursors. Therefore, vinyl-functionalized silirenes were generated by substituting vinyl trichlorosilane with KHMDS (potassium hexamethyldisilazide) in a salt metathesis reaction to afford the vinyl dichloro-silane species. Subsequent reduction with a lithium/sodium alloy in the presence of 2-butene resulted in the formation of the vinyl-silirane, which was finally transformed into the “modular” vinyl-silirene via the silylene-transfer-reaction by employing the respective alkyne [1-phenyl-2-(trimethylsilyl)acetylene]. The “modular” silirene was then used in a hydrosilylation reaction with the presented hydrosilanes or PMHS. The employed hydrosilylation catalyst was subsequently removed by filtration through a combination of celite/ $\text{Al}_2\text{O}_3$ . A residue Pt concentration of less than 0.005 ppm could be detected by inductively coupled plasma optical emission spectroscopy (ICP-OES) measurements, demonstrating the successful separation of the noble metal from the product. This way, we were able to synthesize higher functional silirene crosslinker **L3** and polysiloxane-based linker **L4**. Additionally, bifunctional linker **L2** was re-synthesized via this procedure by combining tetramethyldisiloxane with the modular silirene to validate the applicability of this alternative method.

### Photo-curing

We tested the curing capability of our silirene based linkers L1–L4 in combination with different functionalized polysiloxanes. For this purpose, all commercially purchased polysiloxanes (Figure 1) were degassed and dried prior to the photocuring experiments. Heat and vacuum drying were sufficient for hydrid- and vinyl-terminated PDMS, while hydroxy-functionalized silicones were additionally filtered over dry neutral alumina and stored over 3 Å molecular sieve for several days. We employed polysiloxanes of comparable chain length with termination of Si–H (**P1**,  $n \approx 380$ ,  $M_w \approx 28 \text{ kg mol}^{-1}$ ), Si–OH (**P2**,  $n \approx 480$ ,  $M_w \approx 36 \text{ kg mol}^{-1}$ ), and Si–vinyl (**P3**,  $n \approx 380$ ,  $M_w \approx 28 \text{ kg mol}^{-1}$ ). Mixtures of PDMS and silirene-crosslinkers L1–L4 were combined under inert atmosphere and stirred until a homogenous phase was obtained. The respective mixtures were irradiated at 365 nm (LED) for several hours to afford the hardening of the employed silicones. Linker L1 and L2 were not able to form an elastomer with polysiloxane **P1** in mixing ratios of  $R=0.5$ , 1, 2, or 4 ( $R$  = number of silirene-moieties/number of PDMS functional groups). This is no surprise, since bifunctional linkers can only yield in a chain elongation with terminated silicones. Presumably, this can be attributed to the described issue of forming a rearrangement product during the photo-reaction. Due to its reduced efficiency, photo-curing with only two active silirene centers appears to be insufficient. It is noteworthy that the crosslinker **L2** was much better miscible with the employed silicones compared to **L1**. We suspect that the *tert*-butyl moiety experiences more repulsion in the PDMS matrix in contrast to the silazane  $[\text{N}(\text{TMS})_2]$  group of **L2**. Furthermore, no elastomer formation was observed by utilizing crosslinker **L3** in combination with **P1**, however an increase of viscosity for the irradiated sample was detected. We surmise that the increase of silirene groups partly enables to combine the respective PDMS chains, leading to a chain elongation. Hence, resulting in an increase of viscosity, without forming a silicone network. We further investigated the curing process in an oscillatory rheometer, modified with a lower glass-plate to allow simultaneous irradiation with different LEDs and monitoring of the curing event. This way, we were able to observe not only an increase of the respective complex viscosity  $|\eta^*|$  of **L3** with hydride terminated PDMS **P1**, but also an increase in the loss modulus  $G''$ , while no significant change in the storage modulus  $G'$  was detectable (Figure 2). This further supports the assumption of a chain elongation rather than a network formation. Nevertheless, utilizing the polymeric silirene linker **L4** with hydride terminated silicone **P1** resulted in successful curing of the linear polymer chains. For all mixing ratios ( $R=0.8$ ,

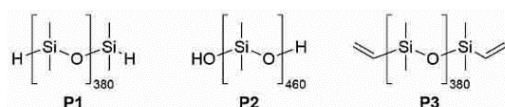


**Figure 1.** Terminal functionalized PDMS **P1–P3** utilized for photocuring with silirene-based linkers.

1, and 2) of linker to PDMS the solidification could be observed. The curing speed of the afforded elastomers is dependent on the employed ratio. Thus, fastest hardening was observed with the highest tested ratio of  $R=2$ , which reached the sol–gel point  $[\tan(\delta)=1]^{[30]}$  at 47 min, while almost 6.5 h were required in the case of  $R=0.8$  to reach this transition point. This ratio  $R$  represents the minimal concentration of linker for which a successful curing could be observed, we did not obtain any elastomers below this ratio. Additionally, by varying the silirene ratio  $R$ , the final elastomer properties can be modified as well. The complex viscosity  $|\eta^*|$  increases from  $102 \text{ Pa s}^{-1}$  for  $R=0.8$  to  $1540 \text{ Pa s}^{-1}$  for  $R=2$ , indicating a denser network with increasing ratio. The dissipation factor  $\tan(\delta)$  decreases from 0.78 to 0.21, which implies an increase in the elasticity of the final elastomer (Figure 2, left graphic). Thus, we can conclude that with higher linker concentrations we obtain denser cured silicone elastomers.

Furthermore, curing of hydroxy-terminated PDMS **P2** and vinyl-terminated PDMS **P3** with **L4** was feasible as well under equal conditions. Elastomers resulting from hydroxy-functionalized PDMS **P2** shared similar properties to the ones originating from **P1**. In comparison, this curing proceeded generally slower, which can be shown by reaching the respective sol–gel transition point at extended times. For example, the crossing of  $\tan(\delta)=1$  for **L4** with **P2** with a ratio  $R=2$  occurred after 135 min, while a low ratio of  $R=0.8$  delayed this transition to 8.6 h. Yet, after the finalization of the photocuring, the final dissipation factors  $\tan(\delta)$  were obtained in a similar range from 0.93 to 0.32 (from  $R=0.8$  to 2), compared to elastomers created from **P1**. To our surprise, crosslinking of vinyl-terminated PDMS **P3** with **L4** proceeded much faster in all employed mixing ratios.

In contrast to before, **P3** at a ratio of  $R=2$  solidified already after 28 min, almost half the required time for curing of **P1** at the same conditions. Even at a substoichiometric ratio of  $R=0.8$  the transition point was reached within 125 min, indicating the accelerated curing process. Further, final dissipation factors ranging from 0.23 to 0.05, indicating a more elastic rubber product in comparison. We hypothesize that the  $[2+1]$  cyclo-addition to the respective silirane proceeds faster compared to the insertion reaction into either the Si–H or Si–OH bond in the polysiloxane, thus resulting in this observable difference in the curing speed. Nevertheless, the resulting elastomers afforded comparable final viscosities. For instance, the complex viscosity  $|\eta^*|$  of **P3** at  $R=2$  resulted in a value of  $2656 \text{ Pa s}$  compared to  $2688 \text{ Pa s}$  for **P2**. Combining these results, we were able to cure these three different siloxane moieties with one crosslinker structure on the basis of multifunctional silirenes. This way, all tested linear polysiloxanes could be transformed into the respective elastomers via soft UV-irradiation under metal-free conditions. As additional proof for the light-mediated nature of the crosslinking process, we repeated the curing experiments of all three silicones **P1–P3** with discontinuous irradiation periods. We could observe in all cases an increase of the storage modulus during irradiation, while deactivating the light source resulted in flattening of the respective modulus rate. By switching the light back on, the storage modulus continued to



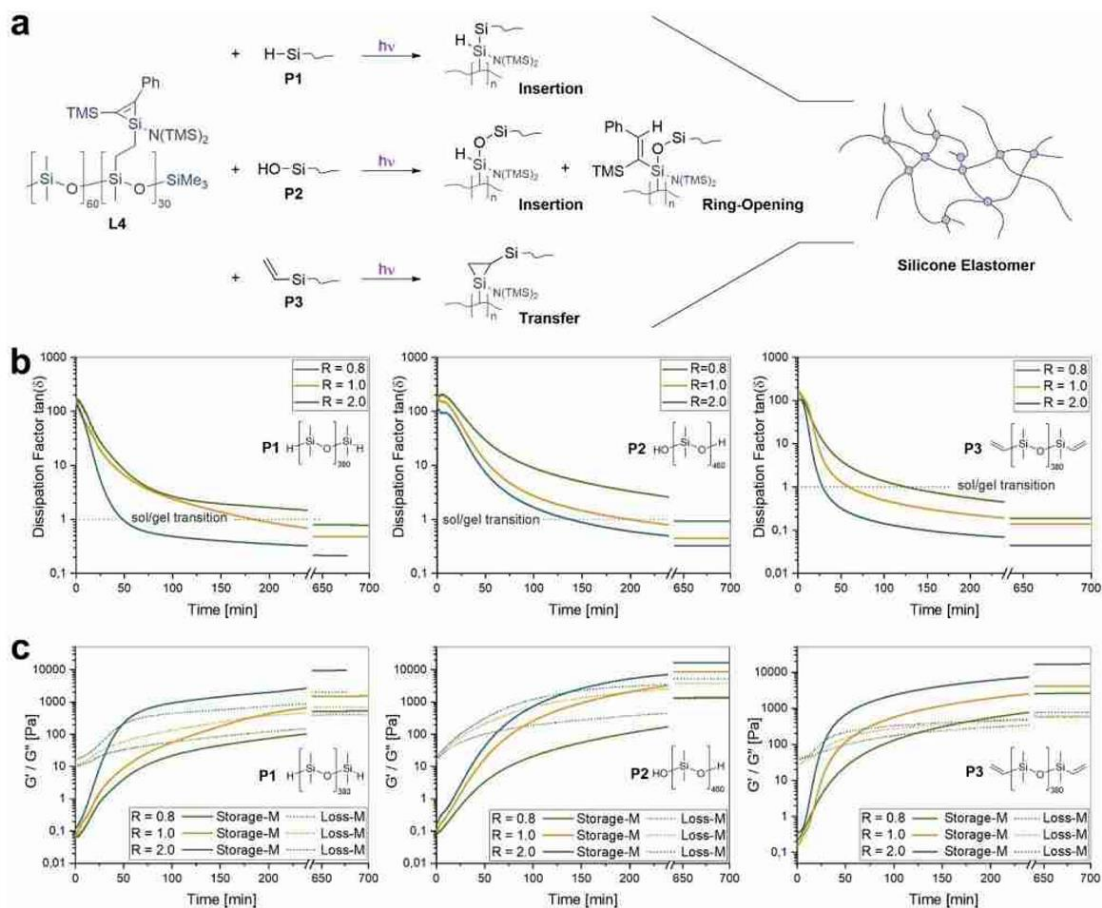


**Figure 2.** Photo-curing of terminal functionalized PDMS P1–P3 with multifunctional silirene linker L4. (a) Proposed crosslinking reactions of linker L4 with hydride- (P1), hydroxy- (P2), and vinyl- (P3) functionalized PDMS. (b) Dissipation factor  $\tan(\delta)$  vs. curing time with the depicted sol-gel transition point at  $\tan(\delta) = 1$  measured by oscillatory rheology ( $f = 1$  Hz,  $\gamma = 5\%$ ) for the photo-curing of linker L4 with PDMS P1–P3 at silirene/PDMS-moiety ratios  $R$  of 0.8–2.0. (c) Storage  $G'$  and loss modulus  $G''$  vs. curing time for the respective curing reactions of linker L4 with PDMS P1–P3 at silirene/PDMS-moiety ratios  $R$  of 0.8–2.0.

raise again, demonstrating the propagation of the respective curing.

## Conclusion

Herein we demonstrated the photo curing of linear polysiloxanes by employing multifunctional silirenes as crosslinkers, which serves as an alternative curing method. Initial investigation of small monofunctional silirenes in a model study provided evidence for the photolability and reactivity with the utilized functionalities. Substitution of the three-membered ring-system allowed effective tunability towards required absorption properties. Undesired rearrangement reactions via the photo-activation could be attenuated by minimizing silyl-

substitution or reduction of the reaction temperature. Based on these results, silirene E14 was chosen as the most suitable chemical motif for the following curing agents. Multifunctional silirenes L1–L4 were successfully obtained either via the silylene transfer reaction or utilization of modular silirenes. Bifunctional linkers L1 and L2 and tetrafunctional linker L3 were unable to create any silicone elastomers due to the reduced reaction selectivity caused by the formation of the rearrangement product. Polymeric linker L4 compensates this issue by introducing a higher number of silirenes per linker-scaffold, and finally enables a light-mediated curing of silicones. Reproducible curing of hydride-, hydroxy-, or vinyl-functionalized polysiloxanes allows a versatile application for the most common silicone moieties used in industry, without the use of any metal-based catalyst. Mechanical properties of the elasto-

mers can be controlled by the mixing ratios. Employing higher concentrations of crosslinker L4 resulted in faster cured, harder silicone rubbers. Further, it was shown that the curing duration is dependent on the utilized polydimethylsiloxane (PDMS) functionalities. Longest irradiation times were required for the curing of hydroxy-terminated PDMS, while fastest solidification occurred for vinyl-functionalized PDMS. The presented method provides exemplary structures for this type of curing, yet additional modifications are required to further improve its efficiency in terms of synthesis, stability, or reaction rates. Especially the suppression of the rearrangement side reaction would help to considerably enhance the curing capability. Nevertheless, the presented results provide the proof of concept for a light controlled, metal- and additive-free curing process through multifunctional silirenes. Additionally, a major advantage is the broad applicability of the silirene linkers towards different PDMS functionalities. In summary, these features result in a genuine alternative to the conventional catalyst or heat-based curing methods.

### Acknowledgements

We acknowledge our principal funding source for this work, the WACKER Chemie AG. Dr. Wolfgang Schindler, Dr. Maximilian Moxter and Dr. Niklas Wienkenhöver are acknowledged for helpful discussions and advice. Open Access funding enabled and organized by Projekt DEAL.

### Conflict of Interest

The authors declare the following conflicts of interest: One patent application was filed (PCT/EP2021/064438) covering the methods reported in this paper.

### Data Availability Statement

The data that support the findings of this study are available in the supplementary material of this article.

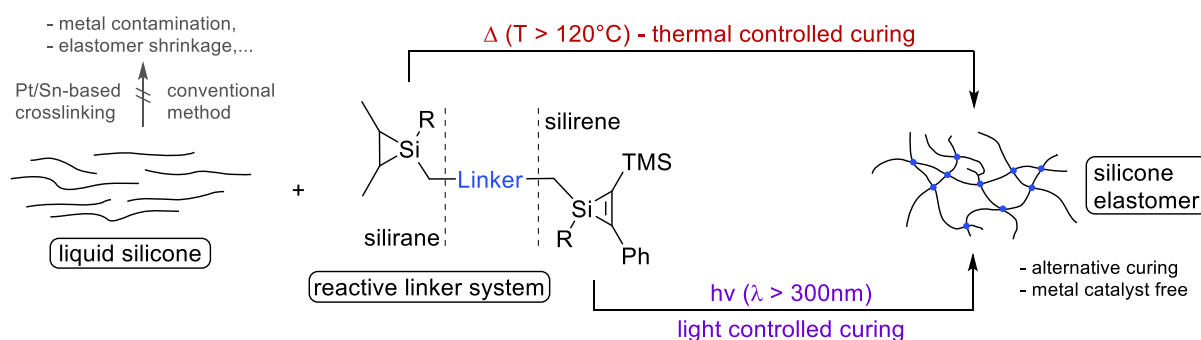
**Keywords:** metal-free · photo-curing · polysiloxanes · silacyclopropene · silylene

- [1] a) *Silicon in organic, organometallic, and polymer chemistry* (Ed.: M. A. Brook), Wiley, New York, 2000; b) *Thermal Properties of Polysiloxanes* (Ed.: P. R. Dvornic), Springer, Dordrecht, 2000; c) J. E. Mark, D. W. Schaefer, G. Lin, *The polysiloxanes*, Oxford University Press, New York, 2015.
- [2] a) *Handbook of thermoset plastics* (Ed.: H. Dodiuk), William Andrew, Norwich, 2022; b) M. Androit, *Silicones in industrial applications*, Inorganic Polymers, 2007.
- [3] GrandViewResearch Inc., *Silicone Market Size, Share & Trends Analysis Report by Product, by End-use, by Region, And Segment Forecasts, 2021–2028*, Report ID: GVR-1-68038-063-7, 2020.
- [4] *Polymer handbook* (Eds.: J. Brandrup, E. H. Immergut, E. A. Gulke, A. Abe, D. Bloch), Wiley, New York, 1999.
- [5] I. E. Markó, S. Stérin, O. Buisine, G. Berthon, G. Michaud, B. Tinant, J.-P. Declercq, *Adv. Synth. Catal.* **2004**, *346*, 1429.
- [6] National Research Council, *The Role of the Chemical Sciences in Finding Alternatives to Critical Resources: A Workshop Summary*, The National Academies Press, Washington D. C., 2012.
- [7] M. Y. Wong, A. F. Schneider, G. Lu, Y. Chen, M. A. Brook, *Green Chem.* **2019**, *21*, 6483.
- [8] G. Lu, A. F. Schneider, M. Vanderpol, E. K. Lu, M. Y. Wong, M. A. Brook, *Ind. Eng. Chem. Res.* **2021**, *60*, 15019.
- [9] F. A. D. Herz, M. Nobis, D. Wendel, P. Pahl, P. J. Altmann, J. Tillmann, R. Weidner, S. Inoue, B. Rieger, *Green Chem.* **2020**, *22*, 4489.
- [10] K. Goswami, A. L. Skov, A. E. Daugaard, *Chem. Eur. J.* **2014**, *20*, 9230.
- [11] R. Sønderbæk-Jørgensen, S. Meier, K. Dam-Johansen, A. L. Skov, A. E. Daugaard, *Macromol. Mater. Eng.* **2022**, 2200157.
- [12] C. Choi, J. L. Self, Y. Okayama, A. E. Levi, M. Gerst, J. C. Speros, C. J. Hawker, J. Read de Alaniz, C. M. Bates, *J. Am. Chem. Soc.* **2021**, *143*, 9866.
- [13] R. T. Conlin, P. P. Gaspar, *J. Am. Chem. Soc.* **1976**, *98*, 3715.
- [14] a) F. Lips, A. Mansikkamäki, J. C. Fettinger, H. M. Tuononen, P. P. Power, *Organometallics* **2014**, *33*, 6253; b) S. Ishida, T. Iwamoto, M. Kira, *Heteroat. Chem.* **2011**, *22*, 432; c) J. A. Baus, N. Laskowski, R. Tacke, *Chem. Ber.* **2016**, *2016*, 5182; d) Y. E. Türkmen in *Comprehensive Heterocyclic Chemistry IV* (Ed.: D. Black), Elsevier Science & Technology, San Diego, 2022, pp. 506–533.
- [15] M. Ishikawa, A. Naka, J. Ohshita, *Asian J. Org. Chem.* **2015**, *4*, 1192.
- [16] a) J. Ohshita, N. Honda, K. Nada, T. Iida, T. Mihara, Y. Matsuo, A. Kunai, A. Naka, M. Ishikawa, *Organometallics* **2003**, *22*, 2436; b) M. Ishikawa, K. Nishimura, H. Sugisawa, M. Kumada, *J. Organomet. Chem.* **1980**, *194*, 147; c) M. Ishikawa, H. Sugisawa, M. Kumada, H. Kawakami, T. Yamabe, *Organometallics* **1983**, *2*, 974.
- [17] a) M. Ishikawa, H. Sugisawa, T. Fuchikami, M. Kumada, T. Yamabe, H. Kawakami, K. Fukui, Y. Ueki, H. Shizuka, *J. Am. Chem. Soc.* **1982**, *104*, 2872; b) A. Sekiguchi, T. Tanaka, M. Ichinohe, K. Akiyama, S. Tero-Kubota, *J. Am. Chem. Soc.* **2003**, *125*, 4962; c) D. Seyferth, S. C. Vick, *J. Organomet. Chem.* **1977**, *125*, C11.
- [18] a) L. Wang, Y. Li, Z. Li, M. Kira, *Coord. Chem. Rev.* **2022**, *457*, 214413; b) C. Shan, S. Yao, M. Drieß, *Where silylene-silicon centres matter in the activation of small molecules*, Technische Universität Berlin, 2020.
- [19] R. R. Aysin, L. A. Leites, S. S. Bukalov, *Organometallics* **2020**, *39*, 2749.
- [20] M. S. Gordon, *J. Am. Chem. Soc.* **1980**, *102*, 7419.
- [21] a) T. Roychowdhury, C. V. Cushman, R. A. Synowicki, M. R. Linford, *Surf. Sci. Spectra* **2018**, *25*, 26001; b) D. Cai, A. Neyer, R. Kuckuk, H. M. Heise, *J. Mol. Struct.* **2010**, *976*, 274.
- [22] P. Boudjouk, E. Black, R. Kumarathasan, *Organometallics* **1991**, *10*, 2095.
- [23] S. Qiu, C. Zhang, R. Qiu, G. Yin, J. Huang, *Adv. Synth. Catal.* **2018**, *360*, 313.
- [24] R. West, L. C. Quass, *J. Organomet. Chem.* **1969**, *18*, 55.
- [25] a) S. Sekigawa, T. Shimizu, W. Ando, *Tetrahedron* **1993**, *49*, 6359; b) W. Uhlig, *J. Organomet. Chem.* **1997**, *545–546*, 281.
- [26] a) T. J. Barton, G. T. Burns, *Tetrahedron Lett.* **1983**, *24*, 159; b) M. Zielinski, M. Trommer, W. Sander, *Organometallics* **1999**, *18*, 2791; c) T. J. Barton, S. A. Burns, G. T. Burns, *Organometallics* **1983**, *2*, 199; d) M. Trommer, W. Sander, C. Marquard, *Angew. Chem. Int. Ed.* **1994**, *33*, 766.
- [27] M. Ishikawa, T. Fuchikami, M. Kumada, *J. Am. Chem. Soc.* **1977**, *99*, 245.
- [28] a) P. Boudjouk, U. Samaraweera, R. Sooriyakumaran, J. Chrusciel, K. R. Anderson, *Angew. Chem. Int. Ed.* **1988**, *27*, 1355; b) M. Ishikawa, M. Kumada in *Advances in Organometallic Chemistry* (Eds.: F. Stone, R. West), Academic Press, 1981, pp. 51–95.
- [29] M. Nobis, S. Inoue, B. Rieger, *Chem. Commun.* **2022**, *58*, 11159.
- [30] T. G. Mezger, *The Rheology Handbook*, Vincentz Network, 2012.

Manuscript received: October 21, 2022  
 Revised manuscript received: November 20, 2022  
 Accepted manuscript online: November 29, 2022  
 Version of record online: ■■■, ■■■■

## 7. Summary and Prospects

Throughout this work, alternative curing concepts in the context of metal-free and additive-free crosslinking of functionalized polysiloxanes have been investigated. Industrial curing of silicones is based on hydrosilylation, condensation or radical curing reactions. Albeit their effectiveness and advantages, each of these methods suffers from specific drawbacks, like rubber shrinkage, occurrence of side reactions or metal contamination of the final product. In regards of these problems, alternative curing methods have been developed on the basis of three-membered silacycles and their respective transient silylene species. The chemical motif of silylenes was chosen to avoid introducing additional heteroatoms into the silicone matrix and possibly deteriorating the final elastomer properties, while obtaining a highly reactive and fast curing agent, which can compete with conventional methods. As a first concept the thermally induced curing with multifunctional silacyclopropanes has been introduced. These organosilicon compounds function as crosslinker agents and can be utilized via two different reaction pathways. The silirane based linker scaffolds can directly be employed with hydroxy terminated polysiloxanes to afford the desired elastomer through a ring opening reaction of the silacycles with the hydroxy functionality. A second reaction pathway is facilitated by the thermal activation of these linker agents to generate the respective transient silylene species. Above the activation temperature of approximately 120 °C the silirane undergoes a fragmentation and transforms into the respective silylene. Thus, enabling the silylene linker to perform insertion reactions into hydride, hydroxy and alkoxy functionalized polysiloxanes. While the silirane linker compounds are stable at room temperature and can be pre-combined with the silicone material to afford a one-component curing mixture, the curing duration can be controlled and accelerated through an increase in temperature.<sup>[271]</sup>



**Scheme 39.** Alternative concepts based on silirane or silirene containing linker scaffolds for PDMS crosslinking.

To further broaden the scope of application, an additional curing concept has been developed by exploiting the photo activity of the unsaturated silacyclopropene moieties. Initial investigations on small monofunctional silirenes in a model study provided evidence for the photo lability and reactivity with common polysiloxane functionalities, including silanols, hydrosilanes, and vinylsilanes. Substitution of the 3-membered ring-system allowed effective tunability towards the required absorption properties. Due to the absorption of the silicone matrix the respective activation wavelength for the silirene had to be above 300 nm to be effectively exploited. Undesired rearrangement reactions through the photo-activation could be attenuated by minimizing silyl-substitution or reduction of the reaction temperature. Multifunctional silirene linker scaffolds were successfully obtained either via the silylene transfer reaction or utilization of modular silirenes. Bifunctional and tetrafunctional linkers were unable to create any silicone elastomers due to the reduced reaction selectivity caused by the formation of the rearrangement product. Polymeric crosslinkers compensate this issue by introducing a higher number of silirenes per linker-scaffold, and finally enables a light-mediated curing of silicones. Curing of hydroxy, hydride, or vinyl functionalized polysiloxanes allows a versatile application for common silicone moieties used in industry. These results provide the proof of concept for a light controlled, metal- and additive-free curing process through multifunctional silirenes. Additionally, a major advantage is the broad applicability of the silirene linkers towards different PDMS functionalities. In summary, these features result in a genuine alternative to the conventional catalyst or heat-based curing methods.<sup>[269]</sup> Regarding the synthesis of silirene linkers based on polymeric silicone structures, a new technique to afford higher functional silirenes was developed, overcoming the limiting scope of conventional synthesis procedures. The synthesis of silirenes and siliranes is a complex and delicate reaction sequence, prone to overreduction and various types of side reactions. With an increasing number of silirene moieties accumulating on one molecule or linker structure, this synthesis step becomes more and more intricate, eventually prohibiting the synthesis of highly functionalized silirenes entirely. By introducing monofunctional silirenes as modular building blocks, an access is provided to create higher functional silirene substrates. The covalent bonding of these modular units was afforded through a hydrosilylation reaction of the vinyl containing silirene unit with a Si-H containing material. Thus, the implementation of silirenes onto hydride functionalized PDMS via this facile grafting method allowed the generation of the desired polysiloxane based high functional silirene linker scaffolds.<sup>[272]</sup>

In conclusion, several new curing concepts to create polysiloxane elastomers have successfully been addressed. Thus, alternative and more sustainable possibilities have been demonstrated for silicone crosslinking, without the use of metal catalysis or hazardous additives. On the basis of three-membered silacycles and their respective transient silylene species both a thermal, as well as a photochemical curing process could be realized. Major advantages besides the metal omission and the consequent resource conservation, are the wide scope of applicable silicone functionalities, the controllable activation for various use cases and the possibility to create one component crosslinking mixtures. However, the reported concepts serve as an initial proof of concept for this type of curing and are a first step towards innovative curing methods. Nevertheless, additional research would help to better assess the potential of these concept in larger scales or industrial applications. The impact of this research will help to challenge the described economic and environmental issues and will directly contribute to the vision for more sustainable polymer materials and their production.

## 8. Literature

- [1] J. E. Mark, D. W. Schaefer, G. Lin, *The polysiloxanes*, Oxford University Press, New York, **2015**.
- [2] F. Ganachaud, S. Boileau, B. Boury, *Silicon Based Polymers. Advances in Synthesis and Supramolecular Organization*, Springer Netherlands, s.l., **2008**.
- [3] R. G. Jones, W. Ando, J. Chojnowski, *Silicon-Containing Polymers. The Science and Technology of Their Synthesis and Applications*, Springer Netherlands, Dordrecht, s.l., **2000**.
- [4] GrandViewResearch Inc., *Silicone Market Size, Share & Trends Analysis Report by Product, by End-use, by Region, And Segment Forecasts, 2021 - 2028*, Report ID: GVR-1-68038-063-7, **2020**.
- [5] H. Staudinger, *Ber. dtsch. Chem. Ges. A/B* **1920**, 53, 1073.
- [6] H. Frey, T. Johann, *Polym. Chem.* **2020**, 11, 8.
- [7] A. Taguet, B. Améduri, P. Penczek, *Crosslinking in materials science. Technical applications*, Springer, Berlin, London, **2011**.
- [8] *Polymer Surfaces and Interfaces*, Springer, Berlin, Heidelberg, **2008**.
- [9] N. Rubio, H. Au, H. S. Leese, S. Hu, A. J. Clancy, M. S. P. Shaffer, *Macromolecules* **2017**, 50, 7070.
- [10] S. Borova, P. Stahlhut, V. Tokarev, R. Luxenhofer, *Crosslinking of Hydrophilic Polymers Using Polyperoxides*, **2020**.
- [11] R. Januszewski, M. Dutkiewicz, M. Nowicki, I. Kownacki, *Polymer Testing* **2020**, 106516.
- [12] A. Bhattacharya, J. W. Rawlins, P. Ray, *Polymer grafting and crosslinking*, John Wiley, Hoboken, N.J., **2009**.
- [13] M. Kryszewski, *Polymer Blends. Volume 2: Processing, Morphology, and Properties*, Springer, New York, NY, **1984**.
- [14] J. J. Chruściel (Ed.) *Silicon-based polymers and materials*, De Gruyter, Berlin, Boston, **2022**.
- [15] G. Barroso, Q. Li, R. K. Bordia, G. Motz, *J. Mater. Chem. A* **2019**, 7, 1936.
- [16] M. E. Brito, H.-T. Lin, K. Plucknett (Eds.) *Ceramic transactions*, v. 142, American Ceramic Society, Westerville, Ohio, **2003**.
- [17] R. D. Miller, J. Michl, *Chem. Rev.* **1989**, 89, 1359.
- [18] F. S. Kipping, J. E. Sands, *J. Chem. Soc., Trans.* **1921**, 119, 830.
- [19] F. S. Kipping, *J. Chem. Soc., Trans.* **1924**, 125, 2291.
- [20] L. A. Harrah, J. M. Zeigler, *Macromolecules* **1987**, 20, 601.
- [21] R. D. Miller, R. Sooriyakumaran, *Macromolecules* **1988**, 21, 3120.
- [22] R. Horiguchi, Y. Onishi, S. Hayase, *Macromolecules* **1988**, 21, 304.
- [23] G. F. Parkin, K. Meyer, D. O'Hare (Eds.) *Comprehensive Organometallic Chemistry IV*, Elsevier, San Diego, **2022**.
- [24] S. M. Chen, L. D. David, K. J. Haller, C. L. Wadsworth, R. West, *Organometallics* **1983**, 2, 409.
- [25] R. D. Miller, D. Hofer, Mckean, C. G. Willson, R. West, P. Trefonas III in *by LF Thompson, CG Willson, and JM Frechet, ACS Symposium Series, New York*, pp. 293–310.
- [26] M. Fujino, H. Isaka, *J. Chem. Soc., Chem. Commun.* **1989**, 466.

- [27] S. Gauthier, D. J. Worsfold, *Macromolecules* **1989**, *22*, 2213.
- [28] R. H. Cragg, R. G. Jones, A. C. Swain, S. J. Webb, *J. Chem. Soc., Chem. Commun.* **1990**, 1147.
- [29] M. Cypryk, J. Chrusciel, E. Fossum, K. Matyjaszewski, *Makromolekulare Chemie. Macromolecular Symposia* **1993**, *73*, 167.
- [30] E. Fossum, K. Matyjaszewski, *Macromolecules* **1995**, *28*, 1618.
- [31] J. Chrusciel, K. Matyjaszewski, *J. Polym. Sci. A Polym. Chem.* **1996**, *34*, 2243.
- [32] K. Sakamoto, K. Obata, H. Hirata, M. Nakajima, H. Sakurai, *J. Am. Chem. Soc.* **1989**, *111*, 7641.
- [33] K. Sakamoto, M. Yoshida, H. Sakurai, *Macromolecules* **1990**, *23*, 4494.
- [34] P. Wisian-Neilson, H. R. Allcock, K. J. Wynne (Eds.) *ACS symposium series, Vol. 572*, American Chemical Society, Washington, DC, **1994**.
- [35] J. Weis, N. Auner (Eds.) *Organosilicon chemistry V. From molecules to materials*, Wiley-VCH, Weinheim, **2003**.
- [36] K. Hatada, T. Kitayama, O. Vogl (Eds.) *Plastics engineering, Vol. 40*, M. Dekker, New York, NY, **1997**.
- [37] F. Gauvin, J. F. Harrod, H. G. Woo, *Advances in organometallic chemistry* **1998**, *42*, 363.
- [38] T. D. Tilley, *Acc. Chem. Res.* **1993**, *26*, 22.
- [39] J. Y. Corey, *Advances in Silicon Chemistry* **1991**, 327.
- [40] S. Yajima, Y. Hasegawa, J. Hayashi, M. Iimura, *J Mater Sci* **1978**, *13*, 2569.
- [41] R. West, L. D. David, P. I. Djurovich, K. L. Stearley, K. S. V. Srinivasan, H. Yu, *J. Am. Chem. Soc.* **1981**, *103*, 7352.
- [42] J. Kido, K. Nagai, Y. Okamoto, T. Skotheim, *Appl. Phys. Lett.* **1991**, *59*, 2760.
- [43] A. Feigl, A. Bockholt, J. Weis, B. Rieger in *Advances in polymer science* (Ed.: A. M. Muzafarov), Springer Berlin Heidelberg, Berlin, Heidelberg, **2011**, pp. 1–31.
- [44] G. Fritz, *Angew. Chem. Int. Ed. Engl.* **1987**, *26*, 1111.
- [45] J. Simon, *Adv. Mater.* **1989**, *1*, 132.
- [46] Z.-F. Zhang, C. S. Scotto, R. M. Laine in *Ceramic engineering & science proceedings, v. 15, no. 4-5* (Eds.: J. B. Wachtman, K. V. Logan), American Ceramic Society, Westerville, Ohio, **1994**, pp. 152–161.
- [47] M. Birot, J.-P. Pillot, J. Dunogues, *Chem. Rev.* **1995**, *95*, 1443.
- [48] W. A. Kriner, *J. Polym. Sci. A-1 Polym. Chem.* **1966**, *4*, 444.
- [49] D. R. Weyenberg, L. E. Nelson, *J. Org. Chem.* **1965**, *30*, 2618.
- [50] B. Boury, R. J. P. Corriu, D. Leclercq, P. H. Mutin, J. M. Planeix, A. Vioux, *Organometallics* **1991**, *10*, 1457.
- [51] Y. Pang, S. Ijadi-Maghsoodi, T. J. Barton, *Macromolecules* **1993**, *26*, 5671.
- [52] E. D. Babich, *Polymeric Materials Encyclopedia, JC Salamone, Ed., CRC Press, New York* **1996**, *10*, 7621.
- [53] L. V. Interrante, I. Rushkin, Q. Shen, *Appl. Organometal. Chem.* **1998**, *12*, 695.
- [54] W. Habel, A. Oelschläger, P. Sartori, *Journal of Organometallic Chemistry* **1993**, *463*, 47.
- [55] L. V. Interrante, Q. Shen in *Silicon-Containing Polymers* (Eds.: R. G. Jones, W. Ando, J. Chojnowski), Springer Netherlands, Dordrecht, **2000**, pp. 247–321.
- [56] G. Levin, J. B. Carmichael, *J. Polym. Sci. A-1 Polym. Chem.* **1968**, *6*, 1.

- [57] A. Soum in *Silicon-Containing Polymers* (Eds.: R. G. Jones, W. Ando, J. Chojnowski), Springer Netherlands, Dordrecht, **2000**, pp. 323–349.
- [58] Jerzy J. Chruściel in *Silicon-based polymers and materials* (Ed.: J. J. Chruściel), De Gruyter, Berlin, Boston, **2022**.
- [59] B. J. Aylett, *Organomet. Chem. Rev* **1968**, *3*, 151.
- [60] Richard M. Laine, Yigal D. Blum, Doris Tse, Robert Glaser in *ACS symposium series, Vol. 360* (Ed.: M. Zeldin), American Chemical Soc, Washington, DC, **1988**, pp. 124–142.
- [61] D. Seyferth, G. H. Wiseman, C. Prud'homme, *J American Ceramic Society* **1983**, *66*, C-13-C-14.
- [62] A. Stock, K. Somieski, *Ber. dtsch. Chem. Ges. A/B* **1921**, *54*, 740.
- [63] W. Fink, *Angew. Chem.* **1966**, *78*, 803.
- [64] Y. Blum, R. M. Laine, *Organometallics* **1986**, *5*, 2081.
- [65] J. C. Salamone, *Polymeric materials encyclopedia*, CRC Press, Taylor & Francis Group, Boca Raton, FL, **2020**.
- [66] E. Duguet, M. Schappacher, A. Soum, *Polym. Int.* **1994**, *33*, 129.
- [67] D. Seyferth, J. M. Schwark, R. M. Stewart, *Organometallics* **1989**, *8*, 1980.
- [68] S. Bruzaud, A. Soum, *Macromol. Chem. Phys.* **1996**, *197*, 2379.
- [69] J. C. Baldwin, M. F. Lappert, J. B. Pedley, J. A. Treverton, *J. Chem. Soc., A* **1967**, 1980.
- [70] S. J. Clarson, J. J. Fitzgerald (Eds.) *ACS symposium series, Vol. 964*, American Chemical Soc, Washington, DC, **2007**.
- [71] C. R. Krüger, E. G. Rochow, *J. Polym. Sci. A Gen. Pap.* **1964**, *2*, 3179.
- [72] J. M. Zeigler, J. M. Zeigler, F. W. G. Fearon (Eds.) *Advances in chemistry series, Vol. 224*, ACS, Washington, D.C., **1991**.
- [73] S. J. Clarson, J. A. Semlyen, J. A. Semlyen, *Siloxane polymers*, Prentice Hall, Englewood Cliffs, NJ, **1993**.
- [74] H. R. Allcock, *Heteroatom ring systems and polymers*, Academic Press: New York, **1967**.
- [75] W. Noll, *Chemistry and Technology of Silicones*, Elsevier Science, Oxford, **1968**.
- [76] S. N. Borisov, *Organosilicon Heteropolymers and Heterocompounds*, Springer, New York, NY, **1970**.
- [77] H. R. Allcock, *Sci Am* **1974**, *230*, 66.
- [78] H. G. Elias, *Macromolecules. Volume 2: Synthesis, Materials, and Technology*, Springer, New York, NY, **1984**.
- [79] J. E. Mark, *Macromolecules* **1978**, *11*, 627.
- [80] E. L. Warrick, O. R. Pierce, K. E. Polmanteer, J. C. Saam, *Rubber Chemistry and Technology* **1979**, *52*, 437.
- [81] E. G. Rochow, *CHEMTECH* **1980**, *10*, 532.
- [82] M. J. Owen, *CHEMTECH* **1981**, *11*, 288.
- [83] Carraher, C. E., Jr., J. E. Sheats, *Advances in organometallic and inorganic polymer science*, New York, **1982**.
- [84] A. L. Smith, *Analysis of silicones*, Wiley, New York, **1974**.
- [85] B. Arkles, *CHEMTECH* **1983**, *13*, 542.
- [86] M. Zeldin (Ed.) *Inorganic and organometallic polymers. Macromolecules containing silicon, phosphorus, and other inorganic elements*, American Chemical Soc, Washington, DC, **1989**.



- [87] E. G. Rochow, *Silicon and silicones: about stone-age tools, antique pottery, modern ceramics, computers, space materials*, Springer-Verlag: Berlin, **1987**.
- [88] G. Koerner, M. Schulze, J. Weis, *Silicones, Chemistry and Technology*, CRC Press: Boca Raton, FL, **1991**.
- [89] M. A. Brook, *Silicon in organic, organometallic, and polymer chemistry*, Wiley, New York, **2000**.
- [90] J. E. Mark, *Progress in Polymer Science* **2003**, *28*, 1205.
- [91] J. E. Mark, H. R. Allcock, R. West, *Inorganic polymers*, Oxford University Press, New York, New York, **2005**.
- [92] E. Hey-Hawkins, M. Hissler (Eds.) *Smart Inorganic Polymers. Synthesis, Properties, and Emerging Applications in Materials and Life Sciences*, Wiley-VCH, Weinheim, **2019**.
- [93] A. Ladenburg, *Ann. Chem. Pharm.* **1872**, *164*, 300.
- [94] J. Ackermann, V. Damrath, *Chem. Unserer Zeit* **1989**, *23*, 86.
- [95] F. S. Kipping, L. L. Lloyd, *J. Chem. Soc., Trans.* **1901**, *79*, 449.
- [96] D. Wendel, D. Reiter, A. Porzelt, P. J. Altmann, S. Inoue, B. Rieger, *Journal of the American Chemical Society* **2017**, *139*, 17193.
- [97] A. C. Filippou, B. Baars, O. Chernov, Y. N. Lebedev, G. Schnakenburg, *Angew. Chem. Int. Ed. Engl.* **2014**, *53*, 565.
- [98] R. Schliebs, J. Ackermann, *Chem. Unserer Zeit* **1987**, *21*, 121.
- [99] imarcgroup Silicones Market: Global Industry Trends, Share, Size, Growth, Opportunity and Forecast 2022-2027. <https://www.imarcgroup.com/silicones-market> (accessed 03.11.2022).
- [100] B. Elvers, F. Ullmann (Eds.) *Ullmann's encyclopedia of industrial chemistry / ed Vol. B, Basic knowledge, Vol. 4*, VCH, Weinheim, **1992**.
- [101] B. Hardman, A. Torkelson, *Silicones: Encyclopedia of Polymer Science and Engineering*. 2nd ed. Koschwitz, J. I., Ed. Wiley-Interscience, New York, **1989**.
- [102] F. O. Stark, J. R. Falender, A. P. Wright, *Silicones, Comprehensive Organometallic Chemistry*, Pergamon Press: Oxford, **1982**.
- [103] L. N. Lewis in *ACS symposium series, Vol. 729* (Ed.: S. J. Clarson), American Chemical Society, Washington, D.C., **2000**, pp. 11–19.
- [104] C. H. van Dyke, *The Bond to Halogens and Halogenoids*, ed. AG. McDiarmid, Marcel Dekker, New York, **1972**.
- [105] L. Birkofer, O. Stuhl, *The chemistry of organic silicon compounds*, Wiley, New York, **1989**.
- [106] R. J. Voorhoeve (Ed.) *Organohalosilanes: Precursors to Silicones*, Elsevir, Amsterdam, **1969**.
- [107] M. P. Clarke, *Journal of Organometallic Chemistry* **1989**, *376*, 165.
- [108] Z. Rappoport, Y. Apeloig (Eds.) *The chemistry of functional groups, Vol. 2*, John Wiley & Sons, Ltd, Chichester, UK, **1998**.
- [109] R. L. Halm, R. H. Zapp, Dow Corning, Us. Pat., 4966986, **1989**.
- [110] K. M. Lewis, R. A. Cameron, J. M. Larnerd, B. Kanner, Union Carbide, Us. Pat., 4973725, **1989**.
- [111] W. Noll, *Physiological Behaviour*, Academic Press: Orlando, FL, **1968**.
- [112] G. N. Bokerman, S. K. Freeburne, L. M. Schuelke and D.G. VanKoevering, Dow Corning, US. Pat., 5075479, **1991**.

- [113] J. N. Kostas, Hercules Inc., U.S. Pat., 5491249, **1996**.
- [114] K. Itoh, T. Shinohara, H. Kizaki, S. Tanaka, Y. Satou and K. Umemura, Shin-Etsu, Us. Pat., 5473037, **1995**.
- [115] G. Allen (Ed.) *Comprehensive polymer science. The synthesis, characterization, reactions & applications of polymers*, Pergamon Pr, Oxford, **1989**.
- [116] F. Normand, X. W. He, J. M. Widmaier, G. C. Meyer, J. E. Herz, *European Polymer Journal* **1989**, 25, 371.
- [117] J. Burkhardt, K. Wegehaupt, Wacker, U.S. Pat., 4203913, **1980**.
- [118] J. Burkhardt, W. Streckel, A. Bilek, Wacker, E.P. 0258640/1988, **1988**.
- [119] W. T. Grubb, *J. Am. Chem. Soc.* **1954**, 76, 3408.
- [120] S. J. Clarson, Z. Wang, J. E. Mark, *European Polymer Journal* **1990**, 26, 621.
- [121] J. Chojnowski, K. Kaźmierski, S. Rubinsztajn, W. Stańczyk, *Makromol. Chem.* **1986**, 187, 2039.
- [122] W. Sarich, A. Surkus, D. Lange, E. Popowski, H. Kelling, *Z. anorg. allg. Chem.* **1990**, 581, 199.
- [123] M. Cypryk, S. Rubinsztajn, J. Chojnowski, *Journal of Organometallic Chemistry* **1993**, 446, 91.
- [124] S. Rubinsztajn, M. Cypryk, J. Chojnowski, *Macromolecules* **1993**, 26, 5389.
- [125] S. Rubinsztajn, M. Cypryk, J. Chojnowski, *Journal of Organometallic Chemistry* **1989**, 367, 27.
- [126] M. Guibergia-Pierron, G. Sauvet, *European Polymer Journal* **1992**, 28, 29.
- [127] G. Helary, G. Sauvet, *European Polymer Journal* **1992**, 28, 37.
- [128] X. W. He, J. M. Widmaier, J. E. Herz, G. C. Meyer, *European Polymer Journal* **1988**, 24, 1145.
- [129] K. Kaźmierski, J. Chojnowski, J. McVie, *European Polymer Journal* **1994**, 30, 515.
- [130] J. Chojnowski, M. Cypryk, W. Fortuniak, K. Kaźmierski, R. G. Taylor, *Journal of Organometallic Chemistry* **1996**, 526, 351.
- [131] G. Odian, G. G. Odian, *Principles of polymerization*, Wiley-Interscience, New York, **2004**.
- [132] A. Molenberg, M. Möller, *Macromol. Rapid Commun.* **1995**, 16, 449.
- [133] J. D. Kress, P. C. Leung, G. J. Tawa, P. J. Hay, *Journal of the American Chemical Society* **1997**, 119, 1954.
- [134] P. Dubois, O. Coulembier, J.-M. Raquez, *Handbook of ring-opening polymerization*, Wiley-VCH, Weinheim, **2009**.
- [135] M. D. Ninago, A. J. Satti, J. A. Ressia, A. E. Ciolino, M. A. Villar, E. M. Vallés, *J. Polym. Sci. A Polym. Chem.* **2009**, 47, 4774.
- [136] H. Qayouh, M. Lahcini, J.-L. Six, H. R. Kricheldorf, *J. Appl. Polym. Sci.* **2012**, 124, 4114.
- [137] C. M. Kuo, S. J. Clarson, *J Inorg Organomet Polym* **2012**, 22, 577.
- [138] L. Wilczek, S. Rubinsztajn, J. Chojnowski, *Die Makromolekulare Chemie* **1986**, 187, 39.
- [139] J. V. Crivello, R. Malik in *ACS Symposium Series*, American Chemical Society, Washington, DC, **2003**, pp. 284–295.
- [140] A. Apedaile, J. Liggat, J. Parkinson, G. Nikiforidis, L. Berlouis, M. Patel, *J. Appl. Polym. Sci.* **2012**, 123, 2601.
- [141] I. YILGÖR, J. S. RIFFLE, J. E. McGRATH in *ACS Symposium Series*, American Chemical Society, Washington, DC, **2003**, pp. 161–174.

- [142] J. E. McGrath, P. M. Sormani, C. S. Elsbernd, S. Kilic, *Makromolekulare Chemie. Macromolecular Symposia* **1986**, *6*, 67.
- [143] W. Noll, *Chemistry and Technology of Silicones*, Elsevier Science, Saint Louis, **2014**.
- [144] M.G. Voronokov, V.P. Mileshekevich, Y.A. Yuzhelevskii, *The Siloxane Bond. Consultants Bureau*, **1978**.
- [145] L. Pauling, *The nature of the chemical bond*, Cornell University Press, Ithaca, **1960**.
- [146] N. B. Hannay, C. P. Smyth, *J. Am. Chem. Soc.* **1946**, *68*, 171.
- [147] F. Stone, D. Seyferth, *Journal of Inorganic and Nuclear Chemistry* **1955**, *1*, 112.
- [148] H.-H. Grapengeter, B. Alefeld, R. Kosfeld, *Colloid & Polymer Sci* **1987**, *265*, 226.
- [149] R. L. P.R. Dvornic, *High temperature siloxane elastomers*, Hllthig and Wept, Basel, **1990**.
- [150] J. R. Durig, M. J. Flanagan, V. F. Kalasinsky, *The Journal of Chemical Physics* **1977**, *66*, 2775.
- [151] D. W. Scott, J. F. Messerly, S. S. Todd, G. B. Guthrie, I. A. Hossenlopp, R. T. Moore, A. Osborn, W. T. Berg, J. P. McCullough, *J. Phys. Chem.* **1961**, *65*, 1320.
- [152] S. J. Clarson, *Silicones and Silicone-Modified Materials: A Concise Overview*, American Chemical Society, Washington, DC, **2000**.
- [153] K. E. Polmanteer, M. J. Hunter, *Journal of Applied Polymer Science* **1959**, *1*, 3.
- [154] L. H. Sommer, F. A. Mitch, G. M. Goldberg, *J. Am. Chem. Soc.* **1949**, *71*, 2746.
- [155] P. R. Dvornic, J. D. Jovanovic, M. N. Govedarica, *Journal of Applied Polymer Science* **1993**, *49*, 1497.
- [156] A. J. Barry, *Journal of Applied Physics* **1946**, *17*, 1020.
- [157] S. Xu, R. G. Lehmann, J. R. Miller, G. Chandra, *Environ. Sci. Technol.* **1998**, *32*, 1199.
- [158] J. E. Mark, *Acc. Chem. Res.* **2004**, *37*, 946.
- [159] R.R. McGregor, *Silicones and their uses*, McGraw Hill, New York, **1954**.
- [160] L.-H. Lee (Ed.) *Polymer Science and Technology, Vol. 5*, Springer, Boston, MA, **1975**.
- [161] R. F. WILLIS, *Nature* **1969**, *221*, 1134.
- [162] M. Shansong, T. Mei, T. Shunqing, Z. Changren, *J. Mater. Sci.* **2003**, *22*, 343.
- [163] D. Fallahi, H. Mirzadeh, M. T. Khorasani, *Journal of Applied Polymer Science* **2003**, *88*, 2522.
- [164] Y. Sugahara, S. Okada, K. Kuroda, C. Kato, *Journal of Non-Crystalline Solids* **1992**, *139*, 25.
- [165] H.-K. Chu, R. P. Cross, D. I. Crossan, *Journal of Organometallic Chemistry* **1992**, *425*, 9.
- [166] J. March, *Advanced organic chemistry. 7th Edition*, Wiley, New York, **2007**.
- [167] P. E. Dietze, *J. Org. Chem.* **1993**, *58*, 5653.
- [168] H. Slebocka-Tilk, R. S. Brown, *J. Org. Chem.* **1985**, *50*, 4638.
- [169] F. W. van der Weij, *Die Makromolekulare Chemie* **1980**, *181*, 2541.
- [170] R. G. Jones, W. Ando, J. Chojnowski (Eds.) *Silicon-Containing Polymers*, Springer Netherlands, Dordrecht, **2000**.
- [171] S. C. Shit, P. Shah, *Natl. Acad. Sci. Lett.* **2013**, *36*, 355.
- [172] A. K. Roy, *Advances in organometallic chemistry* **2007**, *55*, 1.
- [173] I. E. Markó, S. Stérin, O. Buisine, G. Berthon, G. Michaud, B. Tinant, J.-P. Declercq, *Adv. Synth. Catal.* **2004**, *346*, 1429.
- [174] B. Marciniec, *Hydrosilylation. A Comprehensive Review on Recent Advances*, Springer Netherlands, Dordrecht, **2009**.

- [175] R. A. Benkeser, S. Dunny, G. S. Li, P. G. Nerlekar, S. D. Work, *J. Am. Chem. Soc.* **1968**, *90*, 1871.
- [176] M. L. Dunham, D. L. Bailey, R. Y. Mixer, *Ind. Eng. Chem.* **1957**, *49*, 1373.
- [177] M. Newcomb, *Tetrahedron* **1993**, *49*, 1151.
- [178] M. Y. Wong, A. F. Schneider, G. Lu, Y. Chen, M. A. Brook, *Green Chem.* **2019**, *21*, 6483.
- [179] G. Lu, A. F. Schneider, M. Vanderpol, E. K. Lu, M. Y. Wong, M. A. Brook, *Ind. Eng. Chem. Res.* **2021**, *60*, 15019.
- [180] T. Rambarran, F. Gonzaga, M. A. Brook, *Macromolecules* **2012**, *45*, 2276.
- [181] E. M. Burgess, R. Carithers, L. McCullagh, *J. Am. Chem. Soc.* **1968**, *90*, 1923.
- [182] M. A. Brook, *Chemistry European Journal* **2018**, *24*, 8458.
- [183] C. Choi, J. L. Self, Y. Okayama, A. E. Levi, M. Gerst, J. C. Speros, C. J. Hawker, J. Read de Alaniz, C. M. Bates, *Journal of the American Chemical Society* **2021**, *143*, 9866.
- [184] K. Goswami, A. L. Skov, A. E. Daugaard, *Chemistry – A European Journal* **2014**, *20*, 9230.
- [185] R. Sønderbæk-Jørgensen, S. Meier, K. Dam-Johansen, A. L. Skov, A. E. Daugaard, *Macro Materials & Eng* **2022**, 2200157.
- [186] M. L. Lepage, C. Simhadri, C. Liu, M. Takaffoli, L. Bi, B. Crawford, A. S. Milani, J. E. Wulff, *Science (New York, N.Y.)* **2019**, *366*, 875.
- [187] N. J. Hill, R. West, *Journal of Organometallic Chemistry* **2004**, *689*, 4165.
- [188] R. West, M. J. Fink, J. Michl, *Science* **1981**, *214*, 1343.
- [189] S. Masamune, Y. Hanzawa, S. Murakami, T. Bally, J. F. Blount, *J. Am. Chem. Soc.* **1982**, *104*, 1150.
- [190] M. Weidenbruch, *Chem. Rev.* **1995**, *95*, 1479.
- [191] D. Seyferth, D. C. Annarelli, *Journal of the American Chemical Society* **1975**, *97*, 2273.
- [192] W. Ando, Y. Hamada, A. Sekiguchi, *Tetrahedron Letters* **1984**, *25*, 5057.
- [193] K. R. Pichaandi, J. T. Mague, M. J. Fink, *Journal of Organometallic Chemistry* **2015**, *791*, 163.
- [194] R. R. Aysin, L. A. Leites, S. S. Bukalov, *Organometallics* **2020**, *39*, 2749.
- [195] D. Seyferth, S. C. Vick, M. L. Shannon, *Organometallics* **1984**, *3*, 1897.
- [196] M. Ishikawa, A. Naka, J. Ohshita, *Asian J. Org. Chem.* **2015**, *4*, 1192.
- [197] T. Iwamoto, S. Ishida in *Organosilicon Compounds*, Elsevier, **2017**, pp. 361–532.
- [198] R. West, M. Denk, *Pure and Applied Chemistry* **1996**, *68*, 785.
- [199] M. Denk, R. Lennon, R. Hayashi, R. West, A. V. Belyakov, H. P. Verne, A. Haaland, M. Wagner, N. Metzler, *Journal of the American Chemical Society* **1994**, *116*, 2691.
- [200] B. Gehrhus, M. F. Lappert, *Journal of Organometallic Chemistry* **2001**, *617-618*, 209.
- [201] Y. Mizuhata, T. Sasamori, N. Tokitoh, *Chem. Rev.* **2009**, *109*, 3479.
- [202] G. Trinquier, *J. Am. Chem. Soc.* **1990**, *112*, 2130.
- [203] M. Driess, H. Grützmacher, *Angew. Chem.* **1996**, *108*, 900.
- [204] P. P. Power, *Chem. Rev.* **1999**, *99*, 3463.
- [205] A. F. Hill, M. J. Fink, *Advances in organometallic chemistry*, Academic Press, Amsterdam, **2008**.
- [206] L. Wang, Y. Li, Z. Li, M. Kira, *Coordination Chemistry Reviews* **2022**, *457*, 214413.
- [207] P. Jutzi, D. Kanne, C. Krüger, *Angew. Chem. Int. Ed. Engl.* **1986**, *25*, 164.
- [208] M. Denk, R. Lennon, R. Hayashi, R. West, A. V. Belyakov, H. P. Verne, A. Haaland, M. Wagner, N. Metzler, *J. Am. Chem. Soc.* **1994**, *116*, 2691.

- [209] G.-H. Lee, R. West, T. Müller, *J. Am. Chem. Soc.* **2003**, *125*, 8114.
- [210] I. Alvarado-Beltran, A. Baceiredo, N. Saffon-Merceron, V. Branchadell, T. Kato, *Angew. Chem.* **2016**, *128*, 16375.
- [211] A. Rosas-Sánchez, I. Alvarado-Beltran, A. Baceiredo, N. Saffon-Merceron, S. Massou, V. Branchadell, T. Kato, *Angew. Chem.* **2017**, *129*, 10685.
- [212] V. Jouikov, V. Krasnov, *Journal of Organometallic Chemistry* **1995**, *498*, 213.
- [213] M. J. S. Dewar, *J. Am. Chem. Soc.* **1984**, *106*, 669.
- [214] D. Cremer, *Tetrahedron* **1988**, *44*, 7427.
- [215] K. Exner, P. v. R. Schleyer, *J. Phys. Chem. A* **2001**, *105*, 3407.
- [216] A. Skancke, D. van Vechten, J. F. Liebman, P. N. Skancke, *Journal of Molecular Structure* **1996**, *376*, 461.
- [217] H. Wang, *Comprehensive Organic Name Reactions*, Wiley, New York, **2010**.
- [218] R. L. Lambert, D. Seyferth, *J. Am. Chem. Soc.* **1972**, *94*, 9246.
- [219] M. Ishikawa, M. Kumada, *Journal of Organometallic Chemistry* **1972**, *42*, 325.
- [220] W. Ando, M. Fujita, H. Yoshida, A. Sekiguchi, *J. Am. Chem. Soc.* **1988**, *110*, 3310.
- [221] M. Kira, S. Ishida, T. Iwamoto, A. de Meijere, M. Fujitsuka, O. Ito, *Angew. Chem. Int. Ed.* **2004**, *43*, 4510.
- [222] T. Iwamoto, M. Kobayashi, K. Uchiyama, S. Sasaki, S. Nagendran, H. Isobe, M. Kira, *Journal of the American Chemical Society* **2009**, *131*, 3156.
- [223] P. Boudjouk, E. Black, R. Kumarathasan, *Organometallics* **1991**, *10*, 2095.
- [224] A. F. Holleman, *Lehrbuch der anorganischen Chemie*, De Gruyter, Berlin, Boston, **2019**.
- [225] P. Boudjouk, U. Samaraweera, R. Sooriyakumaran, J. Chrusciel, K. R. Anderson, *Angew. Chem. Int. Ed. Engl.* **1988**, *27*, 1355.
- [226] H. M. Cho, K. Bok, S. H. Park, Y. M. Lim, M. E. Lee, M.-G. Choi, K. M. Lee, *Organometallics* **2012**, *31*, 5227.
- [227] D. Seyferth, D. C. Annarelli, S. C. Vick, D. P. Duncan, *Journal of Organometallic Chemistry* **1980**, *201*, 179.
- [228] J. Ciraković, T. G. Driver, K. A. Woerpel, *J. Am. Chem. Soc.* **2002**, *124*, 9370.
- [229] J. Ciraković, T. G. Driver, K. A. Woerpel, *J. Org. Chem.* **2004**, *69*, 4007.
- [230] T. G. Driver, K. A. Woerpel, *J. Am. Chem. Soc.* **2004**, *126*, 9993.
- [231] W. S. Palmer, K. A. Woerpel, *Organometallics* **2001**, *20*, 3691.
- [232] F. Lips, J. C. Fettinger, A. Mansikkamäki, H. M. Tuononen, P. P. Power, *Journal of the American Chemical Society* **2014**, *136*, 634.
- [233] D. A. W. Wendel, *Synthesis and Reactivity of Acyclic Silylenes: On the Way to Metal-free Catalysis*, Dissertation, Technische Universität München, Garching, **2018**.
- [234] K. R. Pichaandi, J. T. Mague, M. J. Fink, *Journal of Organometallic Chemistry* **2011**, *696*, 1957.
- [235] D. H. Pae, M. Xiao, M. Y. Chiang, P. P. Gaspar, *J. Am. Chem. Soc.* **1991**, *113*, 1281.
- [236] D. Seyferth, *Journal of Organometallic Chemistry* **1975**, *100*, 237.
- [237] J. T. Shaw, K. A. Woerpel, *J. Org. Chem.* **1997**, *62*, 442.
- [238] P. M. Bodnar, W. S. Palmer, B. H. Ridgway, J. T. Shaw, J. H. Smitrovich, K. A. Woerpel, *J. Org. Chem.* **1997**, *62*, 4737.
- [239] A. K. Franz, K. A. Woerpel, *Acc. Chem. Res.* **2000**, *33*, 813.
- [240] P. T. Nguyen, W. S. Palmer, K. A. Woerpel, *J. Org. Chem.* **1999**, *64*, 1843.

- [241] Z. Nevárez, K. A. Woerpel, *Organic letters* **2007**, *9*, 3773.
- [242] F.A.D. Herz, *Neue metallfreie Vernetzungsverfahren für Polysiloxane unter Verwendung multifunktionaler Silirane und Silylene*, Dissertation, Technische Universität München, Garching, **2020**.
- [243] A. Rey Planells, A. Espinosa Ferao, *Inorganic chemistry* **2022**.
- [244] M. S. Gordon, *J. Am. Chem. Soc.* **1980**, *102*, 7419.
- [245] M. Ishikawa, K. Nishimura, H. Sugisawa, M. Kumada, *J. Organomet. Chem.* **1980**, *194*, 147.
- [246] M. E. Volpin, Y. D. Koreshkov, V. G. Dulova, D. N. Kursanov, *Tetrahedron* **1962**, *18*, 107.
- [247] W. H. Atwell, D. R. Weyenberg, *Angew. Chem. Int. Ed. Engl.* **1969**, *8*, 469.
- [248] W. H. Atwell, D. R. Weyenberg, *J. Am. Chem. Soc.* **1968**, *90*, 3438.
- [249] R. T. Conlin, P. P. Gaspar, *J. Am. Chem. Soc.* **1976**, *98*, 3715.
- [250] D. Seyferth, D. C. Annarelli, S. C. Vick, *J. Am. Chem. Soc.* **1976**, *98*, 6382.
- [251] D. Seyferth, S. C. Vick, *J. Organomet. Chem.* **1977**, *125*, C11.
- [252] M. Ishikawa, K.-I. Nakagawa, M. Ishiguro, F. Ohi, M. Kumada, *J. Organomet. Chem.* **1978**, *152*, 155.
- [253] M. Ishikawa, H. Sugisawa, K. Yamamoto, M. Kumada, *Journal of Organometallic Chemistry* **1979**, *179*, 377.
- [254] S. Yao, Y. Xiong, M. Driess, *Organometallics* **2011**, *30*, 1748.
- [255] S. Yao, C. van Wüllen, X.-Y. Sun, M. Driess, *Angew. Chem. Int. Ed. Engl.* **2008**, *47*, 3250.
- [256] S. Ishida, T. Iwamoto, M. Kira, *Heteroatom Chem.* **2011**, *22*, 432.
- [257] B. D. Reken, T. M. Brown, J. C. Fettinger, F. Lips, H. M. Tuononen, R. H. Herber, P. P. Power, *Journal of the American Chemical Society* **2013**, *135*, 10134.
- [258] M. Ishikawa, M. Kumada in *Advances in Organometallic Chemistry* (Eds.: F. Stone, R. West), Academic Press, **1981**, pp. 51–95.
- [259] M. Ishikawa, H. Sugisawa, M. Kumada, T. Higuchi, K. Matsui, K. Hirotsu, *Organometallics* **1982**, *1*, 1473.
- [260] M. Ishikawa, H. Sugisawa, T. Fuchikami, M. Kumada, T. Yamabe, H. Kawakami, K. Fukui, Y. Ueki, H. Shizuka, *J. Am. Chem. Soc.* **1982**, *104*, 2872.
- [261] J. Ohshita, N. Honda, K. Nada, T. Iida, T. Mihara, Y. Matsuo, A. Kunai, A. Naka, M. Ishikawa, *Organometallics* **2003**, *22*, 2436.
- [262] M. Ishikawa, T. Fuchikami, M. Kumada, *Journal of the American Chemical Society* **1977**, *99*, 245.
- [263] M. Ishikawa, T. Fuchikami, M. Kumada, *Journal of Organometallic Chemistry* **1977**, *142*, C45-C48.
- [264] M. Ishikawa, H. Sugisawa, M. Kumada, H. Kawakami, T. Yamabe, *Organometallics* **1983**, *2*, 974.
- [265] M. Ishikawa, K. Nakagawa, S. Katayama, M. Kumada, *J. Am. Chem. Soc.* **1981**, *103*, 4170.
- [266] W. H. Atwell, J. G. Uhlmann, *Journal of Organometallic Chemistry* **1973**, *52*, C21-C23.
- [267] D. Seyferth, D. P. Duncan, S. C. Vick, *J. Organomet. Chem.* **1977**, *125*, C5.
- [268] D. Seyferth, S. C. Vick, M. L. Shannon, T. F. Lim, D. P. Duncan, *Journal of Organometallic Chemistry* **1977**, *135*, C37-C44.
- [269] M. Nobis, J. Futter, M. Moxter, S. Inoue, B. Rieger, *ChemSusChem* **2022**, e202201957.

- [270] National Research Council, *The Role of the Chemical Sciences in Finding Alternatives to Critical Resources: A Workshop Summary*, The National Academies Press, Washington (DC), **2012**.
- [271] F. A. D. Herz, M. Nobis, D. Wendel, P. Pahl, P. J. Altmann, J. Tillmann, R. Weidner, S. Inoue, B. Rieger, *Green Chem.* **2020**, *22*, 4489.
- [272] M. Nobis, S. Inoue, B. Rieger, *Chemical Communications* **2022**, *58*, 11159.

## 9. Appendix

## 9.1. List of Figures

<b>Figure 1.</b> Schematic overview of different polymer association. (I) “Physisorption” describes the reversible attachment of polymers through physical attractive forces. (II) “Grafting from” is the covalent attachment of a monomer to a polymer chain followed by a polymerization, while (III) “grafting to” is referred to the functionalization of the polymer backbone with already finished polymer to create branches. (IV) “Crosslinking” describes the irreversible formation of a polymer network via chemical bonding of the individual polymer chains.....	4
<b>Figure 2.</b> Representation and chemical structure of polysilanes consisting of a continuous silicon-silicon bond. ....	5
<b>Figure 3.</b> Depiction and chemical structure of linear polycarbosilanes of alternating silicon-carbon bonds.....	8
<b>Figure 4.</b> Depiction and chemical structure of linear polysilazanes, with a backbone of repeating Si-N bonds.....	10
<b>Figure 5.</b> General depiction and chemical structure of the Si-O backbone present in a polysiloxane chain. ....	12
<b>Figure 6.</b> Industrial refinement of silica SiO <sub>2</sub> to elemental silicon by a reductive carbothermal reaction. ....	14
<b>Figure 7.</b> Characteristic properties of a polydimethylsiloxane chain, such as bond length, enthalpy, or angle. ....	18
<b>Figure 8.</b> Hydrosilylation mechanism via oxidative addition of the hydrosilane to the platinum, followed by the insertion of the olefine, and finalization by the reductive elimination of the carbosilanes closes the reaction cycle. ....	24
<b>Figure 9.</b> Selection of relevant organosilicon compounds and their description (X = F, Cl, Br, I).....	34
<b>Figure 10.</b> Comparison of singlet-triplet energy difference, hybridization energy, stability and metal character of the divalent compounds within the group 14 elements and orbital depiction of the triplet and singlet ground states. ....	37
<b>Figure 11.</b> Different bonding models for the dimerization of single- and triplet-ground state fragments and their resulting molecular geometry. ....	38
<b>Figure 12.</b> Depiction of stabilization methods for silylene compounds via kinetic or thermodynamic control. ....	40
<b>Figure 13.</b> Comparison of silacyclopropanes and cyclopropanes in regard to bond-lengths, angles, and ring strain. ....	40
<b>Figure 14.</b> Overview of some literature known stable and isolable silacyclopropanes.....	44
<b>Figure 15.</b> Top: Comparison of the calculated C=C bond lengths and apex bond angles of silacyclopropanes, silacyclopropenes, and cyclopropenes in combination with their resulting ring strain energy (RSE). <sup>[243]</sup> Bottom: Depiction of the aromaticity in silacyclopropenes and their respective MO overlap. <sup>[194]</sup> .....	47
<b>Figure 16.</b> Table of Content for the manuscript titled “Application of multifunctional silylenes and siliranes as universal crosslinkers for metal-free curing of silicones” .....	54
<b>Figure 17.</b> Table of content for the manuscript titled “Modular silacyclopropenes: synthesis and application for Si–H containing substrate functionalization” .....	65
<b>Figure 18.</b> Table of content for the manuscript titles “Photo-Activity of Silacyclopropenes and their Application in Metal-Free Curing of Silicones“ .....	71



## 9.2. List of Schemes

<b>Scheme 1.</b> Overview of synthetic processes to generate polysilanes. (a) Reductive Wutz-type coupling of dichlorosilanes. (b) Ring-Opening Polymerization of cyclotetrasilanes. (c) Anionic polymerization of masked disilenes mediated by organolithium compounds. (d) Dehydrogenative coupling of organosilanes by metallocene based catalysts. ....	6
<b>Scheme 2.</b> General procedures to create different polycarbosilanes. (a) Platin catalyzed ROP of disilacyclobutane. <sup>[48]</sup> (b) thermal ROP of monosilacyclobutane. <sup>[52]</sup> (c) Initial Wurtz coupling reaction, subsequent reduction with AlCl <sub>3</sub> and final substitution via Grignard coupling. <sup>[54]</sup> (d) Hydrosilylation polymerization of vinyl dimethylsilane <sup>[50]</sup> and (e) hydrosilylation polymerization of acetylenedimethylsilane. <sup>[51]</sup> .....	9
<b>Scheme 3.</b> Synthesis overview for producing polysilazanes. (a) Polycondensation via aminolysis reaction of dichlorosilane with amines. (b) Cationic ROP initiated by methyl triflate to polymerize cyclodisilazane. (c) Anionic ring opening polymerization of cyclodisilazane mediated via benzyl lithium. ....	11
<b>Scheme 4.</b> Transformation of elemental silicon to organosilicon compounds. (a) Chlorination of silicon, followed by a Grignard reaction. (b) Transformation of silicon into silyl hydrides with subsequent hydrosilylation reaction. (c) "Direct Process" or "Müller-Rochow-Process" to convert silicon directly into the organosilicon species.....	14
<b>Scheme 5.</b> Two-step process to afford polysiloxanes. Initial hydrolysis/methanolysis of the organochlorosilane to obtain linear or cyclic siloxane oligomers. Subsequent polymerization via polycondensation or ROP.....	15
<b>Scheme 6.</b> Polycondensation processes to obtain polysiloxanes via homo- or heterofunctional approaches. ....	16
<b>Scheme 7.</b> Anionic and cationic ring opening polymerization processes of cyclic siloxane monomer units.....	17
<b>Scheme 8.</b> Equilibration of linear and cyclic polysiloxanes to create high molecular polysiloxane material. ....	17
<b>Scheme 9.</b> Condensation curing of hydroxy-terminated polysiloxanes with a variety of silane derivate linkers. ....	21
<b>Scheme 10.</b> Comparison of the condensation curing process RTV-1 (one-component system) and RTV-2 (two-component system) by using tin-based catalysis to generate silicone elastomers.....	22
<b>Scheme 11.</b> Addition curing of hydrid- and vinyl-functionalized PDMS via a transition metal catalyzed hydrosilylation reaction.....	23
<b>Scheme 12.</b> Overview of commonly used radical initiators and inhibitors for the HTV curing process of silicones.....	26
<b>Scheme 13.</b> HTV or Radical curing of polysiloxanes with organic peroxides. Overview of possible reaction pathways dependent on the type of polysiloxane functionality and crosslinking conditions.	27
<b>Scheme 14.</b> Thermal oxidative crosslinking of hydrosilane functionalized PDMS by employing molecular oxygen. ....	28
<b>Scheme 15.</b> Schematic overview of the metal free curing via click ligation of alkyne and azide functionalized PDMS. ....	29
<b>Scheme 16.</b> Piers-Rubinsztajn catalyzed curing of hydride functionalized with multifunctional silyl-ethers.....	30
<b>Scheme 17.</b> Crosslinking of cyclic disulfide functionalized PDMS through UV-light mediated initiation to afford bottlebrush elastomers containing two different types of polymer backbones. ....	31
<b>Scheme 18.</b> Thiol-ene based curing to create PDMS elastomers from vinyl- and thiol-functionalized polysiloxanes. ....	31

---

<b>Scheme 19.</b> Overview of the underlying polysilazane fragmentation mechanism (top) and the resulting curing concept based on the reaction with carbinol functionalized PDMS (bottom).....	32
<b>Scheme 20.</b> Carbene based curing of polysiloxane through thermal or light induced activation of bis-diaziridines.....	33
<b>Scheme 21.</b> Common synthetic approaches to create silylenes by employing different types of silicon precursors.....	35
<b>Scheme 22.</b> Exemplary synthesis of silylenes through thermal or photochemical induced Si-Si cleavage.....	35
<b>Scheme 23.</b> Fragmentation of stable three-membered silacycles to obtain the desired silylenes. ....	36
<b>Scheme 24.</b> Reduction of dihalosilanes with different reducing agents to afford the respective silylenes. ....	36
<b>Scheme 25.</b> Silylene reactivity overview of $\sigma$ -, $\pi$ -bond insertion as well as dimerization and polymerization reactions. <sup>[206]</sup> .....	39
<b>Scheme 26.</b> First synthesis of a stable silacyclopropane by Seyferth et al. in 1972 via the Wurtz-coupling reaction.....	41
<b>Scheme 27.</b> Silane photolysis reaction to create the silirane in the presence of butene reported by Sekiguchi, as well as the mechanistic theory to explain the respective reaction pathway, provided by Kira et al.....	42
<b>Scheme 28.</b> Lithium based reduction of 1,1-dibromosilane through the formation of a silylenoide species. ....	43
<b>Scheme 29.</b> Proposed mechanism of the silver-catalyzed silylene transfer reaction in the presence of styrene.....	44
<b>Scheme 30.</b> Selection of ring-opening reactions of various nucleophiles with silacyclopropanes.....	45
<b>Scheme 31.</b> Overview of different cycloaddition reactions with carbonyls, alkynes, isocyanides, and imines. ....	45
<b>Scheme 32.</b> Equilibrium reaction of siliranes and silylenes, with possible consecutive reactions of the transient silylene. ....	46
<b>Scheme 33.</b> Overview of various synthesis methods to generate silacyclopropenes through different approaches. ....	48
<b>Scheme 34.</b> Thermal dimerization reaction of silacyclopropenes to afford dimeric six-membered silacycles.....	49
<b>Scheme 35.</b> Insertion reactions of silacyclopropenes via one- and two-atom insertion. One-atom insertions proceed via the reaction with silylenes, while two-atom insertions occur in combination with alkynes or aldehydes.....	50
<b>Scheme 36.</b> Overview of differently substituted silacyclopropenes and their different behavior upon irradiation.....	51
<b>Scheme 37.</b> Conceptual crosslinking method based on the application of silylenes with functionalized silicones. ....	53
<b>Scheme 38.</b> Protecting of the silylene through silacyclopropane precursor structures, gaining synthesis and application control.....	53
<b>Scheme 39.</b> Alternative concepts based on silirane or silirene containing linker scaffolds for PDMS crosslinking.....	81

### 9.3. List of Tables

<b>Table 1:</b> General abbreviations. ....	V
<b>Table 2:</b> Abbreviations for formula signs. ....	VI
<b>Table 3:</b> Abbreviations for methods.....	VII

## 9.4. Supporting Information

### 9.4.1. Supporting Information for Chapter 4

Electronic Supplementary Material (ESI) for Green Chemistry.  
This journal is © The Royal Society of Chemistry 2020

#### SUPPORTING INFORMATION

---

### Supporting Information

#### Application of Multifunctional Silylenes and Siliranes as Universal Crosslinkers for Metal-Free Curing of Silicones

Fabian A. D. Herz,<sup>a,b,†</sup> Matthias Nobis,<sup>a,b,†</sup> Daniel Wendel,<sup>a,b</sup> Philipp Pahl,<sup>a</sup> Philipp J. Altmann,<sup>c</sup> Jan Tillmann,<sup>d</sup> Richard Weidner,<sup>d</sup> Shigeyoshi Inoue,<sup>b</sup> and Bernhard Rieger\*<sup>a,b</sup>

a. Technical University of Munich, WACKER-Chair of Macromolecular Chemistry  
Lichtenbergstraße 4, 85748 Garching bei München, Germany.  
E-mail: rieger@tum.de

b. Technical University of Munich, WACKER-Institute of Silicon Chemistry  
Lichtenbergstraße 4, 85748 Garching bei München, Germany.

c. Technical University of Munich, Catalysis Research Center  
Ernst-Otto-Fischer-Straße 1, 85748 Garching bei München, Germany.

d. WACKER Chemie AG, Consortium für elektrochemische Industrie  
Zielstattstraße 20, 81379 München, Germany.

† Authors contributed equally to this work.

## SUPPORTING INFORMATION

## Table of Contents

1.	General Methods and Instrumentation .....	3
2.	Synthesis and Characterization of New Compounds .....	4
2.1.1.	Synthesis of <i>cis</i> -1,1-di- <i>tert</i> -butyl-2,3-dimethylsilirane/ <i>trans</i> -1,1-di- <i>tert</i> -butyl-2,3-dimethylsilirane <b>1</b> .....	4
2.2.	Multifunctional Silirane Crosslinkers 5–10 .....	4
2.2.1.	General Procedure for Multifunctional Silirane Crosslinkers <b>5–10</b> .....	4
2.2.2.	1,3-Bis(1,1-di- <i>tert</i> -butylsilirane-2-yl)-1,1,3,3-tetramethyldisiloxane <b>5</b> .....	5
2.2.3.	Tetrakis(1,1-di- <i>tert</i> -butylsilirane-2-yl)silane <b>6</b> .....	6
2.2.4.	2,4,6,8-Tetrakis(1,1-di- <i>tert</i> -butylsilirane-2-yl)-2,4,6,8-tetramethyl-cyclotetrasiloxane <b>7</b> .....	8
2.2.5.	Tetrakis((1,1-di- <i>tert</i> -butylsilirane-2-yl)methyl)silane <b>8</b> .....	10
2.2.6.	Poly(((1,1-di- <i>tert</i> -butylsilirane-2-yl)methylsiloxane)-co-dimethylsiloxane) Copolymer <b>9</b> .....	12
2.2.7.	Poly(((1,1-di- <i>tert</i> -butylsilirane-2-yl)methylsiloxane)-co-dimethylsiloxane) Copolymer <b>10</b> .....	15
2.3.	Difunctional Silirane Crosslinkers 15-16 .....	18
2.3.1.	1,1,3,3-Tetramethyl-1,3-bis(2-(trichloro-silyl)ethyl)disiloxane <b>12</b> .....	18
2.3.2.	1,3-Bis(2-( <i>tert</i> -butyl-dichlorosilyl)ethyl) 1,1,3,3,-tetramethyldisiloxane <b>13</b> .....	20
2.3.3.	1,1'-((1,1,3,3-tetramethyldisiloxane-1,3-diyl)bis(ethane-2,1-diyl))bis(1,1-dichloro- <i>N,N</i> -bis(trimethylsilyl)-silanamine) <b>14</b> .....	21
2.3.4.	1,3-bis(2-(1-( <i>tert</i> -butyl)-2,3-dimethylsiliran-1-yl)ethyl)-1,1,3,3-tetramethyldisiloxane <b>15</b> .....	23
2.3.5.	1,1'-((1,1,3,3-tetramethyldisiloxane-1,3-diyl)bis(ethane-2,1-diyl))bis(2,3-dimethyl- <i>N,N</i> -bis(trimethylsilyl)siliran-1-amine) <b>16</b> .....	28
2.4.	Screening Reactions and Screening Products .....	34
2.4.1.	Ring opening .....	34
2.4.2.	Silylene Transfer .....	35
2.4.3.	Silylene Insertion .....	36
3.	X-ray Crystallographic Data .....	38
4.	Rheological Measurements .....	41
5.	IR-Spectroscopy Data .....	50
6.	Shore Hardness of Crosslinked Elastomers .....	51
7.	References .....	53

---

## SUPPORTING INFORMATION

---

### 1. General Methods and Instrumentation

All manipulations (except for polymerizations with **16** and OH-terminated PDMS) and were carried out under argon or nitrogen atmosphere using standard Schlenk or glovebox techniques. Glassware was heat-dried under vacuum prior to use. Unless otherwise stated, all chemicals were purchased from *Sigma-Aldrich*, *ABCR* or *TCI Chemicals* and used as received. Compounds for screening reactions were carefully dried and purified prior to use. PDMS-compounds were received from *WACKER Chemie AG* or purchased from *ABCR*. All siloxanes for crosslinking experiments were degassed and dried to avoid problems with oxygen and water. For vinyl- and hydrosiloxanes we applied high vacuum and heat for several days. Carbinol and silanol terminated siloxanes were additionally flashed over dry neutral alumina and 3 Å molecular sieve. *Cis*-2-Butene (2.0) and *Trans*-2-butene (2.0) were purchased from *Linde AG* and used as received. A Li/Na alloy was prepared by melting elemental Li (*Sigma-Aldrich*, 99 %, trace metal basis) and Na (*Sigma-Aldrich*, 99.8 %, sodium basis) in a Ni crucible to 200 °C under argon in a glove-box. After mixing and subsequent cooldown the alloy was cut into small pieces for reductions. Al<sub>2</sub>O<sub>3</sub> (neutral) and carbon black were dried for 72 h at 150 °C in high vacuum. n-Hexane, n-Pentane, THF, Et<sub>2</sub>O, Benzene and toluene were refluxed over sodium/benzophenone or CaH<sub>2</sub>, distilled and deoxygenated prior to use. All solvents were analysed for remaining H<sub>2</sub>O by Karl-Fischer titration prior to use. Deuterated benzene (C<sub>6</sub>D<sub>6</sub>) and toluene (C<sub>7</sub>D<sub>8</sub>) were obtained from *Deutero Deutschland GmbH* and were dried and stored over 3 Å molecular sieves. All NMR samples were prepared under argon in *J. Young* PTFE tubes.

#### NMR-Spectroscopy

NMR spectra were recorded on *Bruker* AV-500C, AV-500 or DRX-400 spectrometers at ambient temperature (300 K). <sup>1</sup>H, <sup>13</sup>C and <sup>29</sup>Si NMR spectroscopic chemical shifts  $\delta$  are reported in ppm relative to tetramethylsilane.  $\delta(^1\text{H})$  and  $\delta(^{13}\text{C})$  were referenced internally to the relevant residual solvent resonances.  $\delta(^{29}\text{Si})$  was referenced to the signal of tetramethylsilane (TMS) ( $\delta = 0$  ppm) as external standard.

#### Mass Spectrometry

Mass spectra (MS-Cl) were recorded on a double focusing *Finnigan* MAT 90 mass spectrometer (isobutene, 150 eV) or TOF LCT 700 from *Waters* equipped with an ion source from *Linden CMS GmbH*. For LIFDI-MS the substances were dissolved in dry solvents and filtrated (syringe-filter, 0.45  $\mu\text{m}$ ) before measuring.

#### UV-Vis Measurements

For UV-Vis measurements a *Varian* Cary 50 Scan photometer was used in combination with custom-made UV-cuvettes with attached vacuum connection. n-Pentane and n-hexane were used as solvents.

#### Rheologic Measurements

Rheologic measurements were conducted with an *Anton Paar* MCR 302 with an additional hood for inert gas and custom-made plates. The transfer of compound mixtures into the rheometer was conducted under protective gas. Measuring frequency  $f = 1$  Hz, gradually decreasing amplitude (starting at 10 %, automatic decrease of 1/10 when moment  $M > 1$  mNm).  $\text{Tan}(\delta)$  values of fully crosslinked (steady viscosity) elastomers are calculated as mean values of the last 100 data points. This is necessary due to high fluctuations when measuring solid elastomers with deformations as low as 0.01 %.

#### Shore Measurements

Shore A and Shore A0 measurements were conducted with a *Sauter* HBA 100-0 or *Zwick/Roell* 3130 tool. The measuring duration was 3 seconds. All given values are average values from 5 measurements. The thickness of measured elastomers was at least 6 mm, some specimens were cut and stacked to reach the required height.

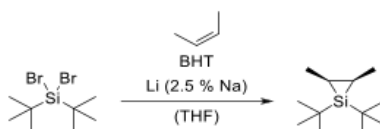
#### Elemental Analysis

Elemental analyses (EA) were conducted with a *EURO EA (HEKA tech)* instrument equipped with a CHNS combustion analyser.

## SUPPORTING INFORMATION

## 2. Synthesis and Characterization of New Compounds

Precursors of silirane **1**  $t\text{Bu}_2\text{SiHCl}$ ,  $t\text{Bu}_2\text{SiH}_2$  and  $t\text{Bu}_2\text{SiBr}_2$  were synthesized according to literature.<sup>[1-4]</sup>  $t\text{Bu}_2\text{SiBr}_2$  was additionally purified by crystallisation from dry MeCN at  $-30\text{ }^\circ\text{C}$ . Highly pure  $t\text{Bu}_2\text{SiBr}_2$  is a colourless waxy solid. Siliranes *cis*-1,1-di-*tert*-butyl-2,3-dimethylsilirane and *trans*-1,1-di-*tert*-butyl-2,3-dimethyl-silirane were synthesized *via* modified procedures described in literature.<sup>[4-6]</sup>

2.1.1. Synthesis of *cis*-1,1-di-*tert*-butyl-2,3-dimethylsilirane/*trans*-1,1-di-*tert*-butyl-2,3-dimethylsilirane **1**

A 500 mL high-pressure Schlenk-tube with a PTFE sealed screw cap was equipped with a PTFE-coated stir bar and was loaded with 30.0 g (99.3 mmol, 1.00 eq.) of  $t\text{Bu}_2\text{SiBr}_2$ , 100 mg (0.45 mmol, 0.005 eq.) 3,5-Di-*tert*-butyl-4-hydroxytoluene (BHT) and 17.5 g (198.6 mmol, 2 eq.) tetrahydrofuran. The reaction tube was cooled down to  $-78\text{ }^\circ\text{C}$  with a dry ice/isopropanol mixture. Present argon atmosphere was removed *in vacuo* and 111.4 g (1.9 mol, 20.0 eq.) *cis*-2-butene was condensed into the cooled reaction mixture by pressurizing it with 1.80 bar of the respective gas. After re-pressurizing with argon, 5.51 g (2.5 % Na, 794.4 mmol, 8.0 eq.) Li/Na alloy chunks were added to the reaction mixture, followed by vigorous stirring at room temperature for 16 h. After full conversion ( $^{29}\text{Si}$ -NMR verification) *cis*-2-butene gas was released and remaining solvent was removed under vacuum. The crude slurry was extracted 5 times with each 50 mL *n*-pentane to precipitate and separate the generated LiBr by filtration. After filtration (syringe-filter) *n*-pentane was removed again and the remaining oil purified by bulb-to-bulb distillation ( $40\text{ }^\circ\text{C}$ ,  $10^{-2}$  mbar,  $\text{N}_2$  cooled trap). 14.4 g (72.6 mmol, 73 %) *cis*-1,1-di-*tert*-butyl-2,3-dimethylsilirane is received as a colourless clear oil.

*cis*- $t\text{Bu}_2\text{Si}(\text{CHMe})_2$ :  $^1\text{H-NMR}$ : (300 K, 500 MHz,  $\text{C}_6\text{D}_6$ )  $\delta = 1.06$  (s, 9H, *t*Bu), 1.04–1.10 (m, 2H, -Si-CH-), 1.17 (s, 9H, *t*Bu), 1.40–1.41 (m, 6H, -CH-Me).  $^{13}\text{C-NMR}$ : (300 K, 125 MHz,  $\text{C}_6\text{D}_6$ )  $\delta = 10.0$  (Si-CH-), 10.3 (Si-CH-), 18.6 (-CH-Me), 20.9 (-CH-Me), 30.0 (*t*Bu-Me), 31.6 (*t*Bu-Me).  $^{29}\text{Si-NMR}$ : (300 K, 100 MHz,  $\text{C}_6\text{D}_6$ )  $\delta = -53.2$ . CI-MS: 197.3 [M-H] $^+$ .

The *trans*-species of **1** is synthesised analogously with *trans*-2-butene. For subsequent silylene transfer reaction both stereoisomers were equally suitable and yielded identical products.

*trans*- $t\text{Bu}_2\text{Si}(\text{CHMe})_2$ :  $^1\text{H-NMR}$ : (297 K, 300 MHz,  $\text{C}_6\text{D}_6$ )  $\delta = 1.06$  (s, 2H, -Si-CH-), 1.09 (s, 18H, *t*Bu), 1.54–1.47 (m, 6H, -CH Me).  $^{29}\text{Si-NMR}$ : (300 K, 100 MHz,  $\text{C}_6\text{D}_6$ )  $\delta = -43.9$ . CI-MS: 197.3 [M-H] $^+$ .

## 2.2. Multifunctional Silirane Crosslinkers 5–10

## 2.2.1. General Procedure for Multifunctional Silirane Crosslinkers 5–10

2.80 mmol (1.00 eq.) of the respective vinyl-functionalized reagent and  $x \cdot 1.20$  eq. silirane **1** were mixed with 5 mL toluene in a 20 mL Schlenk-tube ( $x$  = number of vinyl-moieties at the reagent). While stirring 1 mg (4.01  $\mu\text{mol}$ , 0.0014 eq.) AgOTf was added to the reaction. The mixture was heated up to  $60\text{ }^\circ\text{C}$  and stirred for 16 h. Emerging butene gas was released over a relief valve. Full conversion was verified by  $^1\text{H-NMR}$  (absence of vinyl-H). The solvent and remaining **1** were removed by high vacuum ( $60\text{ }^\circ\text{C}$ ,  $10^{-5}$  mbar) from the product. Separation of the catalyst was carried out by diluting the crude product in 5 mL pentane and subsequent filtration over an appropriate amount of aluminium oxide ( $\text{Al}_2\text{O}_3$ ). The aluminium oxide was further washed with 2 mL pentane. At last the solvent was removed in vacuo to obtain the silirane crosslinkers as colourless viscous fluids. The yield strongly depends on the filtration step. Raw yield is always 100 %, workup loss can be up to 50 %.

## SUPPORTING INFORMATION

2.2.2. 1,3-Bis(1,1-di-*tert*-butylsilylirane-2-yl)-1,1,3,3-tetramethyldisiloxane **5**

$^1\text{H-NMR}$ : (500 MHz,  $\text{C}_6\text{D}_6$ )  $\delta$  = -0.26–0.19 (m, 2H,  $t\text{Bu}_2\text{SiCH}$ ), 0.33–0.38 (m, 12H, Si-Me), 0.6–.78 (m, 4H,  $t\text{Bu}_2\text{SiCH}_2$ ), 1.05–1.07 (m, 18H,  $t\text{Bu}$ ), 1.16–1.18 (m, 18H,  $t\text{Bu}$ ).  $^{29}\text{Si-NMR}$ : (100 MHz,  $\text{C}_6\text{D}_6$ )  $\delta$  = 5.47, -48.42, -48.45, -48.57, -48.73.<sup>1</sup>

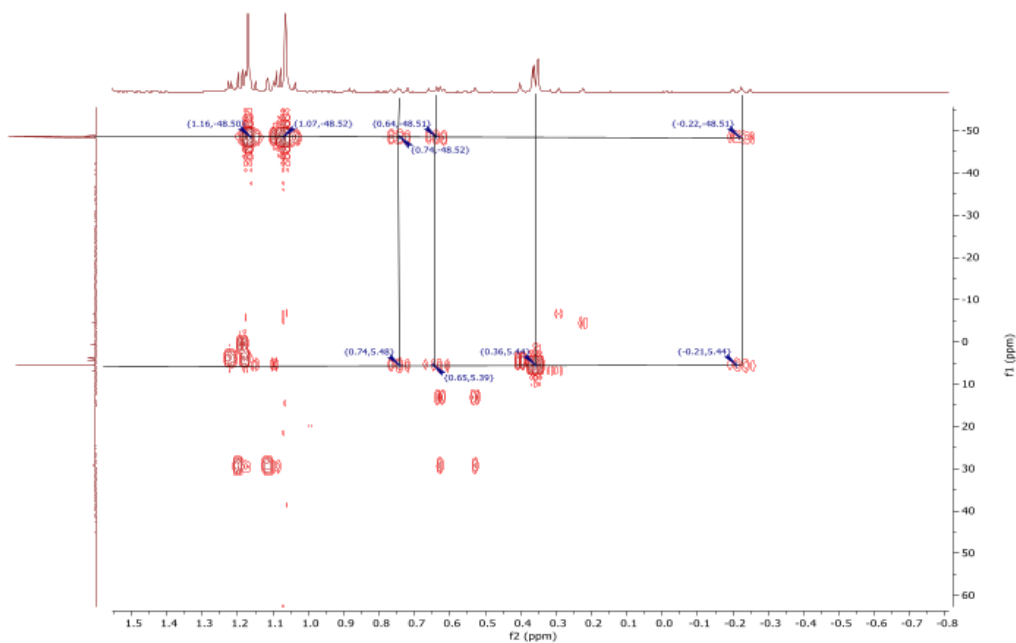


Figure 1:  $^1\text{H}$ - $^{29}\text{Si}$ -HMBC (500 MHz/100 MHz,  $\text{C}_6\text{D}_6$ ) of compound **5**. Raw product contains monosubstituted species and sideproducts derived from  $^t\text{Bu}_2\text{SiMe}_2$ -silylirane **1**.

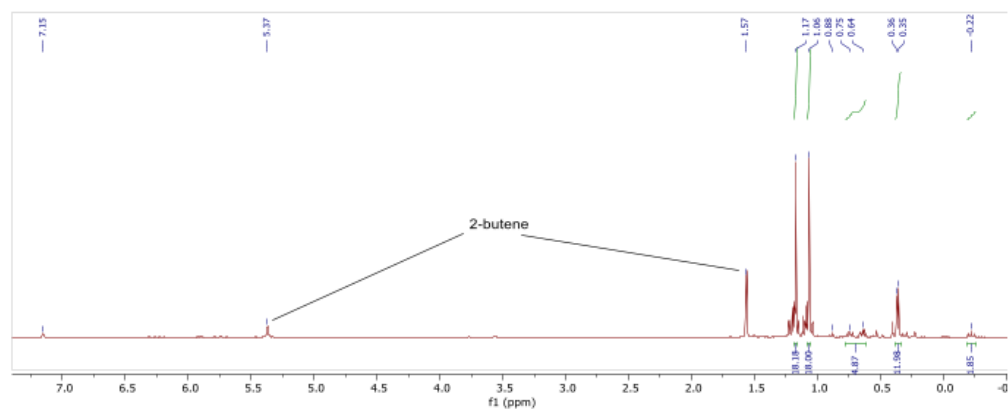


Figure 2:  $^1\text{H}$ -NMR (500 MHz,  $\text{C}_6\text{D}_6$ ) of compound **5**. Raw product contains monosubstituted species and sideproducts derived from  $^t\text{Bu}_2\text{SiMe}_2$ -silylirane **1**.

<sup>1</sup> Compound **5** is a mixture of various stereoisomers, which results in multiple signals for e.g. silylirane-Si.

## SUPPORTING INFORMATION

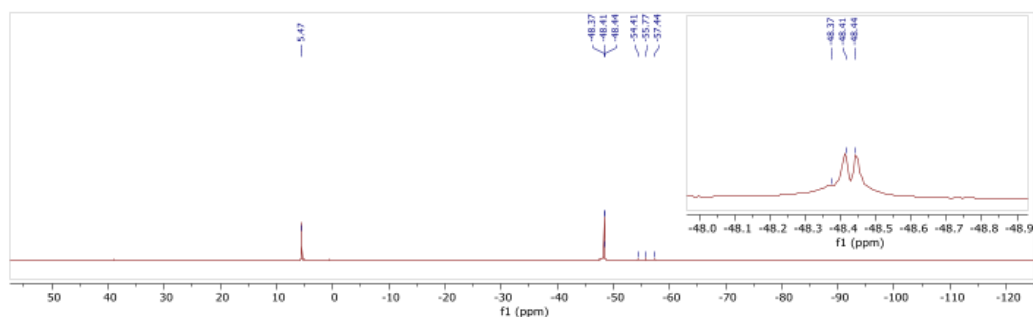


Figure 3:  $^{29}\text{Si}$ -ig-NMR (100 MHz,  $\text{C}_6\text{D}_6$ ) of compound 5. Raw product contains monosubstituted species and sideproducts derived from  $^1\text{Bu}_2\text{SiMe}_2$ -silirane 1.

2.2.3. Tetrakis(1,1-di-*tert*-butylsilirane-2-yl)silane 6

Yield: 91 %.  $^1\text{H-NMR}$ : (500 MHz,  $\text{C}_6\text{D}_6$ )  $\delta$  = 0.10–0.29 (m, 4H,  $-\text{CH}-$ ), 0.62–0.88 (m, 8H,  $-\text{CH}_2-$ ), 1.18–1.22 (m, 36H, *t*Bu), 1.31–1.34 (m, 36H, *t*Bu).  $^{29}\text{Si-NMR}$ : (100 MHz,  $\text{C}_6\text{D}_6$ )  $\delta$  = -46.5–(-43.9) ( $-\text{Si}-\text{tBu}_2$ ), 5.0–5.2 ( $\text{Si}-\text{CH}_2-$ ).  $\text{CI-MS}$ : 704.2 [ $\text{M}^+$ ].

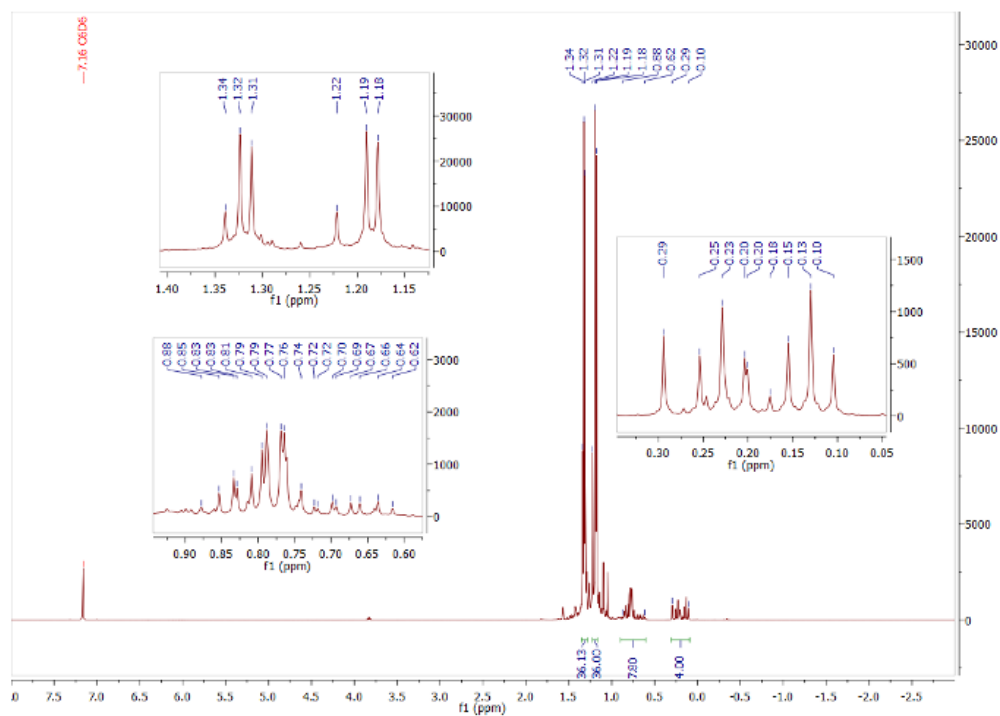


Figure 4:  $^1\text{H-NMR}$  (500 MHz,  $\text{C}_6\text{D}_6$ ) of compound 6. Contains diastereomers and  $^1\text{Bu}_2\text{SiMe}_2$  silirane. When integrated over entire signal-areas the integrals relate to the molecular structure.



## SUPPORTING INFORMATION

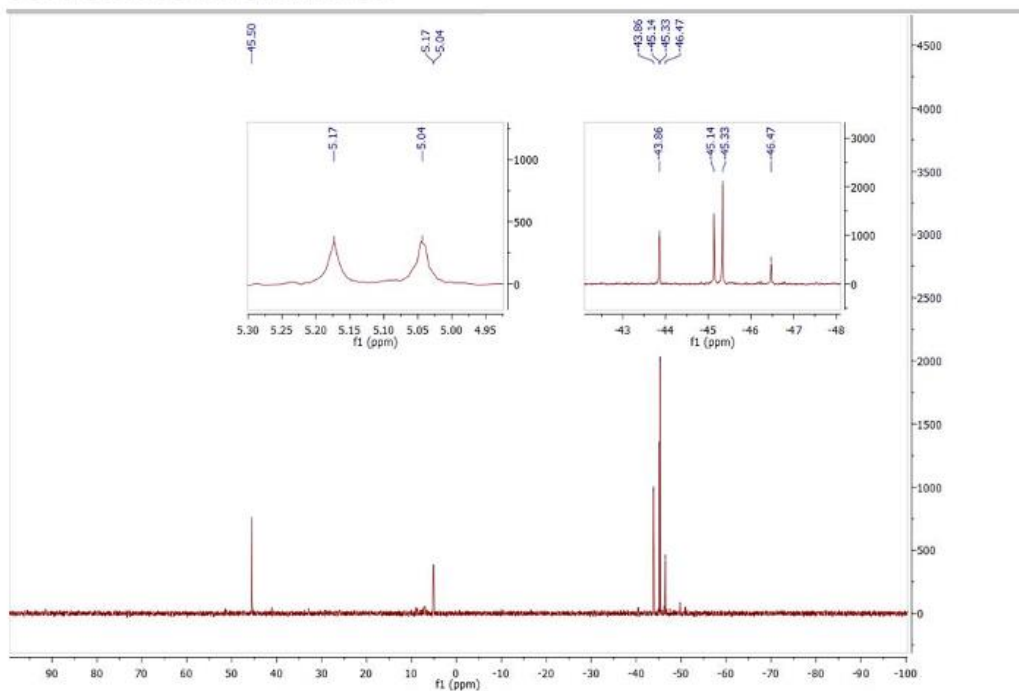


Figure 5:  $^{29}\text{Si}$ -ig-NMR (100 MHz,  $\text{C}_6\text{D}_6$ ) of compound 6. Contains diastereomers and  $^t\text{Bu}_2\text{SiMe}_2$  silyrane.

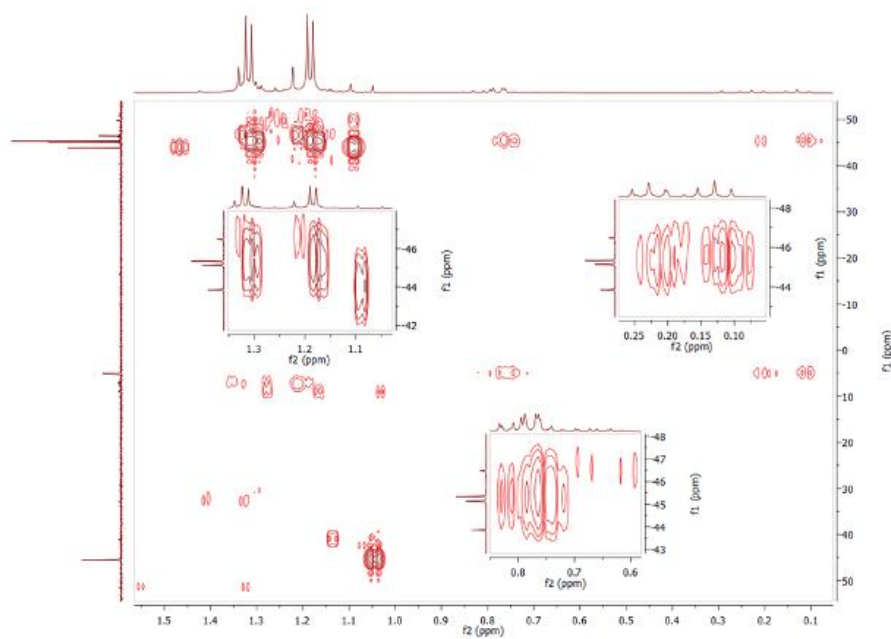


Figure 6:  $^1\text{H}$ - $^{29}\text{Si}$ -HMBC (500 MHz/100 MHz,  $\text{C}_6\text{D}_6$ ) of compound 6.

## SUPPORTING INFORMATION

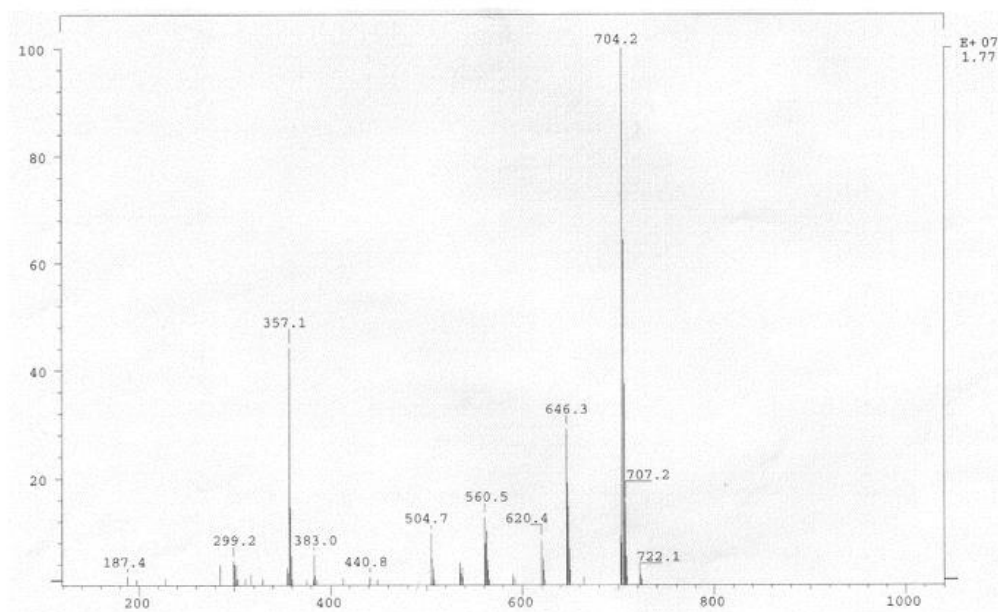


Figure 7: CI-MS spectrum of compound 6.

#### 2.2.4. 2,4,6,8-Tetrakis(1,1-di-*tert*-butylsilylirane-2-yl)-2,4,6,8-tetramethyl-cyclotetrasiloxane 7

Yield: 85 %. <sup>1</sup>H-NMR: (500 MHz, C<sub>6</sub>D<sub>6</sub>) δ = -0.16–0.02 (m, 4H, -CH-), 0.46–0.66 (m, 12H, Si-Me), 0.77–0.88 (m, 8H, -CH<sub>2</sub>-), 1.04–1.13 (m, 36H, *t*Bu), 1.24–1.31 (m, 36H, *t*Bu). <sup>29</sup>Si-NMR: (100 MHz, C<sub>6</sub>D<sub>6</sub>) δ = -49.8–(-49.0) (-Si-*t*Bu<sub>2</sub>), -23.8–(-21.9) (-Si-O-). CI-MS: 911.4[M]<sup>+</sup>, 769.8 [M-Si(*t*Bu)<sub>2</sub>]<sup>+</sup>, 628.1 [M-2Si(*t*Bu)<sub>2</sub>]<sup>+</sup>.

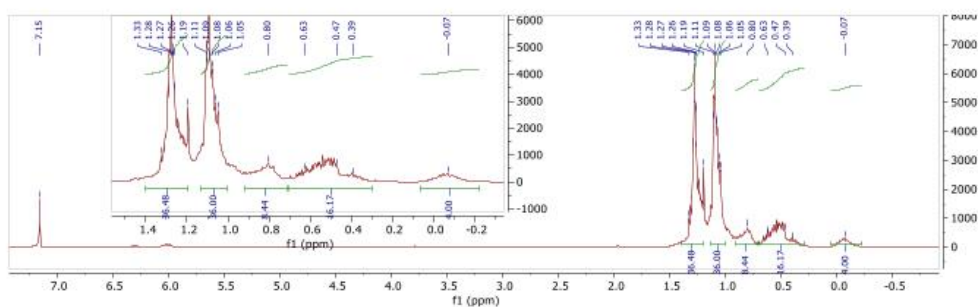


Figure 8: <sup>1</sup>H-NMR (500 MHz, C<sub>6</sub>D<sub>6</sub>) of compound 7. Contains diastereomers. When integrated over entire signal-areas the integrals relate to the molecular structure.

## SUPPORTING INFORMATION

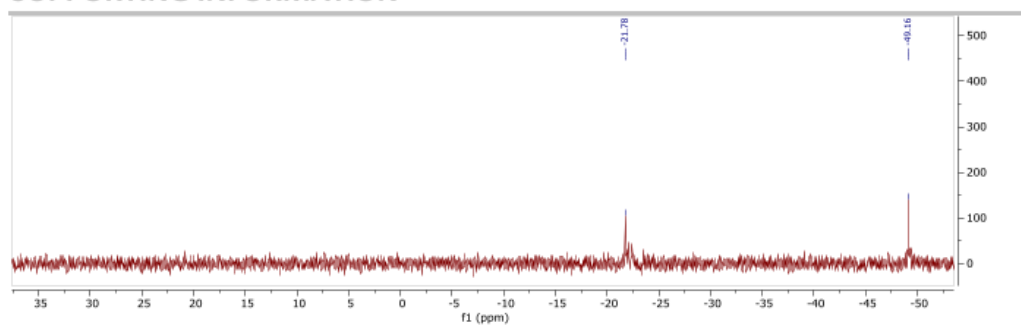


Figure 9:  $^{29}\text{Si}$ -ig-NMR (100 MHz,  $\text{C}_6\text{D}_6$ ) of compound 7. Contains diastereomers.

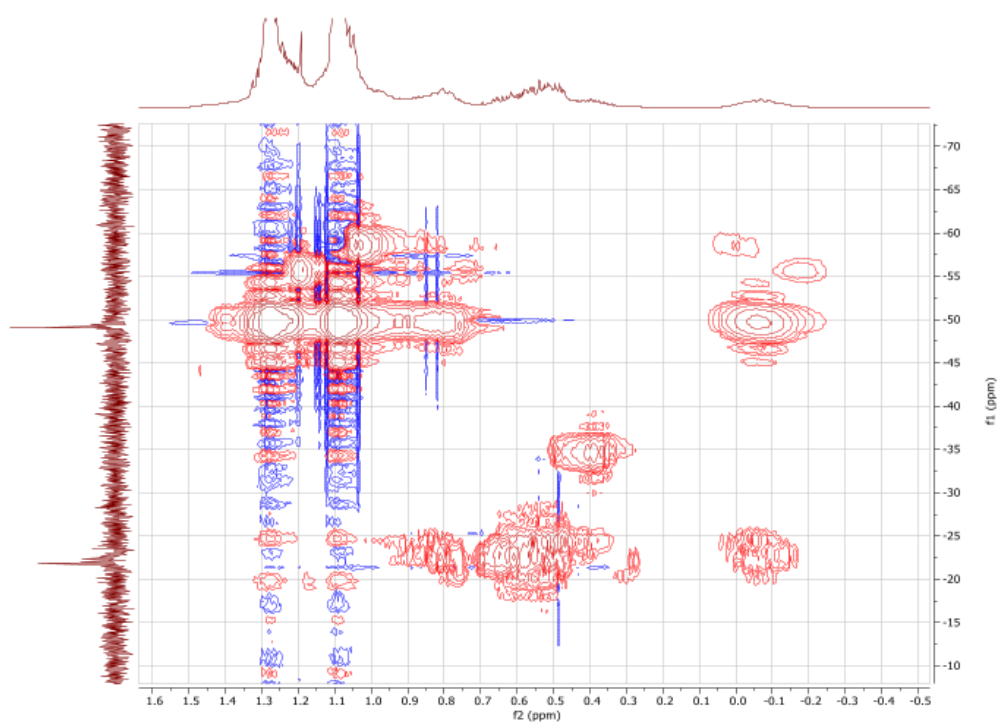


Figure 10:  $^1\text{H}$ - $^{29}\text{Si}$ -HMBC (500 MHz/100 MHz,  $\text{C}_6\text{D}_6$ ) of compound 7.

## SUPPORTING INFORMATION

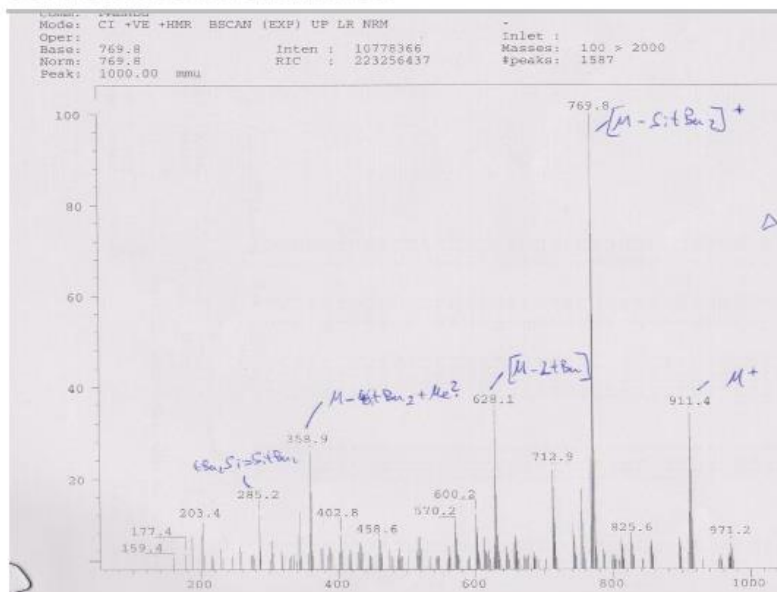
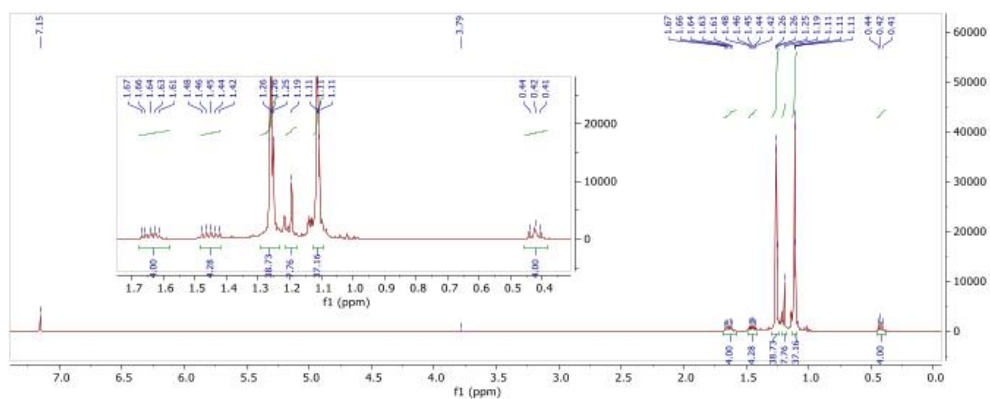


Figure 11: CI-MS spectrum of compound 7.

2.2.5. Tetrakis((1,1-di-*tert*-butylsilirane-2-yl)methyl)silane **8**

**Yield:** 82 %. **<sup>1</sup>H-NMR:** (500 MHz, C<sub>6</sub>D<sub>6</sub>) δ = 0.39–0.44 (m, 4H, tBu<sub>2</sub>SiCH), 1.10–1.11 (m, 36H, tBu), 1.19–1.22 (m, 8H, Si(CH<sub>2</sub>)<sub>4</sub>), 1.25–1.26 (m, 36H, tBu), 1.40–1.47 (m, 4H, tBu<sub>2</sub>SiCH<sub>2</sub>), 1.60–1.66 (m, 4H, tBu<sub>2</sub>SiCH<sub>2</sub>). **<sup>29</sup>Si-NMR:** (100 MHz, C<sub>6</sub>D<sub>6</sub>) δ = 5.0 (Si-(CH<sub>2</sub>)<sub>4</sub>), -49.5 (Si-tBu<sub>2</sub>). **CI-MS:** 760.0[M]<sup>+</sup>, 285.2 [Si<sub>2</sub>tBu<sub>4</sub>]<sup>+</sup>.

Figure 12: <sup>1</sup>H-NMR (500 MHz, C<sub>6</sub>D<sub>6</sub>) of compound **8**. Contains diastereomers.

## SUPPORTING INFORMATION

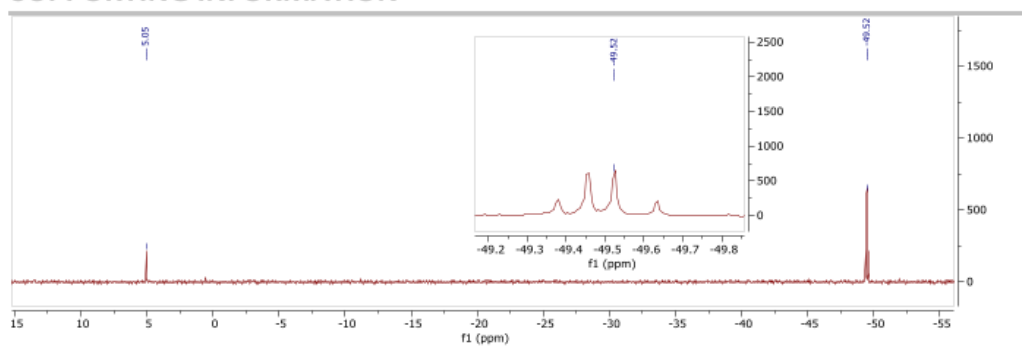


Figure 13:  $^{29}\text{Si}$ -ig-NMR (100 MHz,  $\text{C}_6\text{D}_6$ ) of compound **8**. Contains diastereomers.

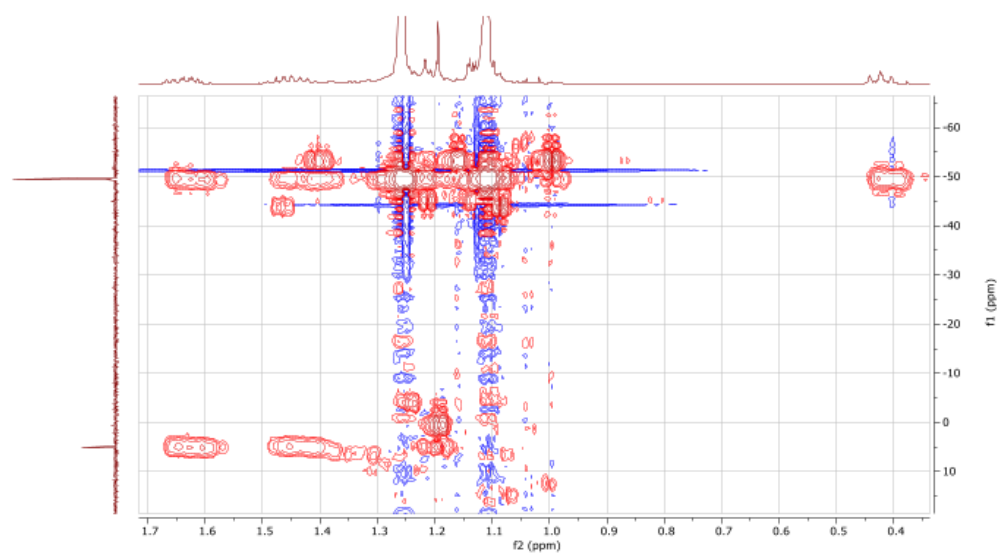


Figure 14:  $^1\text{H}$ - $^{29}\text{Si}$ -HMBC (500 MHz/100 MHz,  $\text{C}_6\text{D}_6$ ) of compound **8**.

## SUPPORTING INFORMATION

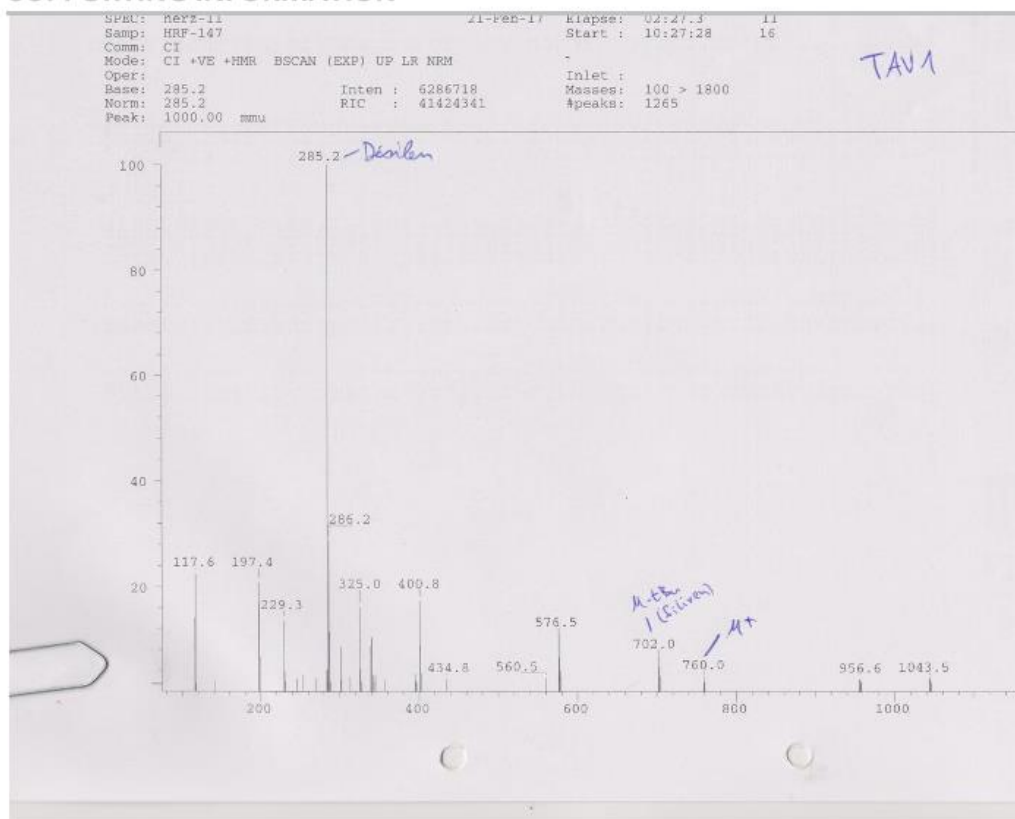


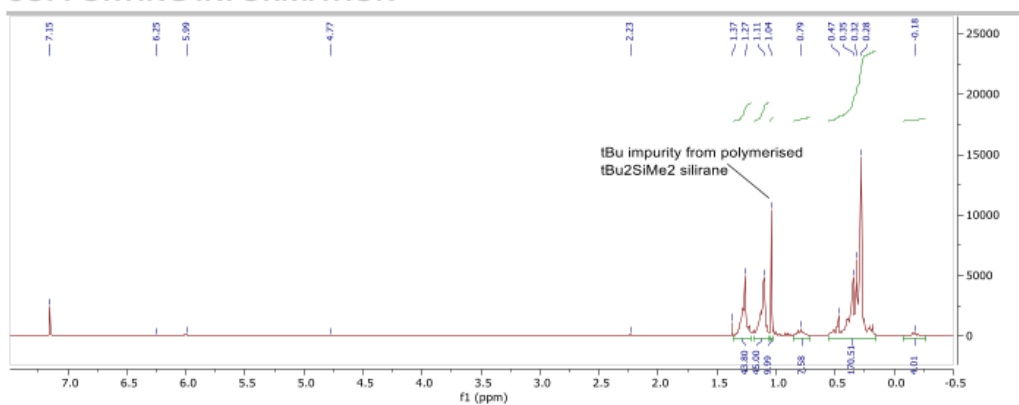
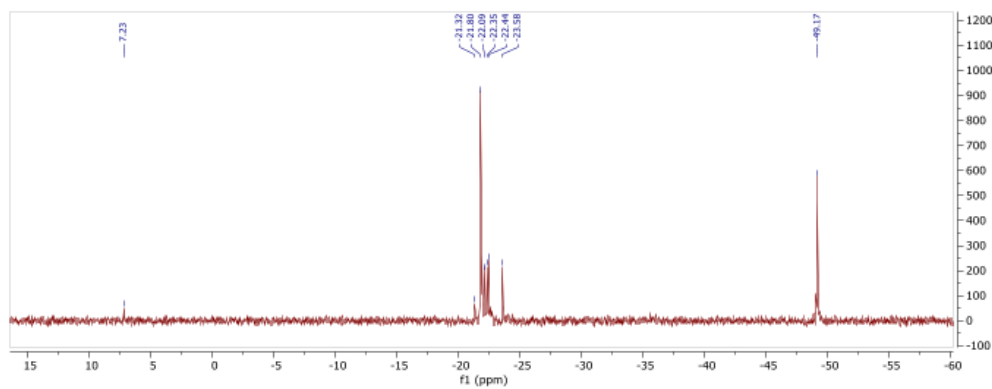
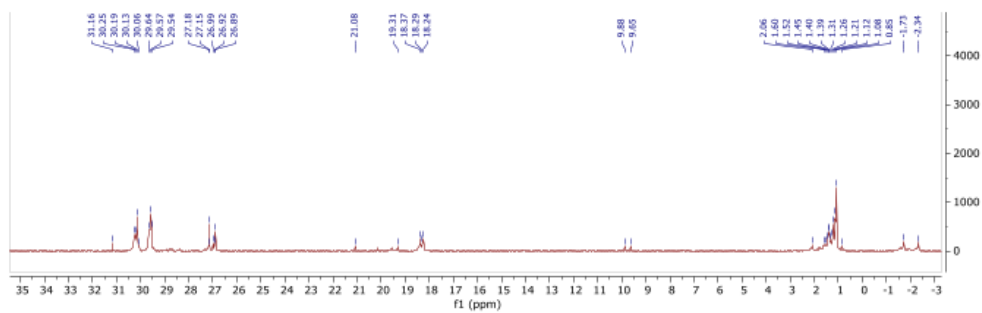
Figure 15: CI-MS spectrum of compound 8.

2.2.6. Poly(((1,1-di-*tert*-butylsilirane-2-yl)methylsiloxane)-co-dimethylsiloxane) Copolymer 9

**Yield:** 85 %. **<sup>1</sup>H-NMR:** (500 MHz, C<sub>6</sub>D<sub>6</sub>)  $\delta$  = -0.18 (m, 5H, *t*Bu<sub>2</sub>SiCH), 0.17–0.56 (m, 159H, Si-Me), 0.70–0.87 (m, 10H, *t*Bu<sub>2</sub>SiCH<sub>2</sub>), 1.06–1.17 (m, 45H, *t*Bu), 1.21–1.34 (m, 45H, *t*Bu). **<sup>29</sup>Si-NMR:** (100 MHz, C<sub>6</sub>D<sub>6</sub>)  $\delta$  = -21.3–(-22.7) (-Si/Me<sub>2</sub>-O-), -23.66 (-Si/MeR-O-), -49.17 (-Si-*t*Bu<sub>2</sub>).<sup>2</sup>

<sup>2</sup> Only a single analysis method was conducted (NMR). MS was not possible due to high *M<sub>w</sub>* and lability of siliranes. EA not meaningful, since compound 9 and 10 are a mixture of polymers of different length with a statistical distribution. NMR can be regarded as structural proof and proof of purity due to complete disappearance of vinyl protons in <sup>1</sup>H-NMR and correlations between silirane-Si and PDMS-backbone. Furthermore, the structure is confirmed by successful polymerizations with these compounds.

## SUPPORTING INFORMATION

Figure 16: <sup>1</sup>H-NMR (500 MHz, C<sub>6</sub>D<sub>6</sub>) of compound 9.Figure 17: <sup>29</sup>Si-NMR (100 MHz, C<sub>6</sub>D<sub>6</sub>) of compound 9.Figure 18: <sup>13</sup>C-NMR (125 MHz, C<sub>6</sub>D<sub>6</sub>) of compound 9.

## SUPPORTING INFORMATION



Figure 19:  $^1\text{H}$ - $^{29}\text{Si}$ -HMBC (500 MHz/100 MHz,  $\text{C}_6\text{D}_6$ ) of compound 9.

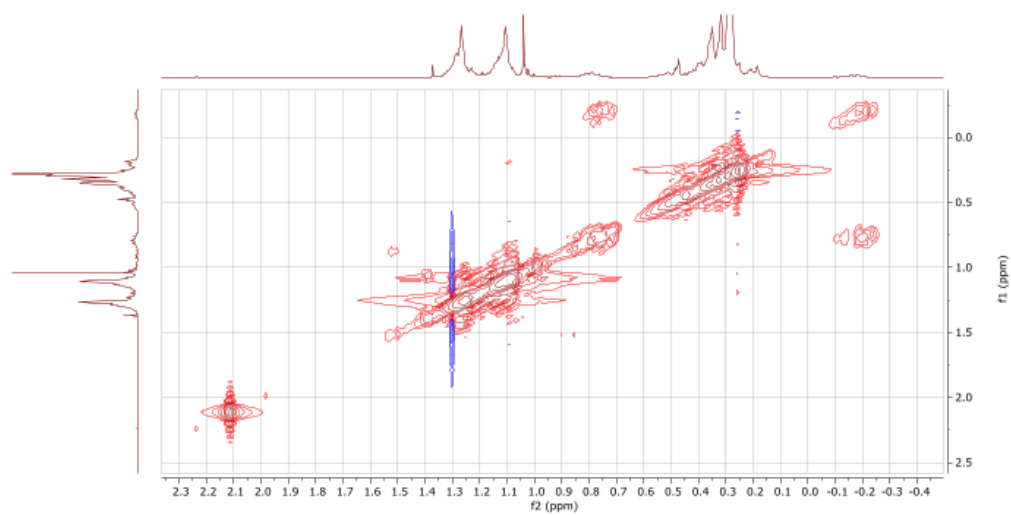


Figure 20:  $^1\text{H}$ -COSY (100 MHz,  $\text{C}_6\text{D}_6$ ) of compound 9. Correlation of silirane protons.



## SUPPORTING INFORMATION

2.2.7. Poly(((1,1-di-*tert*-butylsilirane-2-yl)methylsiloxane)-*co*-dimethylsiloxane) Copolymer **10**

**Yield:** 85 %. **<sup>1</sup>H-NMR:** (500 MHz, C<sub>6</sub>D<sub>6</sub>)  $\delta$  = -0.20 (m, tBu<sub>2</sub>SiCH), 0.17–0.56 (m, Si-Me), 0.73–0.90 (m, tBu<sub>2</sub>SiCH<sub>2</sub>), 1.06–1.19 (m, tBu), 1.21–1.34 (m, tBu). **<sup>29</sup>Si-NMR:** (100 MHz, C<sub>6</sub>D<sub>6</sub>)  $\delta$  = -21.3–(-21.3) (-Si/Me<sub>2</sub>-O-), -23.66 (-Si/MeR-O-), -49.17 (-Si-tBu<sub>2</sub>).<sup>3</sup>

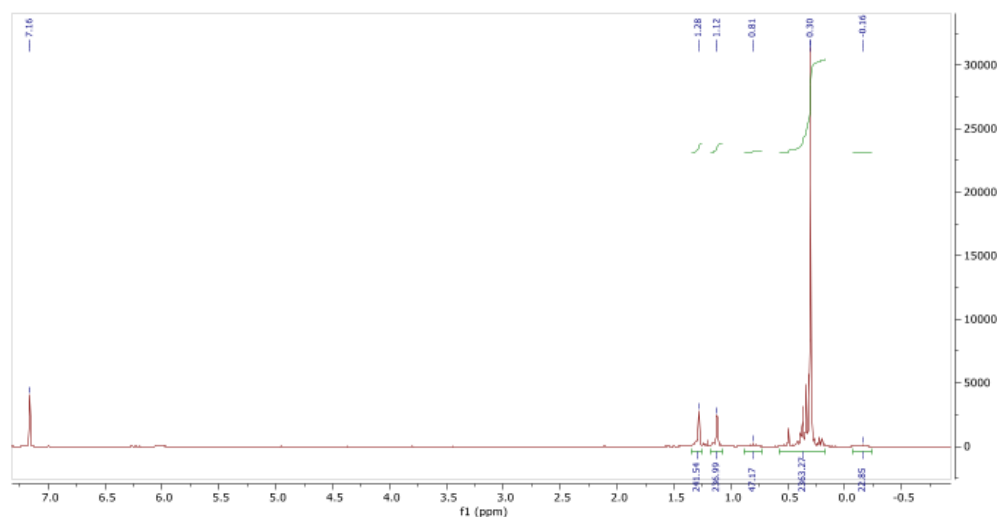


**Figure 21:** <sup>1</sup>H-NMR (500 MHz, C<sub>6</sub>D<sub>6</sub>) of compound **10**.

<sup>3,2</sup> Only a single analysis method was conducted (NMR). MS was not possible due to high  $M_w$  and lability of siliranes. EA not meaningful, since compound **9** and **10** are a mixture of polymers of different length with a statistical distribution. NMR can be regarded as structural proof and proof of purity due to complete disappearance of vinyl protons in <sup>1</sup>H-NMR and correlations between silirane-Si and PDMS-backbone. Furthermore, the structure is confirmed by successful polymerizations with these compounds.

## SUPPORTING INFORMATION

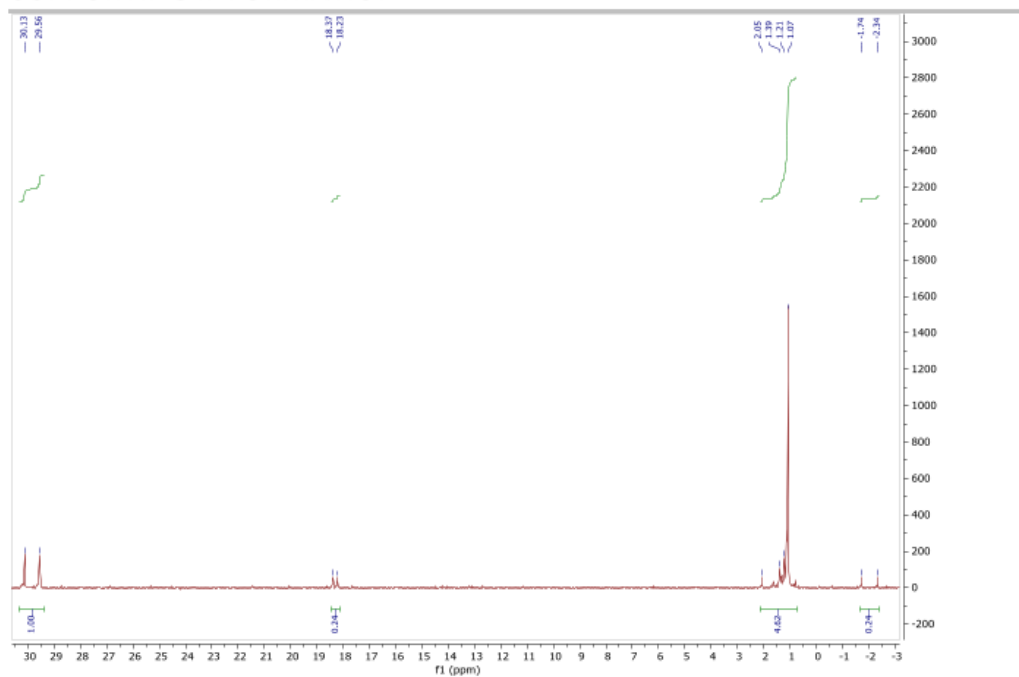


Figure 22:  $^{13}\text{C}$ -NMR (100 MHz,  $\text{C}_6\text{D}_6$ ) of compound 10.

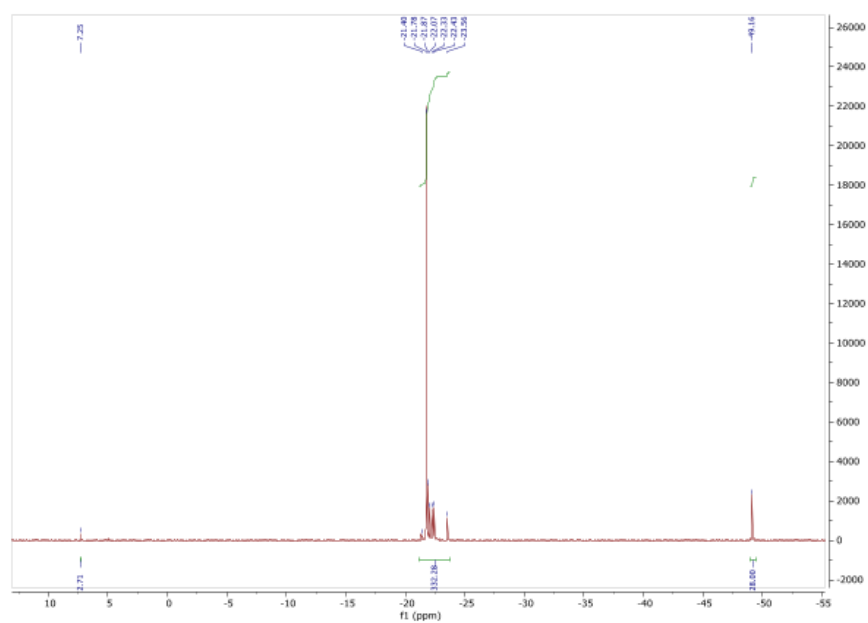


Figure 23:  $^{29}\text{Si}$ -inept-NMR (100 MHz,  $\text{C}_6\text{D}_6$ ) of compound 10.

## SUPPORTING INFORMATION

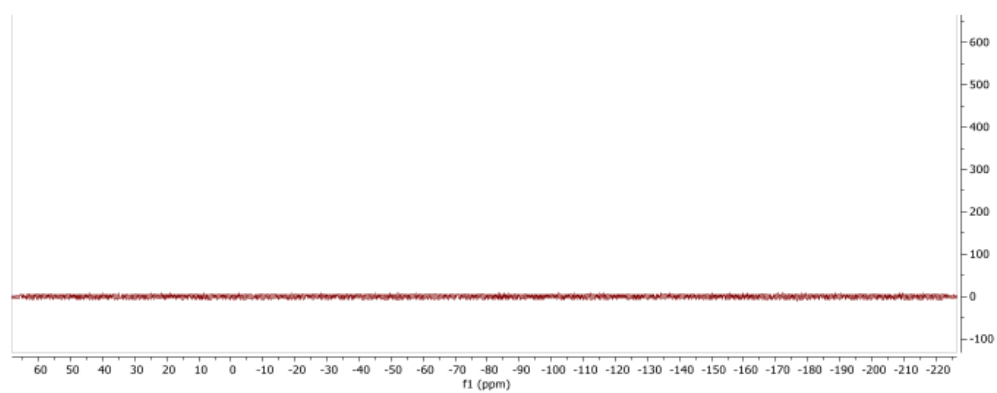


Figure 24:  $^{19}\text{F}$ -NMR (470 MHz,  $\text{C}_6\text{D}_6$ ) of compound **10** to demonstrate complete AgOTf removal.

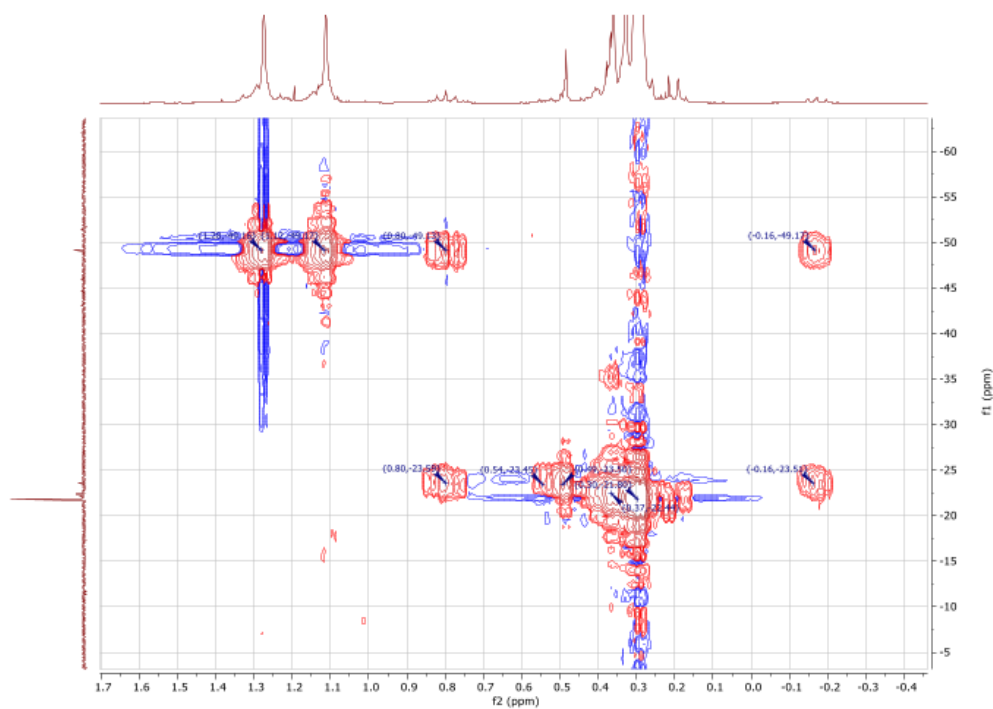


Figure 25:  $^1\text{H}$ - $^{29}\text{Si}$ -HMBC (500 MHz/100 MHz,  $\text{C}_6\text{D}_6$ ) of compound **10**.

## SUPPORTING INFORMATION

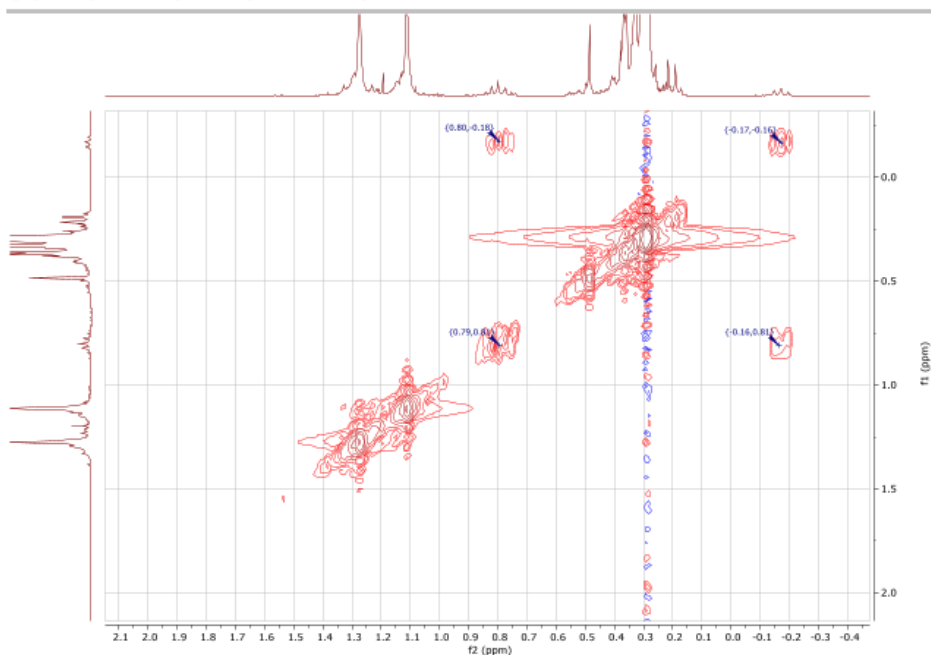
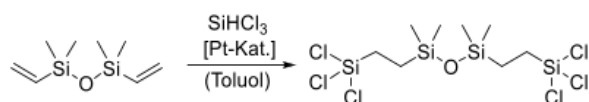


Figure 26:  $^1\text{H}$ -COSY (100 MHz,  $\text{C}_6\text{D}_6$ ) of compound **10**. Correlation of silirane protons.

### 2.3. Difunctional Silirane Crosslinkers 15-16

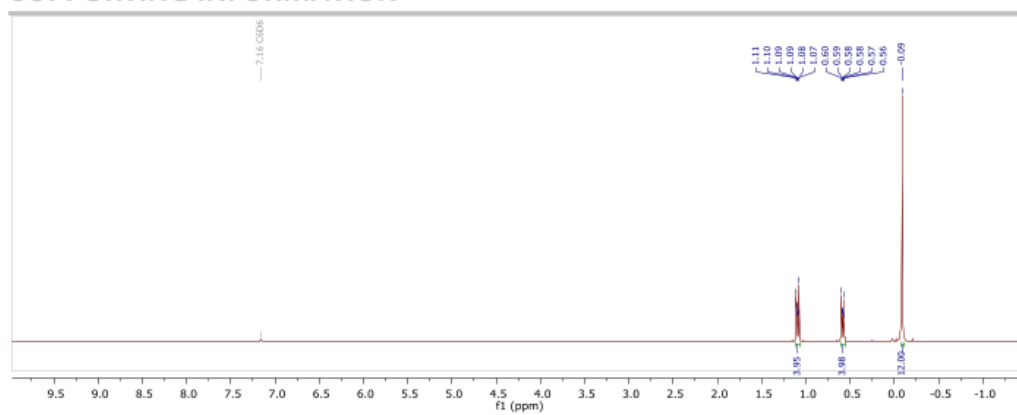
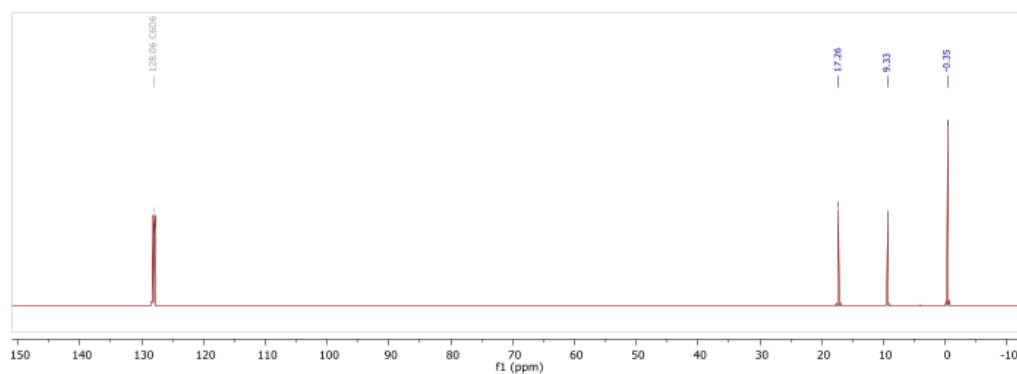
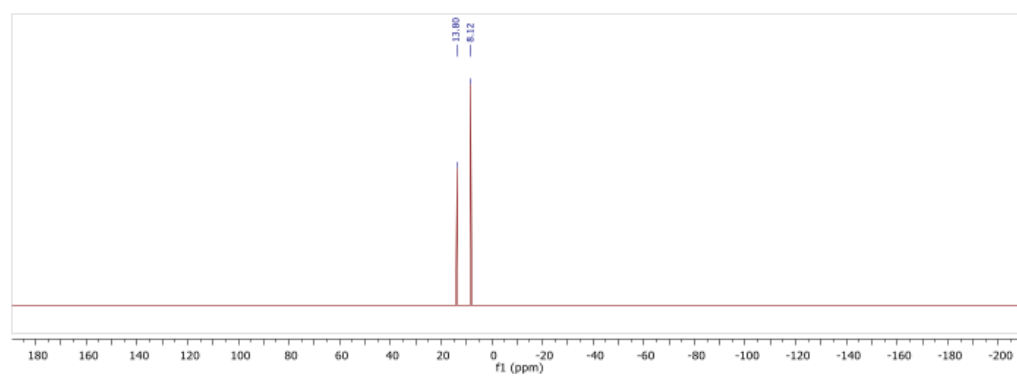
#### 2.3.1. 1,1,3,3-Tetramethyl-1,3-bis(2-(trichloro-silyl)ethyl)disiloxane **12**



A 250 mL Schenk-flask with a PTFE-coated stir bar was loaded with 100 g (740 mmol, 4.00 eq.) trichlorosilane and 30 mL toluene. 34.4 g (180 mmol, 1.00 eq.) divinyltetramethyldisiloxane was added under an inert atmosphere. Subsequently 0.05 mL *Karstedt*-catalyst (2.1 – 2.4 % Pt in xylene) was added to the reaction mixture and stirred for 18 h at room temperature. After removing solvent and excess trichlorosilane under vacuum the clear, yellow liquid was filtered over dry neutral aluminiumoxide to separate remaining Pt-catalyst from the reaction. 81.3 g (177 mmol) of the product was obtained as a clear, colourless liquid.

**Yield:** 95 %.  $^1\text{H-NMR}$ : (500 MHz,  $\text{C}_6\text{D}_6$ )  $\delta$  = 0.10 (s, 12H), 0.55–0.60 (m, 4H), 1.05–1.10 (m, 4H).  $^{13}\text{C-NMR}$ : (125 MHz,  $\text{C}_6\text{D}_6$ )  $\delta$  = 0.4, 9.3, 17.3.  $^{29}\text{Si-NMR}$ : (100 MHz,  $\text{C}_6\text{D}_6$ )  $\delta$  = 8.1, 13.8. **EA:** experimental (calculated) C 20.93 (21.01), H 4.63 (4.41) %.

## SUPPORTING INFORMATION

Figure 27:  $^1\text{H-NMR}$  (500 MHz,  $\text{C}_6\text{D}_6$ ) of compound **12**.Figure 28:  $^{13}\text{C-NMR}$  (125 MHz,  $\text{C}_6\text{D}_6$ ) of compound **12**.Figure 29:  $^{29}\text{Si-NMR}$  (100 MHz,  $\text{C}_6\text{D}_6$ ) of compound **12**.

## SUPPORTING INFORMATION

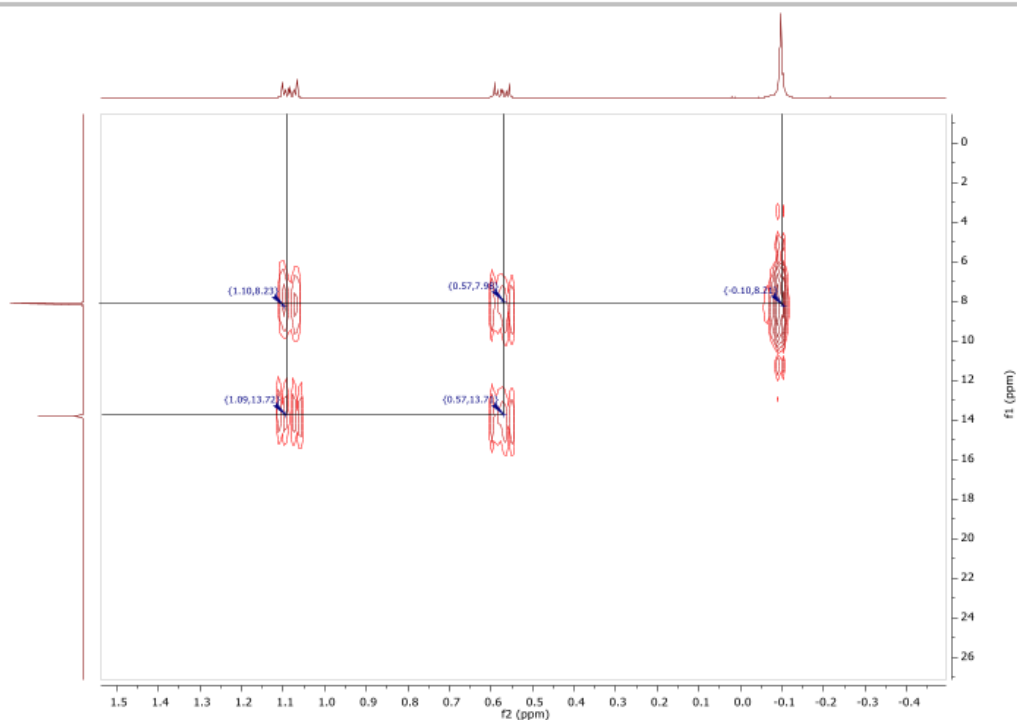
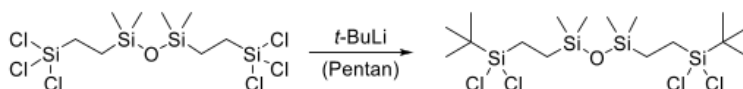


Figure 30:  $^1\text{H}$ - $^{29}\text{Si}$ -HMBC (500 MHz/100 MHz,  $\text{C}_6\text{D}_6$ ) of compound **12**.

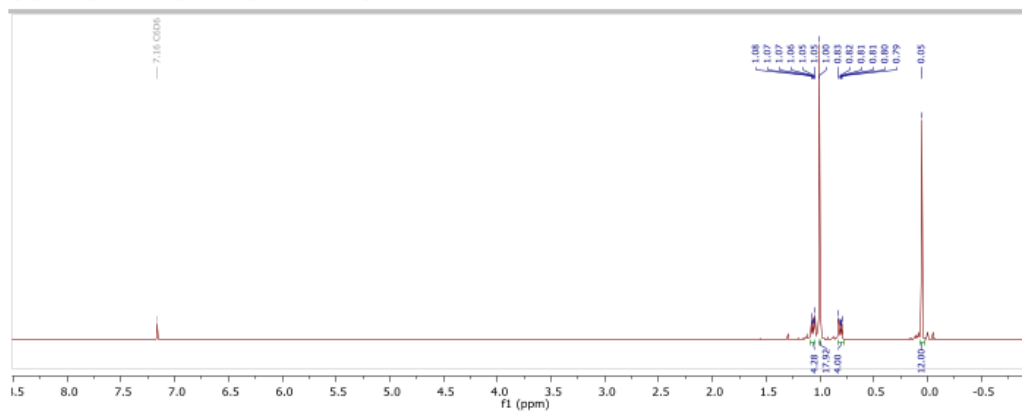
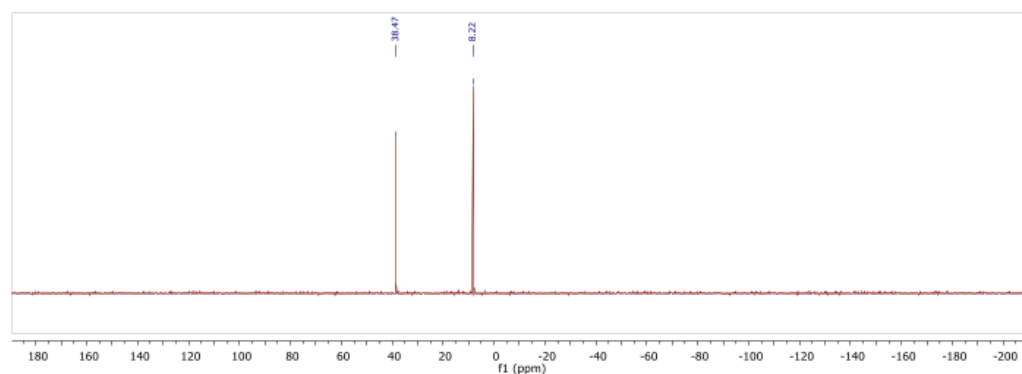
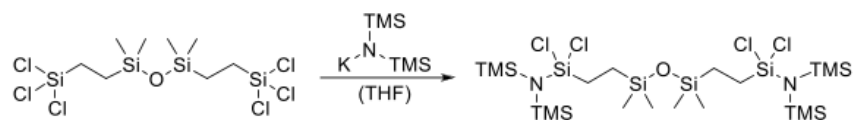
### 2.3.2. 1,3-Bis(2-(*tert*-butyl-dichlorosilyl)ethyl) 1,1,3,3-tetramethyldisiloxane **13**



A 250 mL Schenk-round-bottom flask was equipped with a PTFE-coated stir bar and filled with 30.0 g (65.6 mmol, 1.00 eq.) 1,1,3,3-Tetramethyl-1,3-bis(2-(trichloro-silyl)-ethyl)disiloxane **12** and 75 mL pentane. Subsequently the reaction mixture was cooled down to 0 °C, while 8.40 g (131 mmol, 2.00 eq.) *tert*-butyllithium solution (1.7 M) was slowly added through a dropping funnel over the period of 30 min. Then the reaction was stirred vigorously for 8 h at 0 °C before it was allowed to warm up to room temperature again. Emerged lithium chloride was separated from the crude product by filtration. The occurred suspension was separated from generated lithium chloride by filtration and solvent was removed *in vacuo* to give a yellowish solid. The crude product was purified by sublimation in a high vacuum (110 °C,  $10^{-5}$  mbar), giving 22.0 g (43.9 mmol) of **13** as a white solid.

**Yield:** 67 %.  $^1\text{H-NMR}$ : (500 MHz,  $\text{C}_6\text{D}_6$ )  $\delta$  = 0.05 (s, 12H), 0.78–0.82 (m, 4H), 1.00 (s, 18H), 1.04–1.08 (m, 4H).  $^{29}\text{Si-NMR}$ : (100 MHz,  $\text{C}_6\text{D}_6$ )  $\delta$  = 8.2, 38.5. **EA:** experimental (calculated) C 38.25 (38.39), H 7.76 (7.65) %.

## SUPPORTING INFORMATION

Figure 31:  $^1\text{H-NMR}$  (500 MHz,  $\text{C}_6\text{D}_6$ ) of compound **13**.Figure 32:  $^{29}\text{Si-NMR}$  (100 MHz,  $\text{C}_6\text{D}_6$ ) of compound **13**.2.3.3. 1,1'-((1,1,3,3-tetramethyldisiloxane-1,3-diyl)bis(ethane-2,1-diyl))bis(1,1-dichloro-*N,N*-bis(trimethylsilyl)-silanamine) **14**

In a 250 mL Schlenk round-bottom flask 10.0 g (21.9 mmol, 1.00 eq.) 1,1,3,3-Tetramethyl-1,3-bis(2-(tri-chloro-silyl)ethyl)disiloxane **12** was charged with 40 mL THF and cooled to 0 °C. A solution of 8.27 g (43.7 mmol, 2.00 eq.) potassium bis(trimethylsilyl)amide diluted in 30 mL THF was slowly added to the reaction flask through a dropping funnel over 30 minutes. The reaction mixture was stirred at room temperature for 6 h subsequently. Remaining solvent was removed under vacuum, then the crude product was solved in 40 mL pentane again. The so formed suspension was filtered and washed with 10 mL pentane again. Then the solvent was removed *in vacuo* to result in 12.5 g (17.7 mmol) **14** as a clear, light yellow liquid.

## SUPPORTING INFORMATION

Yield: 81 %.  $^1\text{H-NMR}$ : (500 MHz,  $\text{C}_6\text{D}_6$ )  $\delta$  = 0.07 (s, 12H), 0.33 (s, 36H), 0.83–0.87 (m, 4H), 1.25–1.29 (m, 4H).  $^{29}\text{Si-NMR}$ : (100 MHz,  $\text{C}_6\text{D}_6$ )  $\delta$  = 2.2, 6.4, 8.5. EA: experimental (calculated) C 33.49 (33.97), H 7.96 (7.98), N 3.94 (3.96) %.

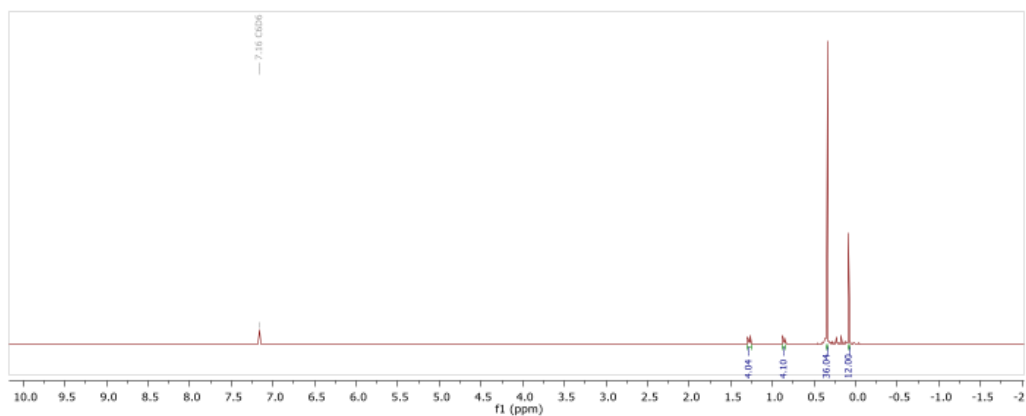


Figure 33:  $^1\text{H-NMR}$  (500 MHz,  $\text{C}_6\text{D}_6$ ) of compound **14**.

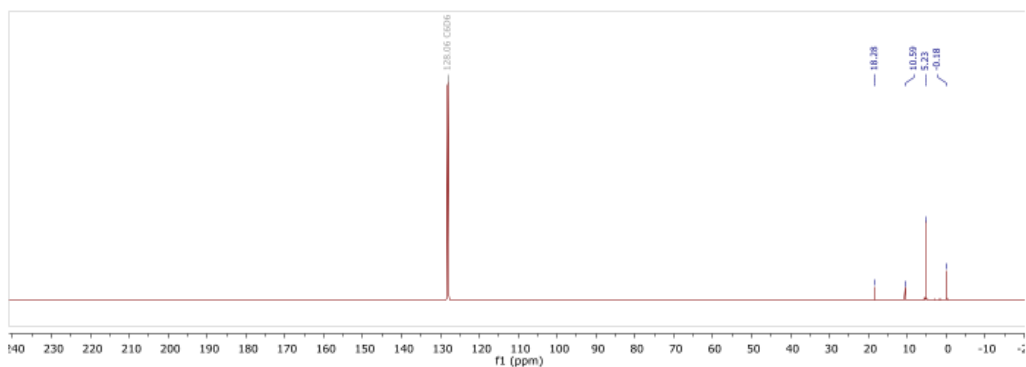


Figure 34:  $^{13}\text{C-NMR}$  (125 MHz,  $\text{C}_6\text{D}_6$ ) of compound **14**.

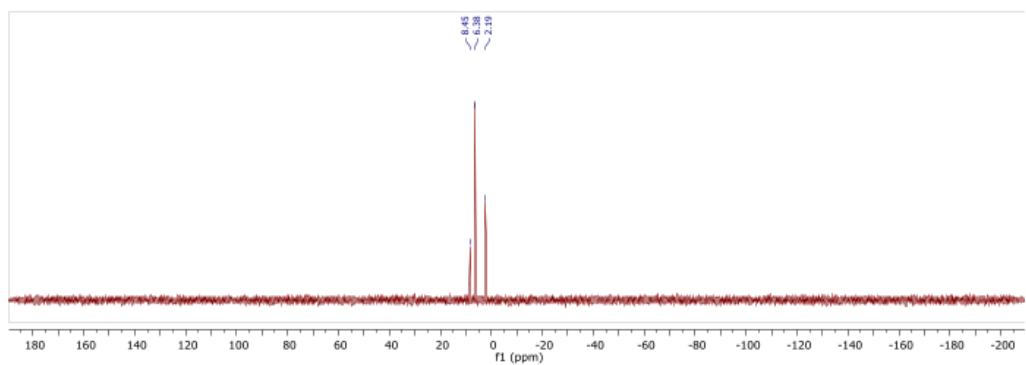


Figure 35:  $^{29}\text{Si-NMR}$  (100 MHz,  $\text{C}_6\text{D}_6$ ) of compound **14**.



## SUPPORTING INFORMATION

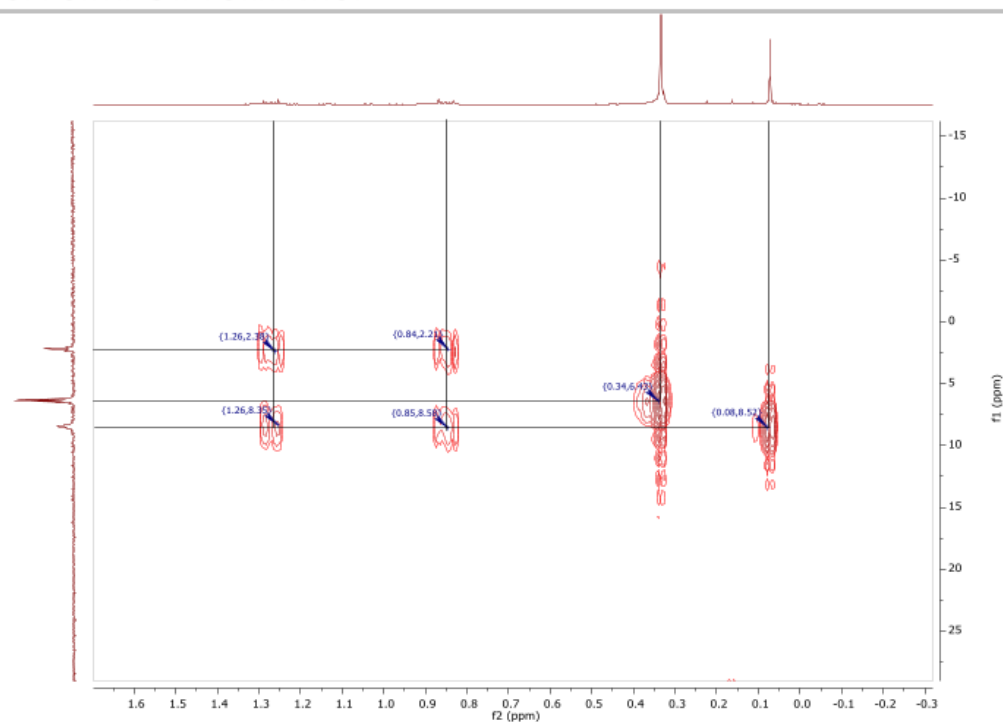
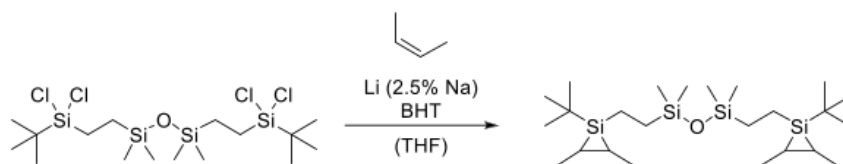


Figure 36:  $^1\text{H}$ - $^{29}\text{Si}$ -HMBC (500 MHz/100 MHz,  $\text{C}_6\text{D}_6$ ) of compound **14**.

#### 2.3.4. 1,3-bis(2-(1-(*tert*-butyl)-2,3-dimethylsilyran-1-yl)ethyl)-1,1,3,3-tetramethyldisiloxane **15**



A 250 mL Schlenk-tube was equipped with a PTFE-coated stir bar and was loaded with 10.0 g (20.0 mmol, 1.00 eq.) of **13**, 50 mL THF and 20 mg (0.09 mmol, 0.001 eq.) 3,5-Di-*tert*-butyl-4-hydroxytoluene (BHT) to suppress radical side reactions. The reaction tube was cooled down to  $-78^\circ\text{C}$  with a dry ice/isopropanol mixture. Present argon atmosphere was removed *in vacuo* and 33.6 g (600 mmol, 30.0 eq.) *cis*-2-butene was condensed onto the cooled reaction mixture by pressurizing it with 1.80 bar of the respective gas. After re-pressurizing with argon, 2.10 g (300 mmol, 15.0 eq.) Li/Na alloy chunks (2.5 % Na) were added to the reaction mixture, followed by vigorous stirring at room temperature for 7 days. By the end of the reduction, *cis*-2-butene gas and remaining solvent was removed under vacuum. The slurry crude was diluted in 50 mL pentane to precipitate and separated the generated lithium chloride by filtration. The product was collected by removing the remaining solvent *in vacuo* to afford 7.80 g (16.7 mmol, 86 %) of the silylene-crosslinker **15** as a colourless oil with high viscosity.

The product was a mixture of diastereomeric *cis*- and *trans*-isomers. Small amounts of a constitutional isomer from the respective 1-butene could be found due to the containing impurities of isomers in the used *cis*-2-butene gas. The three different species could be assigned by  $^1\text{H}$ - $^{29}\text{Si}$ -HMBC NMR measurements, but no distinct differentiation of the respective *cis/trans* species could be achieved.

## SUPPORTING INFORMATION

*Cis/Trans* species: 67 % relative ratio.  $^1\text{H-NMR}$ : (500 MHz,  $\text{C}_6\text{D}_6$ )  $\delta$  = 0.15–0.16 (m, 12H), 0.86–0.89 (m, 8H), 1.04 (s, 18H), 1.11–1.12 (m, 4H) 1.36–1.38 (m, 12H).  $^{29}\text{Si-NMR}$ : (100 MHz,  $\text{C}_6\text{D}_6$ )  $\delta$  = -49.7, 7.3. **LIFDI-MS**: 469.95 [ $\text{M}$ ] $^+$ , 413.99 [ $\text{M}-\text{C}_6\text{H}_6$ ] $^+$ , 358.03 [ $\text{M}-\text{C}_6\text{H}_6$ ] $^+$ .

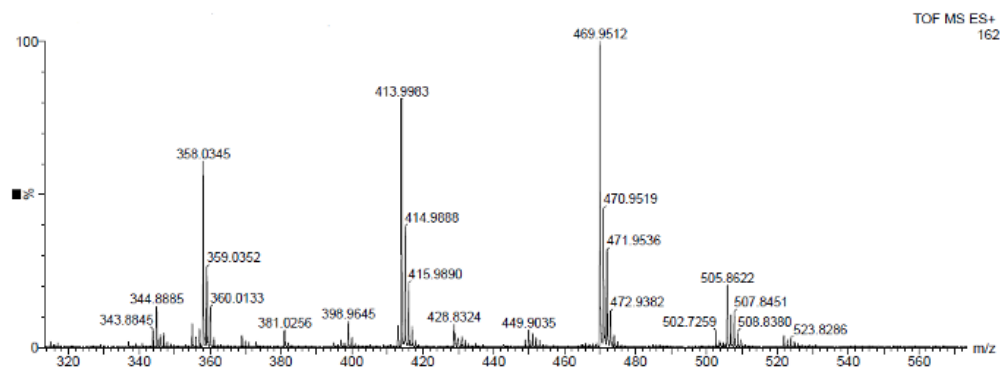


Figure 37: LIFDI-MS spectrum of compounds **15**.

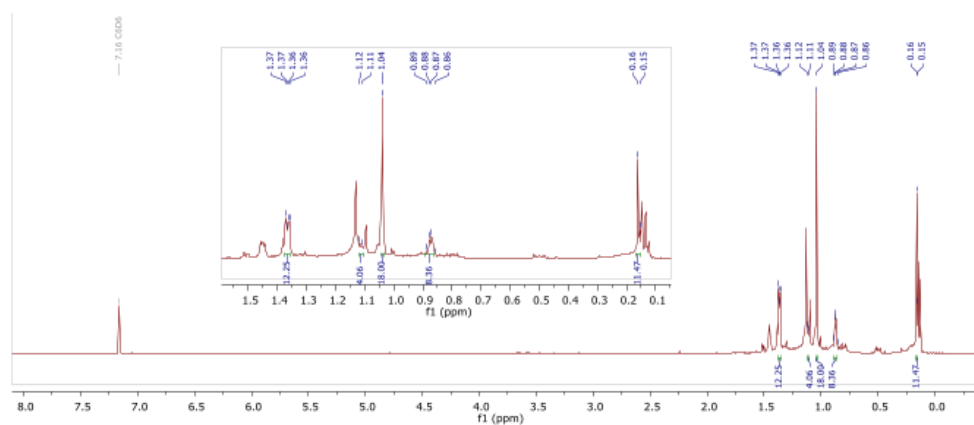


Figure 38:  $^1\text{H-NMR}$  (500 MHz,  $\text{C}_6\text{D}_6$ ) of compound **15** (*cis/trans*-species).

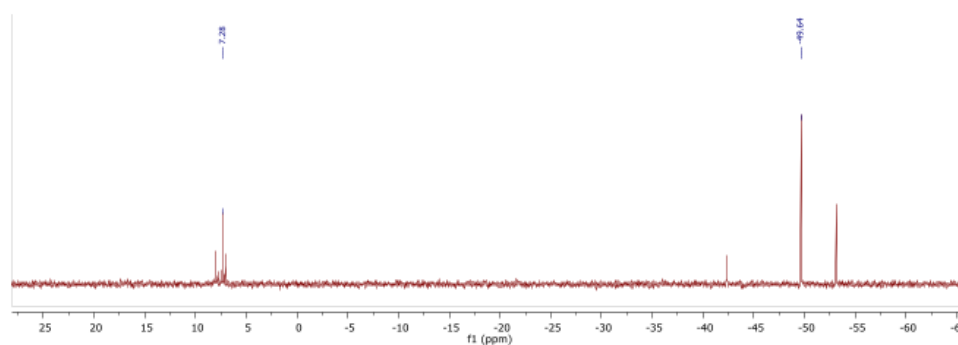


Figure 39:  $^{29}\text{Si-NMR}$  (100 MHz,  $\text{C}_6\text{D}_6$ ) of compound **15** (*cis/trans*-species).

## SUPPORTING INFORMATION

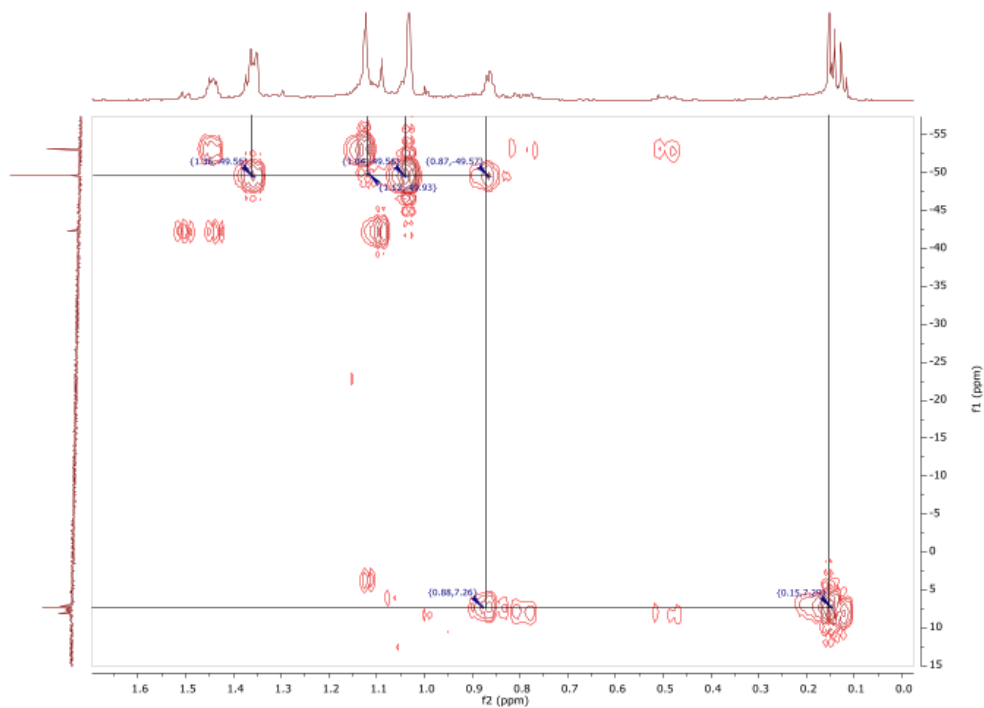


Figure 40:  $^1\text{H}$ - $^{29}\text{Si}$ -HMBC (500 MHz/100 MHz,  $\text{C}_6\text{D}_6$ ) of compound **15** (cis/trans-species).

*Trans/Cis* species: 24 % relative ratio.  $^1\text{H}$ -NMR: (500 MHz,  $\text{C}_6\text{D}_6$ ):  $\delta$  = 0.12–0.14 (m, 12H), 0.46–0.52 (m, 4H), 0.74–0.78 (m, 4H), 1.12 (s, 18H), (m, 4H), 1.43–1.45 (m, 12H).  $^{29}\text{Si}$ -NMR: (100 MHz,  $\text{C}_6\text{D}_6$ ):  $\delta$  = -53.1, 8.0. LIFDI-MS: 469.95 [ $\text{M}$ ] $^+$ , 413.99 [ $\text{M}-\text{C}_4\text{H}_8$ ] $^+$ , 358.03 [ $\text{M}-\text{C}_8\text{H}_{16}$ ] $^+$ .

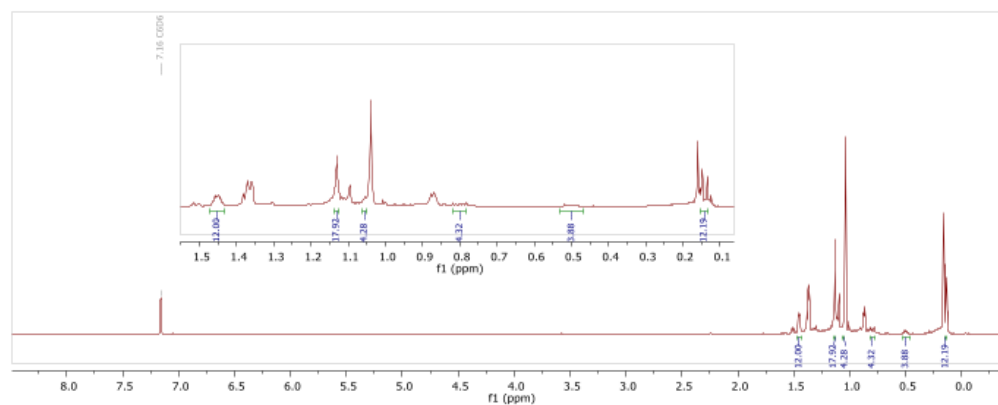


Figure 41:  $^1\text{H}$ -NMR (500 MHz,  $\text{C}_6\text{D}_6$ ) of compound **15** (trans/cis-species).

## SUPPORTING INFORMATION

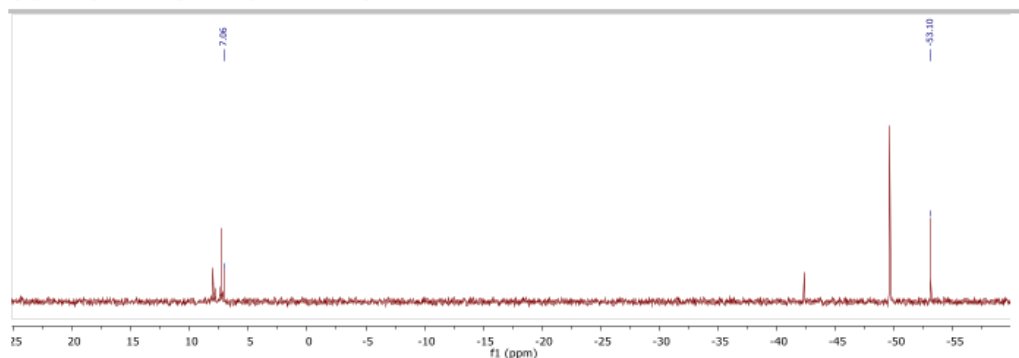


Figure 42:  $^{29}\text{Si}$ -NMR (100 MHz,  $\text{C}_6\text{D}_6$ ) of compound **15** (trans/cis-species).

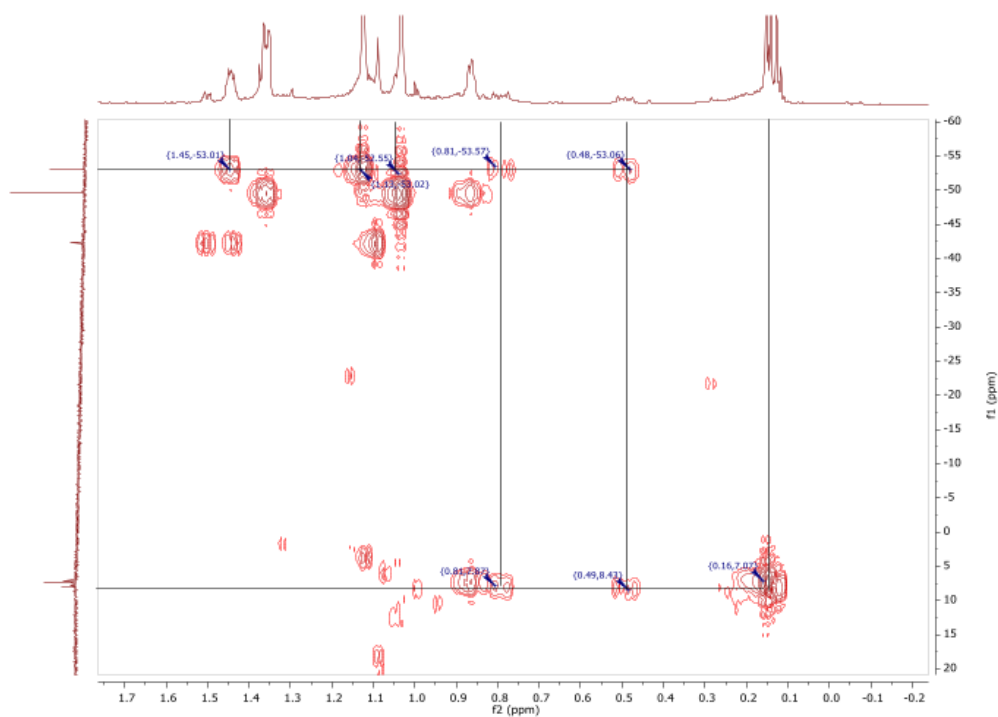


Figure 43:  $^1\text{H}$ - $^{29}\text{Si}$ -HMBC (500 MHz/100 MHz,  $\text{C}_6\text{D}_6$ ) of compound **15** (trans/cis-species).

1-butene-species: 9 % relative ratio.  $^1\text{H}$ -NMR: (500 MHz,  $\text{C}_6\text{D}_6$ )  $\delta$  = 0.07–0.10 (m, 12H), 0.59–0.68 (m, 4H), 0.79–0.81 (m, 4H), 1.08 (s, 18H), 1.18–1.19 (m, 2H), 1.19–1.20 (m, 4H), 1.39–1.40 (m, 4H), 1.47–1.49 (m, 6H).  $^{29}\text{Si}$ -NMR: (100 MHz,  $\text{C}_6\text{D}_6$ )  $\delta$  = -42.3, 6.9. LIFDI-MS: 469.95 [M] $^+$ , 413.99 [M-C $_4\text{H}_8$ ] $^+$ , 358.03 [M-C $_8\text{H}_{16}$ ] $^+$ .

## SUPPORTING INFORMATION

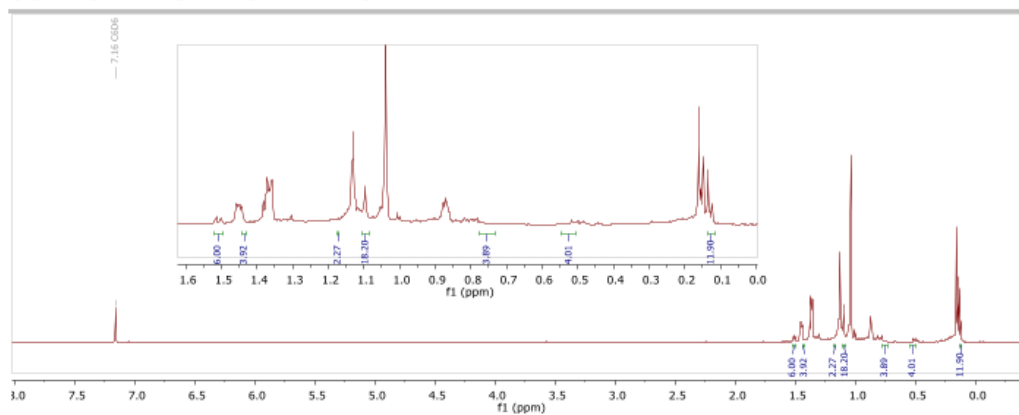


Figure 44:  $^1\text{H-NMR}$  (500 MHz,  $\text{C}_6\text{D}_6$ ) of compound **15** (1-butene species).

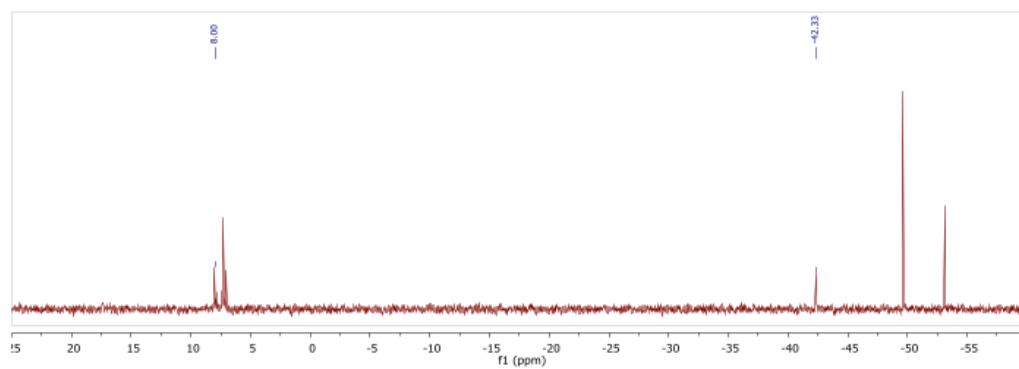


Figure 45:  $^{29}\text{Si-NMR}$  (100 MHz,  $\text{C}_6\text{D}_6$ ) of compound **15** (1-butene species).

## SUPPORTING INFORMATION

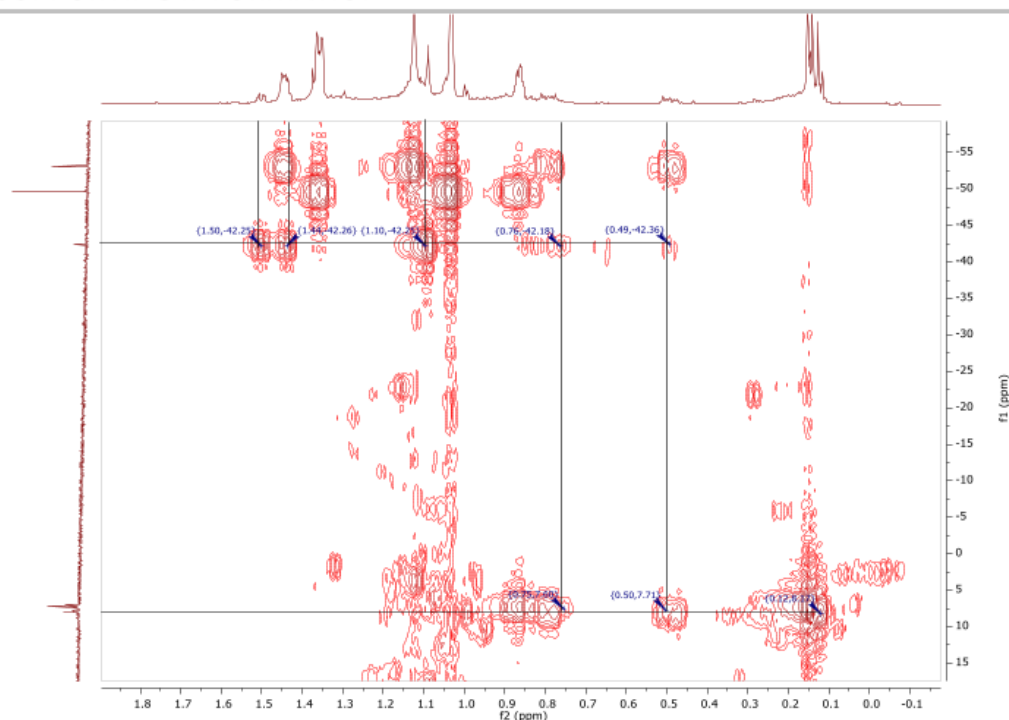
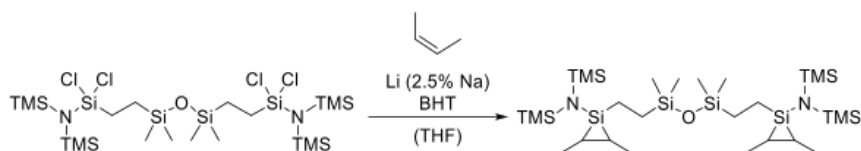


Figure 46:  $^1\text{H}$ - $^{29}\text{Si}$ -HMBC (500 MHz/100 MHz,  $\text{C}_6\text{D}_6$ ) of compound **15** (1-butene species).

2.3.5. 1,1'-((1,1,3,3-tetramethyldisiloxane-1,3-diyl)bis(ethane-2,1-diyl))bis(2,3-dimethyl-N,N-bis(trimethylsilyl)siliran-1-amine)  
**16**



A 250 mL Schlenk-tube was equipped with a PTFE-coated stir bar and was loaded with 10.0 g (14.1 mmol, 1.00 eq.) of **14**, 50 mL THF and 20 mg (0.09 mmol, 0.001 eq.) 3,5-Di-*tert*-butyl-4-hydroxytoluene (BHT) to suppress radical side reactions. The reaction tube was cooled down to  $-78\text{ }^\circ\text{C}$  with a dry ice/isopropanol mixture. Present argon atmosphere was removed *in vacuo* and 30.6 g (424.2 mmol, 30.0 eq.) *cis*-2-butene was condensed onto the cooled reaction mixture by pressurizing it with 1.80 bar of the respective gas. After re-pressurizing with argon, 1.47 g (212.1 mmol, 15.0 eq.) Li/Na alloy chunks (2.5 % Na) were added to the reaction mixture, followed by vigorous stirring at room temperature for 7 days. By the end of the reduction, *cis*-2-butene gas and remaining solvent was removed under vacuum. The slurry crude was diluted in 50 mL pentane to precipitate and separated the generated lithium chloride by filtration. The product was collected by removing the remaining solvent *in vacuo* to afford 5.46 g (8.06 mmol, 57 %) of the silylene-crosslinker **16** as a colourless oil.

The product was a mixture of diastereomeric *cis*- and *trans*-isomers. Small amounts of a constitutional isomer from the respective 1-butene could be found due to the containing impurities of isomers in the used *cis*-2-butene gas. The three different species could be assigned by  $^1\text{H}$ - $^{29}\text{Si}$ -HMBC NMR measurements, but no distinct differentiation of the respective *cis/trans* species could be achieved.

## SUPPORTING INFORMATION

*Cis/Trans* species: 70 % relative ratio. <sup>1</sup>H-NMR: (500 MHz, C<sub>6</sub>D<sub>6</sub>) δ = 0.12–0.13 (m, 12H), 0.22 (s, 36H), 0.77–0.80 (m, 8H), 1.12–1.15 (m, 4H), 1.19–1.21 (m, 12H). <sup>29</sup>Si-NMR: (100 MHz, C<sub>6</sub>D<sub>6</sub>) δ = -50.0, 4.7, 7.8. LIFDI-MS: 675.61 [M]<sup>+</sup>, 619.70 [M-C<sub>4</sub>H<sub>8</sub>]<sup>+</sup>.

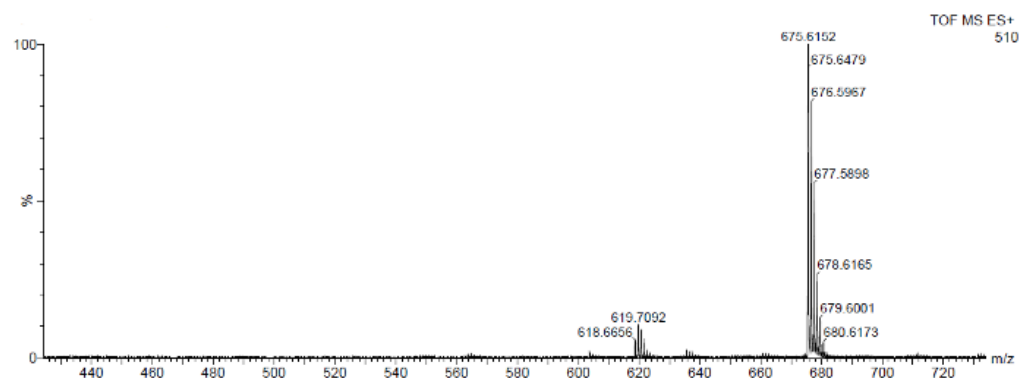


Figure 47: LIFDI-MS spectrum of compounds **16**.

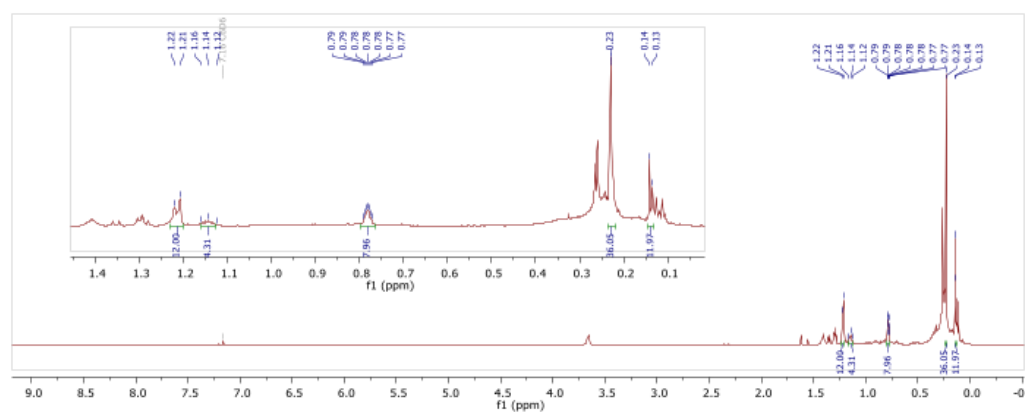


Figure 48: <sup>1</sup>H-NMR (500 MHz, C<sub>6</sub>D<sub>6</sub>) of compound **16** (*cis/trans*-species).

## SUPPORTING INFORMATION

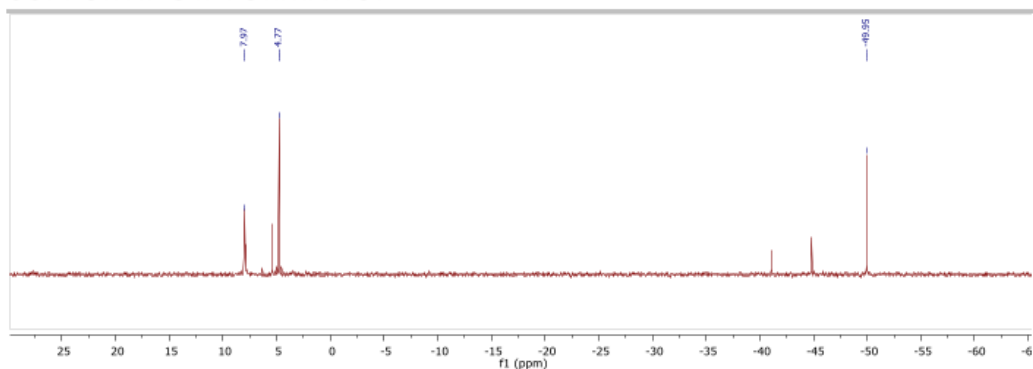


Figure 49:  $^{29}\text{Si}$ -NMR (100 MHz,  $\text{C}_6\text{D}_6$ ) of compound **16** (cis/trans-species).

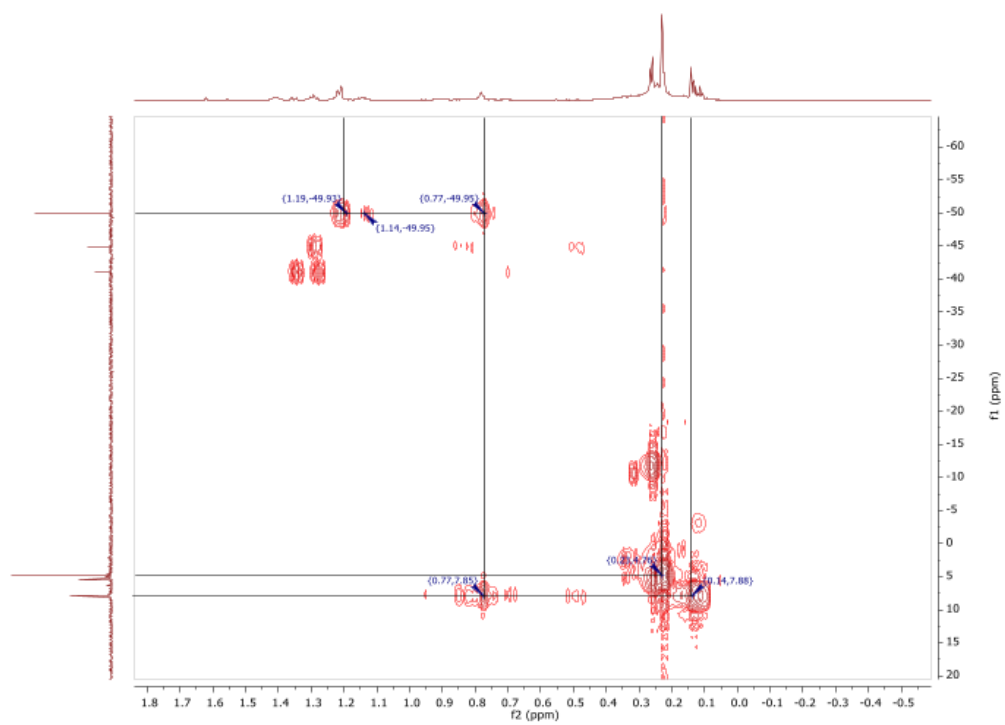
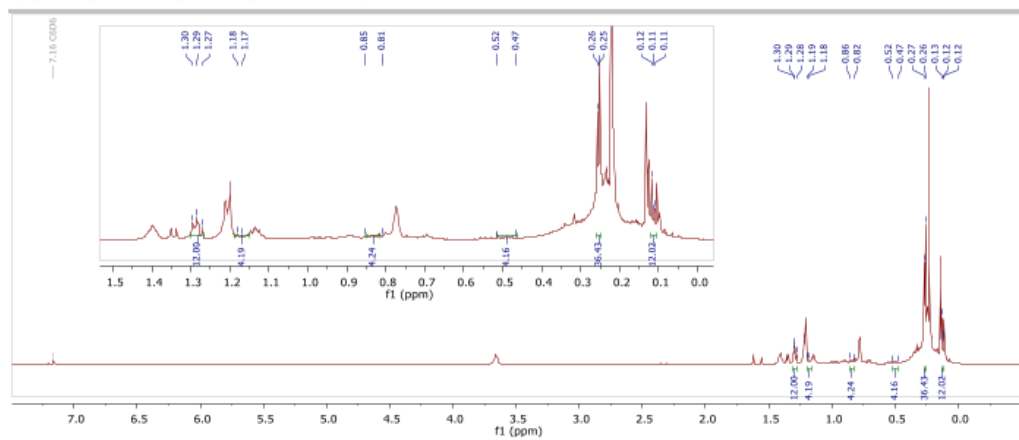
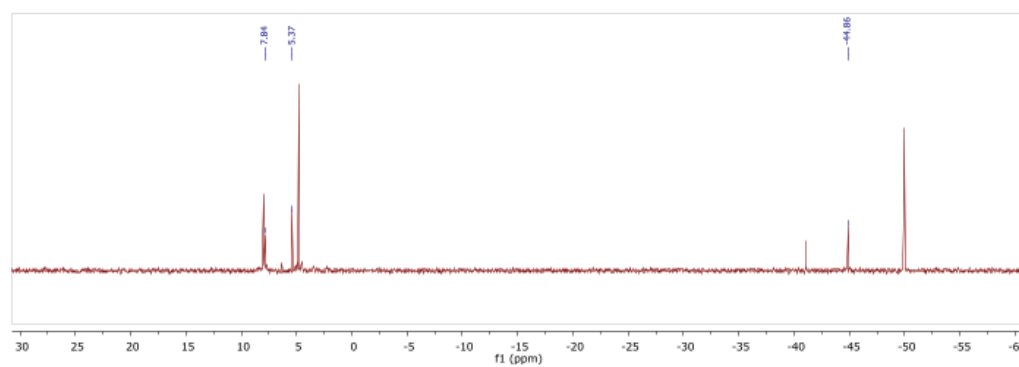


Figure 50:  $^1\text{H}$ - $^{29}\text{Si}$ -HMBC (500 MHz/100 MHz,  $\text{C}_6\text{D}_6$ ) of compound **16** (cis/trans-species).

*Trans/ Cis* species: 70 % relative ratio.  $^1\text{H}$ -NMR: (500 MHz,  $\text{C}_6\text{D}_6$ )  $\delta$  = 0.11–0.12 (m, 12H), 0.25–0.26 (m, 36H), 0.47–0.52 (m, 4H), 0.81–0.85 (m, 4H), 1.17–1.18 (m, 4H), 1.27–1.30 (m, 12H).  $^{29}\text{Si}$ -NMR: (100 MHz,  $\text{C}_6\text{D}_6$ )  $\delta$  = 44.9, 4.70, 7.68. LIFDI-MS: 675.61 [ $\text{M}$ ] $^+$ , 619.70 [ $\text{M}-\text{C}_4\text{H}_8$ ] $^+$ .



## SUPPORTING INFORMATION

Figure S1:  $^1\text{H-NMR}$  (500 MHz,  $\text{C}_6\text{D}_6$ ) of compound **16** (trans/cis-species).Figure S2:  $^{29}\text{Si-NMR}$  (100 MHz,  $\text{C}_6\text{D}_6$ ) of compound **16** (trans/cis-species).

## SUPPORTING INFORMATION

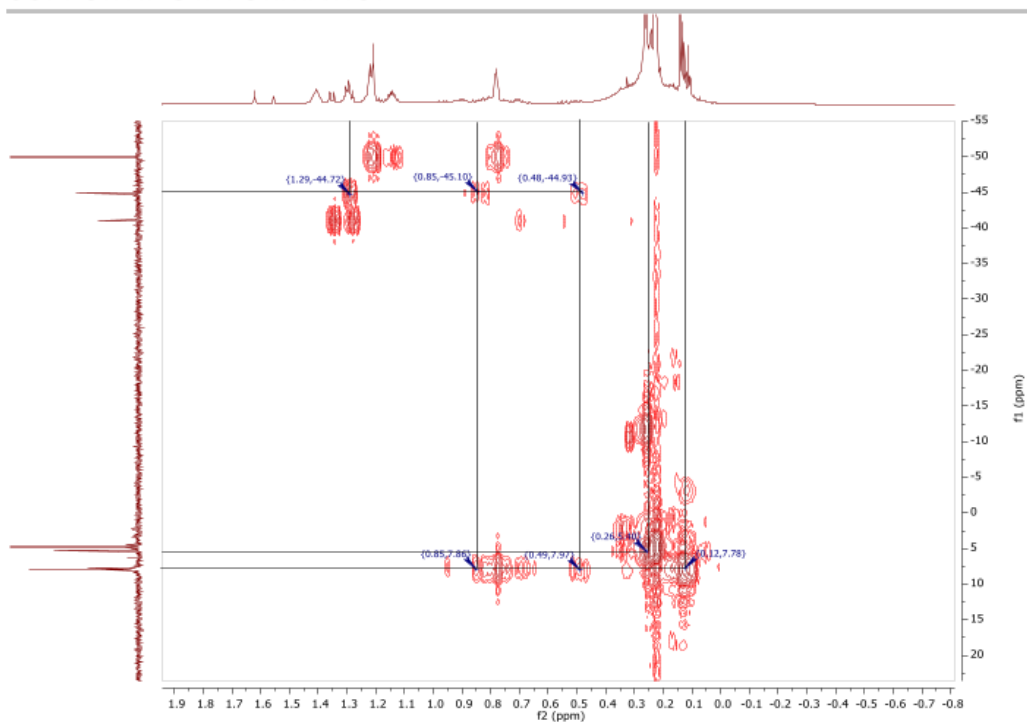


Figure 53:  $^1\text{H}$ - $^{29}\text{Si}$ -HMBC (500 MHz/100 MHz,  $\text{C}_6\text{D}_6$ ) of compound **16** (trans/cis-species).

1-butene-species: 12 % relative ratio.  $^1\text{H-NMR}$ : (500 MHz,  $\text{C}_6\text{D}_6$ )  $\delta$  = 0.09–0.10 (m, 12H), 0.23–0.24 (m, 36H), 0.52–0.57 (m, 4H), 0.67–0.74 (m, 8H), 0.93–0.99 (m, 4H), 1.27 (m, 2H), 1.34–1.35 (m, 6H).  $^{29}\text{Si-NMR}$ : (100 MHz,  $\text{C}_6\text{D}_6$ )  $\delta$  = -41.1, 5.3, 7.8. LIFDI-MS: 675.61 [M] $^+$ , 619.70 [M-C $_4\text{H}_8$ ] $^+$ .

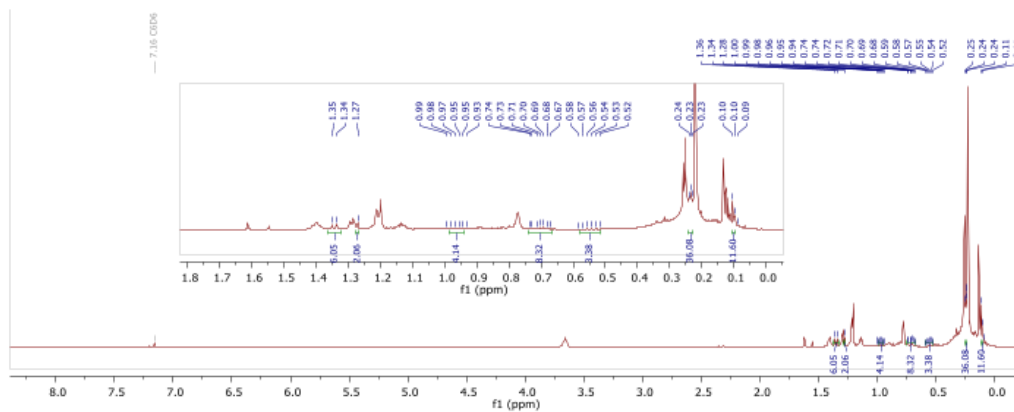


Figure 54:  $^1\text{H-NMR}$  (500 MHz,  $\text{C}_6\text{D}_6$ ) of compound **16** (1-butene species).

## SUPPORTING INFORMATION

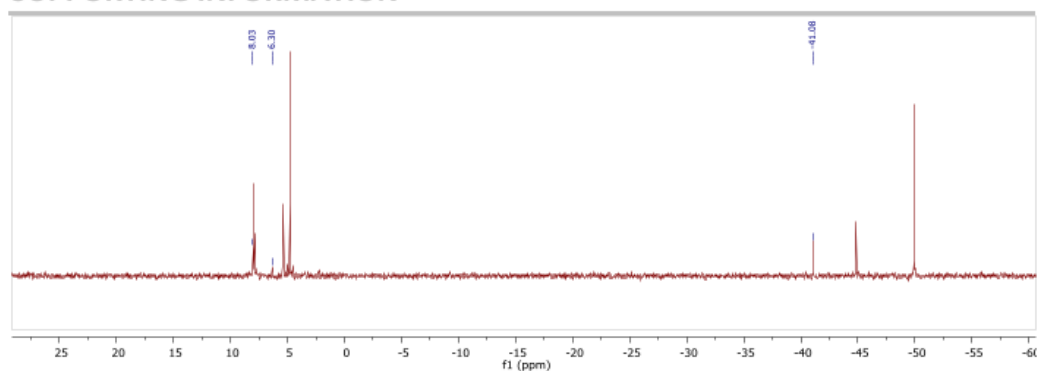


Figure S5:  $^{29}\text{Si}$ -NMR (100 MHz,  $\text{C}_6\text{D}_6$ ) of compound **16** (1-butene species).

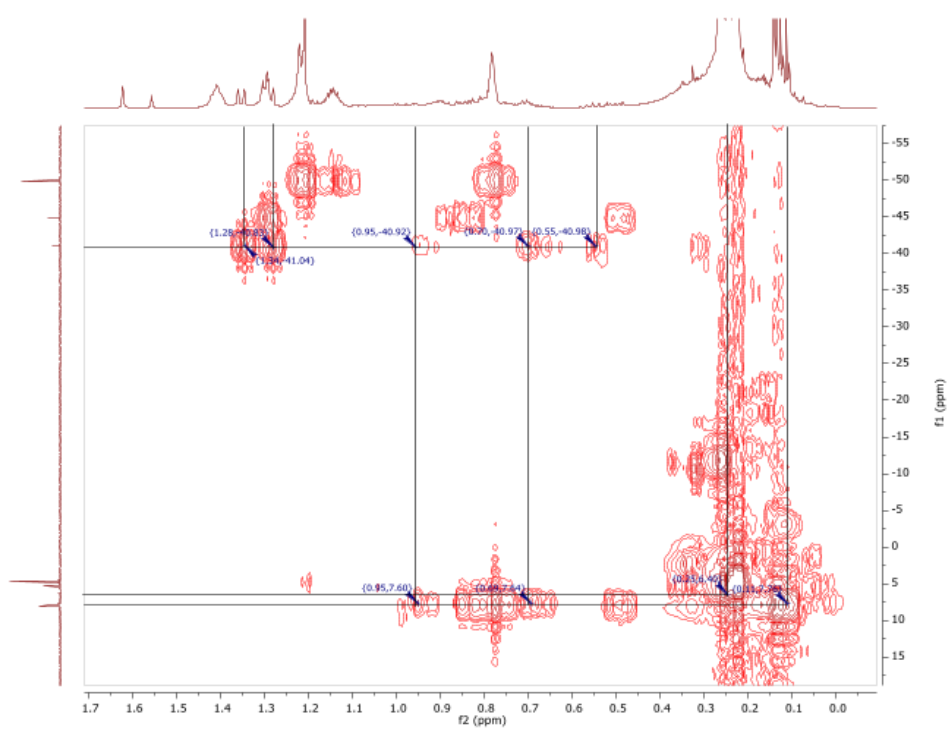


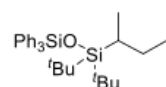
Figure S6:  $^1\text{H}$ - $^{29}\text{Si}$ -HMBC (500 MHz/100 MHz,  $\text{C}_6\text{D}_6$ ) of compound **16** (1-butene species).

## SUPPORTING INFORMATION

## 2.4. Screening Reactions and Screening Products

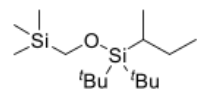
## 2.4.1. Ring opening

**General Procedure:** 30 mg (151.2  $\mu\text{mol}$ , 1.0 eq.) of **1** and 1.0 eq. of the respective silanol or alcohol (dry) are dissolved in 0.6 ml  $\text{C}_6\text{D}_6$  in a high-pressure J-Young NMR-tube. The tube is capped with a PTFE screw-cap. The mixture is heated to 80 °C in an oil-bath until the reactants are consumed or the reaction reached maximum conversion. The reaction progress can be monitored by  $^1\text{H-NMR}$  and/or  $^{29}\text{Si-NMR}$ .  $^{29}\text{Si-ig}$  (inverse gated decoupling) pulse sequence allows quantitative integration of the Si-signals and therefore estimation of reaction progress.

1-(sec-Butyl)-1,1-di-tert-butyl-3,3,3-triphenyldisiloxane

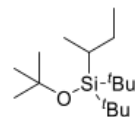
Substrate: Triphenylsilanol

$^1\text{H-NMR}$ : (500 MHz,  $\text{C}_6\text{D}_6$ )  $\delta$  = 0.89 (t, 3 H,  $\text{CH}_2\text{-CH}_3$ ), 1.07 (s, 9 H, tBu), 1.09 (s, 9 H, tBu), 1.19 (d, 3 H,  $\text{CH-CH}_3$ ), 2.00 (dq, 1 H, CH), 1.24 (m, 2 H,  $\text{CH}_2\text{-CH}_3$ ), 7.20 (m, 9 H, Ph), 7.82 (m, 6 H, Ph).  $^{29}\text{Si-NMR}$ : (100 MHz,  $\text{C}_6\text{D}_6$ )  $\delta$  = 6.10 (SitBu<sub>2</sub>), -21.23 (SiPh<sub>3</sub>).

sec-Butyldi-tert-butyl(trimethylsilyl)methoxy)silane

Substrate: Trimethylsilylmethanol

$^1\text{H-NMR}$ : (500 MHz,  $\text{C}_6\text{D}_6$ )  $\delta$  = 0.05 (s, 9 H, SiMe<sub>3</sub>), 0.98 (t, 3 H,  $\text{CH}_2\text{CH}_3$ ), 1.11 (d, 18 H, tBu), 1.14 (s, 3 H,  $\text{CH-CH}_3$ ), 1.24 (m, 1 H,  $\text{CH}_2\text{-CH}_3$ ), 1.87 (dq, 1 H, CH-CH<sub>3</sub>), 3.41 (s, 2 H,  $\text{CH}_2\text{-SiMe}_3$ ) (1 H of  $\text{CH}_2\text{-CH}_3$  superimposed).  $^{29}\text{Si-NMR}$ : (100 MHz,  $\text{C}_6\text{D}_6$ )  $\delta$  = 8.07 (SitBu<sub>2</sub>), -0.75 (SiMe<sub>3</sub>).

tert-Butoxy(sec-butyl)di-tert-butylsilane

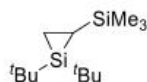
Substrate: tert-Butanol

$^1\text{H-NMR}$ : (500 MHz,  $\text{C}_6\text{D}_6$ )  $\delta$  = 0.87 (m, 1 H,  $\text{CH}_2\text{CH}_3$ ), 0.96 (t, 3 H,  $\text{CH}_2\text{CH}_3$ ), 1.04 (s, 18 H, tBu), 1.11 (d, 3 H,  $\text{CH-CH}_3$ ), 1.21 (m, 1 H,  $\text{CH}_2\text{CH}_3$ ), 1.59 (m, 3 H, OtBu), 1.82 (m, 1 H, CH-CH<sub>3</sub>).  $^{29}\text{Si-NMR}$ : (100 MHz,  $\text{C}_6\text{D}_6$ )  $\delta$  = 9.06 (SitBu<sub>2</sub>).

## SUPPORTING INFORMATION

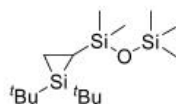
## 2.4.2. Silylene Transfer

**General Procedure:** 2.0 g (10.08 mmol, 1.2 eq.) of **1** and 1.0 eq. of the respective olefin or are dissolved in 5 ml dry toluene in a screw-cap vial with integrated rubber septum. The emerging butene gas must be released over a syringe needle in the septum. The mixture is heated to 80 °C in an oil-bath until the reactants are consumed. The reaction progress can be monitored by <sup>1</sup>H-NMR and/or <sup>29</sup>Si-NMR. <sup>29</sup>Si-ig (inverse gated decoupling) pulse sequence allows quantitative integration of the Si-signals and therefore estimation of reaction progress. Excess **1** is removed in high vacuum. Acceleration of the reaction can be achieved by addition of catalytic amounts AgOTf.<sup>[7-10]</sup> Products can be refined by high-vacuum (10<sup>-3</sup>) bulb-to-bulb distillation.

1,1-Di-tert-butyl-2-(trimethylsilyl)silirane

Substrate: Vinyltrimethylsilane

<sup>1</sup>H-NMR: (500 MHz, C<sub>6</sub>D<sub>6</sub>) δ = -0.31 (dd, 1 H, CH), 0.22 (s, 9 H, SiMe<sub>3</sub>), 0.48 (dd, 1 H, CH), 0.73 (dd, 1 H, CH), 1.04 (s, 9 H, tBu), 1.10 (s, 9 H, tBu).  
<sup>29</sup>Si-NMR: (100 MHz, C<sub>6</sub>D<sub>6</sub>) δ = 1.01 (SiMe<sub>3</sub>), -48.33 (Si(tBu)<sub>2</sub>). <sup>13</sup>C-NMR: (125 MHz, C<sub>6</sub>D<sub>6</sub>) δ = -2.9, -1.3, 1.1, 29.6, 30.0.

1,1-Di-tert-butyl-2-(1,1,3,3,3-pentamethyldisiloxaneyl)silirane

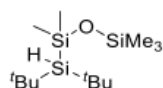
Substrate: Vinylpentamethyldisiloxane

<sup>1</sup>H-NMR: (500 MHz, C<sub>6</sub>D<sub>6</sub>) δ = -0.32 (t, 1 H, CH), 0.16 (s, 9 H, SiMe<sub>3</sub>), 0.28 (s, 3 H, OSiMe), 0.31 (s, 3 H, OSiMe), 0.61 (t, 1 H, CH), 0.69 (m, 1 H, CH), 1.04 (s, 9 H, tBu), 1.16 (s, 9 H, tBu). <sup>29</sup>Si-NMR: (100 MHz, C<sub>6</sub>D<sub>6</sub>) δ = 6.43 (SiMe<sub>3</sub>), 5.77 (SiMe<sub>2</sub>), -48.35 (Si(tBu)<sub>2</sub>).

## SUPPORTING INFORMATION

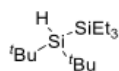
## 2.4.3. Silylene Insertion

**General Procedure:** 30 mg (151.2  $\mu\text{mol}$ , 1.0 eq.) of **1** or 30 mg (133.7  $\mu\text{mol}$ , 1 eq.) of 7,7-di-*tert*-butyl-7-silabicyclo[4.1.0]heptane and an equivalent amount of screening compound (1.0 eq.) is dissolved in 0.6 ml  $\text{C}_6\text{D}_6$  in a high-pressure J-Young NMR-tube. The tube is capped with a PTFE screw-cap. The mixture is heated to 140 °C in an oil-bath (High pressure! Use explosion shield or sand bath) until the reactants are consumed or the reaction reached maximum conversion. The reaction progress can be monitored by  $^1\text{H-NMR}$  and/or  $^{29}\text{Si-NMR}$ .  $^{29}\text{Si-ig}$  (inverse gated decoupling) pulse sequence allows quantitative integration of the Si-signals and therefore estimation of reaction progress.

1-(Di-*tert*-butylsilyl)-1,1,3,3,3-pentamethyldisiloxane

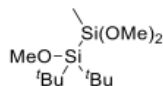
Substrate: Pentamethyldisiloxane

$^1\text{H-NMR}$ : (500 MHz,  $\text{C}_6\text{D}_6$ )  $\delta$  = 0.12 (s, 9 H,  $\text{SiMe}_3$ ), 0.39 (s, 6 H,  $\text{SiMe}_2$ ), 1.17 (s, 18 H, *t*Bu), 3.59 (s, 1 H, Si-H).  $^{29}\text{Si-NMR}$ : (100 MHz,  $\text{C}_6\text{D}_6$ )  $\delta$  = 8.32 ( $\text{SiMe}_3$ ), 5.48 ( $\text{SiMe}_2$ ), -6.58 ( $\text{SiHtBu}_2$ ).

2,2-Di-*tert*-butyl-1,1,1-triethylsilane

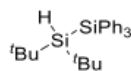
Substrate: Triethylsilane

$^1\text{H-NMR}$ : (500 MHz,  $\text{C}_6\text{D}_6$ )  $\delta$  = 0.77 (q, 6 H,  $\text{CH}_2$ ), 1.05 (t, 9 H, Me), 1.14 (s, 18 H, *t*Bu), 3.69 (s, 1 H, Si-H).  $^{29}\text{Si-NMR}$ : (100 MHz,  $\text{C}_6\text{D}_6$ )  $\delta$  = -6.2 ( $\text{SiHtBu}_2$ ), -8.13 ( $\text{SiEt}_3$ ).

1,1-Di-*tert*-butyl-1,2,2-trimethoxy-2-methyldisilane

Substrate: Trimethoxymethylsilane

$^1\text{H-NMR}$ : (500 MHz,  $\text{C}_6\text{D}_6$ )  $\delta$  = 0.30 (s, 3 H,  $\text{SiMe}$ ), 1.20 (s, 18 H, *t*Bu<sub>2</sub>), 3.37 (s, 6 H,  $\text{SiOMe}_2$ ), 3.63 (s, 3 H,  $\text{SiOMe}$ ).  $^{29}\text{Si-NMR}$ : (100 MHz,  $\text{C}_6\text{D}_6$ )  $\delta$  = 12.07 ( $\text{SiHtBu}_2$ ), -0.83 ( $\text{SiMe}_2\text{OMe}$ ).  $^{13}\text{C-NMR}$ : (125 MHz,  $\text{C}_6\text{D}_6$ )  $\delta$  = 0.7, 22.7, 28.5, 50.1, 54.4.

2,2-Di-*tert*-butyl-1,1,1-triphenylsilane

Substrate: Triphenylsilane

$^1\text{H-NMR}$ : (500 MHz,  $\text{C}_6\text{D}_6$ )  $\delta$  = 1.07 (s, 18 H, *t*Bu<sub>2</sub>), 4.37 (s, 1 H, SiH), 7.12 – 7.19 (m, 9 H, Ph), 7.81 – 7.89 (m, 6 H, Ph).  $^{29}\text{Si-NMR}$ : (100 MHz,  $\text{C}_6\text{D}_6$ )  $\delta$  = -6.0 ( $\text{SiPh}_3$ ), -21.7 ( $\text{SiHtBu}_2$ ).

### SUPPORTING INFORMATION

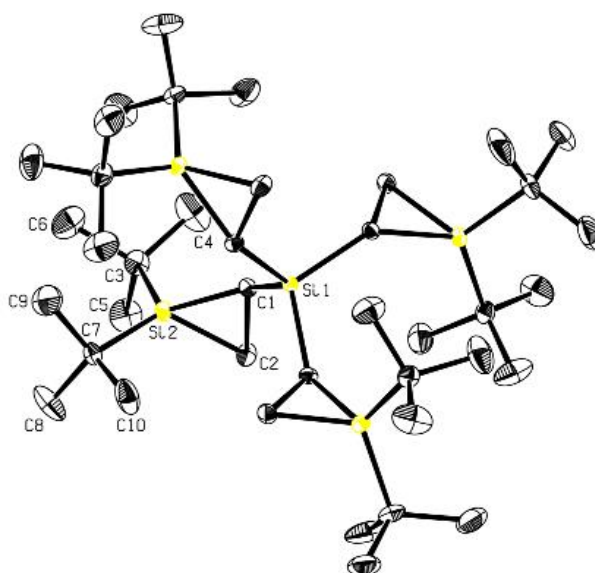
---

#### UV-Vis Experiments

Based on reports from Boudjouk and Fink on photolytic silirane cleavage we investigated the potential for photochemical curing.<sup>[5-6, 11]</sup> UV-VIS measurements revealed absorption maxima for siliranes **1**, **6-10**, **15** and **16** in the range of 210–230 nm. UV-Photolysis of **1** at 254 nm (in cyclohexane-d<sub>12</sub>) in presence of screening compounds gave the expected insertion products (analogously to thermolysis). Due to insufficient absorption this reaction required long irradiation. The requirement for highly energetic UV-C radiation, which is not compatible with siloxanes, disqualifies compounds **6-10**, **15** and **16** for photocrosslinking.

## SUPPORTING INFORMATION

## 3. X-ray Crystallographic Data



## Tetrakis(1,1-di-tert-butylsilirane-2-yl)silane 6

CCDC Deposition Number	1953911
Diffractometer operator	Philipp J. Altmann
Formula weight	176.38
Temperature	100(2) K
Bond precision:	C-C = 0.0031 Å
Wavelength	0.71073 Å
Crystal size	0.070 x 0.085 x 0.149 mm
Crystal habit	clear colourless fragment
Crystal system	tetragonal
Space group	I 41/a
Unit cell dimensions	a = 16.882(2) Å $\alpha = 90^\circ$ b = 16.882(2) Å $\beta = 90^\circ$ c = 16.323(2) Å $\gamma = 90^\circ$
Volume	4652.1(13) Å <sup>3</sup>
Z	16
Density (calculated)	1.007 g/cm <sup>3</sup>
Absorption coefficient	0.177 mm <sup>-1</sup>
F(000)	1576
Diffractometer Bruker	D8 Kappa Apex II
Radiation source	fine-focus sealed tube, Mo
Theta range	2.41 to 25.02°
Index ranges	-20 <= h <= 20, -20 <= k <= 20, -19 <= l <= 19
Reflections collected	74129
Independent reflections	2054 [R(int) = 0.0497]
Coverage of independent refl.	100.0%



## SUPPORTING INFORMATION

Absorption correction	Multi-Scan
Max. and min. transmission	0.9880 and 0.9740
Refinement method	Full-matrix least-squares on F2
Refinement program	SHELXL-2014/7 (Sheldrick, 2014)
Function minimized	$\sum w(\text{Fo}^2 - \text{Fc}^2)^2$
Data / restraints / parameters	2054 / 0 / 108
Goodness-of-fit on F2	1.035
$\Delta/\text{omax}$	0.001
Final R indices	1813 data; $l > 2\sigma(l)$ R1 = 0.0431, wR2 = 0.1071 all data R1 = 0.0496, wR2 = 0.1125
Weighting scheme	$w = 1/[\sigma^2(\text{Fo}^2) + (0.0468P)^2 + 14.2967P]$ where $P = (\text{Fo}^2 + 2\text{Fc}^2)/3$
Largest diff. peak and hole	0.761 and -0.319 eÅ <sup>-3</sup>
R.M.S. deviation from mean	0.059 eÅ <sup>-3</sup>

Bond lengths (Å) for **6**:

Si1-C1 1.8895(19)	Si1-C1 1.8895(19)
Si1-C1 1.8895(19)	Si1-C1 1.8895(19)
Si2-C2 1.836(2)	Si2-C1 1.869(2)
Si2-C7 1.900(2)	Si2-C3 1.914(2)
C1-C2 1.584(3)	C1-H1 1.0
C2-H2A 0.99	C2-H2B 0.99
C3-C4 1.517(3)	C3-C5 1.535(3)
C3-C6 1.557(3)	C4-H4A 0.98
C4-H4B 0.98	C4-H4C 0.98
C5-H5A 0.98	C5-H5B 0.98
C5-H5C 0.98	C6-H6A 0.98
C6-H6B 0.98	C6-H6C 0.98
C7-C8 1.528(3)	C7-C9 1.529(3)
C7-C10 1.536(3)	C8-H8A 0.98
C8-H8B 0.98	C8-H8C 0.98
C9-H9A 0.98	C9-H9B 0.98
C9-H9C 0.98	C10-H10A 0.98
C10-H10B 0.98	C10-H10C 0.98

Bond angles (°) for **6**:

C1-Si1-C1 107.81(6)	C1-Si1-C1 107.81(6)
C1-Si1-C1 112.85(12)	C1-Si1-C1 112.85(12)
C1-Si1-C1 107.81(6)	C1-Si1-C1 107.81(6)
C2-Si2-C1 50.63(8)	C2-Si2-C7 118.74(10)
C1-Si2-C7 121.43(9)	C2-Si2-C3 113.16(10)
C1-Si2-C3 116.84(9)	C7-Si2-C3 118.04(10)
C2-C1-Si2 63.60(10)	C2-C1-Si1 123.25(14)
Si2-C1-Si1 139.44(11)	C2-C1-H1 107.3
Si2-C1-H1 107.3	Si1-C1-H1 107.3
C1-C2-Si2 65.77(10)	C1-C2-H2A 117.1
Si2-C2-H2A 117.1	C1-C2-H2B 117.1
Si2-C2-H2B 117.1	H2A-C2-H2B 114.2
C4-C3-C5 109.9(2)	C4-C3-C6 108.3(2)
C5-C3-C6 106.85(19)	C4-C3-Si2 110.20(15)
C5-C3-Si2 108.57(16)	C6-C3-Si2 112.95(16)
C3-C4-H4A 109.5	C3-C4-H4B 109.5
H4A-C4-H4B 109.5	C3-C4-H4C 109.5
H4A-C4-H4C 109.5	H4B-C4-H4C 109.5
C3-C5-H5A 109.5	C3-C5-H5B 109.5
H5A-C5-H5B 109.5	C3-C5-H5C 109.5
H5A-C5-H5C 109.5	H5B-C5-H5C 109.5
C3-C6-H6A 109.5	C3-C6-H6B 109.5
H6A-C6-H6B 109.5	C3-C6-H6C 109.5
H6A-C6-H6C 109.5	H6B-C6-H6C 109.5
C8-C7-C9 110.7(2)	C8-C7-C10 107.5(2)
C9-C7-C10 107.2(2)	C8-C7-Si2 111.78(16)
C9-C7-Si2 111.38(15)	C10-C7-Si2 108.00(14)

**SUPPORTING INFORMATION**

---

C7-C8-H8A 109.5	C7-C8-H8B 109.5
H8A-C8-H8B 109.5	C7-C8-H8C 109.5
H8A-C8-H8C 109.5	H8B-C8-H8C 109.5
C7-C9-H9A 109.5	C7-C9-H9B 109.5
H9A-C9-H9B 109.5	C7-C9-H9C 109.5
H9A-C9-H9C 109.5	H9B-C9-H9C 109.5
C7-C10-H10A 109.5	C7-C10-H10B 109.5
H10A-C10-H10B 109.5	C7-C10-H10C 109.5
H10A-C10-H10C 109.5	H10B-C10-H10C 109.5

## SUPPORTING INFORMATION

## 4. Rheological Measurements

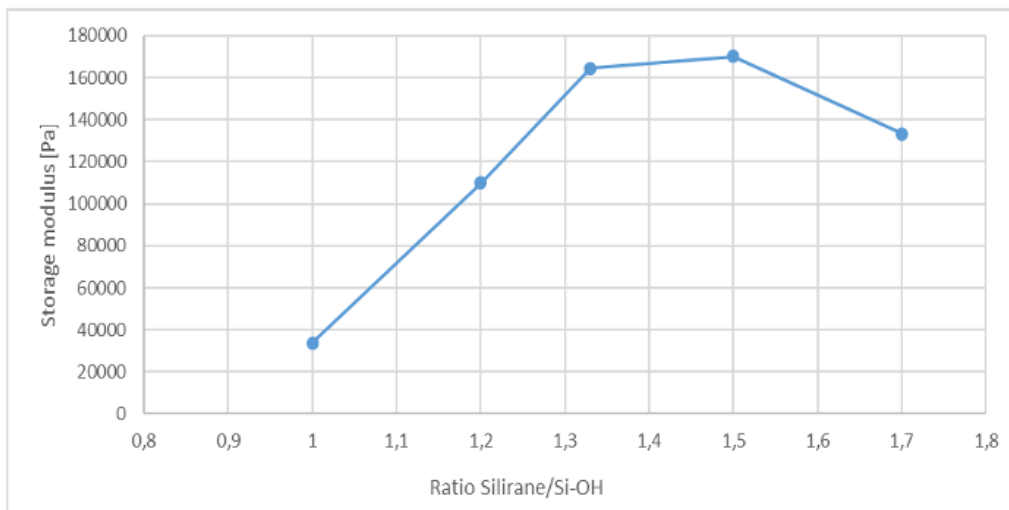


Figure 57: Storage modulus of crosslinked elastomers made from **8** and SiOH-terminated PDMS ( $n \sim 131$ ). Values are taken after full crosslinking (steady viscosity) at 110 °C.

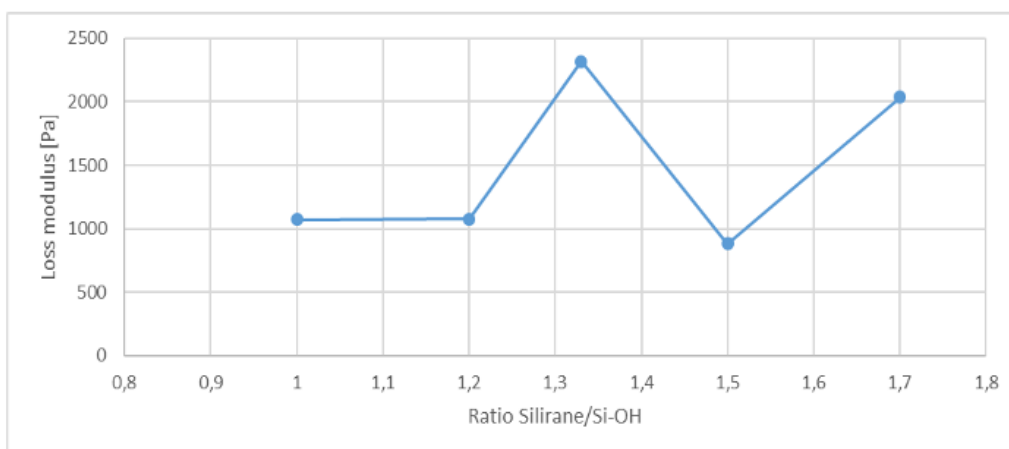


Figure 58: Loss modulus of crosslinked elastomers made from **8** and SiOH-terminated PDMS ( $n \sim 131$ ). Values are taken after full crosslinking (steady viscosity) at 110 °C.

SUPPORTING INFORMATION

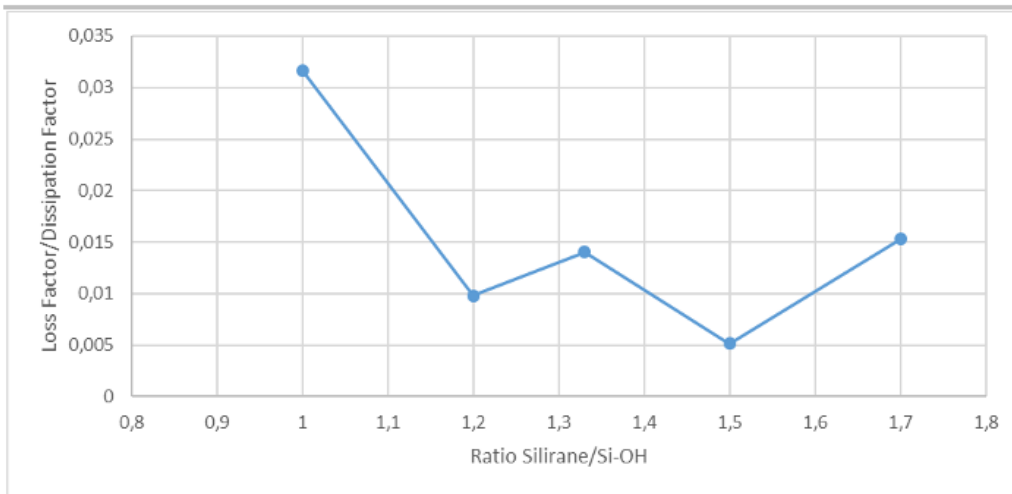


Figure 59: Loss factor  $\tan(\delta)$  of crosslinked elastomers made from **8** and SiOH-terminated PDMS ( $n \sim 131$ ). Values are taken after full crosslinking (steady viscosity) at 110 °C and are mean values of 100 measuring points.

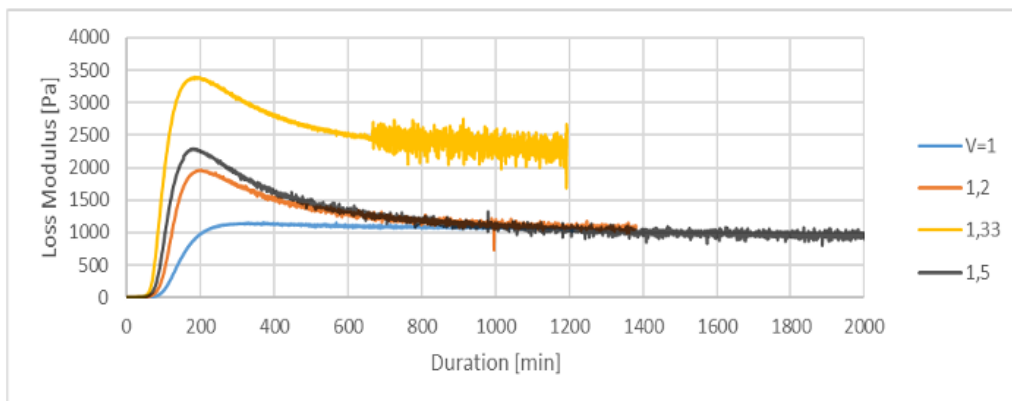


Figure 60: Loss modulus of mixtures made from **8** and SiOH-terminated PDMS ( $n \sim 131$ ) during crosslinking process at 110 °C. V = Ratio Silirane/Si-OH.

SUPPORTING INFORMATION

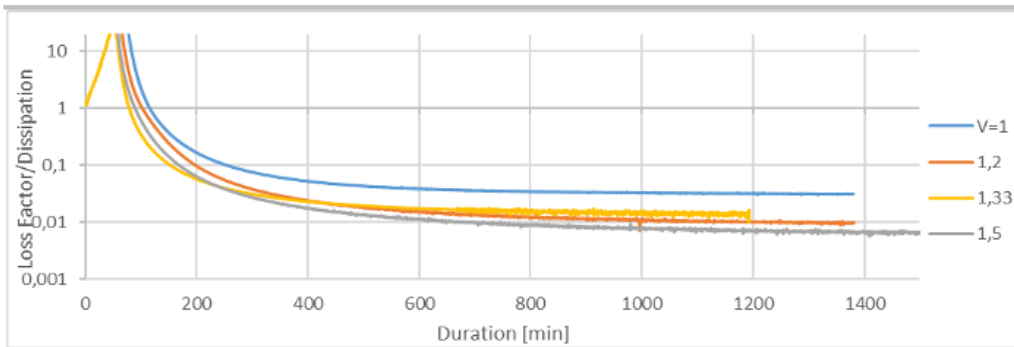


Figure 61: Loss factor  $\tan(\delta)$  of mixtures made from **8** and SiOH-terminated PDMS ( $n \approx 131$ ) during crosslinking process at 110 °C. V = Ratio Silirane/Si-OH.

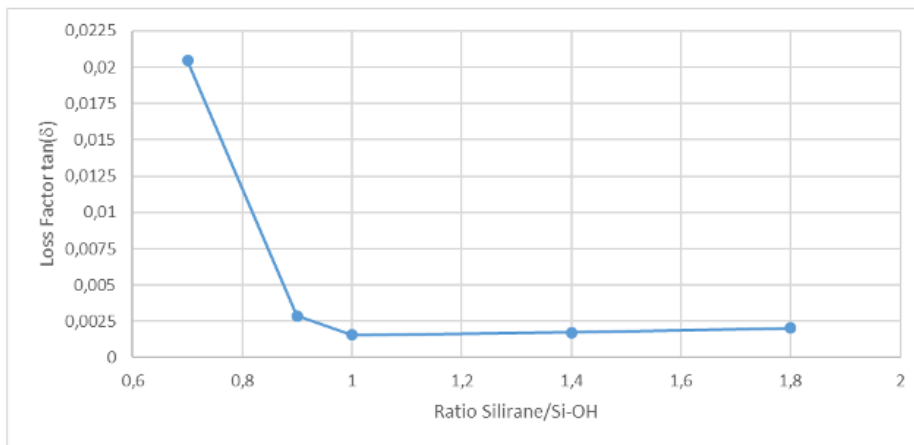


Figure 62: Loss factor  $\tan(\delta)$  of crosslinked elastomers made from **9** and SiOH-terminated PDMS ( $n \approx 131$ ). Values are taken after full crosslinking (steady viscosity) at 110 °C and are mean values of 100 measuring points.

SUPPORTING INFORMATION

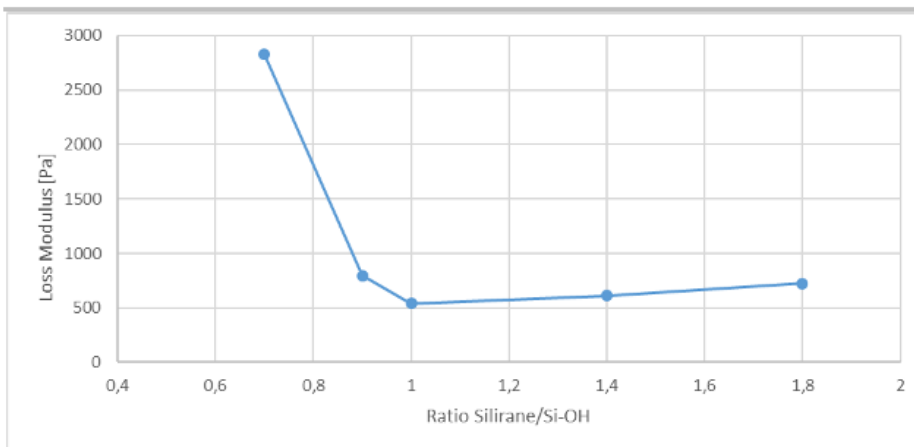


Figure 63: Loss modulus of crosslinked elastomers made from **9** and SiOH-terminated PDMS (n~131). Values are taken after full crosslinking (steady viscosity) at 110 °C.

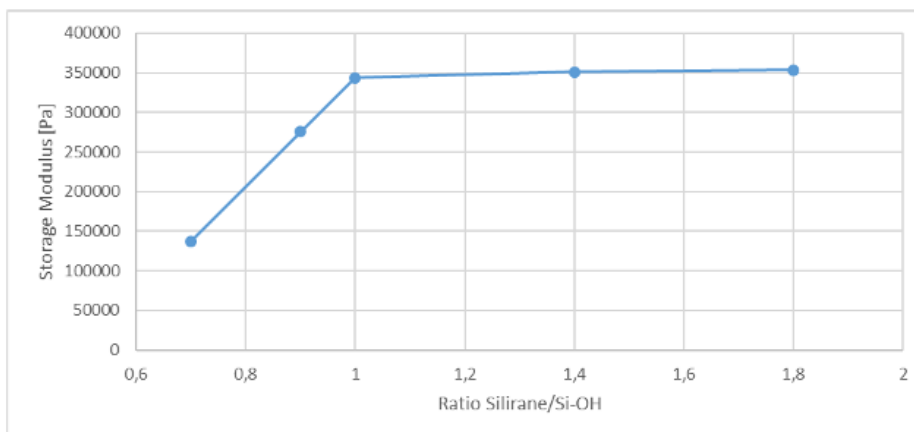


Figure 64: Storage modulus of crosslinked elastomers made from **9** and SiOH-terminated PDMS (n~131). Values are taken after full crosslinking (steady viscosity) at 110 °C.

SUPPORTING INFORMATION

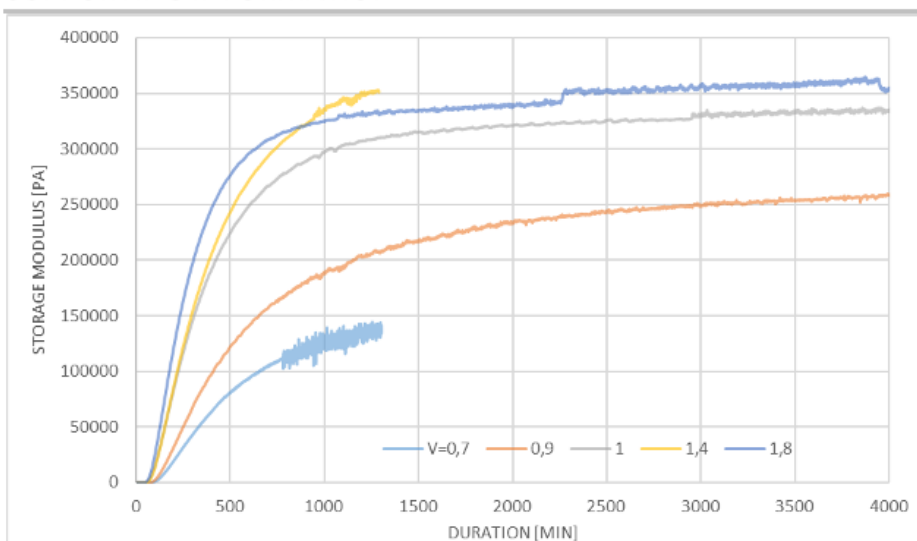


Figure 65: Storage modulus of mixtures made from **9** and SiOH-terminated PDMS ( $n \sim 131$ ) during crosslinking process at 110 °C. V = Ratio Silirane/Si-OH.

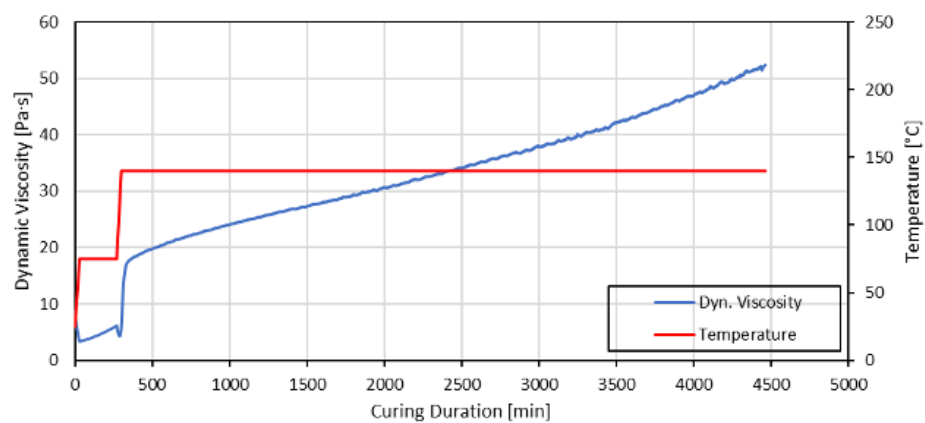


Figure 66: Complex viscosity of crosslinker **15** and Si-OH terminated PDMS ( $n \sim 131$ ) during curing process at different temperatures in a ratio of 2 (Silirane/Si-OH).

SUPPORTING INFORMATION

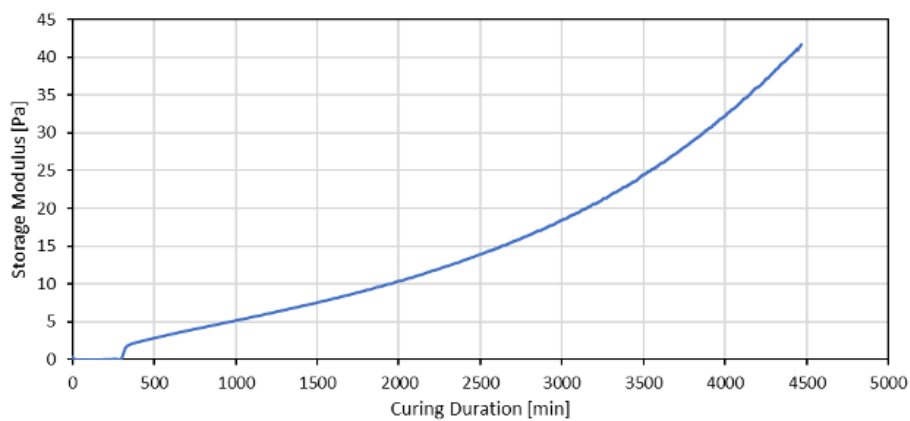


Figure 67: Storage modulus of crosslinker 15 and Si-OH terminated PDMS ( $n \sim 131$ ) during crosslinking process in Silirane/Si-OH ratio of 2.

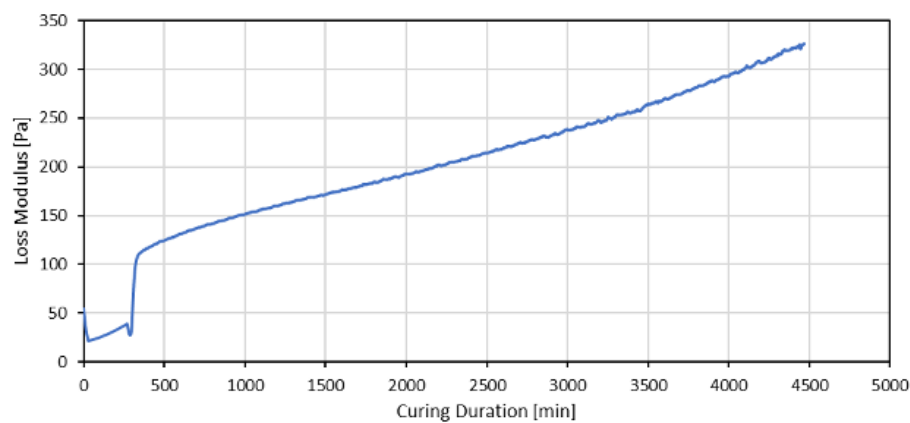


Figure 68: Loss modulus of crosslinker 15 and Si-OH terminated PDMS ( $n \sim 131$ ) during crosslinking process in Silirane/Si-OH ratio of 2.



SUPPORTING INFORMATION

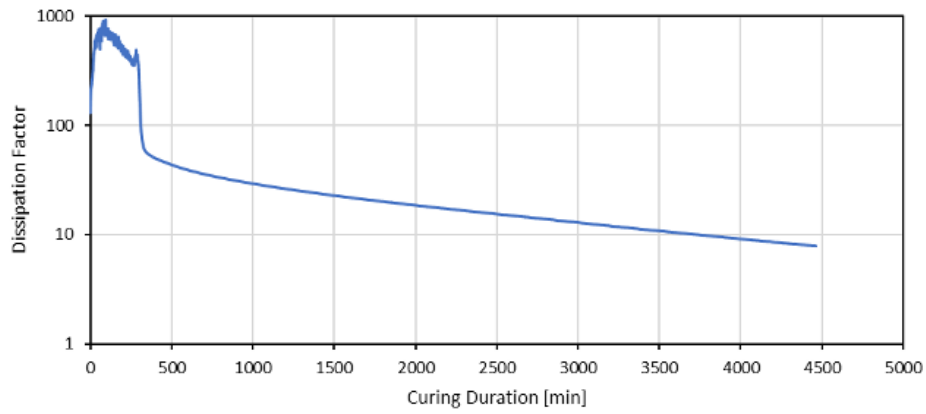


Figure 69: Dissipation factor  $\tan(\delta)$  of crosslinker 15 and Si-OH terminated PDMS ( $n \sim 131$ ) during crosslinking process in Silirane/Si-OH ratio of 2.

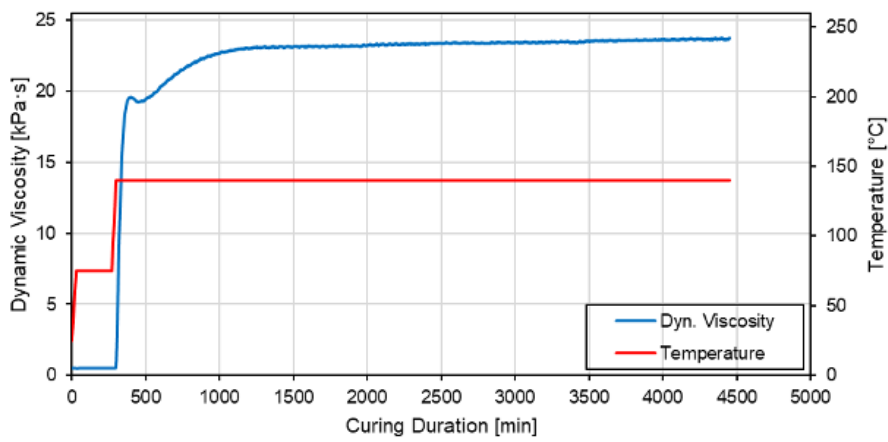


Figure 70: Complex viscosity of crosslinker 16 and Si-OH terminated PDMS ( $n \sim 131$ ) during curing process at different temperatures in a ratio of 2 (Silirane/Si-OH).

SUPPORTING INFORMATION

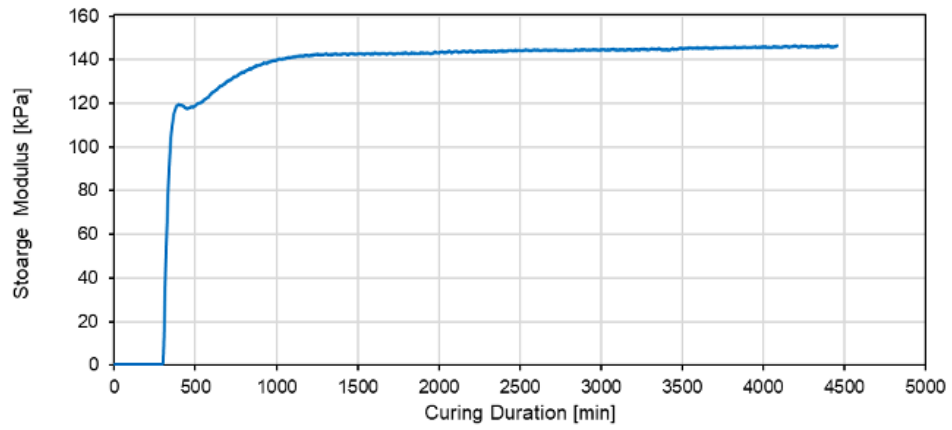


Figure 71: Storage modulus of crosslinker 16 and Si-OH terminated PDMS ( $n \sim 131$ ) during crosslinking process in Silirane/Si-OH ratio of 2.

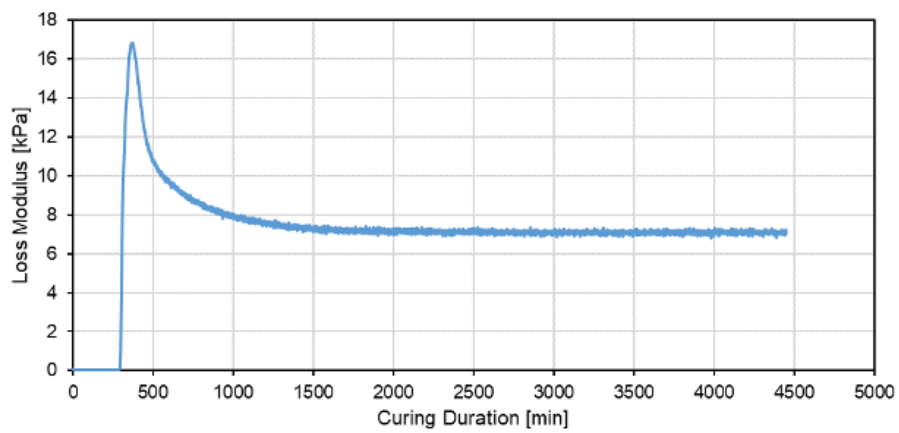


Figure 72: Loss modulus of crosslinker 16 and Si-OH terminated PDMS ( $n \sim 131$ ) during crosslinking process in Silirane/Si-OH ratio of 2.

SUPPORTING INFORMATION

---

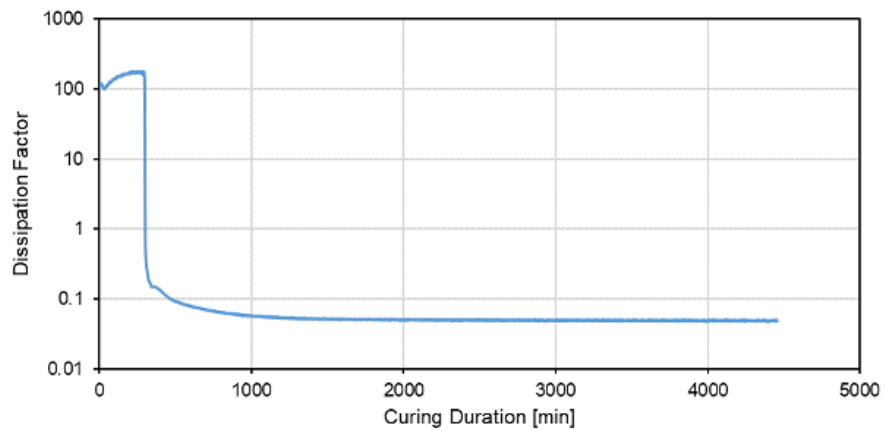
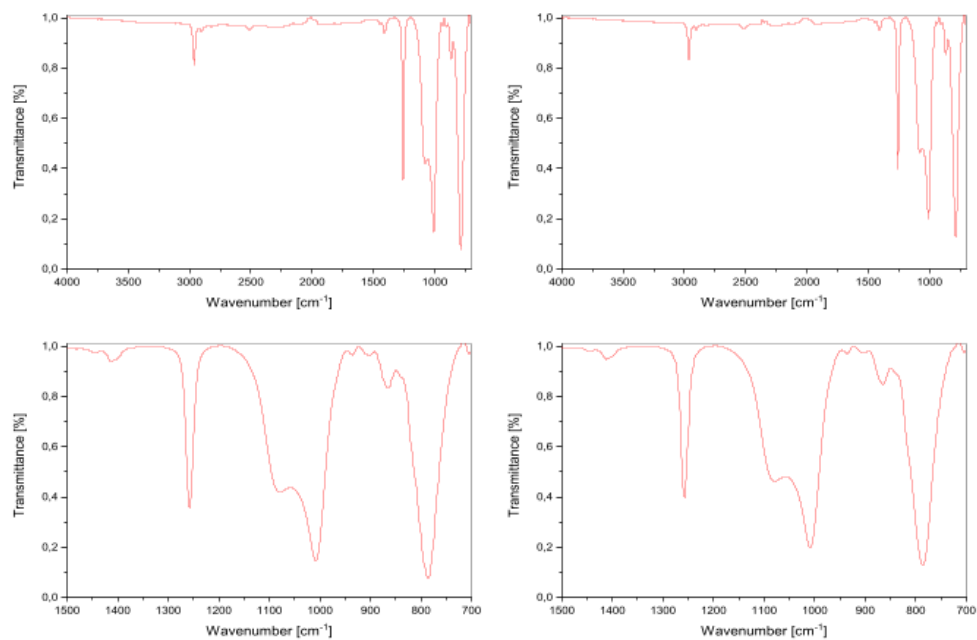


Figure 73: Dissipation factor  $\tan(\delta)$  of crosslinker **16** and Si-OH terminated PDMS ( $n \sim 131$ ) during crosslinking process in Silirane/Si-OH ratio of 2.

## SUPPORTING INFORMATION

## 5. IR-Spectroscopy Data



**Figure 74:** FT-IR-Measurements of elastomer cured with crosslinker **16** and Si-OH terminated PDMS ( $n \sim 131$ , Silirane/Si-OH ratio of 2) before (left) and after 2 h treatment in boiling water (right). Characteristic Si-N-Si band of Tris(trimethylsilyl)amine ("NTMS") at  $908 \text{ cm}^{-1}$  (lit. value at  $915 \text{ cm}^{-1}$ ).<sup>[12]</sup>

## SUPPORTING INFORMATION

## 6. Shore Hardness of Crosslinked Elastomers

**Table 1.** Shore-A Hardness of various crosslinked elastomers. Mixtures were cured at 110 °C for 72 h in inert atmosphere. Shore Hardness was measured after crosslinking and checked again after 8 weeks to detect aging.

Crosslinker	PDMS	Mixing Ratio (Silirane/ funct. Groups PDMS)	Shore-A Hardness
8	9800 g/mol, Si-OH term.	1.0	16.5
8	9800 g/mol, Si-OH term.	1.1	14.5
8	9800 g/mol, Si-OH term.	1.3	6.2
8	9800 g/mol, Si-OH term.	1.5	1.5
9	9800 g/mol, Si-OH term.	1.0	9.8
9	9800 g/mol, Si-OH term.	1.3	5.1
9	9800 g/mol, Si-OH term.	1.5	0
10	9800 g/mol, Si-OH term.	4.0	4.1
10	36000 g/mol, Si-OH term.	6.0	10.5
10	36000 g/mol, Si-OH term.	9.0	13.5
6	13540 g/mol, Si-CH <sub>2</sub> OH term.	1.0	4.1
9	1286 g/mol, Propylamine term.	1.25	27.5
6	9800 g/mol, Si-OH term.	1.0	9.1

**Table 2.** Shore-A0 Hardness of various crosslinked elastomers. Mixtures were cured at 140 °C for 12 h in inert atmosphere. Shore-A0 hardness was measured after crosslinking. Subsequent swelling tests were conducted in toluene at room temperature.

Crosslinker	PDMS	Mixing Ratio (Silirane/ funct. Groups PDMS)	Shore-A0 Hardness	Swelling ratio [%]	Gel fraktion [%]
15	17, 2400 g/mol, Si-H lateral, term.	0.30	50	729	0.83
15	17, 2400 g/mol, Si-H lateral, term.	0.50	55	823	0.85
15	17, 2400 g/mol, Si-H lateral, term.	1.00	60	10.54	0.92
15	18, 55000 g/mol, Si-H lateral	0.33	2	-	0.42
15	18, 55000 g/mol, Si-H lateral	1.00	10	-	0.73
15	18, 55000 g/mol, Si-H lateral	5.00	80	1093	0.95

## SUPPORTING INFORMATION

16	19, 9800 g/mol, Si-OH term.	0.50	11	1410	0.90
16	19, 9800 g/mol, Si-OH term.	1.00	25	690	0.95
16	19, 9800 g/mol, Si-OH term.	2.00	33	380	0.96
16	20, 36000 g/mol, Si-OH term.	0.50	3	1840	0.91
16	20, 36000 g/mol, Si-OH term.	1.00	14	1120	0.95
16	20, 36000 g/mol, Si-OH term.	2.00	20	760	97.3

## SUPPORTING INFORMATION

---

### 7. References

- [1] H. Watanabe, T. Ohkawa, T. Muraoka, Y. Nagai, *Chemistry Letters* **1981**, *10*, 1321-1322.
- [2] M. Weidenbruch, A. Schäfer, R. Rankers, *Journal of Organometallic Chemistry* **1980**, *195*, 171-184.
- [3] N. Wiberg, K. Amelunxen, H. W. Lerner, H. Schuster, H. Nöth, I. Krossing, M. Schmidt-Amelunxen, T. Seifert, *Journal of Organometallic Chemistry* **1997**, *542*, 1-18.
- [4] D. Ostendorf, Dissertation thesis, Universität Oldenburg (Oldenburg), **2001**.
- [5] P. Boudjouk, U. Samaraweera, R. Sooriyakumaran, J. Chrusciel, K. R. Anderson, *Angew. Chem.* **1988**, *100*, 1406-1407.
- [6] P. Boudjouk, U. Samaraweera, R. Sooriyakumaran, J. Chrusciel, K. R. Anderson, *Angew. Chem. Int. Ed.* **1988**, *27*, 1355-1356.
- [7] J. Ćiraković, T. G. Driver, K. A. Woerpel, *J. Am. Chem. Soc.* **2002**, *124*, 9370-9371.
- [8] T. G. Driver, K. A. Woerpel, *J. Am. Chem. Soc.* **2003**, *125*, 10659-10663.
- [9] T. G. Driver, K. A. Woerpel, *Journal of the American Chemical Society* **2004**, *126*, 9993-10002.
- [10] T. G. Driver, in *Silver in Organic Chemistry* (Ed.: M. Harmata), Wiley, Hoboken, **2010**, pp. 183-227.
- [11] K. R. Pichaandi, J. T. Mague, M. J. Fink, *Journal of Organometallic Chemistry* **2015**, *791*, 163-168.
- [12] D. R. Anderson, *Analysis of Silicones*, Wiley, New York, **1974**.

## 9.4.2. Supporting Information for Chapter 5

Electronic Supplementary Material (ESI) for Chemical Communications.  
This journal is © The Royal Society of Chemistry 2022

## Supporting Information for

### Modular Silacyclopropenes: Synthesis and Application for Si-H containing Substrate Functionalization

Matthias Nobis, Shigeyoshi Inoue, Bernhard Rieger\*

#### Table of Contents

A. Experimental Section	S1
a) General Considerations:	S1
b) Synthesis and Characterization of New Compounds	S2
c) Substrate Functionalization	S16
B. References	S34

#### A. Experimental Section

##### a) General Considerations:

All experiments and manipulations were carried out under dry oxygen-free argon atmosphere (Ar 4.6) using standard Schlenk techniques or in a LABmaster sp glovebox from MBraun. Glassware was heat-dried under vacuum prior to use. Solvents were dried by standard methods and freshly distilled prior to use. Dry pentane, Et<sub>2</sub>O, THF and toluene were obtained from a *M. Braun* MB-SPS 800 solvent purification system. Commercially available reagents were purchased from *Sigma-Aldrich*, *Acros*, *Alfa-Aesar*, *abcr* or *TCI* and used as received. The solution NMR spectra were recorded on Bruker Spectrometers AVHD 400 or AVHD 500 cryo with residual solvent signals as internal reference (<sup>1</sup>H NMR: C<sub>6</sub>D<sub>6</sub>, 7.16 ppm. <sup>13</sup>C NMR: C<sub>6</sub>D<sub>6</sub> 128.06 ppm) or an external standard (<sup>29</sup>Si NMR: SiMe<sub>4</sub>, 0.0 ppm). The following abbreviations were used to describe peak patterns when appropriate: br = broad, s = singlet, d = doublet, t = triplet, dd = doublet of doublets, m = multiplet.



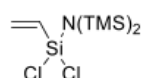
Liquid Injection Field Desorption Ionization Mass Spectrometry (LIFDI-MS) was measured directly from an inert atmosphere glovebox with a Thermo Fisher Scientific Exactive Plus Orbitrap equipped with an ion source from *Linden CMS*.<sup>(S1)</sup>

Elemental analyses were conducted with a Vario EL instrument from *Elementar*. Air-sensitive substances were placed into tin or aluminum boats and kept under argon atmosphere.

UV-Vis spectra were recorded on a Cary 50Scan UV-Visible spectrophotometer from *Varian* with 10·10 mm diameter UV quartz cuvette from *Hellma Analytics*.

## b) Synthesis and Characterization of New Compounds

### Synthesis of dichlorosilane **1**



Synthesis of dichlorosilane **1** was based on the synthesis procedure reported in literature.<sup>(S2)</sup> Modification of the described preparation were the substitution of the lithium-salt with the respective potassium-salt as well as a change of solvent from hexane to THF.

A solution of Trichlorovinylsilane (12.0 g, 74.3 mmol, 1.00 eq) in THF (250 mL) was cooled to 0 °C with an ice-bath. In a second flask a solution of potassium bis(trimethylsilyl)amide (KHMDS) (15.5 g, 78.1 mmol, 1.00 eq) in THF (50 mL) was prepared and cooled to 0 °C as well. The potassium-salt solution was added dropwise to the reaction flask and a rapid formation of the respective KCl-salt occurred. After stirring the solution for 20 min at 0 °C, the reaction was allowed to warm up to room temperature again and was stirred for additional 12 h. After the reaction was completed, the solvent was removed *in vacuo*. The crude product was resolved in 100 ml pentane and the precipitate was removed by filtration through a microfiber glass filter and washed twice with 25 mL pentane. The product was then dried *in vacuo* and further purification was performed by sublimation (2·10<sup>-2</sup> mbar, 100°C) to yield dichlorosilane **1** (18.6 g, 64.9 mmol, 87,4 %) as clear colourless crystals.

<sup>1</sup>H-NMR: (300 K, 500 MHz, C<sub>6</sub>D<sub>6</sub>) δ [ppm] = 0.28 (s, 18 H, Si-(CH<sub>3</sub>)<sub>3</sub>), 5.74 (dd, 1 H, <sup>2</sup>J<sub>HH</sub> = 3.0 Hz, <sup>3</sup>J<sub>HH</sub> = 14.0 Hz, SiCH-CH<sub>2</sub>), 5.98 (dd, 1 H, <sup>2</sup>J<sub>HH</sub> = 3.0 Hz, <sup>3</sup>J<sub>HH</sub> = 20.0 Hz, SiCH-CH<sub>2</sub>), 6.11 (dd, 1 H, <sup>3</sup>J<sub>HH</sub> = 14.0 Hz, <sup>3</sup>J<sub>HH</sub> = 20.0 Hz, Si-CH-CH<sub>2</sub>).

<sup>13</sup>C-NMR: (300 K, 125 MHz, C<sub>6</sub>D<sub>6</sub>) δ [ppm] = 5.09 (Si-(CH<sub>3</sub>)<sub>3</sub>), 135.95 (Si-CH-CH<sub>2</sub>), 136.79 (SiCH-CH<sub>2</sub>).

<sup>29</sup>Si-NMR: (300 K, 100 MHz, C<sub>6</sub>D<sub>6</sub>) δ [ppm] = -14.82 (Si-Cl<sub>2</sub>), 7.03 (Si-(CH<sub>3</sub>)<sub>3</sub>).

EA: calc. [%] for C<sub>8</sub>H<sub>21</sub>Cl<sub>2</sub>NSi<sub>3</sub> = C 33.55, H 7.39, N 4.89; found C 33.73, H 7.41, N 4.84.

LIFDI-MS: m/z = calc. for [C<sub>8</sub>H<sub>21</sub>Cl<sub>2</sub>NSi<sub>3</sub>]<sup>+</sup> = 285.0359 [M]<sup>+</sup>, found 285.0107.



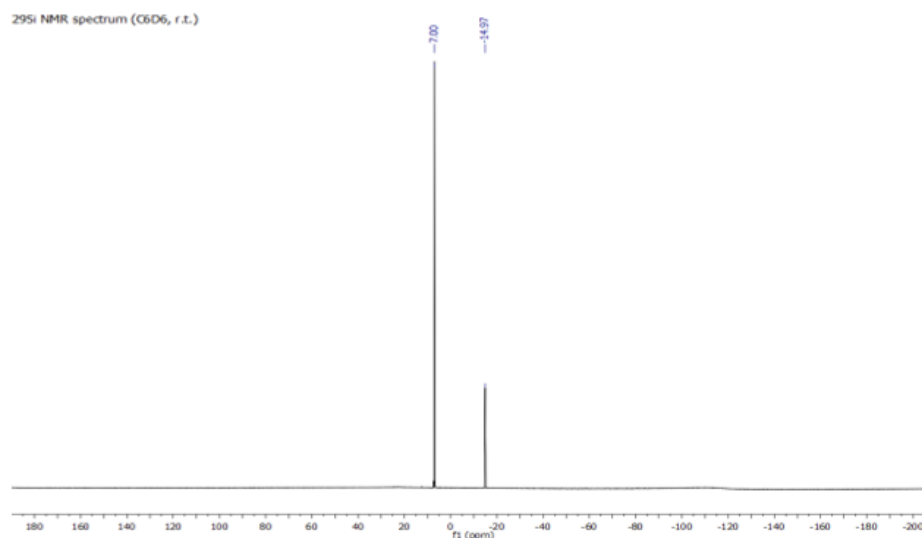
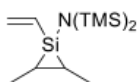


Figure S3:  $^{29}\text{Si}$ -ig NMR spectrum of dichlorosilane **1** ( $\text{C}_6\text{D}_6$ , r.t.).

#### Synthesis of silacyclopropane **2**



A solution of dichlorosilane **1** (4.00 g, 14.0 mmol, 1.00 eq) in THF (10 mL) was prepared in an autoclave and cooled down to  $-30\text{ }^\circ\text{C}$ . *Trans*-but-2-ene (21.9 g, 391 mmol, 28 eq) was condensed to the cold reaction and stirred for 5 min. After letting it warm up to  $-10\text{ }^\circ\text{C}$ , freshly cut pieces of a Lithium/Sodium alloy (969 mg, 137 mmol, 10 eq, 2.5 mol% Na) were added to the reaction mixture. After sealing the autoclave, the reaction was heated to  $50\text{ }^\circ\text{C}$  and stirred for 72 h. Remaining but-2-ene gas was removed and the reaction mixture filtered and washed twice with 10 ml pentane through a glass frit to remove formed lithium salt. The solvent was then removed *in vacuo* and the crude product was purified by a sublimation ( $3 \cdot 10^{-2}$  mbar,  $70\text{ }^\circ\text{C}$ ) to yield silacyclopropane **2** (2.57 g, 9.50 mmol, 68.0 %) as clear colourless crystals.

$^1\text{H-NMR}$ : (300 K, 500 MHz,  $\text{C}_6\text{D}_6$ )  $\delta$  [ppm] = 0.24 (s, 18 H,  $\text{Si}-(\text{CH}_3)_3$ ), 0.27 (dq, 1 H,  $^3J_{\text{HH}} = 7.2\text{ Hz}$ ,  $^3J_{\text{HH}} = 7.2\text{ Hz}$ ,  $\text{Si-CH-CH}_3$ ), 0.69 (dq, 1 H,  $^3J_{\text{HH}} = 7.2\text{ Hz}$ ,  $^3J_{\text{HH}} = 7.2\text{ Hz}$ ,  $\text{Si-CH-CH}_3$ ), 1.28 (d, 3 H,  $^3J_{\text{HH}} = 7.2\text{ Hz}$ ,  $\text{Si-CH-CH}_3$ ), 1.38 (d, 3 H,  $^3J_{\text{HH}} = 7.2\text{ Hz}$ ,  $\text{Si-CH-CH}_3$ ), 5.93 (m, 1 H,  $\text{SiCH-CH}_2$ ), 5.95 (m, 1 H,  $\text{SiCH-CH}_2$ ), 6.08-6.11 (m, 1 H,  $\text{Si-CH-CH}_2$ ).

$^{13}\text{C-NMR}$ : (300 K, 125 MHz,  $\text{C}_6\text{D}_6$ )  $\delta$  [ppm] = 3.60 ( $\text{NSi}-(\text{CH}_3)_3$ ), 16.16 ( $\text{SiCH-CH}_3$ ), 16.35 ( $\text{SiCH-CH}_3$ ), 18.99 ( $\text{Si-CH-CH}_3$ ), 20.22 ( $\text{Si-CH-CH}_3$ ), 135.56 ( $\text{Si-CH-CH}_2$ ), 136.42 ( $\text{SiCH-CH}_2$ ).

$^{29}\text{Si-NMR}$ : (300 K, 100 MHz,  $\text{C}_6\text{D}_6$ )  $\delta$  [ppm] = -53.79 (*Si*-central), 5.71 (*Si*-( $\text{CH}_3$ )<sub>3</sub>).

**EA**: calc. [%] for  $\text{C}_{12}\text{H}_{29}\text{NSi}_3$  = C 53.06, H 10.76, N 5.16; found C 52.73, H 10.66, N 5.18.

**LIFDI-MS**:  $m/z$  = calc. for  $[\text{C}_{12}\text{H}_{29}\text{NSi}_3]^+$ : 271.1608 [M]<sup>+</sup>, found 271.1604.

**UV-Vis**: (n-hexane),  $\lambda_{\text{max}}$  [nm] ( $\epsilon$  [ $\text{Lmol}^{-1}\text{cm}^{-1}$ ]): 256 (3902).

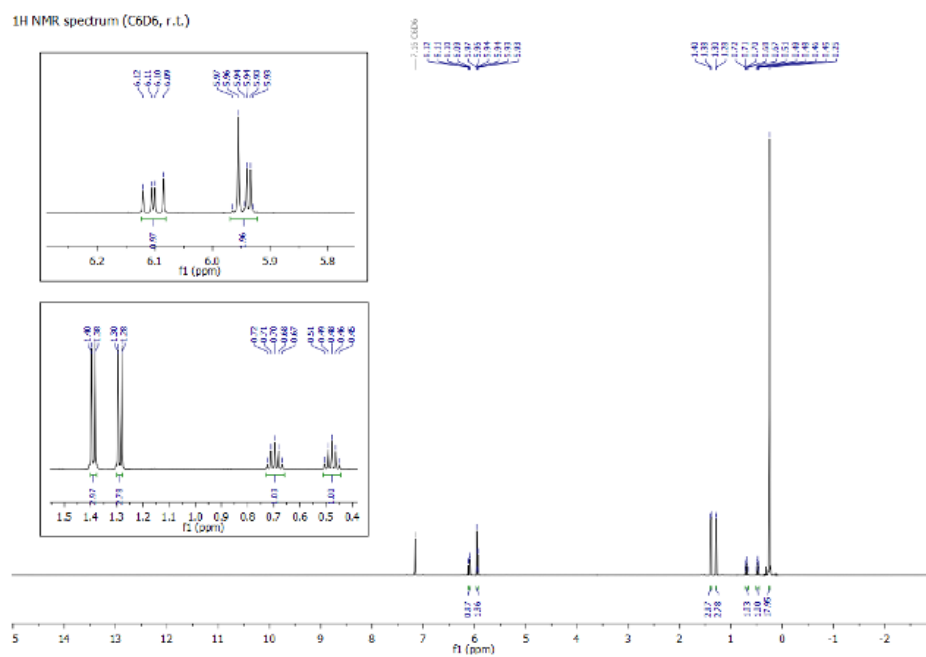


Figure S4: <sup>1</sup>H NMR spectrum of silacyclopropane **2** (C<sub>6</sub>D<sub>6</sub>, r.t.).

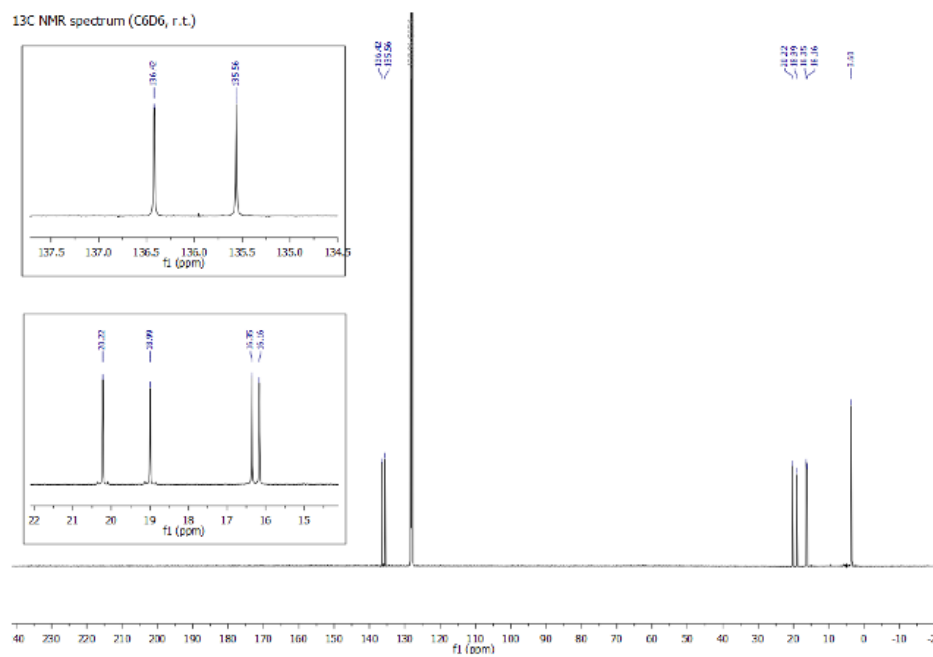


Figure S5: <sup>13</sup>C NMR spectrum of silacyclopropane **2** (C<sub>6</sub>D<sub>6</sub>, r.t.).

S5

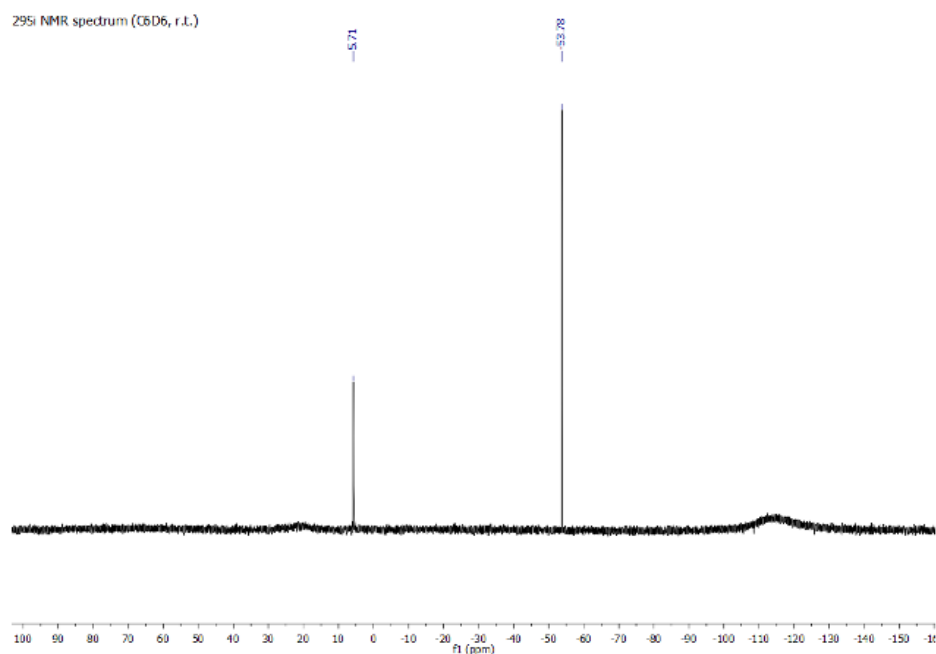


Figure S6:  $^{29}\text{Si}$  NMR spectrum of silacyclopropane **2** ( $\text{C}_6\text{D}_6$ , r.t.).

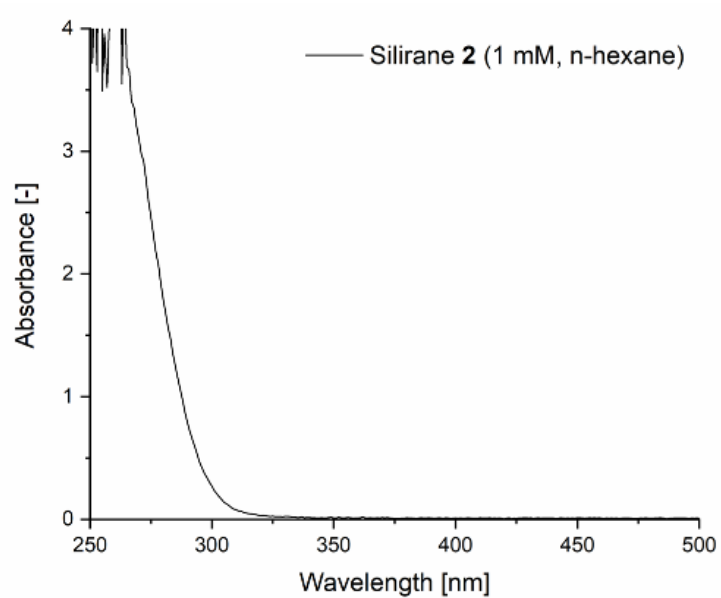
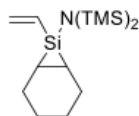


Figure S7: UV-VIS spectrum of silacyclopropane **2** (r.t., n-hexane,  $1.0 \times 10^{-3}$  M).

Synthesis of silacyclopropane **3**

Cyclohexene (4.30 g, 52.4 mmol, 30 eq.) was added to a solution of dichlorosilane **1** (500 mg, 1.75 mmol, 1 eq.) in THF (2 mL) at room temperature. The reaction was cooled down to  $-10\text{ }^{\circ}\text{C}$  and freshly cut pieces of a Lithium/Sodium alloy (969 mg, 137 mmol, 10 eq, 2.5 mol% Na) were added. The mixture was stirred and immediately heated up to  $55\text{ }^{\circ}\text{C}$  for 48 h. After completion the solvent was removed *in vacuo* and the crude was resolved in pentane (20 mL). Additional filtration through a microfiber glass filter and a distillation ( $5\cdot 10^{-2}$  mbar,  $120\text{ }^{\circ}\text{C}$ ), yielded silacyclopropane **3** (180 mg, 0.61 mmol, 35 %) as a colourless liquid. A small portion of not reacted reagent **1** could not be separated by distillation and remained in the product.

**$^1\text{H-NMR}$** : (300 K, 500 MHz,  $\text{C}_6\text{D}_6$ )  $\delta$  [ppm] = 0.23 (s, 18 H, Si-( $\text{CH}_3$ )<sub>3</sub>), 1.30-1.32 (m, 2 H, Si- $\text{CH}_{\text{cyclo}}$ ), 1.35-1.46 (m, 4 H, SiCH $\text{CH}_2\text{-CH}_2$ ), 1.70-1.75 (m, 2 H, SiCH- $\text{CH}_2\text{-CH}_2$ ), 1.93-1.98 (m, 2 H, SiCH- $\text{CH}_2\text{-CH}_2$ ), 6.05-6.11 (m, 1 H, Si- $\text{CH}_{\text{vinyl}}$ ), 6.18-6.26 (m, 2 H, SiCH- $\text{CH}_2_{\text{vinyl}}$ ).

**$^{13}\text{C-NMR}$** : (300 K, 125 MHz,  $\text{C}_6\text{D}_6$ )  $\delta$  [ppm] = 3.73 (SiNSi-( $\text{CH}_3$ )<sub>3</sub>), 15.83 (Si-CH- $\text{CH}_2\text{CH}_2$ ), 21.69 (SiCH- $\text{CH}_2\text{-CH}_2$ ), 24.50 (SiCH $\text{CH}_2\text{-CH}_2$ ), 134.59 (Si-CH- $\text{CH}_2_{\text{vinyl}}$ ), 138.33 (SiCH- $\text{CH}_2_{\text{vinyl}}$ ).

**$^{29}\text{Si-NMR}$** : (300 K, 100 MHz,  $\text{C}_6\text{D}_6$ )  $\delta$  [ppm] = -60.45 ( $\text{Si}_{\text{central}}$ ), 5.55 (N-Si-( $\text{CH}_3$ )<sub>3</sub>).

**EA**: calc. [%] for  $\text{C}_{12}\text{H}_{29}\text{NSi}_3$  = C 56.49, H 10.50, N 4.71; found C 56.03, H 10.86, N 4.99.

$^1\text{H}$  NMR spectrum ( $\text{C}_6\text{D}_6$ , r.t.)

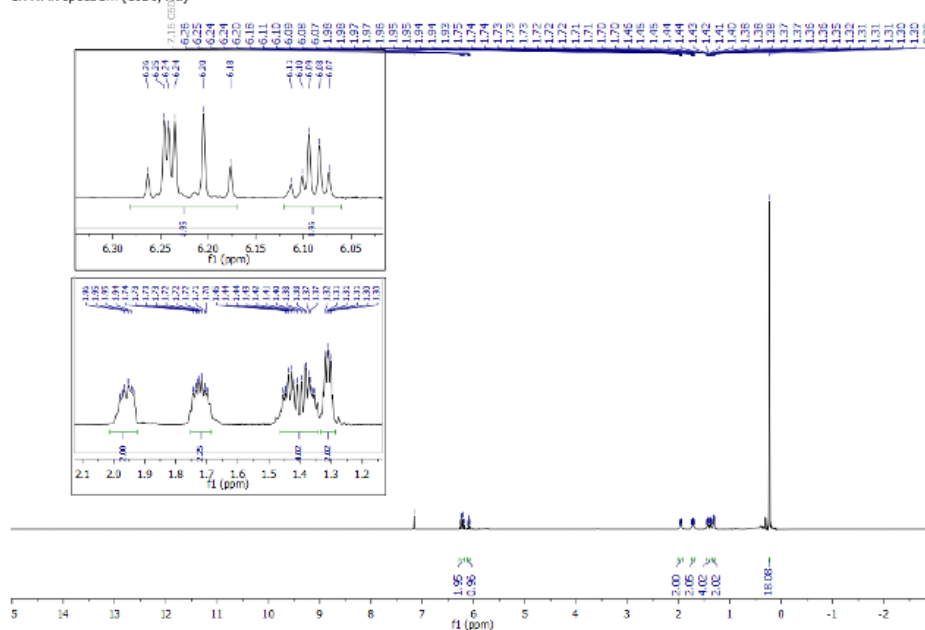


Figure S8:  $^1\text{H}$  NMR spectrum of silacyclopropane **3** ( $\text{C}_6\text{D}_6$ , r.t.).

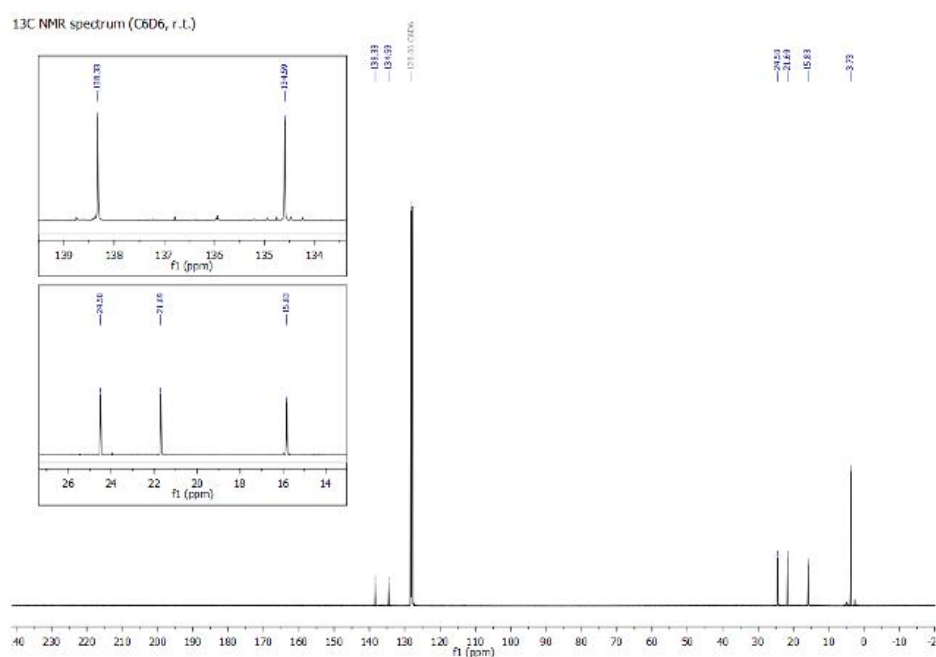


Figure S9: <sup>13</sup>C NMR spectrum of silacyclopropane **3** (C<sub>6</sub>D<sub>6</sub>, r.t.).

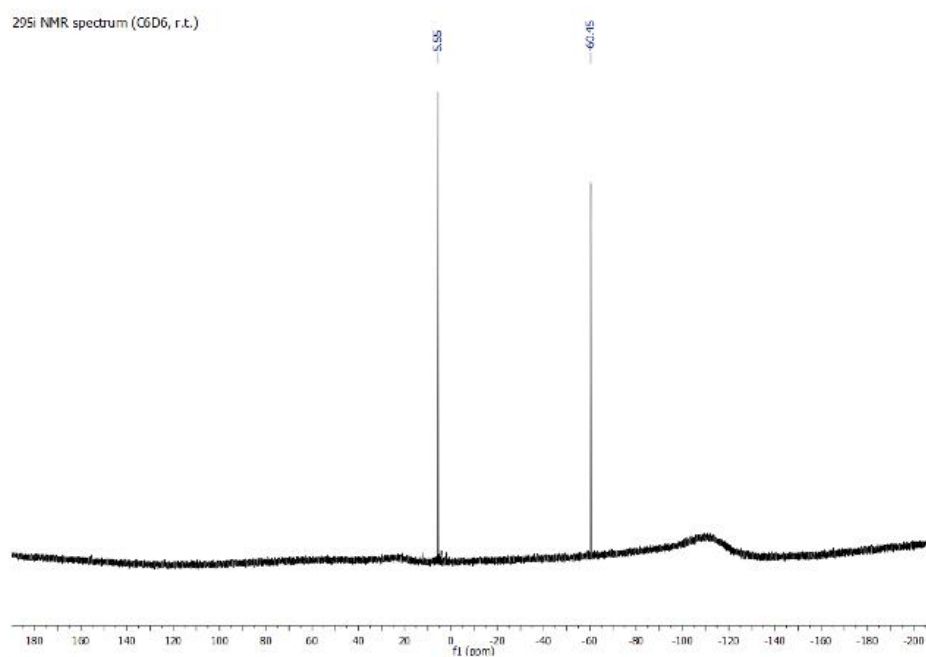
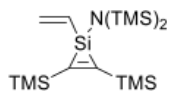


Figure S10: <sup>29</sup>Si NMR spectrum of silacyclopropane **3** (C<sub>6</sub>D<sub>6</sub>, r.t.).

Synthesis of silacyclopropene **4**

Bis-(trimethylsilyl)-acetylene (69.0 mg, 405  $\mu\text{mol}$ , 1.1 eq) was added to a solution of silacyclopropane **2** (100 mg, 368  $\mu\text{mol}$ , 1 eq) in toluene (10 mL). Then 1 mL of a silver-trifluoromethanesulfonate solution (1 mM in toluene) was added as a catalyst. The reaction was stirred at 60 °C for 48 h, while changing to a bright yellow color. The solution was filtrated through an appropriate amount of aluminium oxide ( $\text{Al}_2\text{O}_3$ ) and a syringe filter (PP, 0.5  $\mu\text{m}$ ). Then all volatiles were removed under vacuum, to give silacyclopropene **4** (42.0 mg, 109  $\mu\text{mol}$ , 30 %) as a colourless liquid.

**$^1\text{H-NMR}$** : (300 K, 500 MHz,  $\text{C}_6\text{D}_6$ )  $\delta$  [ppm] = 0.30 (s, 18H,  $\text{SiNSi}-(\text{CH}_3)_3$ ), 0.31 (s, 18 H,  $\text{SiCSi}-(\text{CH}_3)_3$ ), 5.85-5.87 (m, 1 H,  $\text{Si-CH-CH}_2$ ), 6.03-6.08 (m, 2 H,  $\text{SiCH-CH}_2$ ).

**$^{13}\text{C-NMR}$** : (300 K, 125 MHz,  $\text{C}_6\text{D}_6$ )  $\delta$  [ppm] = 0.57 (s,  $\text{SiCSi}-(\text{CH}_3)_3$ ), 3.89 (,  $\text{SiNSi}-(\text{CH}_3)_3$ ), 135.64 ( $\text{Si-CH-CH}_2$ ), 140.42 ( $\text{SiCH-CH}_2$ ), 193.94 ( $\text{Si-C-Si}$ ).

**$^{29}\text{Si-NMR}$** : (300 K, 100 MHz,  $\text{C}_6\text{D}_6$ )  $\delta$  [ppm] = -107.54 ( $\text{Si}_{\text{central}}$ ), -12.47 ( $\text{SiC-Si}-(\text{CH}_3)_3$ ), 4.53 ( $\text{SiN-Si}-(\text{CH}_3)_3$ ).

**LIFDI-MS**:  $m/z = \text{calc. for } [\text{H}_{12}\text{C}_2\text{Si}_3]^+ = 385.1929 \text{ [M]}^+$ , found 385.1916.

**UV-Vis**: (n-hexane),  $\lambda_{\text{max}}$  [nm] ( $\epsilon$  [ $\text{Lmol}^{-1}\text{cm}^{-1}$ ]): 356 (350).

$^1\text{H}$  NMR spectrum ( $\text{C}_6\text{D}_6$ , r.t.)

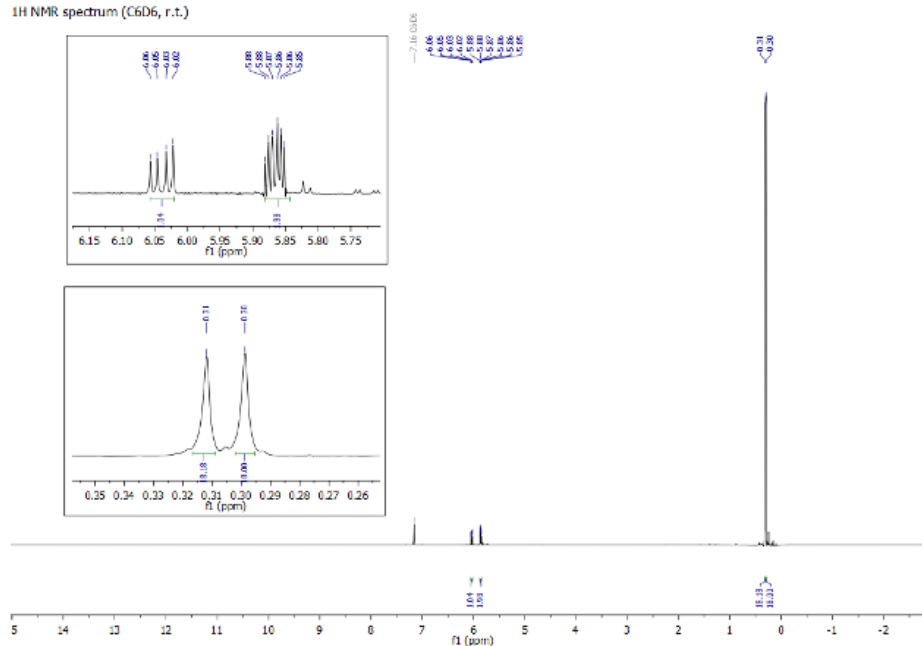


Figure S11:  $^1\text{H}$  NMR spectrum of silacyclopropene **4** ( $\text{C}_6\text{D}_6$ , r.t.).



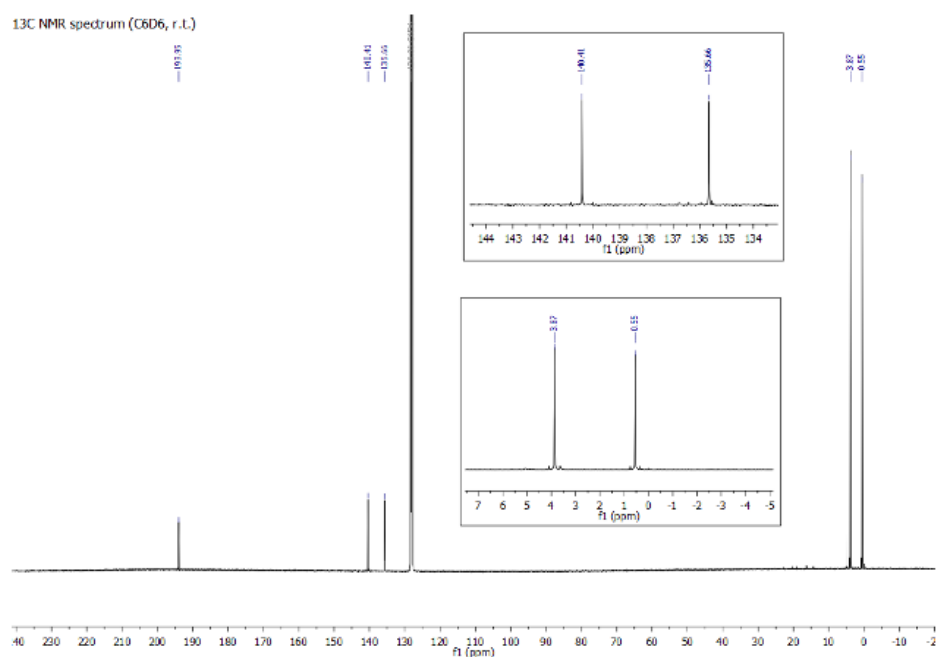


Figure S12: <sup>13</sup>C NMR spectrum of silacyclopene **4** (C<sub>6</sub>D<sub>6</sub>, r.t.).

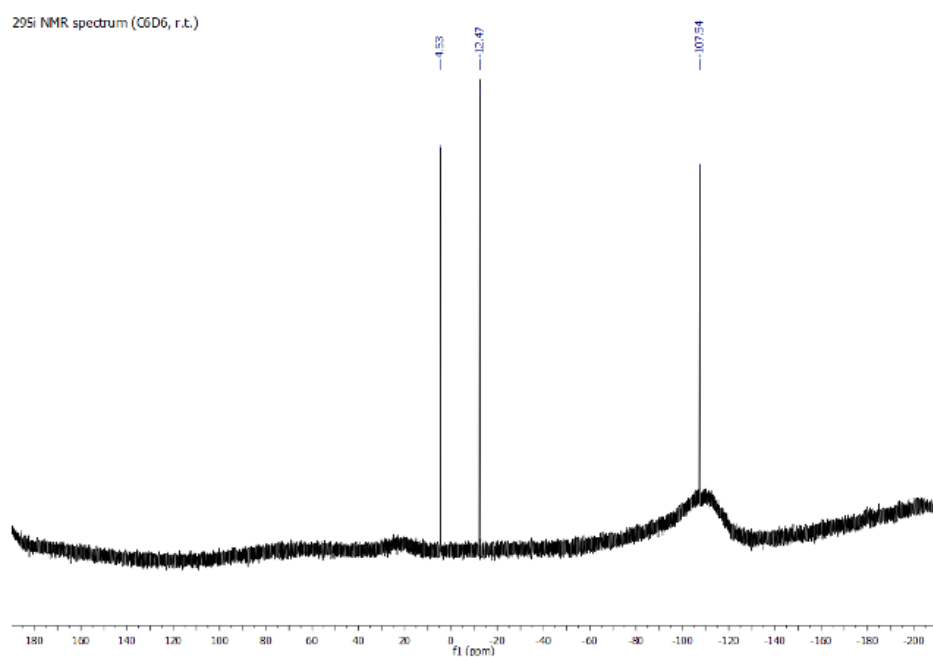


Figure S13: <sup>29</sup>Si NMR spectrum of silacyclopene **4** (C<sub>6</sub>D<sub>6</sub>, r.t.).

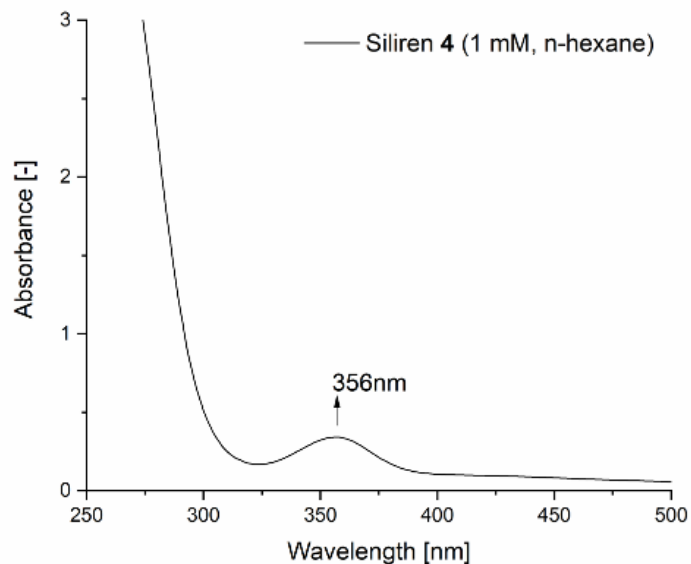
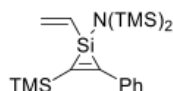


Figure S14: UV-VIS spectrum of silacyclopropene 4 (r.t., n-hexane,  $1.0 \times 10^{-3}$  M).

#### Synthesis of silacyclopropene 5



1-Phenyl-2-trimethyl-silylacetylene (1.11 g, 6.36 mmol, 1.2 eq) was added to a solution of silacyclopropane 2 (1.44 g, 5.30 mmol, 1 eq) in 20 mL toluene. After stirring for 16 h at 100 °C, the reaction was filtered through a syringe filter (PP, 0.5  $\mu$ m). The volatiles were removed under vacuum. Then the residue was purified by a distillation under high vacuum ( $5 \cdot 10^{-5}$  mbar, 120 °C) to yield silacyclopropene 5 (1.50 g, 78 mmol, 72.5 %) as a colourless liquid.

<sup>1</sup>H-NMR: (300 K, 500 MHz, C<sub>6</sub>D<sub>6</sub>)  $\delta$  [ppm] = 0.27 (s, 18 H, NSi-(CH<sub>3</sub>)<sub>3</sub>), 0.31 (s, 9 H, SiCSi-(CH<sub>3</sub>)<sub>3</sub>), 6.00-6.08 (m, 2 H, SiCH-CH<sub>2</sub>), 6.10-6.14 (m, 1 H, Si-CH-CH<sub>2</sub>), 7.04-7.07 (m, 1 H, CH<sub>arm/para</sub>), 7.19-7.23 (m, 2 H, CH<sub>arm/meta</sub>), 7.47-7.50 (m, 2 H, CH<sub>arm/ortho</sub>).

<sup>13</sup>C-NMR: (300 K, 125 MHz, C<sub>6</sub>D<sub>6</sub>)  $\delta$  [ppm] = 0.50 (SiCSi-(CH<sub>3</sub>)<sub>3</sub>), 3.63 (NSi-(CH<sub>3</sub>)<sub>3</sub>), 128.16 (CH<sub>arm/ortho</sub>), 128.35 (CH<sub>arm/meta</sub>), 128.57 (SiC-C<sub>arm</sub>-CH), 136.96 (Si-CH-CH<sub>2</sub>), 138.22 (CH<sub>arm/para</sub>), 139.09 (SiCH-CH<sub>2</sub>), 167.22 (Si-C-Si(CH<sub>3</sub>)<sub>3</sub>), 182.36 (Si-C-C<sub>arm</sub>).

<sup>29</sup>Si-NMR: (300 K, 100 MHz, C<sub>6</sub>D<sub>6</sub>)  $\delta$  [ppm] = -97.51 (Si-central), -12.74 (SiC-Si-(CH<sub>3</sub>)<sub>3</sub>), 4.44 (N-Si-(CH<sub>3</sub>)<sub>3</sub>).

EA: calc. [%] for C<sub>19</sub>H<sub>35</sub>NSi<sub>4</sub> = C 58.54, H 9.05, N 3.59; found C 58.54, H 9.09, N 3.74.

LIFDI-MS: m/z = calc. for [C<sub>8</sub>H<sub>21</sub>Cl<sub>2</sub>NSi<sub>3</sub>]<sup>+</sup> = 389.1847 [M]<sup>+</sup>, found 389.1859.

UV-Vis: (n-hexane),  $\lambda_{\max}$  [nm] ( $\epsilon$  [Lmol<sup>-1</sup>cm<sup>-1</sup>]): 323 (1850).



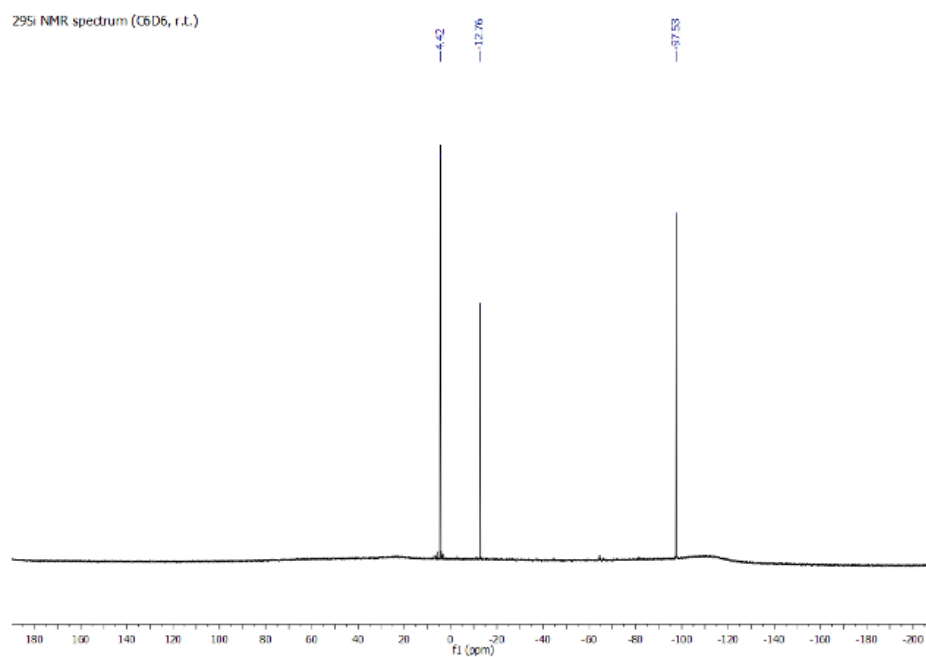


Figure S17:  $^{29}\text{Si}$ -ig NMR spectrum of silacyclopropene **5** ( $\text{C}_6\text{D}_6$ , r.t.).

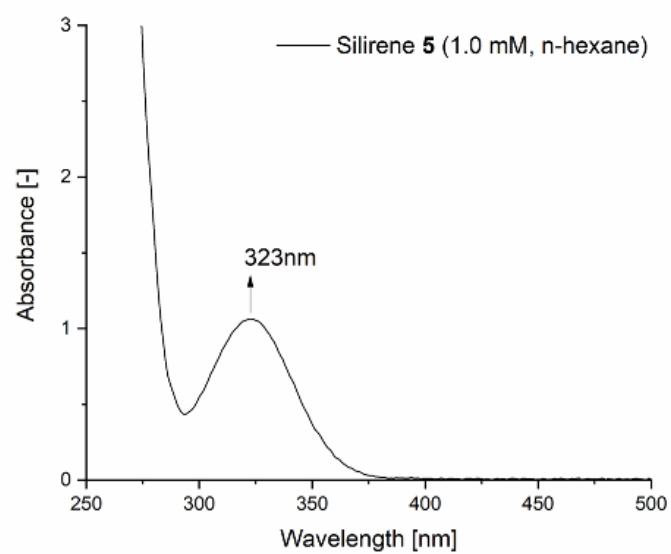
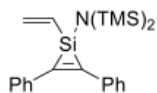


Figure S18: UV-VIS spectrum of silacyclopropene **4** (r.t., n-hexane,  $1.0 \times 10^{-3}$  M).

**Synthesis of silacyclopropene 6**

Diphenylacetylene (72.2 mg, 405  $\mu\text{mol}$ , 1.1 eq) was added to a solution of silacyclopropane **2** (100 mg, 368  $\mu\text{mol}$ , 1 eq) in toluene (10 mL). The reaction was stirred at 100 °C for 24 h, while changing to a yellowish color. The solution was filtrated through an appropriate amount of aluminium oxide ( $\text{Al}_2\text{O}_3$ ) and a syringe filter (PP, 0.5  $\mu\text{m}$ ). Then all volatiles were removed under vacuum, to give silacyclopropene **6** (79.1 mg, 200  $\mu\text{mol}$ , 55 %) as colourless crystals.

**$^1\text{H-NMR}$** : (300 K, 500 MHz,  $\text{C}_6\text{D}_6$ )  $\delta$  [ppm] = 0.29 (s, 18H,  $\text{SiNSi-(CH}_3)_3$ ), 6.08-6.10 (m, 2 H,  $\text{SiCH-CH}_{2,\text{vinyl}}$ ), 6.12-6.13 (m, 1 H,  $\text{Si-CH-CH}_2$ ), 7.01-7.04 (m, 2 H,  $\text{CH}_{\text{arm}/\text{para}}$ ), 7.15 (t, 4 H,  $^3J_{\text{HH}} = 7.7$   $\text{CH}_{\text{arm}/\text{meta}}$ ), 7.58 (d, 4 H,  $^3J_{\text{HH}} = 7.7$  Hz,  $\text{CH}_{\text{arm}/\text{ortho}}$ ).

**$^{13}\text{C-NMR}$** : (300 K, 125 MHz,  $\text{C}_6\text{D}_6$ )  $\delta$  [ppm] = 3.62 ( $\text{SiNSi-(CH}_3)_3$ ), 123.88 ( $\text{CH}_{\text{arm}/\text{para}}$ ), 127.73 ( $\text{CH}_{\text{arm}/\text{meta}}$ ), 128.82 ( $\text{CH}_{\text{arm}/\text{ortho}}$ ), 136.32 ( $\text{SiC-C}_{\text{arm}}-\text{CH}_{\text{arm}}$ ), 137.82 ( $\text{Si-CH-CH}_2$ ), 137.99 ( $\text{SiCH-CH}_2$ ), 159.24 ( $\text{Si-C-C}_{\text{arm}}$ ).

**$^{29}\text{Si-NMR}$** : (300 K, 100 MHz,  $\text{C}_6\text{D}_6$ )  $\delta$  [ppm] = -96.18 ( $\text{Si}_{\text{central}}$ ), 4.41 ( $\text{SiN-Si-(CH}_3)_3$ )

**LIFDI-MS**:  $m/z = \text{calc. for } [\text{H}_{12}\text{C}_{26}\text{Si}_1]^+ = 393.1764$  [M] $^+$ , found 393.1757.

$^1\text{H NMR}$  spectrum ( $\text{C}_6\text{D}_6$ , r.t.)

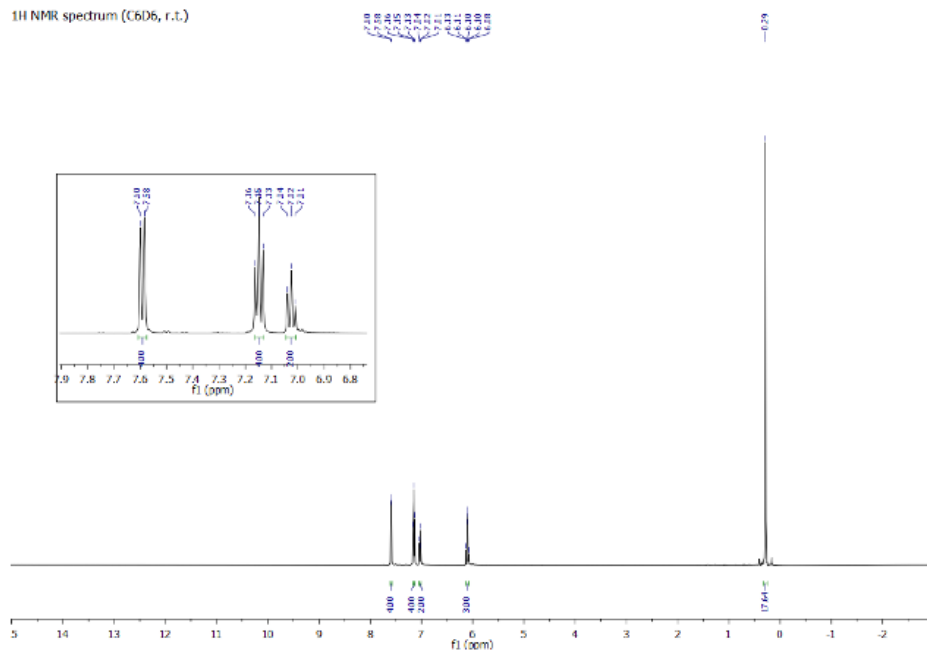


**Figure S19**:  $^1\text{H NMR}$  spectrum of silacyclopropene **6** ( $\text{C}_6\text{D}_6$ , r.t.).

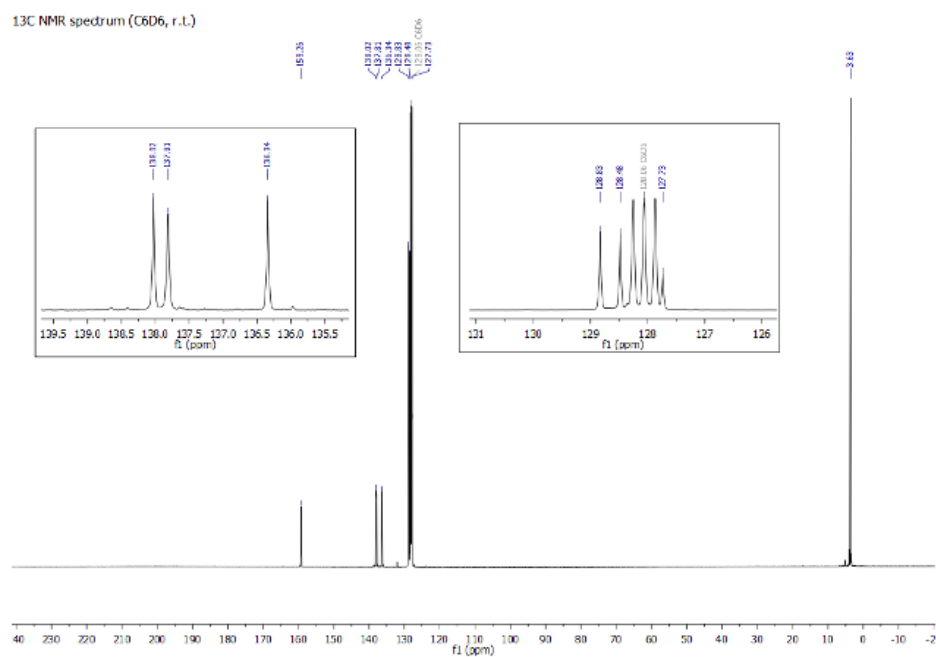


**Figure S20:** <sup>13</sup>C NMR spectrum of silacyclopropene **6** (C<sub>6</sub>D<sub>6</sub>, r.t.).

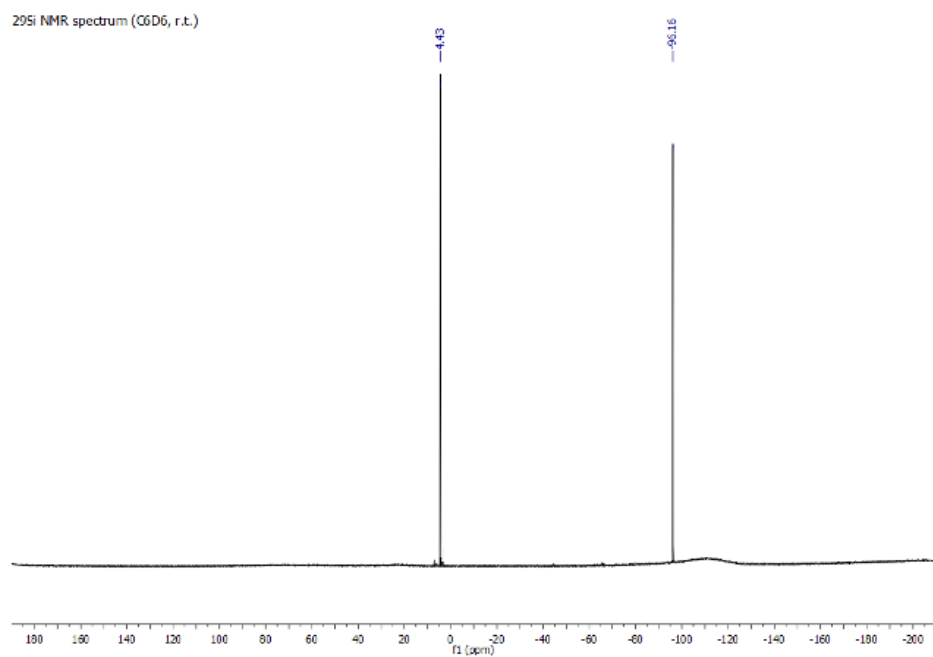
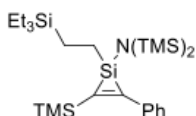


**Figure S21:** <sup>29</sup>Si NMR spectrum of silacyclopropene **6** (C<sub>6</sub>D<sub>6</sub>, r.t.).

### c) Substrate Functionalization

**Procedure for the hydrosilylation of silacyclopropene **5** with triethylsilane with catalysts of I – IV**  
 Silacyclopropene **5** (100 mg, 256  $\mu\text{mol}$ , 1 eq) was added to a solution of triethylsilane (30.6 mg, 256  $\mu\text{mol}$ , 1 eq) in benzene (5 mL). Then 0.13  $\mu\text{mol}$  of the respective catalyst (I-IV)<sup>(53)</sup> was added, and the mixture was stirred at RT or 65 °C for 24 h. All volatiles were removed under vacuum and the residue was redissolved in pentane (5 mL). The reaction was monitored by <sup>1</sup>H-NMR and <sup>29</sup>Si-NMR. The product was purified by filtration through an appropriate amount of aluminium oxide (Al<sub>2</sub>O<sub>3</sub>) and a syringe filter (PP, 0.5  $\mu\text{m}$ ) to remove the applied catalyst.

#### Functionalization of triethylsilane and characterization of **7**



Silacyclopropene **5** (100 mg, 256  $\mu\text{mol}$ , 1 eq) was added to a solution of triethylsilane (30.6 mg, 256  $\mu\text{mol}$ , 1 eq) in benzene (5 mL). Then 2.0 mg (0.24  $\mu\text{mol}$ ) of a Karstead-catalyst solution (2.25 wt.% Pt in xylene) was added, and the mixture was stirred at 65 °C for 12 h. The colour of the reaction changes from a bright yellow to a dark gold/brown over the time. All volatiles were removed under vacuum and the residue was redissolved in pentane (5 mL). The product was purified by filtration through an appropriate amount of aluminium oxide (Al<sub>2</sub>O<sub>3</sub>) and a syringe filter (PP, 0.5  $\mu\text{m}$ ) to remove the applied catalyst. Further distillation under high vacuum ( $3 \cdot 10^{-5}$  mbar, 140 °C) result in the functionalized compound **7** (90.8 mg, 179  $\mu\text{mol}$ , 70 %) as a colourless liquid.

**<sup>1</sup>H-NMR:** (300 K, 500 MHz, C<sub>6</sub>D<sub>6</sub>)  $\delta$  [ppm] = 0.28 (s, 18 H, NSi-(CH<sub>3</sub>)<sub>3</sub>), 0.33 (s, 9 H, SiCSi-(CH<sub>3</sub>)<sub>3</sub>), 0.55 (q, 6 H, <sup>3</sup>J<sub>HH</sub> = 7.9 Hz, Si(CH<sub>2</sub>-CH<sub>3</sub>)<sub>3</sub>), 0.59-0.60 (m, 2 H, NSi-CH<sub>2</sub>-CH<sub>2</sub>Si), 0.93-0.96 (m, 2 H, NSi-CH<sub>2</sub>-CH<sub>2</sub>Si), 0.99 (t, 9 H, <sup>3</sup>J<sub>HH</sub> = 7.9 Hz, Si(CH<sub>2</sub>-CH<sub>3</sub>)<sub>3</sub>), 7.00-7.04 (m, 2 H, CH<sub>arm/meta</sub>), 7.10-7.15 (m, 2 H, CH<sub>arm/ortho</sub>), 7.21-7.28 (m, 1 H, CH<sub>arm/para</sub>).

**<sup>13</sup>C-NMR:** (300 K, 125 MHz, C<sub>6</sub>D<sub>6</sub>)  $\delta$  [ppm] = 0.7 (SiCSi-(CH<sub>3</sub>)<sub>3</sub>), 3.33 (Si(CH<sub>2</sub>-CH<sub>3</sub>)<sub>3</sub>), 3.78 (NSi-(CH<sub>3</sub>)<sub>3</sub>), 5.22 (NSi-CH<sub>2</sub>-CH<sub>2</sub>Si), 7.83 (Si(CH<sub>2</sub>-CH<sub>3</sub>)<sub>3</sub>), 10.71 (NSi-CH<sub>2</sub>-CH<sub>2</sub>Si), 127.6 (CH<sub>arm/para</sub>), 128.4 (CH<sub>arm/meta</sub>), 128.6 (CH<sub>arm/ortho</sub>), 139.2 (SiC-C<sub>arm</sub>), 168.2 (Si-C-C<sub>arm</sub>), 183.2 (Si-C-Si).

**<sup>29</sup>Si-NMR:** (300 K, 100 MHz, C<sub>6</sub>D<sub>6</sub>)  $\delta$  [ppm] = -80.98 (Si<sub>silirene</sub>), -13.21 (SiC-Si-(CH<sub>3</sub>)<sub>3</sub>), 3.35 (N-Si-(CH<sub>3</sub>)<sub>3</sub>), 7.84 (CH<sub>2</sub>-Si-(CH<sub>2</sub>CH<sub>3</sub>)<sub>3</sub>).

**EA:** calc. [%] for C<sub>25</sub>H<sub>51</sub>NSi<sub>5</sub> = C 59.33, H 10.16, N 2.77; found C 59.01, H 10.31, N 2.79.

**LIFDI-MS:** m/z = calc. for [C<sub>25</sub>H<sub>51</sub>NSi<sub>5</sub>]<sup>+</sup>: 505.2868 [M]<sup>+</sup>, found 505.2867.

**UV-Vis:** (n-hexane),  $\lambda_{\text{max}}$  [nm] ( $\epsilon$  [Lmol<sup>-1</sup>cm<sup>-1</sup>]): 316 (1862).

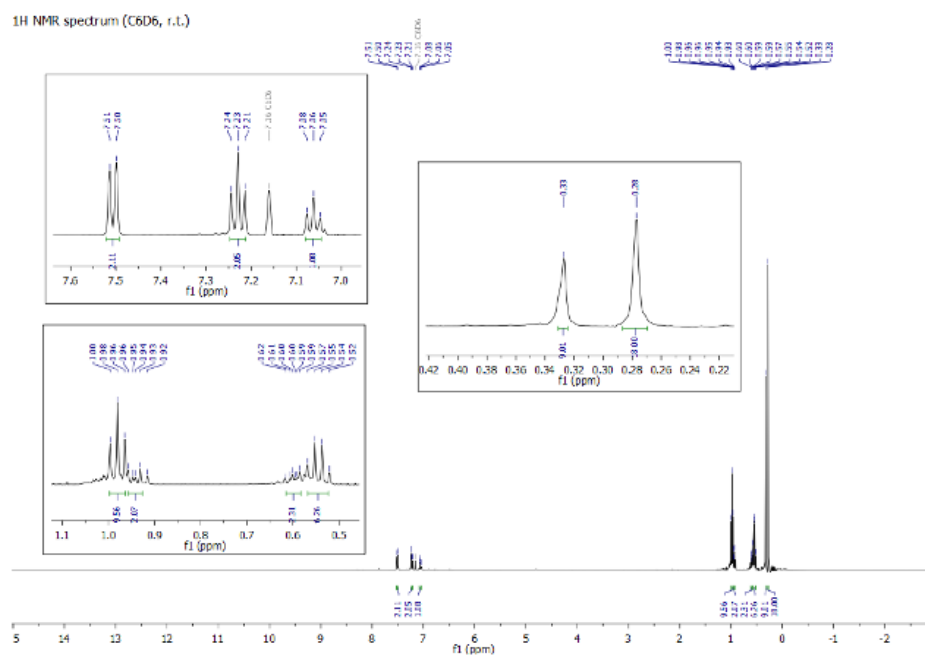


Figure S22: <sup>1</sup>H-NMR spectrum of silacyclopropene **7** (C<sub>6</sub>D<sub>6</sub>, r.t.).

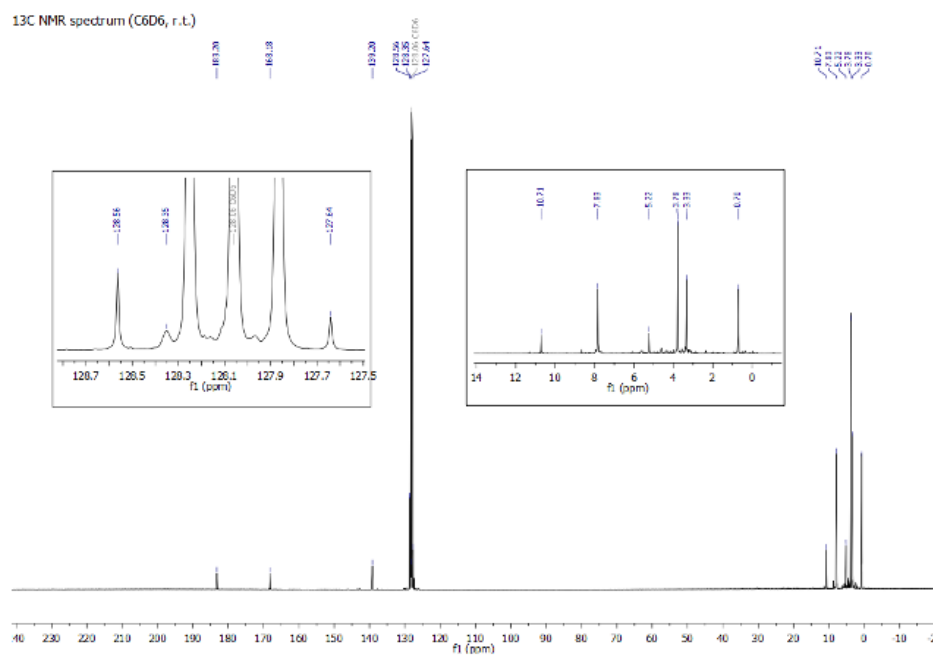


Figure S23: <sup>13</sup>C-NMR spectrum of silacyclopropene **7** (C<sub>6</sub>D<sub>6</sub>, r.t.).



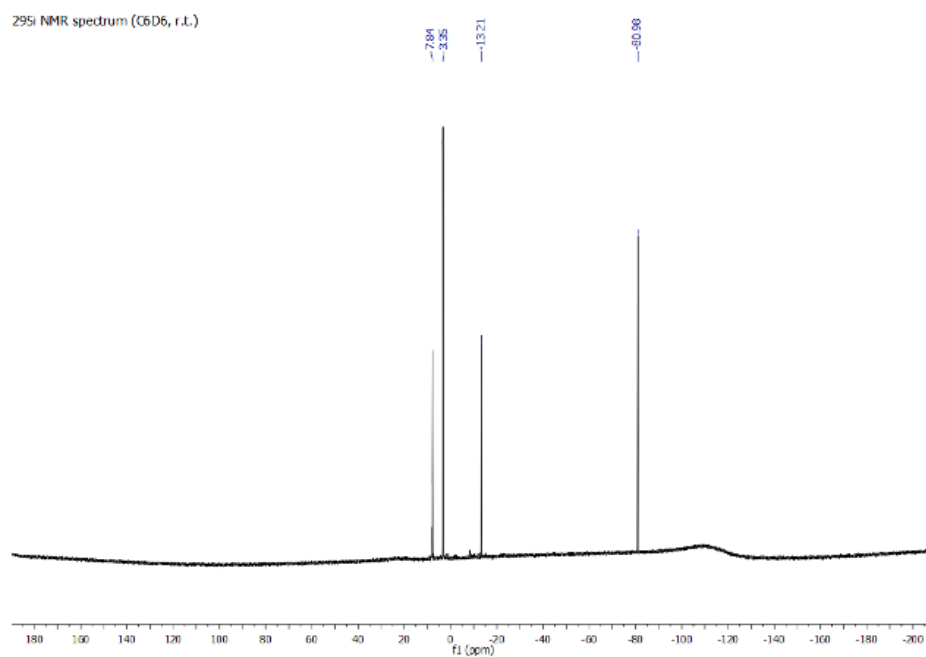


Figure S24:  $^{29}\text{Si}$ -ig NMR spectrum of silacyclopropene **7** ( $\text{C}_6\text{D}_6$ , r.t.).

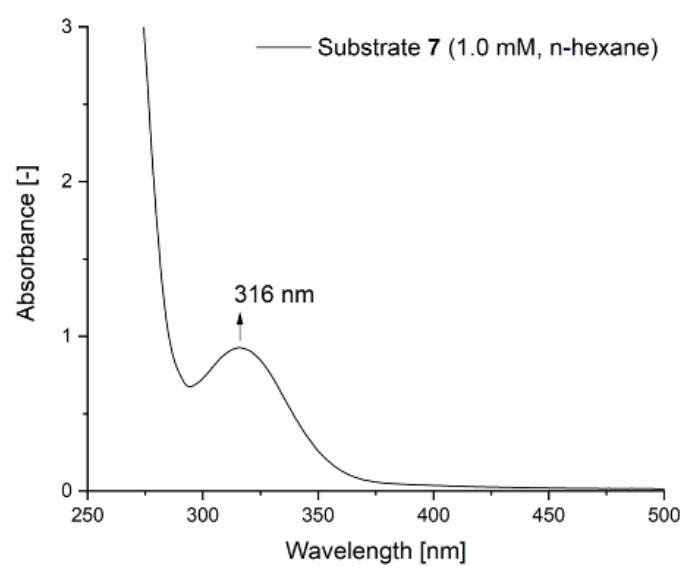
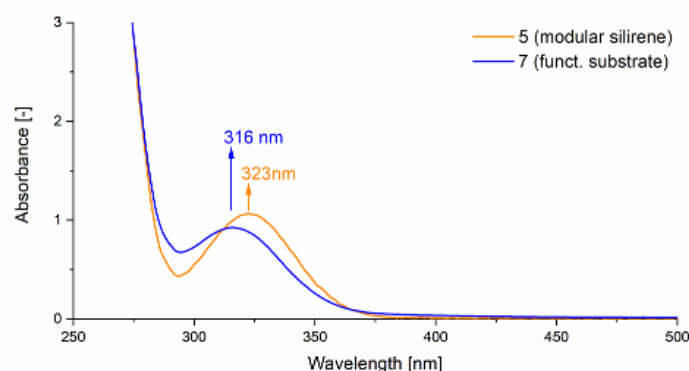
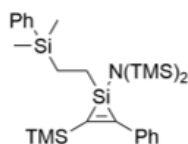


Figure S25: UV-VIS spectrum of silacyclopropene **7** (r.t., n-hexane,  $1.0 \times 10^{-3}$  M).



**Figure S26:** UV-VIS spectra of modular silacyclopriene **5** (orange) and functionalized substrate **7** (blue), (r.t., n-hexane,  $1.0 \times 10^{-3}$  M).

#### Functionalization of dimethylphenylsilane and characterization of **8**



Silacyclopriene **5** (100 mg, 256  $\mu$ mol, 1 eq) was added to a solution of dimethylphenylsilane (35.0 mg, 256  $\mu$ mol, 1 eq) in benzene (5 mL). Then 2.0 mg (0.24  $\mu$ mol) of a Karstead-catalyst solution (2.25 wt.% Pt in xylene) was added, and the mixture was stirred at 65 °C for 12 h. The colour of the reaction changes from a bright yellow to a dark gold/brown over the time. All volatiles were removed under vacuum and the residue was redissolved in pentane (5 mL). The product was purified by filtration through an appropriate amount of aluminium oxide ( $\text{Al}_2\text{O}_3$ ) and a syringe filter (PP, 0.5  $\mu$ m) to remove the applied catalyst. Further distillation under high vacuum ( $3 \cdot 10^{-5}$  mbar, 110 °C) result in the functionalized compound **8** (112 mg, 212  $\mu$ mol, 83 %) as a colourless liquid.

**$^1\text{H-NMR}$ :** (300 K, 500 MHz,  $\text{C}_6\text{D}_6$ )  $\delta$  [ppm] = 0.23 (s, 18 H,  $\text{NSi}-(\text{CH}_3)_3$ ), 0.26 (s, 6 H,  $\text{PhSi}-(\text{CH}_3)_2$ ), 0.32 (s, 9 H,  $\text{SiCSi}-(\text{CH}_3)_3$ ), 0.78-0.83 (m, 2 H,  $\text{NSi-CH}_2-\text{CH}_2\text{Si}$ ), 1.10-1.17 (m, 1 H,  $\text{NSi-CH}_2-\text{CH}_2\text{Si}$ ), 1.24-1.31 (m, 1 H,  $\text{NSi-CH}_2-\text{CH}_2\text{Si}$ ), 7.19-7.24 (m, 6 H,  $\text{CH}_{\text{arm}}$ ), 7.48-7.52 (m, 4 H,  $\text{CH}_{\text{arm}}$ ).

**$^{13}\text{C-NMR}$ :** (300 K, 125 MHz,  $\text{C}_6\text{D}_6$ )  $\delta$  [ppm] = -3.8 ( $\text{PhSi}-(\text{CH}_3)_2$ ), 0.3 ( $\text{SiCSi}-(\text{CH}_3)_3$ ), 3.8 ( $\text{NSi}-(\text{CH}_3)_3$ ), 9.6 ( $\text{NSi-CH}_2-\text{CH}_2\text{Si}$ ), 10.3 ( $\text{NSi-CH}_2-\text{CH}_2\text{Si}$ ), 127.3 ( $\text{CH}_{\text{arm}}$ ), 127.8 ( $\text{CH}_{\text{arm}}$ ), 127.9 ( $\text{CH}_{\text{arm}}$ ), 128.0 ( $\text{CH}_{\text{arm}}$ ), 128.2 ( $\text{CH}_{\text{arm}}$ ), 128.9 ( $\text{CH}_{\text{arm}}$ ), 138.6 ( $\text{C}_{\text{arm}}$ ), 138.7 ( $\text{C}_{\text{arm}}$ ), 167.9 ( $\text{Si-C-C}_{\text{arm}}$ ), 182.6 ( $\text{Si-C-Si}$ ).

**$^{29}\text{Si-NMR}$ :** (300 K, 100 MHz,  $\text{C}_6\text{D}_6$ )  $\delta$  [ppm] = -81.09 ( $\text{Si}_{\text{silirene}}$ ), -13.24 ( $\text{SiC-Si}-(\text{CH}_3)_3$ ), -1.88 ( $\text{Si-PhMe}_2$ ), 3.35 ( $\text{N-Si}-(\text{CH}_3)_3$ ).

**EA:** calc. [%] for  $\text{C}_{25}\text{H}_{51}\text{NSi}_5$  = C 61.64, H 9.01, N 2.66; found C 61.27, H 8.65, N 3.01.

**LIFDI-MS:**  $m/z$  = calc. for  $[\text{C}_{25}\text{H}_{51}\text{NSi}_5]^+$ : 525.2555[M]<sup>+</sup>, found 525.2560.



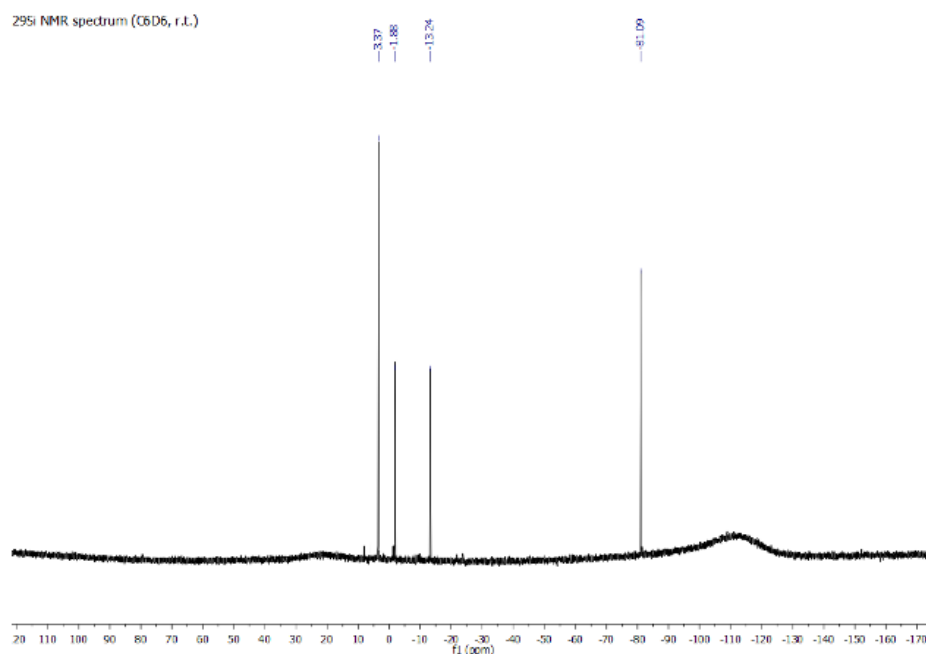
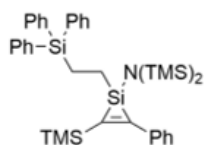


Figure S29:  $^{29}\text{Si}$ -ig NMR spectrum of silacyclopropene **8** ( $\text{C}_6\text{D}_6$ , r.t.).

#### Functionalization of dimethylphenylsilane and characterization of **9**



Silacyclopropene **5** (60.0 mg, 154  $\mu\text{mol}$ , 1 eq) was added to a solution of triphenylsilane (40.8 mg, 154  $\mu\text{mol}$ , 1 eq) in benzene (5 mL). Then 6.4 mg (0.77  $\mu\text{mol}$ ) of a Karstead-catalyst solution (2.25 wt.% Pt in xylene) was added, and the mixture was stirred at 65  $^\circ\text{C}$  for 12 h. The colour of the reaction changes from a bright yellow to a dark gold/brown over the time. All volatiles were removed under vacuum and the residue was redissolved in pentane (5 mL). The product was purified by filtration through an appropriate amount of aluminium oxide ( $\text{Al}_2\text{O}_3$ ) and a syringe filter (PP, 0.5  $\mu\text{m}$ ) to remove the applied catalyst. Further distillation under high vacuum ( $3 \cdot 10^{-5}$  mbar, 130  $^\circ\text{C}$ ) result in the functionalized compound **9** (69.1 mg, 106  $\mu\text{mol}$ , 69 %) as a colourless liquid.

$^1\text{H-NMR}$ : (300 K, 500 MHz,  $\text{C}_6\text{D}_6$ )  $\delta$  [ppm] = 0.19 (s, 18 H,  $\text{NSi}-(\text{CH}_3)_3$ ), 0.32 (s, 9 H,  $\text{SiCSi}-(\text{CH}_3)_3$ ), 0.81-0.87 (m, 2 H,  $\text{NSi-CH}_2\text{-CH}_2\text{Si}$ ), 1.48-1.51 (m, 2 H,  $\text{NSi-CH}_2\text{-CH}_2\text{Si}$ ), 7.11-7.13 (m, 3 H,  $\text{CH}_{\text{arm}}$ ), 7.52-7.54 (m, 2 H,  $\text{CH}_{\text{arm}}$ ), 7.58-7.60 (m, 6 H,  $\text{CH}_{\text{arm}}$ ), 7.62-7.64 (m, 3 H,  $\text{CH}_{\text{arm}}$ ), 7.65-7.68 (m, 6 H,  $\text{CH}_{\text{arm}}$ ).

$^{13}\text{C-NMR}$ : (300 K, 125 MHz,  $\text{C}_6\text{D}_6$ )  $\delta$  [ppm] = 0.7 ( $\text{SiCSi}-(\text{CH}_3)_3$ ), 3.7 ( $\text{NSi}-(\text{CH}_3)_3$ ), 7.6 ( $\text{NSi-CH}_2\text{-CH}_2\text{Si}$ ), 10.3 ( $\text{NSiCH}_2\text{-CH}_2\text{-Si}$ ), 128.2 ( $\text{CH}_{\text{arm}}$ ), 128.4 ( $\text{CH}_{\text{arm}}$ ), 136.0 ( $\text{CH}_{\text{arm}}$ ), 136.2 ( $\text{CH}_{\text{arm}}$ ), 136.9 ( $\text{CH}_{\text{arm}}$ ), 139.1 ( $\text{CH}_{\text{arm}}$ ), 145.2 ( $\text{C}_{\text{arm}}$ ), 151.7 ( $\text{C}_{\text{arm}}$ ), 168.5 ( $\text{Si-C-C}_{\text{arm}}$ ), 182.8 ( $\text{Si-C-Si}$ ).

$^{29}\text{Si-NMR}$ : (300 K, 100 MHz,  $\text{C}_6\text{D}_6$ )  $\delta$  [ppm] = -81.17 ( $\text{Si}_{\text{silirene}}$ ), -13.19 ( $\text{SiC-Si-(CH}_3)_3$ ), -9.53 ( $\text{Si-Ph}_3$ ), 3.50 ( $\text{N-Si-(CH}_3)_3$ ).

**EA**: calc. [%] for  $\text{C}_{37}\text{H}_{51}\text{NSi}_5$  = C 68.34, H 7.91, N 2.15; found C 61.99, H 7.73, N 2.68.

**LIFDI-MS**:  $m/z$  = calc. for  $[\text{C}_{37}\text{H}_{51}\text{NSi}_5]^+$ : 649.2868[M] $^+$ , found 649.2864.

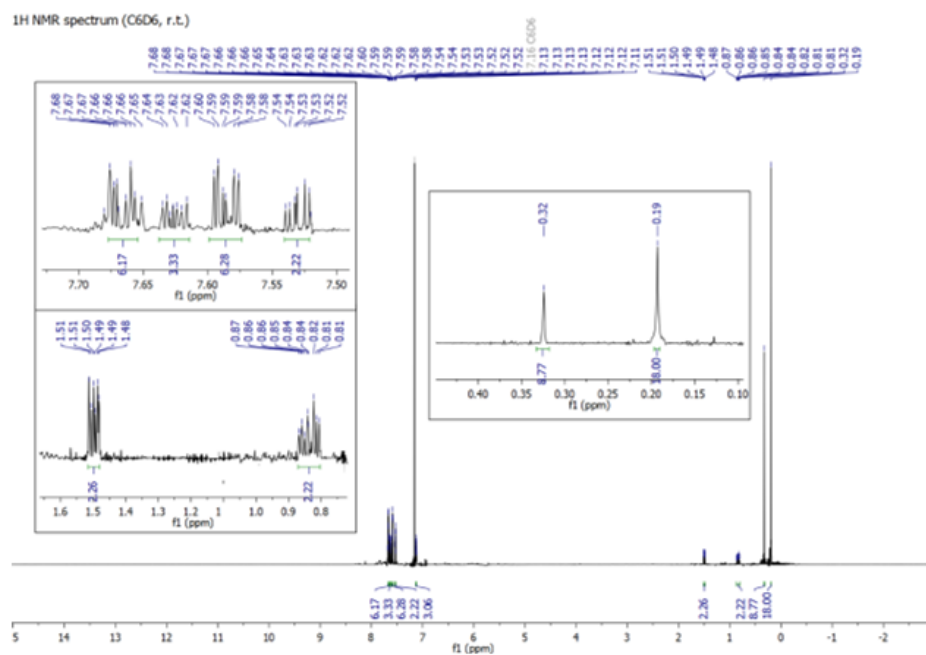


**Figure S30**:  $^1\text{H-NMR}$  spectrum of silacyclopropene **9** ( $\text{C}_6\text{D}_6$ , r.t.).

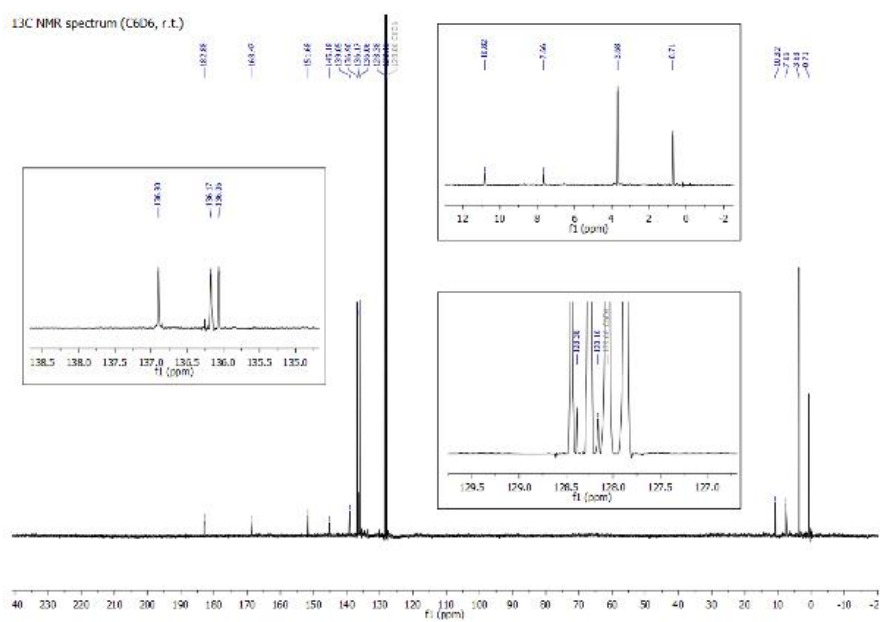


Figure S31: <sup>13</sup>C-NMR spectrum of silacyclopropene **9** (C<sub>6</sub>D<sub>6</sub>, r.t.).

<sup>29</sup>Si NMR spectrum (C<sub>6</sub>D<sub>6</sub>, r.t.)

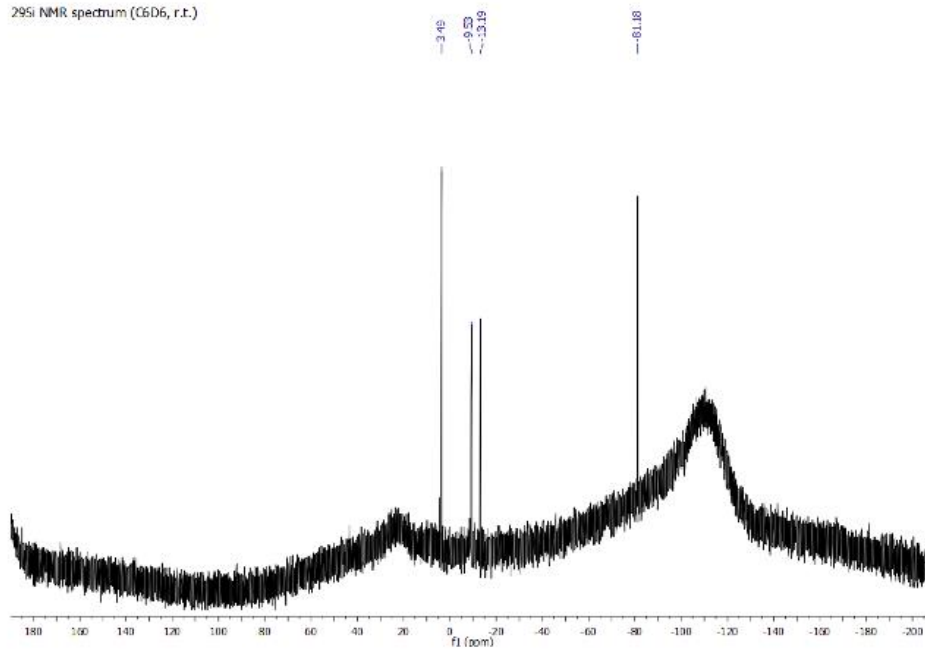
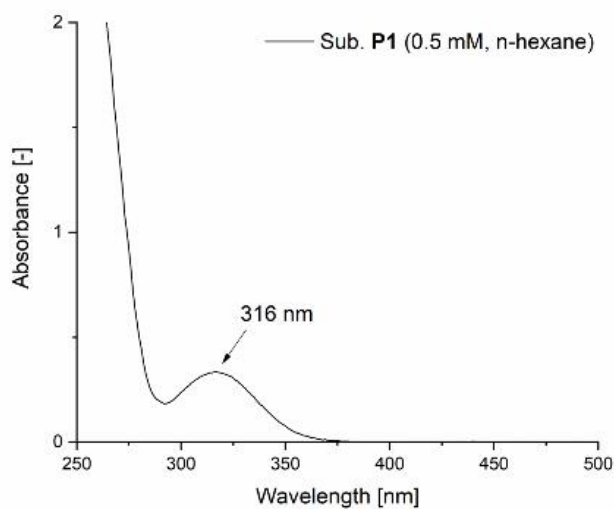


Figure S32: <sup>29</sup>Si-ig NMR spectrum of silacyclopropene **9** (C<sub>6</sub>D<sub>6</sub>, r.t.).

**Functionalization of Tetrakis(dimethylsilyoxy)silane P1**

A solution of substrate **S1** (368  $\mu\text{mol}$ , 81.9 mg, 1 eq) in toluene (10 mL) was added to a solution of silacyclopropene **5** (404  $\mu\text{mol}$ , 109 mg, 1.1 eq) in toluene (5 mL). 16.8 mg (2.05  $\mu\text{mol}$ ) of a Karstead-catalyst solution (2.25 wt.% Pt in xylene) was added, and the mixture was stirred at 65 °C for 12 h. Over the reaction time the colour changed from a bright yellow to a dark orange. All volatiles were removed under vacuum and the obtained residue was redissolved in *n*-hexane (10 mL). The crude was purified by filtration through an appropriate amount of aluminium oxide ( $\text{Al}_2\text{O}_3$ ) and a syringe filter (PP, 0.5  $\mu\text{m}$ ) to remove the applied catalyst. The filter was further washed with *n*-hexane (2 mL). At last, the solvent was removed under vacuum to obtain the functionalized substrate **P1** (105.2 mg, 68 %).



**Figure S33:** UV-VIS spectrum of functionalized substrate **P1** (r.t., *n*-hexane,  $0.5 \times 10^{-3}$  M).

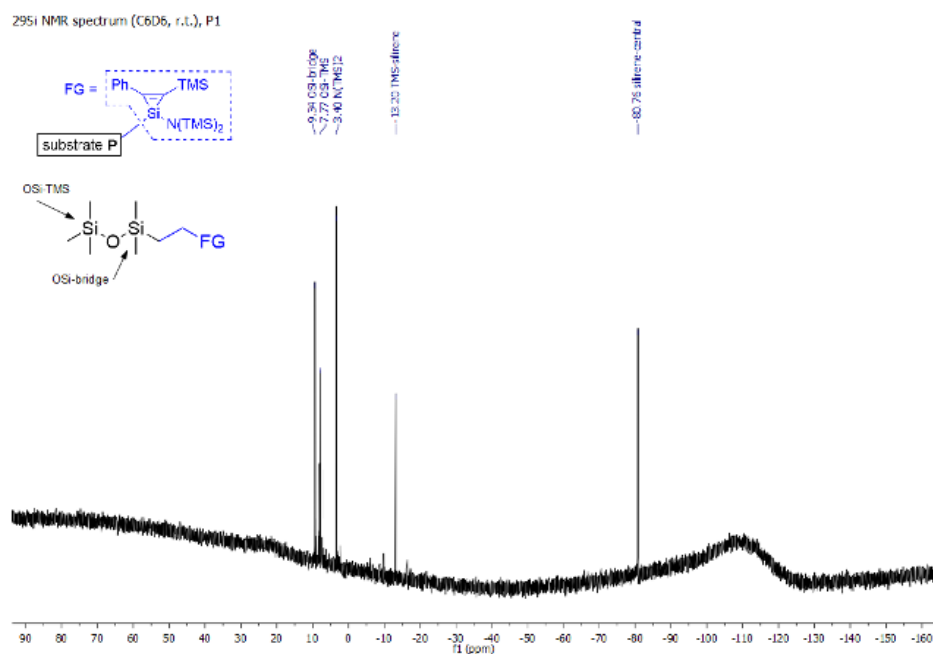
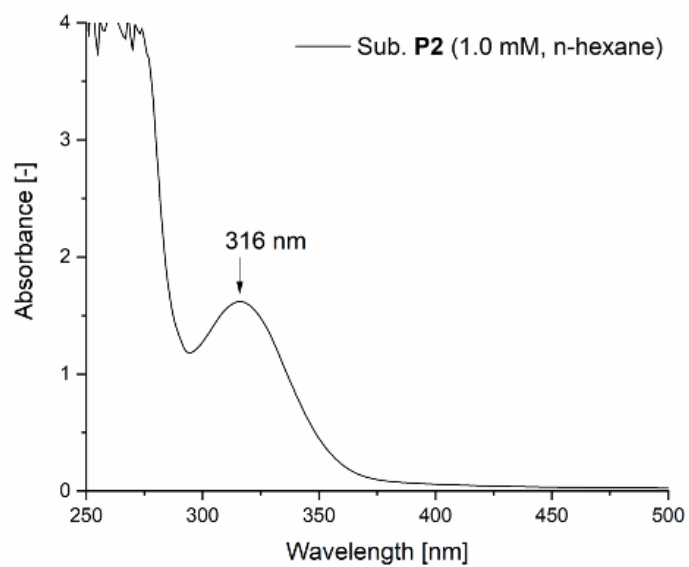


Figure S34: <sup>29</sup>Si-ig NMR spectrum of functionalized substrate **P1** (C<sub>6</sub>D<sub>6</sub>, r.t.).

#### Functionalization of Tetrakis(dimethylsilyoxy)silane **P2**

A solution of substrate **S2** (184  $\mu$ mol, 24.7 mg, 0.5 eq) in toluene (10 mL) was added to a solution of silacyclopropene **5** (404  $\mu$ mol, 109 mg, 1.1 eq) in toluene (5 mL). 16.8 mg (2.05  $\mu$ mol) of a Karstead-catalyst solution (2.25 wt.% Pt in xylene) was added, and the mixture was stirred at 65 °C for 12 h. Over the reaction time the colour changed from a bright yellow to a dark orange. All volatiles were removed under vacuum and the obtained residue was redissolved in *n*-hexane (10 mL). The crude was purified by filtration through an appropriate amount of aluminium oxide (Al<sub>2</sub>O<sub>3</sub>) and a syringe filter (PP, 0.5  $\mu$ m) to remove the applied catalyst. The filter was further washed with *n*-hexane (2 mL). At last, the solvent was removed under vacuum to obtain the functionalized substrate **P2** (79.8 mg, 64 %).





**Figure S35:** UV-VIS spectrum of functionalized substrate **P2** (r.t., n-hexane,  $1.0 \times 10^{-3}$  M).

$^{29}\text{Si}$  NMR spectrum ( $\text{C}_6\text{D}_6$ , r.t.), **P2**

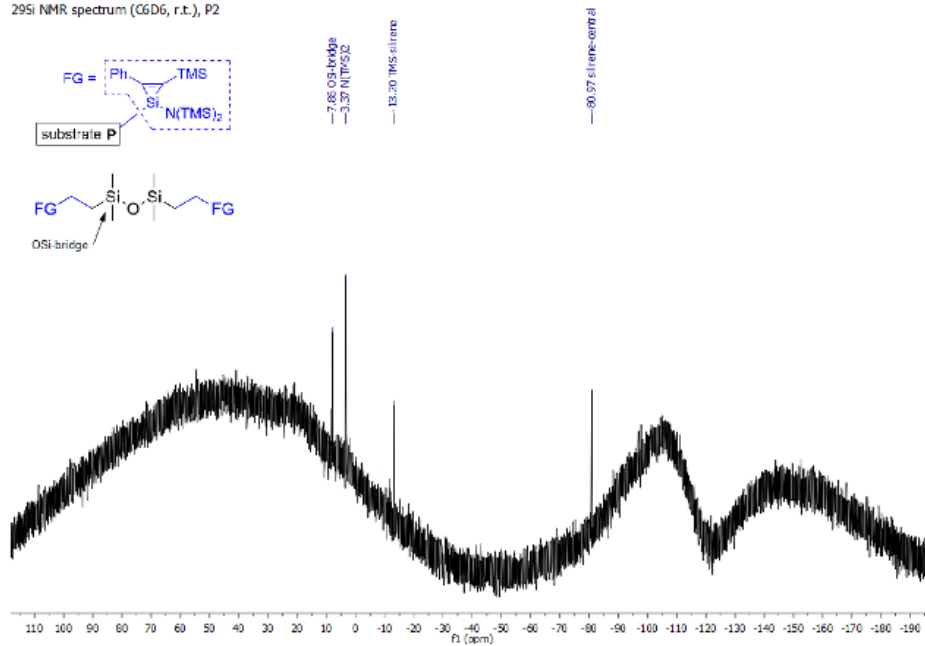


**Figure S36:**  $^{29}\text{Si}$ -ig NMR spectrum of functionalized substrate **P2** ( $\text{C}_6\text{D}_6$ , r.t.).

**Functionalization of Tetrakis(dimethylsilyoxy)silane P3**

A solution of substrate PMHS **53** ( $M = 580$  g/mol, hydrid-terminated,  $92 \mu\text{mol}$ ,  $59.5$  mg,  $0.5$  eq.) in toluene ( $10$  mL) was added to a solution of silacyclopropene **5** ( $202 \mu\text{mol}$ ,  $54.5$  mg,  $1.1$  eq) in toluene ( $5$  mL).  $8.4$  mg ( $1.02 \mu\text{mol}$ ) of a Karstead-catalyst solution ( $2.25$  wt.% Pt in xylene) was added, and the mixture was stirred at  $65$  °C for  $12$  h. Over the reaction time the colour changed from a bright yellow to a dark orange. All volatiles were removed under vacuum and the obtained residue was redissolved in *n*-hexane ( $10$  mL). The crude was purified by filtration through an appropriate amount of aluminium oxide ( $\text{Al}_2\text{O}_3$ ) and a syringe filter (PP,  $0.5 \mu\text{m}$ ) to remove the applied catalyst. The filter was further washed with *n*-hexane ( $2$  mL). At last, the solvent was removed under vacuum to obtain the functionalized substrate **P3** ( $68.6$  mg,  $57$  %).

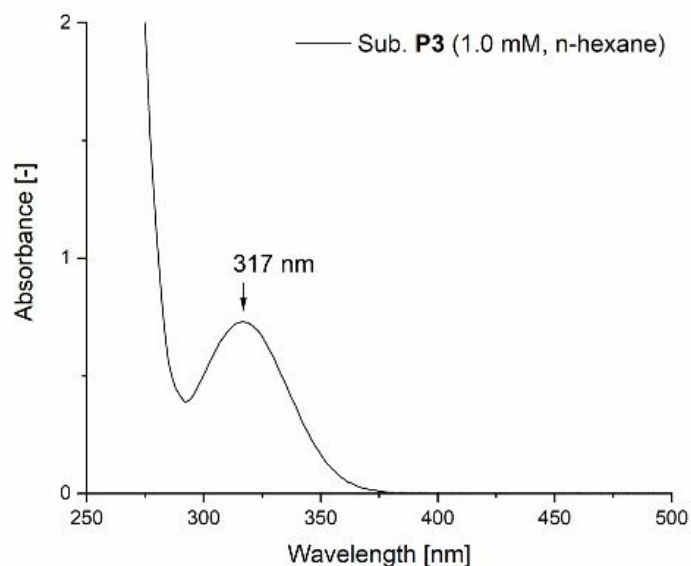


**Figure S37:** UV-VIS spectrum of functionalized substrate **P3** (r.t., *n*-hexane,  $1.0 \times 10^{-3}$  M).

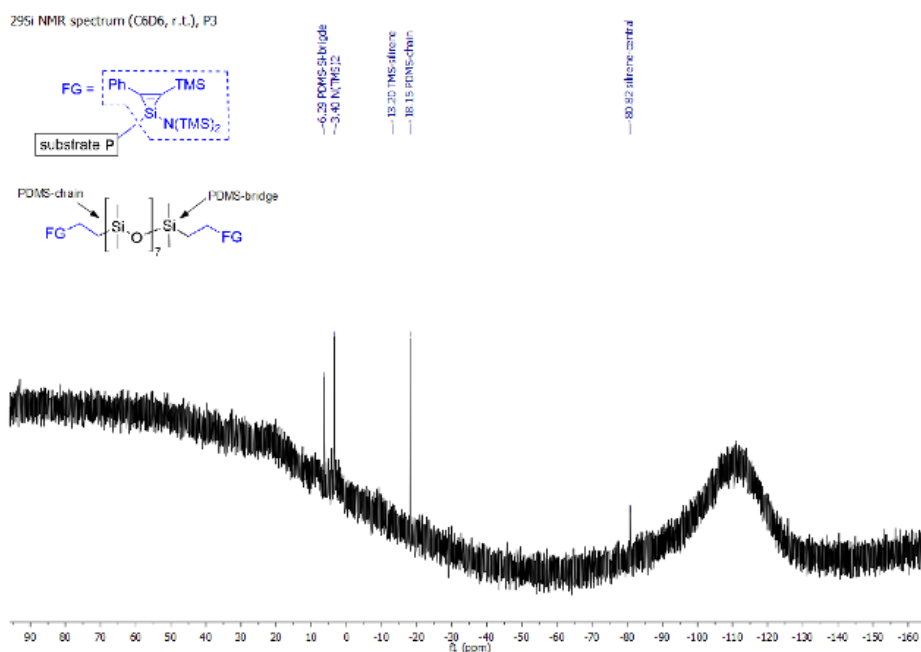
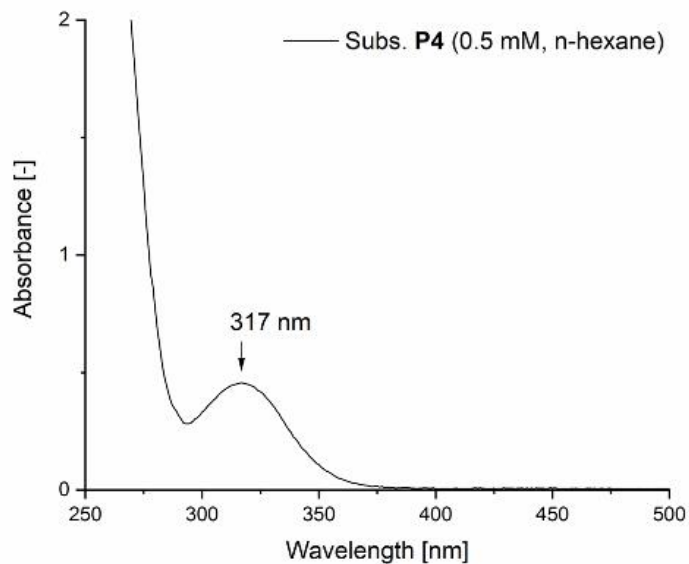


Figure S38: <sup>29</sup>Si NMR spectrum of functionalized substrate P3 (C<sub>6</sub>D<sub>6</sub>, r.t.).

#### Functionalization of Tetrakis(dimethylsilyoxy)silane P4

A solution of substrate PMHS **S3** ( $M = 15000$  g/mol, hydrid-terminated, 92  $\mu\text{mol}$ , 1.38 g, 0.5 eq.) in toluene (10 mL) was added to a solution of silacyclopropene **5** (202  $\mu\text{mol}$ , 54.5 mg, 1.1 eq) in toluene (5 mL). 8.4 mg (1.02  $\mu\text{mol}$ ) of a Karstead-catalyst solution (2.25 wt.% Pt in xylene) was added, and the mixture was stirred at 65 °C for 24 h. Over the reaction time the colour changed from a bright yellow to a dark orange. All volatiles were removed under vacuum and the obtained residue was redissolved in *n*-hexane (10 mL). The crude was purified by filtration through an appropriate amount of aluminium oxide (Al<sub>2</sub>O<sub>3</sub>) and a syringe filter (PP, 0.5  $\mu\text{m}$ ) to remove the applied catalyst. The filter was further washed with *n*-hexane (2 mL). At last, the solvent was removed under vacuum to obtain the functionalized substrate **P3** (677.7 mg, 47 %).



**Figure S39:** UV-VIS spectrum of functionalized substrate **P4** (r.t., n-hexane,  $0.5 \times 10^{-3}$  M).

$^{29}\text{Si}$  NMR spectrum ( $\text{C}_6\text{D}_6$ , r.t.), **P4**

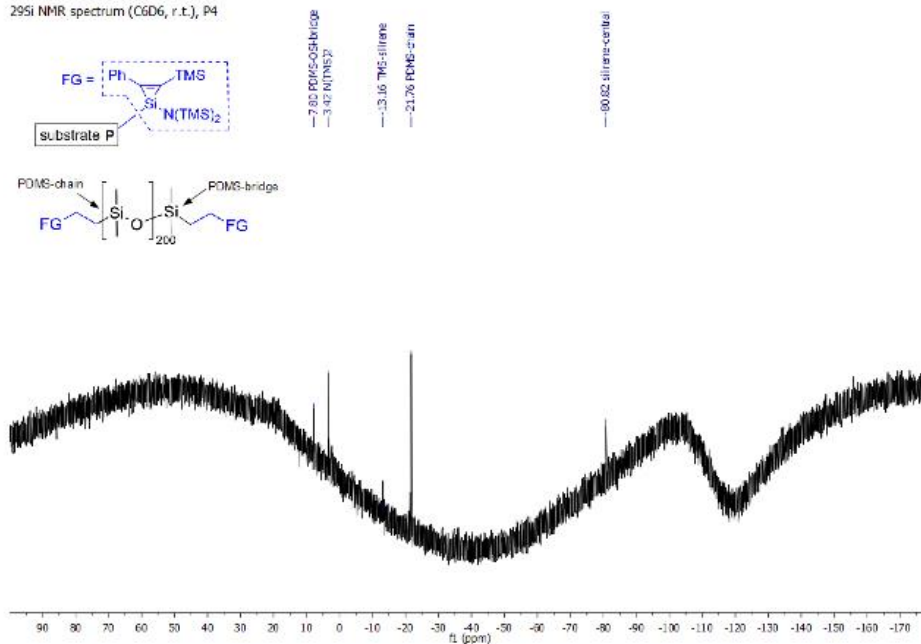


**Figure S40:**  $^{29}\text{Si}$ -ig NMR spectrum of functionalized substrate **P4** ( $\text{C}_6\text{D}_6$ , r.t.).

**Partial functionalization of Tetrakis(dimethylsilyoxy)silane S5**

Silacyclopropene **5** (100 mg, 256  $\mu\text{mol}$ , 1 eq) was added to a solution of tetrakis(dimethylsilyoxy)silane **S5** (44.2 mg, 134.6  $\mu\text{mol}$ , 0.5 eq) in toluene (5 mL). Then 5.6 mg (0.67  $\mu\text{mol}$ ) of a Karstead-catalyst solution (2.25 wt.% Pt in xylene) was added, and the mixture was stirred at 60 °C for 48 h. The colour of the reaction changes from a bright yellow to a dark gold/brown over the time. All volatiles were removed under vacuum and the residue was redissolved in pentane (5 mL). The product was purified by filtration through an appropriate amount of aluminium oxide ( $\text{Al}_2\text{O}_3$ ) and a syringe filter (PP, 0.5  $\mu\text{m}$ ) to remove the applied catalyst and give the compound **P5a** as a colourless, viscous oil. (79.3 mg, 48 %).

**Full functionalization of Tetrakis(dimethylsilyoxy)silane S5**

Silacyclopropene **5** (100 mg, 256  $\mu\text{mol}$ , 1 eq) was added to a solution of tetrakis(dimethylsilyoxy)silane **S5** (22.1 mg, 67.3  $\mu\text{mol}$ , 0.25 eq) in toluene (5 mL). 2.8 mg (0.34  $\mu\text{mol}$ ) of a Karstead-catalyst solution (2.25 wt.% Pt in xylene) was added, and the mixture was stirred at 60 °C for 48 h. The colour of the reaction changes from a bright yellow to a dark gold/brown over the time. All volatiles were removed under vacuum and the residue was redissolved in pentane (5 mL). The product was purified by filtration through an appropriate amount of aluminium oxide ( $\text{Al}_2\text{O}_3$ ) and a syringe filter (PP, 0.5  $\mu\text{m}$ ) to remove the applied catalyst and give the compound **P5b** as a colourless, viscous oil. (61.7 mg, 51 %).

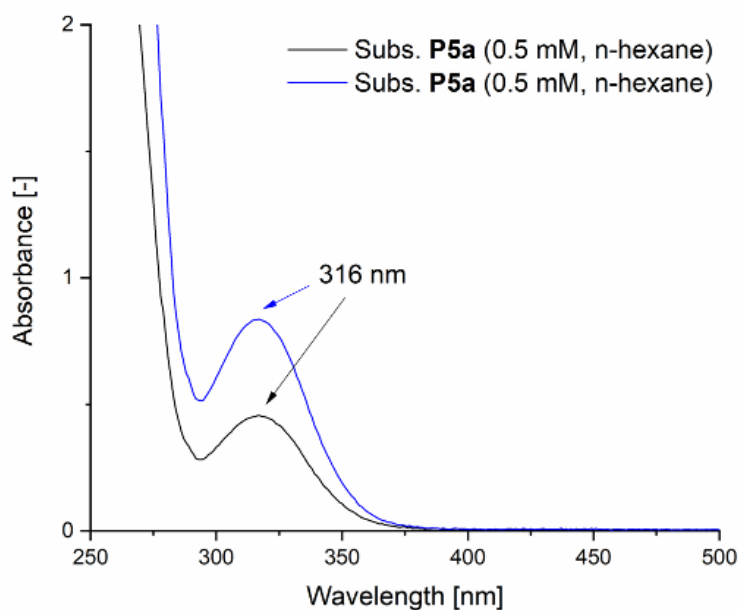
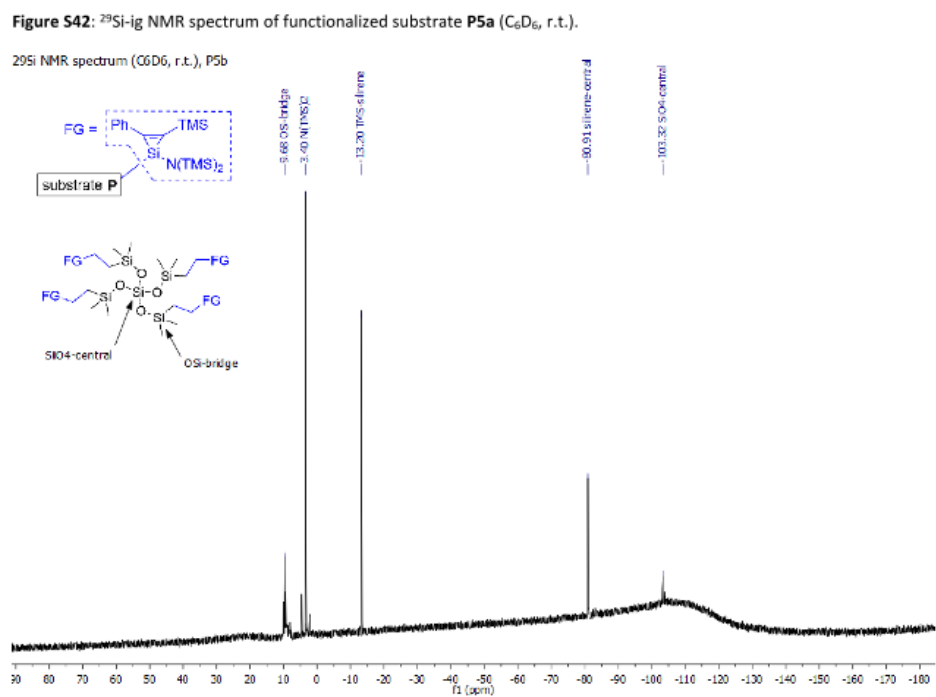
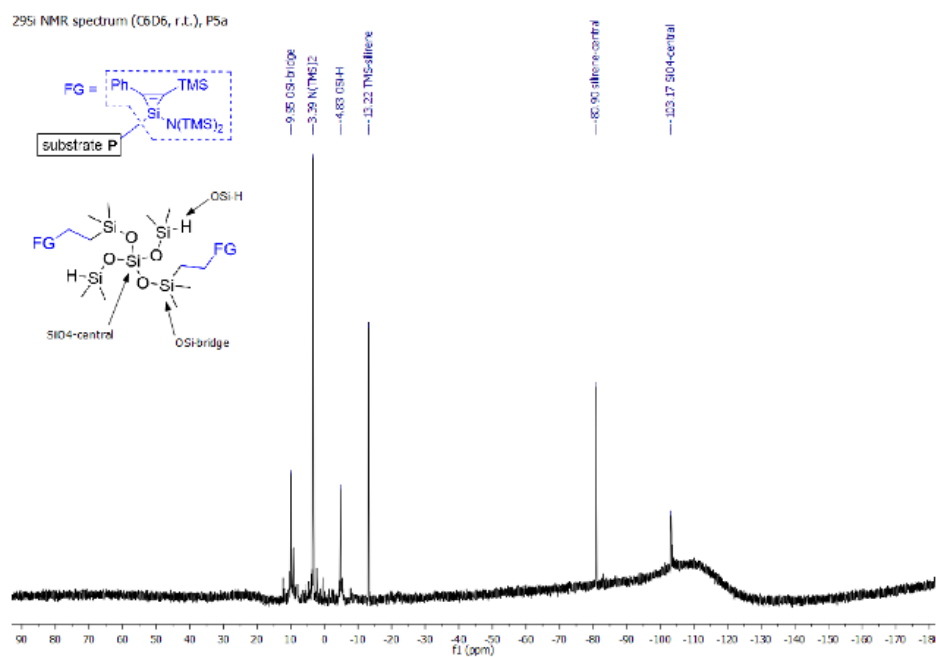


**Figure S41:** UV-VIS spectra of partial modified substrate **P5a** (black) and full modified substrate **P5b** (blue) (r.t., n-hexane,  $0.5 \times 10^{-3}$  M).



**Partial functionalization of lateral polymethylhydrosiloxane (PMHS) S6**

A solution of PMHS (520 mg,  $M = 4900$  g/mol, 4.9 mmol/g Si-H moiety, statistical copolymer of dimethylsiloxane and hydridomethylsiloxane) in toluene (10 mL) was added to a solution of silacyclopropene **5** (500 mg, 1.28 mmol, 0.5 eq per Si-H moiety) in toluene (5 mL). 53.5 mg (6.40  $\mu\text{mol}$ ) of a Karstead-catalyst solution (2.25 wt.% Pt in xylene) was added, and the mixture was stirred at 65 °C for 24 h. Over the reaction time the colour changed from a bright yellow to a dark orange. All volatiles were removed under vacuum and the obtained residue was redissolved in *n*-hexane (10 mL). The crude was purified by filtration through an appropriate amount of aluminium oxide ( $\text{Al}_2\text{O}_3$ ) and a syringe filter (PP, 0.5  $\mu\text{m}$ ) to remove the applied catalyst. The filter was further washed with *n*-hexane (2 mL). At last, the solvent was removed under vacuum to obtain the functionalized PDMS **P6a** as yellowish viscous fluid (530 mg, 51 %).

**Full functionalization of lateral polymethylhydrosiloxane (PMHS) S6**

A solution of PMHS (260 mg,  $M = 4900$  g/mol, 4.9 mmol/g Si-H moiety, statistical copolymer of dimethylsiloxane and hydridomethylsiloxane) in toluene (5 mL) was added to a solution of silacyclopropene **5** (500 mg, 1.28 mmol, 1.0 eq per Si-H moiety) in toluene (5 mL). Then 53.5 mg (6.40  $\mu\text{mol}$ ) of a Karstead-catalyst solution (2.25 wt.% Pt in xylene) was added, and the mixture was stirred at 65 °C for 24 h. Over the reaction time the colour changed from a bright yellow to a dark orange. All volatiles were removed under vacuum and the obtained residue was redissolved in *n*-hexane (10 mL). The crude was purified by filtration through an appropriate amount of aluminium oxide ( $\text{Al}_2\text{O}_3$ ) and a syringe filter (PP, 0.5  $\mu\text{m}$ ) to remove the applied catalyst. The filter was further washed with *n*-hexane (2 mL). At last, the solvent was removed under vacuum to obtain the functionalized PDMS **P6b** as yellowish viscous fluid (378 mg, 48%).

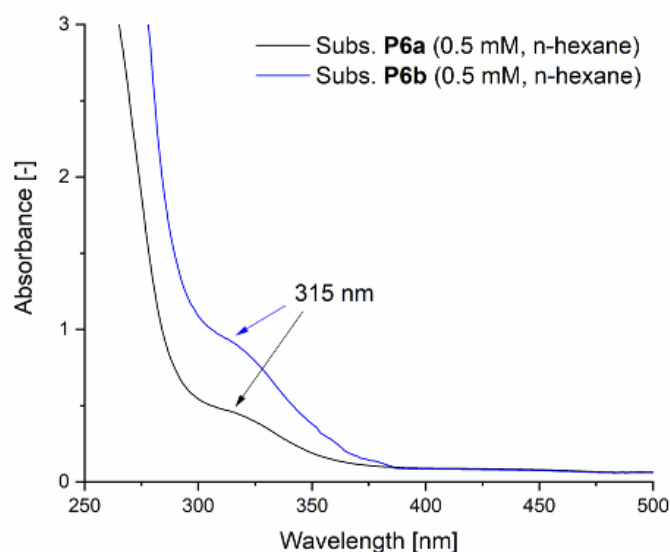


**Figure S44:** UV-VIS spectra of partial modified polysiloxane **P6a** (black) and full modified polysiloxane **P6b** (blue), (r.t., *n*-hexane,  $0.5 \times 10^{-3}$  M).

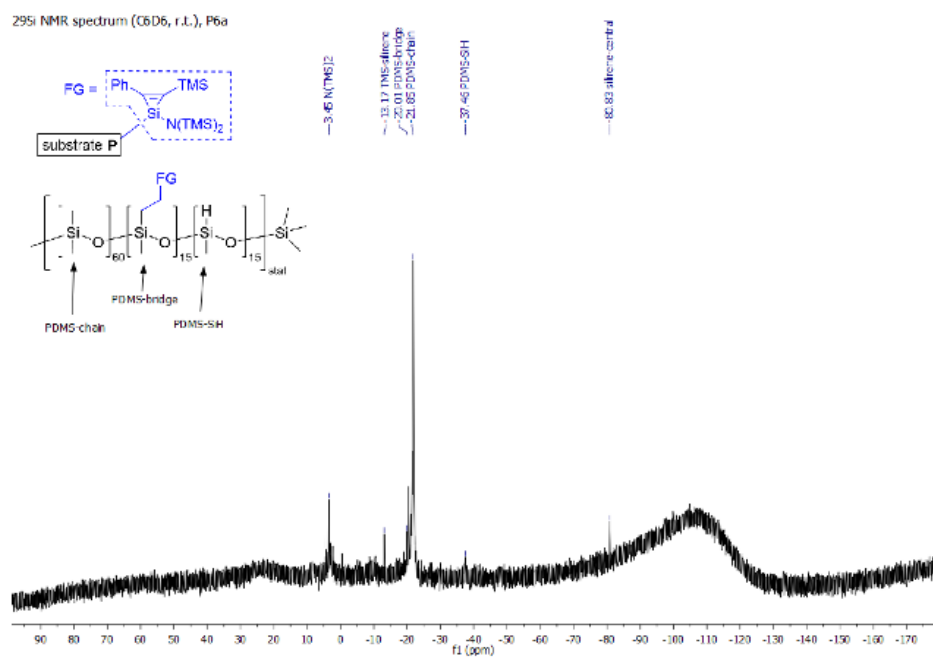


Figure S45: <sup>29</sup>Si-ig NMR spectrum of functionalized substrate P6a (C<sub>6</sub>D<sub>6</sub>, r.t.).

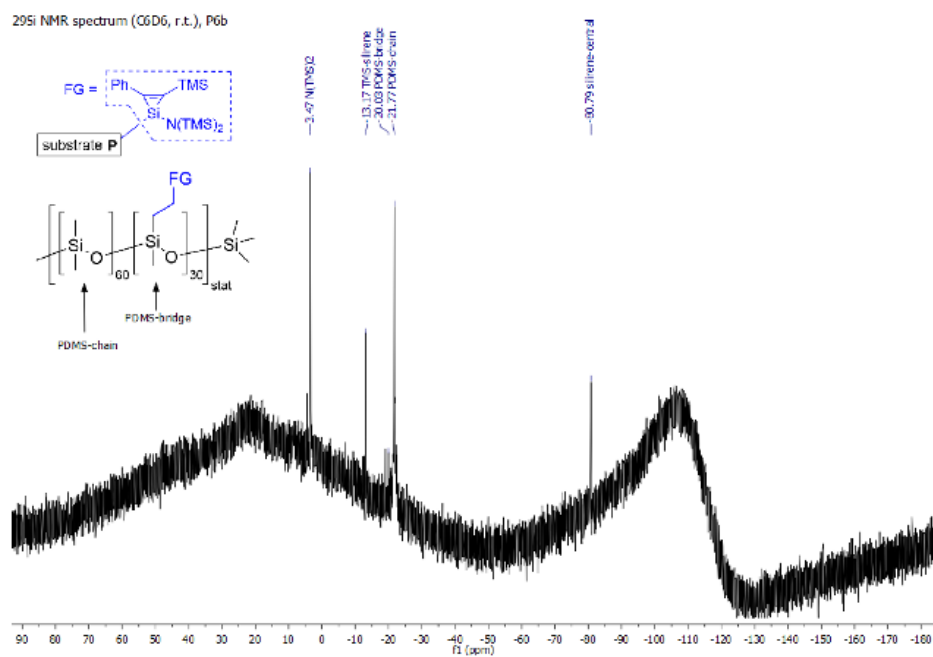
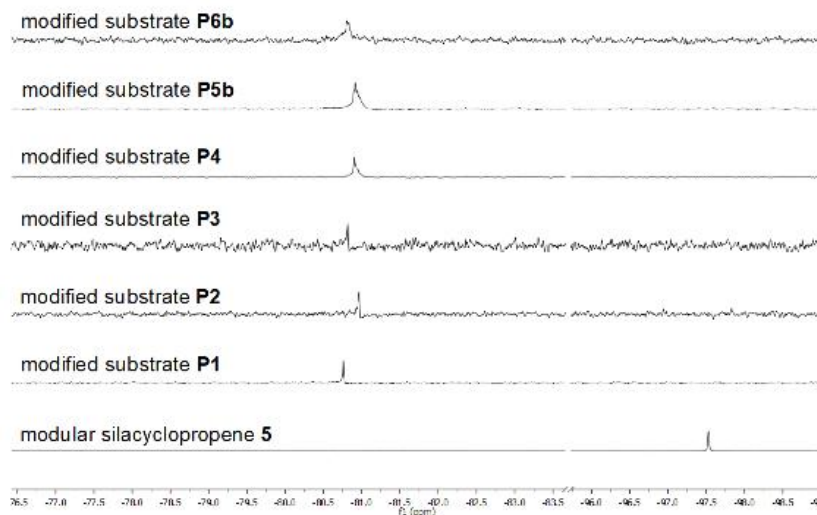


Figure S46: <sup>29</sup>Si-ig NMR spectrum of functionalized substrate P6b (C<sub>6</sub>D<sub>6</sub>, r.t.).





**Figure S47:** Overview of different  $^{29}\text{Si}$  NMR spectra of modified substrates **P1-P6** in comparison to silacyclopropene **5** ( $\text{C}_6\text{D}_6$ , r.t.) after reaction finalization.

## B. References

- (S1) M. Muhr, P. Heiß, M. Schütz, R. Bühler, C. Gemel, M. H. Linden, H. B. Linden and R. A. Fischer, *Dalton Transactions*, 2021, **50**, 9031.
- (S2) a) U. Wannagat and H. Brger, *Z. anorg. allg. Chem.*, 1964, **326**, 309; b) N. Auner, A. W. Weingartner and E. Herdtweck, *Zeitschrift für Naturforschung B*, 1993, **48**, 318;
- (S3) a) I. E. Markó, S. Stérin, O. Buisine, G. Berthon, G. Michaud, B. Tinant and J.-P. Declercq, *Adv. Synth. Catal.*, 2004, **346**, 1429; b) B. D. Karstedt, General Electric, *US Patent*, US 3715334A, **1973**; c) P. B. Hitchcock, M. F. Lappert and N. J. W. Warhurst, *Angew. Chem. Int. Ed. Engl.*, 1991, **30**, 438; d) J. A. Osborn, F. H. Jardine, J. F. Young and G. Wilkinson, *J. Chem. Soc., A*, 1966, 1711;

9.4.3. Supporting Information for Chapter 6

# ChemSusChem

## Supporting Information

### **Photo-Activity of Silacyclopropenes and their Application in Metal-Free Curing of Silicones**

Matthias Nobis, Jonas Futter, Maximilian Moxter, Shigeyoshi Inoue, and Bernhard Rieger\*<sup>©</sup>  
2022 The Authors. ChemSusChem published by Wiley-VCH GmbH. This is an open access article under the terms of the Creative Commons Attribution Non-Commercial License, which permits use, distribution and reproduction in any medium, provided the original work is properly cited and is not used for commercial purposes.

I. Experimental Section	1
a) General Consideration and Analytical Methods	1
b) Synthesis and Characterization of New Compounds	3
1. Synthesis of Acetylenes	3
2. Synthesis of Monofunctional Silirenes	11
3. Synthesis of Multifunctional Silirene-Linkers	22
4. Photoreaction Products	38
c) Figures and Tables	58
1. Rheologic Measurements	58
2. Light Control Reactions	68
3. Thermogravimetric analysis (TGA)	70
4. Differential scanning calorimetry (DSC)	70
5. Swelling Tests	71
6. Emission Spectra	72
II. References	80

## I. Experimental Section

### a) General Consideration and Analytical Methods

All experiments and manipulations were carried out under dry oxygen-free argon or nitrogen atmosphere using standard Schlenk techniques or in a LABmaster sp glovebox from MBraun. Glassware was heat-dried under vacuum prior to use. Solvents were dried by standard methods and freshly distilled prior to use. Dry pentane, Et<sub>2</sub>O, THF and toluene were obtained from a M.Braun MB-SPS 800 solvent purification system. Commercially available reagents were purchased from Sigma-Aldrich, Acros, Alfa-Aesar, abcr or TCI and used as received. PDMS-compounds were received from WACKER Chemie AG or purchased from ABCR. All siloxanes for crosslinking experiments were degassed and dried to avoid problems with oxygen and water. For vinyl- and hydrosiloxanes we applied high vacuum and heat for several days. Silanol terminated siloxanes were additionally flashed over dry neutral alumina and 3 Å molecular sieve. Al<sub>2</sub>O<sub>3</sub> (neutral) and carbon black were dried for 72 h at 150 °C in high vacuum. Cooling baths used were ice/water (0°C) and dry ice/ethanol (-78°C).

Photochemical experiments at  $\lambda_{\text{max}} = 325 \text{ nm}$ ,  $\lambda_{\text{max}} = 340 \text{ nm}$ , or  $\lambda_{\text{max}} = 365 \text{ nm}$ ,  $\lambda_{\text{max}} = 368 \text{ nm}$  were carried out in a Schlenk tube (diameter = 1 cm) with a polished quartz rod as an optical fiber, which was

S1

roughened by sandblasting at one end and the other end attached to the LED (see emission spectra LEDs). The roughed end (length = 5 cm) was completely submerged in the solvent during the reaction, in order to guarantee optimal and reproducible irradiation conditions. The Schlenk tube was cooled using an ethanol bath cooled by a cryostat (Huber TC100E). Photochemical experiments at  $\lambda_{\text{max}} = 254$  nm,  $\lambda_{\text{max}} = 300$  nm,  $\lambda_{\text{max}} = 366$  nm, or  $\lambda_{\text{max}} = 420$  nm were carried out in heat-dried glass tubes in a positive geometry setup (cylindrical array of 16 Philips Black Light Blue fluorescent light tubes, 8 W nominal power,  $\lambda_{\text{max}} = 366$  nm or Luzchem LZC-420 fluorescent light tubes, 8 W nominal power,  $\lambda_{\text{max}} = 420$  nm) with the sample placed in the center of the illumination chamber.

The solution NMR spectra were recorded on Bruker Spectrometers AVHD 400 or AVHD 500 cryo with residual solvent signals as internal reference ( $^1\text{H}$  NMR:  $\text{C}_6\text{D}_6$ , 7.16 ppm.  $^{13}\text{C}$  NMR:  $\text{C}_6\text{D}_6$  128.06 ppm) or an external standard ( $^{29}\text{Si}$  NMR:  $\text{SiMe}_4$ , 0.0 ppm). The following abbreviations were used to describe peak patterns when appropriate: br = broad, s = singlet, d = doublet, t = triplet, dd = doublet of doublets, m = multiplet. A simple baseline correction was applied for all  $^{29}\text{Si}$ -ig-NMR spectra to reduce the signal deriving from the glass-tube.

Liquid Injection Field Desorption Ionization Mass Spectrometry (LIFDI-MS) was measured directly from an inert atmosphere glovebox with a Thermo Fisher Scientific Exactive Plus Orbitrap equipped with an ion source from Linden CMS.<sup>[1]</sup>

Inductive coupled plasma optical emission spectrometry (ICP-OES) was carried out on an Agilent 700Series ICP Optical Emission Spectrometer (725 ICP-OES, radial viewed system) to determine the content of platinum in the synthesized products after multiple filtration procedures. Respective samples were dissolved in concentrated HCl and subsequently diluted with bidistilled water. An essential metal standard was prepared from several defined samples with Pt-concentration ranging from 1 ppm to 50 ppm (platinum AAS standard, Sigma Aldrich). Determination of the Pt concentration was conducted by analyzing the wavelength of 203.646 nm.

Elemental analyses were conducted with a Vario EL instrument from Elementar. Air-sensitive substances were placed into tin or aluminum boats and kept under argon atmosphere.

UV-Vis spectra were recorded on a Cary 50Scan UV-Visible spectrophotometer from Varian with 10 x 10 mm diameter UV quartz cuvette with a screw cap PTFE sealing from Hellma Analytics. n-Hexane or n-pentane were used as solvents for all measurements.

Rheologic measurements were conducted using a commercial shear rheometer (Anton Paar, MCR 302) with a parallel plate (PP) geometry (bottom plate: I-PP50/SS d = 50 mm, measuring head: PP25, d = 25 mm). Photo-based curing were performed with a glass-based bottom plate setup (P-PTD 200/GL) to allow UV-irradiation during the rheological measurement. For this, all measurements were done with a plate separation of d = 0.10 mm and 150  $\mu\text{L}$  sample volume. An additional hood was installed to ensure an inert gas atmosphere (continuous nitrogen flow) during the measurements. The transfer of compound mixtures into the rheometer was conducted under protective gas (nitrogen). Temperature control of the bottom plate was set to 20  $^\circ\text{C}$  and kept constant over the measurement time. Measuring frequency was  $f = 1$  Hz and gradually decreasing amplitude (starting at  $\gamma = 5$  %, automatic decrease of 1/10 when moment  $M > 1$  mNm) to avoid network destruction at high shear-deformation.

Thermogravimetric analysis (TGA) is performed from 2 mg samples on a TGA Q5000 by TA Instruments. Samples are heated from room temperature to 800  $^\circ\text{C}$  with a heat rate of 10 K/min under argon. Analysis of mass loss and determination of T5% is done using TA Analysis software.

Differential scanning calorimetry (DSC) was measured using a DSC Q2000 by TA instruments in exo-

down mode. Sample size is about 6 mg in non-hermetic aluminum pans in the range of -140 °C to 300 °C depending on the sample. Analysis is performed using TA Analysis.

## b) Synthesis and Characterization of New Compounds

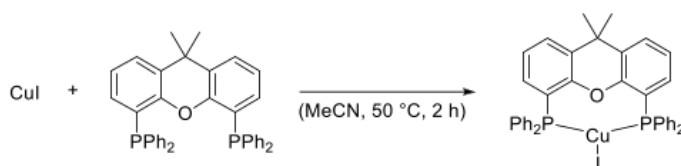
### 1. Synthesis of Acetylenes

All acetylenes, which are not listed in the following were commercially purchased, dried over CaH<sub>2</sub>, and distilled once to ensure pure and dry reactants.

#### General Procedure for diaryl-substituted acetylenes

Diarylacetylenes **A5** and **A6** were synthesized according to literature, described by Huang *et al.*<sup>[2,3]</sup> Pd(OAc)<sub>2</sub> (35.5 mg, 158 μmol, 0.01 eq.), CuI-Xantphos (122 mg, 158 μmol, 0.01 eq.), Cs<sub>2</sub>CO<sub>3</sub> (10.3 g, 31.7 mmol, 2.00 eq.), respective arylbromide or aryl iodide (15.8 mmol, 1.00 eq.) and bis(trimethylsilyl)-ethyne (1.62 g, 9.49 mmol, 0.60 eq.) were stirred in DMF (38 mL) at 60 °C for 18 hours. The reaction progress was monitored by TLC. DMF was evaporated under reduced pressure. The black residue was extracted with water (75 mL) and DCM (3 × 75 mL). The combined organic layers were dried over anhydrous MgSO<sub>4</sub>, filtered and concentrated. The crude product was sublimed to obtain the diarylacetylene in high purity.

#### CuI-Xantphos

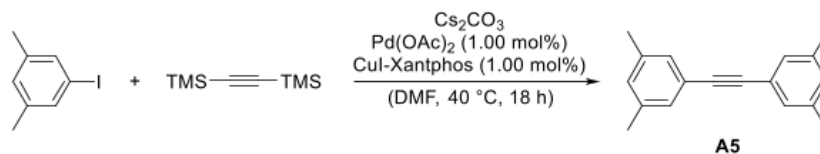


A suspension of CuI (500 mg, 2.63 mmol, 1.00 eq.) in acetonitrile (25 mL) was stirred at 50 °C until all solids dissolved. Xantphos was added in one portion to the yellowish solution, whereupon a white precipitate formed immediately. The suspension was stirred at 50 °C for 2 hours and at room temperature overnight. The reaction mixture was filtered, and the wet cake was washed with acetonitrile (2 × 5 mL) and dried under reduced pressure. CuI-Xantphos was obtained as a white powder. Yield: 2.01 g (99%).

<sup>1</sup>H NMR (400 MHz, CD<sub>2</sub>Cl<sub>2</sub>) δ (ppm): 7.58 (d, 2H, <sup>3</sup>J<sub>HH</sub> = 7.7 Hz, CH<sub>3</sub>-C-C-CH), 7.45 - 7.38 (m, 8H, P-C-CH-CH), 7.35 (t, 4H, <sup>3</sup>J<sub>HH</sub> = 7.4 Hz, P-C-(CH)<sub>2</sub>-CH), 7.26 (t, 8H, <sup>3</sup>J<sub>HH</sub> = 7.4 Hz, P-C-CH), 7.13 (t, 2H, <sup>3</sup>J<sub>HH</sub> = 7.7 Hz, CH<sub>3</sub>-C-C-CH-CH), 6.63 - 6.58 (m, 2H, O-C-C-CH), 1.66 (s, 6H, CH<sub>3</sub>)

<sup>31</sup>P NMR (162 MHz, CD<sub>2</sub>Cl<sub>2</sub>) δ (ppm): -17.89.

The analytical data obtained matched those reported in the literature.<sup>[3]</sup>

**1,2-Bis(3,5-dimethylphenyl)ethyne (A5)**

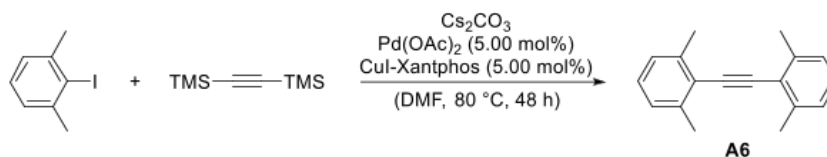
Volatile impurities were removed in *vacuo*. The crude product was sublimed at  $10^{-6}$  mbar and 60 °C to give a white powder. Yield: 790 mg (65%).

TLC: Rf = 0.25 (silica, *n*-pentane) [UV]

<sup>1</sup>H NMR (400 MHz, CDCl<sub>3</sub>) δ (ppm): 7.16 (s, 4H, C-C-CH), 6.96 (s, 2H, CH<sub>3</sub>-C-CH), 2.31 (s, 12H, CH<sub>3</sub>).

<sup>13</sup>C NMR (100 MHz, CDCl<sub>3</sub>) δ (ppm): 138.00 (CH<sub>3</sub>-C-CH), 130.19 (CH<sub>3</sub>-C-CH), 129.42 (C-C-CH), 123.20 (CH-C-C), 89.19 (C-C), 21.27 (CH<sub>3</sub>).

EA: calc. [%] for C<sub>18</sub>H<sub>18</sub>: C, 92.26; H, 7.74; found: C, 92.20; H, 7.68.

**1,2-Bis(2,6-dimethylphenyl)ethyne (A6)**

Volatile impurities were removed in *vacuo*. The crude product was sublimed at  $10^{-2}$  mbar and 155 °C to give a white powder. Yield: 458 mg (38%).

TLC: Rf = 0.22 (silica, *n*-pentane) [UV]

<sup>1</sup>H NMR (400 MHz, DMSO-*d*<sub>6</sub>) δ (ppm): 7.23 - 7.12 (m, 6H, CH), 2.49 (s, 12H, CH<sub>3</sub>).

<sup>13</sup>C NMR (100 MHz, DMSO-*d*<sub>6</sub>) δ (ppm): 139.49 (CH<sub>3</sub>-C-CH), 128.06 (CH-CH-CH), 126.96 (C-CH-CH), 122.69 (CH<sub>3</sub>-C-C), 95.52 (C-C), 21.18 (CH<sub>3</sub>).

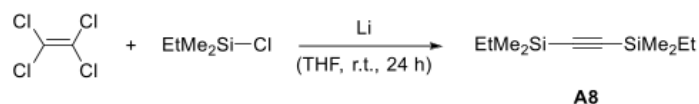
EA: calc. [%] for C<sub>18</sub>H<sub>18</sub>: C, 92.26; H, 7.74; found: C, 91.72; H, 7.74.

**General procedure for symmetrically silyl- or germyl-substituted alkynes (A8-10 and A18) using tetrachloroethylene**

S4

Symmetrical acetylenes **A8-10** and **A18** were prepared according to literature procedures.<sup>[4]</sup> Tetrachloroethylene (1.00 eq.) was added dropwise over a period of 20 minutes to a suspension of finely-cut lithium wire (7.00 eq.) and the respective halogen compound (2.50 eq.) in THF (0.35 M) at room temperature. The resulting mixture was stirred for 24 hours. The reaction was quenched with saturated NaHCO<sub>3</sub> solution, and three times extracted with diethyl ether. The combined organic layers were dried over anhydrous MgSO<sub>4</sub>, filtered and concentrated. Sublimation or distillation gave the corresponding silyl- or germyl-substituted alkynes.

#### 1,2-Bis(ethyldimethylsilyl)ethyne (**A8**)



Distillation at 10<sup>-2</sup> mbar and room temperature gave 1,2-bis(ethyldimethylsilyl)ethyne (**A8**) as a colorless liquid. Yield: 1.72 g (91%).

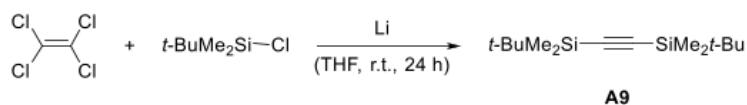
<sup>1</sup>H NMR (500 MHz, C<sub>6</sub>D<sub>6</sub>) δ (ppm): 1.04 (t, 6H, <sup>3</sup>J<sub>HH</sub> = 7.9 Hz, CH<sub>2</sub>-CH<sub>3</sub>), 0.57 (q, 4H, <sup>3</sup>J<sub>HH</sub> = 7.9 Hz, CH<sub>2</sub>-CH<sub>3</sub>), 0.13 (s, 12H, Si-CH<sub>3</sub>).

<sup>13</sup>C NMR (125 MHz, C<sub>6</sub>D<sub>6</sub>) δ (ppm): 113.45 (C-C), 7.94 (CH<sub>2</sub>-CH<sub>3</sub>), 7.24 (CH<sub>2</sub>-CH<sub>3</sub>), -2.48 (Si-CH<sub>3</sub>).

<sup>29</sup>Si NMR (100 MHz, C<sub>6</sub>D<sub>6</sub>) δ (ppm): -15.67.

EA: calc. [%] for C<sub>10</sub>H<sub>22</sub>Si<sub>2</sub>: C, 60.52; H, 11.17; Si, 28.30; found: C, 60.66; H, 11.02; Si, 27.97.

#### 1,2-Bis(*tert*-butyldimethylsilyl)ethyne (**A9**)



Sublimation at 10<sup>-2</sup> mbar and 65 °C gave 1,2-bis(*tert*-butyldimethylsilyl)ethyne (**A9**) as a white solid. Yield: 1.89 g (78%).

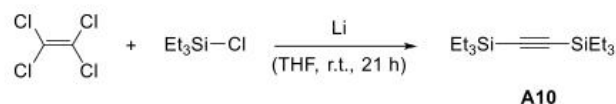
<sup>1</sup>H NMR (500 MHz, C<sub>6</sub>D<sub>6</sub>) δ (ppm): 1.02 (s, 18H, C-CH<sub>3</sub>), 0.11 (s, 12H, Si-CH<sub>3</sub>).

<sup>13</sup>C NMR (125 MHz, C<sub>6</sub>D<sub>6</sub>) δ (ppm): 113.38 (C-C), 26.25 (C-CH<sub>3</sub>), 16.73 (C-CH<sub>3</sub>), -4.49 (Si-CH<sub>3</sub>).

<sup>29</sup>Si NMR (100 MHz, C<sub>6</sub>D<sub>6</sub>) δ (ppm): -9.21.

EA: calc. [%] for C<sub>14</sub>H<sub>30</sub>Si<sub>2</sub>: C, 66.06; H, 11.88; Si, 22.07; found: C, 66.22; H, 12.17; Si, 22.13.

#### 1,2-Bis(triethylsilyl)ethyne (**A10**)



Volatile impurities were removed in *vacuo*. Di distillation at  $10^{-2}$  mbar and  $35\text{ }^\circ\text{C}$  gave 1,2-bis(triethylsilyl)ethyne (**A10**) as a colorless liquid. Yield: 1.58 g (65%).

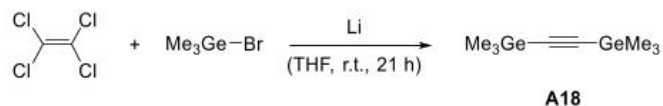
$^1\text{H NMR}$  (500 MHz,  $\text{C}_6\text{D}_6$ )  $\delta$  (ppm): 1.08 (t, 18H,  $^3J_{\text{HH}} = 7.9$  Hz,  $\text{CH}_3$ ), 0.61 (q, 12H,  $^3J_{\text{HH}} = 7.9$  Hz,  $\text{CH}_2$ ).

$^{13}\text{C NMR}$  (125 MHz,  $\text{C}_6\text{D}_6$ )  $\delta$  (ppm): 113.09 (C-C), 7.81 ( $\text{CH}_3$ ), 4.78 ( $\text{CH}_2$ ).

$^{29}\text{Si NMR}$  (100 MHz,  $\text{C}_6\text{D}_6$ )  $\delta$  (ppm): -8.23.

EA: calc. [%] for  $\text{C}_{14}\text{H}_{30}\text{Si}_2$ : C, 66.06; H, 11.88; Si, 22.07; found: C, 62.07; H, 11.62; Si, 22.14.

#### 1,2-Bis(trimethylgermyl)ethyne (**A18**)



Sublimation at  $10^{-2}$  mbar and  $80\text{ }^\circ\text{C}$  gave 1,2-bis(trimethylgermyl)ethyne (**A18**) as a white solid. Yield: 1.52 g (81%).

$^1\text{H NMR}$  (500 MHz,  $\text{CDCl}_3$ )  $\delta$  (ppm): 0.34 (s, 18H,  $\text{CH}_3$ ).

$^{13}\text{C NMR}$  (125 MHz,  $\text{CDCl}_3$ )  $\delta$  (ppm): 112.12 (C-C), 0.16 (Ge- $\text{CH}_3$ ).

EA: calc. [%] for  $\text{C}_8\text{H}_{18}\text{Ge}_2$ : C, 37.03; H, 6.99; Ge, 55.98; found: C, 37.43; H, 7.21.

#### General Procedure for symmetrically silyl- and phosphine-substituted alkynes (**A11**, **A12**, and **A19**) using trichloroethylene

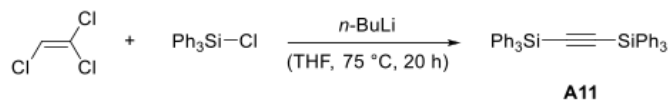
Symmetrical acetylenes **A11-12**, and **A19** were prepared according to literature procedures.<sup>[5-7]</sup> *n*-Butyllithium (2.5 M in hexane, 3.00 eq.) was added to a 1:1 THF/diethyl ether mixture or pure THF (0.30 M) and stirred at  $-78\text{ }^\circ\text{C}$  for ten minutes. A solution of trichloroethylene in diethyl ether or THF (1.00 eq., 0.36 M) was added over a period of 15 minutes. The reaction mixture was allowed to warm up to room temperature and stirred for two hours, whereupon white lithium chloride precipitates. The addition of the respective silyl or phosphine chloride dissolved in diethyl ether or THF (2.05 eq., 0.75 M) occurred fast while cooling the mixture with an ice bath or slowly at room temperature. The resulting reaction solution was refluxed until full conversion of the silyl or phosphine chloride was observed. The reaction progress was monitored by  $^{29}\text{Si}$  or  $^{31}\text{P}$  NMR spectroscopy. Solvents were removed under reduced pressure. The resulting residue was quenched with aqueous  $\text{NaHCO}_3$  solution, and three times

S6



extracted with diethyl ether. The organic layers were dried over anhydrous  $\text{MgSO}_4$ , filtered and concentrated. Subsequent sublimation or distillation gave the corresponding silyl- or phosphine-substituted alkynes.

### 1,2-Bis(triphenylsilyl)ethyne (A11)



The white solid obtained from the extraction was dried under reduced pressure to give bis(triphenylsilyl)ethyne (**A11**) as a white solid. Yield: 1.45 g (62%).

**TLC:**  $R_f = 0.52$  (silica, *n*-pentane/EtOAc 95:5) [UV]

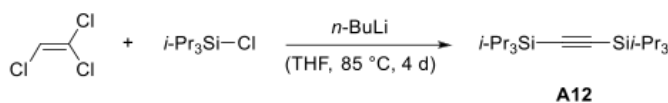
**$^1\text{H}$  NMR** (500 MHz,  $\text{DMSO}-d_6$ )  $\delta$  (ppm): 6.64 - 6.43 (m, 30H, CH).

**$^{13}\text{C}$  NMR** (125 MHz,  $\text{DMSO}-d_6$ )  $\delta$  (ppm): 135.39 (C-CH), 132.47 (C-CH), 131.05 ((CH)<sub>2</sub>-CH-(CH)<sub>2</sub>), 128.95 (CH-CH-C), 114.53 (C-C).

**$^{29}\text{Si}$  NMR** (100 MHz,  $\text{DMSO}-d_6$ )  $\delta$  (ppm): -29.99.

**EA:** calc. [%] for  $\text{C}_{38}\text{H}_{30}\text{Si}_2$ : C, 84.08; H, 5.57; Si, 10.35; found: C, 82.86; H, 5.51; Si, 9.85.

### 1,2-Bis(tri-*iso*-propylsilyl)ethyne (A12)



Volatile impurities were removed in *vacuo*. Double distillation at  $10^{-6}$  mbar and  $65^\circ\text{C}$  gave 1,2-bis(tri-*iso*-propylsilyl)ethyne (**A12**) as a colorless liquid. Yield: 1.60 g (54%).

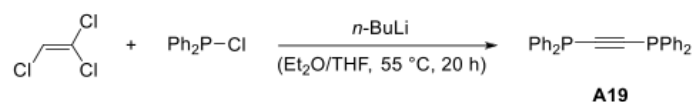
**$^1\text{H}$  NMR** (500 MHz,  $\text{C}_6\text{D}_6$ )  $\delta$  (ppm): 1.17 (d, 36H,  $^3J_{\text{HH}} = 7.2$  Hz,  $\text{CH}_3$ ), 1.10 - 1.02 (m, 6H, CH).

**$^{13}\text{C}$  NMR** (125 MHz,  $\text{C}_6\text{D}_6$ )  $\delta$  (ppm): 112.51 (C-C), 18.89 ( $\text{CH}_3$ ), 11.52 (CH).

**$^{29}\text{Si}$  NMR** (100 MHz,  $\text{C}_6\text{D}_6$ )  $\delta$  (ppm): -2.71.

**EA:** calc. [%] for  $\text{C}_{20}\text{H}_{42}\text{Si}_2$ : C, 70.92; H, 12.50; Si, 16.58; found: C, 71.01; H, 12.50; Si, 16.16.

### 1,2-Bis(diphenylphosphaneyl)ethyne (A19)



A white solid crystallized from the pentane filtrate, which was separated and dried under reduced pressure to give 1,2-bis(diphenylphosphaneyl)ethyne (**A19**). Yield: 1.56 g (55%).

**TLC:** Rf = 0.83 (silica, *n*-pentane/EtOAc 9:1) [UV]

**<sup>1</sup>H NMR** (400 MHz, DMSO-*d*<sub>6</sub>) δ (ppm): 7.60 (td, 8H, <sup>3</sup>J<sub>HH</sub> = 6.8 Hz, 6.3 Hz, <sup>3</sup>J<sub>HP</sub> = 3.6 Hz, P-C-CH), 7.46 - 7.39 (m, 12H, CH-(CH)<sub>3</sub>-CH).

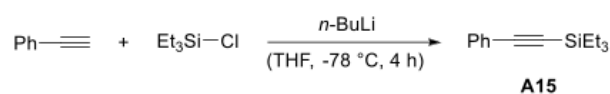
**<sup>13</sup>C NMR** (100 MHz, DMSO-*d*<sub>6</sub>) δ (ppm): 134.70 (d, <sup>1</sup>J<sub>CP</sub> = 4.0 Hz, P-C-CH), 132.20 (d, <sup>2</sup>J<sub>CP</sub> = 21.6 Hz, P-C-CH), 129.65 ((CH)<sub>2</sub>-CH-(CH)<sub>2</sub>), 129.17 - 128.97 (m, P-C-CH-CH), 106.87 (C-C).

**<sup>31</sup>P NMR** (162 MHz, DMSO-*d*<sub>6</sub>) δ (ppm): -33.80.

**EA:** calc. [%] for C<sub>26</sub>H<sub>20</sub>P<sub>2</sub>: C, 79.18; H, 5.11; P, 15.71; found: C, 79.30; H, 5.09; P, 15.51.

**General procedure for silyl- and phosphine-substituted phenylacetylenes (A15-17 and A20)**

Phenylacetylene (1.00 eq.) and THF (0.50 M) were placed in a round-bottom flask, cooled to  $-78\text{ }^{\circ}\text{C}$  and stirred for ten minutes. *n*-Butyllithium (1.6 M in hexane, 1.05 eq.) was added dropwise and the solution was stirred for 30 minutes. The respective silyl or phosphine chloride (1.05 eq.) was added at  $-78\text{ }^{\circ}\text{C}$  over a period of ten minutes and the reaction mixture was allowed to warm up to room temperature and stirred for four hours. The reaction was quenched with saturated  $\text{NaHCO}_3$  solution, and three times extracted with diethyl ether. The combined organic layers were dried over anhydrous  $\text{MgSO}_4$ , filtered and concentrated. Subsequent distillation or purification by flash column chromatography gave the corresponding silyl- or phosphine-substituted phenylacetylenes (**A15-17** and **A20**).

**Triethyl(phenylethynyl)silane (A15)**

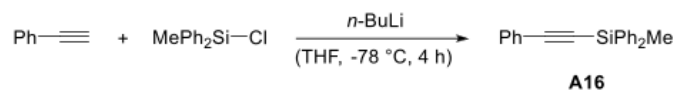
Volatile impurities were removed in *vacuo*. Sublimation at  $10^{-2}$  mbar and  $75\text{ }^{\circ}\text{C}$  gave triethyl(phenylethynyl)silane (**A15**) as a colorless liquid. Yield: 2.35 g (93%).

**$^1\text{H}$  NMR** (500 MHz,  $\text{C}_6\text{D}_{12}$ )  $\delta$  (ppm): 7.38 - 7.33 (m, 2H, C-CH), 7.18 - 7.12 (m, 3H, CH-CH-CH), 1.06 (t, 9H,  $^3J_{\text{HH}} = 7.9\text{ Hz}$ ,  $\text{CH}_3$ ), 0.66 (q, 6H,  $^3J_{\text{HH}} = 7.9\text{ Hz}$ ,  $\text{CH}_2$ ).

**$^{13}\text{C}$  NMR** (125 MHz,  $\text{C}_6\text{D}_{12}$ )  $\delta$  (ppm): 132.64 (C-CH), 128.45 (CH-CH-CH), 128.34 (CH-CH-CH), 124.75 (C-CH), 107.30 (Si-C-C), 91.13 (Si-C-C), 7.83 ( $\text{CH}_3$ ), 5.24 ( $\text{CH}_2$ ).

**$^{29}\text{Si}$  NMR** (100 MHz,  $\text{C}_6\text{D}_{12}$ )  $\delta$  (ppm):  $-7.47$ .

EA: calc. [%] for  $\text{C}_{14}\text{H}_{20}\text{Si}$ : C, 77.71; H, 9.32; found: C, 77.08; H, 9.17.

**Methyldiphenyl(phenylethynyl)silane (A16)**

Distillation at  $10^{-2}$  mbar and  $120\text{ }^{\circ}\text{C}$  resulted in a colorless liquid, which was purified *via* flash column chromatography (silica, eluent: *n*-pentane  $\rightarrow$  *n*-pentane/EtOAc 98:2  $\rightarrow$  *n*-pentane/EtOAc 95:5). Methyldiphenyl(phenylethynyl)silane (**A16**) was obtained as a colorless liquid. Yield: 2.47 g (94%).

TLC: Rf = 0.52 (silica, *n*-pentane/EtOAc 95:5) [UV]

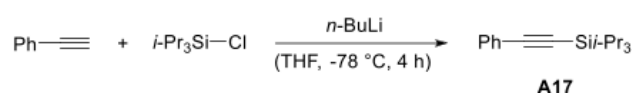
**<sup>1</sup>H NMR** (500 MHz, C<sub>6</sub>D<sub>6</sub>)  $\delta$  (ppm): 7.83 - 7.79 (m, 4H, Si-C-CH), 7.43 (dd, 2H, <sup>3</sup>J<sub>HH</sub> = 8.1 Hz, <sup>4</sup>J<sub>HH</sub> = 1.6 Hz, C-C-CH), 7.22 - 7.18 (m, 6H, Si-C-CH-(CH)<sub>3</sub>), 6.94 - 6.87 (m, 3H, C-C-CH-(CH)<sub>3</sub>), 0.74 (s, 3H, CH<sub>3</sub>).

**<sup>13</sup>C NMR** (125 MHz, C<sub>6</sub>D<sub>6</sub>)  $\delta$  (ppm): 135.71 (Si-C-CH), 135.08 (Si-C-CH), 132.49 (C-C-CH), 130.04 (Si-C-(CH)<sub>2</sub>-CH), 129.04 (C-C-(CH)<sub>2</sub>-CH), 128.54 (C-C-CH-CH), 128.38 (Si-C-CH-CH), 123.32 (C-C-CH), 109.03 (Si-C-C), 91.11 (Si-C-C), -1.74 (CH<sub>3</sub>).

**<sup>29</sup>Si NMR** (100 MHz, C<sub>6</sub>D<sub>6</sub>)  $\delta$  (ppm): -25.48.

EA: calc. [%] for C<sub>21</sub>H<sub>18</sub>Si: C, 84.51; H, 6.08; found: C, 84.16; H, 6.01.

#### Tri-*iso*-propyl(phenylethynyl)silane (A17)



Volatile impurities were removed in *vacuo*. Sublimation at 10<sup>-2</sup> mbar and 120 °C gave tri-*iso*-propyl(phenylethynyl)silane (**A17**) as a colorless liquid. Yield: 2.03 g (80%).

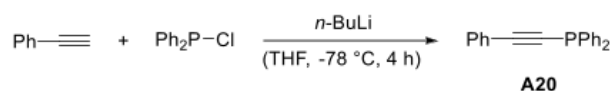
**<sup>1</sup>H NMR** (500 MHz, C<sub>6</sub>D<sub>12</sub>)  $\delta$  (ppm): 7.39 - 7.36 (m, 2H, C-CH), 7.17 - 7.14 (m, 3H, CH-(CH)<sub>3</sub>-CH), 1.15 - 1.14 (m, 18H, CH<sub>3</sub>), 1.14 - 1.12 (m, 3H, Si-CH).

**<sup>13</sup>C NMR** (125 MHz, C<sub>6</sub>D<sub>12</sub>)  $\delta$  (ppm): 132.65 (C-CH), 128.46 (CH-CH-CH), 128.37 (CH-CH-CH), 124.77 (C-CH), 108.24 (Si-C-C), 90.16 (Si-C-C), 19.06 (CH<sub>3</sub>), 12.23 (Si-CH).

**<sup>29</sup>Si NMR** (100 MHz, C<sub>6</sub>D<sub>12</sub>)  $\delta$  (ppm): -2.15.

EA: calc. [%] for C<sub>17</sub>H<sub>26</sub>Si: C, 79.00; H, 10.14; found: C, 77.51; H, 10.09.

#### Diphenyl(phenylethynyl)phosphane (A20)



Distillation at 10<sup>-5</sup> mbar and 170 °C gave diphenyl(phenylethynyl)phosphane (**A20**) as a white solid. Yield: 2.23 g (80%).

**<sup>1</sup>H NMR** (400 MHz, DMSO-*d*<sub>6</sub>)  $\delta$  (ppm): 7.66 (td, 4H, <sup>3</sup>J<sub>HP</sub> = 8.2 Hz, <sup>4</sup>J<sub>HP</sub> = 1.7 Hz, P-C-CH), 7.61 (dd, 2H, <sup>3</sup>J<sub>HP</sub> = 7.7 Hz, <sup>4</sup>J<sub>HP</sub> = 1.8 Hz, C-C-CH), 7.49 - 7.38 (m, 9H, CH-(CH)<sub>3</sub>-CH).

**<sup>13</sup>C NMR** (100 MHz, DMSO-*d*<sub>6</sub>)  $\delta$  (ppm): 135.44 (d, <sup>1</sup>J<sub>CP</sub> = 6.7 Hz, P-C-CH), 132.14 (d, <sup>2</sup>J<sub>CP</sub> = 20.7 Hz, P-C-CH), 131.71 (d, <sup>4</sup>J<sub>CP</sub> = 1.7 Hz, C-C-CH), 129.62 (C-C-(CH)<sub>2</sub>-CH), 129.44 (C-C-

S10

CH-CH), 129.00 (d,  $^3J_{CP} = 7.7$  Hz, P-C-CH-CH), 128.86 (P-C-(CH)<sub>2</sub>-CH), 121.58 (d,  $^3J_{CP} = 1.1$  Hz, C-C-CH), 107.92 (d,  $^2J_{CP} = 3.9$  Hz, P-C-C), 85.27 (d,  $^1J_{CP} = 6.9$  Hz, P-C-C).

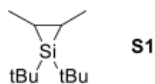
$^{31}\text{P}$  NMR (162 MHz, DMSO-*d*<sub>6</sub>)  $\delta$  (ppm): -35.06.

EA: calc. [%] for C<sub>20</sub>H<sub>15</sub>P: C, 83.90; H, 5.28; found: C, 83.54; H, 5.29.

## 2. Synthesis of Monofunctional Silirenes

### 1,1-Di-*tert*-butyl-2,3-dimethylsilirane (S1)

Precursors of silirane **S1** *t*Bu<sub>2</sub>SiHCl, *t*Bu<sub>2</sub>SiH<sub>2</sub> and *t*Bu<sub>2</sub>SiBr<sub>2</sub> were synthesized according to literature.<sup>[8-10]</sup> *t*Bu<sub>2</sub>SiBr<sub>2</sub> was additionally purified by crystallisation from dry MeCN at -30 °C to give *t*Bu<sub>2</sub>SiBr<sub>2</sub> as a colorless solid. Silirane *trans*-1,1-di-*tert*-butyl-2,3-dimethyl-silirane was synthesized via modified procedures described in literature.<sup>[11,12]</sup>



A 500 mL high-pressure Schlenk-tube with a PTFE sealed screw cap was equipped with a PTFE-coated stir bar and was loaded with 30.0 g (0.99 mol, 1.00 eq.) of *t*Bu<sub>2</sub>SiBr<sub>2</sub>, 100 mg (0.45 mmol) 3,5-Di-*tert*-butyl-4-hydroxytoluene (BHT) and 17.5 g (0.19 mmol, 2 eq.) tetrahydrofuran. The reaction tube was cooled down to -78 °C with a dry ice/isopropanol mixture. Present argon atmosphere was removed *in vacuo* and 111.4 g (1.90 mol, 20.0 eq.) *trans*-2-butene was condensed into the cooled reaction mixture by pressurizing it with 1.80 bar of the respective gas. After re-pressurizing with argon, 5.51 g (2.5 % Na, 0.79 mol, 8.0 eq.) Li/Na alloy chunks were added to the reaction mixture, followed by vigorous stirring at room temperature for 16 h. After full conversion ( $^{29}\text{Si}$ -NMR verification) *cis*-2-butene gas was released and remaining solvent was removed under vacuum. The crude slurry was extracted 5 times with each 50 mL *n*-pentane to precipitate and separate the generated LiBr by filtration. After filtration (syringe-filter) *n*-pentane was removed again and the remaining oil purified by bulb-to-bulb distillation (40 °C, 10<sup>-2</sup> mbar, N<sub>2</sub> cooled trap). 14.4 g (72.6 mmol, 73 %) *trans*-1,1-di-*tert*-butyl-2,3-dimethylsilirane (**S1**) is received as a colourless clear oil.

$^1\text{H}$ -NMR: (300 K, 500 MHz, C<sub>6</sub>D<sub>6</sub>)  $\delta$  = 1.40–1.41 (m, 6H, -CH-*Me*), 1.17 (s, 9H, *t*Bu), 1.10–1.04 (m, 2H, -Si-CH-) 1.06 (s, 9H, *t*Bu).

$^{13}\text{C}$ -NMR: (300 K, 125 MHz, C<sub>6</sub>D<sub>6</sub>)  $\delta$  = 10.0 (Si-CH-), 10.3 (Si-CH-), 18.6 (-CH-*Me*), 20.9 (-CH-*Me*), 30.0 (*t*Bu-Me), 31.6 (*t*Bu-Me).

$^{29}\text{Si}$ -NMR: (300 K, 100 MHz, C<sub>6</sub>D<sub>6</sub>)  $\delta$  = -53.2.

CI-MS: 197.3 [M-H]<sup>+</sup>.

The analytical data obtained matched those reported in the literature.<sup>[12]</sup>

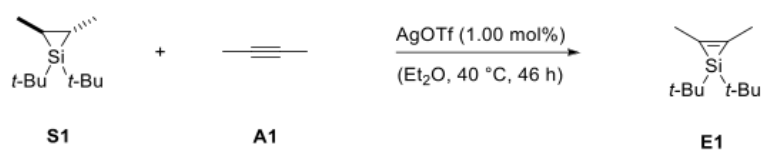
### General Procedure for Silirene E1-E20

All silirenes synthesized in this work are produced via a silylene-transfer-reaction. This reaction was performed either in a thermal initiated reaction or by utilization of a silver catalyst (AgOTf) according to literature known procedures.<sup>[13-15]</sup> Most silirenes were accessible via both reaction procedures. Classification which reaction procedure to employ was determined by higher product yield and/or purity.

**Silver-catalysed synthesis:** 1,1-Di-*tert*-butyl-2,3-dimethylsilirane (**S1**) (1.00 eq.) and the respective alkyne (1.10 eq.) were dissolved in diethyl ether (0.10 M) and stirred for five minutes to ensure . AgOTf (1.00 mol%) was added and the reaction mixture was stirred at 35 °C or 40 °C until full conversion of 1,1-di-*tert*-butyl-2,3-dimethylsilirane (**S1**). The reaction progress was monitored by <sup>29</sup>Si and <sup>1</sup>H NMR spectroscopy. The solvent was removed under reduced pressure. Subsequent distillation, sublimation or crystallization gave the corresponding silirenes.

**Thermal controlled synthesis:** 1,1-Di-*tert*-butyl-2,3-dimethylsilirane (**S1**) (1.00 eq.) and the respective alkyne (1.10 eq.) were dissolved in toluene (0.10 M) and stirred for five minutes. The reaction mixture was stirred at 135 °C until full conversion of 1,1-di-*tert*-butyl-2,3-dimethylsilirane (**S1**). The reaction progress was monitored by <sup>29</sup>Si and <sup>1</sup>H NMR spectroscopy. The solvent was removed under reduced pressure. Subsequent distillation or sublimation gave the corresponding silirenes.

#### 1,1-Di-*tert*-butyl-2,3-dimethyl-silirene (**E1**)



Volatile impurities were removed in *vacuo*. Sublimation at 10<sup>-2</sup> mbar and 125 °C gave 1,1-Di-*tert*-butyl-2,3-dimethyl-silirene (**E1**) as a colorless solid. Yield: 62 mg (78%).

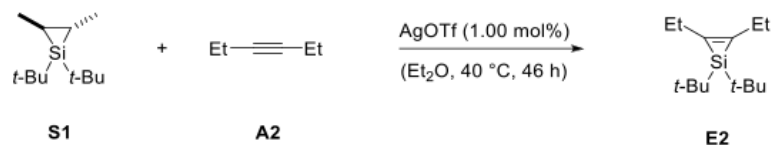
<sup>1</sup>H NMR (500 MHz, C<sub>6</sub>D<sub>12</sub>) δ (ppm): 2.06 (s, 6H, C-Me), 1.08 (s, 18H, SiC-(CH)<sub>3</sub>).

<sup>29</sup>Si NMR (100 MHz, C<sub>6</sub>D<sub>12</sub>) δ (ppm): -67.53.

UV-Vis (*n*-hexane) λ<sub>max</sub>/nm (ε): 212 (37700), 246 (1280).

LIFDI-MS: *m/z* = calc. for [C<sub>12</sub>H<sub>24</sub>Si]<sup>+</sup>: 196.1647 ([M]<sup>+</sup>); found 196.1670.

EA: calc. [%] for C<sub>12</sub>H<sub>24</sub>Si: C, 73.38; H, 12.32; Si, 14.3; found: C, 73.83; H, 12.01.

**1,1-Di-*tert*-butyl-2,3-diethyl-silirene (E2)**

Volatile impurities were removed in *vacuo*. Sublimation at  $10^{-2}$  mbar and  $140^\circ\text{C}$  gave 1,1-Di-*tert*-butyl-2,3-diethyl-silirene (**E2**) as a colorless solid. Yield: 100 mg (72%).

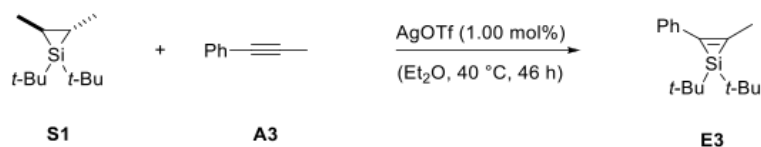
$^1\text{H NMR}$  (500 MHz,  $\text{C}_6\text{D}_{12}$ )  $\delta$  (ppm): 2.46-2.43 (m, 4H, C- $\text{CH}_2\text{-CH}_3$ ), 1.18-1.10 (m, 6H,  $\text{CCH}_2\text{-CH}_3$ ), 1.10 (s, 18H, C- $\text{CH}_3$ )<sub>3</sub>.

$^{29}\text{Si NMR}$  (100 MHz,  $\text{C}_6\text{D}_{12}$ )  $\delta$  (ppm): -66.57.

UV-Vis (*n*-hexane)  $\lambda_{\text{max}}/\text{nm}$  ( $\epsilon$ ): 225 (26200).

LIFDI-MS:  $m/z = \text{calc. for } [\text{C}_{12}\text{H}_{24}\text{Si}]^+$ : 224.1960 ( $[\text{M}]^+$ ); found 224.1938.

EA: calc. [%] for  $\text{C}_{14}\text{H}_{28}\text{Si}$ : C, 74.91; H, 12.57; Si, 12.51; found: C, 74.88; H, 12.96.

**1,1-Di-*tert*-butyl-2methyl-3-phenyl-silirene (E3)**

Volatile impurities were removed in *vacuo*. Sublimation at  $10^{-2}$  mbar and  $145^\circ\text{C}$  gave 1,1-Di-*tert*-butyl-2-methyl-3-phenyl-silirene (**E3**) as a colorless solid. Yield: 160 mg (82%).

$^1\text{H NMR}$  (500 MHz,  $\text{C}_6\text{D}_{12}$ )  $\delta$  (ppm): 7.55-7.53 (m, 2H,  $\text{CH}_{\text{arm,o}}$ ), 7.27-7.23 (m, 2H,  $\text{CH}_{\text{arm,m}}$ ), 7.11-7.08 (m, 1H,  $\text{CH}_{\text{arm,p}}$ ), 2.34 (s, 3H, SiC- $\text{CH}_3$ ), 1.12 (s, 18H, C- $\text{CH}_3$ )<sub>3</sub>.

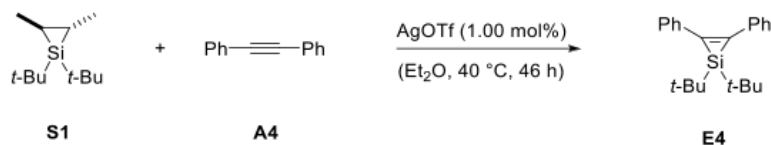
$^{13}\text{C NMR}$  (125 MHz,  $\text{C}_6\text{D}_{12}$ )  $\delta$  (ppm): 150.97 (Si-C-Ph), 149.96 (Si-C- $\text{CH}_3$ ), 136.15 (SiC- $\text{C}_{\text{arm}}$ ), 129.94 ( $\text{C}_{\text{arm,m}}$ ), 128.82 ( $\text{C}_{\text{arm,o}}$ ), 127.25 ( $\text{C}_{\text{arm,p}}$ ), 30.31 (SiC- $\text{C}(\text{CH}_3)_3$ ), 21.71 (Si-C- $\text{C}(\text{CH}_3)_3$ ), 15.81 (SiC- $\text{CH}_3$ ).

$^{29}\text{Si NMR}$  (100 MHz,  $\text{C}_6\text{D}_{12}$ )  $\delta$  (ppm): -68.35.

UV-Vis (*n*-hexane)  $\lambda_{\text{max}}/\text{nm}$  ( $\epsilon$ ): 260 (29740).

LIFDI-MS:  $m/z = \text{calc. for } [\text{C}_{17}\text{H}_{26}\text{Si}]^+$ : 258.1804 ( $[\text{M}]^+$ ); found 258.1812.

EA: calc. [%] for  $\text{C}_{17}\text{H}_{26}\text{Si}$ : C, 79.00; H, 10.14; Si, 10.87; found: C, 78.95; H, 10.38.

**1,1-Di-*tert*-butyl-2,3-diphenyl-silirene (E4)**

Volatile impurities were removed in *vacuo*. Sublimation at  $10^{-2}$  mbar and 160 °C gave 1,1-Di-*tert*-butyl-2,3-diphenyl-silirene (**E4**) as a colorless solid. Yield: 126 mg (84%).

**$^1\text{H}$  NMR** (500 MHz,  $\text{C}_6\text{D}_{12}$ )  $\delta$  (ppm): 7.65-7.62 (m, 4H,  $\text{CH}_{\text{arm,o}}$ ), 7.20-7.17 (m, 4H,  $\text{CH}_{\text{arm,m}}$ ), 7.10-7.02 (m, 2H,  $\text{CH}_{\text{arm,p}}$ ), 1.16 (s, 18H,  $\text{C-CH}_3$ )<sub>3</sub>.

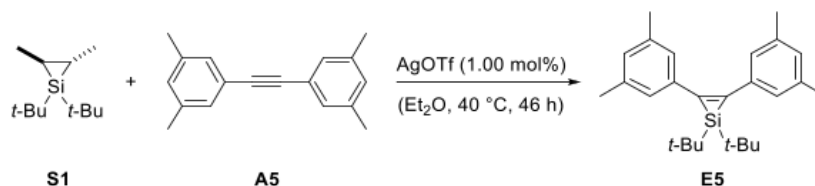
**$^{13}\text{C}$  NMR** (125 MHz,  $\text{C}_6\text{D}_{12}$ )  $\delta$  (ppm): 151.48 (C-C), 136.27 (CH-C-CH<sub>3</sub>), 136.78 (C-C-CH), 129.42 ((CH<sub>3</sub>-C)<sub>2</sub>-CH), 127.51 (C-C-CH), 30.73 (Si-C-CH<sub>3</sub>), 22.38 (Si-C-CH<sub>3</sub>), 21.53 (CH-C-CH<sub>3</sub>).

**$^{29}\text{Si}$  NMR** (100 MHz,  $\text{C}_6\text{D}_{12}$ )  $\delta$  (ppm): -67.14.

**UV-Vis** (*n*-hexane)  $\lambda_{\text{max}}$ /nm ( $\epsilon$ ): 290 (18620).

**LIFDI-MS**:  $m/z$  = calc. for  $[\text{C}_{22}\text{H}_{28}\text{Si}]^+$ : 320.1960 ( $[\text{M}]^+$ ); found 320.19.

**EA**: calc. [%] for  $\text{C}_{22}\text{H}_{28}\text{Si}$ : C, 82.43; H, 8.80; Si, 8.76; found: C, 81.88; H, 9.50.

**1,1-Di-*tert*-butyl-2,3-bis(3,5-dimethylphenyl)-silirene (E5)**

The silirene **E5** precipitates from the reaction solution. Filtration and drying under reduced pressure gave 1,1-di-*tert*-butyl-2,3-bis(3,5-dimethylphenyl)-silirene (**E5**) as a white solid. Yield: 76.2 mg (45%).

**$^1\text{H}$  NMR** (500 MHz,  $\text{C}_6\text{D}_{12}$ )  $\delta$  (ppm): 7.14 (s, 4H, C-C-CH), 6.78 (s, 2H, (CH<sub>3</sub>-C)<sub>2</sub>-CH), 2.25 (s, 12H, CH-C-CH<sub>3</sub>), 1.17 (s, 18H, Si-C-CH<sub>3</sub>).

**$^{13}\text{C}$  NMR** (125 MHz,  $\text{C}_6\text{D}_{12}$ )  $\delta$  (ppm): 151.51 (C-C), 137.71 (CH-C-CH<sub>3</sub>), 136.78 (C-C-CH), 129.42 ((CH<sub>3</sub>-C)<sub>2</sub>-CH), 127.51 (C-C-CH), 30.73 (Si-C-CH<sub>3</sub>), 22.38 (Si-C-CH<sub>3</sub>), 21.53 (CH-C-CH<sub>3</sub>).

**$^{29}\text{Si}$  NMR** (100 MHz,  $\text{C}_6\text{D}_{12}$ )  $\delta$  (ppm): -63.38.

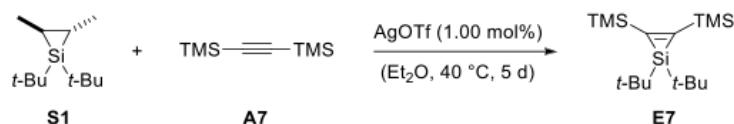
**UV-Vis** (*n*-hexane)  $\lambda_{\text{max}}$ /nm ( $\epsilon$ ): 210 (36600), 234 (29900), 274 (12400), 296 (11600).

**LIFDI-MS**:  $m/z$  = calc. for  $[\text{C}_{26}\text{H}_{36}\text{Si}]^+$ : 376.2586 ( $[\text{M}]^+$ ); found 376.2589.



EA: calc. [%] for C<sub>26</sub>H<sub>36</sub>Si: C, 82.91; H, 9.63; Si, 7.46; found: C, 81.49; H, 9.41; Si, 7.20.

#### 1,1-Di-*tert*-butyl-2,3-bis(trimethylsilyl)-silirene (E7)



Sublimation at 10<sup>-6</sup> mbar and 80 °C gave 1,1-di-*tert*-butyl-2,3-bis(trimethylsilyl)-silirene (**E7**) as a colorless solid. Yield: 293 mg (75%).

<sup>1</sup>H NMR (500 MHz, C<sub>6</sub>D<sub>6</sub>) δ (ppm): 1.03 (s, 18H, SiC-CH<sub>3</sub>), 0.27 (s, 18H, CSi-(CH<sub>3</sub>)<sub>3</sub>).

<sup>13</sup>C NMR (125 MHz, C<sub>6</sub>D<sub>6</sub>) δ (ppm): 184.83 (Si-C-Si), 31.10 (SiC-CH<sub>3</sub>), 20.43 (Si-C-CH<sub>3</sub>), 0.28 (CSi-(CH<sub>3</sub>)<sub>3</sub>).

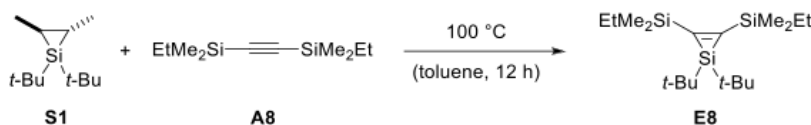
<sup>29</sup>Si NMR (100 MHz, C<sub>6</sub>D<sub>6</sub>) δ (ppm): -13.14 (Si-(CH)<sub>3</sub>), -86.47 (Si-*t*Bu<sub>2</sub>).

UV-Vis (*n*-hexane) λ<sub>max</sub>/nm (ε): 225 (19400), 348 (456).

LIFDI-MS: *m/z* = calc. for [C<sub>16</sub>H<sub>36</sub>Si<sub>3</sub>]<sup>+</sup>: 312.2125 ([M]<sup>+</sup>); found 312.2120.

EA: calc. [%] for C<sub>16</sub>H<sub>36</sub>Si<sub>3</sub>: C, 61.45; H, 11.60; Si, 26.49; found: C, 61.02; H, 12.07; Si, 26.10.

#### 1,1-Di-*tert*-butyl-2,3-bis(ethyl-dimethylsilyl)-silirene (E8)



Volatile impurities were removed in *vacuo*. Sublimation at 10<sup>-6</sup> mbar and 120 °C gave 1,1-di-*tert*-butyl-2,3-bis(ethyl-dimethylsilyl)-silirene (**E8**) as a colorless solid. Yield: 105 mg (58%).

<sup>1</sup>H NMR (500 MHz, C<sub>6</sub>D<sub>12</sub>) δ (ppm): 1.02 (t, 6H, <sup>3</sup>J<sub>HH</sub> = 7.9 Hz, CH<sub>2</sub>-CH<sub>3</sub>), 0.98 (s, 18H, C-CH<sub>3</sub>), 0.69 (qd, 4H, <sup>3</sup>J<sub>HH</sub> = 7.9 Hz, <sup>4</sup>J<sub>HH</sub> = 0.6 Hz, CH<sub>2</sub>-CH<sub>3</sub>), 0.16 (s, 12H, Si-CH<sub>3</sub>).

<sup>13</sup>C NMR (125 MHz, C<sub>6</sub>D<sub>12</sub>) δ (ppm): 185.10 (Si-C-C-Si), 31.32 (C-CH<sub>3</sub>), 20.88 (C-CH<sub>3</sub>), 9.06 (CH<sub>2</sub>-CH<sub>3</sub>), 8.04 (CH<sub>2</sub>-CH<sub>3</sub>), -1.95 (Si-CH<sub>3</sub>).

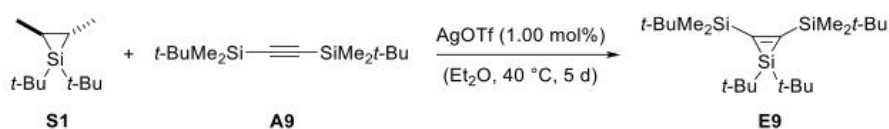
<sup>29</sup>Si NMR (100 MHz, C<sub>6</sub>D<sub>12</sub>) δ (ppm): -10.34 (Si-Me<sub>2</sub>Et), -87.57 (Si-*t*Bu).

UV-Vis (*n*-hexane) λ<sub>max</sub>/nm (ε): 213 (15900), 280 (919), 324 (443).

LIFDI-MS: *m/z* = calc. for [C<sub>18</sub>H<sub>40</sub>Si<sub>3</sub>]<sup>+</sup>: 340.2438 ([M]<sup>+</sup>); found 340.2428.

EA: calc. [%] for  $C_{18}H_{40}Si_3$ : C, 63.44; H, 11.83; Si, 24.72; found: C, 63.46; H, 11.51; Si, 24.28.

**1,1-Di-*tert*-butyl-2,3-bis(*tert*-butyldimethylsilyl)-silirene (E9)**



Sublimation at  $10^{-6}$  mbar and  $120^\circ\text{C}$  gave 1,1-di-*tert*-butyl-2,3-bis(*tert*-butyldimethylsilyl)-silirene (**E9**) as a white solid. Yield: 125 mg (60%).

$^1\text{H NMR}$  (500 MHz,  $C_6D_{12}$ )  $\delta$  (ppm): 1.04 (s, 18H,  $SiMe_2-C-CH_3$ ), 1.03 (s, 18H,  $Si-C-CH_3$ ), 0.16 (s, 12H,  $Si-CH_3$ ).

$^{13}\text{C NMR}$  (125 MHz,  $C_6D_{12}$ )  $\delta$  (ppm): 186.26 ( $Si-C-C-Si$ ), 31.49 ( $Si-C-CH_3$ ), 27.48 ( $SiMe_2-C-CH_3$ ), 21.39 ( $Si-C-CH_3$ ), 17.65 ( $SiMe_2-C-CH_3$ ), -3.44 ( $Si-CH_3$ ).

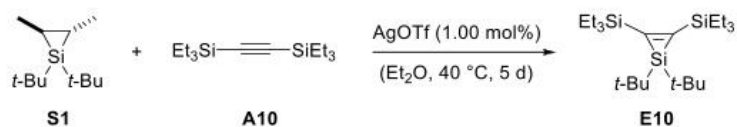
$^{29}\text{Si NMR}$  (100 MHz,  $C_6D_{12}$ )  $\delta$  (ppm): -5.41 ( $Si-Me_2t-Bu$ ), -90.23 ( $Si-t-Bu$ ).

UV-Vis (*n*-hexane)  $\lambda_{\text{max}}/nm$  ( $\epsilon$ ): 223 (17900), 281 (1080), 327 (623).

LIFDI-MS:  $m/z$  = calc. for  $[C_{22}H_{48}Si_3]^+$ : 396.3064 ( $[M]^+$ ); found 396.3061.

EA: calc. [%] for  $C_{22}H_{48}Si_3$ : C, 66.58; H, 12.19; Si, 21.23; found: C, 66.53; H, 12.45; Si, 20.72.

**1,1-Di-*tert*-butyl-2,3-bis(triethylsilyl)-silirene (E10)**



Sublimation at  $10^{-6}$  mbar and  $120^\circ\text{C}$  gave 1,1-di-*tert*-butyl-2,3-bis(triethylsilyl)-silirene (**E10**) as a colorless solid. Yield: 112 mg (53%).

$^1\text{H NMR}$  (500 MHz,  $C_6D_6$ )  $\delta$  (ppm): 1.10 (t, 18H,  $^3J_{\text{HH}} = 7.9$  Hz,  $CH_2-CH_3$ ), 1.08 (s, 18H,  $C-CH_3$ ), 0.82 (qd, 12H,  $^3J_{\text{HH}} = 7.9$  Hz,  $^4J_{\text{HH}} = 0.7$  Hz,  $CH_2-CH_3$ ).

$^{13}\text{C NMR}$  (125 MHz,  $C_6D_6$ )  $\delta$  (ppm): 183.88 ( $Si-C-C-Si$ ), 31.15 ( $C-CH_3$ ), 20.62 ( $C-CH_3$ ), 8.13 ( $CH_2-CH_3$ ), 5.10 ( $CH_2-CH_3$ ).

$^{29}\text{Si NMR}$  (100 MHz,  $C_6D_6$ )  $\delta$  (ppm): -6.34 ( $Si-Et_3$ ), -90.04 ( $Si-t-Bu$ ).

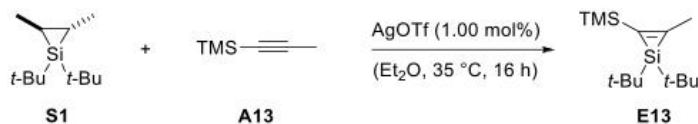
UV-Vis (*n*-hexane)  $\lambda_{\text{max}}/nm$  ( $\epsilon$ ): 215 (17700), 282 (652), 328 (350).

LIFDI-MS:  $m/z$  = calc. for  $[C_{22}H_{48}Si_3]^+$ : 396.3064 ( $[M]^+$ ); found 396.3063.

S16

EA: calc. [%] for  $C_{22}H_{48}Si_3$ : C, 66.58; H, 12.19; Si, 21.23; found: C, 66.82; H, 12.31; Si, 20.63.

**1,1-Di-*tert*-butyl-2-methyl-3-(trimethylsilyl)-silirene (E13)**



Sublimation at  $10^{-6}$  mbar and  $100^\circ\text{C}$  gave 1,1-di-*tert*-butyl-2-methyl-3-(trimethylsilyl)-silirene (**E13**) as a colorless solid. Yield: 104 mg (65%).

$^1\text{H NMR}$  (500 MHz,  $C_6D_{12}$ )  $\delta$  (ppm): 2.33 (s, 3H, SiC-CH<sub>3</sub>), 1.06 (s, 18H, SiC-(CH<sub>3</sub>)<sub>3</sub>), 0.27 (SiCSi-(CH<sub>3</sub>)<sub>3</sub>)

$^{13}\text{C NMR}$  (125 MHz,  $C_6D_{12}$ )  $\delta$  (ppm): 173.85 (Si-C-Me), 154.50 (Si-C-Si), 30.55 (SiC-(CH<sub>3</sub>)<sub>3</sub>), 21.07 (Si-C-(CH<sub>3</sub>)<sub>3</sub>), 20.07 (SiC-CH<sub>3</sub>), 0.53 (Si-(CH<sub>3</sub>)<sub>3</sub>).

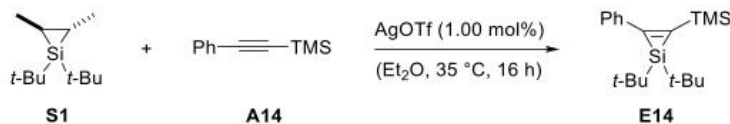
$^{29}\text{Si NMR}$  (100 MHz,  $C_6D_{12}$ )  $\delta$  (ppm): -13.23 (Si-Me<sub>3</sub>), -71.48 (Si-*t*Bu).

UV-Vis (*n*-hexane)  $\lambda_{\text{max}}$ /nm ( $\epsilon$ ): 215 (19840), 278 (2487).

LIFDI-MS:  $m/z$  = calc. for  $[C_{13}H_{30}Si_2]^+$ : 255.1920 ( $[M]^+$ ); found 255.1924.

EA: calc. [%] for  $C_{13}H_{30}Si_2$ : C, 66.06; H, 11.88; Si, 22.07; found: C, 66.21; H, 11.80.

**1,1-Di-*tert*-butyl-2-phenyl-3-(trimethylsilyl)-silirene (E14)**



Sublimation at  $10^{-6}$  mbar and  $135^\circ\text{C}$  gave 1,1-di-*tert*-butyl-2-phenyl-3-(trimethylsilyl)-silirene (**E14**) as a colorless solid. Yield: 149 mg (79%).

$^1\text{H NMR}$  (500 MHz,  $C_6D_{12}$ )  $\delta$  (ppm): 7.65-7.61 (m, 2H, CH<sub>arm,o</sub>), 7.27-7.22 (m, 2H, CH<sub>arm,m</sub>), 7.12-7.07 (m, 1H, CH<sub>arm,p</sub>), 1.10 (s, 18H, C-(CH<sub>3</sub>)<sub>3</sub>), 0.33 (s, 9H, Si-(CH<sub>3</sub>)<sub>3</sub>).

$^{13}\text{C NMR}$  (125 MHz,  $C_6D_{12}$ )  $\delta$  (ppm): 177.30 (Si-C-Ph), 152.31 (Si-C-Si), 136.23 (C-CH), 129.62 (C-CH), 128.50 (C-CH-CH), 128.11 ((CH)<sub>2</sub>-CH-(CH)<sub>2</sub>), 30.58 (SiC-(CH<sub>3</sub>)<sub>3</sub>), 21.12 (Si-C-(CH<sub>3</sub>)<sub>3</sub>), 0.23 (Si-(CH<sub>3</sub>)<sub>3</sub>).

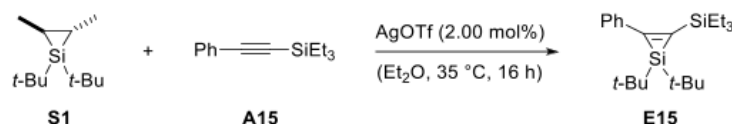
$^{29}\text{Si NMR}$  (100 MHz,  $C_6D_{12}$ )  $\delta$  (ppm): -14.01 (Si-(CH<sub>3</sub>)<sub>3</sub>), -72.12 (Si-*t*Bu).

UV-Vis (*n*-hexane)  $\lambda_{\text{max}}$ /nm ( $\epsilon$ ): 250 (26500), 325 (1635).

**LIFDI-MS:**  $m/z = \text{calc. for } [C_{19}H_{32}Si_2]^+$ : 316.2043 ( $[M]^+$ ); found 316.2039.

**EA:** calc. [%] for  $C_{19}H_{32}Si_2$ : C, 72.07; H, 10.19; Si, 17.74; found: C, 72.20; H, 10.04; Si, 17.49.

**1,1-Di-*tert*-butyl-2-phenyl-3-(triethylsilyl)-silirene (E15)**



Sublimation at  $10^{-6}$  mbar and 120 °C gave 1,1-di-*tert*-butyl-2-phenyl-3-(triethylsilyl)-silirene (**E15**) as a colorless solid. Yield: 126 mg (70%).

**$^1\text{H NMR}$**  (500 MHz,  $C_6D_{12}$ )  $\delta$  (ppm): 7.45 (dd, 2H,  $^3J_{\text{HH}} = 8.3$  Hz,  $^4J_{\text{HH}} = 1.3$  Hz,  $\text{CH}_{\text{am},o}$ ), 7.25 (tq, 2H,  $^3J_{\text{HH}} = 8.3$  Hz, 7.4 Hz,  $\text{CH}_{\text{am},m}$ ), 7.13 (t, 1H,  $^3J_{\text{HH}} = 7.4$  Hz,  $^4J_{\text{HH}} = 1.3$  Hz,  $\text{CH}_{\text{am},p}$ ), 1.09 (s, 18H, C- $\text{CH}_3$ ), 1.00 (t, 9H,  $^3J_{\text{HH}} = 7.9$  Hz,  $\text{CH}_2\text{-CH}_3$ ), 0.79 (qd, 6H,  $^3J_{\text{HH}} = 7.9$  Hz,  $^4J_{\text{HH}} = 0.8$  Hz,  $\text{CH}_2\text{-CH}_3$ ).

**$^{13}\text{C NMR}$**  (125 MHz,  $C_6D_{12}$ )  $\delta$  (ppm): 176.39 (C-C-C), 154.79 (Si-C-Si), 138.03 (C-CH), 129.57 (C-CH), 128.68 (C-CH-CH), 128.23 ((CH) $_2$ -CH-(CH) $_2$ ), 30.98 (C- $\text{CH}_3$ ), 21.75 (C- $\text{CH}_3$ ), 8.19 (CH $_2$ -CH $_3$ ), 5.99 (CH $_2$ -CH $_3$ ).

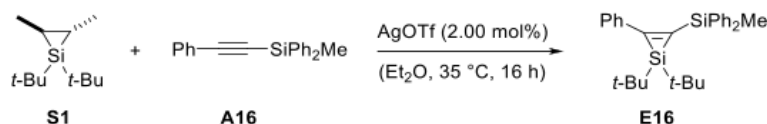
**$^{29}\text{Si NMR}$**  (100 MHz,  $C_6D_{12}$ )  $\delta$  (ppm): -6.06 (Si- $\text{Et}_3$ ), -73.17 (Si-*t*-Bu).

**UV-Vis** (*n*-hexane)  $\lambda_{\text{max}}/\text{nm}$  ( $\epsilon$ ): 248 (9940), 260 (18850), 272 (17000), 323 (3530).

**LIFDI-MS:**  $m/z = \text{calc. for } [C_{22}H_{38}Si_2]^+$ : 358.2503 ( $[M]^+$ ); found 358.2512.

**EA:** calc. [%] for  $C_{22}H_{38}Si_2$ : C, 73.66; H, 10.68; Si, 15.66; found: C, 73.31; H, 10.84; Si, 15.32.

**1,1-Di-*tert*-butyl-2-(methyldiphenylsilyl)-3-phenyl-silirene (E16)**



Sublimation at  $10^{-6}$  mbar and 140 °C gave 1,1-di-*tert*-butyl-2-(methyldiphenylsilyl)-3-phenyl-silirene (**E16**) as a colorless solid. Yield: 110 mg (55%).

**$^1\text{H NMR}$**  (500 MHz,  $C_6D_{12}$ )  $\delta$  (ppm): 7.55 (dt, 4H,  $^3J_{\text{HH}} = 6.4$  Hz,  $^4J_{\text{HH}} = 1.7$  Hz, Si-C- $\text{CH}$ ), 7.34 (dd, 2H,  $^3J_{\text{HH}} = 8.0$  Hz, 1.6 Hz, C-C- $\text{CH}$ ), 7.26 - 7.22 (m, 2H, Si-C-(CH) $_2$ - $\text{CH}$ ), 7.22 - 7.18 (m, 4H, Si-C- $\text{CH-CH}$ ), 7.12 - 7.04 (m, 3H, C-C- $\text{CH-(CH)}_3$ ), 1.04 (s, 18H, C- $\text{CH}_3$ ), 0.73 (s, 3H, Si- $\text{CH}_3$ ).

$^{13}\text{C}$  NMR (125 MHz,  $\text{C}_6\text{D}_{12}$ )  $\delta$  (ppm): 177.73 (C-C-C), 153.89 (Si-C-Si), 138.28 (Si-C-CH), 136.55 (C-C-CH), 135.50 (Si-C-CH), 130.81 (C-C-CH), 129.52 (Si-C-(CH)<sub>2</sub>-CH), 128.65 (C-C-(CH)<sub>2</sub>-CH), 128.57 (C-C-CH-CH), 128.23 (Si-C-CH-CH), 30.89 (C-CH<sub>3</sub>), 21.81 (C-CH<sub>3</sub>), -1.37 (Si-CH<sub>3</sub>).

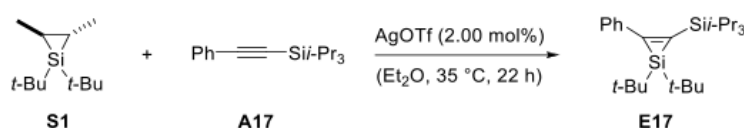
$^{29}\text{Si}$  NMR (100 MHz,  $\text{C}_6\text{D}_{12}$ )  $\delta$  (ppm): -22.07 (Si-Ph<sub>2</sub>Me), -72.69 (Si-*t*-Bu).

UV-Vis (*n*-hexane)  $\lambda_{\text{max}}$ /nm ( $\epsilon$ ): 212 (53700), 249 (16400), 261 (17850), 327 (1980).

LIFDI-MS:  $m/z$  = calc. for  $[\text{C}_{29}\text{H}_{36}\text{Si}_2]^+$ : 440.2348 ( $[\text{M}]^+$ ); found 440.2356.

EA: calc. [%] for  $\text{C}_{29}\text{H}_{36}\text{Si}_2$ : C, 79.02; H, 8.23; Si, 12.74; found: C, 78.86; H, 8.27; Si, 12.48.

### 1,1-Di-*tert*-butyl-2-phenyl-3-(triisopropylsilyl)-silirene (E17)



Sublimation at  $10^{-6}$  mbar and 120 °C gave 1,1-di-*tert*-butyl-2-phenyl-3-(triisopropylsilyl)-silirene (**E17**) as a colorless solid. Yield: 118 mg (58%).

$^1\text{H}$  NMR (500 MHz,  $\text{C}_6\text{D}_{12}$ )  $\delta$  (ppm): 7.47 (dd, 2H,  $^3J_{\text{HH}} = 8.2$  Hz,  $^4J_{\text{HH}} = 1.3$  Hz, C-CH), 7.24 (tq, 2H,  $^3J_{\text{HH}} = 8.2$  Hz, 7.3 Hz, C-CH-CH), 7.13 (tt, 1H,  $^3J_{\text{HH}} = 7.3$  Hz,  $^4J_{\text{HH}} = 1.3$  Hz, C-(CH)<sub>2</sub>-CH), 1.34 - 1.27 (m, 3H, CH-CH<sub>3</sub>), 1.14 (d, 18H,  $^3J_{\text{HH}} = 7.3$  Hz, CH-CH<sub>3</sub>), 1.12 (s, 18H, C-CH<sub>3</sub>).

$^{13}\text{C}$  NMR (125 MHz,  $\text{C}_6\text{D}_{12}$ )  $\delta$  (ppm): 177.63 (C-C-C), 153.79 (Si-C-Si), 138.40 (C-CH), 129.52 (C-CH), 128.62 (C-CH-CH), 128.15 ((CH)<sub>2</sub>-CH-(CH)<sub>2</sub>), 31.20 (C-CH<sub>3</sub>), 22.16 (C-CH<sub>3</sub>), 19.67 (CH-CH<sub>3</sub>), 13.40 (Si-CH).

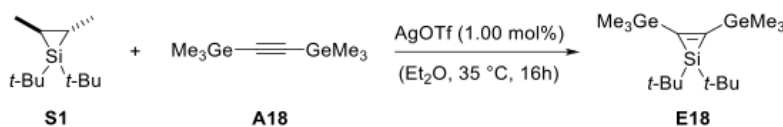
$^{29}\text{Si}$  NMR (100 MHz,  $\text{C}_6\text{D}_{12}$ )  $\delta$  (ppm): -3.55 (Si-*i*-Pr<sub>3</sub>), -75.85 (Si-*t*-Bu).

UV-Vis (*n*-hexane)  $\lambda_{\text{max}}$ /nm ( $\epsilon$ ): 220 (34200), 262 (17000), 272 (17200), 325 (3150).

LIFDI-MS:  $m/z$  = calc. for  $[\text{C}_{25}\text{H}_{44}\text{Si}_2]^+$ : 400.2982 ( $[\text{M}]^+$ ); found 400.2982.

EA: calc. [%] for  $\text{C}_{25}\text{H}_{44}\text{Si}_2$ : C, 74.92; H, 11.07; Si, 14.01; found: C, 74.67; H, 11.33; Si, 13.85.

### 1,1-Di-*tert*-butyl-2,3-bis(trimethylgermyl)-silirene (E18)



S19

Sublimation at  $10^{-5}$  mbar and  $120\text{ }^{\circ}\text{C}$  gave 1,1-di-*tert*-butyl-2,3-bis(trimethylgermyl)-silirene (**E18**) as a colorless solid. Yield: 102 mg (51%).

$^1\text{H NMR}$  (500 MHz,  $\text{C}_6\text{D}_{12}$ )  $\delta$  (ppm): 1.05 (s, 18H, Si-C- $\text{CH}_3$ ), 0.40 (s, 18H, Ge- $\text{CH}_3$ ).

$^{13}\text{C NMR}$  (125 MHz,  $\text{C}_6\text{D}_{12}$ )  $\delta$  (ppm): 181.31 (Si-C-Ge), 30.96 (Si-C- $\text{CH}_3$ ), 20.33 (Si-C- $\text{CH}_3$ ), -0.35 (Ge- $\text{CH}_3$ ).

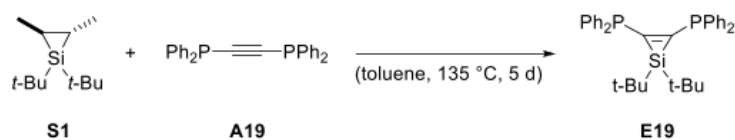
$^{29}\text{Si NMR}$  (100 MHz,  $\text{C}_6\text{D}_{12}$ )  $\delta$  (ppm): -82.20.

UV-Vis (*n*-hexane)  $\lambda_{\text{max}}/\text{nm}$  ( $\epsilon$ ): 218 (84000), 333 (900).

LIFDI-MS:  $m/z$  = calc. for  $[\text{C}_{16}\text{H}_{36}\text{Ge}_2\text{Si}]^+$ : 402.1019 ( $[\text{M}]^+$ ); found 402.1030.

EA: calc. [%] for  $\text{C}_{16}\text{H}_{36}\text{Ge}_2\text{Si}$ : C, 47.83; H, 9.03; Ge, 36.15; Si, 6.99; found: C, 47.21; H, 8.69; Ge, 36.47; Si, 7.12.

**(1,1-Di-*tert*-butyl-silirene-2,3-diyl)bis(diphenylphosphane) (E19)**



Sublimation at  $10^{-6}$  mbar and  $120\text{ }^{\circ}\text{C}$  gave (1,1-di-*tert*-butyl-silirene-2,3-diyl)bis(diphenylphosphane) (**E19**) as a colorless solid. Yield: 108 mg (57%).

$^1\text{H NMR}$  (500 MHz,  $\text{C}_6\text{D}_{12}$ )  $\delta$  (ppm): 7.56 - 7.51 (m, 4H, C-( $\text{CH}_2$ ) $_2$ -CH), 7.21 - 7.17 (m, 8H, C-CH-CH), 7.12 - 7.07 (m, 8H, C-CH), 0.92 (s, 18H, C- $\text{CH}_3$ ).

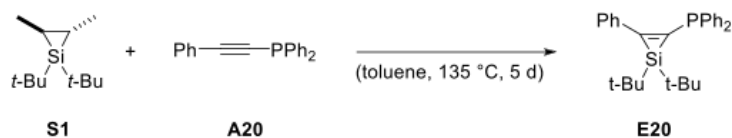
$^{13}\text{C NMR}$  (125 MHz,  $\text{C}_6\text{D}_{12}$ )  $\delta$  (ppm): 163.62 (P-C-C-P), 137.03 (P-C-CH), 133.24 (( $\text{CH}_2$ ) $_2$ -CH), 132.94 (C-CH), 127.82 (C-CH-CH), 29.68 (C- $\text{CH}_3$ ), 21.42 (C- $\text{CH}_3$ ).

$^{29}\text{Si NMR}$  (100 MHz,  $\text{C}_6\text{D}_{12}$ )  $\delta$  (ppm): -67.29.

$^{31}\text{P NMR}$  (203 MHz,  $\text{C}_6\text{D}_{12}$ )  $\delta$  (ppm): -6.60.

UV-Vis (*n*-hexane)  $\lambda_{\text{max}}/\text{nm}$  ( $\epsilon$ ): 212 (50900), 245 (26100), 315 (5770).

LIFDI-MS:  $m/z$  = calc. for  $[\text{C}_{34}\text{H}_{38}\text{P}_2\text{Si}]^+$ : 536.2218 ( $[\text{M}]^+$ ); found 536.2167.

**(1,1-Di-*tert*-butyl-3-phenyl-siliren-2-yl)diphenylphosphane (E20)**

Sublimation at  $10^{-6}$  mbar and 115 °C gave (1,1-di-*tert*-butyl-3-phenyl-siliren-2-yl)diphenylphosphane (**E20**) as a colorless solid. Yield: 288 mg (61%).

**$^1\text{H}$  NMR** (500 MHz,  $\text{C}_6\text{D}_6$ )  $\delta$  (ppm): 7.81 - 7.30 (m, 15H, CH), 1.06 (s, 18H, C- $\text{CH}_3$ ).

**$^{13}\text{C}$  NMR** (125 MHz,  $\text{C}_6\text{D}_6$ )  $\delta$  (ppm): 163.76 (C-C-C), 152.12 (P-C-Si), 139.25 (C-C-CH), 135.04 (C-C-(CH) $_2$ -CH), 133.65 (P-C-CH), 133.11 (P-C-(CH) $_2$ -CH), 132.15 (C-C-CH-CH), 131.10 (C-C-CH), 128.69 (P-C-CH-CH), 128.35 (P-C-CH), 30.38 (C- $\text{CH}_3$ ), 21.65 (C- $\text{CH}_3$ ).

**$^{29}\text{Si}$  NMR** (100 MHz,  $\text{C}_6\text{D}_6$ )  $\delta$  (ppm): -72.68.

**$^{31}\text{P}$  NMR** (203 MHz,  $\text{DMSO-}d_6$ )  $\delta$  (ppm): -10.64.

**UV-Vis** (*n*-hexane)  $\lambda_{\text{max}}/\text{nm}$  ( $\epsilon$ ): 214 (38200), 266 (15700), 325 (4940).

**LIFDI-MS**:  $m/z$  = calc. for  $[\text{C}_{28}\text{H}_{33}\text{PSi}]^+$ : 428.2089 ( $[\text{M}]^+$ ); found 428.2088.

### 3. Synthesis of Multifunctional Silirene-Linkers

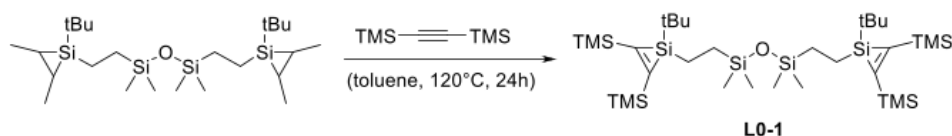
#### Synthesis of bi-functional silacyclopropene-linkers

General synthesis procedure via silylene transfer reaction for linker **L1-2**:

The reactant silacyclopropanes for linker **L1** and **L2** were synthesized according to the literature procedure given by Rieger *et al.*<sup>[16]</sup>

Silacyclopropane (1.0 eq.) and the respective alkyne (3.0 eq.) were dissolved in toluene (0.10 M) and stirred for five minutes. The reaction mixture was stirred at 135 °C until full conversion of the respective silacyclopropane. The reaction progress was monitored by <sup>29</sup>Si and <sup>1</sup>H NMR spectroscopy. The solvent was removed under reduced pressure. Subsequent distillation and filtration over Celite and dry neutral alumina gave the corresponding silacyclopropene linker scaffolds.

#### 1,3-bis(2-(1-(tert-butyl)-2,3-bis(trimethylsilyl)-1H-silirene-1-yl)ethyl)-1,1,3,3-tetramethyldisiloxane (**L0-1**)



**Yield:** 130.5 mg (186.5 μmol, 58.5 %), yellowish viscous oil.

**<sup>1</sup>H NMR** (500 MHz, C<sub>6</sub>D<sub>6</sub>) δ (ppm): 1.02 (s, 18H, SiC-(CH<sub>3</sub>)<sub>3</sub>), 0.99-0.95 (m, 4H, tBuSi-CH<sub>2</sub>-CH<sub>2</sub>SiO), 0.41-0.35 (m, 4H, tBuSiCH<sub>2</sub>-CH<sub>2</sub>-SiO), 0.31 (s, 36H, CSi-(CH<sub>3</sub>)<sub>3</sub>), 0.12 (s, 12H, OSi-(CH<sub>3</sub>)<sub>2</sub>).

**<sup>13</sup>C NMR** (125 MHz, C<sub>6</sub>D<sub>6</sub>) δ (ppm): 185.91 (Si-C-TMS), 29.53 (SiC-(CH<sub>3</sub>)<sub>3</sub>), 18.52 (SiCH<sub>2</sub>-CH<sub>2</sub>-SiO), 13.01 (Si-C-(CH<sub>3</sub>)<sub>3</sub>), 0.19 (CSi-(CH<sub>3</sub>)<sub>3</sub>), 0.02 (OSi-(CH<sub>3</sub>)<sub>2</sub>), -0.06 (Si-CH<sub>2</sub>-CH<sub>2</sub>SiO).

**<sup>29</sup>Si NMR** (100 MHz, C<sub>6</sub>D<sub>6</sub>) δ (ppm): 7.63 (CH<sub>2</sub>-Si-O), -12.88 (C-Si-(CH<sub>3</sub>)<sub>3</sub>), -86.89 (C-Si-tBu).

**UV-Vis** (*n*-hexane) λ<sub>max</sub>/nm (ε): 225 (17800), 348 (1090).

**EA:** calc. [%] for C<sub>32</sub>H<sub>74</sub>OSi<sub>8</sub>: C, 54.94; H, 10.66; O, 2.29; Si, 28.30; found: C, 55.65; H, 10.12; Si, 28.51.



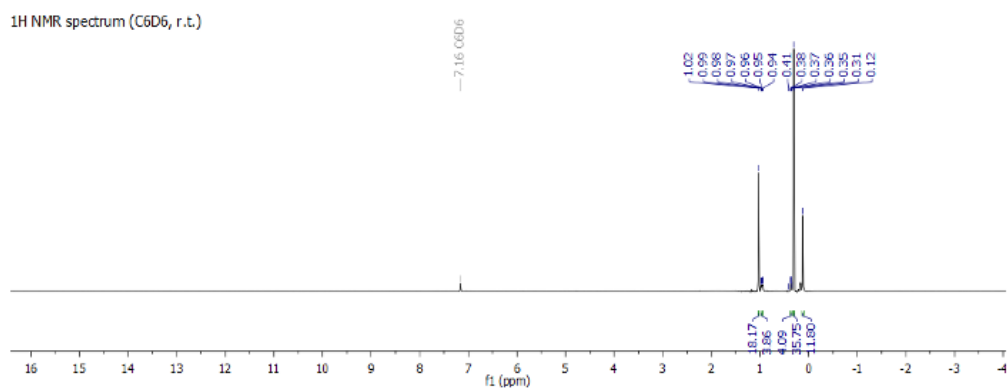


**Figure S1.** <sup>1</sup>H-NMR (500 MHz, C<sub>6</sub>D<sub>6</sub>) of linker molecule **L0-1**.

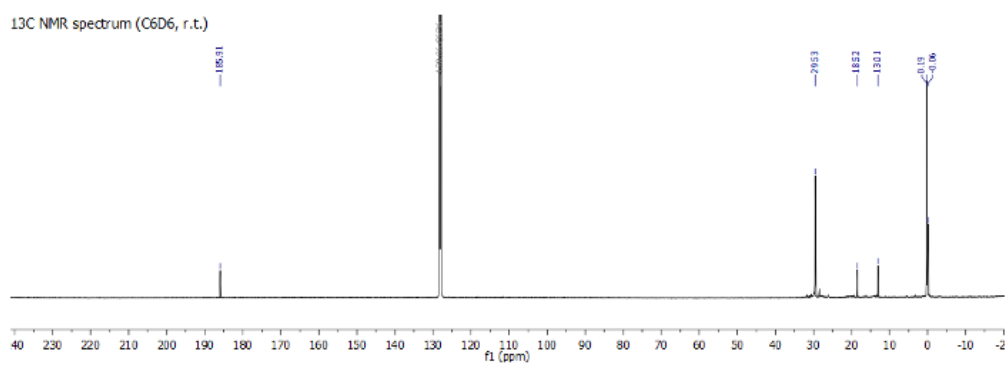


**Figure S2.** <sup>13</sup>C-NMR (125 MHz, C<sub>6</sub>D<sub>6</sub>) of linker molecule **L0-1**.

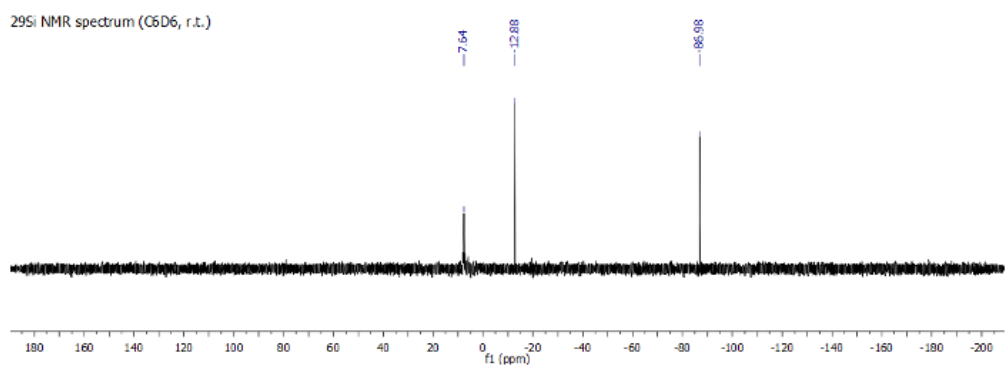


**Figure S3.** <sup>29</sup>Si-NMR (100 MHz, C<sub>6</sub>D<sub>6</sub>) of linker molecule **L0-1**.

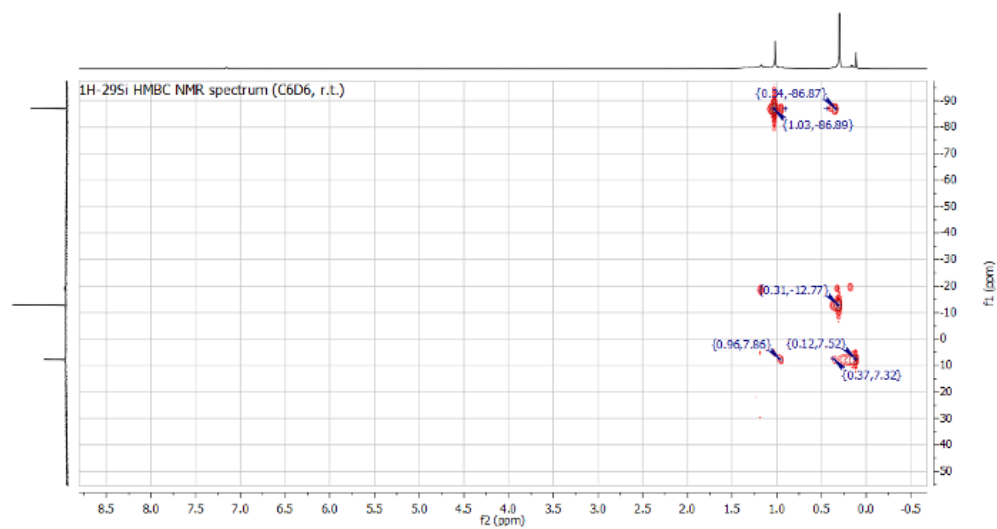


**Figure S4.**  $^1\text{H}$ - $^{29}\text{Si}$ -HMBC (500 MHz/100 MHz,  $\text{C}_6\text{D}_6$ ) of linker molecule **L0-1**.

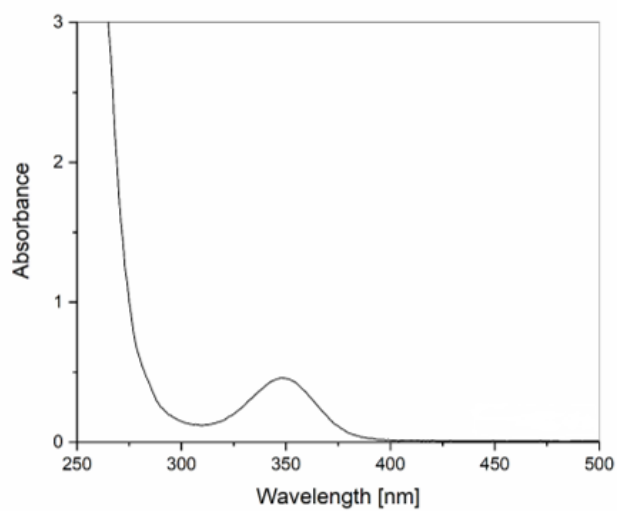
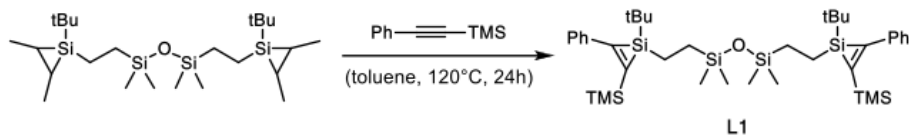


**Figure S5.** UV-VIS spectra of crosslinker **L0-1** (r.t., n-hexane,  $0.5 \times 10^{-3}$  M).

**1,3-bis(2-(1-(tert-butyl)-2-phenyl-3-(trimethylsilyl)-1H-siliren-1-yl)ethyl)-1,1,3,3-tetramethyl-disiloxane (L1)**



**Yield:** 230.2 mg (325.4  $\mu\text{mol}$ , 76.6 %), yellow viscous oil.

**$^1\text{H}$  NMR** (500 MHz,  $\text{C}_6\text{D}_6$ )  $\delta$  (ppm): 7.66-7.63 (m, 4H,  $\text{CH}_{\text{arm}}$ ), 7.27-7.23 (m, 4H,  $\text{CH}_{\text{arm}}$ ), 7.12-7.08 (m, 2H,  $\text{CH}_{\text{arm}}$ ), 1.09 (s, 18H,  $\text{SiC}-(\text{CH}_3)_3$ ), 0.98-0.89 (m, 4H,  $\text{tBuSi-CH}_2\text{-CH}_2\text{SiO}$ ), 0.58-0.49 (m, 4H,  $\text{tBuSiCH}_2\text{-CH}_2\text{-SiO}$ ), 0.35 (s, 18H,  $\text{CSi}-(\text{CH}_3)_3$ ), 0.08 (s, 12H,  $\text{OSi}-(\text{CH}_3)_2$ ).

**$^{13}\text{C}$  NMR** (125 MHz,  $\text{C}_6\text{D}_6$ )  $\delta$  (ppm): 174.51 ( $\text{Si-C-Ph}$ ), 158.71 ( $\text{Si-C-TMS}$ ), 137.65 ( $\text{C}_{\text{arm}}$ ), 132.27 ( $\text{C}_{\text{arm}}$ ), 129.51 ( $\text{C}_{\text{arm}}$ ), 128.75 ( $\text{C}_{\text{arm}}$ ), 29.17 ( $\text{SiC}-(\text{CH}_3)_3$ ), 19.27 ( $\text{SiCH}_2\text{-CH}_2\text{-SiO}$ ), 12.64 ( $\text{SiC}-(\text{CH}_3)_3$ ), 0.66 ( $\text{CSi}-(\text{CH}_3)_3$ ), 0.02 ( $\text{OSi}-(\text{CH}_3)_2$ ), -0.09 ( $\text{Si-CH}_2\text{-CH}_2\text{SiO}$ ).

**$^{29}\text{Si}$  NMR** (100 MHz,  $\text{C}_6\text{D}_6$ )  $\delta$  (ppm): 7.76 ( $\text{CH}_2\text{-Si-O}$ ), -13.69 ( $\text{C-Si}-(\text{CH}_3)_3$ ), -72.16 ( $\text{C-Si-tBu}$ ).

**UV-Vis** ( $n$ -hexane)  $\lambda_{\text{max}}/\text{nm}$  ( $\epsilon$ ): 250 (22100), 321 (870).

**EA:** calc. [%] for  $\text{C}_{38}\text{H}_{66}\text{OSi}_6$ : C, 64.52; H, 9.40; O, 2.26; Si, 23.82; found: C, 65.06; H, 10.02; Si, 23.49.

$^1\text{H}$  NMR spectrum ( $\text{C}_6\text{D}_6$ , r.t.)

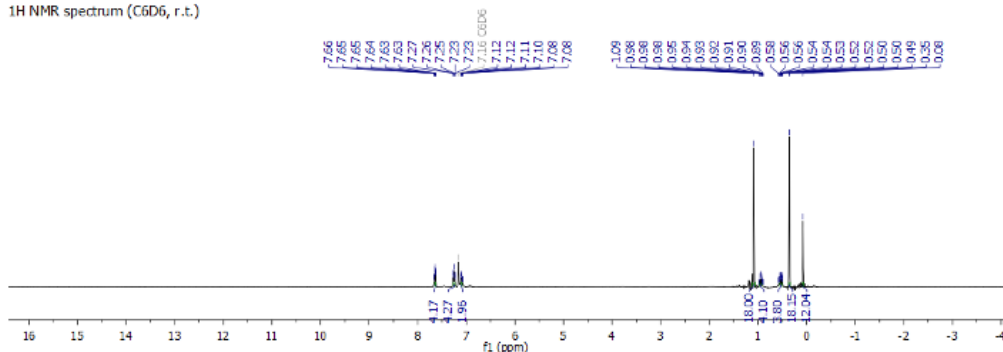


**Figure S6.**  $^1\text{H}$ -NMR (500 MHz,  $\text{C}_6\text{D}_6$ ) of linker molecule **L1**.

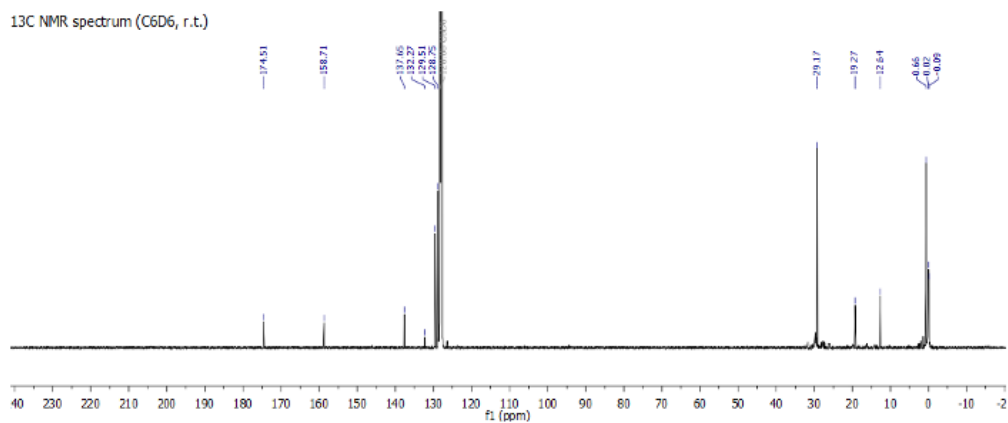


**Figure S7.** <sup>13</sup>C-NMR (125 MHz, C<sub>6</sub>D<sub>6</sub>) of linker molecule **L1**.

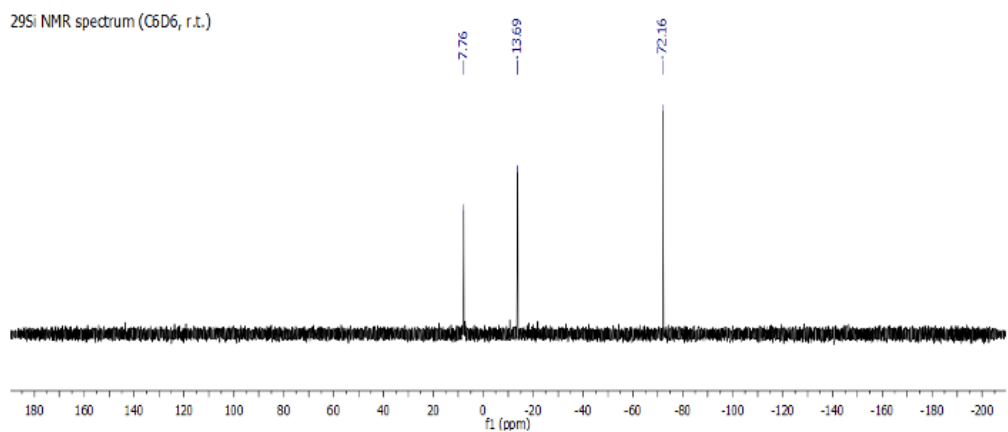


**Figure S8.** <sup>29</sup>Si-NMR (100 MHz, C<sub>6</sub>D<sub>6</sub>) of linker molecule **L1**.

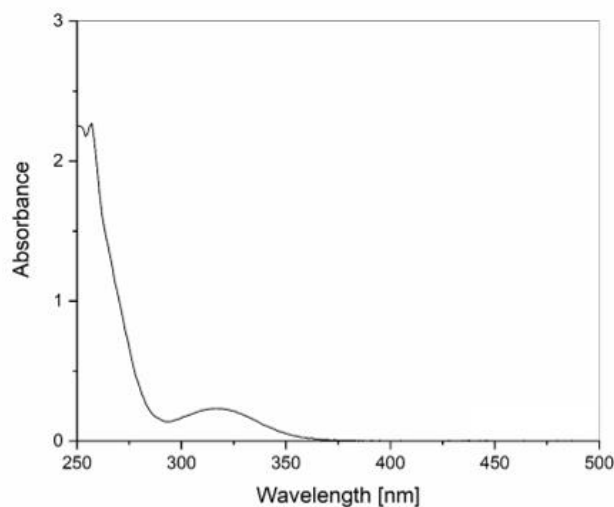
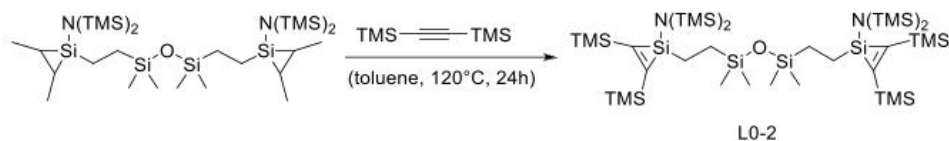


**Figure S9.** UV-VIS spectra of crosslinker **L1** (r.t., n-hexane,  $0.5 \times 10^{-3}$  M).

**1,1'-((1,1,3,3-tetramethyldisiloxane-1,3-diyl)bis(ethane-2,1-diyl))bis(N,N,2,3-tetrakis(trimethylsilyl)-1H-silirene-1-amine) (L0-2)**



**Yield:** 189.3 mg (208.9  $\mu$ mol, 61.3 %), yellow viscous oil.

**$^1\text{H}$  NMR** (500 MHz,  $\text{C}_6\text{D}_6$ )  $\delta$  (ppm): 1.11-1.07 (m, 4H, tBuSi- $\text{CH}_2$ - $\text{CH}_2$ SiO), 0.42-0.38 (m, 4H, tBuSi $\text{CH}_2$ - $\text{CH}_2$ -SiO), 0.35 (s, 36H, CSi-( $\text{CH}_3$ ) $_3$ ), 0.31 (s, 36H, NSi-( $\text{CH}_3$ ) $_3$ ), 0.15 (s, 12H, OSi-( $\text{CH}_3$ ) $_2$ ).

**$^{13}\text{C}$  NMR** (125 MHz,  $\text{C}_6\text{D}_6$ )  $\delta$  (ppm): 195.21 (Si-C-TMS), 12.61 (Si $\text{CH}_2$ - $\text{CH}_2$ -SiO), 9.44 (Si- $\text{CH}_2$ - $\text{CH}_2$ SiO), 3.63 (NSi-( $\text{CH}_3$ ) $_3$ ), 0.36 (CSi-( $\text{CH}_3$ ) $_3$ ), -0.43 (OSi-( $\text{CH}_3$ ) $_2$ ).

**$^{29}\text{Si}$  NMR** (100 MHz,  $\text{C}_6\text{D}_6$ )  $\delta$  (ppm): 7.67 ( $\text{CH}_2$ -Si-O), 3.41 (N-Si-( $\text{CH}_3$ ) $_3$ ), -13.05 (C-Si-( $\text{CH}_3$ ) $_3$ ), -92.29 (C-Si-N(TMS) $_2$ ).

**UV-Vis** (n-hexane)  $\lambda_{\text{max}}$ /nm ( $\epsilon$ ): 225 (9950), 352 (622).

**EA:** calc. [%] for  $\text{C}_{36}\text{H}_{92}\text{OSi}_{12}$ : C, 47.72; H, 10.23; N, 3.09; O, 1.77; Si, 37.19; found: C, 47.65; H, 10.07; N, 3.61; Si, 37.36.

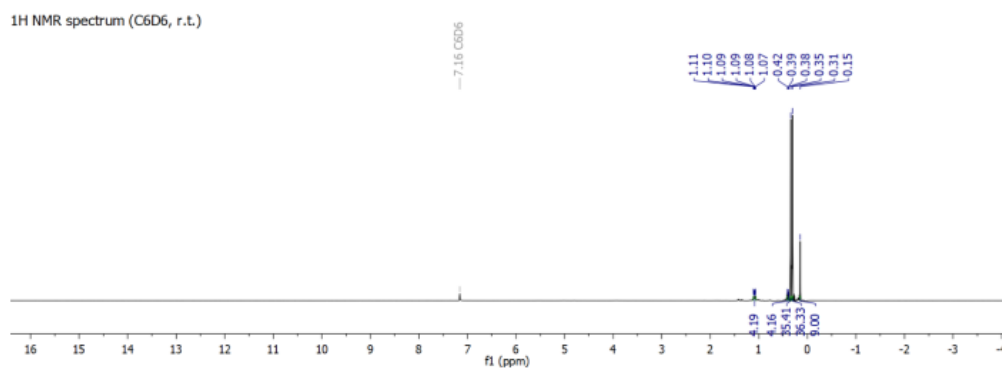


**Figure S10.** <sup>1</sup>H-NMR (500 MHz, C<sub>6</sub>D<sub>6</sub>) of linker molecule **L0-2**.

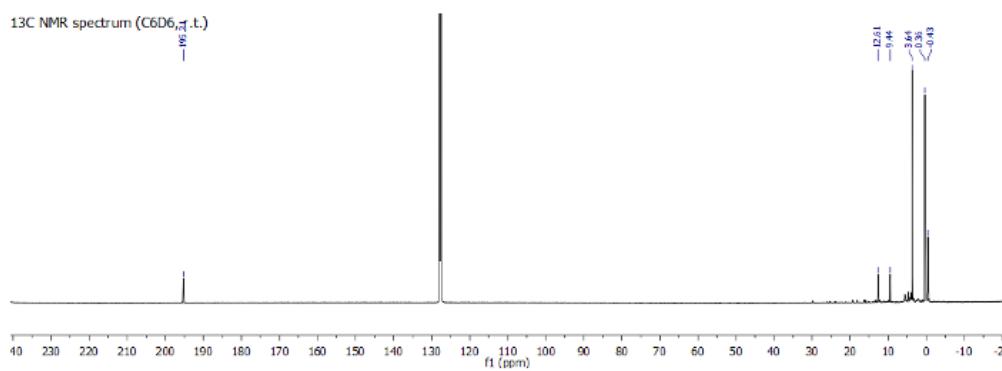


**Figure S11.** <sup>13</sup>C-NMR (125 MHz, C<sub>6</sub>D<sub>6</sub>) of linker molecule **L0-2**.

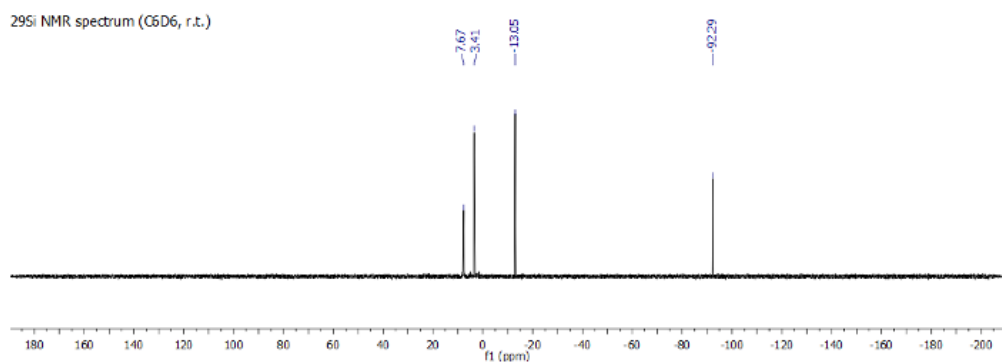


**Figure S12.** <sup>29</sup>Si-NMR (100 MHz, C<sub>6</sub>D<sub>6</sub>) of linker molecule **L0-2**.

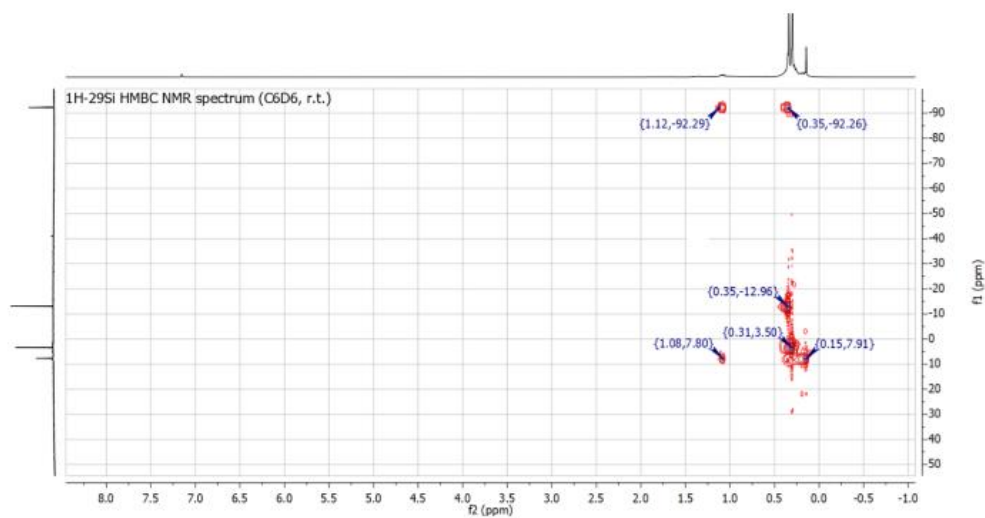


**Figure S13.**  $^1\text{H}$ - $^{29}\text{Si}$ -HMBC (500 MHz/100 MHz,  $\text{C}_6\text{D}_6$ ) of linker molecule **L0-2**.

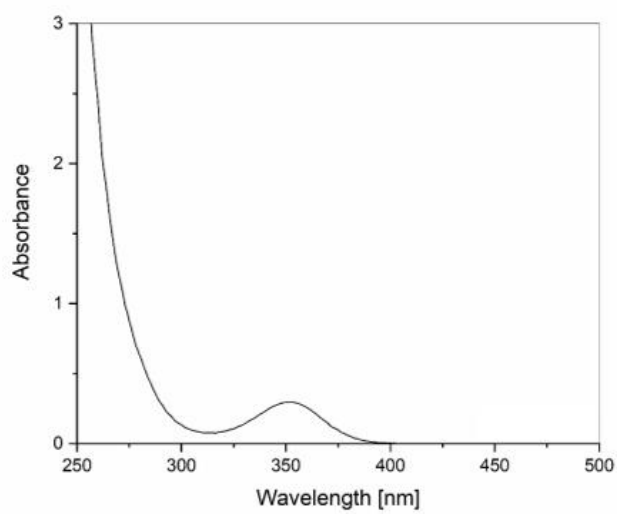
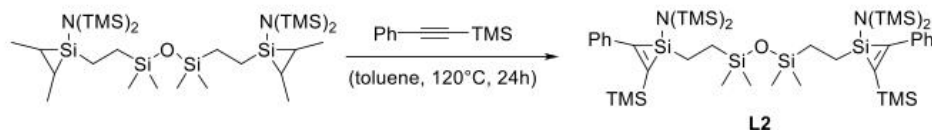


**Figure S14.** UV-VIS spectra of crosslinker **L0-2** (r.t., n-hexane,  $0.5 \times 10^{-3}$  M).

**1,1'-((1,1,3,3-tetramethyldisiloxane-1,3-diyl)bis(ethane-2,1-diyl))bis(2-phenyl-N,N,3-tris(trimethylsilyl)-1H-silirene-1-amine) (L2)**



**Yield:** 157.0 mg (171.8  $\mu$ mol, 72.9 %), yellow/orange viscous oil.

**<sup>1</sup>H NMR** (500 MHz, C<sub>6</sub>D<sub>6</sub>)  $\delta$  (ppm): 7.53-7.51 (m, 4H, CH<sub>arm</sub>), 7.26-7.22 (m, 4H, CH<sub>arm</sub>), 7.09-7.05 (m, 2H, CH<sub>arm</sub>), 1.26-1.17 (m, 4H, tBuSi-CH<sub>2</sub>-CH<sub>2</sub>SiO), 0.68-0.62 (m, 4H, tBuSiCH<sub>2</sub>-CH<sub>2</sub>-SiO), 0.34 (s, 18H, CSi-(CH<sub>3</sub>)<sub>3</sub>), 0.29 (s, 36H, NSi-(CH<sub>3</sub>)<sub>3</sub>), 0.20 (s, 12H, OSi-(CH<sub>3</sub>)<sub>2</sub>).

**<sup>13</sup>C NMR** (125 MHz, C<sub>6</sub>D<sub>6</sub>)  $\delta$  (ppm): 183.23 (Si-C-Ph), 168.28 (Si-C-TMS), 139.14 (C<sub>arm</sub>), 128.56 (C<sub>arm</sub>), 128.35 (C<sub>arm</sub>), 127.66 (C<sub>arm</sub>), 12.69 (SiCH<sub>2</sub>-CH<sub>2</sub>-SiO), 10.18 (Si-CH<sub>2</sub>-CH<sub>2</sub>SiO), 3.79 (NSi-(CH<sub>3</sub>)<sub>3</sub>), 0.69 (CSi-(CH<sub>3</sub>)<sub>3</sub>), 0.01 (OSi-(CH<sub>3</sub>)<sub>2</sub>).

**<sup>29</sup>Si NMR** (100 MHz, C<sub>6</sub>D<sub>6</sub>)  $\delta$  (ppm): 7.94 (CH<sub>2</sub>-Si-O), 3.41 (N-Si-(CH<sub>3</sub>)<sub>3</sub>), -13.19 (C-Si-(CH<sub>3</sub>)<sub>3</sub>), -80.80 (C-Si-N(TMS)<sub>2</sub>).

**UV-Vis** (*n*-hexane)  $\lambda_{\max}$ /nm ( $\epsilon$ ): 250 (20150), 322 (2035).

**EA:** calc. [%] for C<sub>42</sub>H<sub>83</sub>N<sub>2</sub>OSi<sub>2</sub>: C, 55.19; H, 9.26; N, 3.06; O, 1.75; Si, 30.73; found: C, 54.72; H, 9.90; N, 3.67; Si, 27.97.

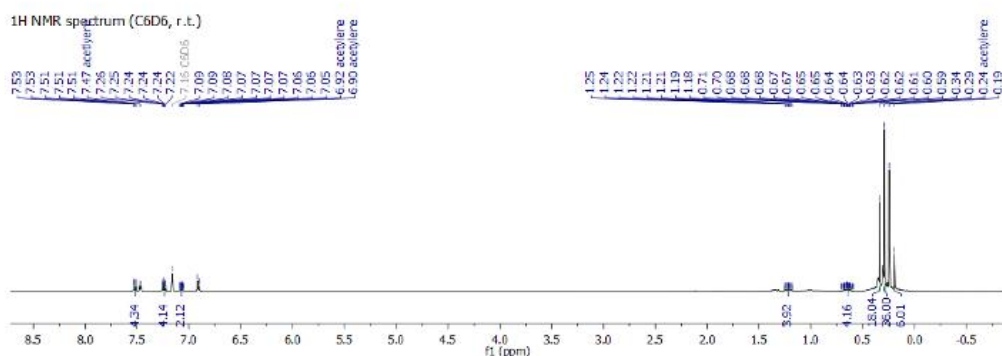


**Figure S15.** <sup>1</sup>H-NMR (500 MHz, C<sub>6</sub>D<sub>6</sub>) of linker molecule **L2**, with residue acetylene reactant.



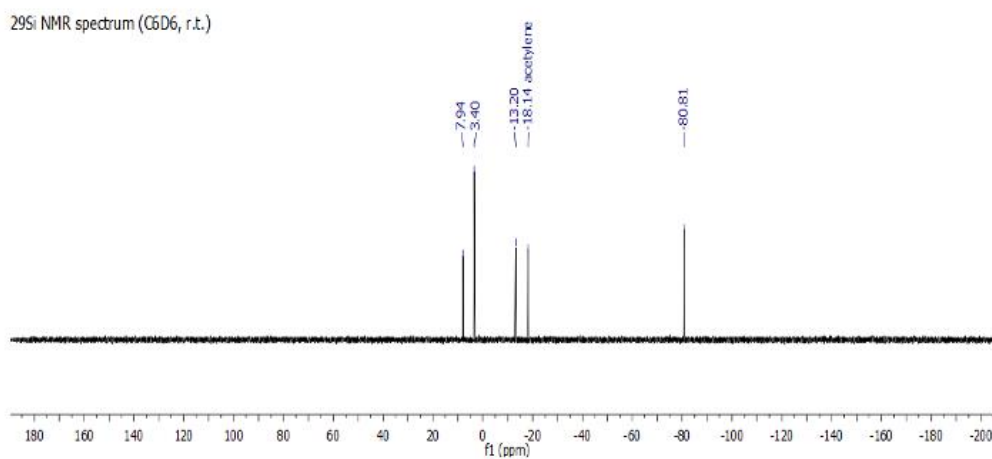


**Figure S16.** <sup>29</sup>Si-NMR (100 MHz, C<sub>6</sub>D<sub>6</sub>) of linker molecule **L2**, with residue acetylene reactant.

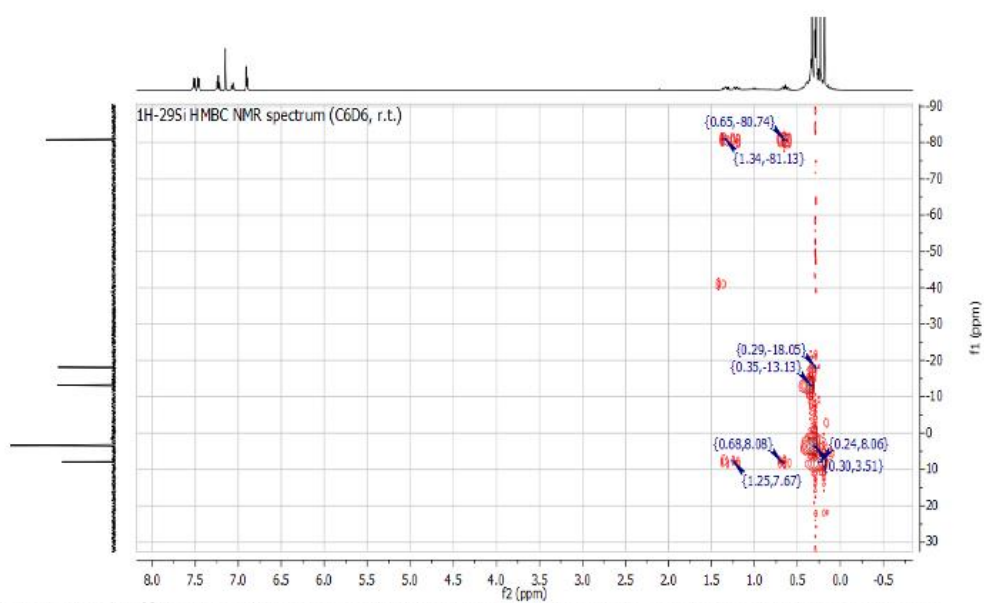


**Figure S17.** <sup>1</sup>H-<sup>29</sup>Si-HMBC (500 MHz/100 MHz, C<sub>6</sub>D<sub>6</sub>) of linker molecule **L2**, via silylene transfer.

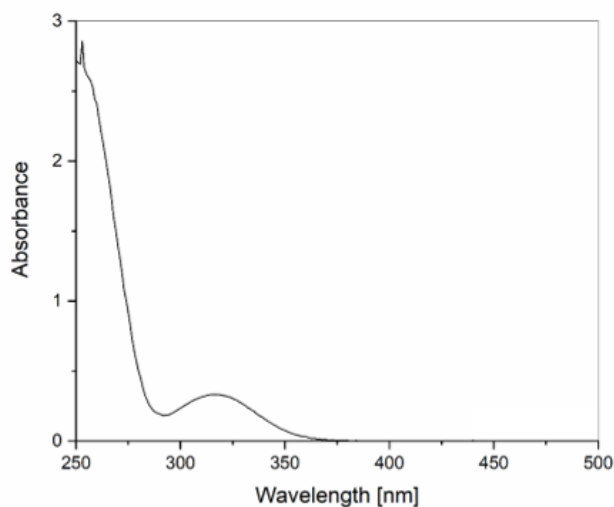
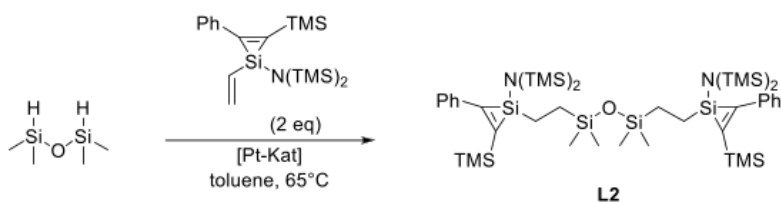


**Figure S18.** UV-VIS spectra of crosslinker **L2** (r.t., n-hexane,  $0.5 \times 10^{-3}$  M), via silylene transfer.

An alternative route to synthesise crosslinker **L2** was presented by Rieger *et al.* via the technique of modular silirenes.<sup>[16]</sup>

A solution of tetramethyldisiloxane (184  $\mu\text{mol}$ , 24.7 mg, 0.5 eq) in toluene (10 mL) was added to a solution of vinyl-silacyclopropene (404  $\mu\text{mol}$ , 109 mg, 1.1 eq) in toluene (5 mL). 16.8 mg (2.05  $\mu\text{mol}$ ) of a Karstead-catalyst solution (2.25 wt.% Pt in xylene) was added, and the mixture was stirred at 65 °C for 12 h. Over the reaction time the colour changed from a bright yellow to a dark orange. All volatiles were removed under vacuum and the obtained residue was redissolved in n-hexane (10 mL). The crude was purified by filtration through an appropriate amount of aluminium oxide ( $\text{Al}_2\text{O}_3$ ) and a syringe filter (PP, 0.5  $\mu\text{m}$ ) to remove the applied catalyst. The filter was further washed with n-hexane (2 mL). At last, the solvent was removed under vacuum to obtain the functionalized substrate **P2** (79.8 mg, 64 %).

The same reaction product could be obtained and coinciding analytic data were obtained for both synthesis pathways.



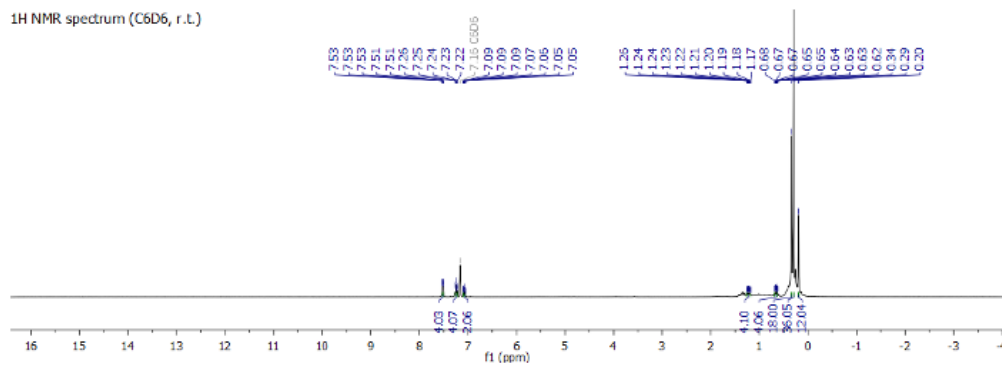
S32

**Yield:** 79.8 mg (64 %), colorless viscous oil.

**UV-Vis** (*n*-hexane)  $\lambda_{\text{max}}/\text{nm}$  ( $\epsilon$ ): 250 (20650), 322 (2140).

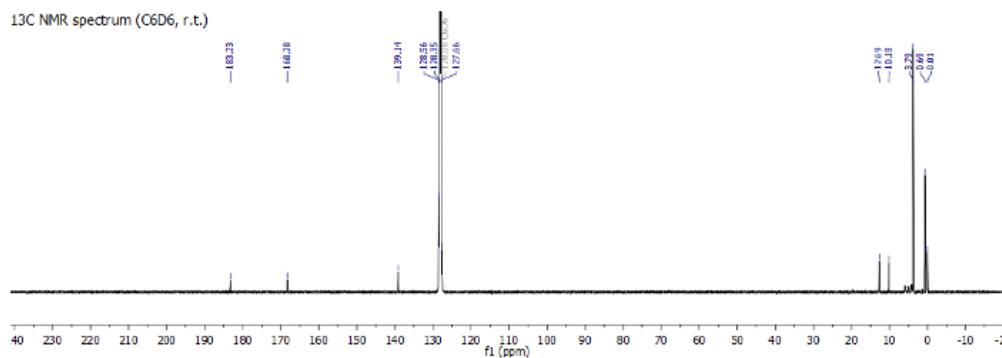
**EA:** calc. [%] for  $\text{C}_{42}\text{H}_{83}\text{N}_2\text{OSi}_2$ : C, 55.19; H, 9.26; N, 3.06; O, 1.75; Si, 30.73; found: C, 55.41; H, 9.10; N, 3.55; Si, 30.39.

$^1\text{H}$  NMR spectrum ( $\text{C}_6\text{D}_6$ , r.t.)

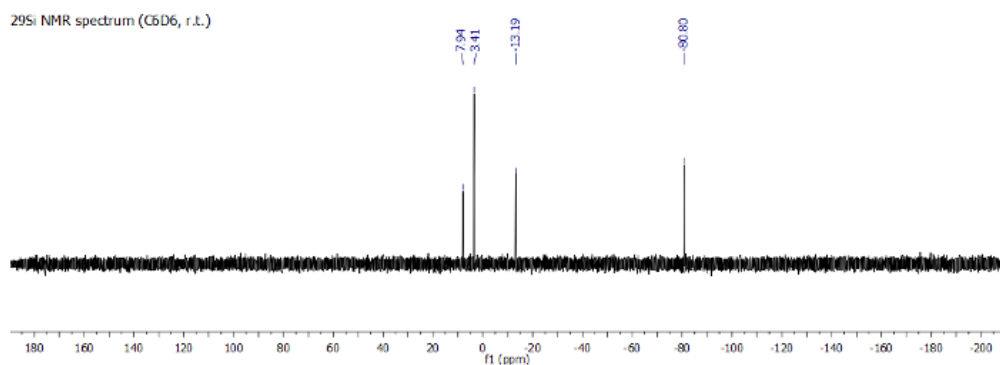


**Figure S19.**  $^1\text{H}$ -NMR (500 MHz,  $\text{C}_6\text{D}_6$ ) of linker molecule **L2**.

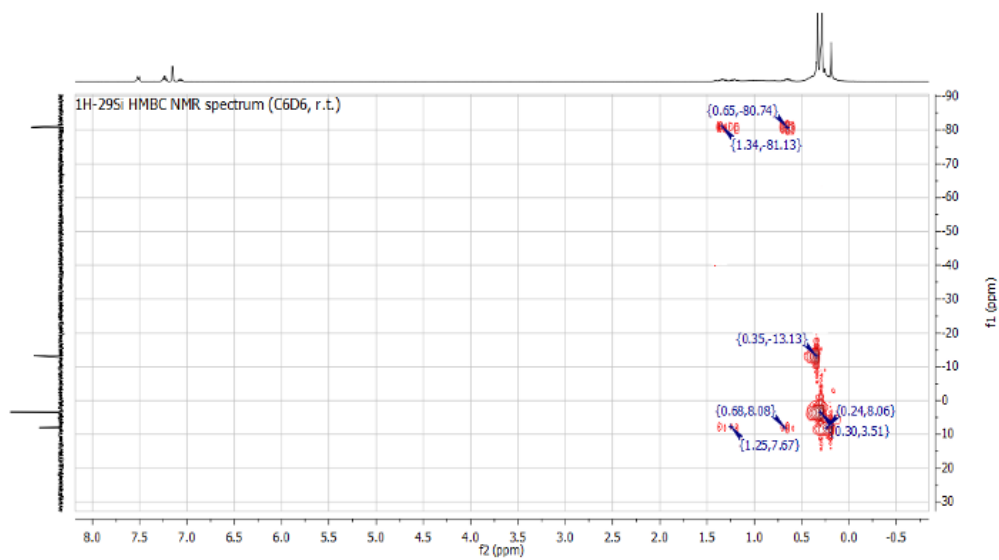
$^{13}\text{C}$  NMR spectrum ( $\text{C}_6\text{D}_6$ , r.t.)



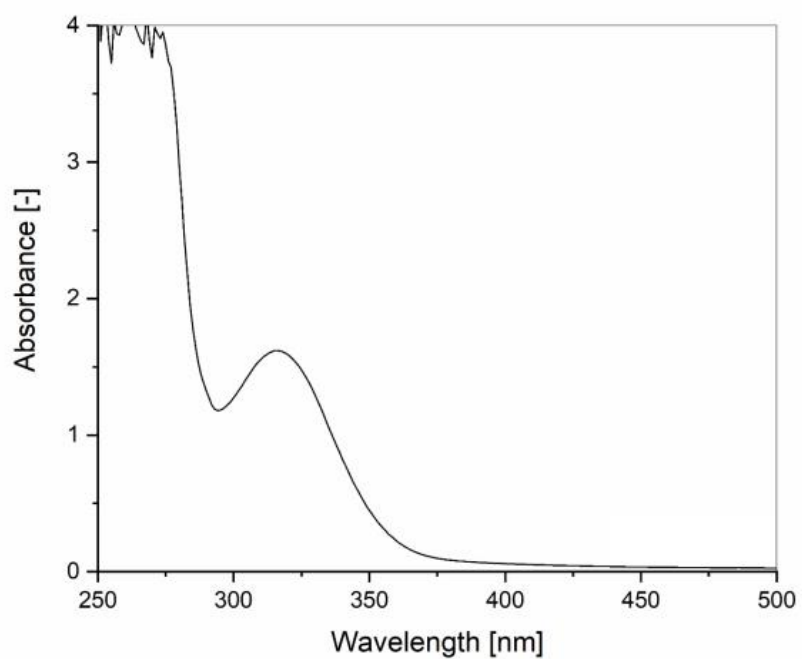
**Figure S20.**  $^{13}\text{C}$ -NMR (125 MHz,  $\text{C}_6\text{D}_6$ ) of linker molecule **L2**.



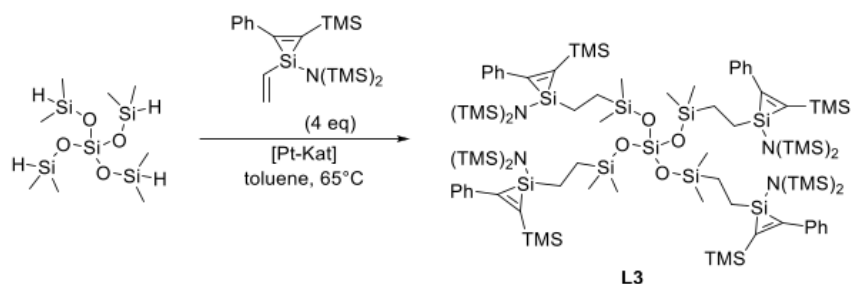
**Figure S21.** <sup>29</sup>Si-NMR (100 MHz, C<sub>6</sub>D<sub>6</sub>) of linker molecule **L2**.



**Figure S22.** <sup>1</sup>H-<sup>29</sup>Si-HMBC (500 MHz/100 MHz, C<sub>6</sub>D<sub>6</sub>) of linker molecule **L2**.



**Figure S23.** UV-VIS spectra of crosslinker **L2** (r.t., n-hexane,  $1.0 \times 10^{-3}$  M), via modular silirenes.

Synthesis of crosslinker **L3** and **L4** via the utilization of modular silirenes

The crosslinker **L3** were synthesized according to the literature procedure provided by Rieger *et al.*<sup>[16]</sup>

Modular vinyl-silacyclopropene (100 mg, 256  $\mu\text{mol}$ , 1 eq) was added to a solution of tetrakis-(dimethylsilyloxy)-silane (22.1 mg, 67.3  $\mu\text{mol}$ , 0.25 eq) in toluene (5 mL). 1.0 mg (0.12  $\mu\text{mol}$ ) of a Karstead-catalyst solution (2.25 wt.% Pt in xylene) was added, and the mixture was stirred at 60 °C for 48 h. The colour of the reaction changes from a bright yellow to a dark gold/brown over the time. All volatiles were removed under vacuum and the residue was redissolved in pentane (5 mL). The product was purified by filtration through an appropriate amount of aluminium oxide (Al<sub>2</sub>O<sub>3</sub>) and a syringe filter (PP, 0.5  $\mu\text{m}$ ) to remove the applied catalyst and give crosslinker **L3** as a colourless, viscous oil.

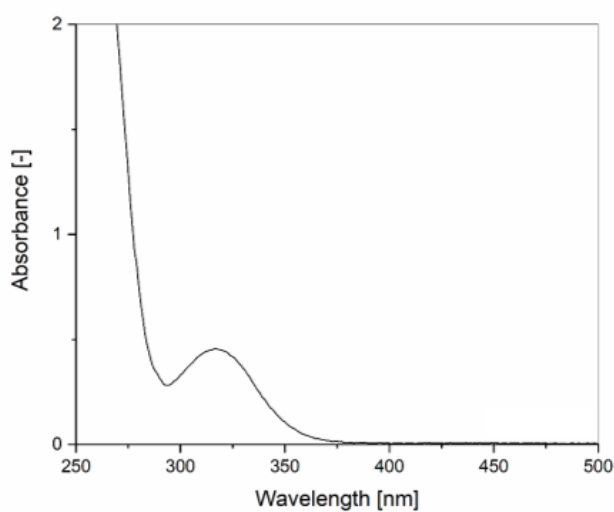
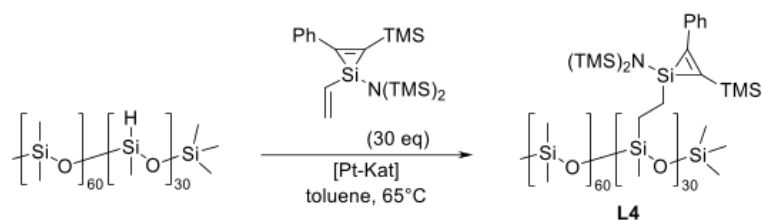


Figure S24. UV-VIS spectra of crosslinker **L3** (r.t., n-hexane,  $0.5 \times 10^{-3}$  M).



The crosslinker **L3** were synthesized according to the literature procedure provided by Rieger *et al.*<sup>[16]</sup>

A solution of PMHS (260 mg,  $M = 4900$  g/mol, 4.9 mmol/g Si-H moiety, statistical copolymer of dimethylsiloxane and hydridomethylsiloxane) in toluene (5 mL) was added to a solution of vinylsilacyclopentene (500 mg, 1.28 mmol, 1.0 eq per Si-H moiety) in toluene (5 mL). Then 53.5 mg (6.40  $\mu$ mol) of a Karstead-catalyst solution (2.25 wt.% Pt in xylene) was added, and the mixture was stirred at 65 °C for 24 h. Over the reaction time the colour changed from a bright yellow to a dark orange. All volatiles were removed under vacuum and the obtained residue was redissolved in *n*-hexane (10 mL). The crude was purified by filtration through an appropriate amount of aluminium oxide ( $\text{Al}_2\text{O}_3$ ) and a syringe filter (PP, 0.5  $\mu$ m) to remove the applied catalyst. The filter was further washed with *n*-hexane (2 mL). At last, the solvent was removed under vacuum to obtain crosslinker **L4** as yellowish viscous fluid.

Successful removal of the employed Pt-based catalyst was analyzed via ICP-OES. Prior to the applied filtration a Pt-concentration of 39.48 ppm (mg/L) was determined, while a sample after filtration resulted in a concentration of 0.0046 ppm (mg/L).

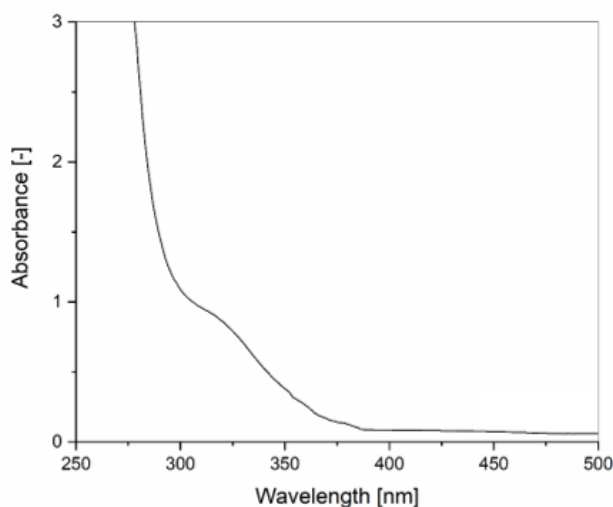


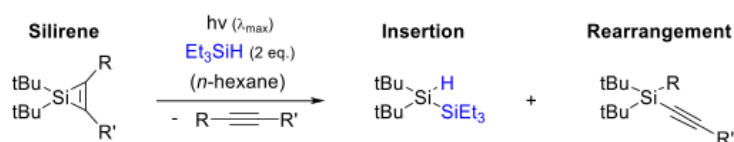
Figure S25. UV-VIS spectra of crosslinker **L4** (r.t., *n*-hexane,  $0.5 \times 10^{-3}$  M).

## 4. Photoreaction Products



**Figure S26.** Irradiation set-up for all photoreactions. Additional covers were arranged to protect the staff from harmful UV-light. Schematic layout of the setup (right) and actual images of the setup (left).

**General Procedure: Photoreaction of silirenes **E** with triethylsilane  $\text{Et}_3\text{SiH}$ .**



Silacyclopene **E** (50  $\mu\text{mol}$ , 1.00 eq.) and triethylsilane (100  $\mu\text{mol}$ , 2.00 eq.) was added to a heat-dried quartz-glass Schlenk-tube (*Duran*) in 3 mL *n*-hexane. The phototube was irradiated subsequently at given wavelength ( $\lambda_{\text{max}} = 254, 300, 325, 340, 365, \text{ or } 420 \text{ nm}$ ), temperature (25, -40, -80  $^\circ\text{C}$ ), and time (30 min – 3 d). After finalization, the reaction solution was carefully concentrated at ambient temperatures under weak vacuum to remove all solvent. The reaction mixture was resolved in 0.5 mL deuterated benzene ( $\text{C}_6\text{D}_6$ ) and directly analyzed further in the NMR.

Determination of the relative ratio of the reaction products was performed by comparing the integral of the *t*-Bu-moieties in the  $^1\text{H}$ -NMR of both products (insertion vs. rearrangement). Assignment of the respective signals (*t*-Bu-moieties in  $^1\text{H}$ - and central Si-atom  $^{29}\text{Si}$ -NMR) was realized via 2D-NMR experiments ( $^1\text{H}$ - $^{29}\text{Si}$  HMBC).



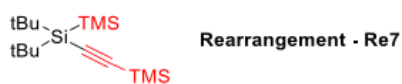
$^1\text{H}$  NMR (500 MHz,  $\text{C}_6\text{D}_6$ )  $\delta$  (ppm): 3.69 (s, 1H, Si-H), 1.14 (s, 18H, SiC-( $\text{CH}_3$ )<sub>3</sub>), 1.05 (t, 9H,  $^3J_{\text{HH}} = 8.0 \text{ Hz}$ , Si( $\text{CH}_2$ - $\text{CH}_3$ )<sub>3</sub>), 0.77 (q, 6H,  $^3J_{\text{HH}} = 8.0 \text{ Hz}$ , Si( $\text{CH}_2$ - $\text{CH}_3$ )<sub>3</sub>).

$^{29}\text{Si}$  NMR (100 MHz,  $\text{C}_6\text{D}_6$ )  $\delta$  (ppm): -6.19 ( $\text{tBu}_2$ -Si-H), -8.13 (Si-Et<sub>3</sub>).

The analytical data obtained matched those reported in the literature.<sup>[17]</sup>







**$^1\text{H}$  NMR** (500 MHz,  $\text{C}_6\text{D}_6$ )  $\delta$  (ppm): 1.20 (s, 18H,  $\text{SiC}(\text{CH}_3)_3$ ), 0.32 (s, 9H,  $\text{Si-Si}(\text{CH}_3)_3$ ), 0.17 (s, 9H,  $\text{SiCC-Si}(\text{CH}_3)_3$ ).

**$^{29}\text{Si}$  NMR** (100 MHz,  $\text{C}_6\text{D}_6$ )  $\delta$  (ppm): -14.60 ( $\text{tBu}_2\text{-Si}$ ), -18.86 ( $\text{Si-SiMe}_3$ ), -19.73 ( $\text{SiCC-SiMe}_3$ ).

The analytical data obtained matched those reported in the literature.<sup>[18,19]</sup>

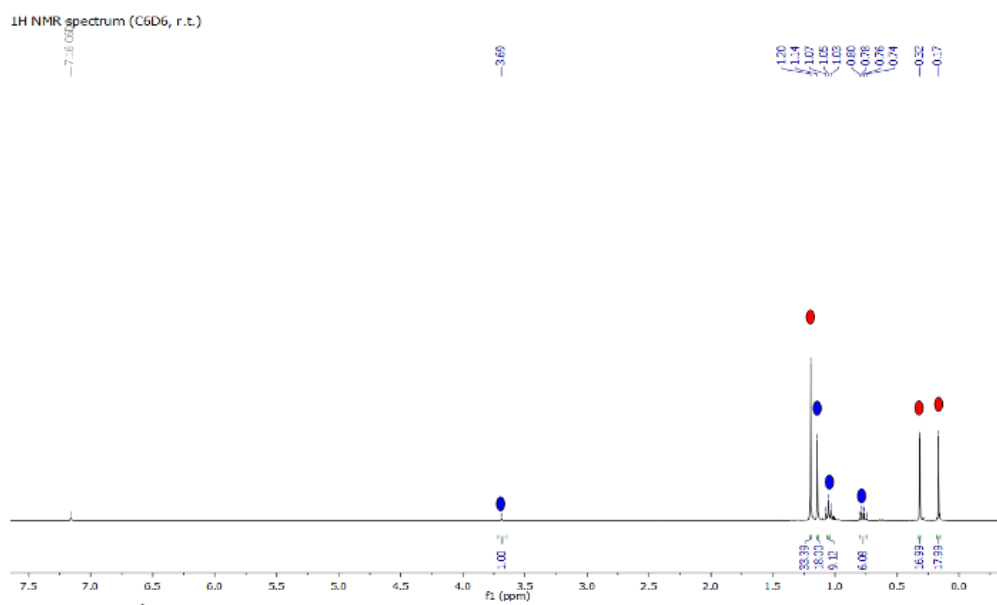


**Figure S27.**  $^1\text{H}$ -NMR (500 MHz,  $\text{C}_6\text{D}_6$ ) of photoreaction of **E7**, with the insertion (blue) and rearrangement (red) product mixture.

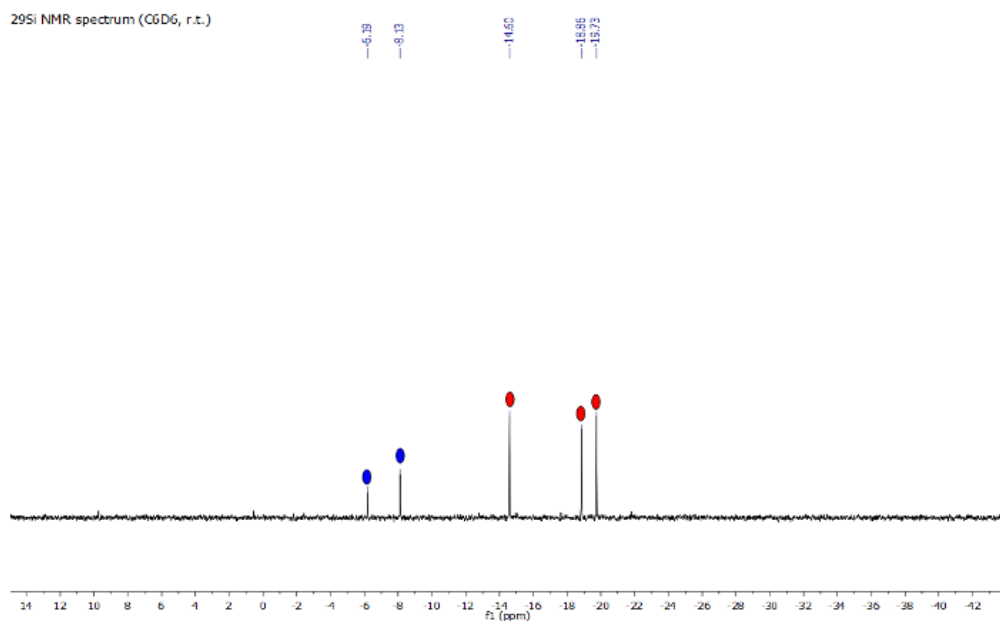


**Figure S28.**  $^{29}\text{Si}$ -NMR (100 MHz,  $\text{C}_6\text{D}_6$ ) of photoreaction of **E7**, with the insertion (blue) and rearrangement (red) product mixture.



**Figure S29.**  $^1\text{H}$ - $^{29}\text{Si}$ -HMBC (500 MHz/100 MHz,  $\text{C}_6\text{D}_6$ ) of photoreaction of **E7**, with the insertion (blue) and rearrangement (red) product mixture.

S41



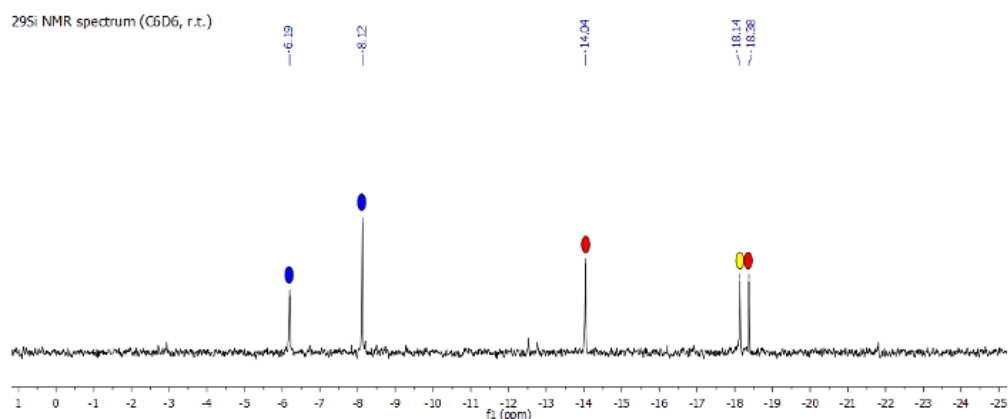


**Figure S31.** <sup>29</sup>Si-NMR (100 MHz, C<sub>6</sub>D<sub>6</sub>) of photoreaction of **E14**, with the insertion (blue), eliminated acetylene (yellow), and rearrangement (red) product mixture.



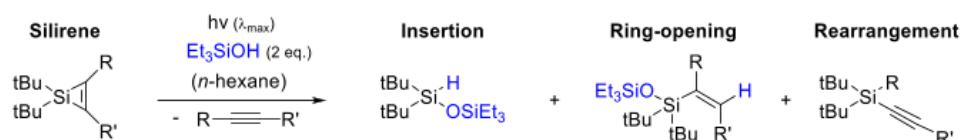
**Figure S32.** <sup>1</sup>H-<sup>29</sup>Si-HMBC (500 MHz/100 MHz, C<sub>6</sub>D<sub>6</sub>) of photoreaction of **E14**, with the insertion (blue), eliminated acetylene (yellow), and rearrangement (red) product mixture.

**Table S2.** Overview of photoreaction of silirenes **E7/E14** with triethylsilane under various conditions.

Silirene <b>E</b>	Et <sub>3</sub> SiH [eq.]	Irradiation $\lambda_{\max}$ [nm]	Solvent	Temperature [°C]	Reaction time <sup>a</sup>	Relative ratio <sup>b</sup> [rel.%] Insertion / Rearrangement
E7	2	365	<i>n</i> -hexane	25	30 min	34 / 66
E7	0	365	<i>n</i> -hexane	25	30 min	0 / 100
E7	10	365	<i>n</i> -hexane	25	30 min	35 / 65
E7	100	365	<i>n</i> -hexane	25	30 min	36 / 64
E7	2	420	<i>n</i> -hexane	25	60 min	34 / 66
E7	2	300	<i>n</i> -hexane	25	30 min	35 / 65
E7	2	365	toluene	25	30 min	33 / 67
E7	2	365	C <sub>6</sub> D <sub>12</sub>	25	30 min	35 / 65
E7	2	365	<i>n</i> -hexane	-40	24 h	50 / 50
E7	2	365	<i>n</i> -hexane	-80	72 h	79 / 21
E14	2	365	<i>n</i> -hexane	25	30 min	65 / 35
E14	0	365	<i>n</i> -hexane	25	30 min	0 / 100
E14	100	365	<i>n</i> -hexane	25	30 min	65 / 35
E14	2	420	<i>n</i> -hexane	25	- <sup>c</sup>	- / -
E14	2	300	<i>n</i> -hexane	25	30 min	63 / 37
E14	2	365	toluene	25	30 min	65 / 35
E14	2	365	C <sub>6</sub> D <sub>12</sub>	25	30 min	64 / 36
E14	2	365	<i>n</i> -hexane	-40	24 h	81 / 19
E14	2	365	<i>n</i> -hexane	-80	72 h	93 / 7

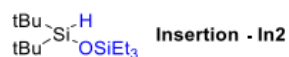
<sup>a</sup> Reaction time until full depletion of silirene **E** is observed. <sup>b</sup> Relative ratios were calculated by integral comparison of the <sup>1</sup>H-NMR-signals of the respective *t*-Bu-moieties for the insertion and the rearrangement product. <sup>c</sup> No reaction of silirene **E20** could be observed, all starting material were recovered.

**General Procedure: Photoreaction of silirenes **E** with triethylsilanol Et<sub>3</sub>SiOH.**



Silacyclopropene **E** (50  $\mu\text{mol}$ , 1.00 eq.) and triethylsilanol (100  $\mu\text{mol}$ , 2.00 eq.) was added to a heat-dried quartz-glass Schlenk-tube (*Duran*) in 3 mL *n*-hexane. The phototube was irradiated subsequently at a wavelength of  $\lambda_{\max} = 365$  nm, or 420 nm (LED), at ambient temperature for 30 min. After finalization, the reaction solution was carefully concentrated at ambient temperatures under weak vacuum to remove all solvent. The reaction mixture was resolved in 0.5 mL deuterated benzene (C<sub>6</sub>D<sub>6</sub>) and directly analyzed further in the NMR.

Determination of the relative ratio of the reaction products was performed by comparing the integral of the *t*-Bu-moieties in the <sup>1</sup>H-NMR of both products (insertion vs. ring-opening vs. rearrangement). Assignment of the respective signals (*t*-Bu-moieties in <sup>1</sup>H- and central Si-atom <sup>29</sup>Si-NMR) was realized via 2D-NMR experiments (<sup>1</sup>H-<sup>29</sup>Si HMBC).



**<sup>1</sup>H NMR** (500 MHz, C<sub>6</sub>D<sub>6</sub>)  $\delta$  (ppm): 4.33 (s, 1H, Si-H), 1.05 (s, 18H, SiC-(CH<sub>3</sub>)<sub>3</sub>), 1.01 (t, 9H, <sup>3</sup>J<sub>HH</sub> = 7.95 Hz, Si(CH<sub>2</sub>-CH<sub>3</sub>)<sub>3</sub>), 0.62 (q, 6H, <sup>3</sup>J<sub>HH</sub> = 7.95 Hz, Si-(CH<sub>2</sub>-CH<sub>3</sub>)<sub>3</sub>).

**<sup>29</sup>Si NMR** (100 MHz, C<sub>6</sub>D<sub>6</sub>)  $\delta$  (ppm): 10.99 (tBu<sub>2</sub>-Si-H), 4.51 (O-Si-Et<sub>3</sub>).

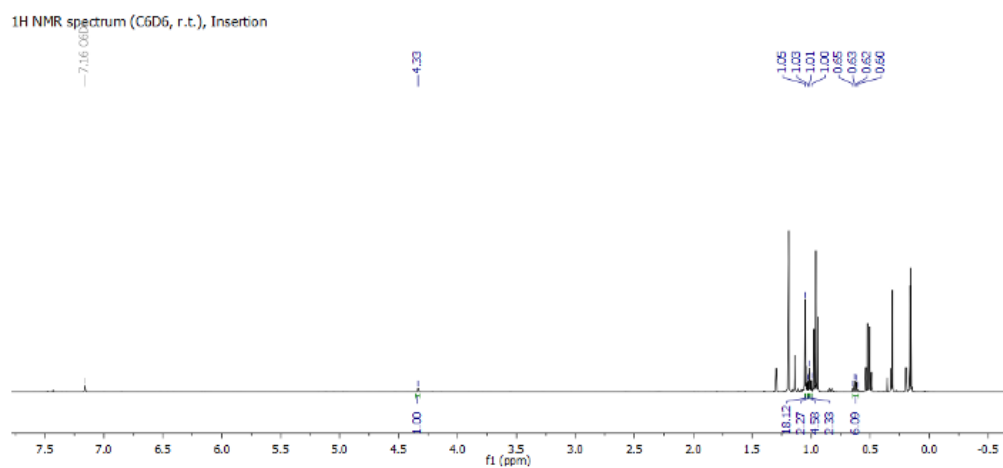


**Figure S33.** <sup>1</sup>H-NMR (500 MHz, C<sub>6</sub>D<sub>6</sub>) of photoreaction of **E7** with triethylsilanol, with the assigned insertion product.

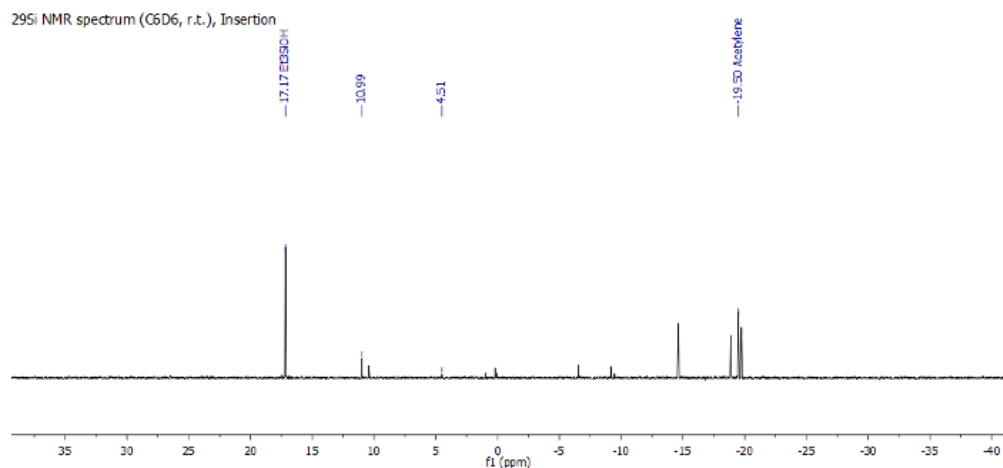


**Figure S34.** <sup>29</sup>Si-NMR (100 MHz, C<sub>6</sub>D<sub>6</sub>) of photoreaction of **E7** with triethylsilanol, with the assigned insertion product.

S45





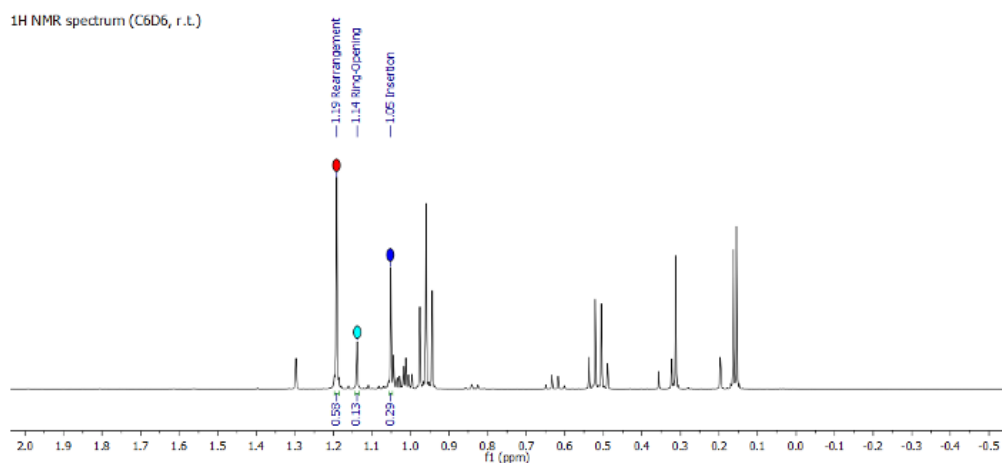


**Figure S36.** <sup>1</sup>H-NMR (500 MHz, C<sub>6</sub>D<sub>6</sub>) of photoreaction of **E7** and triethylsilanol, with the *t*Bu-signals of the insertion (dark blue), ring-opening (light blue), and rearrangement (red) product mixture.

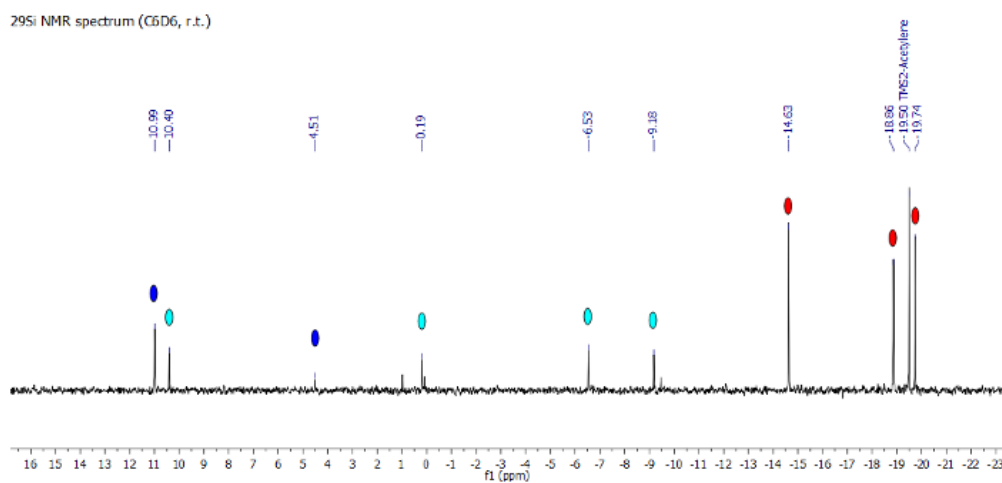


**Figure S37.** <sup>29</sup>Si-NMR (100 MHz, C<sub>6</sub>D<sub>6</sub>) of photoreaction of **E7** and triethylsilanol, with the insertion (dark blue), ring-opening (light blue), and rearrangement (red) product mixture.



<sup>1</sup>H NMR (500 MHz, C<sub>6</sub>D<sub>6</sub>)  $\delta$  (ppm): 7.43 (s, 1H, SiC-CH), 1.14 (s, 18H, SiC-(CH<sub>3</sub>)<sub>3</sub>), 1.02 (t, 9H, <sup>3</sup>J<sub>HH</sub> = 7.61 Hz, Si(CH<sub>2</sub>-CH<sub>3</sub>)<sub>3</sub>), 0.83 (q, 6H, <sup>3</sup>J<sub>HH</sub> = 7.61 Hz, Si-(CH<sub>2</sub>-CH<sub>3</sub>)<sub>3</sub>), 0.32 (s, 9H, SiC-Si(CH<sub>3</sub>)<sub>3</sub>), 0.20 (s, 9H, SiCC-Si(CH<sub>3</sub>)<sub>3</sub>).

**<sup>29</sup>Si NMR** (100 MHz, C<sub>6</sub>D<sub>6</sub>)  $\delta$  (ppm): 10.40 (O-Si-Et<sub>3</sub>), 0.19 (SiCC-SiMe<sub>3</sub>), -6.53 (tBu<sub>2</sub>-Si), -9.18 (SiC-SiMe<sub>3</sub>).

The analytical data obtained matched those reported in the literature.<sup>[17]</sup>

<sup>1</sup>H NMR spectrum (C<sub>6</sub>D<sub>6</sub>, r.t.), Ring-opening

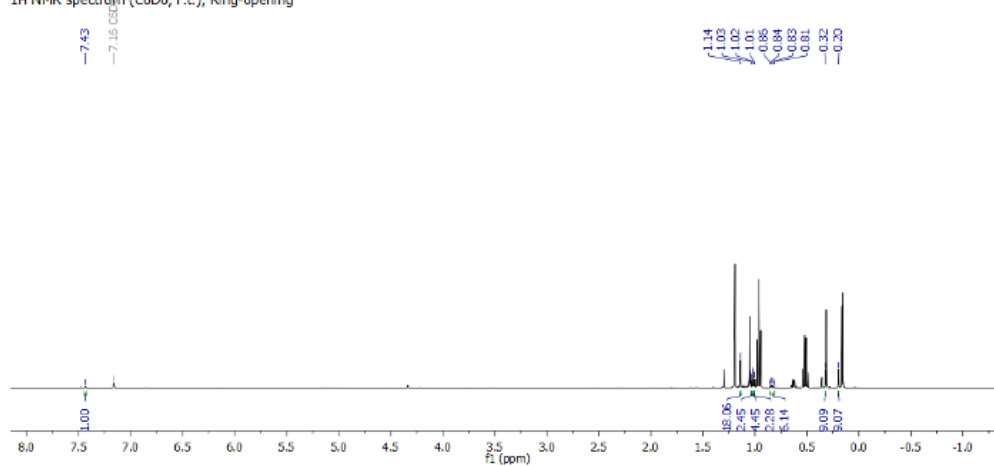


**Figure S38.** <sup>1</sup>H-NMR (500 MHz, C<sub>6</sub>D<sub>6</sub>) of photoreaction of **E7** with triethylsilanol, with the assigned ring-opening product.

<sup>29</sup>Si NMR spectrum (C<sub>6</sub>D<sub>6</sub>, r.t.), Ring-Opening

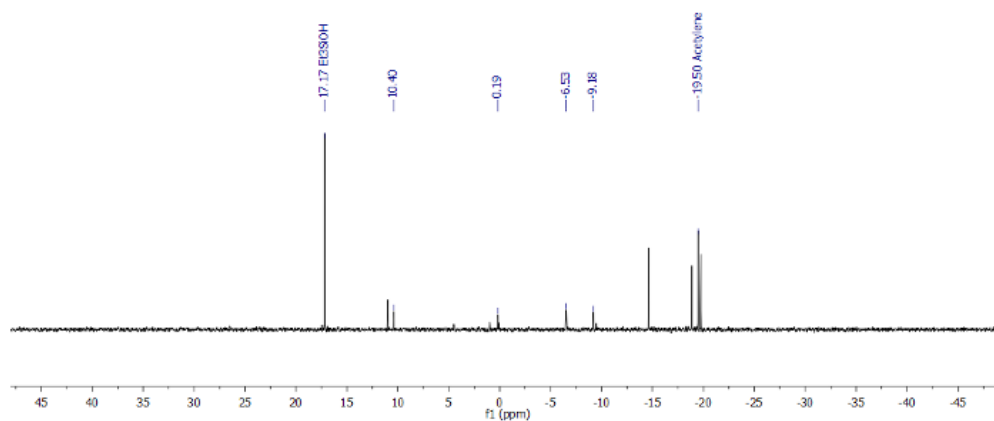


**Figure S39.** <sup>29</sup>Si-NMR (100 MHz, C<sub>6</sub>D<sub>6</sub>) of photoreaction of **E7** with triethylsilanol, with the assigned ring-opening product.

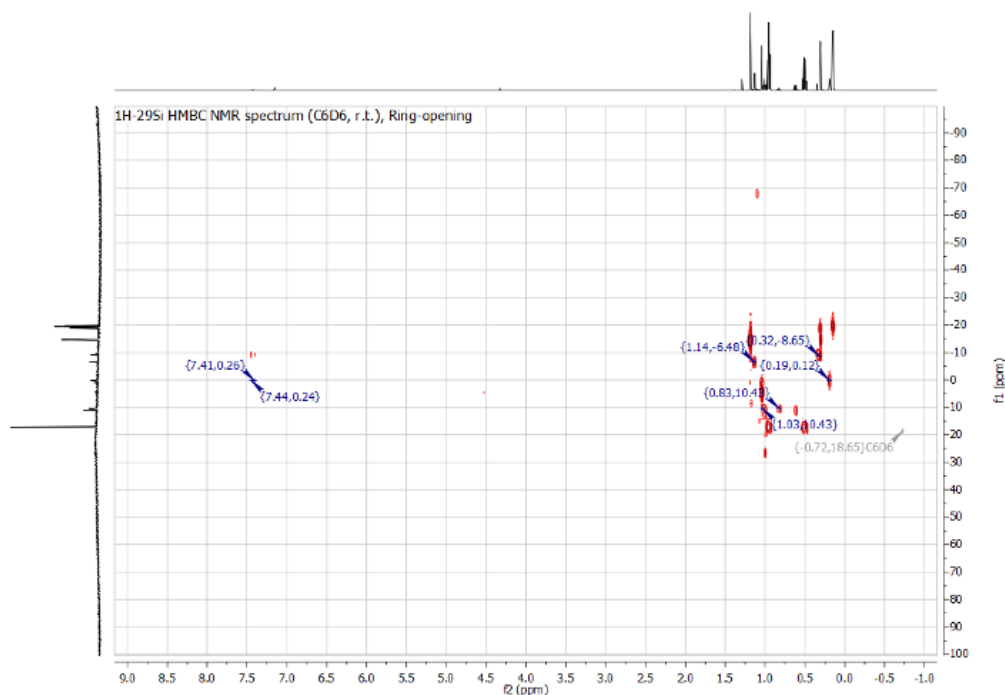
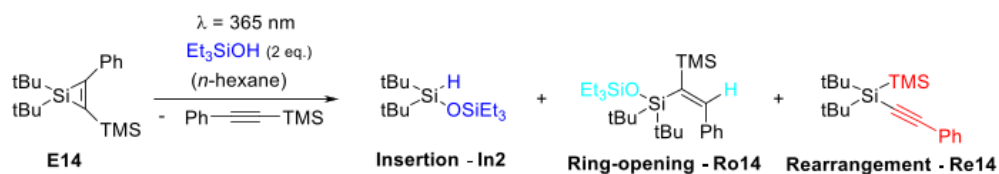


**Figure S40.**  $^1\text{H}$ - $^{29}\text{Si}$ -HMBC (500 MHz/100 MHz,  $\text{C}_6\text{D}_6$ ) of photoreaction of **E7** with triethylsilanol, with the assigned ring-opening product.

#### Photoreaction of silirene **E14** with triethylsilanol



Silacyclopropene **E14** (50  $\mu\text{mol}$ , 1.00 eq.) and triethylsilanol (100  $\mu\text{mol}$ , 2.00 eq.) was added to a heat-dried quartz-glass Schlenk-tube (*Duran*) in 3 mL *n*-hexane. The phototube was irradiated subsequently at a wavelength of  $\lambda_{\text{max}} = 365 \text{ nm}$  at ambient temperature for 30 minutes. After finalization, the reaction solution was carefully concentrated at ambient temperatures under weak vacuum to remove all solvent. The reaction mixture was resolved in 0.5 mL deuterated benzene ( $\text{C}_6\text{D}_6$ ) and directly analyzed further in the NMR.

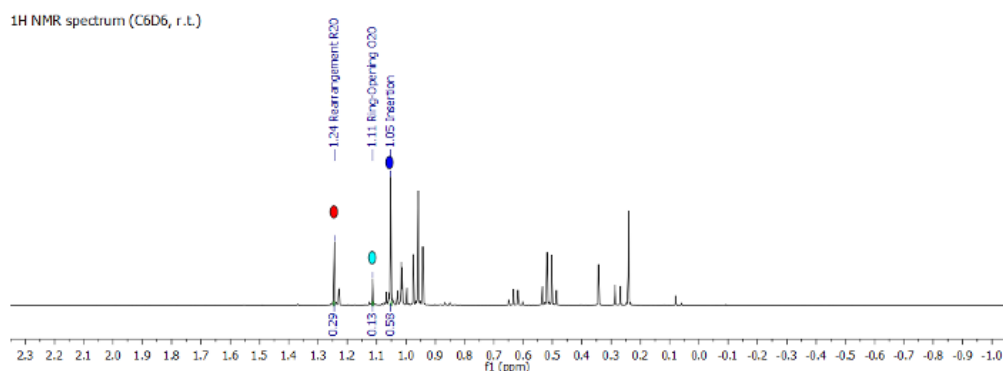


**Figure S41.** <sup>1</sup>H-NMR (500 MHz, C<sub>6</sub>D<sub>6</sub>) of photoreaction of **E14** and triethylsilanol, with the *t*Bu-signals of the insertion (dark blue), ring-opening (light blue), and rearrangement (red) product mixture.

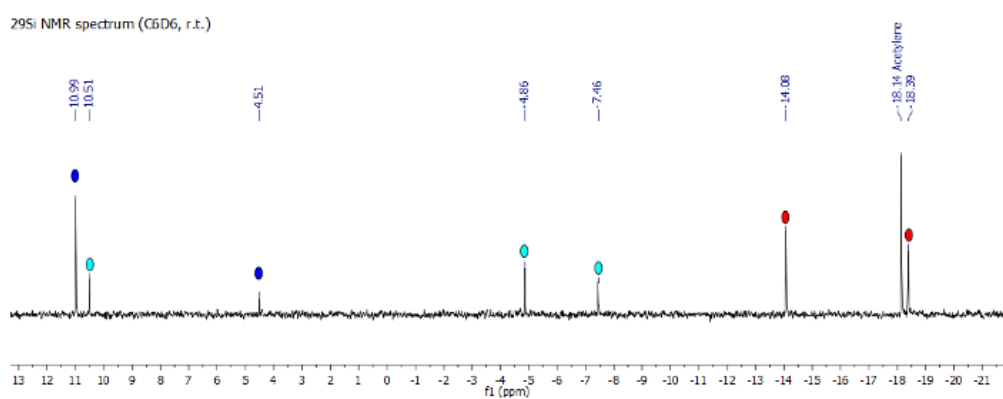
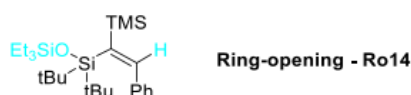


**Figure S42.** <sup>29</sup>Si-NMR (100 MHz, C<sub>6</sub>D<sub>6</sub>) of photoreaction of **E14** and triethylsilanol, with the insertion (dark blue), ring-opening (light blue), and rearrangement (red) product mixture.



<sup>1</sup>H NMR (500 MHz, C<sub>6</sub>D<sub>6</sub>)  $\delta$  (ppm): 7.43-7.42 (m, 2H, H<sub>arm.</sub>), 7.03-7.01 (m, 2H, H<sub>arm.</sub>), 6.91-6.90 (m, 1H, H<sub>arm.</sub>), 6.52 (s, 1H, SiC-CH), 1.11 (s, 18H, SiC-(CH<sub>3</sub>)<sub>3</sub>), 1.06 (t, 9H, <sup>3</sup>J<sub>HH</sub> = 7.53 Hz, Si(CH<sub>2</sub>-CH<sub>3</sub>)<sub>3</sub>), 0.86 (q, 6H, <sup>3</sup>J<sub>HH</sub> = 7.53 Hz, Si-(CH<sub>2</sub>-CH<sub>3</sub>)<sub>3</sub>), 0.29 (s, 9H, SiC-Si(CH<sub>3</sub>)<sub>3</sub>).

<sup>29</sup>Si NMR (100 MHz, C<sub>6</sub>D<sub>6</sub>)  $\delta$  (ppm): 10.51 (O-Si-Et<sub>3</sub>), -4.86 (tBu<sub>2</sub>-Si), -7.46 (SiC-SiMe<sub>3</sub>).

The analytical data obtained are consistent with those reported in the literature.<sup>[17]</sup>

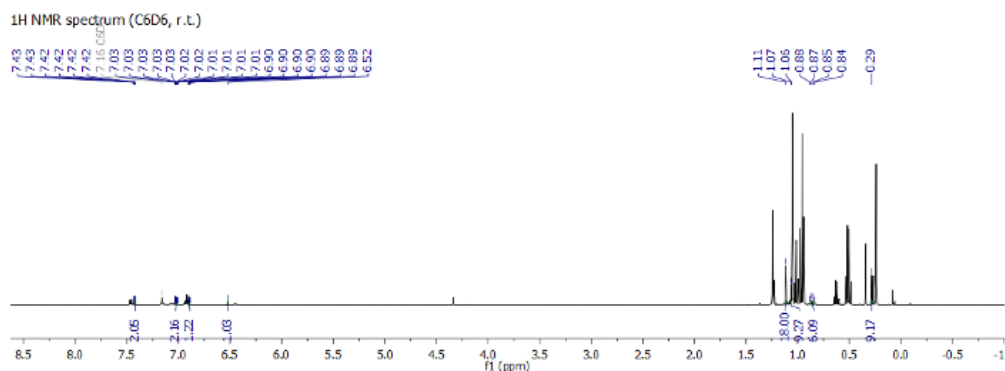


**Figure S43.** <sup>1</sup>H-NMR (500 MHz, C<sub>6</sub>D<sub>6</sub>) of photoreaction of **E14** with triethylsilanol, with the assigned ring-opening product.

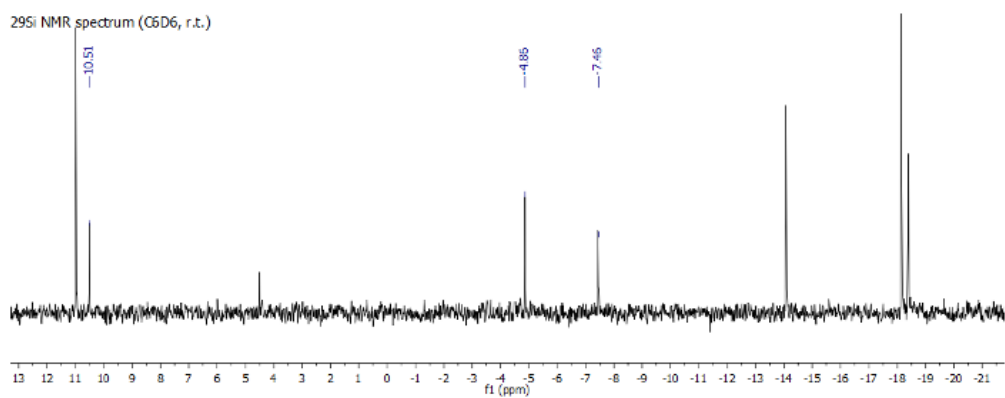


**Figure S44.** <sup>29</sup>Si-NMR (100 MHz, C<sub>6</sub>D<sub>6</sub>) of photoreaction of **E14** with triethylsilanol, with the assigned ring-opening product.

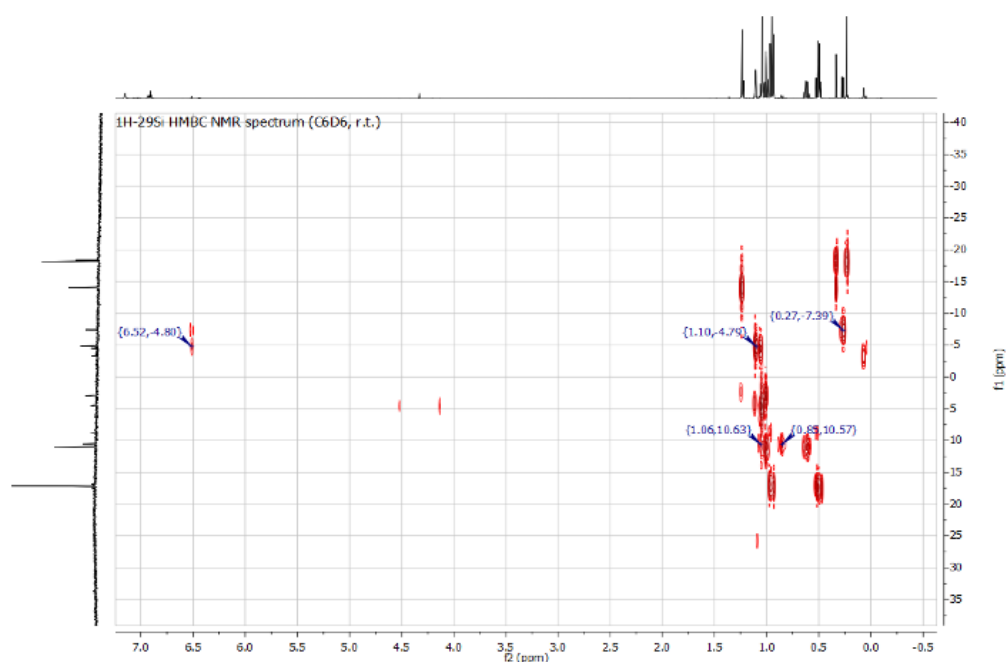


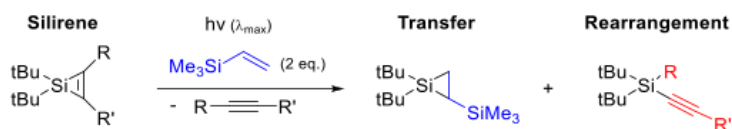
**Figure S45.**  $^1\text{H}$ - $^{29}\text{Si}$ -HMBC (500 MHz/100 MHz,  $\text{C}_6\text{D}_6$ ) of photoreaction of **E14** with triethylsilanol, with the assigned ring-opening product.

**Table S3.** Overview of photoreaction of silirenes **E7/E14** with triethylsilanol (in n-hexane), under various conditions.

Silirene <b>E</b>	$\text{Et}_3\text{SiOH}$ [eq.]	Irradiation $\lambda_{\text{max}}$ [nm]	Temperature [ $^{\circ}\text{C}$ ]	Reaction time <sup>a</sup>	Relative ratio <sup>b</sup> [rel.%]		
					Insertion	Ring-Opening	Rearrangement
E7	2	365	25	30 min	29 /	13 /	58
E7	0	365	25	30 min	0 /	0 /	100
E7	10	365	25	30 min	28 /	16 /	56
E7	2	420	25	30 min	30 /	17 /	53
E7	2	365	-40	30 h	48 /	6 /	46
E14	2	365	25	30 min	59 /	14 /	27
E14	0	365	25	30 min	0 /	0 /	100
E14	10	365	25	30 min	57 /	13 /	30
E14	2	420	25	- <sup>c</sup>	- /	- /	-
E14	2	365	-40	30 h	79 /	5 /	16

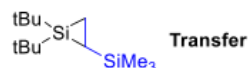
<sup>a</sup> Reaction time until full depletion of silirene **E** is observed. <sup>b</sup> Relative ratios were calculated by integral comparison of the  $^1\text{H}$ -NMR-signals of the respective *t*-Bu-moieties for the insertion, ring-opening, and the rearrangement product. <sup>c</sup> No reaction of silirene **E14** could be observed, all starting material were recovered.

**General Procedure: Photoreaction of silirenes **E** with trimethyl-vinylsilane  $\text{Me}_3\text{SiCHCH}_2$ .**



Silacyclopropene **E** (50  $\mu\text{mol}$ , 1.00 eq.) and trimethyl-vinylsilane (100  $\mu\text{mol}$ , 2.00 eq.) was added to a heat-dried quartz-glass Schlenk-tube (*Duran*) in 3 mL *n*-hexane. The phototube was irradiated subsequently at given wavelength ( $\lambda_{\text{max}} = 365$ , or 420 nm), temperature (25, -40, -80  $^\circ\text{C}$ ), and time (30 min – 3 d). After finalization, the reaction solution was carefully concentrated at ambient temperatures under weak vacuum to remove all solvent. The reaction mixture was resolved in 0.5 mL deuterated benzene ( $\text{C}_6\text{D}_6$ ) and directly analyzed further in the NMR.

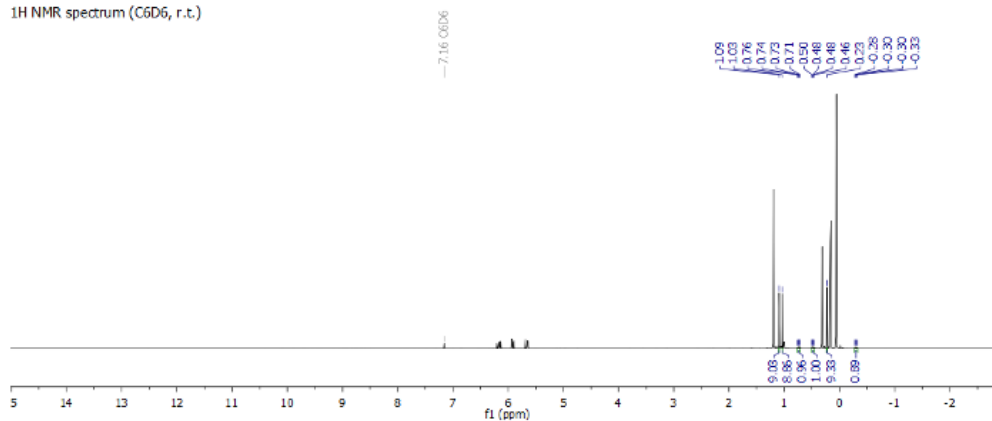
Determination of the relative ratio of the reaction products was performed by comparing the integral of the *t*-Bu-moieties in the  $^1\text{H}$ -NMR of both products (transfer vs. rearrangement). Assignment of the respective signals (*t*-Bu-moieties in  $^1\text{H}$ - and central Si-atom  $^{29}\text{Si}$ -NMR) was realized via 2D-NMR experiments ( $^1\text{H}$ - $^{29}\text{Si}$  HMBC).



**$^1\text{H}$  NMR** (500 MHz,  $\text{C}_6\text{D}_6$ )  $\delta$  (ppm): 1.09 (s, 9H, SiC-( $\text{CH}_3$ )<sub>3</sub>), 1.03 (s, 9H, SiC-( $\text{CH}_3$ )<sub>3</sub>), 0.73 (dd, 1H,  $^2J_{\text{HH}} = 13.0$  Hz,  $^3J_{\text{HH}} = 10.2$  Hz *t*BuSi-( $\text{CH}_2$ )-CHSi), 0.48 (dd, 1H,  $^3J_{\text{HH}} = 11.7$  Hz,  $^3J_{\text{HH}} = 10.2$  Hz *t*BuSiCH<sub>2</sub>-( $\text{CH}$ )-Si), 0.23 (s, 9H, Si-( $\text{CH}_3$ )<sub>3</sub>), -0.30 (dd, 1H,  $^2J_{\text{HH}} = 13.0$  Hz,  $^3J_{\text{HH}} = 11.7$  Hz *t*BuSi-( $\text{CH}_2$ )-CHSi).

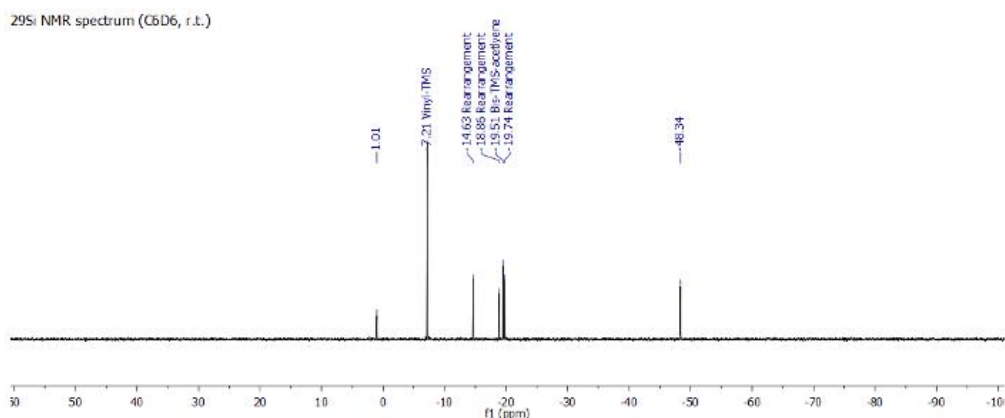
**$^{29}\text{Si}$  NMR** (100 MHz,  $\text{C}_6\text{D}_6$ )  $\delta$  (ppm): 1.01 ( $\text{Si}_{\text{TMS}}$ ), -48.34 ( $\text{Si}_{\text{tBu}}$ ).

$^1\text{H}$  NMR spectrum ( $\text{C}_6\text{D}_6$ , r.t.)

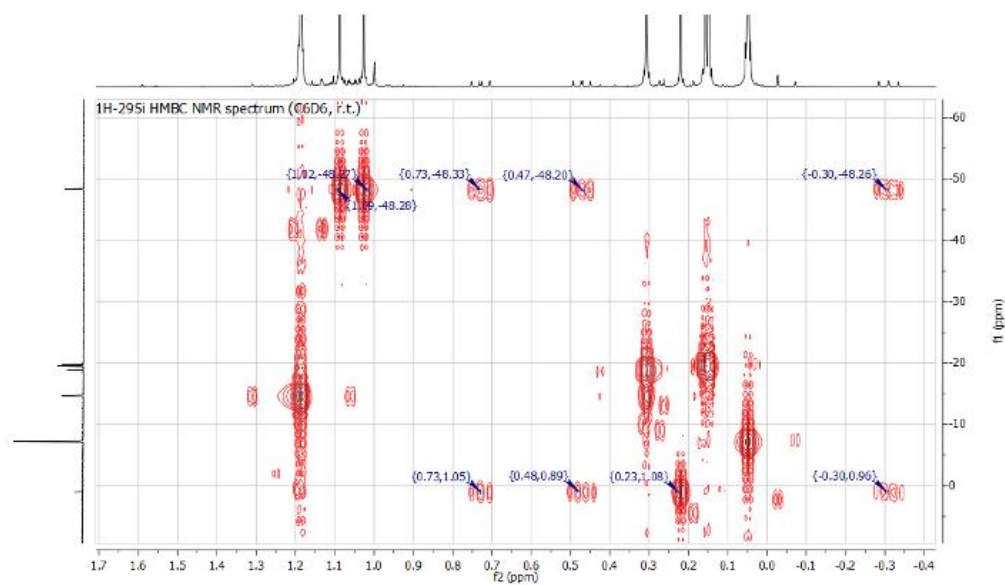


**Figure S46.**  $^1\text{H}$ -NMR (500 MHz,  $\text{C}_6\text{D}_6$ ) of photoreaction of **E7** with vinyltrimethylsilane, with the assigned silirane product.

S53

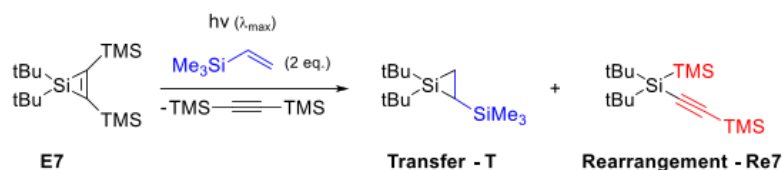


**Figure S47.** <sup>29</sup>Si-NMR (100 MHz, C<sub>6</sub>D<sub>6</sub>) of photoreaction of **E7** with triethylsilanol, with the assigned silirane product.

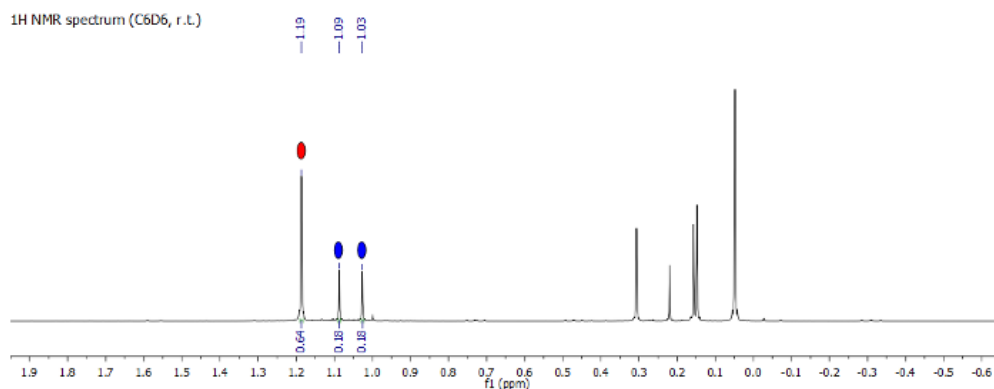


**Figure S48.** <sup>1</sup>H-<sup>29</sup>Si-HMBC (500 MHz/100 MHz, C<sub>6</sub>D<sub>6</sub>) of photoreaction of **E7** with vinyltrimethylsilane, with the assigned silirane product.

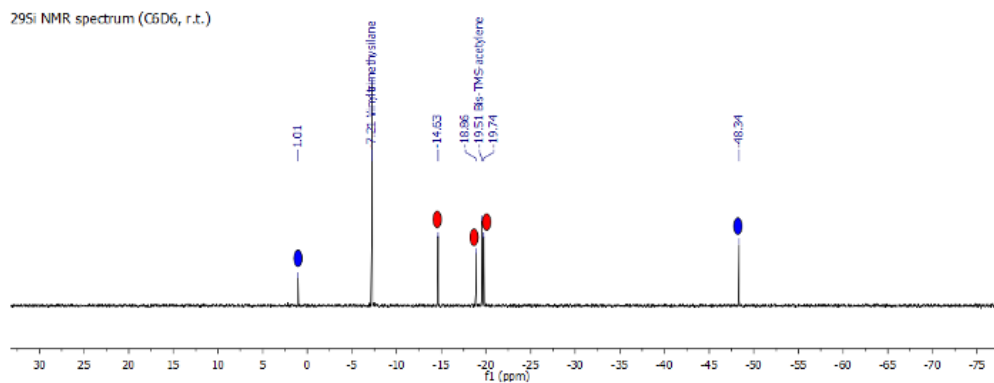


Photoreaction of silirene **E7** with triethylsilanol

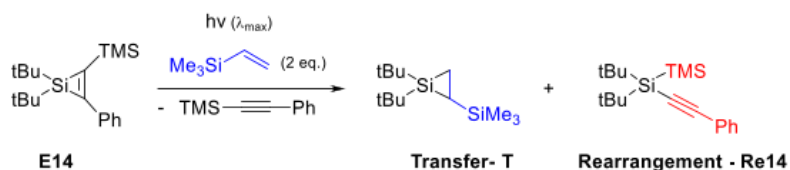
Silacyclopentene **E7** (50  $\mu\text{mol}$ , 1.00 eq.) and trimethyl-vinylsilane (100  $\mu\text{mol}$ , 2.00 eq.) was added to a heat-dried quartz-glass Schlenk-tube (*Duran*) in 3 mL *n*-hexane. The phototube was irradiated subsequently at a wavelength of  $\lambda_{\text{max}} = 365$  for time 30 min. After finalization, the reaction solution was carefully concentrated at ambient temperatures under weak vacuum to remove all solvent. The reaction mixture was resolved in 0.5 mL deuterated benzene ( $\text{C}_6\text{D}_6$ ) and directly analyzed further in the NMR.



**Figure S49.** <sup>1</sup>H-NMR (500 MHz,  $\text{C}_6\text{D}_6$ ) of photoreaction of **E7** and vinyltrimethylsilane, with the *t*Bu-signals of the **transfer** (blue), and **rearrangement** (red) product **Re7** mixture.



**Figure S50.** <sup>29</sup>Si-NMR (100 MHz,  $\text{C}_6\text{D}_6$ ) of photoreaction of **E7** and triethylsilanol, with the insertion (dark blue), and **rearrangement** (red) product mixture.

Photoreaction of silirene **E20** with triethylsilanol

Silacyclopene **E14** (50  $\mu\text{mol}$ , 1.00 eq.) and trimethyl-vinylsilane (100  $\mu\text{mol}$ , 2.00 eq.) was added to a heat-dried quartz-glass Schlenk-tube (*Duran*) in 3 mL *n*-hexane. The phototube was irradiated subsequently at a wavelength of  $\lambda_{\text{max}} = 365$  for time 30 min. After finalization, the reaction solution was carefully concentrated at ambient temperatures under weak vacuum to remove all solvent. The reaction mixture was resolved in 0.5 mL deuterated benzene ( $\text{C}_6\text{D}_6$ ) and directly analyzed further in the NMR.

$^1\text{H}$  NMR spectrum ( $\text{C}_6\text{D}_6$ , r.t.)

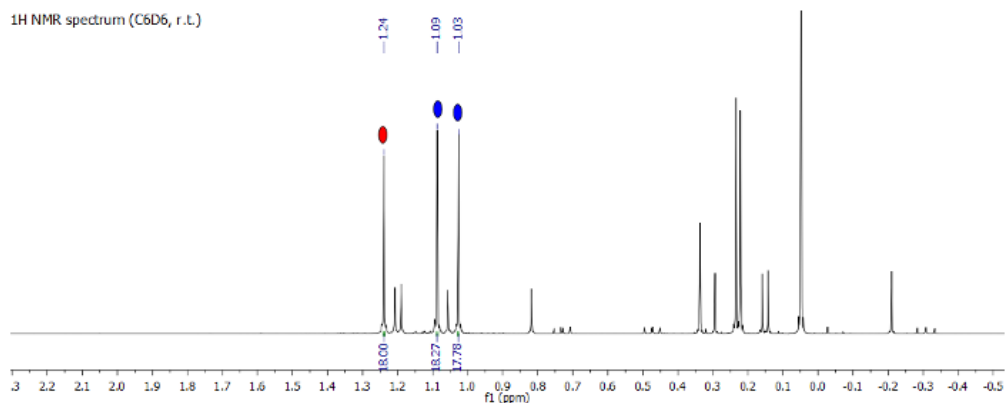


**Figure S51.**  $^1\text{H}$ -NMR (500 MHz,  $\text{C}_6\text{D}_6$ ) of photoreaction of **E14** and vinyltrimethylsilane, with the *t*Bu-signals of the transfer (blue) and rearrangement (red) **Re14** product mixture.

$^{29}\text{Si}$  NMR spectrum ( $\text{C}_6\text{D}_6$ , r.t.)

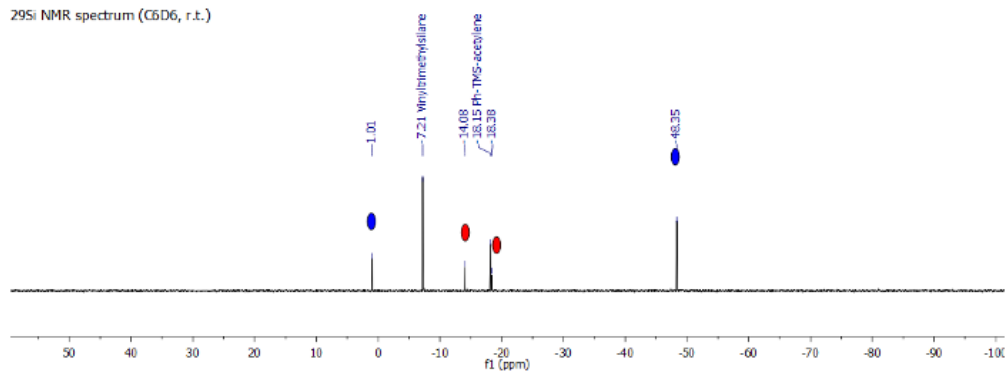


**Figure S52.**  $^{29}\text{Si}$ -NMR (100 MHz,  $\text{C}_6\text{D}_6$ ) of photoreaction of **E14** and vinyltrimethylsilane, with the transfer (blue), and rearrangement (red) **Re14** product mixture.

**Table S4.** Overview of photoreaction of silirenes **E7/14** with vinyltrimethylsilane (in *n*-hexane), under various conditions.

Silirene <b>E</b>	Me <sub>3</sub> Si-Vinyl [eq.]	Irradiation $\lambda_{\text{max}}$ [nm]	Solvent	Temperature [°C]	Reaction time <sup>a</sup>	Relative ratio <sup>b</sup> [rel.%] Transfer / Rearrangement
E7	2	365	<i>n</i> -hexane	25	30 min	36 / 64
E7	10	365	<i>n</i> -hexane	25	30 min	36 / 64
E7	2	420	<i>n</i> -hexane	25	60 min	37 / 63
E7	2	300	<i>n</i> -hexane	25	30 min	33 / 67
E7	2	365	C <sub>6</sub> D <sub>6</sub>	25	30 min	35 / 65
E7	2	365	<i>n</i> -hexane	-40	30 h	53 / 47
E14	2	365	<i>n</i> -hexane	25	30 min	69 / 31
E14	2	420	<i>n</i> -hexane	25	30 min	- / - <sup>c</sup>
E14	2	300	<i>n</i> -hexane	25	30 min	65 / 35
E14	2	265	<i>n</i> -hexane	25	30 min	- / - <sup>d</sup>
E14	2	365	<i>n</i> -hexane	-40	30 h	78 / 22

<sup>a</sup> Reaction time until full depletion of silirene **E** is observed. <sup>b</sup> Relative ratios were calculated by integral comparison of the <sup>1</sup>H-NMR-signals of the respective *t*-Bu-moieties for the transfer and the rearrangement product. <sup>c</sup> No reaction of silirene **E14** could be observed, all starting material were recovered. <sup>d</sup> Full decomposition of silirene **E14**, without explicit product formation visible (presumably further decomposition of the silirane product by hard UV-light).

## c) Figures and Tables

## 1. Rheologic Measurements

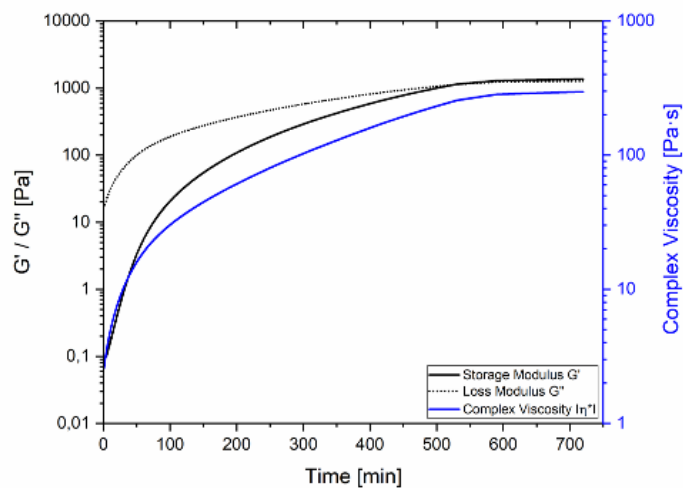


**Figure S53.** Storage, loss modulus and complex viscosity of crosslinked elastomer made from **L4** and terminal Si-OH PDMS ( $n \sim 484$ ) in a ratio of 0.8 (silirene/Si-OH), while irr. with  $\lambda = 365\text{nm}$  (LED).

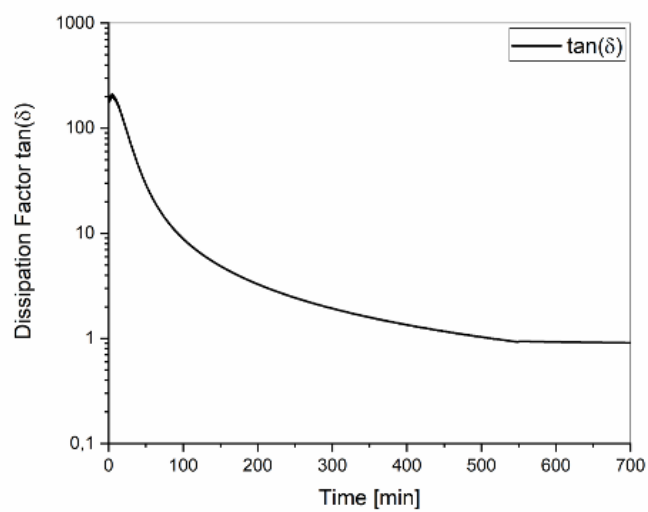


**Figure S54.** Dissipation factor  $\tan(\delta)$  of crosslinker **L4** and terminal Si-OH PDMS ( $n \sim 484$ ) in a ratio of 0.8 (silirene/Si-OH), while irradiation with  $\lambda = 365\text{nm}$  (LED).

S58

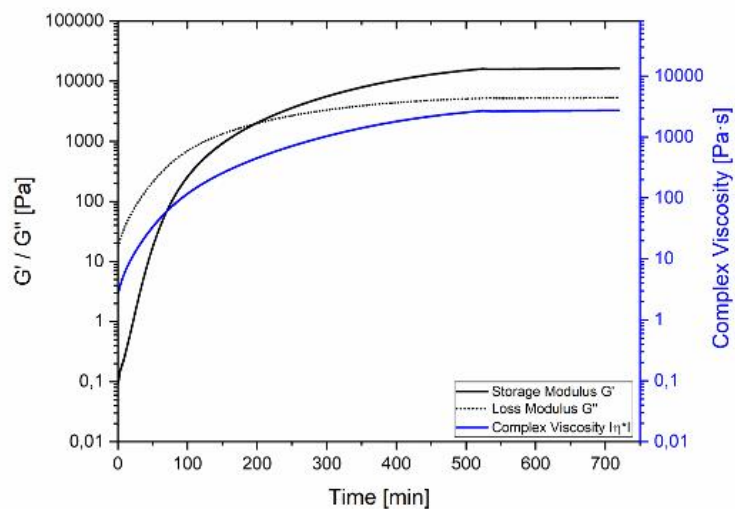


**Figure S55.** Storage, loss modulus and complex viscosity of crosslinked elastomer made from **L4** and terminal Si-OH PDMS ( $n \sim 484$ ) in a ratio of 1.0 (silirene/Si-OH), while irr. with  $\lambda = 365\text{nm}$  (LED).

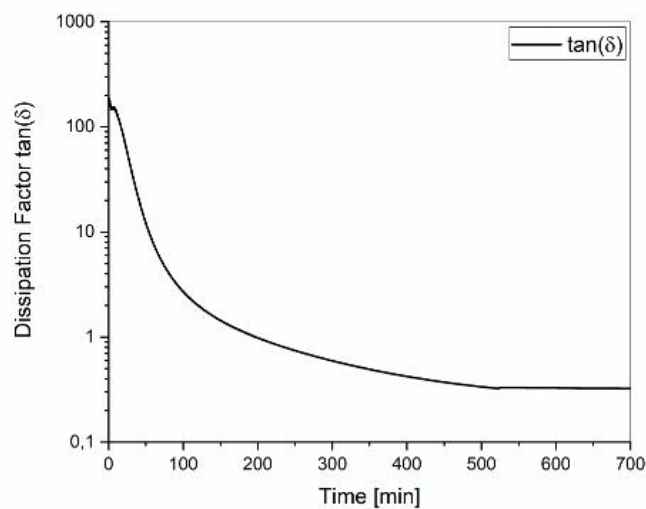


**Figure S56.** Dissipation factor  $\tan(\delta)$  of crosslinker **L4** and terminal Si-OH PDMS ( $n \sim 484$ ) in a ratio of 1.0 (silirene/Si-OH), while irradiation with  $\lambda = 365\text{nm}$  (LED).

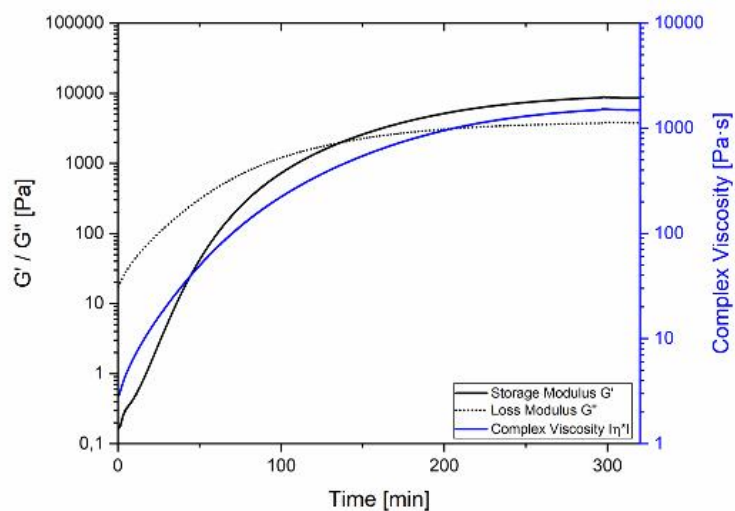


**Figure S57.** Storage, loss modulus and complex viscosity of crosslinked elastomer made from **L4** and terminal Si-OH PDMS ( $n \sim 484$ ) in a ratio of 2.0 (silirene/Si-OH), while irr. with  $\lambda = 365\text{nm}$  (LED).

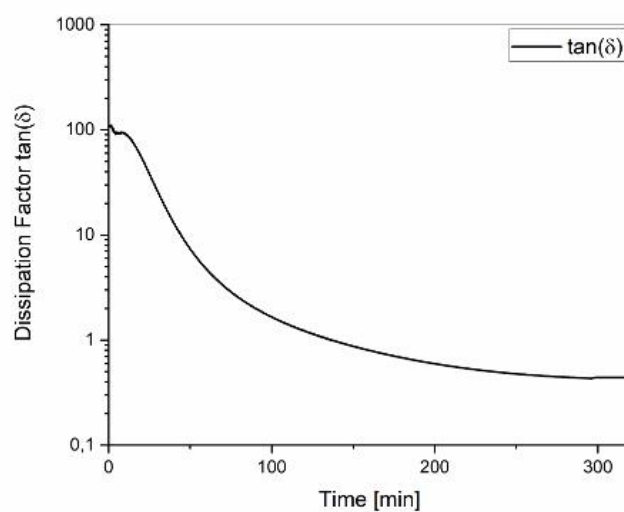


**Figure S58.** Dissipation factor  $\tan(\delta)$  of crosslinker **L4** and terminal Si-OH PDMS ( $n \sim 484$ ) in a ratio of 2.0 (silirene/Si-OH), while irradiation with  $\lambda = 365\text{nm}$  (LED).

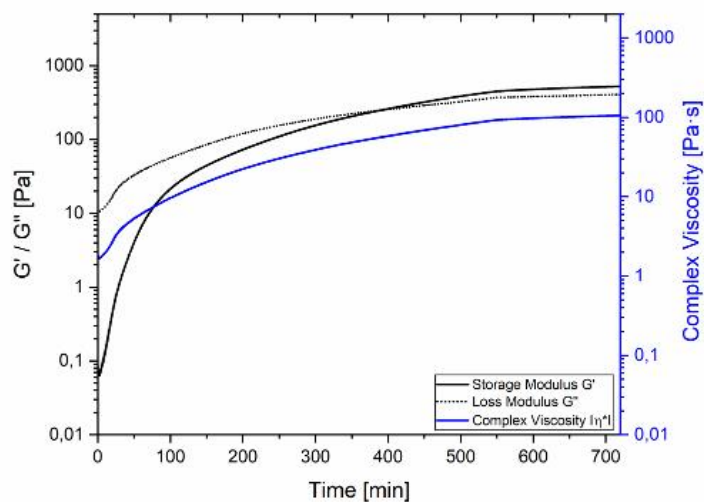


**Figure S59.** Storage, loss modulus and complex viscosity of crosslinked elastomer made from **L4** and terminal Si-H PDMS ( $n \sim 378$ ) in a ratio of 0.8 (silirene/Si-H), while irradiation with  $\lambda = 365\text{nm}$  (LED).

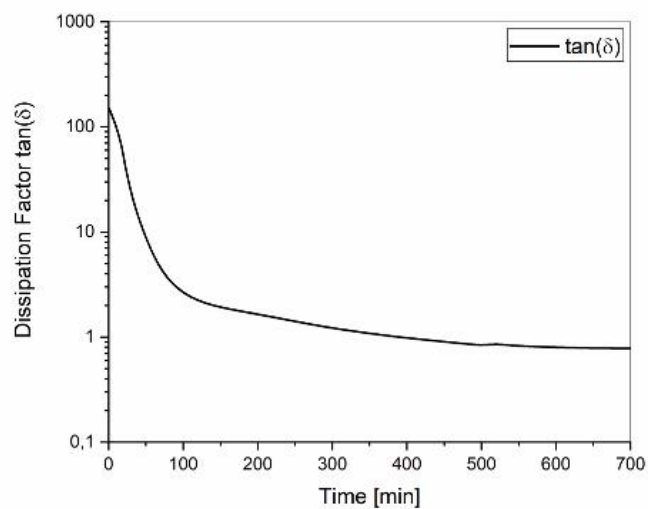


**Figure S60.** Dissipation factor  $\tan(\delta)$  of crosslinker **L4** and terminal Si-H PDMS ( $n \sim 378$ ) in a ratio of 0.8 (silirene/Si-H), while irradiation with  $\lambda = 365\text{nm}$  (LED).

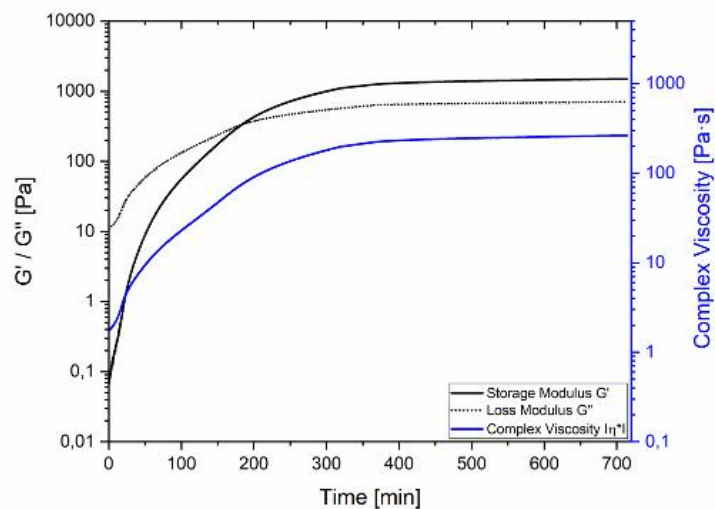


**Figure S61.** Storage, loss modulus and complex viscosity of crosslinked elastomer made from **L4** and terminal Si-H PDMS ( $n \sim 378$ ) in a ratio of 1.0 (silirene/Si-H), while irradiation with  $\lambda = 365\text{nm}$  (LED).

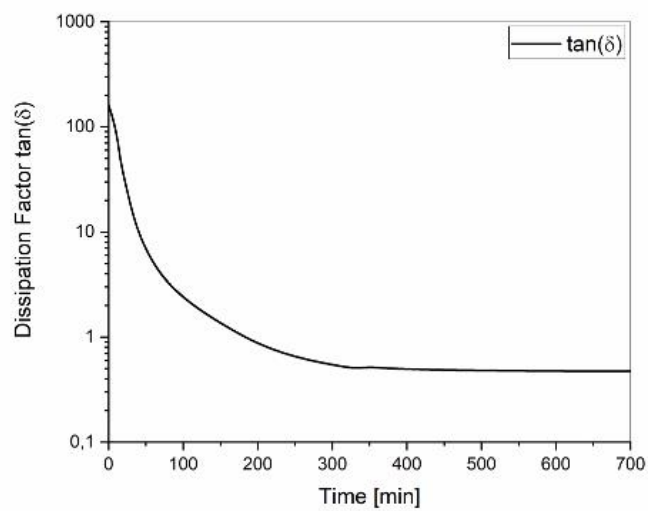


**Figure S62.** Dissipation factor  $\tan(\delta)$  of crosslinker **L4** and terminal Si-H PDMS ( $n \sim 378$ ) in a ratio of 1.0 (silirene/Si-H), while irradiation with  $\lambda = 365\text{nm}$  (LED).

S62



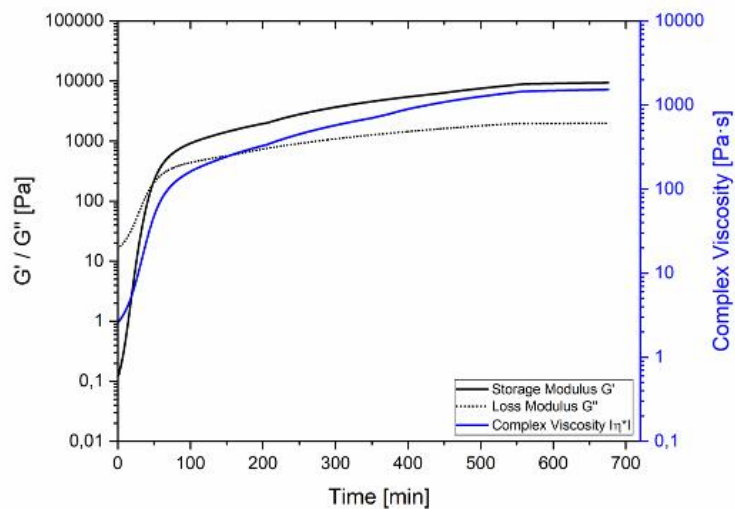


**Figure S63.** Storage, loss modulus and complex viscosity of crosslinked elastomer made from **L4** and terminal Si-H PDMS ( $n \sim 378$ ) in a ratio of 2.0 (silirene/Si-H), while irradiation with  $\lambda = 365\text{nm}$  (LED).

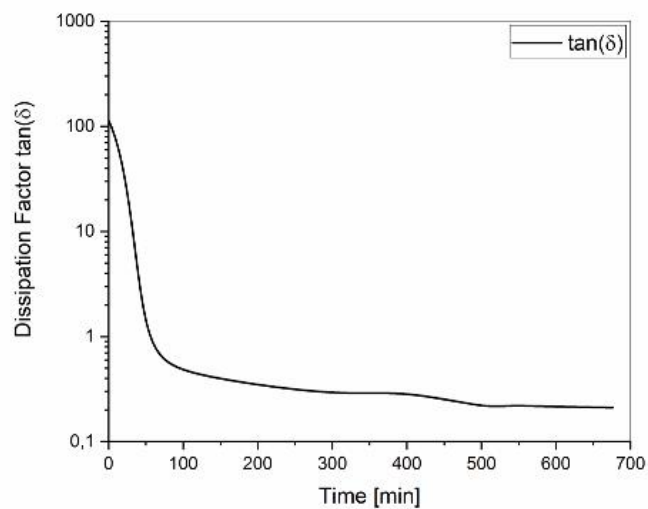


**Figure S64.** Dissipation factor  $\tan(\delta)$  of crosslinker **L4** and terminal Si-H PDMS ( $n \sim 378$ ) in a ratio of 2.0 (silirene/Si-H), while irradiation with  $\lambda = 365\text{nm}$  (LED).

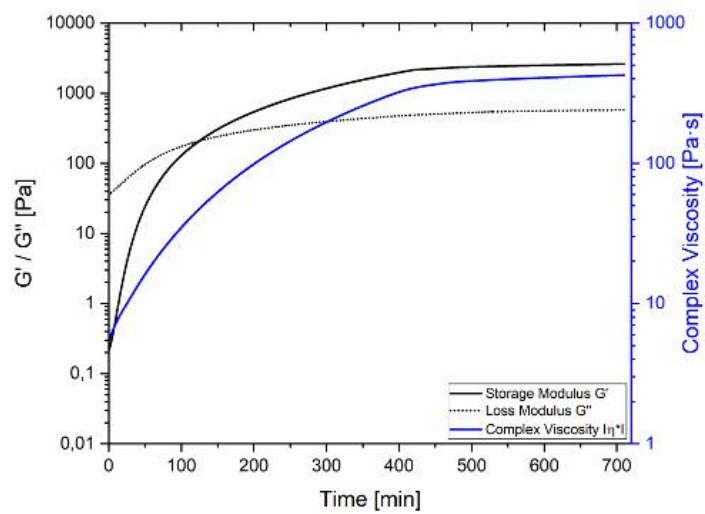


**Figure S65.** Storage, loss modulus and complex viscosity of crosslinked elastomer made from **L4** and terminal Si-vinyl PDMS ( $n \sim 376$ ) in a ratio of 0.8 (silirene/Si-vinyl), while irr. with  $\lambda = 365\text{nm}$  (LED).

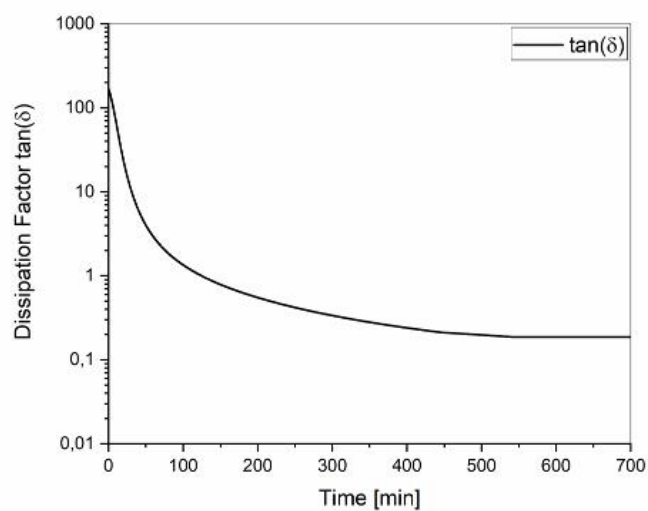


**Figure S66.** Dissipation factor  $\tan(\delta)$  of crosslinker **L4** and terminal Si-vinyl PDMS ( $n \sim 376$ ) in a ratio of 0.8 (silirene/Si-vinyl), while irradiation with  $\lambda = 365\text{nm}$  (LED).

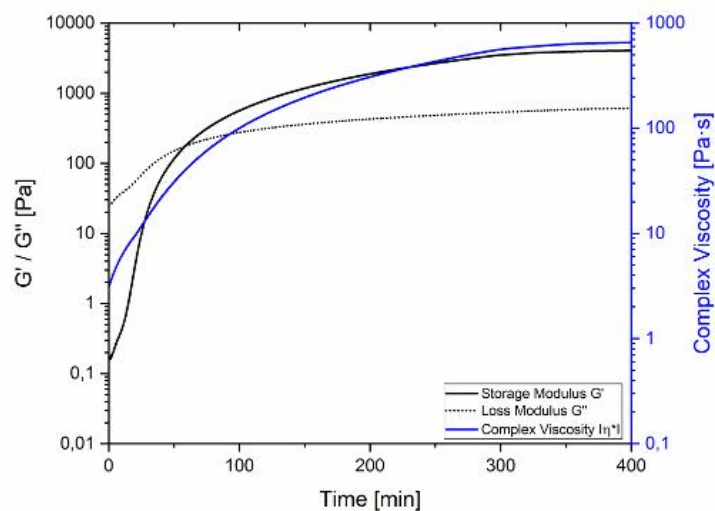


**Figure S67.** Storage, loss modulus and complex viscosity of crosslinked elastomer made from **L4** and terminal Si-vinyl PDMS ( $n \sim 376$ ) in a ratio of 1.0 (silirene/Si-vinyl), while irr. with  $\lambda = 365\text{nm}$  (LED).

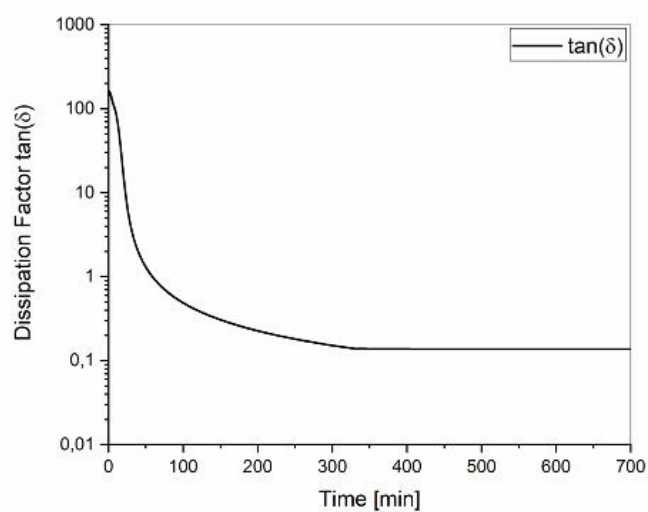


**Figure S68.** Dissipation factor  $\tan(\delta)$  of crosslinker **L4** and terminal Si-vinyl PDMS ( $n \sim 376$ ) in a ratio of 1.0 (silirene/Si-vinyl), while irradiation with  $\lambda = 365\text{nm}$  (LED).

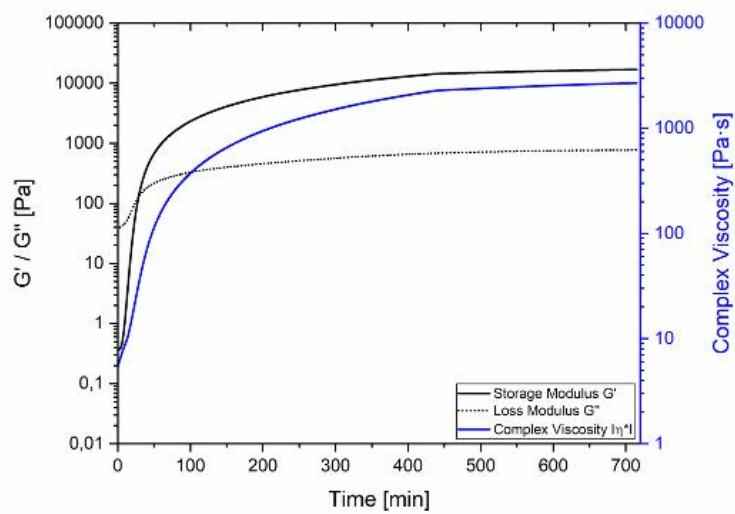


**Figure S69.** Storage, loss modulus and complex viscosity of crosslinked elastomer made from **L4** and terminal Si-vinyl PDMS ( $n \sim 376$ ) in a ratio of 2.0 (silirene/Si-vinyl), while irr. with  $\lambda = 365\text{nm}$  (LED).

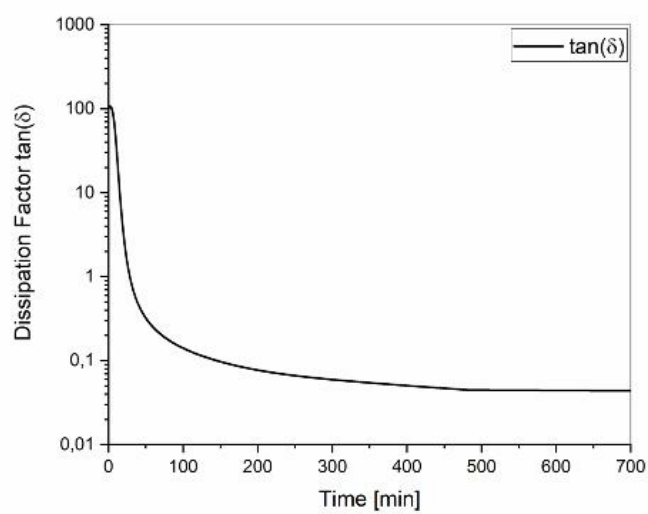


**Figure S70.** Dissipation factor  $\tan(\delta)$  of crosslinker **L4** and terminal Si-vinyl PDMS ( $n \sim 376$ ) in a ratio of 2.0 (silirene/Si-vinyl), while irradiation with  $\lambda = 365\text{nm}$  (LED).

**Table S5.** Overview of curing experiments with crosslinker **L4** and the respective PDMS. Determination of the time-point of the sol/gel transition ( $t_{SG}$ ), values for the final dissipation factor ( $\tan(\delta)$ ), complex viscosity ( $|\eta^*|$ ), storage modulus ( $G'$ ), and loss modulus ( $G''$ ).

PDMS	ratio	$t_{SG}$ [min] <sup>III</sup>	$\tan(\delta)_{final}$	$ \eta^* _{final}$ [Pa·s]	$G'_{final}$ [Pa]	$G''_{final}$ [Pa]
<b>term. Si-OH</b>	0.8	518	0.93	299,7	1363.6	1274.2
<b>term. Si-OH</b>	1.0	190	0.42	1478	8773	3803
<b>term. Si-OH</b>	2.0	135	0.32	2688	16379	5266
<b>term. Si-H</b>	0.8	395	0.78	101.7	512.5	398.2
<b>term. Si-H</b>	1.0	183	0.47	264.4	1492	696.7
<b>term. Si-H</b>	2.0	47	0.21	1543	9523	1960
<b>term. Si-vinyl</b>	0.8	125	0.23	650.7	2588	577.6
<b>term. Si-vinyl</b>	1.0	59	0.14	1765	4072	603.0
<b>term. Si-vinyl</b>	2.0	28	0.046	2656	16379	787.5

<sup>III</sup> sol/gel-transition was defined at  $\tan(\delta) = 1$  and sets the crossover point for  $G' = G''$ .

## 2. Light Control Reactions

The following measurements have been performed to identify and proof for a solely light-controlled curing process. By turning off and on the light-source the curing progress can be stopped (by turning off the light) and started/continued again (by turning on the light). To exclude thermal initiated curing by the heat of the light-source the measurement system was actively cooled to 20°C during the whole process.

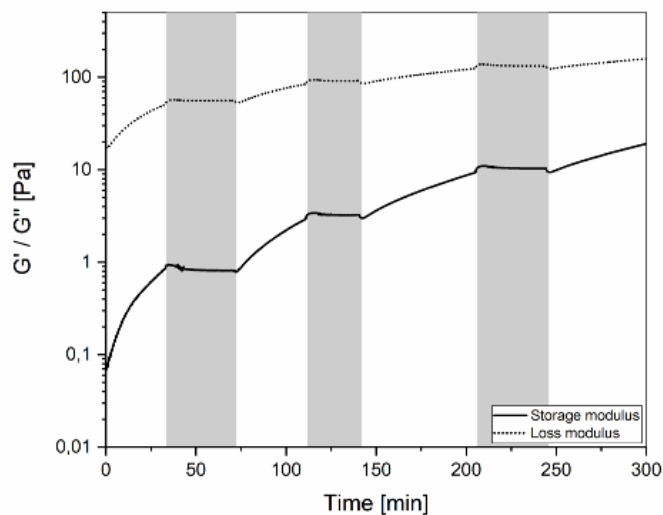


**Figure S 71.** Control photo-curing with crosslinker **X** and terminal Si-vinyl PDMS (n~376) in a ratio of 0.5. White areas display curing with irradiation ( $\lambda = 365\text{nm}$ ), grey areas without irradiation.

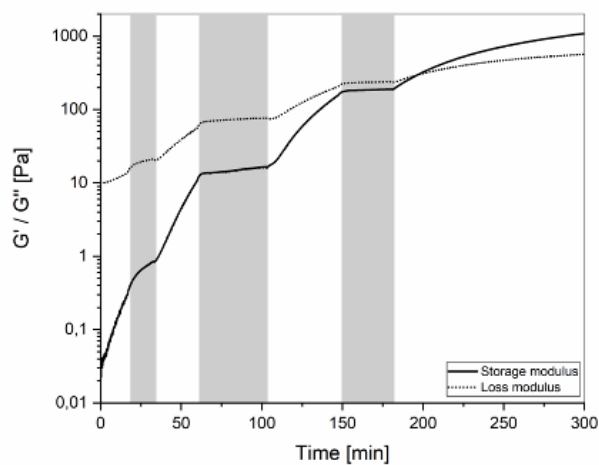


**Figure S72.** Control photo-curing with crosslinker X and terminal Si-OH PDMS (n~484) in a ratio of 2.0. White areas display curing with irradiation ( $\lambda = 365\text{nm}$ ), grey areas without irradiation.

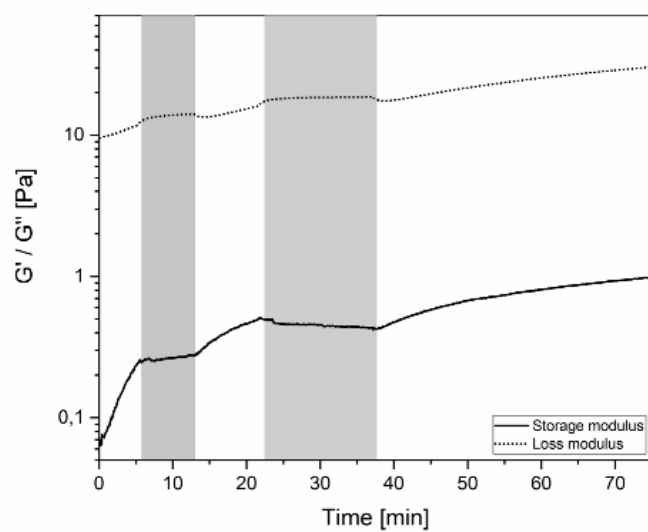


**Figure S73.** Control photo-curing with crosslinker X and terminal Si-H PDMS (n~378) in a ratio of 0.5. White areas display curing with irradiation ( $\lambda = 365\text{nm}$ ), grey areas without irradiation.

### 3. Thermogravimetric analysis (TGA)

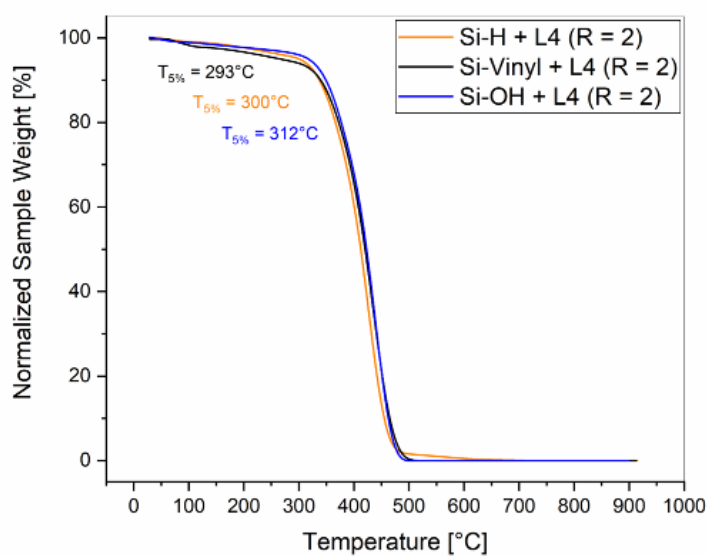


**Figure S 74.** Thermogravimetric analysis of silicone elastomers afforded from PMHS Si-H (orange), PDMS Si-OH (blue), and PDMS Si-vinyl (black).

### 4. Differential scanning calorimetry (DSC)

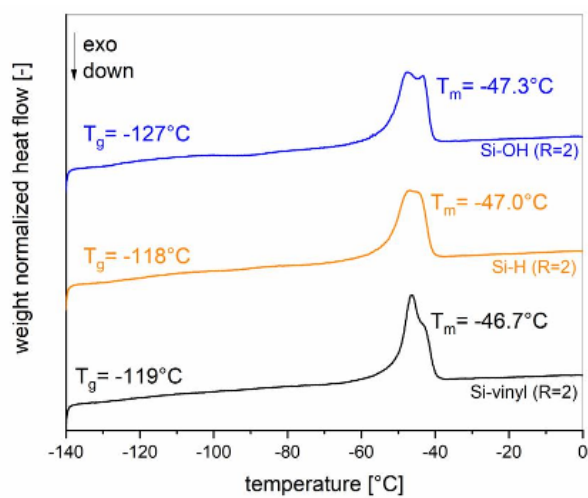


**Figure S 75.** Differential scanning calorimetry of silicone elastomers afforded from PMHS Si-H (orange), PDMS Si-OH (blue), and PDMS Si-vinyl (black).



## 5. Swelling Tests

Three replicas of each dried hydrogel were swollen in toluene at room temperature for 3 days to achieve equilibrium swelling. The swollen samples were subsequently removed from the swelling solution and dried at 40 °C in vacuum to remove all solvent. The gel-fraction was defined as  $F_g = [M_{\text{cured}} / M_{\text{dried}}]$ , while the swelling ratio was calculated as  $S = [(M_{\text{swollen}} - M_{\text{dried}}) / M_{\text{dried}}]$ .

**Table S 6.** asd

Sample (Ratio)	$M_{\text{cured}}$ [mg]	$M_{\text{dried}}$ [mg]	$M_{\text{swollen}}$ [mg]	$F_g$ [%]	$S$ [%]
Si-H (0.8)	203	159	957	78	502
Si-H (1.0)	201	166	880	83	430
Si-H (2.0)	210	197	649	94	229
Si-OH (0.8)	198	154	1024	78	565
Si-OH (1.0)	206	176	852	85	384
Si-OH (2.0)	204	190	732	93	285
Si-vinyl (0.8)	206	175	910	85	420
Si-vinyl (1.0)	207	180	885	87	392
Si-vinyl (2.0)	212	202	631	95	212

## 6. Emission Sepetra

DUV325-SD353EL

## Basic Information

Type	Deep UV SMD
Description	DEEP UV SMD LEDs - 325 nm / 45 mW
Manufacturer / Supplier	n/a / Roithner
Order number / Date of purch.	n/a / 04/2022
Internal lot / serial number	2022-04 / LED325

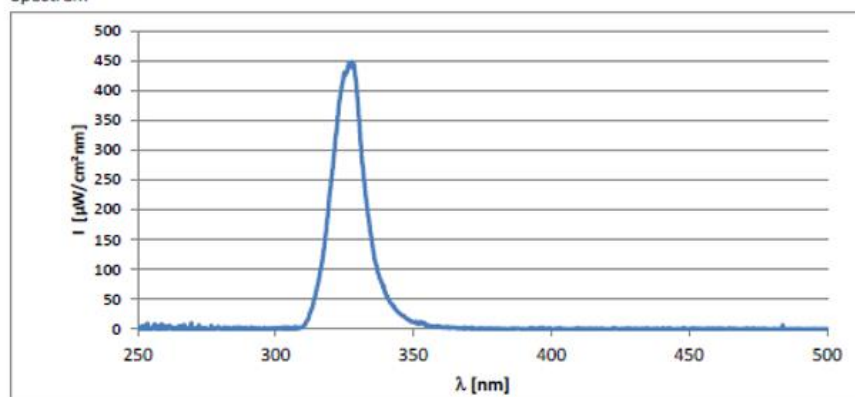
## Specification Manufacturer

Type / size	single emitter / ca. 2.3 x 2.3 mm
Mechanical specification	UV glass lens, 65 deg. Beam angle
Electrical specification	350 mA, UF 5.0 V
Wavelength (range, typ.)	320-330 nm, typ. n/a
Spectral width (FWHM)	15 nm
Datasheet	n/a

## Characterization

Description of measurement	Measured with Ocean-optics USB4000 spectrometer using a calibrated setup (cosine corrector/fibre). The distance between the emitting surface and the surface of the cosine corrector was 20 mm. The LED was operated at 350 mA on a passive heat-sink at approx. 20 °C	
Measured dominant wavelength / Int.	328 nm	448 $\mu\text{W}/\text{mm}^2\text{nm}$
Measured spectral width (FWHM)	13 nm	
Integral Reference intensity / range	6802 $\mu\text{W}/\text{cm}^2$	310-380 nm

## Spectrum

Figure S76. Datasheet with emission spectrum of LED ( $\lambda_{\text{max}} = 325 \text{ nm}$ ).

S72

## DUV340-SD353EL

## Basic Information

Type	Deep UV SMD
Description	DEEP UV SMD LEDs - 340 nm / 44 mW
Manufacturer / Supplier	n/a / Roithner
Order number / Date of purch.	n/a / 04/2022
Internal lot / serial number	2022-04 / LED340

## Specification Manufacturer

Type / size	single emitter / ca. 2.3 x 2.3 mm
Mechanical specification	UV glass lens, 65 deg beam angle
Electrical specification	350 mA, UF 5.5 V
Wavelength (range, typ.)	335-345 nm, typ. n/a
Spectral width (FWHM)	10 nm
Datasheet	n/a

## Characterization

Description of measurement	Measured with Ocean-optics USB4000 spectrometer using a calibrated setup (cosine corrector/fibre). The distance between the emitting surface and the surface of the cosine corrector was 20 mm. The LED was operated at 350 mA on a passive heat-sink at approx. 20 °C	
Measured dominant wavelength / Int.	339 nm	700 $\mu\text{W}/\text{mm}^2\text{nm}$
Measured spectral width (FWHM)	9 nm	
Integral Reference intensity / range	7743 $\mu\text{W}/\text{cm}^2$	310-380 nm

## Spectrum

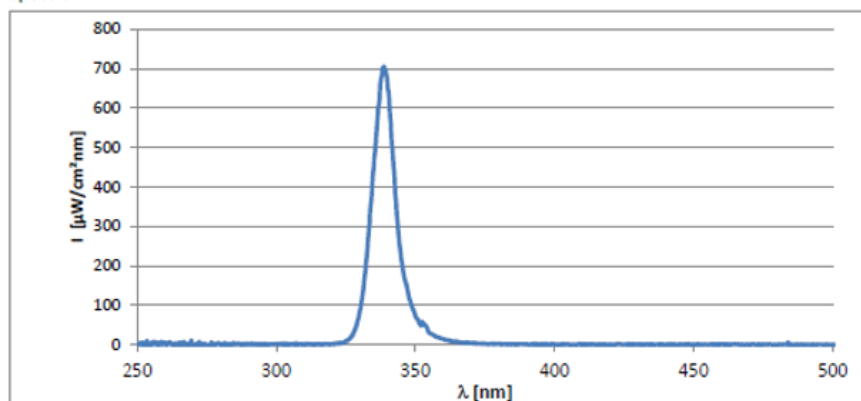
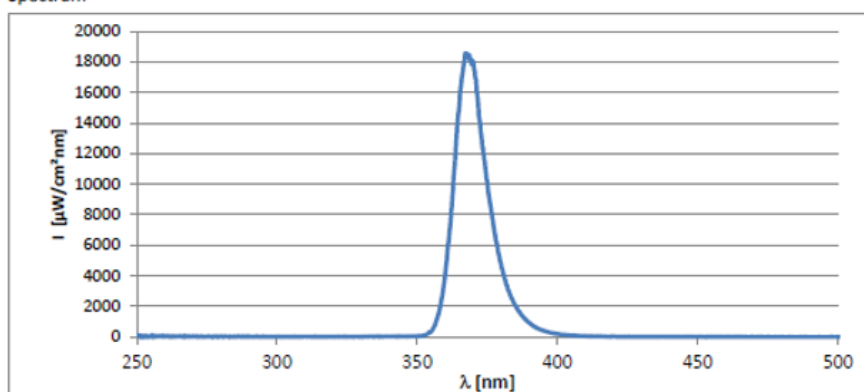


Figure S77. Datasheet with emission spectrum of LED ( $\lambda_{\text{max}} = 340$  nm).

## LZ4-V4UV0R-0000

Basic Information	
Type	Deep UV SMD
Description	DEEP UV SMD LEDs - 365 nm / 44 mW
Manufacturer / Supplier	n/a / Mouser
Order number / Date of purch.	n/a / 05/2022
Internal lot / serial number	2022-04 / LED365
Specification Manufacturer	
Type / size	single emitter / ca. 2.3 x 2.3 mm
Mechanical specification	UV glass lens, 110 deg beam angle
Electrical specification	700 mA, UF 15.2 V
Wavelength (range, typ.)	365 nm, typ. n/a
Spectral width (FWHM)	15 nm
Datasheet	n/a
Characterization	
Description of measurement	Measured with Ocean-optics USB4000 spectrometer using a calibrated setup (cosine corrector/fibre). The distance between the emitting surface and the surface of the cosine corrector was 20 mm. The LED was operated at 350 mA on a passive heat-sink at approx. 20 °C
Measured dominant wavelength / Int.	367 nm                      18229 $\mu\text{W}/\text{mm}^2\text{nm}$
Measured spectral width (FWHM)	13 nm
Integral Reference intensity / range	149600 $\mu\text{W}/\text{cm}^2$ 310-380 nm
Spectrum	



**Figure S78.** Datasheet with emission spectrum of LED ( $\lambda_{\text{max}} = 365 \text{ nm}$ ).

Datasheet LED040		366 / 10W
Basic Information	Ultra-High-Power UV-A-LED	
Type	High-Power-LED	
Description		
Manufacturer / Supplier	Mouser	
Order number / Date of purch.	LZ4-44UV00-0000 / 06/2016	
Internal lot / serial number	2016-01 / LED040	
Specification Manufacturer		
Type / size	quattro emitter / not spec.	
Mechanical specification		
Electrical specification	700 mA @18V	
Wavelength (range, typ.)		
Spectral width (FWHM)		
Datasheet	LZ4-04UV-series	
Characterization		
Description of measurement	Measured with Ocean-optics USB4000 spectrometer using a calibrated setup (cosine corrector/fibre). The distance between the emitting surface and the surface of the cosine corrector was 20 mm. The LED was operated at 500 mA on a passive heat-sink at approx. 20 °C	
Measured wavelength	368 nm	
Measured spectral width	12 nm	
Integral Reference intensity	18605 $\mu\text{W}/\text{cm}^2$ (350-425 nm @ 20 mm distance, 4 mmsine corr.)	
Spectrum		

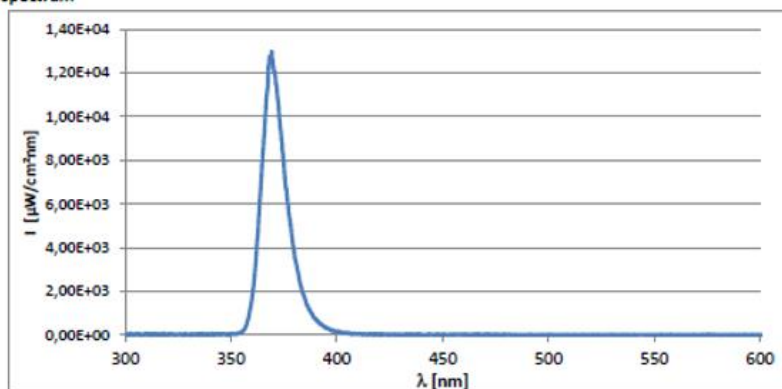


Figure S79. Datasheet with emission spectrum of LED ( $\lambda_{\text{max}} = 368$  nm).

## Datasheet FLT014

RPR-2537A

## Basic Information

Type	Fluorescent light tube
Description	S. N. E. Ultraviolet Co. RPR-2537 Å
Manufacturer / Supplier	n/a / Ryonet
Order number / Date of purch.	n/a / n/a
Internal lot / serial number	n/a / FLT014

## Specification Manufacturer

Type / size	T5 tube, G5 socket
Mechanical specification	16 mm diameter, 288 mm length
Electrical specification	n/a
Wavelength (range, typ.)	254 nm
Spectral width (FWHM)	n/a
Datasheet	n/a

## Characterization

Description of measurement	Measured with Ocean-optics USB4000 spectrometer using a calibrated setup (cosine corrector/fibre). The cosine corrector was placed at 20 mm distance from a single fluorescent tube at half height.	
----------------------------	--	--

Measured dominant wavelength / Int.	253 nm	311 $\mu\text{W}/\text{mm}^2\text{nm}$
Measured spectral width (FWHM)	2 nm	
Integral Reference intensity / range	6089 $\mu\text{W}/\text{cm}^2$	245-270 nm

## Spectrum

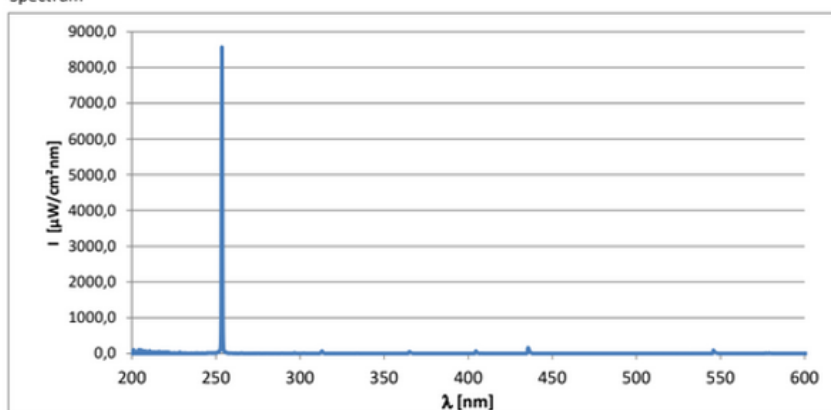


Figure S80. Datasheet with emission spectrum of FLT ( $\lambda_{\text{max}} = 254 \text{ nm}$ ).

S76

## Datasheet FLT012

RPR3000

## Basic Information

Type	Fluorescent light tube
Description	Rayonet RPR-3000A
Manufacturer / Supplier	n/a / Southern New England Ultraviolet Company
Order number / Date of purch.	n/a / n/a
Internal lot / serial number	n/a / FLT012

## Specification Manufacturer

Type / size	T5 tube, G5 socket
Mechanical specification	16 mm diameter, 288 mm length
Electrical specification	8 W
Wavelength (range, typ.)	300 nm
Spectral width (FWHM)	~ 40 nm
Datasheet	n/a

## Characterization

Description of measurement	Measured with Ocean-optics USB4000 spectrometer using a calibrated setup (cosine corrector/fibre). The cosine corrector was placed at 20 mm distance from a single fluorescent tube at half height.
----------------------------	--

Measured dominant wavelength / Int.	313 nm	138 $\mu\text{W}/\text{mm}^2\text{nm}$
Measured spectral width (FWHM)	40 nm	
Integral Reference intensity / range	4725 $\mu\text{W}/\text{cm}^2$	260-380 nm

## Spectrum

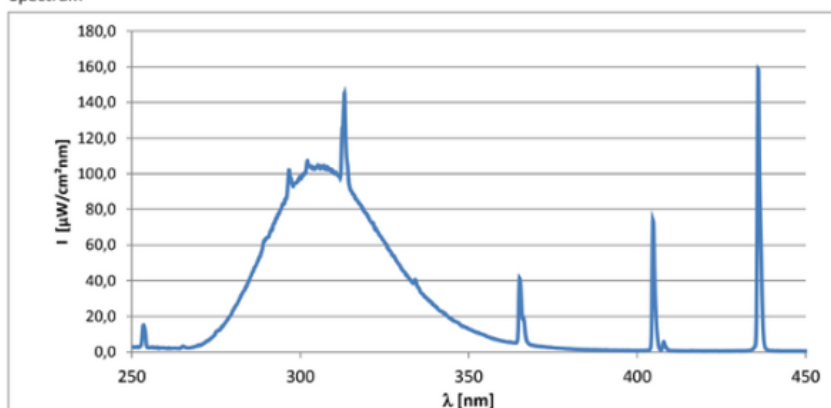


Figure S81. Datasheet with emission spectrum of FLT ( $\lambda_{\text{max}} = 300$  nm).

S77

## Datasheet FLT015

## RPR-Set1-UV-A

## Basic Information

Type	Fluorescent light tube
Description	Set1 (UV-A)
Manufacturer / Supplier	n/a / Rayonet
Order number / Date of purch.	n/a / n/a
Internal lot / serial number	Set1 / FLT015

## Specification Manufacturer

Type / size	T5 tube, G5 socket
Mechanical specification	16 mm diameter, 288 mm length
Electrical specification	8 W
Wavelength (range, typ.)	350 nm
Spectral width (FWHM)	~ 30 nm
Datasheet	

## Characterization

Description of measurement	Measured with Ocean-optics USB4000 spectrometer using a calibrated setup (cosine corrector/fibre). The cosine corrector was placed at 20 mm distance from a single fluorescent tube at half height.	
Measured dominant wavelength / Int.	365 nm	104 $\mu\text{W}/\text{mm}^2\text{nm}$
Measured spectral width (FWHM)	18 nm	
Integral Reference intensity / range	2194 $\mu\text{W}/\text{cm}^2$	300-450 nm

## Spectrum

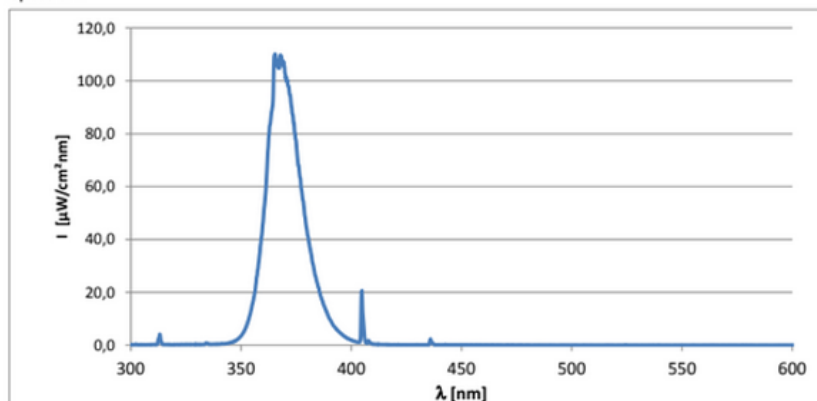


Figure S82. Datasheet with emission spectrum of FLT ( $\lambda_{\text{max}} = 366 \text{ nm}$ ).



## Datasheet FLT022

LZC-420

## Basic Information

Type	Fluorescent light tube
Description	Luzchem LZC-420
Manufacturer / Supplier	n/a / Luzchem
Order number / Date of purch.	n/a / 07/2017
Internal lot / serial number	2017-07 / FLT022

## Specification Manufacturer

Type / size	T5 tube, G5 socket
Mechanical specification	16 mm diameter, 288 mm length
Electrical specification	8 W
Wavelength (range, typ.)	400 - 440 nm
Spectral width (FWHM)	~ 30 nm
Datasheet	LES-420-016

## Characterization

Description of measurement	Measured with Ocean-optics USB4000 spectrometer using a calibrated setup (cosine corrector/fibre). The cosine corrector was placed at 20 mm distance from a single fluorescent tube at half height.
----------------------------	--

Measured dominant wavelength / Int.	421 nm	121 $\mu\text{W}/\text{mm}^2\text{nm}$
Measured spectral width (FWHM)	30 nm	
Integral Reference intensity / range	4142 $\mu\text{W}/\text{cm}^2$	350-500 nm

## Spectrum

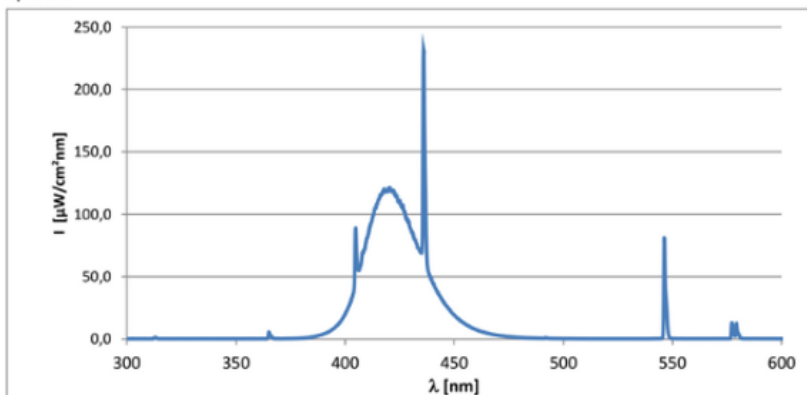


Figure S83. Datasheet with emission spectrum of FLT ( $\lambda_{\text{max}} = 420 \text{ nm}$ ).

S79

## II. References

- [1] M. Muhr, P. Heiß, M. Schütz, R. Bühler, C. Gemel, M. H. Linden, H. B. Linden, R. A. Fischer, *Dalton Transactions* **2021**, 50, 9031.
- [2] J. Huang, J. Chan, Y. Chen, C. J. Borths, K. D. Baucom, R. D. Larsen, M. M. Faul, *Journal of the American Chemical Society* **2010**, 132, 3674.
- [3] S. Qiu, C. Zhang, R. Qiu, G. Yin, J. Huang, *Adv. Synth. Catal.* **2018**, 360, 313.
- [4] R. West, L. C. Quass, *Journal of Organometallic Chemistry* **1969**, 18, 55.
- [5] W. Uhlig, *Journal of Organometallic Chemistry* **1997**, 545-546, 281.
- [6] S. Sekigawa, T. Shimizu, W. Ando, *Tetrahedron* **1993**, 49, 6359.
- [7] J. J. Eisch, B. W. Kotowicz, *Chem. Ber.* **1998**, 1998, 761.
- [8] H. Watanabe, T. Ohkawa, T. Muraoka, Y. Nagai, *Chem. Lett.* **1981**, 10, 1321.
- [9] M. Weidenbruch, A. Schäfer, R. Rankers, *Journal of Organometallic Chemistry* **1980**, 195, 171.
- [10] N. Wiberg, K. Amelunxen, H.-W. Lerner, H. Schuster, H. Nöth, I. Krossing, M. Schmidt-Amelunxen, T. Seifert, *Journal of Organometallic Chemistry* **1997**, 542, 1.
- [11] P. Boudjouk, U. Samaraweera, R. Sooriyakumaran, J. Chrisciell, K. R. Anderson, *Angew. Chem.* **1988**, 100, 1406.
- [12] P. Boudjouk, U. Samaraweera, R. Sooriyakumaran, J. Chrusiell, K. R. Anderson, *Angew. Chem. Int. Ed. Engl.* **1988**, 27, 1355.
- [13] T. G. Driver, K. A. Woerpel, *J. Am. Chem. Soc.* **2004**, 126, 9993.
- [14] D. Seyferth, D. C. Annarelli, S. C. Vick, *J. Am. Chem. Soc.* **1976**, 98, 6382.
- [15] T. G. Driver, K. A. Woerpel, *J. Am. Chem. Soc.* **2003**, 125, 10659.
- [16] M. Nobis, S. Inoue, B. Rieger, *Chemical Communications* **2022**, 58, 11159.
- [17] F. A. D. Herz, M. Nobis, D. Wendel, P. Pahl, P. J. Altmann, J. Tillmann, R. Weidner, S. Inoue, B. Rieger, *Green Chem.* **2020**, 22, 4489.
- [18] M. Ishikawa, M. Kumada in *Advances in Organometallic Chemistry*, pp. 51–95.
- [19] M. Ishikawa, A. Naka, J. Ohshita, *Asian J. Org. Chem.* **2015**, 4, 1192.

## 9.5. License Agreements

## 9.5.1. License Agreement for Chapter 4



This is a License Agreement between Matthias Nobis ("User") and Copyright Clearance Center, Inc. ("CCC") on behalf of the Rightsholder identified in the order details below. The license consists of the order details, the Marketplace Order General Terms and Conditions below, and any Rightsholder Terms and Conditions which are included below.

All payments must be made in full to CCC in accordance with the Marketplace Order General Terms and Conditions below.

Order Date	06-Nov-2022	Type of Use	Republish in a thesis/dissertation
Order License ID	1287233-1	Publisher	ROYAL SOC OF CHEM
ISSN	1463-9262	Portion	Chapter/article

## LICENSED CONTENT

Publication Title	Green chemistry : an international journal and green chemistry resource : GC	Rightsholder	Royal Society of Chemistry
Article Title	Application of Multifunctional Silylenes and Siliranes as Universal Crosslinkers for Metal-Free Curing of Silicones	Publication Type	Journal
Author/Editor	Royal Society of Chemistry (Great Britain)	Start Page	4489
Date	01/01/1999	End Page	4497
Language	English	Issue	14
Country	United Kingdom of Great Britain and Northern Ireland	Volume	22

## REQUEST DETAILS

Portion Type	Chapter/article	Rights Requested	Main product
Page Range(s)	4489-4497	Distribution	Worldwide
Total Number of Pages	9	Translation	Original language of publication
Format (select all that apply)	Print, Electronic	Copies for the Disabled?	No
Who Will Republish the Content?	Author of requested content	Minor Editing Privileges?	No
Duration of Use	Life of current edition	Incidental Promotional Use?	No
Lifetime Unit Quantity	Up to 499	Currency	EUR

## NEW WORK DETAILS

Title	Three-Membered Silacycles and Silylenes in Thermal and Photochemical Curing of Polysiloxanes	Institution Name	Technical University Munich
Instructor Name	Matthias Nobis	Expected Presentation Date	2023-01-01

## ADDITIONAL DETAILS

Order Reference Number	N/A	The Requesting Person/Organization to Appear on the License	Matthias Nobis
------------------------	-----	---	----------------

## REUSE CONTENT DETAILS

Title, Description or Numeric Reference of the Portion(s)	Application of Multifunctional Silylenes and Siliranes as Universal Crosslinkers for Metal-Free Curing of Silicones	Title of the Article/Chapter the Portion Is From	Application of Multifunctional Silylenes and Siliranes as Universal Crosslinkers for Metal-Free Curing of Silicones
Editor of Portion(s)	Herz, Fabian Andreas; David; Nobis, Matthias; Wendel, Daniel Wolfgang; Pahl, Philipp; Altmann, Philipp Johannes; Weidner, Richard; Tillmann, Jan; Inoue, Shigeyoshi; Rieger, Bernhard	Author of Portion(s)	Herz, Fabian Andreas; David; Nobis, Matthias; Wendel, Daniel Wolfgang; Pahl, Philipp; Altmann, Philipp Johannes; Weidner, Richard; Tillmann, Jan; Inoue, Shigeyoshi; Rieger, Bernhard
Volume of Serial or Monograph	22	Issue, if Republishing an Article From a Serial	14
Page or Page Range of Portion	4489-4497	Publication Date of Portion	2020-01-01

## Marketplace Order General Terms and Conditions

The following terms and conditions ("General Terms"), together with any applicable Publisher Terms and Conditions, govern User's use of Works pursuant to the Licenses granted by Copyright Clearance Center, Inc. ("CCC") on behalf of the applicable Rightsholders of such Works through CCC's applicable Marketplace transactional licensing services (each, a "Service").

1) **Definitions.** For purposes of these General Terms, the following definitions apply:

"License" is the licensed use the User obtains via the Marketplace platform in a particular licensing transaction, as set forth in the Order Confirmation.

"Order Confirmation" is the confirmation CCC provides to the User at the conclusion of each Marketplace transaction. "Order Confirmation Terms" are additional terms set forth on specific Order Confirmations not set forth in the General Terms that can include terms applicable to a particular CCC transactional licensing service and/or any Rightsholder-specific terms.

"Rightsholder(s)" are the holders of copyright rights in the Works for which a User obtains licenses via the Marketplace platform, which are displayed on specific Order Confirmations.

"Terms" means the terms and conditions set forth in these General Terms and any additional Order Confirmation Terms collectively.

"User" or "you" is the person or entity making the use granted under the relevant License. Where the person accepting the Terms on behalf of a User is a freelancer or other third party who the User authorized to accept the General Terms on the User's behalf, such person shall be deemed jointly a User for purposes of such Terms.

"Work(s)" are the copyright protected works described in relevant Order Confirmations.

2) **Description of Service.** CCC's Marketplace enables Users to obtain Licenses to use one or more Works in accordance with all relevant Terms. CCC grants Licenses as an agent on behalf of the copyright rightsholder identified in the relevant Order Confirmation.

3) **Applicability of Terms.** The Terms govern User's use of Works in connection with the relevant License. In the event of any conflict between General Terms and Order Confirmation Terms, the latter shall govern. User acknowledges that Rightsholders have complete discretion whether to grant any permission, and whether to place any limitations on any grant, and that CCC has no right to supersede or to modify any such discretionary act by a Rightsholder.

## 9.5.2. License Agreement for Chapter 5



This is a License Agreement between Matthias Nobis ("User") and Copyright Clearance Center, Inc. ("CCC") on behalf of the Rightsholder identified in the order details below. The license consists of the order details, the Marketplace Order General Terms and Conditions below, and any Rightsholder Terms and Conditions which are included below.

All payments must be made in full to CCC in accordance with the Marketplace Order General Terms and Conditions below.

Order Date	06-Nov-2022	Type of Use	Republish in a thesis/dissertation
Order License ID	1287233-2	Publisher Portion	THE SOCIETY, Chapter/article
ISSN	1359-7345		

## LICENSED CONTENT

Publication Title	Chemical communications : Chem comm	Publication Type	Journal
Article Title	Modular Silacyclopropenes: Synthesis and Application for Si H containing Substrate Functionalization	Start Page	11159
		End Page	11162
		Issue	79
		Volume	58
		URL	<a href="http://www.rsc.org/Publishing/Journals/cc/Article.asp?Type=CurrentIssue">http://www.rsc.org/Publishing/Journals/cc/Article.asp?Type=CurrentIssue</a>
Author/Editor	ROYAL SOCIETY OF CHEMISTRY (GREAT BRITAIN)		
Date	01/01/1996		
Language	English		
Country	United Kingdom of Great Britain and Northern Ireland		
Rightsholder	Royal Society of Chemistry		

## REQUEST DETAILS

Portion Type	Chapter/article	Rights Requested	Main product
Page Range(s)	11159-11162	Distribution	Worldwide
Total Number of Pages	4	Translation	Original language of publication
Format (select all that apply)	Print, Electronic	Copies for the Disabled?	No
Who Will Republish the Content?	Author of requested content	Minor Editing Privileges?	No
Duration of Use	Life of current edition	Incidental Promotional Use?	No
Lifetime Unit Quantity	Up to 499	Currency	EUR

## NEW WORK DETAILS

Title	Three-Membered Silacycles and Silylenes in Thermal and Photochemical Curing of Polysiloxanes	Institution Name	Technical University Munic
		Expected Presentation Date	2023-01-01
Instructor Name	Matthias Nobis		

## ADDITIONAL DETAILS

Order Reference Number	N/A	The Requesting Person/Organization to Appear on the License	Matthias Nobis
------------------------	-----	---	----------------

## REUSE CONTENT DETAILS

Title, Description or Numeric Reference of the Portion(s)	Modular Silacyclopropenes: Synthesis and Application for Si H containing Substrate Functionalization	Title of the Article/Chapter the Portion Is From	Modular Silacyclopropenes: Synthesis and Application for Si H containing Substrate Functionalization
Editor of Portion(s)	Nobis, Matthias; Inoue, Shigeyoshi; Rieger, Bernhard	Author of Portion(s)	Nobis, Matthias; Inoue, Shigeyoshi; Rieger, Bernhard
Volume of Serial or Monograph	58	Issue, if Republishing an Article From a Serial	79
Page or Page Range of Portion	11159-11162	Publication Date of Portion	2022-10-04

## Marketplace Order General Terms and Conditions

The following terms and conditions ("General Terms"), together with any applicable Publisher Terms and Conditions, govern User's use of Works pursuant to the Licenses granted by Copyright Clearance Center, Inc. ("CCC") on behalf of the applicable Rightsholders of such Works through CCC's applicable Marketplace transactional licensing services (each, a "Service").

1) **Definitions.** For purposes of these General Terms, the following definitions apply:

"License" is the licensed use the User obtains via the Marketplace platform in a particular licensing transaction, as set forth in the Order Confirmation.

"Order Confirmation" is the confirmation CCC provides to the User at the conclusion of each Marketplace transaction. "Order Confirmation Terms" are additional terms set forth on specific Order Confirmations not set forth in the General Terms that can include terms applicable to a particular CCC transactional licensing service and/or any Rightsholder-specific terms.

"Rightsholder(s)" are the holders of copyright rights in the Works for which a User obtains licenses via the Marketplace platform, which are displayed on specific Order Confirmations.

"Terms" means the terms and conditions set forth in these General Terms and any additional Order Confirmation Terms collectively.

"User" or "you" is the person or entity making the use granted under the relevant License. Where the person accepting the Terms on behalf of a User is a freelancer or other third party who the User authorized to accept the General Terms on the User's behalf, such person shall be deemed jointly a User for purposes of such Terms.

"Work(s)" are the copyright protected works described in relevant Order Confirmations.

2) **Description of Service.** CCC's Marketplace enables Users to obtain Licenses to use one or more Works in accordance with all relevant Terms. CCC grants Licenses as an agent on behalf of the copyright rightsholder identified in the relevant Order Confirmation.

3) **Applicability of Terms.** The Terms govern User's use of Works in connection with the relevant License. In the event of any conflict between General Terms and Order Confirmation Terms, the latter shall govern. User acknowledges that Rightsholders have complete discretion whether to grant any permission, and whether to place any limitations on any grant, and that CCC has no right to supersede or to modify any such discretionary act by a Rightsholder.

4) **Representations; Acceptance.** By using the Service, User represents and warrants that User has been duly authorized by the User to accept, and hereby does accept, all Terms.

## 9.5.3. License Agreement for Chapter 6



This is a License Agreement between Matthias Nobis ("User") and Copyright Clearance Center, Inc. ("CCC") on behalf of the Rightsholder identified in the order details below. The license consists of the order details, the Marketplace Order General Terms and Conditions below, and any Rightsholder Terms and Conditions which are included below.

All payments must be made in full to CCC in accordance with the Marketplace Order General Terms and Conditions below.

Order Date	07-Dec-2022	Type of Use	Republish in a thesis/dissertation
Order License ID	1298164-1	Publisher	WILEY - VCH VERLAG GMBH & CO. KGAA
ISSN	1864-5631	Portion	Chapter/article

## LICENSED CONTENT

Publication Title	ChemSusChem	Language	English
Article Title	Photo-Activity of Silacyclopropenes and their Application in Metal-Free Curing of Silicones.	Country	Germany
		Rightsholder	John Wiley & Sons - Books
		Publication Type	Journal
Author/Editor	Asian Chemical Editorial Society., EU ChemSoc., Società chimica italiana.		
Date	01/01/2008		

## REQUEST DETAILS

Portion Type	Chapter/article	Rights Requested	Main product
Page Range(s)	?	Distribution	Worldwide
Total Number of Pages	9	Translation	Original language of publication
Format (select all that apply)	Print, Electronic	Copies for the Disabled?	No
Who Will Republish the Content?	Author of requested content	Minor Editing Privileges?	No
Duration of Use	Life of current edition	Incidental Promotional Use?	No
Lifetime Unit Quantity	Up to 499	Currency	EUR

## NEW WORK DETAILS

Title	Dissertation	Institution Name	Technical University Munich
Instructor Name	Matthias Nobis	Expected Presentation Date	2023-01-09

## ADDITIONAL DETAILS

The Requesting Person/Organization to Appear on the License	Matthias Nobis
---	----------------

## REUSE CONTENT DETAILS

<b>Title, Description or Numeric Reference of the Portion(s)</b>	Photo-Activity of Silacyclopropenes and their Application in Metal-Free Curing of Silicones	<b>Title of the Article/Chapter the Portion Is From</b>	Photo-Activity of Silacyclopropenes and their Application in Metal-Free Curing of Silicones
<b>Editor of Portion(s)</b>	Nobis, Matthias; Futter, Jonas; Moxter, Maximilian; Inoue, Shigeyoshi; Rieger, Bernhard	<b>Author of Portion(s)</b>	Nobis, Matthias; Futter, Jonas; Moxter, Maximilian; Inoue, Shigeyoshi; Rieger, Bernhard
<b>Volume of Serial or Monograph</b>	x	<b>Publication Date of Portion</b>	2022-11-29
<b>Page or Page Range of Portion</b>	x		

## RIGHTSHOLDER TERMS AND CONDITIONS

No right, license or interest to any trademark, trade name, service mark or other branding ("Marks") of WILEY or its licensors is granted hereunder, and you agree that you shall not assert any such right, license or interest with respect thereto. You may not alter, remove or suppress in any manner any copyright, trademark or other notices displayed by the Wiley material. This Agreement will be void if the Type of Use, Format, Circulation, or Requestor Type was misrepresented during the licensing process. In no instance may the total amount of Wiley Materials used in any Main Product, Compilation or Collective work comprise more than 5% (if figures/tables) or 15% (if full articles/chapters) of the (entirety of the) Main Product, Compilation or Collective Work. Some titles may be available under an Open Access license. It is the Licensors' responsibility to identify the type of Open Access license on which the requested material was published, and comply fully with the terms of that license for the type of use specified Further details can be found on Wiley Online Library <http://olabout.wiley.com/WileyCDA/Section/id-410895.html>.

## SPECIAL RIGHTSHOLDER TERMS AND CONDITIONS

This is an open access article under the terms of the Creative Commons Attribution-NonCommercial License, which permits use, distribution and reproduction in any medium, provided the original work is properly cited and is not used for commercial purposes.

## Marketplace Order General Terms and Conditions

The following terms and conditions ("General Terms"), together with any applicable Publisher Terms and Conditions, govern User's use of Works pursuant to the Licenses granted by Copyright Clearance Center, Inc. ("CCC") on behalf of the applicable Rightsholders of such Works through CCC's applicable Marketplace transactional licensing services (each, a "Service").

1) **Definitions.** For purposes of these General Terms, the following definitions apply:

"License" is the licensed use the User obtains via the Marketplace platform in a particular licensing transaction, as set forth in the Order Confirmation.

"Order Confirmation" is the confirmation CCC provides to the User at the conclusion of each Marketplace transaction. "Order Confirmation Terms" are additional terms set forth on specific Order Confirmations not set forth in the General Terms that can include terms applicable to a particular CCC transactional licensing service and/or any Rightsholder-specific terms.

"Rightsholder(s)" are the holders of copyright rights in the Works for which a User obtains licenses via the Marketplace platform, which are displayed on specific Order Confirmations.

"Terms" means the terms and conditions set forth in these General Terms and any additional Order Confirmation Terms collectively.

"User" or "you" is the person or entity making the use granted under the relevant License. Where the person accepting the Terms on behalf of a User is a freelancer or other third party who the User authorized to accept the General Terms on the User's behalf, such person shall be deemed jointly a User for purposes of such Terms.

"Work(s)" are the copyright protected works described in relevant Order Confirmations.

2) **Description of Service.** CCC's Marketplace enables Users to obtain Licenses to use one or more Works in accordance with all relevant Terms. CCC grants Licenses as an agent on behalf of the copyright rightsholder identified in the relevant Order Confirmation.



## 9.6. Statutory Declaration

Ich, **Matthias Fabian Nobis**, erkläre an Eides statt, dass ich die bei der promotionsführenden Einrichtung

**TUM School of Natural Sciences**

---

der TUM zur Promotionsprüfung vorgelegte Arbeit mit dem Titel:

**“Three-Membered Silacycles and Silylenes in Thermal and Photochemical Curing of Polysiloxanes”**

---

unter der Anleitung und Betreuung durch: Prof. Dr. Dr. h. c. Bernhard Rieger

ohne sonstige Hilfe erstellt und bei der Abfassung nur die gemäß § 7 Abs. 6 und 7 angegebenen Hilfsmittel benutzt habe.

Ich habe keine Organisation eingeschaltet, die gegen Entgelt Betreuer\*innen für die Anfertigung von Dissertationen sucht, oder die mir obliegenden Pflichten hinsichtlich der Prüfungsleistungen für mich ganz oder teilweise erledigt.

Ich habe die Dissertation in dieser oder ähnlicher Form in keinem anderen Prüfungsverfahren als Prüfungsleistung vorgelegt.

Teile der Dissertation wurden in den genannten Fach-Journalen (Green Chem, ChemComm, ChemSusChem) veröffentlicht.

Ich habe den angestrebten Doktorgrad noch nicht erworben und bin nicht in einem früheren Promotionsverfahren für den angestrebten Doktorgrad endgültig gescheitert.

Ich habe bereits am \_\_\_\_\_ bei der promotionsführenden Einrichtung \_\_\_\_\_ der Hochschule \_\_\_\_\_ unter Vorlage einer Dissertation mit dem Thema \_\_\_\_\_

die Zulassung zur Promotion beantragt mit dem Ergebnis:

---

Ich habe keine Kenntnis über ein strafrechtliches Ermittlungsverfahren in Bezug auf wissenschaftsbezogene Straftaten gegen mich oder eine rechtskräftige strafrechtliche Verurteilung mit Wissenschaftsbezug.

Die öffentlich zugängliche Promotionsordnung sowie die Richtlinien zur Sicherung guter wissenschaftlicher Praxis und für den Umgang mit wissenschaftlichem Fehlverhalten der TUM sind mir bekannt, insbesondere habe ich die Bedeutung von § 27 PromO (Nichtigkeit der Promotion) und § 28 PromO (Entzug des Doktorgrades) zur Kenntnis genommen. Ich bin mir der Konsequenzen einer falschen Eidesstattlichen Erklärung bewusst.

Mit der Aufnahme meiner personenbezogenen Daten in die Alumni-Datei bei der TUM bin ich

einverstanden,  nicht einverstanden.

---

München, 19.01.2023